

# ICOEST

**UKRAINE**

**4TH INTERNATIONAL CONFERENCE ON  
ENVIRONMENTAL SCIENCE AND TECHNOLOGY**

**SEPTEMBER 19-23 2018**

**BOOK OF PROCEEDINGS**

[www.icoest.eu](http://www.icoest.eu)

**Organized by**



**Partners**



**4th INTERNATIONAL CONFERENCE ON ENVIRONMENTAL SCIENCE AND TECHNOLOGY  
(ICOEST)**

**ISBN 978-605-81426-2-6**

**BOOK OF PROCEEDING OF THE  
4th INTERNATIONAL CONFERENCE ON ENVIRONMENTAL SCIENCE AND TECHNOLOGY  
(ICOEST)**

**19–23 September 2018, Kiev, UKRAINE**

**Edited by**

Prof. Dr. Özer Çınar

**Published, 2018**

**info@icoest.eu**

**www.icoest.eu**

This work is subject to copyright. All rights are reserved, whether the whole or part of the material is concerned. Nothing from this publication may be translated, reproduced, stored in a computerized system or published in any form or in any manner, including, but not limited to electronic, mechanical, reprographic or photographic, without prior written permission from the publisher.

**info@icoest.eu**

The individual contributions in this publication and any liabilities arising from them remain the responsibility of the authors.

The publisher is not responsible for possible damages, which could be a result of content derived from this publication.

## SCIENTIFIC COMMITTEE

1. Prof.Dr. Adisa Parić – University of Sarajevo - Bosnia and Herzegovina
2. Prof.Dr. Ana Vovk-Korže - University of Maribor - Slovenia
3. Prof.Dr. Arslan Saral – Yıldız Technical University - Turkey
4. Prof.Dr. Ayşegül Pala – Dokuz Eylül University - Turkey
5. Prof.Dr. Cumali Kınacı - İstanbul Technical University - Turkey
6. Prof.Dr. Dragan Vinterhalter - University of Belgrade - Serbia
7. Prof.Dr. Dragutin T. Mihailović - University of Novi Sad - Serbia
8. Prof.Dr. Edina Muratović – University of Sarajevo - Bosnia and Herzegovina
9. Prof.Dr. Esad Prohic - University of Zagreb - Croatia
10. Prof.Dr. Hasan Merdun - Akdeniz University - Turkey
11. Prof.Dr. Jasna Huremović – University of Sarajevo - Bosnia and Herzegovina
12. Prof.Dr. Lada Lukić Bilela – University of Sarajevo - Bosnia and Herzegovina
13. Prof.Dr. Lukman Thalib - Qatar University - Qatar
14. Prof.Dr. M. Asghar Fazel - University of Environment - Iran
15. Prof.Dr. Mehmet Kitiş - Süleyman Demirel University - Turkey
16. Prof.Dr. Muhammad Arshad Javed - Universiti Teknologi Malaysia - Malaysia
17. Prof.Dr. Noureddine Djebli - Mostaganeml University - Algeria
18. Prof.Dr. Nuri Azbar - Ege University - Turkey
19. Prof.Dr. Özer Çınar - Yıldız Technical University - Turkey
20. Prof.Dr. Rifat Skrijelj - University of Sarajevo - Bosnia and Herzegovina
21. Prof.Dr. Samir Đug - University of Sarajevo - Bosnia and Herzegovina
22. Prof.Dr. Suad Bećirović - International University of Novi Pazar - Serbia
23. Prof.Dr. Tanju Karanfil - Clemson University - USA
24. Prof.Dr. Vladyslav Sukhenko - National University of Life and Environmental Sciences of Ukraine (Kyiv) - Ukraine
25. Assoc. Prof.Dr. Alaa Al Hawari - Qatar University - Qatar
26. Assoc. Prof.Dr. Cevat Yaman - Gebze Technical University - Turkey
27. Assoc. Prof. Dr. Kateryna Syera - National University of Life and Environmental Sciences of Ukraine (Kyiv) - Ukraine
28. Assoc. Prof.Dr. Mostafa Jafari - Research Institute of Forests and Rangelands - Iran
29. Assoc. Prof.Dr. Nusret Drešković - University of Sarajevo - Bosnia and Herzegovina
30. Assoc. Prof.Dr. Yuriy Kravchenko - National University of Life and Environmental Sciences of Ukraine (Kyiv) - Ukraine
31. Assist. Prof.Dr. Ahmad Talebi - University of Environment - Iran
32. Assist. Prof.Dr. Ahmet Aygün - Bursa Technical University - Turkey
33. Assist. Prof.Dr. Mostafa Panahi - Islamic Azad University - Iran
34. Assist. Prof.Dr. Rishee K. Kalaria - Navsari Agricultural University - India
35. Assist. Prof.Dr. Šasan Rabieh - Shahid Beheshti University - Iran
36. Assist. Prof.Dr. Ševkija Okerić - University of Sarajevo - Bosnia and Herzegovina
37. Dr. Hasan Bora Usluer - Galatasaray University - Turkey
38. Dr. Zsolt Hetesi - National University of Public Service, Budapest - Hungary
39. Dr. Zsolt T. Németh - National University of Public Service, Budapest - Hungary



## **ORGANIZATION COMMITTEE**

### **Chairman(s) of the Conference**

Prof. Dr. Özer Çınar – Yıldız Technical University

### **Members of the Committee**

Prof. Dr. M. Asghar Fazel (Co-Chairman) – University of Environment  
Dr. Gábor Baranyai (Co-Chairman) – National University of Public Service, Budapest  
Prof. Dr. Samir Đug, University of Sarajevo  
Assist. Prof. Dr. Sasan Rabieh Shahid Beheshti University  
Assist. Prof. Dr. Ševkija Okerić - University of Sarajevo  
Assist. Prof. Dr. Nusret Drešković - University of Sarajevo  
Assist. Prof. Dr. Ranko Mirić - University of Sarejevo  
Musa Kose - Zenith Group Sarajevo  
Ismet Uzun - Zenith Group Sarajevo  
Alma Ligata - Zenith Group Sarajevo  
Ajdin Perco - Faktor.ba

## **WELCOME TO ICOEST 2018**

*On behalf of the organizing committee, we are pleased to announce that the 3th International Conference on Environmental Science and Technology (ICOEST-2018) is held from September 19 to 23, 2018 in Kiev. ICOEST 2018 provides an ideal academic platform for researchers to present the latest research findings and describe emerging technologies, and directions in Environmental Science and Technology. The conference seeks to contribute to presenting novel research results in all aspects of Environmental Science and Technology. The conference aims to bring together leading academic scientists, researchers and research scholars to exchange and share their experiences and research results about all aspects of Environmental Science and Technology. It also provides the premier interdisciplinary forum for scientists, engineers, and practitioners to present their latest research results, ideas, developments, and applications in all areas of Environmental Science and Technology. The conference will bring together leading academic scientists, researchers and scholars in the domain of interest from around the world. ICOEST 2018 is the oncoming event of the successful conference series focusing on Environmental Science and Technology. The scientific program focuses on current advances in the research, production and use of Environmental Engineering and Sciences with particular focus on their role in maintaining academic level in Science and Technology and elevating the science level such as:*

*Water and waste water treatment, sludge handling and management, Solid waste and management, Surface water quality monitoring, Noise pollution and control, Air pollution and control, Ecology and ecosystem management, Environmental data analysis and modeling, Environmental education, Environmental planning, management and policies for cities and regions, Green energy and sustainability, Water resources and river basin management. The conference's goals are to provide a scientific forum for all international prestige scholars around the world and enable the interactive exchange of state-of-the-art knowledge. The conference will focus on evidence-based benefits proven in environmental science and engineering experiments.*

***Best regards,***

***Prof. Dr.Özer ÇINAR***

CONTENT	COUNTRY	PAGE
Assesment of Some Physical and Chemical Characteristics of Soil in Samsun Tekkekoy Region with GIS	TURKEY	1.
Near Field Dilution of Wastewater Discharges in Oludeniz	TURKEY	8.
A useful Way to Dispose of Phenolic-rich Agro-industrial Wastes: Mushroom Cultivation	TURKEY	16.
Social, Environmental and Economic Effects of Hydroelectric Power Plants: Keban HEPP Sample	TURKEY	24
An Environmentally Friendly Plant in Terms of Oxygen Supply: Hemp	TURKEY	31
Petaloid Monocotyledonous Flora of Bingol Province (Turkey)	TURKEY	35
Ammonia Removal From Landfill Leachate Using MAP Precipitation Method	TURKEY	41
Geological, Mineralogical and Geochemical Features of the Kiziltepe (Aladag) Skarn Deposit (Ezine/Canakkale-North West Turkey)	TURKEY	48
A skarn deposit in the Kazdaglari Region: Saricayir (Yenice/Canakkale - Northwest Turkey) Iron-Copper Skarn Deposit	TURKEY	56
The Landscape Design Project of Sey Bath Geosite (Kizilcahamam-Camlidere) Under Geopark and Geotourism Concept	TURKEY	64
A Study on the Determination of the Effects of Carbon Structures of FAME Fuels on Fuel Properties	TURKEY	73
Comparison of Performance and Combustion Characteristics of Methyl Ester and Ethanol Used In a Common Rail Diesel Engine	TURKEY	81
Improvement of Engineering Properties of Sandy Soils by Bacillus simplex	TURKEY	87
Environmental Risks of Bumblebee Commercialization and Suggestions for Prevention	TURKEY	94
Determination of the microbial composition of 1-year shelf-life lyophilized bacteria with DGGE method	TURKEY	98
Chemical And Mineralogical Properties Of Salt And Soda Lake Muds Used As Peloids In Konya Basin, Turkey	TURKEY	105
Lithofacies And Geochemical Properties Of Neogen Deposits At South Of Tuzgolu-Turkey	TURKEY	111
Tannase Production and Enzyme Characterization from Bacillus coagulans	TURKEY	119
Effect of Nano-Silica Addition on Kaolin-Based Brick Properties	TURKEY	127
Use of Alginate – Clinoptilolite Beads for the Removal of Mixed Heavy Metals: Effect of Clinoptilolite Size and Alginate – Clinoptilolite Ratio	TURKEY	133

Legislations of Ministry of Environment and Urbanization in Turkey for Sustainable Construction	<i>TURKEY</i>	138
Temporal Coastal Change Analysis in Kizilirmak Delta and Yesilirmak Delta	<i>TURKEY</i>	143
Effects of Catalysts on Bio-oil of Fast Pyrolysis of Greenhouse Vegetable Wastes	<i>TURKEY</i>	148
Investigation of Catalysts and Bio-oil in Co-pyrolysis of Greenhouse Vegetable Wastes and Coal	<i>TURKEY</i>	153
Investigation of the Use of Adsorbents Derived from Waste Shells with Addition of PAn/K2S2O8 in Laundry Wastewater Treatment by Adsorption Methods	<i>TURKEY</i>	158
Investigation of Bisphenol A Solutions Treatability by Using Ozone Based Oxidation Processes	<i>TURKEY</i>	164
Removal of Diclofenac from Aqueous Solution by Microwave Enhanced Persulfate Oxidation: Optimization Using Taguchi Design	<i>TURKEY</i>	172
Microwave Assisted Sludge Disintegration: Optimization of Operating Parameters	<i>TURKEY</i>	179
Multi Response Optimization of Nanofiltration Process for Carbamazepine Removal	<i>TURKEY</i>	185
Mineralogical, Chemical And Physical Properties And Suitability For Therapy Of Peloids In Susurluk (Balikesir, Turkey)	<i>TURKEY</i>	193
Experiences on sustainable tourism development in Turkey	<i>TURKEY</i>	199
Quantification Of Microorganism Composition Of Biohydrogen Production From The Dry Fermentation System By Real-Time Q-Pcr	<i>TURKEY</i>	208
Recent advances in membrane fouling control in wastewater treatment processes	<i>TURKEY</i>	215
The Importance of Ventilation for Indoor Air Quality	<i>TURKEY</i>	222
Effect of Common-Rail Diesel Engine Bioethanol-Biodiesel-Eurodiesel Mixtures on Engine Performance and Emissions	<i>TURKEY</i>	226
Determination of Optimum Operational Conditions for the Removal of 2-Methylisoborneol and Geosmin from Drinking Water by Peroxone Process	<i>TURKEY</i>	233
A Case Study for Waste to Energy Conversion: MCw Plasma Gasifier	<i>TURKEY</i>	239
Microwave Plasma Gasification Process of Polyethylene	<i>TURKEY</i>	245
The Effect of Environmental Pollutants on Honeybees ( <i>Apis mellifera</i> L.)	<i>TURKEY</i>	250
Comparison of the thermal performances of concretes containing waste	<i>TURKEY</i>	255

rubber for energy efficient buildings		
Mathematical Modeling and Performance Analysis of Solar Assisted Heat Pump Wheat Drying System with Energy Storage Tank	<i>TURKEY</i>	263
Adsorption of methylene blue by using activated carbon prepared by olive seed	<i>TURKEY</i>	272
The Microwave Oven Curing of Fly Ash-Based Geopolymer Mortars	<i>TURKEY</i>	278
Use of 3D City Modeling Techniques in Urban Planning : A Case Study of Selahiye	<i>TURKEY</i>	285

## Assesment of Some Physical and Chemical Characteristics of Soil in Samsun Tekkekoy Region with GIS

*Occan Coluk<sup>1</sup>, Ayse Kuleyin<sup>2</sup>, Aziz Sisman<sup>3</sup>*

### *Abstract*

*Geographical Information Systems have become one of the primary tools in environmental management, as in many applications. Geographical Information System applications are used especially in studies of natural resource management, resource inventory, assessment of wild life, environmental protection, risk assessment, air emission tracking, land assessment and selection, environmental effect studies, ecological and geological studies, soil analyses, infrastructure management with erosion assessment, waste management, planning, housing, etc. Information systems in which data about the soil are assessed are a significant source of information for all disciplines related with soil.*

*In this study, basic physical and chemical characteristics of soil samples taken from 0-20 cm deep from land from Tekkekoy town of Samsun province were assessed and thematic maps were produced using Geographical Information Systems. The purpose of the study was to make the results of the study set up a substructure in the interpretation and assessment of other studies to be conducted on the region.*

**Keywords:** Soil, Geographical Information Systems, Environmental management, KDK, Organic Matter.

### 1. INTRODUCTION

Soil is a three dimensional and natural living being which covers the surface of terrestrial environment around the world in the form of a thin layer, which occurs as a result of the disintegration of various rocks and minerals with the influence of environmental factors and which consists of inorganic and organic materials and specific amounts of air and water and acts as a source of attachment and nutritional source for plants (1). Physical and chemical characteristics of soil are generally found through laboratory analyses. Some of the physical soil characteristics found by using various devices and analysis methods are proportional compound of soil texture (sand, silt and clay amount%), structural (clustered structure) characteristics, bulk density, specific weight, water holding capacity, porosity and infiltration capacity. Some of the chemical characteristics of soil are characteristics such as “soil reaction (pH), organic matter amount, soil’s level of being able to absorb and release nutritional elements (cation change capacity), the type and amount of cations absorbed by soil (changeable cations), the type and amount of anions in the soil (non-absorbable), amount of lime”. Basic physical and chemical characteristics of soils such as pH, organic matter, cation exchange capacity (CEC), lime and texture are used in examining and associating the results of many studies related with different disciplines. In studies about soil pollution, the values of parameters discussed in examining and interpreting the behaviour of contaminants in soil are taken into consideration.

Geographical Information Systems (GIS) is an information system which collects, keeps, processes and presents graphical and non-graphical data obtained through spatial based observations to users in an integrated way (2). With a more comprehensive approach, GIS is a numerical system consisting of regularly brought together compounds so that location based data can be collected, stored, processed, managed, analysed and examined for the purposes of providing decision support in tracking, planning and managing natural and socioeconomic environment (3,4,5).

<sup>1</sup> Environmental Engineer, Ondokuz Mayıs University, Department of Environmental Engineering, 55139, Samsun, ozcancoluk@gmail.com

<sup>2</sup> Assoc. Prof. .Dr., Ondokuz Mayıs University, Department of Environmental Engineering, 55139, Samsun, akuleyin@omu.edu.tr

<sup>3</sup> Assoc. Prof. .Dr., University, Department of Geomatic Engineering, 55139, Samsun, asisman@omu.edu.tr

GIS is an important tool since it enables examining environmental data based on location with different themes. GIS mediates the integration of economic, social and environmental policies; analysis of data by collecting the data in a common data base and also making correct decisions for necessary changes to increase the quality of environment and environmental management in addition to tracking the state and sustainability of natural resources (2).

One of the most important reasons why GIS is preferred by various occupations as a tool for decision making is the fact that graphical and non-graphical data are analysed multi-directionally as a whole. A GIS application keeps information about the world in thematic layers associated with location. This simple but very powerful and multi-directional content contributes to the solution of real world problems. The most important component of GIS is data. Graphical data about location and attribute data or data in tables are obtained from necessary sources and examination and analysis can be done by making associations between data. In examination processes, the records in the data base are listed according to one or more criteria and the results are thus obtained. In analysis, the data are exposed to some mathematical or statistical operations and new results are obtained.

In the current study some spatial analysis were used to examine and interpret data collected from the study area. The study area was assessed according to various parameters. With the GIS application conducted, the existing and possible future states of the area were examined environmentally.

## 2. MATERIAL METHOD

### 2.1. Study Area

Study area is within Tekkekoy town which is 1 km inland to the south from the 13th kilometer of Samsun – Trabzon highway. Tekkekoy is a town of the province of Samsun. It is built in the area where Tekkekoy river leads to coastal plain. The continuation of Carsamba plain constitutes one third of the soil in town. Carsamba town is in the east and South of the town, while Canik town is in the west, Black Sea is in the North and Asarcik town is in the southeast. The key feature of the town in which the study is conducted is the fact that it contains heavy industry facilities in addition to fertile agricultural land. The study area is shown in Figure 2.1. Figure 2.2 shows the satellite image of sample points taken from the area.

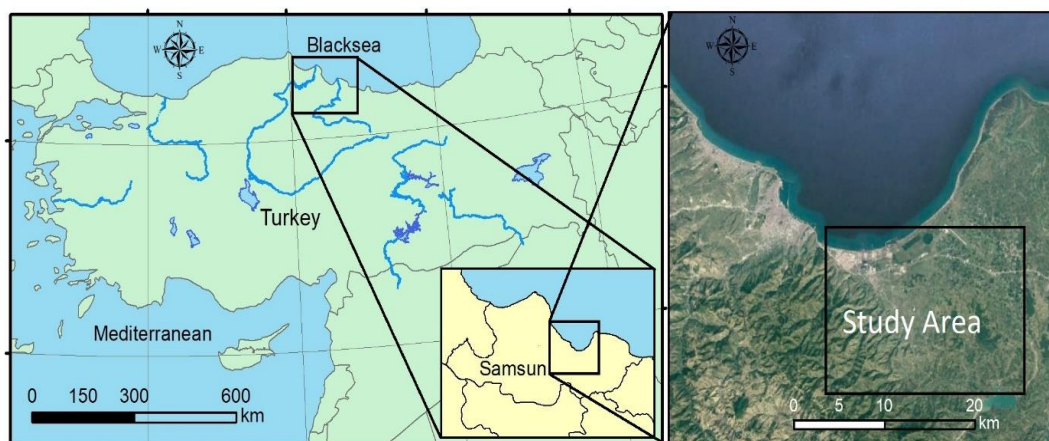


Figure 2.1. Satellite image of the study area (Google Earth)





Figure 2.2. Google earth image of the sampling points

### 2.2. Determination Of Soil Characteristics

The study area was examined and places for sampling were decided after satellite images and physical maps were obtained. The samples were taken from 0-15 cm soil depth as reported by Jackson (6) and brought to laboratory in polyethylene bags. The samples were dried in air, ground and prepared for analysis after sifting from 2 mm sieve. Before the heavy metal adsorption capacities of the soils were examined, moisture %, organic matter %, CEC and pH values, which are some of the physical and chemical characteristics, were found. pH of the samples taken was found with potentiometric method in saturation mud by using pH-meter. Organic matter contents of the samples were found through "Walkley-Black" wet oxidation method and while organic matter content was expressed as weight ratio (%) (7), cation change capacities were found with ammonium content distillation method and this value was assessed as CEC and the amount of other cations fixed in soil (7). Table 3.1 shows the coordinates of sample points and the values of the related parameters.

### 2.2. GIS Application

CEC, Organic matter %, Moisture % and pH values of the samples found with the aforementioned methods were analysed using ArcGIS software and thematic maps were obtained in line with the determined parameters. Thematic maps were obtained with Inverse Distance Weighted (IDW) method. IDW method is one of the commonly used interpolation methods. The method is based on the determination of pixel values via the average values of sample data points around each pixel. The sample points closest to the cell (pixel) are given greater weights. As they get farther to the assumption location, the influence of points gets smaller. The solution is to consider sufficient number of points and to create surface for small areas. The number of points differs according to the amount and distribution of sample points and surface character. In this study, data obtained from sufficient number of sample points were examined with IDW, location analysis was conducted and thematic maps were obtained.

Similar GIS studies are planned for other physical and chemical parameters in the continuation of the study.

## 3. RESULTS AND DISCUSSION

Table 3.1 shows the values of soil samples brought to laboratory from the sampling area according to some soil parameters determined. IDW method was used on samples taken from 46 points in the study area according to four parameters. The thematic maps of data are shown in Figure 3.1., Figure 3.2., Figure 3.3., and Figure. 3.4. When Table 3.1 is examined, it can be seen that CEC values are between 5 and 60, Organic matter % values are between 0,74 and 4,08, moisture % values are between 0 and 10,3 and pH values are between 4,57 and 7,97.



Table 3.1. Coordinates and study parameter values of the samples

Point number	Coordinates		CEC	Org. Matter %	pH	Moisture %
N1	K 41.143760	D 36.506195	27,00	0,87	7,68	6,66
N2	K 41.171418	D 36.487656	60,00	3,30	4,57	7,62
N3	K 41.172452	D 36.487999	60,00	0,96	6,06	0,00
N4	K 41.149448	D 36.503105	5,00	1,21	6,70	8,46
N5	K 41.180204	D 36.491089	18,20	1,08	6,52	6,44
N6	K 41.191573	D 36.508598	22,60	2,06	6,91	5,83
N7	K 41.168575	D 36.524391	22,60	0,85	6,33	8,38
N8	K 41.148414	D 36.537437	16,00	1,65	5,59	5,80
N9	K 41.140721	D 36.530228	22,60	1,83	6,27	5,96
N10	K 41.145553	D 36.553574	33,60	1,62	6,14	8,16
N11	K 41.179171	D 36.575546	24,80	2,19	7,55	6,49
N12	K 41.205006	D 36.583099	38,00	2,09	7,56	4,06
N13	K 41.235737	D 36.579666	53,40	3,04	7,72	5,89
N14	K 41.173370	D 36.570380	29,20	0,74	7,27	4,97
N15	K 41.212496	D 36.508255	22,60	0,78	7,36	2,88
N16	K 41.124499	D 36.302972	44,60	3,02	7,55	7,78
N17	K 41.208106	D 36.523361	57,80	3,02	6,59	10,30
N18	K 41.200356	D 36.595116	31,40	3,44	6,97	5,91
N19	K 41.201131	D 36.605415	49,00	2,47	7,97	6,81
N20	K 41.194673	D 36.606102	35,80	2,40	7,71	6,00
N21	K 41.189764	D 36.609192	31,40	2,51	7,53	4,46
N22	K 41.178654	D 36.616402	27,00	3,13	7,65	4,08
N23	K 41.174003	D 36.644554	24,80	3,10	7,93	3,23
N24	K 41.230831	D 36.56868	24,80	2,03	7,72	3,82
N25	K 41.243223	D 36.552887	31,40	2,23	7,91	4,32
N26	K 41.215396	D 36.480983	39,60	1,39	6,04	5,87
N27	K 41.195403	D 36.485105	39,60	1,90	5,92	5,93
N28	K 41.163929	D 36.501855	50,60	2,22	7,37	6,91
N29	K 41.225148	D 36.512857	59,40	2,30	7,24	8,99
N30	K 41.219497	D 36.543015	33,00	1,80	7,38	4,50
N31	K 41.208901	D 36.553228	44,00	2,52	7,54	7,43
N32	K 41.194141	D 36.531491	33,00	1,08	6,99	6,10
N33	K 41.185384	D 36.546234	26,40	2,11	5,92	5,53
N34	K 41.169404	D 36.549849	35,20	1,16	6,50	7,16
N35	K 41.183986	D 36.521015	22,00	1,83	5,98	6,77
N36	K 41.156727	D 36.521518	39,6	2,45	4,93	6,08
N37	K 41.158682	D 36.556131	22,00	0,21	7,58	4,81
N38	K 41.194180	D 36.572167	22,00	1,63	6,66	6,68
N39	K 41.187673	D 36.597280	50,60	2,22	7,24	5,32
N40	K 41.154267	D 36.623287	39,60	4,08	6,83	3,65
N41	K 41.176835	D 36.592581	24,20	2,27	6,37	5,10
N42	K 41.164867	D 36.599400	28,60	1,80	5,65	5,23
N43	K 41.191355	D 36.635018	17,60	1,76	7,47	3,20
N44	K 41.202539	D 36.627203	37,40	1,67	7,45	3,68
N45	K 41.214357	D 36.623209	30,80	2,01	7,36	3,43
N46	K 41.221415	D 36.593202	57,20	2,14	7,42	5,30

### Legend

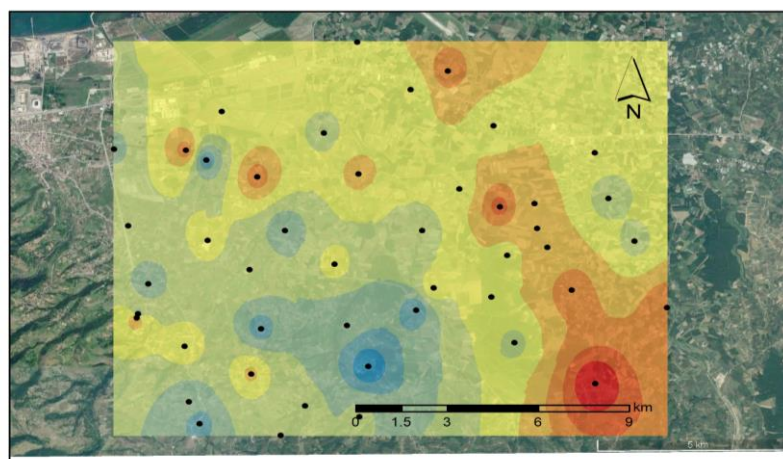
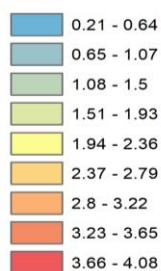


Figure. 3. 1. Thematic map of Organic Matter (OM) % values

When the thematic map shown in Figure 3.1 is examined, it can be seen that organic matter % values of soil samples are between 0 and 5%. When the distribution of the values in the colour scale is examined, similar results are generally seen in areas close to each other and it can be seen that they have the same colour tones. Different colours in some points are helpful in interpreting the characteristics of the area and the areas in which soil samples differ from each other.

### Legend

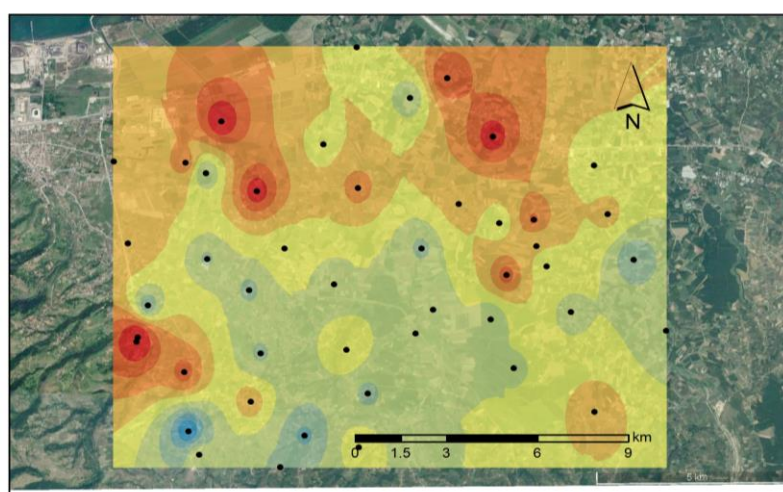
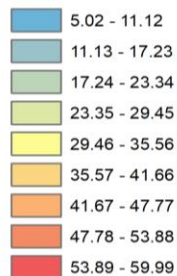


Figure. 3. 2. Thematic map of CEC meq/100 ml values

Similarly, when the distribution of CEC values in the colour scale of the area is examined, similar results are generally seen in areas close to each other and it can be seen that they have the same colour tones. As in the previous map, colours different from the colour tones of that area in some points help us in seeing the points where soil samples differ from each other and in interpreting these with other parameters.

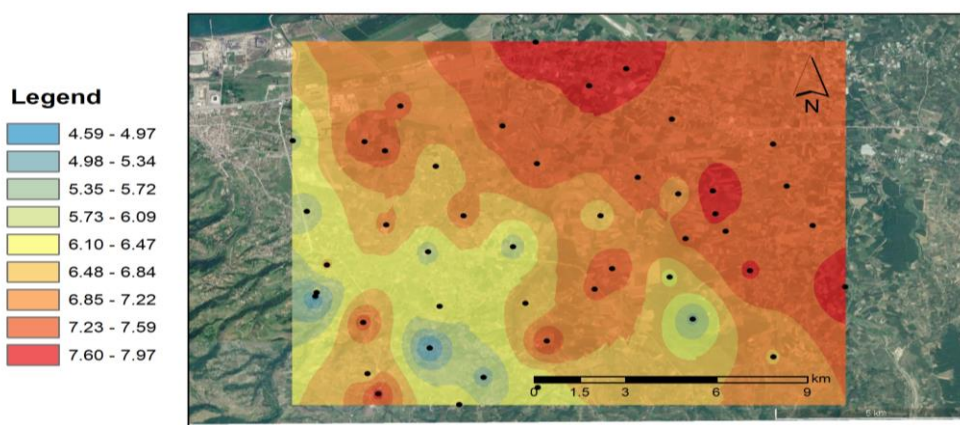


Figure. 3. 3. Thematic map of pH values

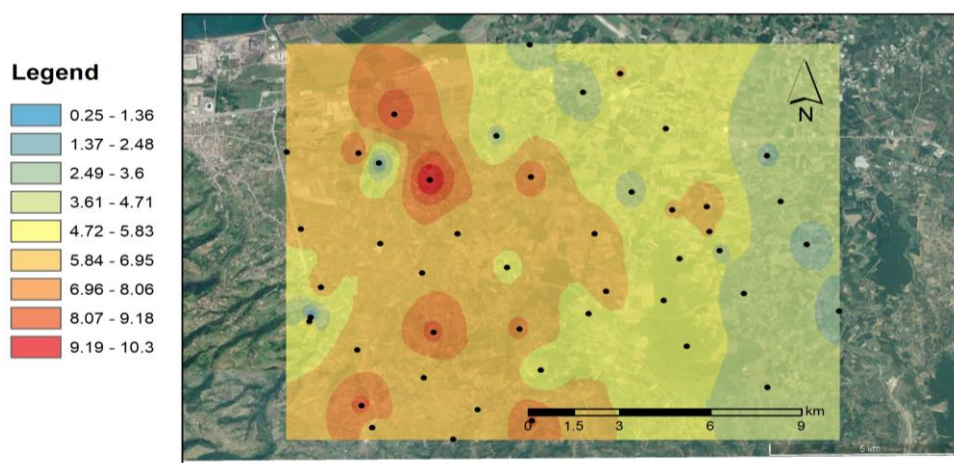


Figure. 3. 4. Thematic map of Moisture % values

In Figure 3.3. and Figure 3.4. location analysis was conducted for pH and Moisture values, respectively. In pH values, different colour tones can be seen at a few points within close areas. The application conducted showed that the highest pH values of the soil samples were in the east of the area in general. Moisture% values in Figure 3.4 showed a scattered map. There is a variation of colours distributed in every point of the area. This result shows us that the area has a scattered structure in terms of moisture %.

## 4. CONCLUSION

With GIS shaped in parallel with the development in information technologies, fast and effective results can be obtained about the variability of data obtained from big areas without loss of time during the data collection phase. GIS has become one of the commonly used tools in the management of environment. It is possible to see the applications especially in natural resource management (resource inventory, assessment of wild life, etc.), protection of the environment (risk assessment, air emission tracking, assessment and choice of land, studies of environmental influence, etc), ecological and geological studies (soil analyses, erosion assessment, etc.) and infrastructure (infrastructure management, waste management, planning, structuring, etc.). Information systems in which data about soil are assessed are important information sources for all disciplines related with soil.

As can be seen, the determined basic physical and chemical characteristics of soil samples taken from 0-20 cm deep in Tekkekoy town of Samsun province were assessed with GIS and the data obtained were transferred to GIS data base. With GIS application, it was possible to easily examine the distribution of 224 data in the study area.

It is thought that this application is very useful especially in terms of showing the conditions of contaminant parameters of soil samples taken from the study area and also showing the general characteristics of the study area.

## REFERENCES

- [1]. Karasuloglu, G., (2007). Organik Kirleticilerin Yuzey Aktif Maddelerin Varliginda Elektrokinetik Yontemlerle Toprakten Giderilmesinin Arastirilmesi. Yuksek Lisans Tezi, Gebze Yuksek Teknoloji Enstitusu Muhendislik ve Fen Bilimleri Enstitusu, Kocaeli, 96 s.
- [2]. Yomralioglu, T., (2000), Cografi Bilgi Sistemleri, Temel Kavramlar ve Uygulamalar, DGN Bilgi Sistemleri A.S., Sayfa 49
- [3]. Maras, H., (1999), Cografi Veri Tabani Guncellestirmesine Yonelik Cografi Bilgi Sistemi Tasarimi ve Uygulaması, Doktora Tezi, I.T.U. Fen Bilimleri Enstitusu, Istanbul.
- [4]. Heywood, I., Cornelius, S., Carver, S., (2006). An Introduction to Geographical Information Systems. Prentice Hall. 3rd edition.
- [5]. Maras, E. E., Maras, H. H., Maras, S. S., Alkis, Z. (2011). CBS Verilerinden Cevresel Gurultu Haritalarinin Hazirlanmasinda Kullanilan Tahmin Yonteminin Analizi. Harita Dergisi. Sayi 145.
- [6]. Jackson M.L, (1962). Soil Chemical Analysis, (Prentice Hall, Inc. Eaglewood Cliffs, N.Y., pp 219-221)
- [7]. Bayrakli, F., (1987). Toprak ve bitki analizleri. Ondokuz Mayis Universitesi yayinlari, Yayin no:17, s:77.

## Near Field Dilution of Wastewater Discharges in Oludeniz

Asu Inan<sup>1</sup>, Lale Balas<sup>2</sup>

### Abstract

*The main cause of wastewater discharges is the use of sea outfalls with the increasing industrialization and urbanization, which are chosen through the assimilation capacity of seas as an economical alternative to refinery systems. Uncontrolled discharges into the ambient sea water have an adverse effect on the ecosystem and incorrect selection of the location of the sea outfall causes that the wastewater comes back to the coastal zone and deposit in the ecosystem. In this study, the near field dilution of wastewater discharges was modeled and the behaviors of pollutant clouds were analyzed using VISUAL PLUMES, CORMIX, HYDROTAM 3D for Oludeniz. Following effects of different parameters (total effluent discharge, velocity and direction of current) on the near field dilution of wastewater discharges were examined with different scenarios in summer and winter conditions. Wind climate, wave climate and current pattern of Oludeniz were determined by HYDROTAM-3D and were used as input for near field dilution calculation.*

**Keywords:** Wastewater discharges, near field dilution, VISUAL PLUMES, CORMIX, HYDROTAM 3D, Oludeniz

### 1. INTRODUCTION

The coastal environment is used as a source of food and recreation and as a final sink for wastes. There is an obvious potential conflict. With the increasing industrialization and urbanization, urban and industrial communities wastes have been disposed off in the coastal waters nowadays and the need for coastal pollution control has increased considerably. The disposal is carried out by constructing a pipeline on the sea bed with a multiport diffuser. The wastewater having a density close to that of fresh water, rises to the surface and entrains the surrounding sea water and becomes diluted. If the ambient sea water is stratified, the diluted waste mixture may be trapped below the sea surface where its density is almost same as the sea water density (near field dilution,  $S_1$ ). However, if the water depth is shallow as in the most of the coastal waters, the diluted waste mixture rises up to the water surface with a density which is less than the salty sea water ( $S_1$ ). and it is further diluted by the sea currents and by the turbulence (far field dilution,  $S_2$ ) [1]. The near field mixing is a result of buoyancy and initial momentum. It is significant over distances of 10m to 1000m and duration of 1-10 minutes. The far field mixing is due to the advection and diffusion by the coastal currents and turbulence [2]. In the meantime as the physical dilutions, the pathogens die away and become inactive ( $S_3$ ). The quality of water near the coast is an outcome of the net result of any treatment, inactivation and dilution of discharged waste [3].

Various models have been developed to predict near field dilution. Some of them simulate the first dilution in still, uniform and unstratified ambient water, but there are more complex models too. In this study, CORMIX

<sup>1</sup> Corresponding author: Gazi University, Department of Civil Engineering, 06570, Maltepe/Ankara, Turkey.  
[asuina@gazi.edu.tr](mailto:asuina@gazi.edu.tr)

<sup>2</sup> Gazi University, Department of Civil Engineering, 06570, Maltepe/Ankara, Turkey, [lalebal@gmail.com](mailto:lalebal@gmail.com)



[4], Visual Plumes [5] and HYDROTAM 3D [6, 7, 8] are used to predict near field dilution. The results of these three models are compared.

## 2. STUDY FIELD

The study area is located in the region of sea outfall of Oludeniz (Hata! Başvuru kaynağı bulunamadı.).

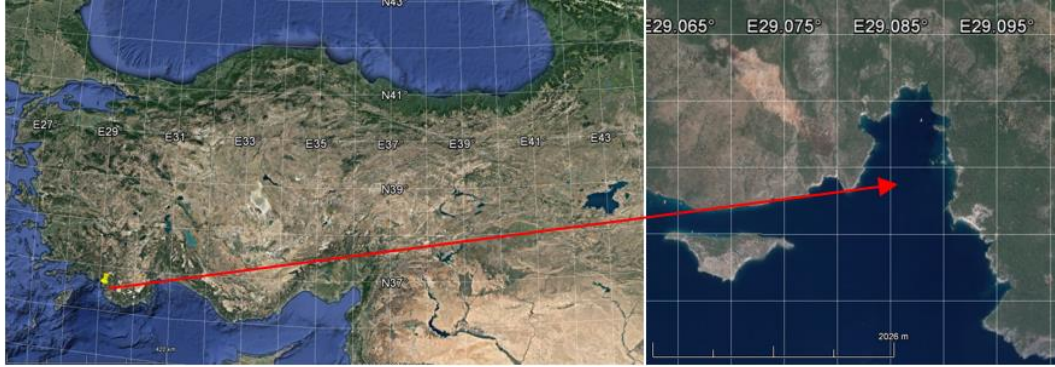


Figure 1: Geographical Location of study area [9]

### 2.1. Wind and Wave Climate

The wind roses providing the directional distribution of wind speeds are obtained from the measured wind data between the years 2000-2016 of ECMWF (36.5N-29E).

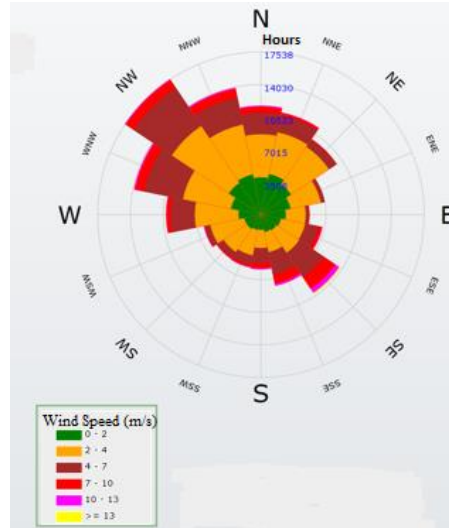


Figure 2: Annual Wind Rose

Due to studies of wind measurements of the Station of ECMWF, the interval of the dominant direction of the wind is determined as WNW-NNW. In winter season, winds blowing from SW are dominant and in summer season, winds blowing from W are dominant. Results of long term wind statistics show that the monthly average for wind speed is 3.5m/s and extreme value of wind speed changes between 9-17m/s.

Dominant wave directions are determined in the interval of S and SW based on long term wave statistics. Predictions of the significant wave heights are obtained from the data of ECMWF between the years 2000-2016 for the coordinate 36.5<sup>0</sup>N-26.9<sup>0</sup>E. The annual and seasonal wave roses are shown in Figure 3.

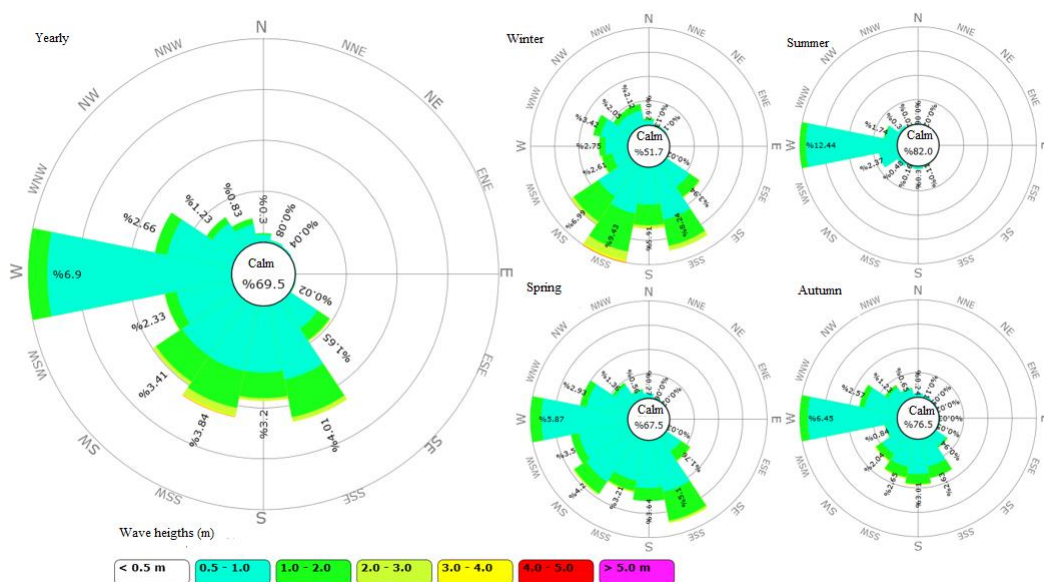


Figure 3: Wave Rose

## 2.2. Current Climate

In this study, currents due to wind, tide and wave breaking are modeled using HYDROTAM-3D. Circulation in coastal regions is generally irregular and turbulent. In the model, the connection between average motion and turbulent motion is emerged with mass transport due to vertical and horizontal eddy viscosities and vertical and horizontal eddy diffusion. The temperature of sea water, salinity and density are taken as constant in the numerical model.

Measurements of the winds for every 6 hours obtained from the data of ECMWF between the years 2000-2016 for the coordinate  $36.5^{\circ}\text{N}$ - $26.9^{\circ}\text{E}$  are used to predict the time series of current pattern. The seasonal current roses at the sea surface and at the sea bottom are given in Figure 4. In the study field, surface waters are drifted with a speed 25-30cm/s to SE-SW under the effect of the waves caused by the wind blowing from NW and bottom waters are drifted with a speed 2-4cm/s to NW-NE.

The highest values of current velocity are reached generally in winter. At the sea surface, currents move in the direction of NNW-NNE with the average speed of 25-30cm/s and at the bottom, they move in the direction of SSW-SW with the average speed of 10cm/s. Seasonal current roses at the sea surface and at the sea bottom are illustrated in Figure 4.

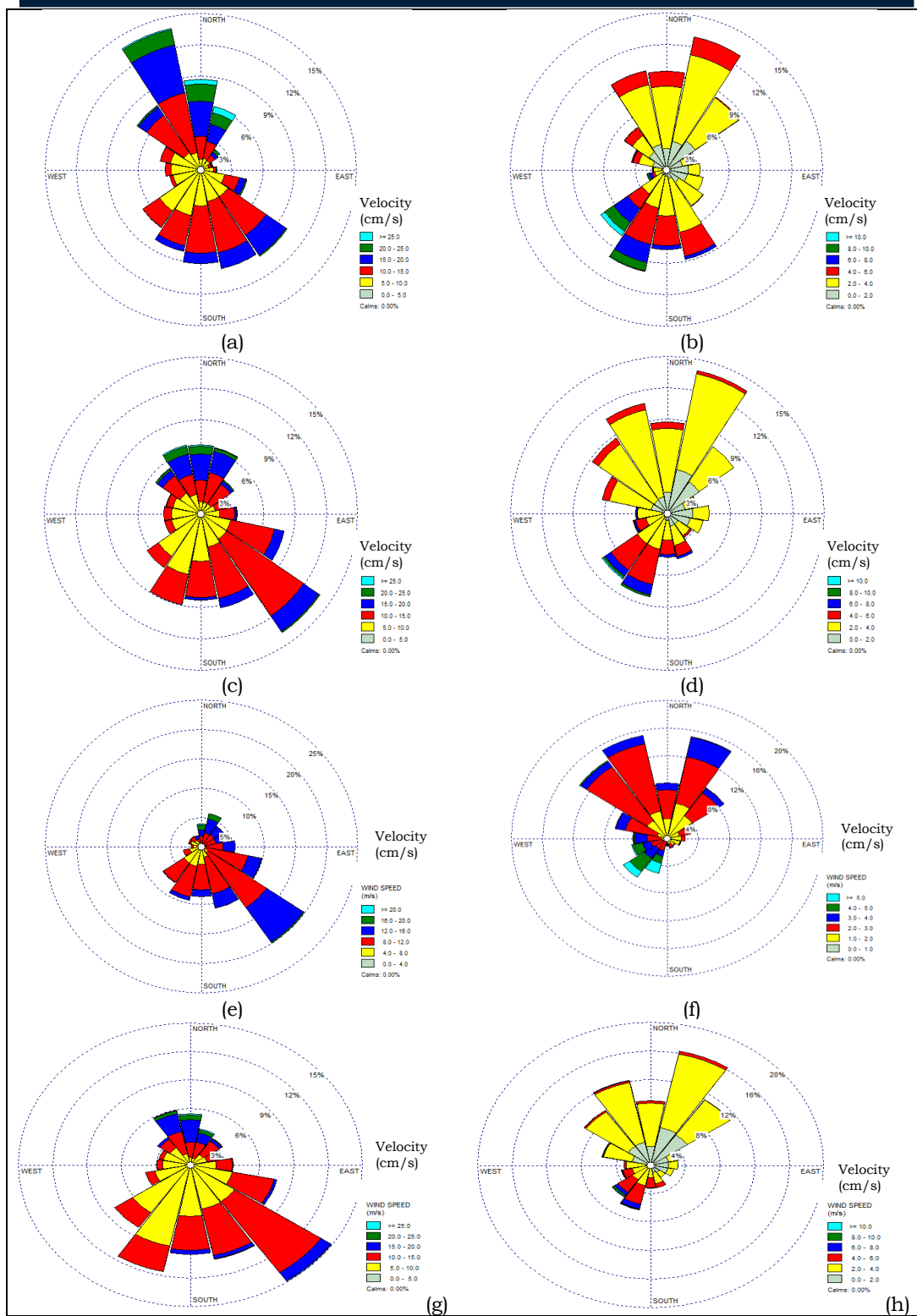


Figure 4: Seasonal current roses a) Winter- at the sea surface b) Winter- at the sea bottom c) Spring- at the sea surface d) Spring- at the sea bottom e) Summer- at the sea surface f) Summer- at the sea bottom g) Autumn- at the sea surface h) Autumn- at the sea bottom



### 3. MODELING OF NEAR FIELD DILUTION

A sea outfall is planned in Oludeniz. The parameters are considered for 40 years. The wastewater discharges are examined in two steps. 1.step and 2.step indicate the discharges of the present population and the population in other forty years. The values of the wastewater discharges are given in Table 1. The properties of the effluent are summarized: The effluent density ( $\rho_0$ ) is 999 kg/m<sup>3</sup>, the viscosity of the effluent ( $\nu_0$ ) is 10<sup>-6</sup> m<sup>2</sup>/s, the maximum bacteria concentration after the refinement ( $C_0$ ) is 10<sup>7</sup> TC/100ml. Decay coefficients ( $k$ ) are 1.541 1/hour in summer and 0.77 1/hour in winter. The properties of the diffuser of the sea outfall in Oludeniz are presented in Table 2.

Table 1: Wastewater discharges in Oludeniz

Discharge (m <sup>3</sup> /s)	1.Step	2. Step
Minimum	0.070067	0.092589
Project	0.178603	0.238128
Maximum	0.207703	0.277147

Table 2: The properties of the diffuser of the sea outfall in Oludeniz

Q, Discharge (m <sup>3</sup> /s)	0.05-0.3	L, Diffuser Length (m)	40
N, Number of alternating ports	6	D, Water depth (m)	-45
D, Port diameter (m)	0.12	Alignment	Same direction with the diffuser line

CORMIX, Visual Plumes and HYDROTAM 3D are performed to predict near field dilution in the study area and they are compared with each other. Effects of the wastewater discharge, current velocity and current direction on the near field dilution are analysed. The density of sea water is calculated as a function of salinity and temperature in the hydrodynamic models. The parameters except for the discharge are taken as constant for the discharge sensitivity analysis. The range of the discharge is selected depending on the present and in other forty years values of the discharges. They change from 0.05 m<sup>3</sup>/s to nearly 0.3 m<sup>3</sup>/s. Based on the measurements, current velocity is taken as 0.1m/s, salinity in winter is 38ppt, temperature in winter is 16°C, salinity in winter is 39ppt, temperature in winter is 27°C [10]. The discharge sensitivity in winter and summer are shown in Figure 5 and Figure 6, respectively.

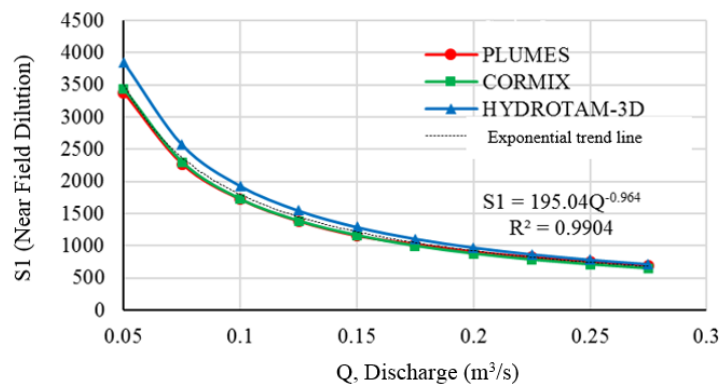


Figure 5: Discharge sensitivity in winter conditions

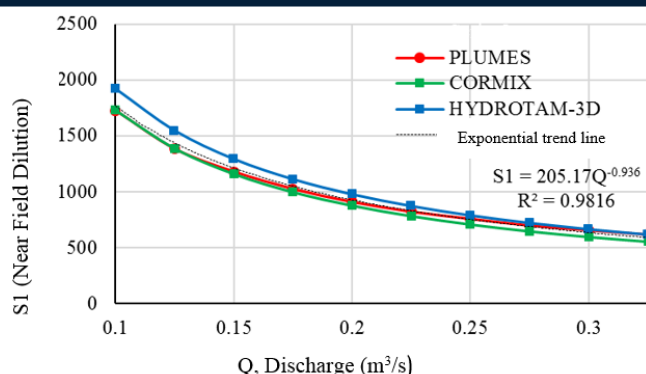


Figure 6: Discharge sensitivity in summer conditions

It is observed in Figure 5 and Figure 6, that as the discharge increases near field dilution is in accordance with the exponential function and the change of the near field dilution is small for the discharges greater than 0.15 m³/s. The near field dilution is  $595 \leq S1 \leq 3375$  for all examined discharges so the condition for near field dilution ( $S1 > 40$ ) is satisfied [11].

Effects of current velocity on the near field dilution is examined and showed in Figure 7 and Figure 8. Figure 7 and Figure 8 give the predictions in winter season and in summer season, respectively.

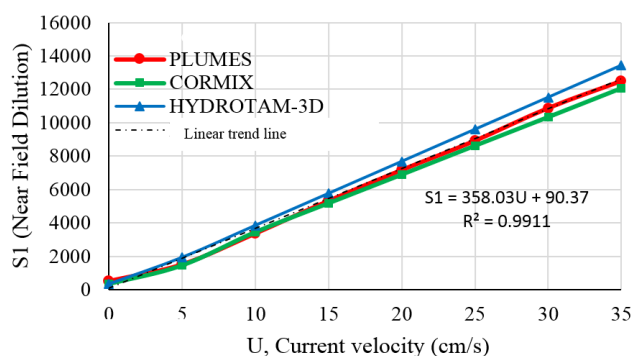


Figure 7: Sensitivity of current velocity in winter conditions

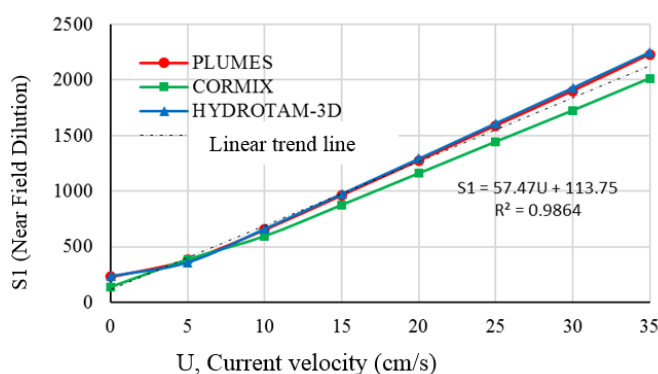


Figure 8: Sensitivity of current velocity in summer conditions

If the current velocity is zero, it means that there is any current or no wind blows. So near field dilution is minimum. As velocity of current increases, near field dilution increases approximately linearly. Linear trend line includes the prediction of all three hydrodynamic models. When the current velocity changes from 0 to 35cm/s, near field dilution changes from 231 to 2013. Near field dilution for all studied currents is greater than 40.

Another important parameter of near field dilution is current direction. The effects of current direction on the near dilution are shown for winter and summer conditions in Figure 9 and Figure 10, respectively. If the current direction is parallel to the diffuser, near field dilution is minimum, conversely if they are perpendicular, near field dilution is maximum. Also the minimum value of the predictions of the near field dilution satisfies the condition that the near field dilution must be 40 at least.

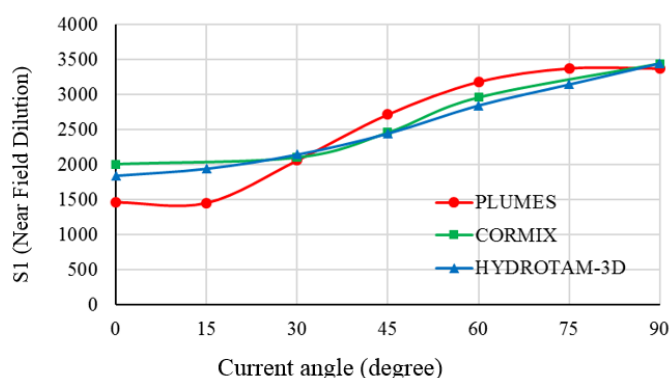


Figure 9: Effect of current direction on near field dilution in winter conditions

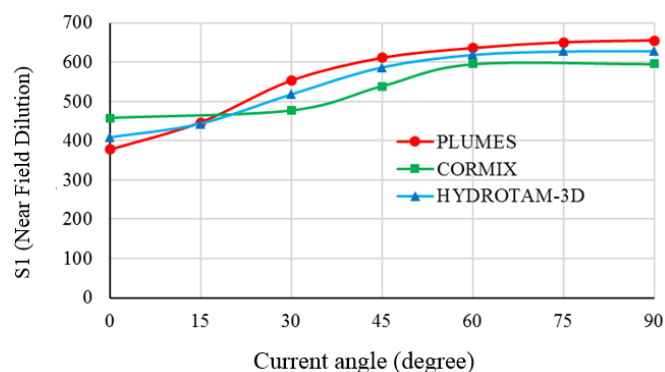


Figure 10: Effect of current direction on near field dilution in summer conditions

## 4. CONCLUSIONS

In this study, wind and wave climates, wind-wave-wave breaking induced currents, near field dilutions of the pollutant cloud for the coastal area of Oludeniz sea outfall are modeled numerically with CORMIX, Visual Plumes, HYDROTAM-3D. The wind rose providing the directional distribution of wind speeds is obtained from the measured wind data between the years 2000-2016 of ECMWF (36.5N-29E). Due to wind measurements of ECMWF (36.5N-29E), the interval of dominant direction of wind is determined as WNW-NNW. Predictions of long term wind statistics show that the monthly average for wind speed is 3.5m/s and extreme value of wind speed changes between 9-17m/s. Dominant wave directions are determined in the interval of S and SW based on long term wave statistics. In the study field, surface waters are drifted with a speed 25-30cm/s to SE-SW under the effect of the waves caused by the wind blowing from NW and bottom waters are drifted with a speed 2-4cm/s to NW-NE. The effects of the wastewater discharge, the current velocity and the angle between the current direction and diffuser alignment on the near field dilution are examined. It is

confirmed at this study conditions that near field dilution  $S_1$  is greater than 40. As current speed increases or wastewater discharge decreases, near field dilution increases. If the angle between the current direction and diffuser alignment is approximately perpendicular then near field dilution reaches its maxima.

### REFERENCES

- [1] X. Tian, P.J.W. Roberts, G.J. Daviero, *Marine wastewater discharges from multiport diffusers I: Unstratified stationary water*, Journal of Hydraulic Engineering, vol.130 no.12. pp. 1137-1146, 2004.
- [2] P.J.W., Roberts, H.J Salas, F.M. Reiff, M. Libhaber, A. Labbe, J.C. Thomson, *Marine Wastewater Outfalls and Treatment Systems*, IWA Publishing, 2010.
- [3] I.R. Wood, R.G. Bell, D.L. Wilkinson, *Ocean Disposal of Wastewater*, Advanced Series on Ocean Engineering, Vol.8., World Scientific Publishing Co.Pte.Ltd., 1993.
- [4] R.L. Doneker, G.H. Jirka, *CORMIX User Manual: A Hydrodynamic Mixing Zone Model and Decision Support System for Pollutant Discharges into Surface Waters*, EPA-823-K-07-001, 2007.
- [5] W.E. Frick, *Visual plumes mixing zone modelling software*, *Environmental Modeling and Software*, vol., 19, pp. 645-654, 2004.
- [6] L. Balas, *Simulation of Pollutant Transport in Marmaris Bay*, China Ocean Engineering, Nanjing Hydraulics Research Institute (NHRI), vol. 15, no.4, pp. 565-578, 2002.
- [7] L. Balas, A. Inan, A. Numanoglu Genc, *Modelling of Dilution of Thermal Discharges in Enclosed Coastal Waters*, Research Journal of Chemistry and Environment, vol. 17, no. 10, 82-89, 2013.
- [8] HYDROTAM-3D, *Three Dimensinal Hydrodynamic Transport Model*, <http://hydrotam.com>, (2018), (Accessed 15 February 2018).
- [9] Google Earth, <https://www.google.com/earth/>, (2018), (Accessed 10 January 2018).
- [10] DENAM, Modeling of Wind and Wave Climates, Current Pattern and Water Quality for Oludeniz Sea Outfall, Sea and Aquatic Application and Research Center, Gazi University, 2017.
- [11] RWPC, Regulation of Water Pollution Control, Official Gazette, 31.12.2004, No: 25687, Clause 35, 2004.

## A useful Way to Dispose of Phenolic-rich Agro-industrial Wastes: Mushroom Cultivation

Funda Atila<sup>1</sup>

### Abstract

*The by-products resulting from the agricultural productions are arised in extrem quantities every year. Some agricultural by-pruducts such as olive press waste, green walnut husks, tea wastes, coffee pulp etc. have been recognized as phenolic-rich wastes. The high polyphenol content in these wastes could have negative impact on soil and flora, if they are not disposed properly. Moreover, some studies have investigated the toxicity of phenolic compounds on aquatic organisms. Burning of these wastes may cause to increase amount of carbondioxide in atmosphere. Conversion of phenolic-rich wastes by different processes is therefore a desired aim. Mushroom has been used either as a therapeutic and protein-rich foods for many centuries. Mushrooom cultivation on agricultural wastes could be a promising method to reduce the the environmental pollution problems as well as production of tasty and healthy foods. This paper reviews the potential uses of phenolic-rich materials as substrate in cultivation of edible and medical mushrooms.*

**Keywords:** Coffee Husk; Green Walnut Husk; Grape Pomace; Mushroom Cultivation; Olive Press Wastes; Tea Wastes.

### 1. INTRODUCTION

Phenol is aromatic hydrocarbon and produced through both natural and anthropogenic processes [1]. US Environmental Protection Agency classified phenols as Priority Pollutants. They exhibit several toxic effects including chromosomal aberrations [2], endocrine disrupting effect [3,4], serious kidney and liver damage [5], mutagenicity and carcinogenicity [6].

Phenolic-rich agro-industrial wastes have no value as commercially. If inattentively disposed of in the surrounding environment by burying, burning, or dumping at unplanned and uncontrolled landfills, these wastes lead to climate change and environmental pollution. For that reason, there is a tendency to find a way to convert into valuable resources through proper management, with their utilization leading to reduced environmental pollution and further economic growth. Phenolic-rich agro-industrial wastes have potential to biochemically dissolved to produce several products like production of biogas, bio-ethanol etc. These wastes could also represent a possible source for mushroom cultivation as growing substrate.

Mushrooms are distinct both from plants and animals and belong to a separate group in the Fungi Kingdom. They are classified as a group of macrofungus. Chang and Miles [7] have defined mushroom as a macrofungus with a fruitbody, large enough to be seen by the naked eye and to be taken by hand. They have not got leaves, buds or flowers, yet, they form fruit and produce spores. Mushrooms, can synthesize and excrete different enzymes to degrade lignocellulosic materials such as and forestry residues, which can then be absorbed by the mushrooms for their nutrients [8]. Recent estimates of the number of fungi on the world changed between 2.2 and 3.4 million species [9].

Wild mushrooms are consumed by humans since ancient times. But commercial mushroom cultivation was started in France in 1650's by *Agaricus bisporus* cultivation. Mushroom production has increased steadily after World War II, and the production of edible and medical mushrooms such as *Pleurotus* spp., *Lentinula edodes*,

<sup>1</sup>Corresponding author: Ahi Evran University, Faculty of Agriculture, Department of Horticulture, 40200 Kirsehir-Turkey, [funda.atila@ahievran.edu.tr](mailto:funda.atila@ahievran.edu.tr)

*Flammulina velutipes*, *Ganoderma lucidum* have also shown great increase in the past few decades [10]. The total production of mushrooms in the world was only 1 million ton in 1978 [11] whereas the world production of cultivated edible mushrooms reached 34 million tones in 2013 [12]. During those 35 years, production increased by 3300%.

Technologies and innovations for human development are expanding every day. The world population have reached 7.6 billion inhabitants as of May 2018 [13]. It is estimated to reach 11.2 billion in 2100. However, humankind, particularly in some less developed countries, face three basic problems such as inadequate nutrition, increasing health problems, and increasing environmental pollution [14]. It is expected that the importance of these problems is set to rise as the world's population continues to increase.

Mushroom cultivation techniques is gaining importance in recent years to reuse or disposal of the solid organic wastes. Mushrooms can convert lignocellulosic materials into high quality food rich in protein, vitamins, dietary fibres, mineral salts and low in fat [15,16]. Taste of mushrooms frequently is descired as umami. Mushroom cultivation is not only a source for tasty and protein-rich food, it can also contribute to the production of effective medicinal products [14,17,18]. Many species of mushrooms have been used in traditional medicine for thousands of years. Mushrooms contain several biologically active substances including high-molecular-weight polysaccharides, glucans, chitinous substances, lectins, and secondary metabolites such as terpenoids, phenols, alkaloids, antibiotics.

Many of phenolic-rich agricultural wastes, such as tea waste, viticulture waste, tea waste, coffee pulp etc. can be provided at abundant and inexpensive cost in the different part of the world. Use of phenolic rich wastes as a raw material in cultivation of mushroom could be also useful ecological and environmental as well as economical. Kues [19] reported that *Basidiomycota* mushrooms are useful tools for the degradation of uncontrollable pollutants such as phenols, polyaromatic hydrocarbons, bisphenols, phenolic or non-phenolic textile dyes, halogenated aromatics, , naphthols etc. White-rot fungi can secrete some ligninolytic enzymes such as peroxidases and polyphenol oxidases destroying phenolic compounds [20,21].

As you can see, mushroom cultivation could be may contribute to the solution of these three key underlying problems that mentioned before. Finally, the aim of the presented review is to discuss the disposal of phenolic content rich agricultural wastes by mushroom cultivation. Moreover, the ability of mushrooms to remove phenolic compounds has also been investigated.

## 2. USES OF SOME PHENOLIC-RICH AGRO-INDUSTRIAL WASTES ON MUSHROOM CULTIVATION

A huge amount of phenolic-rich agro-industrial wastes and effluents are produced every year through the oil, juice, beverage, wine industries. These wastes are lignocellulosic, rich in source of nutrients, abundantly available and cheap. They contain high concentration of oil, phenol, lignin, cellulose, hemicellulose, ash, nitrogen and dissolved solids as shown in Table 1. In the following section, some of studies about the possibility of using of these phenolic rich agro-industrial wastes as growing media in the mushrooms production were presented.

Table 1. The composition of some of phenolic-rich agro-industrial wastes

	Ash (%)	Lipits (%)	Protein (%)	Hemicellulose (%)	Lignin (%)	Cellulose (%)	Sources
Olive press cake	1.4-2.4	3.9-8.7	2.9-4.8	7.9-11.0	8.5-14.2	14.5-24.1	[22]
Grape pomace	5.5	-	12.2	-	2.2-2.3	-	[23,24]
Tea waste	5.2	-	12.3	18.9	37.8	28.8	[25,26]
Coffee husk	5.4	0.5-3.0	8.0-11.0	7.0	9.0	43.0	[27]
Green walnut husk	18.6	-	8.3	3.5	13.5	17.7	Atila, F. (unpublished)

### 2.1. Olive Mill Wastes

Olive mill wastes are major environmental problem in Mediterranean Basin, due to its high phenol concentrations, that have a toxic impact for water, air, plants and soil microorganisms [28,29]. The two-phase extraction system generated about 0.8 ton of solid waste for per ton of processed olives [30]. According to the data, annual production of olive mill wastes reaches to million of tons in the world. So, large amounts of generated olive mills wastes should be disposed by appropriate methods to prevent environmental damage.

Kalmis and Sargin [31] suggested that 25–50% concentrations of olive mill wastewater (OMWW) can be used at for the moistening of the wheat straw substrate for *Pleurotus sajor-caju* and *Pleurotus cornucopiae* var. *citrinopileatus* cultivation. This can be a promising alternative method for the mushroom cultivation and disposal of OMWW. However, 75% OMWW or 100% OMWW was not adaptable with cultivation of these mushroom species. Zervakis et al. [32] also reported that the 75% OMWW has toxic effects on mycelial growth and yield of *Pleurotus eryngii* and *Pleurotus pulmonarius*. It was determined that when 75% OMWW was used in wetting of substrates, colonisation period was prolonged and BEs of *Pleurotus eryngii* and *Pleurotus pulmonarius* decreased 50%.

Kalmis et al. [33] investigate the feasibility of using OMWW as an alternative moisturing agent for *Pleurotus ostreatus* cultivation. Moreover they determined that effect of OMWW on some food quality characteristics of mushrooms. the use of 25%OMWW was suitable for *P. ostreatus* cultivation. Although food quality was not effected by increasing concentration of OMWW in the moisturing mixture, fruitbody shape was deformed in high concentrations of OMWW. The use of OMWW up to 25% as moisturizer could be suggested for *Pleurotus ostreatus* cultivation. In addition, it could be an environmentally friendly and practical solution for disposal of OMWW

Ruiz-Rodriguez et al. [34] used wheat straw supplemented with 0 up to 90% olive mill waste for cultivation seven *Pleurotus ostreatus* strains. They reported that all *P. ostreatus* strains could grow but high OMW concentrations resulted in a prolonged cultivation period, losses of yield, biological efficiency and fruiting bodies quality. OMW concentrations did not affected total phenolic content and antioxidant activity of fruitbodies and phenolic compounds from OMW were not detected in the fruiting bodies.

Atila [35] reported that sawdust substrate could be supplemented with 25-75% portions of OMW to prepare the growing media for *Pleurotus djamor*, *Pleurotus eryngii* and *Pleurotus citrinopileatus* cultivation and using OMW as a substrate in mushroom cultivation provides an eco-friendly method for disposing of OMW.

Altieri et al [36] and Parati et al. [37] suggested composted olive mill solid waste for cultivation of *Agaricus bisporus*.

Koutrotsios et al [38] reported that *Hericium erinaceus* exhibited high yield in OMWW and olive pruning residues-based media. Moreover it was observed that phenolics and toxicity were decrease on OMWW. Uses of olive press cake was also suggested for *Hericium erinaceus* [39] and *Hericium americanum* production [40] in other previous studies.

According to results from several studies, using by-products from the olive oil industry in mushroom cultivation could help to reduce the environmental impact and production costs.

### 2.2. Grape Pomace

Grape (*Vitis* spp.) is produced 70 million tons every year in the world [41]. Grape pomace, consisting of the seed, skin, and stem, is the main solid organic waste from winery industries. Grape pomace represent, in general, 20–30% of the original grape weight [42]. This waste has highly lignified fibre, so its use as animal feed is limited. Moreover, these residues also have highpolyphenol content. Makris et al. [43] reported that that extracts of grape seeds (either white or red) contain 10.3–11.1% of total polyphenols. Christ and Burrit [44] reported that the wine industry might have a negative impact on local water resources.

A relatively few studies have focused on the use of grape pomace as a substrate for mushrooms production. Koutrotsios et al [45] cultivated *Pleurotus ostreatus*, *Pleurotus eryngii*, and *Pleurotus nebrodensis* on growing media containing grape marc substrate. Grape marc substrates led to large increase of fruit-bodies content in total phenolics, antioxidant activity,  $\beta$ -glucans as well as mushroom yield.

Sanchez et al [46] evaluated the bioconversion of vineyard pruning and grape pomace by cultivation of *Pleurotus* spp. Biological efficiency and bioconversion of vineyard pruning and grape pomace ranged from 37.2 to 78.7% and from 16.7 to 38.8%, respectively. They suggested that uses of viticulture residues on *Pleurotus* spp. cultivation has great potential.

Pardo et al. [47] composted by- products from grape cultivation and wine industry such as vine shoots, grape stalks and grape pomace under controlled conditions for cultivation of two varieties of *Agaricus bisporus*. It was reported that composted vine shoots, grape stalks and grape pomace did not exhibit higher biologically efficient than traditional compost, but these substrates could be economically viable and environmentally advantageous.

### 2.3. Coffee Husk

Coffee is the second largest traded product in the world after petroleum Grape (*Vitis* spp.) is produced 70 million tons every year in the world [48], The coffee industry creates The coffee industry generates over ten million tonnes of residues in the world every year [49]. Generally, most coffee husk is burned to remove this toxic waste.

These by-products are rich in nutrients, caffeine, tannins and polyphenols [50]. Phenolic content of coffee husk limits the uses of it [51]. Maziero [52] studied the production of *Pleurotus* with coffee husk for, but it was no



obtained success. Beaux and Soccol [53] used the coffee husk for *Lentinus edodes* production. They reported poor mycelial growth in comparison to other substrates in this substrate. Tan and Chang [54] studied the effect of tannic acid and caffeine on the growth of *L. edodes*. The results showed that tannic acid and caffeine have a toxic effect on the growth of *L. edodes*. Fan et al., [55] reported that the toxic content was higher in the coffee husk than that in the coffee pulp. Previous studies shown that immersion in water [56] or boiling [57] the coffee husk can be an effective method to remove toxic compounds from the substrate and to increase mushroom yield. Martinez et al. [58] confirmed that the toxic materials can be minimised by hot water treatment, but it also was noted that the other residue (waste water) would lead to environmental pollution [59].

On the other hand some previous studies showed that *Pleurotus ostreatus* has ability in producing fruiting body in coffee husk and coffee pulp. Leifa et al. [60] investigated the possibility of using coffee husk and coffee spent-ground as substrates for the cultivation of *Flammulina velutipes*. They reported that using as substrate coffee husk and coffee spent-ground is appropriate for cultivation of *F. velutipes*. evaluated the feasibility of using coffee husks as substrate for *P. ostreatus* and *P. sajor-caju* cultivation. They reported about 97% of BE *P. ostreatus*. The results of Fan et al. [55] showed that it is possible to use coffee husk for *Pleurotus* spp. cultivation.

### 2.4. Tea Wastes

Tea is one of the most popular beverages in the world. A large amount of tea waste is left after extracting water-soluble components from tea leaves. Therefore, accumulated tea waste is a significant problem for many tea processing industries. Yang et al. [61] suggested that the substrates containin 40–60% tea waste could be used as growing substrate for *Pleurotus ostreatus* cultivation substrate with high yield, biological efficiency and relatively shorter cropping time. It was investigated that the possibility of using tea production waste as a new casing material in *Agaricus bisporus* cultivation by Gulser and Peksen [62]. They did not suggest using tea production waste alone as a casing material in *Agaricus bisporus* cultivation, but also they reported a mixture of tea production waste with peat in 1:1 (v:v) ratio increased the mushroom yield. Chukowry et al [63] obtained satisfactory results from substrate mixture containing 75 % sugarcane bagasse and 25 % tea wastes on cultivation of *Pleurotus ostreatus*. They reported using tea wastes as supplement material to prepare mushroom growing medium could reduced cost of fruiting bag preparation. Baktemur et al. [64] suggested that tea waste can be used successfully as substrate material in *Pleurotus* cultivation. Tea waste was also used in *Ganoderma lucidum* production by Peksen and Yakupoglu [26] and the successful results were obtained.

### 2.5. Green Walnut Husks

The consumption of walnuts is increased by the highly nutritional properties of the seed as well. The main by-product of walnut processing is the green husk. Generated amounts of green walnut husk are quite high. Yilmaz et al [65] reported that the ratio of fresh green walnut husk biomass to total fresh green walnut biomass varied between 65.37%-43.22%. There is a low utilization ratio of green husk because of its toxic content, called juglone. Juglone is an organic compound and occurs naturally in leaves, roots, husks, and bark of plants in Juglandaceae family [66]. Also, Stampar *et al.* [67] has shown that within walnut green husk, juglone is the major phenolic compound. Burying or spreading of green walnut hulls to the soil can cause phytotoxicity. Several studies showed that juglone has inhibitory effects [68,69] and allelopathic activity on several plants [70].

To the best of our knowledge, no study has been conducted to date on the use of green walnut husks in the preparation of mushroom growing media. The high quantities of these waste materials indicate the need for their assessment as an economical substrate for mushroom cultivation. Using green walnut husk on mushroom cultivation could provide extra income to walnut producers and help disposal of green husk.

## 3. DEGRADATION OF PHENOLIC COMPOUNDS FROM AGRO-INDUSTRIAL WASTES BY MUSHROOMS

It is also possible to enhance nutrition quality of agricultural wastes through mushroom cultivation. It has been emphasized in many studies that protein and mineral content of the agricultural wastes may be increased by mushroom cultivation [39,40,60]. In addition to improving the nutrient content of the agricultural wastes, several studies are focused on the elimination of phenolic compounds. Ntugias et al [71] evaluated utilization of olive mill wastewater for cultivation of 49 diverse white-rot strains. They found that using of olive mill wastewater for cultivation of white-rot fungi resulted to the increments of total phenolics (>60%) and reduction of color in mushroom fruit bodies. Moreover, culture extracts from some strains reduced olive mill wastewater phenolics within a nine days period.



Tsioulpas et al. [62] investigated the ability of several *Pleurotus* spp. strains to eliminate phenolic compounds from OMW. In addition, they also studied the toxicity of the treated substrates, in order to select strains able to detoxify OMW. They concluded that *Pleurotus* spp. strains can be grown in OMW and the strains have ability to remove a significant portion of phenolic compounds from OMW.

Zerva et al. [73] reported the use of OMWW for mushroom cultivation can lead to valorization of this toxic waste but also they highlighted the ability of *Pleurotus citrinopileatus* LGAM 28684 and *Irpex lacteus* LGAM 238 species in terms of complete degradation of the phenolics content in OMWW. Saavedra et al. [74] suggested *Pleurotus ostreatus* was effective in elimination of phenolic compounds, the initial concentration in the wet olive cake being reduced by around 90% in the wet olive cake treated with *P. ostreatus*. They reported the spent substrate could be used as soil amendments. Sanchez et al. [46] also reported some antinutritional factors of grape pomace such as phenolic components can be diminished by *Pleurotus* spp. using a solid state fermentation. Echeverria and Nuti [49] reported that caffeine (60%) and tannins (70%) content decrease in coffee husk after mushroom cultivation.

Wong and Wang [75] demonstrated that *Pleurotus sajor-caju* has ability to elimination of tannin in coffee spent ground. Brand et al. [76] reported the content of caffeine and phenolic compounds in coffee pulp as 0.75% caffeine and 3.7% phenolic compounds, while in coffee husks it was 1.2% caffeine and 9.3% phenolic compounds. It is noted that the toxic compounds (caffeine and phenolic compounds) in Brazilian coffee husk are much higher than in coffee pulp, so it is more difficult to treat coffee husk than pulp.

Fan et al. [55] evaluated use of coffee husk for *Pleurotus ostreatus* and *Pleurotus sajor-caju* cultivation. It was determined tannin content (79.2%) and caffeine content (60.7%) was decreased in substrate after cultivation. Although tannic concentration decreased in the medium, it was not determined tannic acid in the mycelia. This result concluded that *Pleurotus* spp. had the capacity of degrading tannic acid.

Sampedro et al [77] reported that olive mill waste is a promising substrate for mushroom cultivation. However, mushroom need long colonization times to reach stabilization of the organic matter and for removal of toxic content from the waste.

Leifa et al. [60] reported that caffeine (10.2%) and tannins (20.4%) contents decrease in coffee husk after *Flammulina velutipes* cultivation. The decrease of tannin content was 28% in coffee spent ground. They [60] suggested that caffeine or tannins were not adsorbed by *F. velutipes* fruitbody. They attributed the decrease in caffeine or tannin content of spent mushroom substrates to degradation of these contents by the mycelium. However Echeverria and Nuti [49] reported that caffeine was found in the fruiting body in some cases and this is a evidence that caffeine was not completely degraded.

### Concluding Remarks

Accumulation of phenol-rich agro-industrial wastes in large quantities in places or disposal of them by burning causes environmental problems. The enzymes of *Basidiomycota* are efficient tools for the destruction of phenols from agro and industrial wastes. The use of phenolic-rich agricultural wastes for production of mushroom is a promising method of elimination these toxic contents. Phenol-rich agro-industrial wastes are rich in nutrient composition as well as bioactive compounds. The use of these wastes as mushroom growing substrates not only help to solve environmental problems, but also can prevent loss of valuable materials and reduce the mushroom production cost. Furthermore, phenolic-rich agro-industrial wastes can improve health preventive compounds in fruitbody such as antioxidants. Thus, mushroom production and distribution can serve as agents for promoting healthy society.

In conclusion, mushroom cultivation can lead to a agricultural revolution in the world, especially in less-developed countries. It has a great potential for generating great environmental and socio-economic impacts in human life. Moreover, spent mushroom substrates could be used to feed ruminants because toxic content decrease while protein increase.

### ACKNOWLEDGMENT

This work was supported by the Kirsehir Ahi Evran University Research Council 2018 Grant No. ZRT.A4.18.020

### REFERENCES

- [1]. A.A. Gami, M.Y. Shukor, K.A. Khalil, F.A Dahalan, A. Khalid and S.A. Ahmad, "Phenol and its toxicity" *J Environ Microbiol Toxicol.*, vol. 2, pp. 11–24, 2014.
- [2]. M.C. Silva, J. Gaspar, I.D. Silva, D. Leão and J. Rueff, "Induction of chromosomal aberrations by phenolic compounds: possible role of reactive oxygen species," *Mutat Res.*, vol. 540 pp.29–42, 2003.
- [3]. X. Peng, Y.Yua, C.Tanga, J. Tana, Q. Huang and Z. Wang, "Occurrence of steroid estrogens, endocrine-disrupting phenols, and acid pharmaceutical residues in urban riverine water of the Pearl River Delta, South China," *Sci Total Environ.*, vol.397, pp.158–166, 2008.
- [4]. J. Li, M. Ma and Z. Wang, "In vitro profiling of endocrine disrupting effects of phenols," *Toxicol in Vitro*, vol. 24 pp.201–207, 2010.
- [5]. O.O. Olujimi, O.S. Fatoki, J.P. Odendaal, J.O. Okonkwo, "Endocrine disrupting chemicals (phenol and phthalates) in the South African environment: a need for more monitoring," *Water SA*, vol.36, pp. 671–682, 2010.
- [6]. P.P. Zhang, Y. Wen, J. An, Y.X. Yu, M.H. Wu and X.Y. Zhang, "DNA damage induced by three major metabolites of 1,3-butadiene in human hepatocyte L02 cells". *Mutat Res.*, vol. 747, pp. 240–245, 2012.
- [7]. S.T Chang and P.G. Miles, Mushroom biology: A new discipline. *The Mycologist*, vol. 6, pp.64–65, 1992.
- [8]. S.T. Chang, and P.G. Miles, *Mushroom: Cultivation, nutritional value, medicinal effect, and environmental impact*, 2nd ed., Boca Raton, FL: CRC Press., 2004.
- [9]. D.L. Hawksworth and R. Lucking, "Fungal diversity revisited: 2.2 to 3.8 million species". *Microbiol Spectrum.*, vol.5 Article ID. FUNK–0052– 2016, 2017.
- [10]. S.T. Chang and J.A. Buswell, "Development of the world mushroom industry: Applied mushroom biology and international mushroom organizations". *Int J Med Mushroom.*, vol. 10, pp.195–208, 2008.
- [11]. Q. Tan, H. Cao, New development of the mushroom industry in China institute of edible fungi, Shanghai Academy of Agricultural Sciences, Shanghai 201106, P. R. China, 2010, [http://wsmbmp.org/Bulletin\\_2\\_Content.html](http://wsmbmp.org/Bulletin_2_Content.html).
- [12]. D.J. Royse,, J. Baars and Q. Tan, Current overview of mushroom production in the world. D.C. Zied, Ed., *Edible and medicinal mushrooms: Technology and applications*. New York: John Wiley & Sons, 2017.
- [13]. (2018) Wikipedia website. [Online]. Available: ([https://en.wikipedia.org/wiki/World\\_population](https://en.wikipedia.org/wiki/World_population)).
- [14]. S.T. Chang, and S.P. Wasser, "The role of culinary–medicinal mushrooms on human welfare with a pyramid model for human health," *Int J Med Mushroom.*, vol.14, pp. 93–134, 2012.
- [15]. F.S. Reis, L.Barros, A. Martins and I.C.F.R. Ferreira, "Chemical composition and nutritional value of the most widely appreciated cultivated mushrooms: an inter– species comparative study," *Food Chem Toxicol.*, vol.50, pp.191–197, 2012.
- [16]. X.M. Wang, J. Zhang, , L.H., Wub, Y.L., Zhao, T., Li, JQ Li, , YZ.,Wang, HG.Liu, "A mini–review of chemical composition and nutritional value of edible wild–grown mushroom from China," *Food Chem.*, vol. 151, pp. 279–285, 2014.
- [17]. S. P. Wasser, "Medicinal mushroom science: History, current status, future trends, and unsolved problems," *Int J Med Mushroom.*, vol.12, pp.1–16, 2010.
- [18]. S.P. Wasser, "Medicinal mushroom science: Current perspectives, advances, evidences, and challenges," *Biomed J.*, vol.35, pp. 516–528, 2014.
- [19]. U. Kues, "Fungal enzymes for environmental management," *Curr Opin Biotech.*, vol.33, pp. 268–278, 2015.
- [20]. L. Martirani, P. Giardina, L. Marzullo and G. Sannia, "Reduction of phenolic content and toxicity in olive oil mill waste waters with the ligninolytic fungus *Pleurotus ostreatus*," *Water Res.*, vol.30, pp. 1914–1918, 1996.
- [21]. G. Olivieri, A. Marzocchella, P. Salatino, P. Giardina, G. Cennamob and G. Sannia, "Olive mill wastewater remediation by means of *Pleurotus ostreatus*," *Biochem Eng J.*, vol. 31, pp.180–187, 2006.
- [22]. A.G. Vlyssides, M. Loizidou, K. Gimouhopoulos and A. Zorpas, "Olive oil processing wastes production and their characteristics in relation to olive oil extraction methods", *Frenius Envir Bull.*, vol:7, pp. 308–313, 1998
- [23]. A. Llobera and Jaime Canellas, "Dietary fibre content and antioxidant activity of Manto Negro red grape (*Vitis vinifera*): pomace and stem," *Food Chem.*, vol:101, pp. 659–666, 2007.
- [24]. F. Saura-Calixto, I. Goni, E. Manas and R. Abia, "Klason lignin, condensed tannins and resitant protein as dietary fibre constituents: Determination in Grape Pomaces," *Food Chem.*, vol:39, pp. 299–309, 1991
- [25]. A. Demirbas, "Evaluation of biomass materials as energy sources: Upgrading of tea waste by briquetting process," *Energy Source*, vol:21, pp.2115–220, 1999
- [26]. A. Peksen and G. Yakupoglu, "Tea waste as a supplement for the cultivation of *Ganoderma lucidum*".*World J Microbiol Biotechnol*, vol.25, pp. 611–618, 2009.
- [27]. A.S. Franca, L.S. Oliveira, "Coffee processing solid wastes: current uses and future perspectives". In: F Clumbus (ed) *Agricultural wastes*, Nova Publishers, New York, 2009.
- [28]. M Della Greca, P Monaco, G Pinto, A Pollio, L Previtera, F Temussi, "Phytotoxicity of low molecular weight phenols from olive mill waste waters," *Bull Environ Contam Toxicol.*, vol.67, pp. 352–357, 2001.
- [29]. G. Rana, M. Rinaldi and M.Introna, "Volatilisation of substances after spreading olive oil waste water on the soil in a Mediterranean environment," *Agric Ecosyst Environ.*, vol.96, pp.49–58. 2003.
- [30]. F. Cerrone, M.M. Sánchez–Peinado, B. Juárez–Jimenez, J. González–López and C. Pozo, "Biological treatment of two–phase olive mill wastewater (TPOMW, alpeorujo): polyhydroxyalkanoates (phas) production by azotobacter strains," *J Microbiol Biotechnol.*, vol. 20, pp. 594–601, 2010.
- [31]. E. Kalmis and S. Sargin, "Cultivation of two *Pleurotus* species on wheat straw substrates containing olive mill waste water," *Int Biodeter Biodegr.*, vol.53, pp.43–47, 2004.

- [32]. G. Zervakis, P. Yiatra and C. Balis, "Edible mushrooms from olive oil wastes," *Int Biodeter Biodeg.*, vol.38, pp.237–243, 1996.
- [33]. E. Kalmis, N. Azbar, H. Yildiz and F. Kalyoncu, "Feasibility of using olivemill effluent (OME) as a wetting agent during the cultivation of oyster mushroom," *Bioresour Technol.*, vol. 99, pp.164–169, 2008.
- [34]. A. Ruiz–Rodriguez, C. Soler–Rivas, I. Polonia and J.H. Wichers, "Effect of olive mill waste (OMW) supplementation to oyster mushrooms substrates on the cultivation parameters and fruiting bodies quality," *IntBiodeter Biodegr.*, vol. 64, pp.638–645, 2010.
- [35]. F. Atila, "Cultivation of *Pleurotus* spp., as an alternative solution to dispose olive waste," *J Agric Ecol Res Int.*, vol.12, pp. 1–10, 2017
- [36]. R. Altieri, A. Esposito, F. Parati, A. Lobianco and M. Pepi, "Performance of olive mill solid waste as a constituent of the substrate in commercial cultivation of *Agaricus bisporus*," *Int Biodeter Biodeg.*, vol. 63, pp. 993–997, 2009
- [37]. F. Parati, R. Altieri, A. Esposito, A. Lobianco, M. Pepi, L. Montesi and T. Nair, "Validation of thermal composting process using olive mill solid waste for industrial scale cultivation of *Agaricus bisporus*," *Int Biodeter Biodeg.*, vol. 65, pp. 160–163, 2011.
- [38]. G. Koutrotsios, E. Larou, K.C. Mountzouris and G. Zervakis, "Detoxification of olive millwastewater and bioconversion of olive crop residues into high–value–added biomass by the choice edible mushroom *Hericium erinaceus*," *Appl Biochem Biotechnol.*, vol. 180, pp.195–209, 2016.
- [39]. F. Atila, Y.Tuzel, J.A. Fernandez and A.F. Cano, "The effect of some agro– industrial wastes on yield, nutritional characteristics and antioxidant activities of *Hericium erinaceus* isolates" *Sci Hort.*, vol. 238, pp. 246–254, 2018.
- [40]. F. Atila, Y. Tuzel, A.F. Cano and J.A. Fernandez, "Effect of different lignocellulosic wastes on *Hericium americanum* yield and nutritional characteristics," *J Sci Food Agric.*, vol. 97, pp. 606–612, 2017.
- [41]. FAOSTAT, Food and Agriculture Organization of the United Nations Statistics Division. [Online] <http://faostat3.fao.org/download/Q/QC/E> (Accessed 30 September 2018), 2016.
- [42]. K. Dwyer, F. Hosseinian and M. Rod, "The market potential of grape waste alternatives" *J Food Res.*, vol. 3, pp. 91–106, 2014.
- [43]. D.P. Makris, G. Boskou and N.K. Andrikopoulos, "Polyphenolic content and in vitro antioxidant characteristics of wine industry and other agri–food solid waste extracts" *J Food Compos Anal.*, vol. 20, pp. 125–132, 2007.
- [44]. K.L. Christm and R.L.Burritt, "Critical environmental concerns in wine production: an integrative review," *J Clean Prod.*, vol.53, pp.232–242, 2013.
- [45]. G. Koutrotsios, N. Kalogeropoulos, A.C. Kaliora and G.I. Zervakis, "Toward an increased functionality in oyster (*Pleurotus*) mushrooms produced on grape marc or olive mill wastes serving as sources of bioactive compounds," *J Agric Food Chem.*, vol.66, pp.5971–5983, 2018.
- [46]. A. Sánchez, F. Ysunza, M.J. Beltrán–García and M. Esqueda, "Biodegradation of viticulture wastes by *Pleurotus*: a source of microbial and human food and its potencial use in animal feding," *J Agric Food Chem.*, vol.50, pp. 2537–2542, 2002.
- [47]. A.Pardo, , M.A.Perona and J. Pardo, "Indoor composting of vine by–products to produce substrates for mushroom cultivation," *Spanish J Agric Res.*, vol. 5, pp.417–424, 2007.
- [48]. S.I. Mussatto, E.M.S. Machado, S. Martins and J.A. Teixeira, "Production, composition, and application of coffee and its industrial residues," *Food Bioprocess Technol.*, vol.4, pp.661–672, 2011.
- [49]. M.C. Echeverria and M. Nuti, "Valorisation of the residues of coffee agro–industry: perspectives and limitations," *Open Waste Manage J.*, vol. 10, pp.13–22, 2017.
- [50]. E. Bondesson, A nutritional analysis on the by–product coffee husk and its potential utilization in food production. Bachelor thesis. Faculty of natural Resources and Agricultural Sciences, Uppsala, 2015.
- [51]. A. Pandey, C.R. Soccol, P. Nigam, D. Brand, R. Mohan and S. Roussos, "Biotechnological potential of coffee pulp and coffee husk for bioprocesses," *Biochem Eng J.*, vol.6, pp.153–162, 2000.
- [52]. R. Maziero, Substratos alternativos para o cultivo de *Pleurotus* sp. São Paulo, (Master Science Thesis, Faculdade de Ciências da USP) 1990.
- [53]. M.R. Beaux and C.R. Soccol, "Cultivation of edible mushroom *Lentinula edodes* in agroindustrial residues from Paraná using solidstate fermentatation. Boletim do Centro de Pesquisa e Processamento de Alimentos, vol.14, pp. 11–24, 1996.
- [54]. Y.H. Tan and S.T. Chang, "Effect of growth regulators, enzyme inhibitors and stimulatory additives on the vegetative development and fructification of *L. Edodes*". Proceedings of the twelfth international congress on the science and cultivation of edible fungi. September, Braunschweig, Germany, 1987.
- [55]. L. Fan, A.T. Soccol, A. Pandey, L.P. Vandenberghe de Souza and C.R. Soccol, "Effect of caffeine and tannins on cultivation and fructification of *Pleurotus* on coffee husks". *Braz J Microbiol.*, vol.37, pp. 420–424, 2006.
- [56]. M.D. Nunes, M.C.S. da Silva, J.G.S. Schram, J.S. da Silva, Y. Tamai and M.C.M. Kasuya, "Pleurotus ostreatus, mushrooms production using quick and cheap methods and the challenges to the use of coffee husk as substrate," *Afr J Microbiol Res.*, vol. 11, pp. 1252–1258, 2017.
- [57]. M.C.S. da Silva, J. Naozuka, J.M.R. da Luz, L.S. de Assunção, P.V. Oliveira, M.C.D. Vanetti, D.M.S. Bazzolli and M.C.M. Kasuya, "Enrichment of *Pleurotus ostreatus* mushrooms with selenium in coffee husks," *Food Chem.* vol. 131, pp. 558–563, 2012.
- [58]. C.D.Martinez, C. Soto and G. Guzman, "Cultivo de *Pleurotus ostreatus* en pulpa de café com paja como substrato," *Rev Mex de Micol.*, vol.1, pp.101–108, 1985.
- [59]. L. Fan, A.T. Soccol, A. Pandey and C.R. Soccol, "Cultivation of *Pleurotus* mushrooms on Brazilian coffee husk and effects of caffeine and tannic acid", *Micol Aplic Int.*, vol. 15, pp. 15–21, 2003.
- [60]. F. Leifa, A. Pandey and C.R. Soccol, "Production of *Flammulina velutipes* on coffee husk and coffee spent–ground", *Braz Arch Biol Technol.*, vol. 44, pp. 205–212, 2001.

- [61]. D. Yang, J. Liang, Y. Wang, F. Sun, H. Tao, Q. Xu, L. Zhang, Z. Zhang, C.T. Ho and X. Wan, "Tea waste: An effective and economic substrate for oyster mushroom cultivation," *J Sci Food Agric.* vol.96, pp. 680–684, 2016.
- [62]. C. Gulser and A. Peksen, "Using tea waste as a new casing material in mushroom (*Agaricus bisporus* (L.) Sing.) cultivation," *Bioresour Technol.*, vol. 88, pp.153–156, 2003.
- [63]. N.D. Chukowry, R.D. Nowbuth and B.Lalljee, "Evaluation of tea wastes as an alternative substrate for oyster mushroom cultivation" *Univ Mauritius Res J.*, vol. 15, pp.458–473, 2009.
- [64]. G.Baktemur, H. Taskin, Y.E. Guzelel, O. Buyukalaca and H. Akilli, "Use of the tea wastes in *Pleurotus* cultivation as an alternative substrate material in Turkey under conventional controlled climate," *Int J Adv Sci Eng Technol.*, vol. 6, pp.13–16, 2018.
- [65]. S.Yilmaz, Y. Akca and S. Saclik, "Green husk and inshell biomass production capabilities of six walnut cultivars. *J Int Sci Publ.*, vol. 5, pp.389–397, 2017.
- [66]. S. Ercisli and C. Turkkal, "Allelopathic effects of juglone and walnut leaf extracts on growth, fruit yield and plant tissue composition in strawberry cvs. 'Camarosa' and 'Sweet Charlie,'" *J Hort Sci Biotechnol.*, vol. 80, pp.39–42, 2005.
- [67]. F. Stampar, A. Solar, M. Hudina, R.Veberic and M. Colaric, "Traditional walnut liqueur – cocktail of phenolics," *Food Chem.*, vol. 95, pp. 627–631, 2006.
- [68]. I. Kocacaliskan and I Terzi, "Allelopathic effects of walnut leaf extracts and juglone on seed germination and seedling growth," *J Hort Sci Biotechnol.*, vol.7, pp. 436–440, 2001.
- [69]. I. Terzi, "Allelopathic effects of Juglone and decomposed walnut leaf juice on muskmelon and cucumber seed germination and seedling growth," *Afr J Biotechnol.*, vol.7, pp.1870–1874, 2008.
- [70]. H. Zhang, J.M Gao, W.T. Liu, J.C. Tang, X.C. Zhang, Z.G. Jin, Y.P. Xu and M.A. Shao, Allelopathic substances from walnut (*Juglans regia* L) leaves. *Allelopathy J.*, vol. 21, pp. 354–362, 2008.
- [71]. S., Ntougias P. Baldrian, C. Ehaliotis, F. Nerud, V. Merhautová and G.I. Zervakis, "Olive mill wastewater biodegradation potential of white-rot fungi--Mode of action of fungal culture extracts and effects of ligninolytic enzymes," *Bioresour Technol.*, vol. 189, pp.121–130, 2015.
- [72]. A.Tsioulpas, D. Dimou, D. Iconomou and G.Aggelis, "Phenolic removal in olive oil mill wastewater by strains of *Pleurotus* spp. in respect to their phenol oxidase (laccase) activity," *Bioresour Technol.*, vol.84, pp. 251–257, 2002.
- [73]. A. Zerva, G.I. Zervakis, P. Christakopoulos and E. Topakas, "Degradation of olive mill wastewater by the induced extracellular ligninolytic enzymes of two wood-rot fungi," *J Environ Manag.*, vol.203, pp. 791–798, 2017.
- [74]. M. Saavedra, E. Benitez, C. Cifuentes and R. Nogales, "Enzyme activities and chemical changes in wet olive cake after treatment with *Pleurotus ostreatus* or *Eisenia fetida*," *Biodegradation* vol.17, pp. 93–102, 2006.
- [75]. Y.S. Wong and X. Wang, "Degradation of tannins in spent coffee grounds by *Pleurotus sajor-caju*," *World J Microbiol Biotechnol.*, vol. 7, pp. 573-574, 1991.
- [76]. D. Brand, A. Pandey, S. Roussos and C.R. Soccol, "Biological detoxification of coffee husk by filamentous fungi using a solid state fermentation system," *Enzyme Microb Technol.*, vol.27, pp.127–133, 2000.
- [77]. I. Sampedro, S. Marinari, A. D'Annibale, S. Grego, J.A. Ocampo and I. GarcíaRomera, "Organic matter evolution and partial detoxification in two-phase olive mill waste colonized by white-rot fungi". *Int Biodet Biodeg.*, vol.60, pp.116–125, 2007.

## Social, Environmental and Economic Effects of Hydroelectric Power Plants: Keban HEPP Sample

*Alp Bugra Aydin<sup>1</sup>*

---

### *Abstract*

*Energy is one of the most fundamental requirements for the economic and social development of countries. Energy consumption is rapidly increasing due to factors such as population growth, industrial developments, urbanization and technological progress. As a result of the investigations, it has been determined that the world's energy consumption has increased by 57% more than expected in the last two decades. For this reason, efficient use of energy resources has gained great importance. Today's energy sources are classified as renewable and non-renewable energy. Renewable energy is also referred to as inexhaustible energy because it is continuously renewed in nature. Solar energy, wind energy, geothermal energy, hydroelectric energy, bioenergy, wave energy are defined as renewable energy sources. In this study, the social and economic impacts of hydroelectric energy from renewable energy sources are mentioned. It also mentioned the social and economic impact of the Keban HEPP of great importance for Turkey's economy.*

**Keywords:** Hydroelektric power, renewable energy, social impact, economic impact

---

### 1. INTRODUCTION

Energy resources are significant for the social and economic development of nations. After the Industrial Revolution, individuals' demand for energy resources has increased considerably and a need to diversify the energy resources has emerged. Most of the global energy requirements is fulfilled with fossil resources [1]. However, the existing reserves for these resources are increasingly exhausted, and their use lead to significant environmental problems. The need to produce energy with reliable, clean, inexpensive and sustainable methods increased the interest in renewable energy sources [2].

Renewable energy includes the natural energy resources that are renewed continuously. Renewable energy sources, which lead to lower damages in the environment when compared to conventional energy sources, are available in the nature. According to the Renewable Energy Sources Global Status Report, the renewable power capacity in certain countries in 2011 are presented in Table 1 [3]. According to this report, it was observed that mostly hydraulic energy is used for power generation in several countries.

---

<sup>1</sup> Corresponding author: Firat University, Department of Civil Engineering, Elazig, Turkey. baydin@firat.edu.tr

*Table 1. Renewable Electricity Power Capacity of Countries by Year 2011 (GW) [3],[4]*

Resources	China	ABD	India	Germany	Turkey	Europion Union	World
Wind	62	47	16	29	1.7	94	238
Biomass	4.4	13.7	3.8	7.2	~0	26	72
Solar (Pv)	3.1	4	0.5	25	0	51	70
Geothermal	~0	3.1	0	~0	0.1	0.9	11.2
Solar (Thermal)	0	0.5	~0	0	0	1.1	1.8
Ocean	~0	~0	0	0	0	0.2	0.5
Hydraulic	212	79	42	4.4	17.1	120	970
<b>Total</b>	<b>282</b>	<b>147</b>	<b>62</b>	<b>65</b>	<b>19</b>	<b>294</b>	<b>1360</b>

The term hydroelectricity corresponds to the electrical energy generated by falling or streaming water through the force of gravity. Hydroelectric power plants refer to the structures where this electrical energy is generated. Hydroelectric power plants generate electricity by simply turning the turbines by the water that fall from a certain altitude [5].

HEPPs that significantly contribute to national economies, despite they are considered among renewable-green energy resources, constitute significant threats to the nature due to the irreversible damages they cause in natural life and force living organisms to migrate. In the present study, social, environmental and economic effects of hydroelectric power stations were investigated and the social, environmental and economic impacts of Keban HEPP, which is the third largest hydroelectric plant in Turkey, were discussed.

## 2. SOCIAL, ENVIRONMENTAL AND ECONOMIC IMPACTS OF HYDROELECTRIC POWER PLANTS

The fact that 90% of the total national electricity production in 24 countries and 50% of the total national electricity production in 63 countries are generated by hydroelectric power plants in the world indicates the significance of these plants in energy production [6]. Hydroelectric energy is preferred more than other energy sources due to several technical advantages such as a long economic life, short depreciation period, high productivity, low operating and maintenance costs. It is obvious that the hydraulic power plants with high investment costs would have significant contributions to the national economy when their long-term returns and depreciation periods are considered. The depreciation of certain power plants and their contribution to national economies are presented in Figure 1.



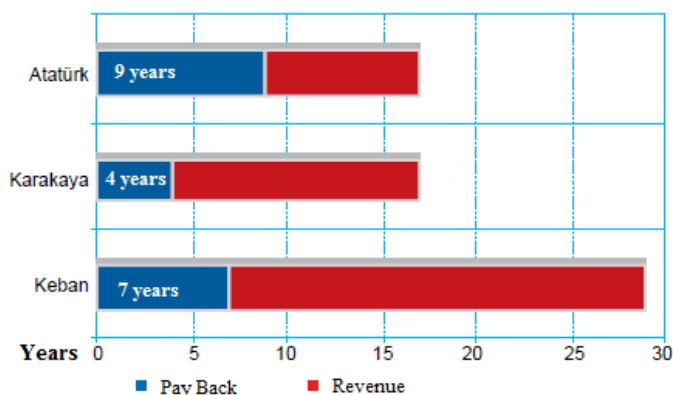


Figure 1. Payback Time for Some HEPP Projects [7]

It is known that the energy sector contributes to local economies after HEPP investments due to the developments in industries such as increasing the employment, improving trade, agricultural activities, forestry and tourism. Hydroelectric power plants, which are economically very productive, are not absolutely clean due to the environmental damages they cause. Hydroelectric power generation has several effects on natural, historical and cultural assets and socioeconomic environment, based on the size of the project [5], [8].

The initial impact of the HEPP projects is observed during the stage of determination of the location of the plant site. Archaeological and cultural studies are of great significance in the areas and settlements that would be affected by HEPPs. However, the lack of proper documentation and conservation/recovery studies leads to the destruction of several cultural heritage sites.

Hydroelectric Power Plant Forest Permit should be obtained from the Ministry of Forestry and Water Affairs based on the characteristics of the construction region. As a result of the economic and political interests during the acquisition of the necessary permits, several forest areas are destroyed or lost. Thus, the risk of erosion in steep and slope areas is doubled. Furthermore, rare or endangered plant and animal species in the area are harmed.

Most environmental and social impacts occur during the construction. Dust and traffic, especially during excavation work, negatively affect the inhabitants of the region. The transportation destination of the excavated earth is also a significant problem. Furthermore, due to the dusting that occurs during the construction of the HEPP, the leaves are covered with dust, reducing the permeability of light, the photosynthesis rate of the leaves, and thus the tree growth is adversely affected [2].

Water intake structures and water transmission lines, which are a part of hydroelectric power plants, disrupt the stream integrity. This causes great damage to natural life and the ecosystem [5].

Since the majority of the water in the stream is used during the operation of the hydroelectric power plants, the water flow rate and velocity are reduced. This has an adverse effect on agricultural irrigation. Furthermore, the amount of dissolved oxygen in the water decreases in parallel with the decrease in water volume. When the required oxygen rate is not available, it is difficult for the living creatures to maintain their lives in the water.

Hydroelectric power plants should be designed considering all these effects during the preliminary studies. Otherwise, environmental ecology and local residents will be adversely affected.

### 3. KEBAN DAM AND HYDROELECTRIC POWER PLANT

Keban Dam is located 45 km northwest of Elazığ provincial center, 65 km northeast of Malatya provincial center and on one of the narrowest straits on the river at 10 km downstream from the point where Karasu and Murat rivers merge. It is the first point suitable for a dam site on the Euphrates River, which is formed by the merger of Karasu and Murat rivers. There are 5 dams and/or HEPPs on the Euphrates River (Figure 2). The first dam constructed on the Euphrates River was the Keban Dam.

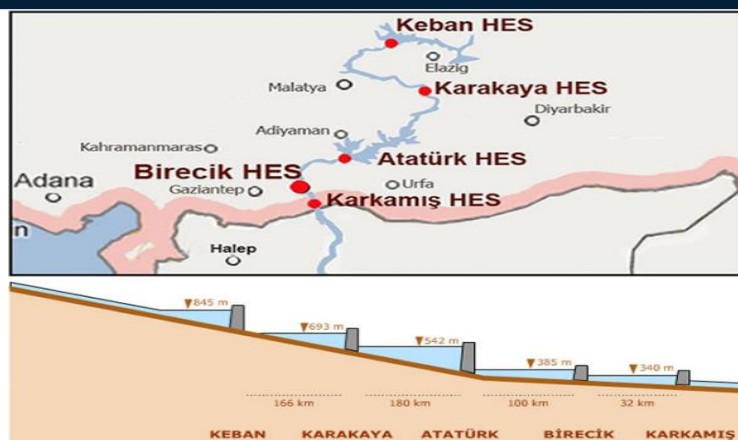


Figure 2. Dams on the Fırat River [9]

The Keban Dam was built between 1965 and 1974 on the Fırat River in the Keban district of Elazığ province. The height of the dam is 210.00 m, the lake volume is 31.000.000 m<sup>3</sup>, the lake is 680.00 km<sup>2</sup> and the length is 125 km. The width of this dam is variable. The construction started in 1965. In 1974, the first 4 large turbines, and in 1981, the remaining 4 turbines were activated. The total power of the dam is 1330 Megawatts and the energy generation based on the years of operation is presented in Table 2 [9].

Table 2. Keban Dam and HES annual electricity production [9]

Years	Production	Province Consumption Rate	Country Consumption Rate
1993	7.168.000.000	%1.635,73	%9,76
1994	6.311.000.000	%1.359,60	%8,11
1995	7.272.000.000	%1.424,37	%8,50
1996	7.350.000.000	%1.299,35	%7,75
1997	7.714.000.000	%1.225,05	%7,31
1998	7.740.000.000	%1.137,49	%6,79
1999	5.743.000.000	%812,22	%4,85
2000	4.512.000.000	%589,40	%3,52
2001	3.822.000.000	%504,81	%3,01
2002	5.266.719.000	%665,81	%3,97
2003	6.375.965.000	%756,94	%4,52
2004	7.904.810.000	%882,97	%5,27



2005	6.694.897.000	%697,70	%4,16
2006	7.280.758.000	%698,61	%4,17
2007	6.104.782.000	%538,41	%3,21
2008	4.958.698.000	%419,48	%2,50
2009	3.958.800.000	%341,81	%2,04
2010	7.958.586.000	%633,75	%3,78
2011	6.331.000.000	%460,64	%2,75
2012	5.654.000.000	%390,91	%2,33
2013	5.975.088.820	%406,42	%2,43
2014	3.296.328.930	%215,36	%1,29
2015	4.780.887.780	%301,18	%1,80
2016	4.965.679.000	%302,72	%1,81

Keban Dam generated 236 billion kilowatt-hours of energy since its inception and contributed significantly to the national economy. In several countries, such structures with a major contribution to the national economy are subject to the EIA (Environmental Impact Assessment) process and the construction site decision is made after the analysis of the site surveys. Thus, based on the archaeological-cultural heritage potential of the site, the project and selected site are changed when necessary, and the destruction of the archaeological heritage in these areas is prevented. The failure to implement the said process in Keban Dam has led to great environmental and social impacts.

According to SHW findings, 5 provinces, 9 districts, 258 towns/villages/hamlets were affected by the construction of this dam. Of these, 94 towns/villages were completely submerged, 1 province, 3 districts and 115 towns / villages were partially affected by the dam (Figure 3) [10].

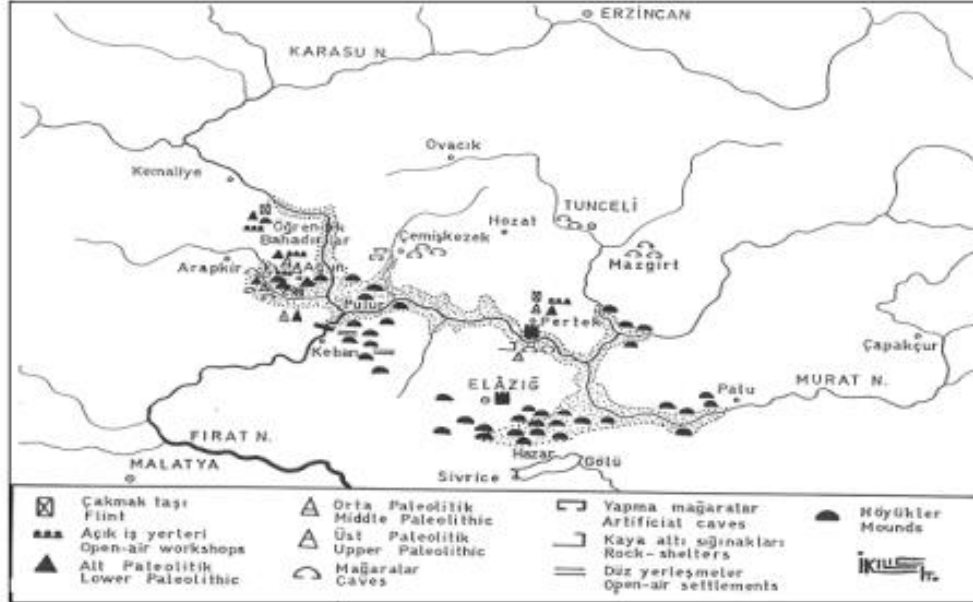


Figure 3. Keban Dam Area - Prehistoric Detection and Dam Basin Relationship [10]

A number of studies were conducted to determine the archaeological/cultural heritage sites in the area and the settlements affected by the dam. With the study titled “Keban Reservoir Recovery Project,” only 65% of the Keban Reservoir could be surveyed [11]. However, the dam construction was completed without any necessary analyses were conducted on any settlement and a great historical heritage site was submerged [10].

For the construction of the Keban Dam, expropriations were conducted in 160 villages, 50 hamlets and 11 neighborhoods and approximately 615 thousand square meters of agricultural land was submerged [12]. These agricultural lands with high crop yields affected the local residents, 30% of whose income depended on agriculture. Submergence of thousands of acres of land led to the migration of the rural population to urban areas. The people in possession of expropriation payments initially contributed economically to the urban centers, however migration of the rural population to urban centers led to formation of an unqualified urban population and urban unemployment increased over time. Furthermore, the rapid increase in urban population led to urban sprawl and inadequate urban infrastructure, constantly increasing environmental problems.

As the agricultural land submerged, fishing became the secondary livelihood of local residents. With the recent regulations, it was determined that 16 cooperatives operate in the reservoir (Figure 4). In this area where 22 species and subspecies in 6 genera live, 40000 tons of fish were caught in 2014 and a large portion of this production was exported to Europe and Japan [13], [14]. In this respect, Keban Reservoir provided economic benefits to local residents.

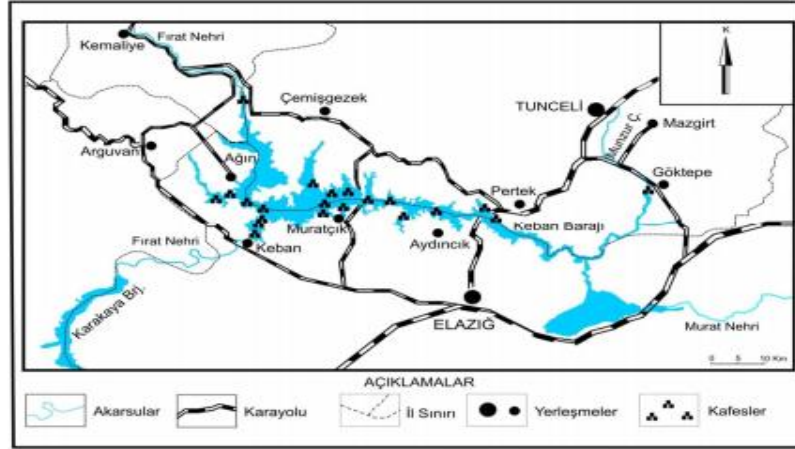


Figure 4. Fish Breeding Area in Keban Dam [13]

## 4. CONCLUSION

National energy requirement increases rapidly due to population increase, industrialization and acceleration in urbanization and economic developments. The rapid increase in the energy demand revealed the necessity of diversifying energy resources. Hence, humans started to search for clean, cheap, sustainable and reliable energy production methods and developed renewable energy sources. Hydroelectric (hydraulic) energy, a renewable energy source, is widely used in several countries. The number of hydropower plants in Turkey increased in recent years due to the hydraulic potential. The country's first major investment in this field was the Keban Dam and Hydroelectric Power Plant. The Keban dam was commissioned in 1974 and produced about 236 billion kWh of energy until today. As mentioned in the present study, Keban Dam and Hydroelectric Power Plant contributed significantly to the Turkish economy, however it had negative environmental and social effects on local and regional residents.

## REFERENCES

- [1]. M. Yılmaz, Türkiye'nin Enerji Potansiyeli ve Yenilenebilir Enerji Kaynaklarının Elektrik Enerjisi Üretimi Açısından Önemi, Ankara Üniversitesi Çevre Bilimleri Dergisi, 4(2), 33-54(2012)
- [2]. E. Turhan, H. Özmen Çagatay, A. Kececi, Hidroelektrik Santrallerin Çevresel ve Sosyal Etkileri: Alakir Vadisi Örneği, 4. Su Yapıları Sempozyumu, 67-76, 2015.
- [3]. E. Koc, M. C. Senel, 2013, The State of Energy in World and Turkey - General Evaluation, Mühendislik ve Makine, vol 54, s. 32-44.
- [4]. REN21, 2012. Renewables 2012 Global Status Report, Renewables Energy Policy Network for the 21st Century (REN21), Paris, France.
- [5]. O. Urker and N. Cobanoğlu, Türkiye'de Hidroelektrik Santraller'in Durumu (Hes'ler) Ve Çevre Politikaları Bağlamında Değerlendirilmesi, Ankara Üniversitesi Sosyal Bilimler Enstitüsü Dergisi, 2012, 3(2) DOI: 10.1501.
- [6]. World Commission on Dams Report: Dams and Development, November 2000.
- [7]. O. Dalkir and E. Sesen, Çevre ve Temiz Enerji: Hidroelektrik, Çevre ve Orman Bakanlığı Devlet Su İşleri Genel Müdürlüğü, 2011.
- [8]. TMMOB SU RAPORU, Küresel Su Politikaları ve Türkiye, 2009.
- [9]. (2018) Online Available <http://www.enerjiatlası.com/hidroelektrik/keban-barajı.html>
- [10]. D. Cakirca, Keban Barajı ile Neleri Kaybettik, 4. Su Yapıları Sempozyumu, ss. 550-561, 2015.
- [11]. Su Yapıları ve İTÜ'lu Süleyman Demirel, İstanbul Teknik Üniversitesi Vakfı, Vol.70, 2015.
- [12]. (2018) Online Available <https://bianet.org/bianet/cevre/73632-tarim-alanlari-kebanin-sulari-altinda-kaldi>
- [13]. B. Güner, Keban Baraj Gölü'nde Kültür Balıkçılığı, Fırat University Journal of Social Science Vol: 25, Sayfa: 1-8, ELAZIG-2015
- [14]. Y. Celayir, M. Pala and F. Yuksel, Keban Baraj Gölü Balıkçılığı, I. Balıklandırma ve Rezervuar Yönetimi Sempozyumu 7 - 9 subat 2006, Antalya.

## An Environmentally Friendly Plant in Terms of Oxygen Supply: Hemp

*Selim Aytac<sup>1</sup>*

### Abstract

*Global warming has been found to be associated with increased concentrations of atmospheric greenhouse gases such as carbon dioxide (CO<sub>2</sub>). CO<sub>2</sub> emitted from the burning of fossil fuels is not absorbed by the vegetation cover, and thus causes the global temperature to rise by continuing to remain in the atmosphere. Industrial hemp uses solar energy to convert atmospheric CO<sub>2</sub> to hydrocarbons and water. In addition, O<sub>2</sub> produced. This absorptive CO<sub>2</sub> is released back into the atmosphere only when the hemp is composted or burned. According to a report, every ton of hemp produced produces 1.63 tonnes of CO<sub>2</sub>. Hemp provides the protection of forests in the production of energy and paper. Hemp stalks release atmospheric carbon dioxide by burning for energy purposes. Hemp plants used a lot of this carbon dioxide released during the growing season. The high amount of oxygen provided by the atmosphere is due to the rapid growth of the hemp and its abundant leaves. Hemp can be processed into building materials. Thus, even though traditional construction is an expensive carbon footprint, hemp can be used to build "zero carbon" structures, ie building materials absorb CO<sub>2</sub> more than the ones produced during construction. In this manuscript, the O<sub>2</sub> / CO<sub>2</sub> usage cycle of the hemp plant will be discussed.*

**Keywords:** Environment, Hemp, Oxygen

### 1. INTRODUCTION

In recent years, the increase in consumer awareness and the search for new and different products of the textile sector, natural fiber is increasing in popularity. In order to meet this growing demand, we also need to produce fiber crops outside of cotton cultivation areas. One of the fiber plants that can be produced outside cotton cultivation areas is hemp. Hemp, which is an industrial plant, is mainly grown for its fiber, seed and oil. Hemp fibers have excellent mechanical properties and are environmentally friendly, biodegradable to meet waste treatment needs.

Considering the last 5 years of statistics, the cultivation of hemp in Europe has increased considerably. There are a number of reasons for the increase of hemp fields. The fact that the production of genotypes with low THC ratios is safe from narcotics. On the other hand, the importance of hemp in different areas has increased in recent years due to factors such as being suitable for environmentally friendly production. In addition to being suitable for environmentally sensitive agriculture, the production of the products obtained from hemp has been done without causing much harm to the environment, has attracted attention in recent years. One of the effects of hemp on environmental sensitivity is the oxygen / carbon dioxide cycle relationship.

### 2. TAXONOMY OF HEMP

Order: *Rosales*

Family: *Cannabaceae*

Genus: *Cannabis*

Species: *Cannabis sativa L.*

<sup>1</sup> Corresponding author: Ondokuzmayis University, Agriculture Faculty, Field Crops Department, 55139, Atakum/Samsun, Turkey. [selim@omu.edu.tr](mailto:selim@omu.edu.tr)

Subspecies:

*Cannabis sativa* var. *vulgaris* L. (Industrial Hemp)

*Cannabis sativa* var. *indica* Lam. (Marihuana)

*Cannabis sativa* subvar. *gigantica* (Huge)

*Cannabis sativa* var. *ruderalis* (Weed).

Hemp is an annual, dioecious, flowering herb. The leaves are palmately compound or digitate, with serrate leaflets. Although different taxonomy has been made, many sources classify hemp as above. Again according to many sources, Hemp is the only species in the Cannabinaceae family.

### 3. BENEFIT FROM HEMP

Hemp is primarily a fiber plant. But; food, feed, construction material, bioplastic, biopolymer, paper, especially in many sectors are used. Figure 1 shows areas where hemp is used.

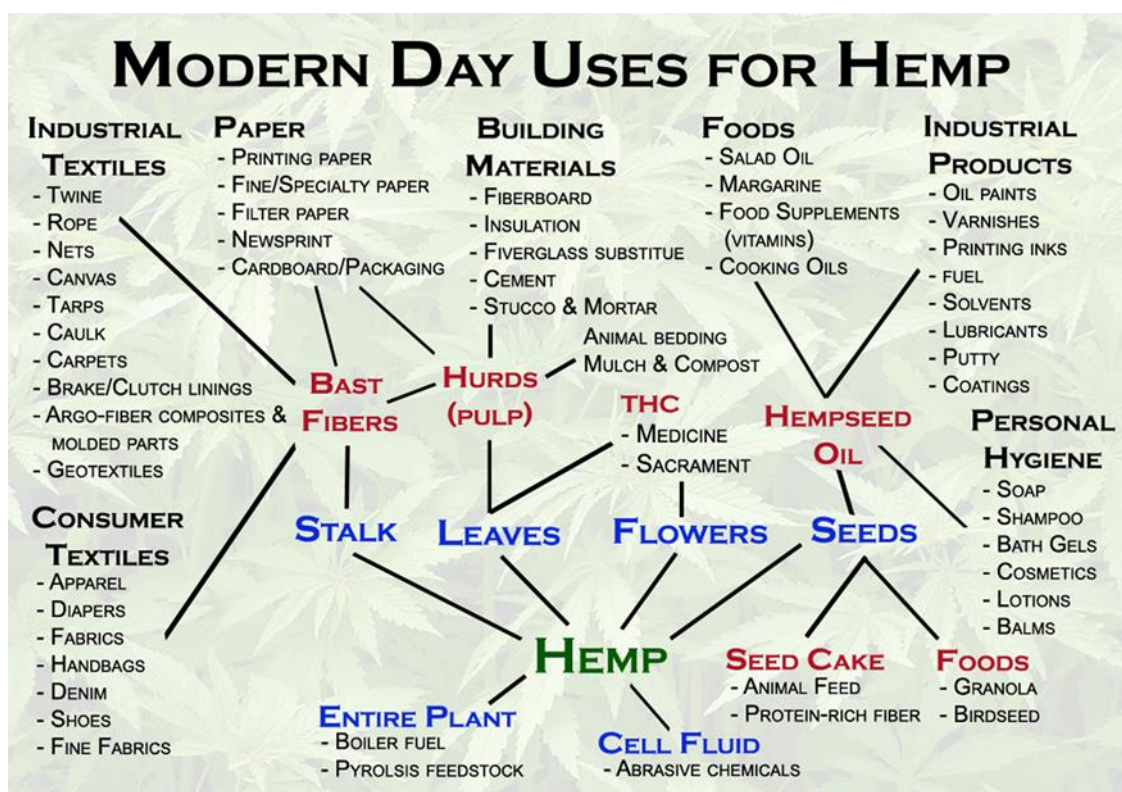


Figure 1. Uses of Hemp [1]

### 4. EFFECT OF O<sub>2</sub> / CO<sub>2</sub>

#### 4.1. Forest Protection

The high amount of oxygen provided by the atmosphere is due to the rapid growth of the hemp and its abundant leaves (Figure 2). . Hemp is a solution for global warming because it replaces more than it uses [2]. Hemp has a faster CO<sub>2</sub> uptake by side, producing productive, annual, versatile biomass without the use of low-yield fertilizers and other chemical inputs. In addition to improving the soil structure, it can produce a wide variety of sustainable raw materials that generally have low environmental impact. Non-sustainable raw materials can



be replaced with Hemp. It can also be used to alter some of the important characteristics of wood-based products, reducing the use of the existing tree population, which in turn leads to their CO<sub>2</sub> uptake [3].



*Figure 2. A view from the hemp field.*

Hemp can produce 7.5-20 tonnes of dry habitat tons per hectare, which is about 4 times that of an average forest [4]. According to Hemp Global Solutions, each ton of hemp grown represents 1.63 tons of CO<sub>2</sub> absorption. And according to the Great Book of Hemp, an average decare of hemp will yield 1.25-2.5 tons of dried stalk [5]. Hemp can take the place of wood fibers, thus contributing to the prevention of global warming as well as protecting the forests [4], [6]. Hemp can replace most of the toxic petrochemical products. Studies on the use of hemp for the production of plant-based cellophane, injection molded products, recycled plastics and biodegradable plastic products are still ongoing [7].

CO<sub>2</sub> emitted from a burning hemp is the same amount of CO<sub>2</sub> that the plant has received from the environment when it lives. Thus, it will not make a negative contribution to the environment, and will produce a so-called carbon cycle system of energy production and slow down the effects of global warming [3].

Hemp cultivation is 400% more efficient in CO<sub>2</sub> absorption than land-based agro-forestry. The rapid growth rate means that we can provide the required amount of industrial biomass in our modern society. Hemp can be transformed into a large number of sustainable raw material solutions to fit the needs of local communities wherever it grows and can protect remaining forest resources and biodiversity. It can be produced once or twice a year in relatively hot climates [8]

#### **4.2 Sustainable Raw Materials**

When hemp is produced in large areas; the products and raw materials derived therefrom may replace many petroleum-based unsustainable products and materials, particularly in construction, by linking them in CO<sub>2</sub> and creating secondary benefits to the global environment[9]. This is a very good example of hempcrete. Hempcrete is made from hemp stalks and can be used instead of bricks. The overall emission balance is very convenient. Thanks to the CO<sub>2</sub> intake during hemp growth and the carbonation of the hen, the hempcrete blocks have a negative carbon footprint and therefore act as effective carbon sinks [10].

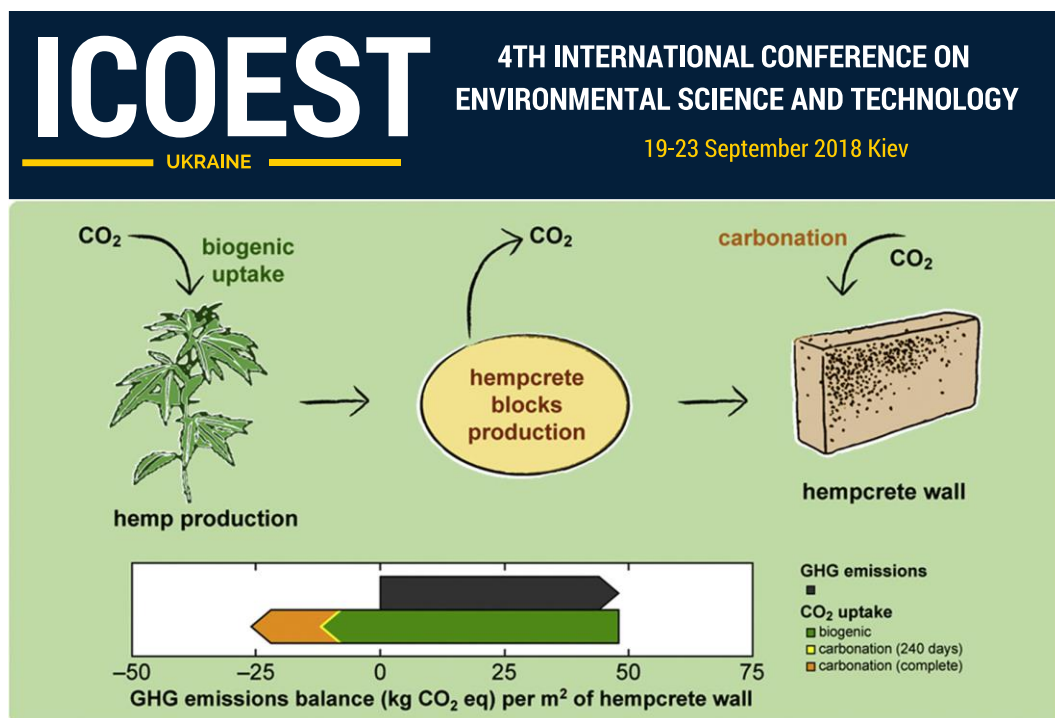


Figure 3. Benefits of Hempcrete [10]

## 5. CONCLUSIONS

Hemp is the THC (marihuana) producing plant. However, in recent years, THC-free varieties have been improved. Hemp has superior properties in terms of oxygen production, carbon dioxide decomposition and permanent bonding to the materials in which it is produced. We must make more use of hemp, which is very useful for the economy and the environment.

## REFERENCES

- [1].2018. <https://oecotextiles.wordpress.com/2010/06/02/characteristics-of-hemp/> Characteristics of hemp
- [2]. 2018. <https://www.drawdown.org/solutions/coming-attractions/industrial-hemp>. Coming Attractions Industrial Hemp.
- [3]. 2018. <https://hempnewstv.wordpress.com/2009/09/28/the-science-behind-carbon-dioxide-reduction-with-hemp/> The Science behind Carbon Dioxide Reduction with Hemp, September 28, 2009)
- [4].2018. <http://www.globalhemp.com/1997/10/north-american-industrial-hemp-council-industrial-hemp-facts-sheet.html> Industrial Hemp Facts
- [5]. 2018. <https://globalhempgroup.com/tag/hemp/>
- [6].2018. [www.ubfdb.org.in](http://www.ubfdb.org.in)
- [7]. 2018. [www.LotusOrganics.com](http://www.LotusOrganics.com)
- [8]. 2018.2018. <http://rebekahshaman.com/hemp-a-climate-change-crop/> Hemp a Climate Change Crop
- [9]. James Vosper BSCHons The Role of Industrial Hemp in Carbon Farming, FRGS. GoodEarth Resources PTY Ltd (ABN 79 124 022 859)
- [10] Al. Arrigonia, R. Pelosatoa P. Melià, G. Ruggieric, S. Sabbadinid , G. Dotellia. "Life cycle assessment of natural building materials: the role of carbonation, mixture components and transport in the environmental impacts of hempcrete block" Journal of Cleaner Production, Volume 149, Pages 1051-106, April 2017

## BIOGRAPH

Selim AYTAC was born in Samsun, Turkey. He completed his graduate of the Ondokuz Mayis University of Field Crops Department. He has completed master's degree and PhD at the Ondokuzmayis Universty. He is an associate professor at the Ondokuzmayis University.



# Petaloid Monocotyledonous Flora of Bingol Province (Turkey)

*Suleyman Mesut Pinar<sup>1</sup>, Mehmet Fidan<sup>2</sup>, Huseyin Eroglu<sup>3</sup>*

---

## Abstract

*This study was carried out to determine the petaloid monocotyledonous flora of Bingol Province. According to grid system of Davis Bingol Province is located B7 square in Turkey. The field studies were carried out to cover the 4 seasons (spring, summer, autumn and winter) in 2017-2018. 82 taxa belonging to 10 families in total were determined in Bingol. 12 of these taxa are endemic to Turkey. Names, photographs and threatened categories (according to IUCN) of taxa are given in this study. This study is part of the Project to Determine Biodiversity of Bingol Province*

**Keywords:** Bingol, endemic, IUCN, monocotyledonous, petaloid, Turkey.

---

## 1. INTRODUCTION

Turkey has a rich flora and various vegetation types with ecological and floristic reasons like; its geographical position, geological structure, having different topographic and soil structures, with the appearance of different climate types within its boundaries, being at the junction of three different plant geography regions and being a gene center of many genera [1]. According to Guner et al. total number of taxa in Turkey is 11.707 including foreign-funded and cultivated plants. Endemic taxa number and endemism rate were determined as respectively 3.649 and 31,82% [2].

Petaloid monocots are so named due to they have conspicuous tepals like petals [3]. Anatolia is one of the most significant geophyte centers in the world, having around 100 seedless vascular geophytes, 1000-1200 dicotyledonous geophytes, 200-250 non-petaloid monocotyledonous geophytes and around 1000 petaloid monocotyledonous geophytes [4].

Bingol is located in East Anatolia Region at Turkey. This area belongs to Irano-Turanian phytogeographic region and situated at B8 frame within the grid system of Davis [5]. The area of Bingol province is 8.253 square kilometers The elevation varies from 1150 to 3000 meters in Bingol. Because of its height, it is covered with snow in about half of the year.

## 2. MATERIALS AND METHODS

Within the Biological Diversity Project, field studies carried out to determine vascular plant species of the Bingol Province were conducted in 2017 and 2018, covering 4 seasons.

In this context, field studies to determine the floristic structure and vegetation of the Bingol Province were carried out periodically between the vegetation periods of the plants. Field work was done almost all of the Bingol province at different vegetation periods and efforts were made to identify the plants.

Plant samples collected at the end of the field studies were brought to the Herbarium of Van Yuzuncu Yil University Science Faculty and diagnosed using Flora of Turkey and the East Aegean Islands [6;7;8].

---

<sup>1</sup> S. Mesut PİNAR: Van Yuzuncu Yil University, Health Faculty, 65080, Tusba/Van, Turkey. [mesutpinar@hotmail.com](mailto:mesutpinar@hotmail.com)

<sup>2</sup> Mehmet FİDAN: Siirt University, Faculty of Science and Literature, 56100, Siirt, Turkey [mfidan7384@hotmail.com](mailto:mfidan7384@hotmail.com)

<sup>3</sup> Corresponding author: Huseyin EROGLU: Van Yuzuncu Yil University, Faculty of Science, 65080, Tusba/Van, Turkey. [huseyineroğlu\\_41@hotmail.com](mailto:huseyineroğlu_41@hotmail.com)

The height, locality, habitat, date and coordinates (using GPS) of the sampling stations and plants were noted. In all field studies, photographs of plants and habitats were taken as much as possible.

All plant species fixed were classified and identified according to the family name, species-subspecies-variety, endemism, and IUCN categories according to Ekim et. al., 2000; IUCN, 2016. [9;10]

### 3. RESULTS AND DISCUSSION

A total of 1254 taxa have been identified during the literature and field studies done by us, including ferns, of which 122 are endemic to Turkey. 81 monocotyl petaloid taxa belongs to 10 families were identified in the study area and 12 of them are endemic. These taxa are given in table 1.

Table 1. Monocotyl petaloids detected in Bingol Province.

FAMILY	SPECIES	SUBSPECIES	VARIETY	IUCN	ENDEMISM
ALISMATACEAE	<i>Alisma lanceolatum</i>				
AMARYLLIDACEAE	<i>Allium ampeloprasum</i>				
AMARYLLIDACEAE	<i>A. armenum</i>			LC	END.
AMARYLLIDACEAE	<i>A. atroviolaceum</i>				
AMARYLLIDACEAE	<i>A. cardiostemon</i>				
AMARYLLIDACEAE	<i>A. kharputense</i>				
AMARYLLIDACEAE	<i>A. paniculatum</i>	<i>paniculatum</i>			
AMARYLLIDACEAE	<i>A. pseudoampeloprasum</i>			VU	
AMARYLLIDACEAE	<i>A. pseudoflavum</i>				
AMARYLLIDACEAE	<i>A. scorodoprasum</i>	<i>jajlae</i>			
AMARYLLIDACEAE	<i>A. scorodoprasum</i>	<i>rotundum</i>			
AMARYLLIDACEAE	<i>A. sintenisii</i>			NT	END.
ARACACEAE	<i>Biarum carduchorum</i>				
ARACACEAE	<i>Lemna trisulca</i>				
ARACACEAE	<i>L. turionifera</i>				
ARACACEAE	<i>Spirodela polyrhiza</i>				
ASPARAGACEAE	<i>Bellevallia fominii</i>			VU	
ASPARAGACEAE	<i>B. leucantha</i>			CR	END.
ASPARAGACEAE	<i>B. paradoxa</i>				
ASPARAGACEAE	<i>B. pseudofominii</i>				END.
ASPARAGACEAE	<i>B. speciosa</i>				
ASPARAGACEAE	<i>Hyacinthus orientalis</i>	<i>chionophilus</i>			
ASPARAGACEAE	<i>Muscari armeniacum</i>				
ASPARAGACEAE	<i>M. comosum</i>				
ASPARAGACEAE	<i>M. neglectum</i>				
ASPARAGACEAE	<i>Ornithogalum arcuatum</i>				
ASPARAGACEAE	<i>O. montanum</i>				
ASPARAGACEAE	<i>O. narbonense</i>				
ASPARAGACEAE	<i>O. oligophyllum</i>				
ASPARAGACEAE	<i>Puschkinia peshmenii</i>				END.
ASPARAGACEAE	<i>Puschkinia scilloides</i>				

ASPARAGACEAE	<i>Scilla siberica</i>	<i>armena</i>		
COLCHICACEAE	<i>Colchicum kotschy</i>			
COLCHICACEAE	<i>C. soboliferum</i>			
COLCHICACEAE	<i>C. szovitsii</i>			
IRIDACEAE	<i>Crocus biflorus</i>	<i>tauri</i>		
IRIDACEAE	<i>C. cancellatus</i>	<i>cancellatus</i>		
IRIDACEAE	<i>C. cancellatus</i>	<i>damascenus</i>		
IRIDACEAE	<i>C. kotschyanus</i>	<i>kotschyanus</i>		
IRIDACEAE	<i>C. pallasii</i>	<i>turcicus</i>		
IRIDACEAE	<i>Gladiolus atrovioleaceus</i>			
IRIDACEAE	<i>G. humilis</i>		EN	END.
IRIDACEAE	<i>G. kotschyanus</i>			
IRIDACEAE	<i>Iris caucasica</i>	<i>caucasica</i>	VU	
IRIDACEAE	<i>I. galatica</i>		LC	END.
IRIDACEAE	<i>I. persica</i>			
IRIDACEAE	<i>I. reticulata</i>	<i>reticulata</i>		
IRIDACEAE	<i>I. sari</i>		LC	END.
IXIOLIRIACEAE	<i>Ixiolirion tataricum</i>	<i>tataricum</i>		
LILIACEAE	<i>Fritillaria alburyana</i>		NT	END.
LILIACEAE	<i>F. latifolia</i>			
LILIACEAE	<i>F. minuta</i>			
LILIACEAE	<i>F. pinardii</i>			
LILIACEAE	<i>Gagea bohémica</i>			
LILIACEAE	<i>G. bulbifera</i>			
LILIACEAE	<i>G. confusa</i>			
LILIACEAE	<i>G. luteoides</i>			
LILIACEAE	<i>G. peduncularis</i>			
LILIACEAE	<i>G. reticulata</i>			
LILIACEAE	<i>G. taurica</i>			
LILIACEAE	<i>G. villosa</i>	<i>villosa</i>		
LILIACEAE	<i>Tulipa armena</i>	<i>armena</i>		
LILIACEAE	<i>T. julia</i>			
LILIACEAE	<i>T. sintenesii</i>		LC	END.
ORCHIDACEAE	<i>Cephalanthera damasonium</i>			
ORCHIDACEAE	<i>C. kotschyana</i>		LC	END.
ORCHIDACEAE	<i>Dactylorhiza iberica</i>			
ORCHIDACEAE	<i>D. osmanica</i>		NT	END.
ORCHIDACEAE	<i>D. umbrosa</i>			
ORCHIDACEAE	<i>Epipactis helleborine</i>			
ORCHIDACEAE	<i>Limodorum abortivum</i>	<i>abortivum</i>		

ORCHIDACEAE	<i>Himantoglossum affine</i> (Boiss.) Schltr.	
ORCHIDACEAE	<i>Ophrys argolica</i>	
ORCHIDACEAE	<i>O. holoserica</i>	<i>heterochila</i>
ORCHIDACEAE	<i>O. reinholdii</i>	<i>straussii</i>
ORCHIDACEAE	<i>Orchis coriophora</i>	<i>coriophora</i>
ORCHIDACEAE	<i>O. mascula</i>	<i>pinetorum</i>
ORCHIDACEAE	<i>O. palustris</i>	<i>palustris</i>
ORCHIDACEAE	<i>O. punctulata</i>	
ORCHIDACEAE	<i>O. tridentata</i>	
XANTHORRHOEACEAE	<i>Asphodeline damascena</i>	<i>damescena</i>
XANTHORRHOEACEAE	<i>Eremurus spectabilis</i>	

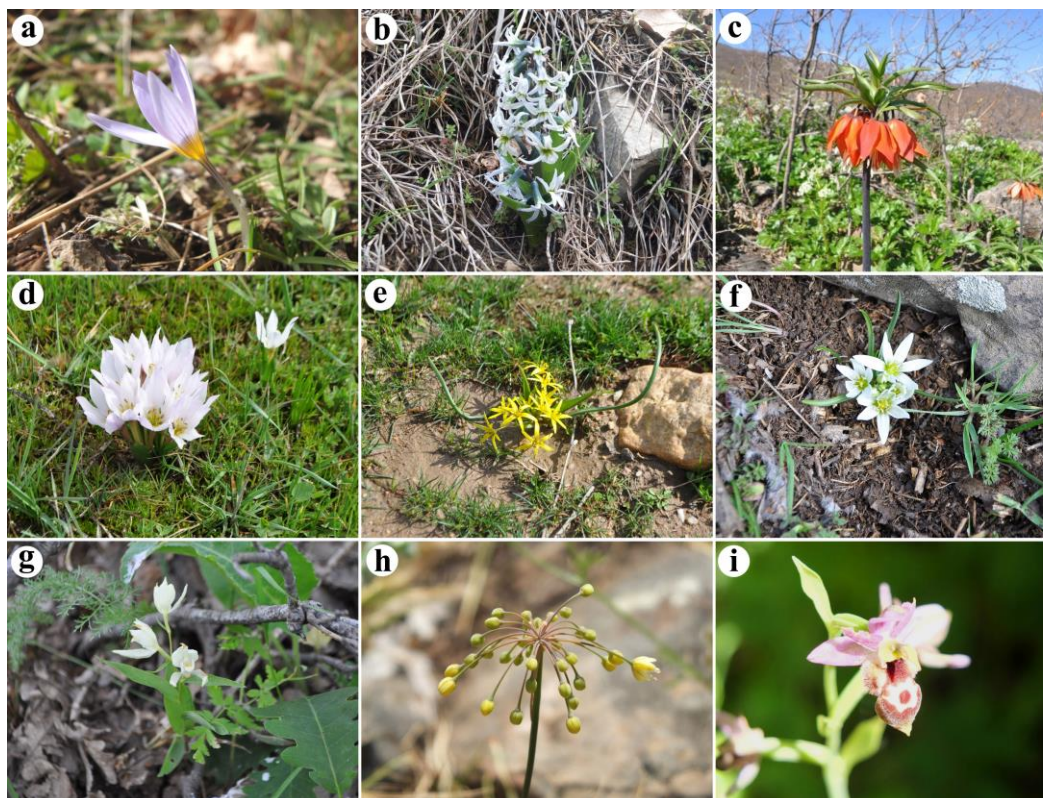
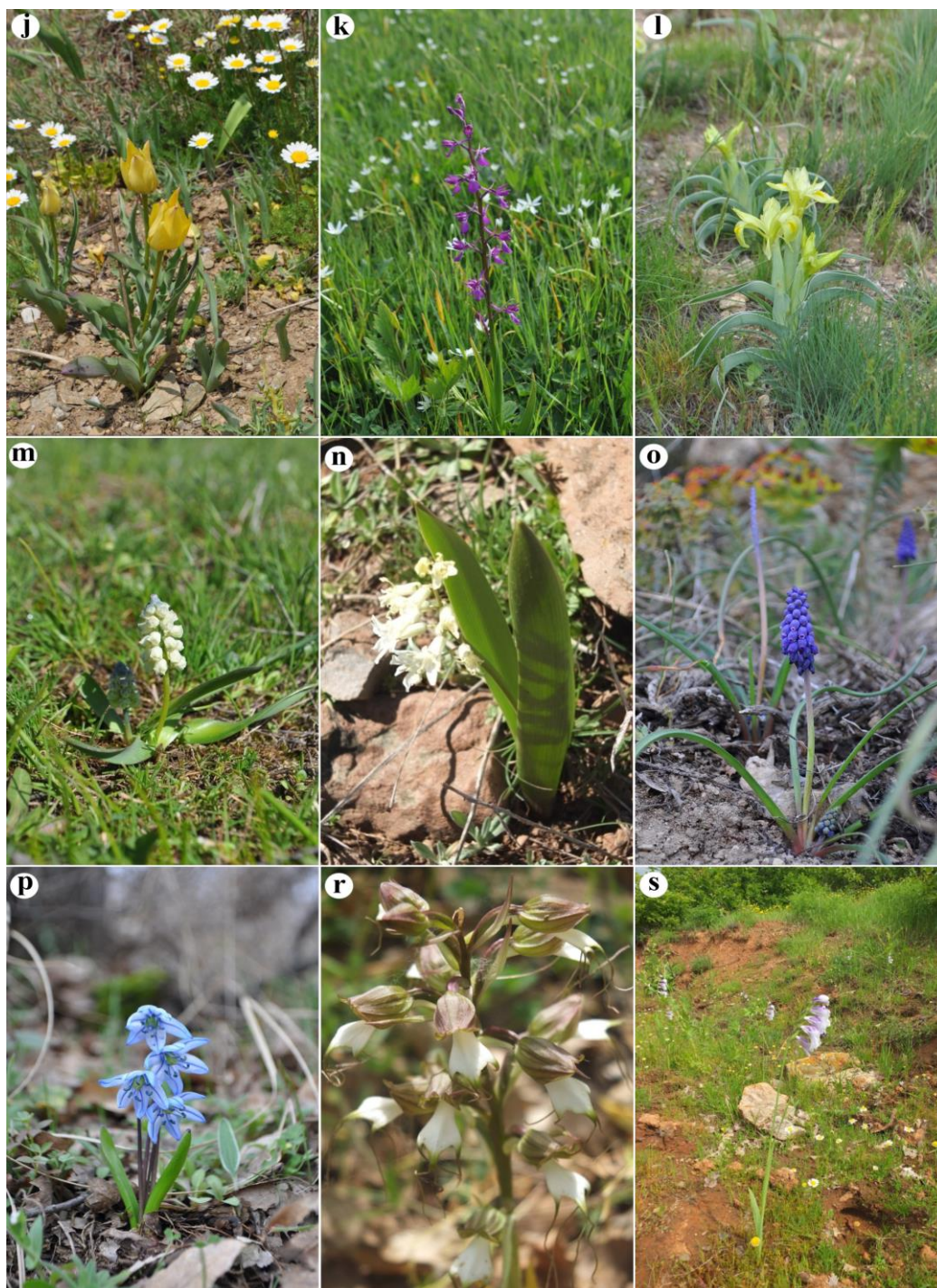


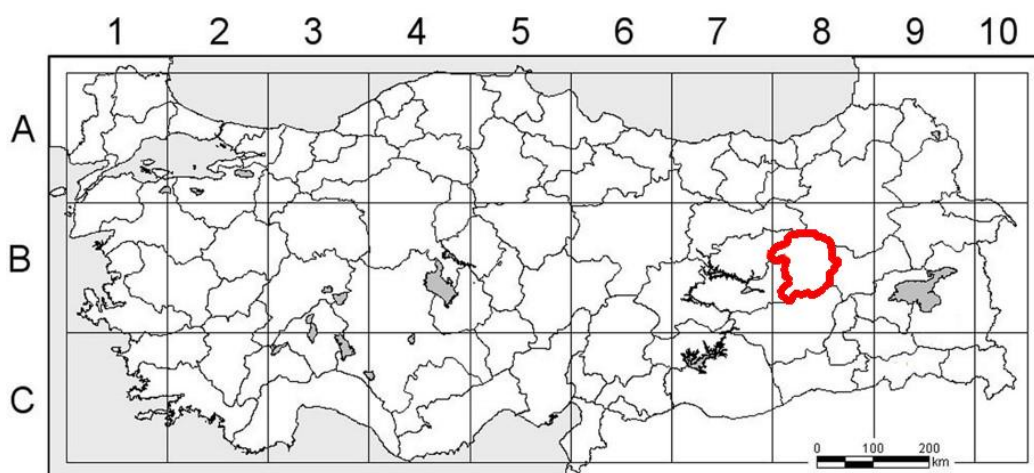
Figure 1: Some monocotyl petaloids from Bingol; **a.** *Crocus biflorus* Mill. subsp. *tauri* (Maw) B.Mathew, **b.** *Hyacinth orientalis* L. subsp. *orientalis*, **c.** *Fritillaria imperialis* L., **d.** *Colchicum szovitsii* Fisch. & C.A.Mey., **e.** *Gagea villosa* (M. Sweet subsp. *villosa*, **f.** *Ornithogalum montanum* Cirillo, **g.** *Cephalanthera kotschyana* Renz & Taubenheim (endemic), **h.** *Eremurus pseudoflavum* Vved., **i.** *Ophrys holoserica* (Burnm.f.) Greuter subsp. *heterochila* Renz & Taubenheim





Continuation of Figure 1: **j.** *Tulipa julia* K.Koch, **k.** *Orchis anatolica* Boiss., **l.** *Iris caucasica* Hoffm. subsp. *caucasica*, *Bellevallia leucantha* K.Perss. (endemic), **n.** *Puschkinia peshmenii* Rix & B.Mathew (endemic), **o.** *Muscari armeniacum* Le ex Baker, **p.** *Scilla siberica* subsp. *armena* (Grossh.) Mordak, **r.** *Himantoglossum affine* (Boiss.) Schltr., **s.** *Gladiolus kotschevii* Boiss.

Monocotyl petaloid plants are important in terms of ecotourism, especially because of having flashy tepals. Increasing such studies will be beneficial for ecotourism. The authors believe that increasing such studies will increase the interest of people in nature and enable the development of ecotourism.



**Figure 2.** Location of the Bingol Province in Turkey

## ACKNOWLEDGEMENTS

The authors would like to thanks to The Republic of Turkey Ministry of Forestry and Water Affairs, General Directorate of Bingol Nature Conservation and National Parks for their support during field works.

## REFERENCES

- [1]. P. H. Davis and I. C. Hedge, The Flora of Turkey; Past, Present and Future. *Candollea*, vol. 30, pp. 331-351, 1975.
- [2]. A., Guner, S. Aslan, T. Ekim, M. Vural and M. T. Babac, Eds., *Turkiye Bitkileri Listesi (Damarli Bitkiler)*. Istanbul, Turkey: Nezahat Gokyigit Botanik Bahcesi ve Flora Arastirmalari Dernegi Yayini, 2012.
- [3]. W. B. Zomlefer, N. H. Williams, W. M. Whitten, and W. S. Judd. Generic circumscription and relationships in the tribe Melanthieae (Liliales, Melanthiaceae), with emphasis on Zigadenus: evidence from ITS and trnL-F sequence data. *American Journal of Botany* vol. 88, pp. 1657-1669, 2001.
- [4]. S. C. Demir and I. Eker. *Petaloid Monocotyledonous Flora Of Bolu Province, Including Annotations On Critical Petaloid Geophytes Of Turkey*, Ankara, Turkey: Pegem Akademi Yayinlari, 2015.
- [5]. P.H. Davis, *Distribution patterns in Anatolia with particular reference to endemism*, in: P.H. Davis, P.C. Harper and I.C. Hedge Eds., *Plant Life of South-West Asia*, Edinburgh, UK: The Botanical Society of Edinburgh, 1971.
- [6]. P. H. Davis, Ed., *Flora of The Turkey and the East Aegean Islands*, Edinburgh, UK: Edinburgh University Press, 1965-1985, vol. 1- 9.
- [7]. P. H. Davis, R. R. Mill and K. Tan, *Flora of Turkey and the East Aegean Islands*, Edinburgh, UK: Edinburgh University Press, 1988, vol. 10.
- [8]. A. Guner, N. Ozhatay, T. Ekim, and K. H. C. Baser, *Flora of Turkey and the East Aegean Islands, (Supplement)*. Edinburgh, UK: Edinburgh University Press, 2000, vol. 11.
- [9]. T. Ekim, M. Koyuncu, M. Vural, H. Duman, Z. Aytac and N. Adiguzel, *Turkiye Bitkileri Kirmizi Kitabı (Egrelti ve Tohumlu Bitkiler)/ Red Data Book of Turkish Plants (Pteridophyta and Spermatophyta)*, Van, Turkey: Turkiye Tabiatini Koruma Dernegi ve Yuzuncu Yil Universitesi, 2000.
- [10]. IUCN (2017), *Guidelines for Using the IUCN Red List Categories and Criteria* Ver. 13, [Online]. Available <http://www.iucnredlist.org/documents/RedListGuidelines.pdf>

## Ammonia Removal From Landfill Leachate Using MAP Precipitation Method

Omer Yeni<sup>1</sup>, Ayse Kuleyin<sup>2</sup>, Yasemin Sisman<sup>3</sup>

### Abstract

Most of the major cities in our country are opposed to the problem of water pollution due to the uncontrolled leachate resulting from the decomposition of solid wastes in irregular landfills. Depending on various problems that are caused, especially eutrophication; waste waters containing high nitrogen, such as leachate, are water that should be considered first. In this study; The preliminary treatment of MAP (Magnesium ammonium phosphate) sedimentation of the leachate which formed on the landfill site storing solid wastes of Samsun Metropolitan Municipality has been examined. For this purpose, optimization of the parameters affecting the MAP settlement has been tried and the conditions for optimum recovery efficiency have been investigated. As a result of MAP precipitation, various stoichiometric ratios were tried with the aim of providing the best ammonia removal efficiency. The maximum ammonia removal was found to be 90.63% at pH 9.5 and the ammonia concentration was from 1792 mg/L 168 mg/L in the MAP precipitation experiments applied in the stoichiometric doses of the leachate. The results of the study were evaluated and the feasibility of the MAP process was examined and the application principles of the process were defined. Experimental data was also evaluated and the regression equations of ammonia removal was obtained using Minitab 16 statistical software..

**Keywords:** MAP precipitation, leachate, ammonia removal

### 1. INTRODUCTION

The leachate containing nitrogen in organic and inorganic form at high concentrations in the structures is highly variable and has a wider range of pollution loads than many industrial wastewaters [1]. Nitrogen compounds are known to cause problems such as depletion of oxygen, toxicity, algae growth and eutrophication in the environment where they are discharged. For this reason, wastewater containing high ammonia needs to be purified by suitable methods before receiving the receiving medium [2].

Nitrification and denitrification processes of nitrogen removal from wastewater are the most frequently used processes in biological treatment [3]. Physico-chemical methods such as ion exchange with biological method and stripping at high pH can be used to remove ammonia nitrogen [4].

The MAP precipitation method is used as one of the alternative methods in obtaining high yields of ammonia nitrogen removal in leachate waters [5]. MAP precipitation has emerged as an alternative treatment method with the advantages that nitrogen and phosphorus can be removed together, the resulting sediments do not contain toxic substances and they have the potential to be used as fertilizers [6].

The decrease in MAP resolution with high temperature and toxicity in high wastewater MAP precipitation makes nitrogen and phosphorus removal more advantageous than biological methods. In the MAP settlement, magnesium and phosphorus are added at the molar concentration equivalent to ammonia, depending on the composition of the wastewater.  $MgNH_4PO_4 \cdot 6H_2O$  precipitate is brought to the well and ammonia is removed. In this study using ammonia precipitation method, ammonia removal from leachate was experimentally investigated and the principles of application of the process were described.

<sup>1</sup>Environmental Engineer, Ondokuz Mayıs University, Department of Environmental Engineering, 55139, Samsun, omer\_yeni.52@hotmail.com

<sup>2</sup> Assoc. Prof. .Dr., Ondokuz Mayıs University, Department of Environmental Engineering, 55139, Samsun, akuleyin@omu.edu.tr

<sup>3</sup> Assoc. Prof. .Dr., University, Department of Geomatic Engineering, 55139, Samsun, ysisman@omu.edu.tr



## 2. MATERIAL METHOD

### 2.1. Experimental Study

Experimental study was carried out on samples of garbage leachate taken at Samsun Metropolitan Municipality Solid Waste Regular Storage Site. The MAP precipitation experiments were carried out on a Velp brand JLT6 model jar test system and for the ammonia nitrogen determination, the Kjeltac System 1002 Distilling Unit Tecator brand Kjeldahl nitrogen detection device. Experiments were carried out at room temperature and pH 9.5.

9 different mixing times have been tried between 2 minutes and 120 minutes with the aim of determining the optimum mixing time in the MAP precipitation process.  $\text{NH}_4\text{-N}$  analyses were carried out on the samples taken after 30 min resting time after stirring at 150 rpm.

In the MAP precipitation process,  $\text{MgSO}_4 \cdot 7\text{H}_2\text{O}$  was used as the magnesium source,  $\text{K}_2\text{HPO}_4$  was used as the phosphate source, and 6N NaOH was used to increase the pH.

Various stoichiometric ( $\text{Mg} : \text{NH}_4 : \text{PO}_4$ ) ratios have been tried for the purpose of achieving the best ammonia removal efficiency as a result of MAP precipitation.

For this purpose, the efficiency of ammonia removal was determined by keeping the others fixed and increasing the Mg rates 4 times. The other components were then held constant and the  $\text{PO}_4\text{-P}$  ratios were increased up to 2.2 times, after which the ratio of both Mg and  $\text{PO}_4\text{-P}$  was increased by keeping the  $\text{NH}_4\text{-H}$  ratio constant. As a result of the experiments ammonia removal efficiencies were measured.

### 2.2. The Regression Model

The regression model is a statistical procedure that allows a researcher to estimate relationship that relates two or more variables. (URL1 <http://uregina.ca/~gingrich/reg.pdf>) Regression analysis is a statistical technique used to determine mathematical relationships between depend variable  $y$  and independent variables  $x$ . (URL2 <http://personal.cb.cityu.edu.hk/msawan/teaching/FB8916/FB8916Ch1.pdf>) The relationship can be describe as different mathematical formula as linear curvilinear exponent. The linear regression analysis is the most used and the simplest methods. The formula of the linear regression analysis can be written as follows,

$$y_i = \beta_0 + \sum_{i=1}^n \beta_i x_i + \varepsilon_i$$

Where  $x_i$  is the independent variable and  $y_i$  is the dependent or response variable,  $\beta_i$  is coefficients,  $\varepsilon_i$  is noise of model. (URL3 <http://www.mit.edu/~6.s085/notes/lecture3.pdf>).

In this study, 38 experiments were realized for determine the ammonia removal respectively. The linear regression analysis was made for these experiments using Minitab 16.

## 3. RESULTS AND EVALUATION

### 3.1. Characterization of the landfill leachate

The characterization of the raw leachate used in the experimental study are given in Table 1. Ammonia, pH, COD and  $\text{PO}_4\text{-P}$  analysis were carried out for each sample taken during the study and the lowest and highest values are given in the table.

Table 1. Characterization of the landfill leachate used in this study.

Parameter	Unit	Average
pH	-	7.5-8.5
$\text{NH}_4\text{-N}$	mg/l	12000-18000
COD	mg/l	15000-40000
$\text{PO}_4\text{-P}$	mg/l	20-30

### 3.2. Determination of MAP Precipitation Conditions

When the results obtained from the characterization study are compared with the literature values, it can be said that the measured concentrations of pollutant parameters are in accordance with the range of values given in the literature.

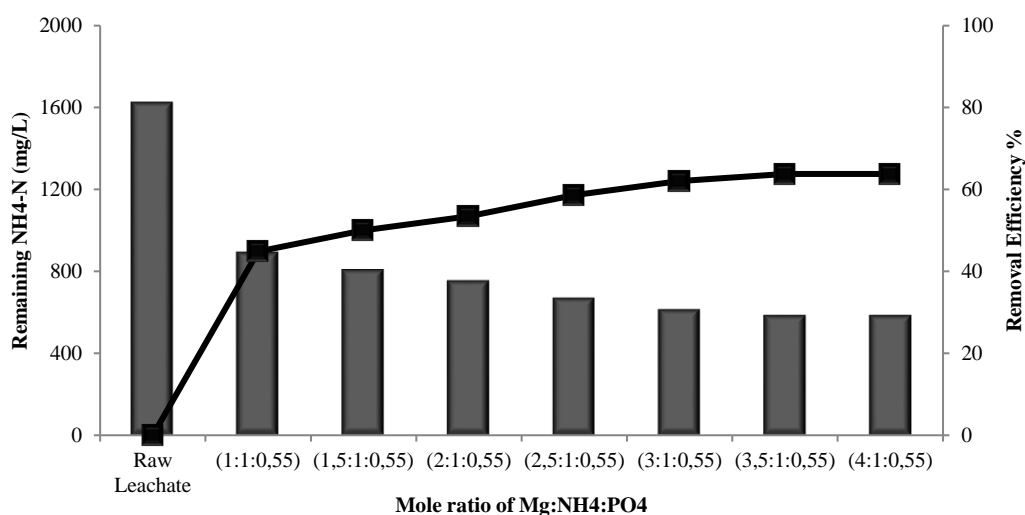
The results of the MAP precipitation experiment, in which the Mg ratios were increased and the other components were kept constant, are given in Table 2.

According to the stoichiometric ratio of MAP precipitation (1: 1: 0,55), ammonia removal was achieved at 44.83%. When the Mg ratio is increased to 4 times, the ammonia elimination efficiencies are reduced, but it is observed that the increase after the 2.5 times Mg ratio is not significant. This indicates the saturation of the leachate to the Mg source.

For ammonia with the highest Mg content (4: 1: 0.55), 63.79% remission was obtained.. The MAP precipitation experiment results, in which the Mg contents are increased and the other components are kept constant, are presented in Figure 1.

**Table 2.** The results of the MAP precipitation experiment in which Mg ratios were increased

(Mg:NH <sub>4</sub> -N:PO <sub>4</sub> )	NH <sub>4</sub> -N	
	Concentration (mg/L)	Removal Efficiency%
Raw Leachate	1624	-
(1:1:0,55)	896	44.83
(1,5:1:0,55)	812	50.00
(2:1:0,55)	756	53.45
(2,5:1:0,55)	672	58.62
(3:1:0,55)	616	62.07
(3,5:1:0,55)	588	63.79
(4:1:0,55)	588	63.79



**Fig. 1.** Ammonia removal efficiencies for the MAP precipitation experiment in which the Mg ratios were increased

The results of the MAP precipitation experiment, in which PO<sub>4</sub>-P ratios were increased and other components were kept constant, are given in Table 3.

According to the stoichiometric ratio of the MAP settlement result (1: 1: 0,55), the ammonia removal rate was 37.5%.

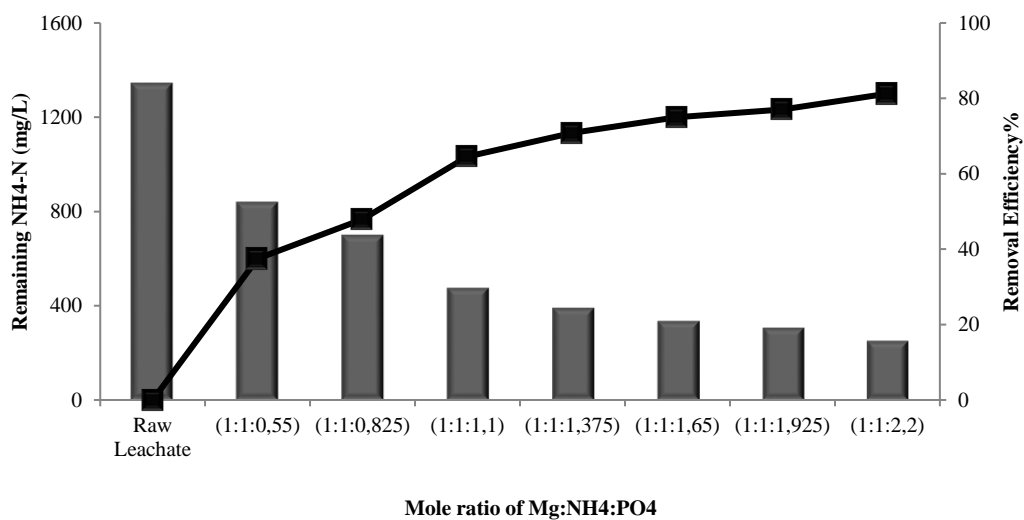
When we increase PO<sub>4</sub>-P ratio up to 2.2 times, a continuous increase in ammonia removal efficiency is observed. This shows that PO<sub>4</sub>-P in the leachate is low and that the leachate is not saturated. Using higher PO<sub>4</sub>-P has not been tried in the effluent even higher than the PO<sub>4</sub>-P concentration.

The best ammonia removal efficiency (1: 1: 2,2) reported in the table was achieved. Ammonia was recovered for 81.25% .

Figure 2 show the results of MAP precipitation trials in which PO<sub>4</sub>-P ratios are increased and other components are kept constant.

**Table 3.** The results of the MAP precipitation experiment in which PO<sub>4</sub>-P ratios were increased

NH <sub>4</sub> -N		
(Mg:NH <sub>4</sub> -N:PO <sub>4</sub> )	Concentration (mg/l)	Removal Efficiency%
Raw Leachate	1344	-
(1:1:0,55)	840	37.50
(1:1:0,825)	700	47.92
(1:1:1,1)	476	64.58
(1:1:1,375)	392	70.83
(1:1:1,65)	336	75.00
(1:1:1,925)	308	77.08
(1:1:2,2)	252	81.25



**Fig.2** Ammonia removal efficiencies for the MAP precipitation experiment in which the PO<sub>4</sub>-P ratios were increased

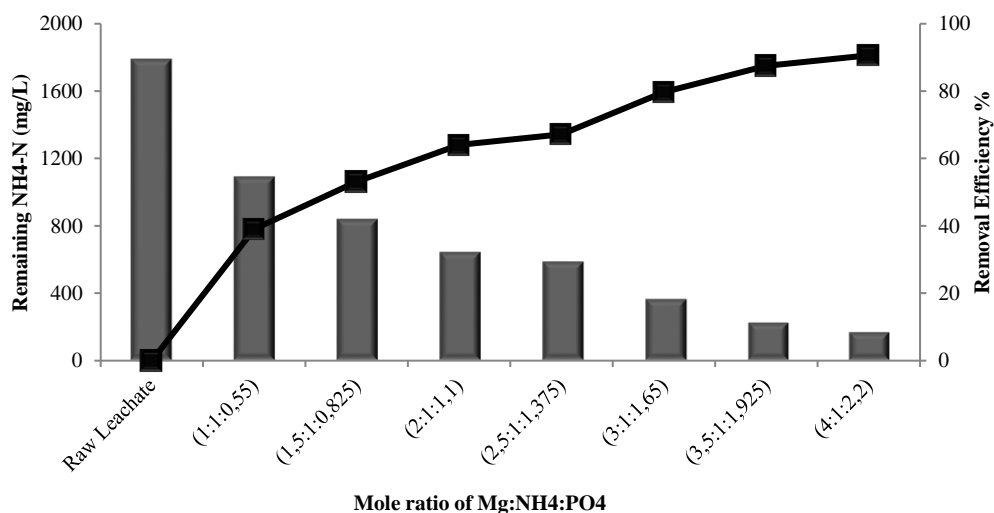
The results of the MAP precipitation experiment, in which both Mg and PO<sub>4</sub>-P ratios are increased and other components are kept constant, are given in Table 4.

According to the stoichiometric ratio of starting MAP settlement (1: 1: 0,55), 39.06% for ammonia were provided. When we increase both Mg and PO<sub>4</sub>-P ratios, a steady increase in recovery efficiency is observed. In this condition, the highest ammonia removal rates (4: 1: 2,2) were achieved, with 90.63% for ammonia in the ratio of (4: 1: 2,2).

Figure 3 show the results of MAP precipitation experiments in which both Mg and PO<sub>4</sub>-P ratios are increased and ammonia concentration is kept constant.

**Table 4.** The results of the MAP precipitation experiment in which both Mg and PO<sub>4</sub>-P ratios were increased

NH <sub>4</sub> -N		
(Mg:NH <sub>4</sub> :PO <sub>4</sub> )	Concentration (mg/l)	Removal Efficiency %
Raw Leachate	1792	-
(1:1:0,55)	1092	39.06
(1,5:1:0,825)	840	53.13
(2:1:1,1)	644	64.06
(2,5:1:1,375)	588	67.19
(3:1:1,65)	364	79.69
(3,5:1:1,925)	224	87.50
(4:1:2,2)	168	90.63



**Fig.3.** Ammonia removal efficiencies for the experiment of MAP precipitation, in which both Mg and PO<sub>4</sub>-P ratios were increased

### 3.3. The regression Analysis

Firstly the Analysis of Variance (ANOVA) results were obtained for ammonia removal from experiments (Table 5)

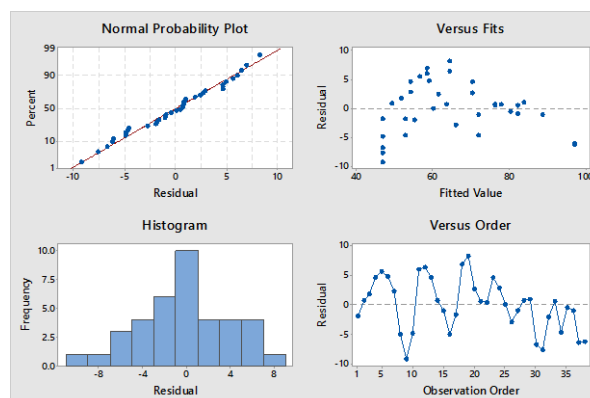
*Table 5. The results of ANOVA for ammonia removal*

Source	Adj SS	Adj MS	F-Value	P-Value
Regression	7744.87	3872.43	189.03	0.000
Mg	917.85	917.85	44.80	0.000
PO4	6165.23	6165.23	300.95	0.000
Model Summary	S	R-sq	R-sq(adj)	R-sq(pred)
	4.52614	91.53%	91.04%	89.90%

Then, the linear regression equations of ammonia removal were calculated from these results.

$$\text{Ammonia Removal} = 29.97 + 4.889 \cdot \text{Mg} + 21.53 \cdot \text{PO4}$$

Finally, the Residual Plots for Ammonia Removal were obtained (Fig.4).



*Fig 4. The Residual Plots for Ammonia Removal*

## 4. DISCUSSION

MAP sedimentation as a pre-treatment process is a method used to achieve high ammonia removal in raw leachate collected on landfill. The best removal (1: 1: 0.55) for removal of high ammonia concentration resulted in a stoichiometric ratio of 37-44%. The best ammonia removal efficiency (4: 1: 2,2) ratio was achieved by 90.63% for stoichiometric chemical use.

When applying the MAP sedimentation method, attention should be paid to the TDS and PO<sub>4</sub>-P parameters that can occur in the high amount of effluent water due to the chemicals used.

According to the statistical analysis results, the different levels of Mg and PO<sub>4</sub> have significant effects on the ammonia removal. The data is very close are to the fitted regression line in ammonia removal (91.53%).

### ACKNOWLEDGMENT

This paper is supported by OMU BAP project numbered PYO.MUH.1904.18.003

### REFERENCES

- [1]. Kabdasli, I., Tunay, O., Cetin, M.S. ve Olmez, T.(2001), Assessment of Magnesium Ammonium Phosphate Precipitation for the Treatment of Leather Tanning Industry Wastewaters, *World Water Congress Efficient Water Management-Making It Happen*, 15-19 Ekim, Berlin, Germany
- [2]. Tunay, O., Kabdasli, I., Orhon, D. ve Kolcak, S.(1997). Ammonia Removal by Magnesium Ammonium Phosphate Precipitation in Industrial Wastewaters, *Wat. Sci. Tech.*, **36**(2-3), 225-228.
- [3]. EPA U. (1993) Process design manual of nitrogen control, vol 625/r-93/010. 625/r-93/010, Cincinnati, Ohio
- [4]. Zengin, G., Olmez, T., Dogruel, S., Kabdasli, I. ve Tunay, O. (2002). Assessment of Source-Based Nitrogen Removal Alternatives in Leather Tanning Industry Wastewater, *Wat.Sci. Tech.*, **45**(12), 205-215.
- [5]. Zdybiewska, M.W. ve Kula, B. (1991). Removal of Ammonia Nitrogen by the Precipitation Method, on the Example of Some Selected Wastewaters, *Wat. Sci. Tech.*, **24**(7), 229-234.
- [6]. Ozturk M (2006). Magnezyum Amonyum Fosfat (Map) Cokturmesi Ile Atiksulardan Azot Ve Fosfor Giderimi. Cumhuriyet Universitesi Fen Bilimleri Enstitusu, Yuksek Lisans Tezi, 73s, Sivas.
- [7]. URL1 <http://uregina.ca/~gingrich/regr.pdf>, accessed in 08.13.2018.
- [8]. URL2 <http://personal.cb.cityu.edu.hk/msawan/teaching/FB8916/FB8916Ch1.pdf> accessed in 08.13.2018.
- [9]. URL3 <http://www.mit.edu/~6.s085/notes/lecture3.pdf>, accessed in 08.13.2018.

## Geological, Mineralogical and Geochemical Features of the Kiziltepe (Aladag) Skarn Deposit (Ezine/Canakkale-North West Turkey)

*Fetullah Arik<sup>1</sup>, Umit Aydin<sup>2</sup>*

### Abstract

*Kiziltepe Skarn Mineralization located 35 km south of the Canakkale and 8 km southwest of Ezine County near the Kestanbol Pluton. Cambrian to Holocene aged magmatic, metamorphic and sedimentary rocks crop out in the study area. The basement of the study area is formed by Pre(?) -Lower Cambrian metasandstone, metaconglomerate, phyllite and chalc schist of low-grade metamorphic Geyikli formation. Recrystallized limestones of the Middle-Late Permian Bozalan Formation cover the Geyikli Formation. Cretaceous Denizgoren Ophiolites thrust over the older units. Upper Oligocene-Lower Miocene Hallaclar Volcanics composed of altered andesite and rhyolite. Kestanbol Pluton represented by quartz-monzonite and monzonite besides monzodiorite syenite and quartz-syenite porphyry are cut the older units. Lower- Middle Miocene Ezine Volcanics composed of pyroxene-andesite and trachyte.*

*Kiziltepe skarn deposit was developed close to Kestanbol Pluton contacts with the carbonaceous rocks of the Bozalan Formation and Denizgoren Ophiolites. Therefore Ca-silicates and some metallic enrichment such as iron, copper, zinc and lead were developed in this altered zone. Mainly garnet (grossular), tremolite/actinolite, epidote and zoisite/clinozoisite paragenesis was observed while minor amount of talc, wollastonite, augite, diopside were determined in the skarn zone. Main ore minerals are magnetite, hematite, chalcopryrite, sphalerite, galenite, cerussite, covellite, digenite, malachite and pyrite.*

*Chemical data obtained from samples reveal that Cu-Pb-Zn > 1% ppm and Au, Ag, Cd, Mo, and Fe<sub>2</sub>O<sub>3</sub> contents reach up to 67.30 ppb, 72.20 ppm, 710 ppm, 936 ppm and 87.95%. Many ancient mining exploitation cavities were coincided located near the Kiziltepe area. 1110 ppb and 724.90 ppb Au values were detected from two samples taken from skarn mineralization.*

**Keywords:** Skarn-type mineralization, geology, geochemistry, ore deposits, Aladag, Kiziltepe, Ezine

### 1. INTRODUCTION

Kiziltepe located 35 km south of the Canakkale city center and 8 km southwest of Ezine County (Canakkale-Turkey) and western edge of the Biga Peninsula (NW Turkey). Ezine county and Aladag, Kemalli, Uskufcu, Kocali and Gokcebayir Villages were known settlements in the study area (Fig. 1).

In this study, it is aimed that geochemical features of contact metamorphic and metasomatic zone mineralization among the granitoidic rocks of Kestanbol Pluton and carbonate rocks of Bozalan Formation together with the altered serpentinites of the Denizgoren Ophiolites. In addition, primary geochemical characteristics of different rock types of Kestanbol Pluton, Denizgoren Ophiolites, Hallaclar Volcanites and dykes.

<sup>1</sup> Konya Technical University, Faculty of Engineering and Natural Sciences, Geological Engineering Department, Selcuklu-Konya / TURKEY, [farik@selcuk.edu.tr](mailto:farik@selcuk.edu.tr)

<sup>2</sup> General Directorate of Mineral Research & Exploration, Ankara / TURKEY, [umitaydin77@gmail.com](mailto:umitaydin77@gmail.com)





Figure 1. Location map of the study area

## 2. MATERIAL AND METHODS

Field and laboratory studies were carried out to understand the geological, mineralogical, petrographical and geochemical characteristics of the exposed units in the study area. During the field studies formation boundaries were updated and hand specimens collected from different rock units and skarn zone. 27 of these samples were chemically analyzed in the General Directorate of Mineral Research & Exploration of Turkey (MTA). In order to investigation of mineralogical and petrographical features 37 thin section samples investigated under polarizan microscope at the MTA, Geological Engineering Departments of Ankara University and Selcuk University. The rest 27 sample collected from skarn zone were polished and investigated under ore microscopy at the Ore Deposit-Geochemistry Division of the Geological Engineering Department of the Ankara University and MTA Laboratories.

In order to determine the geochemical characteristics of the rock units 62 samples were chemically analyzed of their major ( $\text{SiO}_2$ ,  $\text{Al}_2\text{O}_3$ ,  $\text{Fe}_2\text{O}_3$ ,  $\text{MgO}$ ,  $\text{CaO}$ ,  $\text{Na}_2\text{O}$ ,  $\text{K}_2\text{O}$ ,  $\text{TiO}_2$ ,  $\text{P}_2\text{O}_5$ ,  $\text{MnO}$ ,  $\text{Cr}_2\text{O}_3$ ), some minor and trace (Cu, Pb, Zn, Ni, Ga, Nb, Th, V, Zr, Y, Sc) element compositions at the ACME Analytical Laboratories Ltd., Vancouver (Canada). Samples were jaw crushed to 70% passing 10 mesh (2 mm), a 250 g aliquot was riffle split and pulverized to 95% passing 150 mesh (100  $\mu\text{m}$ ) in a mild-steel ring-and-puck mill. Samples after thawing process calibration standards, verification standards and reagent blanks were included in the sample sequence. Sample solutions were aspirated into an ICP emission spectrograph (ICP-ES) (Spectro Ciros Vision) for the determination of the major oxides. The detection limit for the major oxides is 0.01 wt %, excepting for  $\text{SiO}_2$ ,  $\text{Al}_2\text{O}_3$ ,  $\text{Fe}_2\text{O}_3$ ,  $\text{Cr}_2\text{O}_3$  and LOI, of which detection limits are 0.04, 0.03, 0.04, 0.001 and 0.1 wt. %, respectively. Sample solutions were aspirated into an ICP-MS (Perkin-Elmer Elan 6000 or 9000) for the determination the trace including REEs. The limits of detection are 0.05 ppm, excepting Pr, Nd, Sm, Tb and Lu, of which detection limits are 0.02, 0.4, 0.1, 0.01 and 0.01 ppm, respectively. Some sulphide samples exceeded the upper limits of this method and these samples were re-analyzed. In the re-analyzing process 1.0 g sample digested in 100 ml aqua regia ( $\text{HCl-HNO}_3\text{-H}_2\text{O}$ ) and sample solutions analyzed into ICP-AES.

All geochemical data were evaluated with basic and multivariate statistical methods using student t test, correlation coefficient, simple regression and scatter diagrams, cluster analyses and factor analyses.

## 3. RESULT AND DISCUSSION

### 3.1. Geological Settings

Cambrian to Holocene aged 8 different magmatic, metamorphic and sedimentary geological units cropped out in the study area. Pre-Lower Cambrian aged Geyikli Formation forms the basement of the study area and represented by the alternation of low-grade metamorphic featured rocks such as calcschists, metasandstones and phyllites (e.g. [1]-[6]). Middle-Late Permian Bozalan Formation consists of low metamorphic detritic rocks such as gravelly sandstone, quartzite and phyllites from bottom and carbonaceous rocks and marbles to the top recrystallized limestones and extends over the Geyikli Formation by unconformity (e.g. [2]-[4], [7]-[8]). Cretaceous aged Denizgoren Ophiolites usually consists of serpentinized peridotites and emplaced on the other

units by tectonic boundary (e.g. [4], [8]-[10]). Upper Oligocene-Lower Miocene Hallaçlar Volcanics consists of yellow, pink and beige-colored andesite, basalt, spherulitic rhyolite, and pyroclastic rocks with same composition (e.g. [8], [11], [12]). In addition, Upper Oligocene-Lower Miocene aged Kestanbol pluton cuts the older units and mainly represented by intense fractured dirty yellow and pink quartz-monzonites together with basic enclaves such as monzonite, monzodiorite porphyry, monzonite porphyry, syenite porphyry and quartz syenite porphyry (e.g. [11]-[16]). Lower-Middle Miocene aged Ezine Volcanics consist of gray, dark gray, black and greenish-black color, coarse crystalline K-feldspar andesite, trachyandesite, dacite, rhyodacite and andesitic, rhyolitic pyroclastics (e.g. [5]-[6], [8], [12]). Plio-Quaternary aged Bayramic Formation represented by conglomerate, sandstone and mudstone (e.g. [6], [17]). All of the older units overlain unconformably by alluvium consist of slightly consolidated and unconsolidated terrestrial clastics (Figure 2).

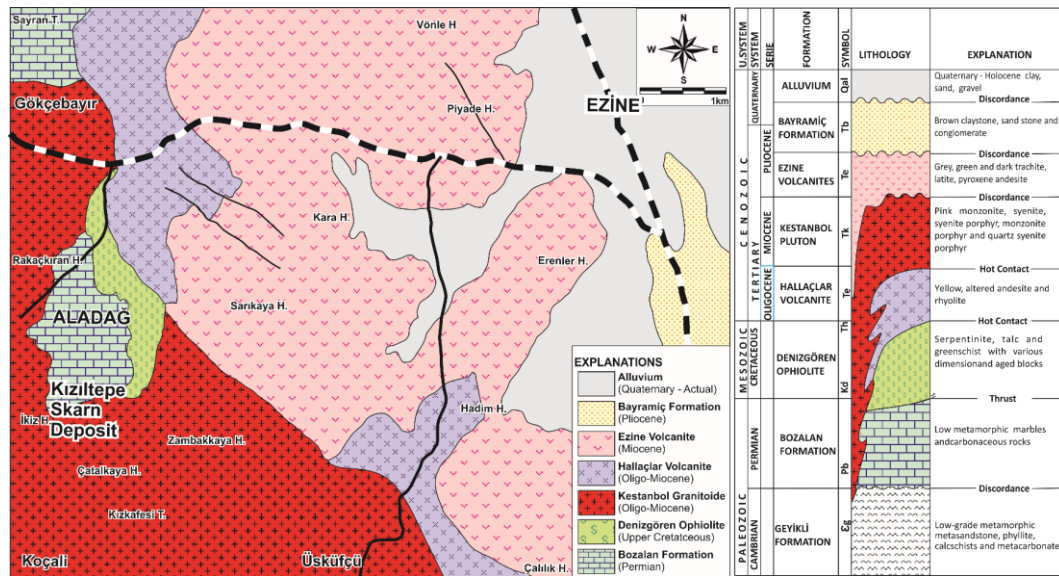


Figure 2. Geological map and tectono-stratigraphical section of the study area (After [6])

### 3.2. Kiziltepe Skarn Mineralization

A contact metamorphic and Cu, Pb, Zn and Fe skarn zone formed developed by the intrusion of the magmatic rocks belonging to Kestanbol Pluton in carbonate rocks of Bozalan Formation and some talc and asbestos formation developed in the altered peridotites of the Denizgören Ophiolites at the Aladag (Figure 3).

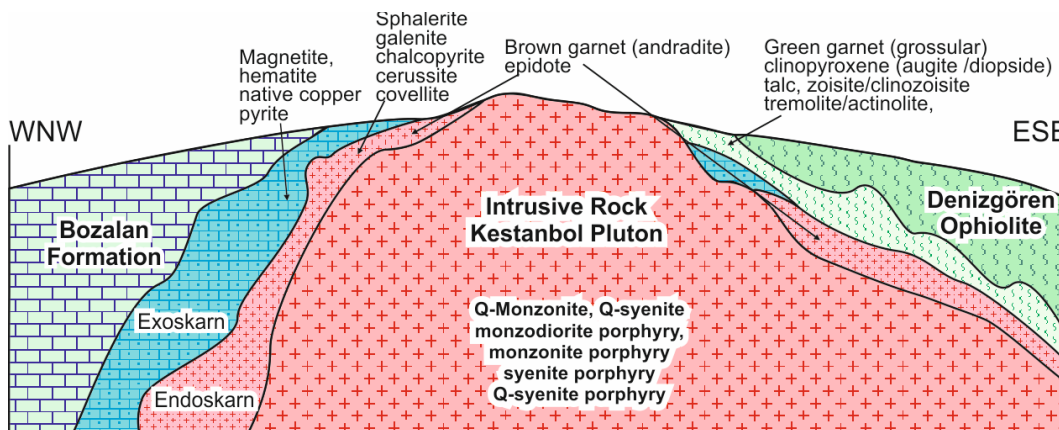


Figure 3. Schematic Cross Section model of Kiziltepe (Aladag) Skarn Zone (Modified from [18]).

Intrusive rock represented by mainly monzonite, Q-monzonite and syenites of the Kestanbol Pluton (e.g. [5]-[6], [9], [18]). Monzonites composed of mainly plagioclase, alkali feldspar, quartz, biotite, hornblende and



minor amount sphene while syenites composed of mainly alkali feldspar, plagioclase, quartz, biotite, hornblende and minor amount sphene. There are some coarse-grained K-feldspar, biotite, quartz, pyroxenes (diopside, augite) in the endoskarn zone. Ore mineral paragenesis are consist of magnetite, hematite, galena, sphalerite, chalcopyrite, cerussite, covellite, malachite, azurite, pyrite, limonite (goethite and lepidocrocite) in skarn zone (Figure 4 c, d, e, f, g).

Magnetite and hematites observed near the pluton contact (Figure 4 d). Hematites were formed by the alteration of magnetites. There are epidote, grossular, tremolite/actinolite, augite, diopside and talc formations near the wall rocks (Figure 4 b and h). Galena, cerussite, sphalerite, chalcopyrite pyrite and covellite were observed in the outer zone of skarn mineralization (Figure 4 c, f, g). Chalcopyrite, pyrite and covellite near the magnetite mineralization. Galena and sphalerite mineralization are near the carbonate rocks. Some galena and sphalerite veins are in the marbles and recrystallized limestones. There are minor amount pyrite and chalcopyrite in the rocks. Some of the pyrites were oxidized from the edges. In addition, cavity filling and / or veins in the form of limonite (lepidocrocites and goethite) are observed in some place. Goethite and lepidocrocites were observed side by side and enlarged intertwined.

Talc and asbestos formation contact between the pluton and ophiolites (Figure 5 b, h). There are malachite, azurite and native copper formations around the Kiziltepe Skarn Zone in and near environs. Some Ca-silicate mineral formed in the contact zone such as tremolite, actinolite, augite, epidote etc. (Figure 4 b, c, h).



Figure 4. Some views of the contact metamorphic zone a) Skarn zone between the Kestanol Pluton and Bozalan Formation, b) Talc and tremolite formations in the contact metamorphic zone between the Kestanol Pluton and Denizgoren ophiolites, c) Copper enrichments in the skarn zone, d) Magnetite vein in the Bozalan Formation, e) Magnetite (mag) and hematite (hem) (+N, X10), f) Magnetite (mag) and sphalerite (sph), (+N, X10), g) Galena (gn) (+N, X63), h) Epidote and tremolite (N, X3.2), e, f and g polished sections, h thin section

### 3.3. Geochemical Characteristics of Kestanbol Pluton and Skarn Zone

The major oxides and some trace element analyzes of the samples taken from the Kestanbol Pluton (Table 1) and endoskarn and exoskarn zones (Table 3 and Table 5) were made.

#### Kestanbol Pluton:

The granitoidic rocks of the Kestanbol pluton contain 63.3% SiO<sub>2</sub>, 16% Al<sub>2</sub>O<sub>3</sub>, 4% Fe<sub>2</sub>O<sub>3</sub>, 1.8% MgO and 3.2% CaO on average (Table 1). In the genetic and petrological investigations carried out in these rocks, it has been determined that the rocks belonging to Kestanbol pluton fall down to the area of volcanic arc granitoids with subalkaline and calcalkaline properties.

Table 1. Major oxides (%) and some trace element (ppm, Au: ppb) analysis and statistical summaries of the granitoidic rocks (S.D.: Standard deviation, S.E.: Standard error, t<sub>h</sub>: Calculated t value; L.L.: The lower limit, U.L.: Upper limit, Sample number: 7, tt: Table t value: 1.94).

NO	SiO <sub>2</sub>	Al <sub>2</sub> O <sub>3</sub>	Fe <sub>2</sub> O <sub>3</sub>	MgO	CaO	Na <sub>2</sub> O	K <sub>2</sub> O	TiO <sub>2</sub>	MnO	Cr <sub>2</sub> O <sub>3</sub>	Ba	Co	Sr	W	Mo	Cu	Pb	Zn	Ni	As	Ag	Au	Sum	
S 33	62.0	16.2	4.62	3.44	3.8	4.9	0.6	0.1	30.0	1231.0	27.5	852.0	128.8	0.6	48.7	19.2	28.0	13.2	1.4	0.1	2.0	99.5	7	
S 34	61.0	15.7	4.42	6.3	2.5	5.4	0.6	0.1	40.0	1334.0	21.4	795.8	66.4	0.3	38.4	39.5	63.0	21.9	1.4	0.1	10.5	99.5	8	
S 55	64.7	15.2	3.81	9.2	3.5	5.2	0.5	0.1	40.0	1160.0	28.6	664.8	173.4	4.9	80.1	30.2	28.0	15.0	3.2	0.1	1.2	99.6	1	
S 56	67.3	15.1	2.41	0.1	8.2	4.7	0.3	0.1	20.0	1171.0	13.7	413.4	58.3	0.2	15.1	30.0	29.0	13.2	0.5	0.1	0.5	99.7	2	
S 57	61.7	15.7	4.82	3.3	3.7	5.0	0.6	0.1	20.0	1354.0	26.4	815.1	114.1	0.5	20.8	18.6	25.0	14.5	1.8	0.1	0.5	99.7	3	
S 58	65.3	15.5	3.71	1.7	3.2	3.6	4.9	0.5	0.1	30.0	1159.0	22.8	679.7	132.5	1.2	6.4	12.9	15.0	15.1	1.3	0.1	0.5	99.6	4
S 65	61.5	16.8	5.01	0.2	6.3	5.6	0.6	0.1	20.0	1474.0	35.1	972.0	72.7	1.7	86.1	7.0	46.0	14.5	7.5	0.1	0.5	99.5	5	
Mean	63.3	15.7	4.11	1.8	3.2	3.3	5.1	0.5	0.1	28.6	1269.0	25.1	741.8	106.6	1.3	42.2	22.5	33.4	15.3	2.4	0.1	10.8	7	
S.D.	2.4	0.6	0.90	6.0	0.9	0.5	0.3	0.1	0.0	9.0	121.5	6.7	178.4	42.4	1.7	31.3	11.3	15.9	3.0	2.4	0.0	0.6	7	
S.E.	0.9	0.2	0.30	2.0	0.3	0.2	0.1	0.0	0.0	3.4	45.9	2.5	67.4	16.0	0.6	11.8	4.3	6.0	1.1	0.9	0.0	0.2	7	
t <sub>h</sub>	70.1	69.8	12.3	7.7	9.5	18.2	42.5	10.8	10.2	8.4	27.6	9.9	11.0	6.7	2.1	3.6	5.3	5.6	13.5	2.7	0.3	0.7	7	
L.L.	61.1	15.2	3.31	1.2	2.4	2.9	4.8	0.4	0.1	20.3	1156.7	18.9	576.8	67.4	1.3	12.1	18.7	12.5	0.2	0.1	0.3	99.5	6	
U.L.	65.5	16.3	4.92	2.4	4.1	3.8	5.4	0.6	0.1	36.9	1381.3	31.3	906.9	145.8	2.9	71.2	32.9	48.2	18.1	4.6	0.1	1.4	7	

#### Endoskarn Zone

The average Cu, Pb and Zn contents of the samples collected from endoskarn zone were 2.7%, 2.5% and 2.7%, respectively. Cu reaching 14.6%, Pb reaching 17.2% and Zn reaching 16.5% are important. Cr is high in some specimens, whereas Mo and W increase in the outer sections of the endoskarn zone (Table 2).

Table 2. Major oxides (%) and some trace element (ppm, Au: ppb) analysis and statistical summaries of the granitoidic rocks (M: Mean, S.S.: Standard deviation, S.E.: Standard error, t<sub>c</sub>: Calculated t value; L.L.: The lower limit, U.L.: Upper limit, Sample number: 16, tt: Table t value: 1.75).

NO	SiO <sub>2</sub>	Al <sub>2</sub> O <sub>3</sub>	Fe <sub>2</sub> O <sub>3</sub>	MgO	CaO	Na <sub>2</sub> O	K <sub>2</sub> O	TiO <sub>2</sub>	MnO	Cr <sub>2</sub> O <sub>3</sub>	Ba	Co	Sr	W	Mo	Cu	Pb	Zn	Ni	As	Ag	Au
S 11	16.2	1.1	6.2	1.1	7.8	0.01	0.02	0.04	0.32	190	2	117	43	49	936	146060	172700	82600	128	56	70	62
S 13	30.1	1.3	36.8	0.1	25.3	0.01	0.01	0.01	0.81	20	3	123	4	141	38	14350	4200	6000	84	68	67	11
S 14	84.1	0.6	0.7	0.6	0.1	0.01	0.01	0.02	0.13	50	2	68	5	269	301	1250	36900	53400	57	2	15	7
S 15	35.1	18.1	14.8	1.3	17.5	0.01	0.09	1.26	0.69	4170	9	28	1897	37	372	12680	9000	18800	384	10	0	1
S 16	44.8	0.9	5.4	0.6	3.0	0.01	0.01	0.02	0.95	40	2	146	54	92	498	6490	78900	165100	67	20	18	15
S 18	33.4	14.3	21.2	0.6	16.5	0.01	0.05	0.89	0.66	3440	8	167	941	43	300	22690	11300	10600	308	43	4	8
S 19	34.1	0.5	27.6	0.1	18.5	0.01	0.01	0.01	0.55	40	1	42	6	178	58	83760	15700	11000	49	229	72	67
S 20	22.7	1.4	29.9	0.2	19.1	0.01	0.01	0.03	0.99	100	5	25	35	221	264	28710	26900	27800	137	28	38	21
S 21	75.3	0.3	0.7	0.2	4.1	0.01	0.01	0.01	0.46	30	3	66	20	210	260	1780	49100	59100	32	8	25	9
S 27	65.2	15.1	2.4	3.5	3.1	1.69	5.20	0.40	0.02	30	1331	14	528	75	3	1169	57	60	14	4	0	6
S 28	52.6	10.1	18.1	3.3	0.4	3.88	0.54	0.30	0.05	20	51	45	67	102	3	40350	200	200	20	3	12	42
S 30	56.0	8.3	5.5	5.9	2.4	1.43	4.12	0.22	0.07	20	1079	21	189	46	3	71710	100	100	14	8	14	34
S 31	58.0	13.0	8.9	3.0	3.1	6.08	3.19	0.43	0.10	130	822	25	286	28	1	9568	95	83	28	2	1	15
S 32	65.0	15.6	3.7	1.8	3.6	3.72	4.86	0.54	0.07	30	938	32	775	193	1	120	23	24	13	1	0	2
S 61	66.1	17.5	4.9	0.8	0.1	0.24	5.19	0.57	0.01	20	1191	14	96	88	9	568	592	109	13	42	3	15
S 62	61.5	16.9	8.7	0.8	0.1	0.14	5.09	0.51	0.01	20	738	18	119	74	23	626	908	204	16	35	1	15
M.	50.0	8.4	12.2	1.5	7.8	1.08	1.78	0.33	0.37	522	387	59	317	115	192	27618	25417	27199	85	35	21	21
S.D.	19.7	7.3	11.3	1.6	8.5	1.87	2.32	0.37	0.36	1289	521	51	511	76	258	40630	45228	44710	110	56	26	20
S.E.	4.9	1.8	2.8	0.4	2.1	0.47	0.58	0.09	0.09	322	130	13	128	19	64	10158	11307	11177	28	14	7	5
t <sub>c</sub>	10.2	4.6	4.3	3.7	3.7	2.31	3.07	3.59	4.10	1.62	2.97	4.69	2.48	6.04	2.98	2.72	2.25	2.43	3.10	2.49	3.24	4.09

In the correlation analyzes conducted to determine the direction and strength of the relationships between the components Fe<sub>2</sub>O<sub>3</sub>; has strong positive correlation with CaO and Mn and strong negative correlation with SiO<sub>2</sub>. Cu shows strong positive correlation with Au, Pb and Ag besides strong negative correlation with SiO<sub>2</sub>. Pb and Zn show strong positive correlation with each other and Mo. According the correlation and cluster analysis trace elements such as Cu, Mo, Pb, Zn, Au, Ag, As and W Show similar behaviors in the geochemical environments different from major components (Table 3).

Table 3. Correlation coefficients between the components of the endoskarn samples

	SiO <sub>2</sub>	Al <sub>2</sub> O <sub>3</sub>	Fe <sub>2</sub> O <sub>3</sub>	MgO	CaO	Na <sub>2</sub> O	K <sub>2</sub> O	TiO <sub>2</sub>	MnO	Cr <sub>2</sub> O <sub>3</sub>	Ba	Co	Sr	W	Mo	Cu	Pb	Zn	Ni	As	Ag	Au
SiO <sub>2</sub>	1.00	0.24	-0.70	0.24	-0.75	0.28	0.50	0.00	-0.66	-0.33	0.49	-0.41	-0.13	0.28	-0.48	-0.60	-0.38	-0.14	-0.55	-0.43	-0.61	-0.47
Al <sub>2</sub> O <sub>3</sub>		1.00	-0.23	0.35	-0.26	0.37	0.69	0.87	-0.49	0.41	0.63	-0.42	0.62	-0.55	-0.42	-0.39	-0.55	-0.58	0.17	-0.34	-0.76	-0.43
Fe <sub>2</sub> O <sub>3</sub>			1.00	-0.33	0.86	-0.18	-0.47	-0.07	0.61	0.19	-0.47	0.22	-0.02	0.08	-0.13	0.16	-0.21	-0.26	0.34	0.53	0.54	0.24
MgO				1.00	-0.44	0.59	0.50	0.13	-0.57	-0.13	0.60	-0.41	0.09	-0.46	-0.35	0.15	-0.28	-0.35	-0.29	-0.39	-0.39	0.09
CaO					1.00	-0.38	-0.55	0.05	0.76	0.43	-0.53	0.33	0.25	0.08	0.14	0.19	-0.02	-0.11	0.60	0.51	0.58	0.10
Na <sub>2</sub> O						1.00	0.39	0.13	-0.51	-0.22	0.42	-0.36	0.05	-0.22	-0.45	-0.14	-0.34	-0.37	-0.36	-0.34	-0.40	-0.05
K <sub>2</sub> O							1.00	0.28	-0.73	-0.30	0.97	-0.62	0.03	-0.29	-0.58	-0.30	-0.45	-0.49	-0.50	-0.27	-0.56	-0.26
TiO <sub>2</sub>								1.00	-0.14	0.80	0.24	-0.17	0.89	-0.54	-0.13	-0.30	-0.40	-0.41	0.62	-0.26	-0.64	-0.44
MnO									1.00	0.34	-0.71	0.55	0.11	0.16	0.42	0.04	0.25	0.48	0.56	0.27	0.45	-0.02
Cr <sub>2</sub> O <sub>3</sub>										1.00	-0.29	0.25	0.87	-0.39	0.25	-0.08	-0.11	-0.09	0.94	-0.07	-0.27	-0.30
Ba											1.00	-0.61	0.04	-0.32	-0.57	-0.25	-0.44	-0.48	-0.49	-0.28	-0.53	-0.24
Co												1.00	-0.06	-0.07	0.57	0.18	0.50	0.58	0.37	0.11	0.35	0.04
Sr													1.00	-0.38	0.05	-0.21	-0.25	-0.22	0.75	-0.23	-0.46	-0.44
W														1.00	-0.08	-0.21	-0.01	0.12	-0.28	0.13	0.28	-0.08
Mo															1.00	0.51	0.92	0.73	0.46	-0.01	0.38	0.26
Cu																1.00	0.62	0.13	0.07	0.46	0.67	0.89
Pb																	1.00	0.74	0.11	0.07	0.51	0.44
Zn																		1.00	0.06	-0.06	0.23	0.08
Ni																			1.00	0.01	-0.02	-0.18
As																				1.00	0.69	0.65
Ag																					1.00	0.68
Au																						1.00

Strong negative

Weak Negative

No correlation

Weak positive

Strong positive

### Exoskarn Zone

The Fe<sub>2</sub>O<sub>3</sub> content of the exoskarn samples is 73.4% on average. Iron source is principally magnetite and hematite, and iron content in andradite, pyrite and chalcopyrite, which is observed in some samples, also affect this result. In the same samples, there are 899 ppm Cu, 76 ppm Pb and 156 ppm Zn on average (Table 4). A sample has 6753 ppm Cu and this value show importance of the exoskarn zone by means of copper. Outer zones of the main ore region heavily weathered at the surface. As a result of this process there are lots of small polluted areas by copper carbonate and oxides around the Kiziltepe deposits.

Table 4. Major oxides (%) and some trace element (ppm, Au: ppb) analysis and statistical summaries of the granitoidic rocks (M: Mean, S.S.: Standard deviation, S.E.: Standard error, tc: Calculated t value; L.L: The lower limit, U.L: Upper limit, Sample number:8, tt: Table t value1.83)

NO	SiO <sub>2</sub>	Al <sub>2</sub> O <sub>3</sub>	Fe <sub>2</sub> O <sub>3</sub>	MgO	CaO	Na <sub>2</sub> O	K <sub>2</sub> O	TiO <sub>2</sub>	MnO	Cr <sub>2</sub> O <sub>3</sub>	Ba	Co	Sr	W	Mo	Cu	Pb	Zn	Ni	As	Ag	Au	Sum
S 1	4.10	37.56	33.9	18.8	0.01	0.01	0.01	0.69	30.05	0.33	1.65	2.04	3.3	0	47.8	321.6	166.0	108.8	139.6	1.4	20.99	76	
S 3	8.80	30.83	34.7	1.80	0.01	0.01	0.02	0.57	70.01	0.38	0.0	5.4	18.00	6	6.0	48.7	164.0	107.7	24.5	0.1	4.8	99.78	
S 4	11.50	52.69	16.2	7.10	0.02	0.01	0.03	0.65	110.06	0.15	6.4	9.9	13.30	5	1.3	32.9	141.0	117.5	34.5	0.1	3.7	99.79	
S 6	20.90	18.64	52.4	8.30	0.01	0.01	0.02	0.55	20.01	0.22	2.9	4.25	7.70	66	753.0	10.3	121.0	76.1	30.00	9	8.2	98.76	
S 7	16.70	22.72	08.9	0.60	0.02	0.01	0.01	0.71	40.01	0.44	6.0	4.5	9.90	9	22.2	112.8	247.0	84.0	59.8	0.6	6.3	99.69	
S 8	10.10	07.84	75.0	0.10	0.01	0.01	0.01	0.53	20.01	0.31	2.8	1.8	14.50	8	10.2	45.4	187.0	18.4	23.00	1	2.7	99.77	
S 9	7.20	07.88	03.2	1.60	0.01	0.01	0.01	0.56	20.01	0.12	29.9	8.4	19.60	5	5.0	18.7	137.0	14.0	14.20	1	1.6	99.77	
S 10	17.90	11.69	24.5	7.30	0.02	0.01	0.01	0.46	20.02	0.20	1.0	6.1	32.60	4	345.8	18.3	88.0	97.3	28.10	1	4.4	99.77	
M.	12.20	23.73	44.8	5.70	0.01	0.01	0.02	0.59	41.32	0.32	85.1	11.5	26.10	9	898.9	76.1	156.4	77.9	44.20	4	6.5	99.64	
S.D.	5.80	16.11	02.0	6.20	0.01	0.00	0.01	0.09	32.72	1	98.8	16.5	16.90	92	368.3	104.3	47.6	40.4	40.80	5	5.8		
S.E.	2.10	06.3	3.90	2.20	0.00	0.00	0.00	0.03	11.60	7	34.9	5.9	6.00	3	837.3	36.9	16.8	14.3	14.40	2	2.1		



t <sub>c</sub>	5.94	0.09	18.9	6.9	2.67	5.1	-5.61	19.5	3.63	1	8.2	2.0	4.43	0	1.1	2.1	9.3	5.5	3.12	4	3.1
L.L.	7.30	10	64.2	3.2	0.50	0.01	0.01	0.01	0.52	13.90	5	202.5	-2.3	12.00	2	-	-116.6	44.1	10.10	0	1.6
U.L.	17.00	36	82.6	6.5	10.90	0.02	0.01	0.02	0.66	68.64	0	367.7	25.4	40.3	1.62	878.8	163.3	196.1	111.8	78.30	8

Fe<sub>2</sub>O<sub>3</sub> has no positive correlation with any component in the correlation analyzes. SiO<sub>2</sub> shows strong positive correlation only with Cu. Trace elements have significant correlations each other's (Table 5). Iron enrichments are independent the other components.

CaO, Sr, Mo, As, Ag and Au have strong positive correlations within each other (Table 5). Accordingly, these components together form a cluster, and have settled down towards the end of the contact metamorphism process.

Table 5. Correlation coefficients between the components of the exoskarn samples

	SiO <sub>2</sub>	Al <sub>2</sub> O <sub>3</sub>	Fe <sub>2</sub> O <sub>3</sub>	MgO	CaO	Na <sub>2</sub> O	K <sub>2</sub> O	TiO <sub>2</sub>	MnO	Cr <sub>2</sub> O <sub>3</sub>	Ba	Co	Sr	W	Mo	Cu	Pb	Zn	Ni	As	Ag	Au
SiO <sub>2</sub>	1.00	-0.25	-0.22	0.14	-0.21	0.46	-0.05	0.13	-0.30	-0.17	-0.36	-0.17	-0.59	0.28	-0.54	0.63	-0.53	-0.18	0.11	-0.39	-0.06	-0.28
Al <sub>2</sub> O <sub>3</sub>		1.00	-0.50	0.28	0.47	0.28	0.74	0.71	0.64	0.85	0.83	-0.07	0.43	-0.06	0.33	-0.14	0.38	0.09	0.79	0.44	0.25	0.39
Fe <sub>2</sub> O <sub>3</sub>			1.00	0.03	-0.86	-0.25	-0.16	-0.13	-0.38	-0.03	0.59	0.12	0.63	-0.64	-0.59	-0.34	-0.58	0.14	-0.67	-0.73	-0.78	-0.79
MgO				1.00	-0.37	0.70	0.28	0.02	0.54	0.41	0.09	0.50	-0.20	-0.71	-0.09	-0.50	0.08	0.72	0.25	0.08	-0.18	-0.17
CaO					1.00	-0.09	0.09	0.05	0.27	-0.03	0.68	-0.23	0.87	0.69	0.76	0.18	0.71	-0.33	0.53	0.79	0.76	0.87
Na <sub>2</sub> O						1.00	0.49	0.18	0.16	0.39	0.30	-0.14	-0.24	-0.37	-0.30	-0.27	-0.17	0.04	0.44	-0.07	-0.26	-0.24
K <sub>2</sub> O							1.00	0.80	0.28	0.85	0.74	-0.53	-0.04	-0.31	-0.19	-0.15	-0.17	-0.13	0.40	-0.10	-0.26	-0.19
TiO <sub>2</sub>								1.00	0.13	0.84	0.46	-0.43	-0.19	-0.02	-0.32	0.25	-0.33	-0.23	0.50	-0.25	-0.19	-0.18
MnO									1.00	0.40	0.46	0.47	0.49	-0.20	0.56	-0.22	0.65	0.69	0.36	0.66	0.53	0.51
Cr <sub>2</sub> O <sub>3</sub>										1.00	0.59	-0.14	-0.05	-0.44	-0.16	-0.28	-0.09	0.08	0.59	-0.06	-0.28	-0.15
Ba											1.00	-0.38	0.62	0.05	0.47	-0.25	0.47	-0.16	0.59	0.54	0.27	0.46
Co												1.00	0.10	-0.29	0.34	-0.27	0.44	0.84	0.02	0.34	0.26	0.26
Sr													1.00	0.38	0.95	-0.18	0.93	0.02	0.35	0.93	0.75	0.91
W														1.00	0.34	0.77	0.22	-0.53	0.18	0.32	0.67	0.58
Mo															1.00	-0.15	0.98	0.26	0.26	0.96	0.82	0.94
Cu																1.00	-0.26	-0.33	-0.01	-0.14	0.38	0.12
Pb																	1.00	0.36	0.33	0.98	0.78	0.91
Zn																		1.00	-0.10	0.28	0.18	0.10
Ni																			1.00	0.43	0.29	0.45
As																				1.00	0.85	0.95
Ag																					1.00	0.93
Au																						1.00

#### 4. CONCLUSIONS

Permian to Holocene magmatic, metamorphic and sedimentary rocks crop out in the study area. In the basement of the study area Middle-Late Permian Bozalan Formation consists of recrystallized limestone and marbles. Cretaceous aged Denizgoren Ophiolites thrust over Bozalan Formation and generally, observed as serpentinite. Oligo-Miocene Hallaçlar Volcanics cuts the older units and composed of altered andesite and rhyolite. Oligo – Miocene Kestanbol Pluton represented by mainly porphyric monzonite and syenites. Miocene aged Ezine Volcanics composed of pyroxene-andesite and trachyte.

A contact metamorphic and skarn zone were developed by the intrusion of the Kestanbol Pluton into carbonaceous rocks of the Bozalan Formation and Denizgoren Ophiolites at the north of the Kiziltepe - Aladag. Ca-silicate and some metallic mineral enrichments such as iron, copper, zinc and lead were developed in the skarn zones. The skarn zone can be divided into endoskarn and exoskarn zones according to the determined mineral paragenesis.

In the endoskarn zone, there are large crystallized K-feldspar, biotite and quartz as well as red-brown garnet (andradite) and galena, sphalerite and chalcopyrite with epidote. It is important to note that, Ag is reached up to 70 ppm besides 2.7% Cu, 2.5% Pb and 2.7% Zn. In the exoskarn zone, there are magnetite, hematite, chalcopyrite and pyrite together with Ca-silicate minerals such as green garnet (grossular), pyroxene (augite, diopside), amphibole (actinolite-tremolite) epidote group (epidote, zoisite and clinozoisite). In this case, 73% of Fe<sub>2</sub>O<sub>3</sub> is important. Secondary copper enrichments (covellite, digenite, cerussite and malachite) are formed near the skarn zone. In addition, talc and amphibole asbestos formed contact in the ophiolites and pluton.

According to the findings obtained from the field, laboratory and statistical studies performed in the Kiziltepe skarn zone, the Kestanbol pluton, which intruded into the carbonate and clastic rocks of the Bozalan formation and the serpentized peridotites of the Denizgoren ophiolites, formed a contact metamorphic zone in this region. Kiziltepe Skarn Deposit and near environs should be detailed investigate for gold, copper, lead, zinc iron formations.

### ACKNOWLEDGMENT

The Authors wish to thank Scientific Research Project Coordination Unit of Selcuk University for supports timely (BAP Project Numbers: 09201047, 10701480, 11601145 and 18701335), Dr. Yesim OZEN for her helpful analysis.

### REFERENCES

- [1]. Bingol, E., Akyurek, B., Korkmazer, B., 1973, Geology of Biga Peninsula and Karakaya formation characteristics. 50th Anniversary Geology Congress of Republic's, 1973, Ankara.
- [2]. Gozler, M.Z., Ergul, E., Akcaoren, F., Genc, S., Akat, U. and Acar, S., 1984. Geology and compilation the area among the East Canakkale Bay, South Marmara Sea- Bandirma-Balikesir-Edremit and Aegean Sea, Rep. Of Min. Res. Expl. Inst. of Turkey, Ankara, 7430. 123p.
- [3]. Okay, A. I., Siyako, M., and Burkan K. A., 1990, Geology and tectonic evolution of Biga Peninsula, Bulletin of Turkey Petroleum Geologist Association, 2/1 83-121.
- [4]. Beccaleto, L. and Jenny, C., 2004. Geology and Correlation of the Ezine Zone: A Rhodope Fragment in NW Turkey? Journal of Earth Sciences (Turkish J. Earth Sci.), 13, 145-176.
- [5]. Aydin, U., 2010, Geological Features and Ore Deposits of Kiziltepe (Ezine/Canakkale), MSc Thesis, Selcuk University, Graduate Natural and Applied Sciences, Geological Engineering Main Science Branch 111 pp.
- [6]. Arik, F. and Aydin, U., 2010, Geological Features and Ore Deposits of Kiziltepe (Ezine/Canakkale) Area, Selcuk University Scientific Research Projects Coordinatories, Project number: 09201047, 97 p.
- [7]. Kalafatcioglu, A., 1963. Geology of Ezine vicinity and Bozcaada, age of limestone and serpentinite, Journal of Min. Res. Expl. Inst. of Turkey, Ankara, 60-70.
- [8]. Donmez, M., Akcay, A.E., Genc, S.C. and Acar, S., 2005, Middle-Upper Eocene volcanism and marine ignimbrites of Biga Peninsula, Journal of Min. Res. Expl. Inst. of Turkey, 131 49-61.
- [9]. Arik, F. And Aydin, U., 2011, Mineralogical and petrographical characteristics of the Aladag skarn deposit (Ezine/Canakkale-West Turkey), Scientific Research and Essays, 6(3), 592-606.
- [10]. Okay, A.I., Satir, M., Maluski, H., Siyako, M., Monie, P., Metzger, R. and Akyuz, S., 1996, Paleo-and Neotethyan events in northwest Turkey. In: Yin A, Harrison M(eds) Tectonics of Asia. Cambridge University Press, Cambridge, 420-441.
- [11]. Krushensky, R., 1976, Neogene calc-alkaline extrusive rocks of the Karalar-Yesiller area Northwest Anatolia: Bulletin of Volcanology, 40. 336-360.
- [12]. Ercan, T., Satir, M., Steinitz, G., Dora, A., Sarifakioglu, E., Adis, C., Walter, H.J. and Yildirim, T., 1995. NW Anatolia Tertiary volcanism in Biga Peninsula, Gokceada, Bozcaada and Tavsan peninsulas characteristics, Journal of Min. Res. Expl. Inst. of Turkey, Ankara, 117, 55-87.
- [13]. Birkle, P. and Satir, M., 1995, Dating, Geochemistry and geodynamic significance of the Tertiary magmatism of the Biga Peninsula, NW-Turkey. Geology of the Black Sea Region, Journal of Min. Res. Expl. Inst. of Turkey, Ankara, 171-180
- [14]. Yilmaz Sahin, S., Orgun, Y., Gungor, Y., Goker, A.F., Gultekin A. H. and Karacik, Z., 2010, Mineral and Whole-rock Geochemistry of the Kestanbol Granitoid (Ezine-Canakkale) and its Mafic Microgranular Enclaves in Northwestern Anatolia: Evidence of Felsic and Mafic Magma Interaction, Turkish Journal of Earth Sciences (Turkish J. Earth Sci.), 19, 101-122.
- [15]. Orgun, Y., Altinsoy, N., Sahin S.Y., Gungor, Y., Gultekin, A.H., Karahan, G. and Karacik, Z., 2007, Natural and anthropogenic radionuclides in rocks and beach sands from Ezine region (Canakkale), Western Anatolia, Turkey. Appl Radiat Isot. 65(6):739-747.
- [16]. Fytikas, M., Innocenti, F., Manetti, P., Peccerillo, A. and Villari, L., 1984. Tertiary to Quaternary evolution of volcanism in the Aegean region. Geol. Soc. Spec. Pub 17, 687-699.
- [17]. Siyako, M., Burkan, K. and Okay, A., 1989. Tertiary geology of Biga and Gelibolu Peninsulas and hydrocarbon facilities. Bulletin of Turkey Petroleum Geologist Association 1, 183-199.
- [18]. Arik, F. and Aydin, U., 2011, "Geochemical features of the Aladag Fe-Cu-Zn-Pb skarn deposit" (Ezine/Canakkale-North West Turkey), Goldschmidt 2011 Conference, Prague, Mineralogical Magazine, 452.



## A skarn deposit in the Kazdaglari Region: Saricayir (Yenice/Canakkale -Northwest Turkey) Iron-Copper Skarn Deposit

*Fetullah Arik<sup>1</sup>, Ilknur Akis<sup>2</sup>*

### *Abstract*

*Saricayir skarn deposit is located around the Saricayir village of Yenice County, 70 km southeast of Canakkale and northeast of the Kazdaglari Region in the northwestern Turkey. Triassic to Oligo-Miocene magmatic, metamorphic and volcanic rocks crop out in the study area. The Karakaya complex is the structural basement of the study area and represented by the Nilufer and Hodul units which are metamorphosed to green schist facies. While Nilufer unit mostly consists of metabasic rocks, Hodul unit dominated by arkosic sandstones was emplaced over the Nilufer unit. Karakaya complex are cut by Oligocene Karadoru granitoid and Saricayir alkali granites and covered unconformably by the Oligocene Can Volcanics, consist of andesitic pyroclastics and lavas. It is aimed that to explain geological, mineralogical and geochemical properties of the skarn zone between the Karadoru Granitoid and the Karakaya Complex's Nilufer and Hodul units in this study.*

*Owing to Nilufer and Hodul units were affected by the intrusion of Karadoru Granitoid and Saricayir alkali granite contact metamorphism and skarn zones have been developed between the Karadoru Granitoid and the Nilufer and Hodul units. Contact metamorphism appears to have extended from albite-epidote hornfels to hornblende hornfels facies. Calc-silicate minerals such as garnet, tremolite and epidote were determined in the skarn zone. In addition, pyrite, chalcopyrite, sphalerite, galena, digenite and cinnabar were observed. Chemical data reveal that Fe<sub>2</sub>O<sub>3</sub>, Pb, Cu, Zn, As, Ag and Au reach up to 57.54%, 8101 ppm, 4656 ppm, 3700 ppm, 2500 ppm, 8.3 ppm and 60.6 ppb respectively.*

**Keywords:** Saricayir granite, Skarn-type mineralization, iron, copper, lead, zinc

### 1. INTRODUCTION

Saricayir skarn deposit is situated 70 km southeast of Canakkale city center and around the Saricayir village of Yenice County (Canakkale-Turkey) northeast of the Kazdaglari Region (Figure 1). Triassic to Oligo-Miocene magmatic, metamorphic and volcanic rocks crop out in the study area. The Karakaya complex is the structural basement of the study area and represented by the Nilufer and Hodul units and cut by Oligocene Karadoru granitoid and Saricayir alkali granites and covered unconformably by the Oligocene Can Volcanics, consist of andesitic pyroclastics and lavas. Owing to Nilufer and Hodul units were affected by the intrusion of Karadoru Granitoid and Saricayir alkali granite contact metamorphism and skarn zones have been developed between the Karadoru Granitoid and the Nilufer and Hodul units.

Garnet, tremolite and epidote were determined in the skarn zone besides pyrite, chalcopyrite, sphalerite, galena, digenite and cinnabar formations. It is aimed that to explain geological and geochemical properties of the contact metamorphic and skarn zone among the granitoidic rocks and the Nilufer and Hodul units.

<sup>1</sup> Konya Technical University, Faculty of Engineering and Natural Sciences, Geological Engineering Department, Selcuklu-Konya / TURKEY, [farik@selcuk.edu.tr](mailto:farik@selcuk.edu.tr)

<sup>2</sup> Selcuk University Graduate of Natural and Applied Sciences Geological Engineering Department, [katre97@hotmail.com](mailto:katre97@hotmail.com)



Figure 5. Location map of the study area

## 2. MATERIAL AND METHODS

In order to determination of geological, mineralogical, petrographical and geochemical characteristics of the units crop out, field and laboratory studies were carried out in the study area. Formation boundaries were updated and total 90 samples collected from different rock units during the field studies. In order to understand mineralogical petrographic analyzes of rock and ore samples collected during field studies, thin section and polishing section studies were conducted. Samples were classified and prepared for chemical analysis in the Selcuk University and sent to the related laboratories. For petrographic studies, 40 thin sections and 12 polishing sections were prepared. Thin sections were prepared in the Pamukkale University Geological Engineering Department. The polished sections were prepared in the laboratories of the Geological Engineering Department of Istanbul Technical University. Thin and polished sections were examined by a polarizing microscope in the laboratories of the Geological Engineering Department of Istanbul Technical University and Selcuk University Geological Engineering Department.

A total of 45 samples taken from the region and other units which are considered to have skarn mineralization were passed through the crusher for chemical analysis and 50 grams of the ground and grinded samples were taken and placed in plastic bags. The prepared samples were analyzed in ACME (Vancouver-Canada) Laboratories for the determination of the major oxides ( $\text{SiO}_2$ ,  $\text{Al}_2\text{O}_3$ ,  $\text{Fe}_2\text{O}_3$ ,  $\text{MgO}$ ,  $\text{CaO}$ ,  $\text{Na}_2\text{O}$ ,  $\text{K}_2\text{O}$ ,  $\text{TiO}_2$ ,  $\text{P}_2\text{O}_5$ ,  $\text{MnO}$ ,  $\text{Cr}_2\text{O}_3$ ) and trace elements (Cu, Pb, Zn, Ni, Ga, Nb, Th, V, Zr, Y, Sc). Samples were jaw crushed to 70% passing 10 mesh (2 mm), a 250 g aliquot was riffle split and pulverized to 95% passing 150 mesh (100  $\mu\text{m}$ ) in a mild-steel ring-and-puck mill. Samples after thawing process calibration standards, verification standards and reagent blanks were included in the sample sequence. Sample solutions were aspirated into an ICP emission spectrograph (ICP-ES) (Spectro Ciros Vision) for the determination of the major oxides. All geochemical data were evaluated with basic and multivariate statistical methods using student t test, correlation coefficient, cluster analyses, simple regression and scatter diagrams.

## 3. RESULT AND DISCUSSION

### 3.1. Geological Settings

In the Biga Peninsula, the Pre-Tertiary rocks are exposed in tectonic and tectonic zones extending from NE-SW. These zones are composed of Izmir-Ankara Zone, Sakarya Zone, Cetmi Melange and Ezine Zones (e.g. [1], [2]). The stratigraphic basement of the Biga Peninsula consists of units belonging to the Sakarya continent. In the study area, the Karakaya complex (e.g. [3]), which is called Sakarya Zone rocks, constitutes the foundation (e.g. [4]). Triassic to Holocene aged metamorphic, magmatic and sedimentary units exposed in the study area (Figure 2) (e.g. [5]-[7]).

Permo-Triassic Nilufer unit (e.g. [8], [9]), which is the most common widespread rock group in the study area, constitutes the lowest structural slice of the Karakaya complex. The unit is mainly represented by dark green, distinctive foliated and fine-grained schists as well as dark gray, lead gray phyllite, sericite-quartz-schist and garnet-schist and gray, blackish gray marble-calcschist block and lenses. The Nilufer unit is exposed to metamorphism in the greenschist facies and the metamorphism grade extends up to the garnet zone, which

represents the higher level of the greenschist facies. The green schists in the Nilufer unit were observed to be intensely deformed in the contact zones with the Hodul unit. As a result of metamorphism, schist, Q-schist, garnet schist and epidote schists were formed (e.g. [1], [3]-[4], [7]). Predominantly lepydoblastic, granolepydoblastic, porphyroblastic and occasionally fibroblastic texture development (especially in the external contact zone). According to these properties, the rocks are called phyllite-schist such as epidote-schist, garnet-schist, and quartz-schist. Plagioclases are mostly polygonal grain-shaped and polysynthetic twins. Crystallized limestone and calcschist blocks and lenses located in Karakaya complex are observed to the south of Ortacagil stream and north of Saricayir - Karadoru village road. A marble block within the Nilufer unit to the east of the Karadoru village remained within the Karadoru Granitoid contact metamorphism and skarn zone (e.g. [5]-[7]).

Cretaceous Hodul Unit (e.g. [4], [12]) covers the Nilufer unit with tectonic contact. It has been affected from low grade metamorphism. In the study area, it presents a narrow area spread to the north of Korcesme Hill. Hodul Unit is represented by yellowish gray-brown arkosic conglomerate, sandstone, black greywacke and light green shales (e.g. [5]-[7]). In addition, it contains green colored spyllitic basalt, diabase and recrystallized limestone and chert gravel and blocks. In the petrographic examinations; 30-40% of actinolite, 10-20% of biotite and 30-40% of tremolite have been determined.

Oligocene Karadoru Granitoid is observed South of the Uzunburun Slope to the north of Karadoru village. Granitoid cut the Nilufer and Hodul Units of Karakaya Complex and developed a contact metamorphism and skarn zone in an area of about 7 square kilometers although it has a very narrow area (e.g. [6]). Karadoru Granitoid was cut with hot contact by Saricayir granite. The granitoids are quite cracked and these cracks were filled with secondary quartz (e.g. [13]). Intense clay deposits due to alteration of feldspars in the Karadoru granitoid are exposed on the Karadoru village road (e.g. [7]). 30-50% quartz, 30-50% plagioclase, 10-20% alkali feldspar and 5-8% biotite paragenesis identified in the petrographic examinations of the samples collected from Karadoru granitoid. The holocrystalline, granular textured rock is called granodiorite (e.g. [14]).

Saricayir granite is represented by pinkish-colored, fine-to medium-grained alkali feldspar granite, and aplitic granites (e.g. [15]). In the last phase of the Karadoru granitoid, Oligocene Saricayir granite, which is a granitic and aplitic-looking granite, is settled (e.g. [14]). It was cut by the Can Volcanics developed at the same period. Almost no mafic minerals are contained. The grain size varies between 0.1 and 3 mm. Epidote are observed along the cracks and joint planes. Mainly quartz (15-30%), plagioclase (5-30%) and orthoclase (30-60%) minor amounts biotite and amphibole were observed. The rocks are composed of holocrystalline, grain-like and semi-euhedral crystals. According to these properties, it is in granite composition and it is called alkali granite (e.g. [5]-[7]).

The Miocene Can Volcanics (e.g. [16]) are represented by beige, yellowish beige and pink colored andesite, dacite and rhyodacitic lava, tuff and agglomerates. The tuff and agglomerates are observed to the east of the Patlak Ridge around the Saricayir village (e.g. [5]-[7]). Can Volcanics are generally composed of pyroclastic levels. There are pumice fragments in the tuffs (e.g. [17]). Volcanic glass and plagioclase microliths, as well as large plagioclase phenocrysts, altered amphibole and biotites were observed. The rocks have hypocrySTALLINE porphyric texture are called andesitic tuffs. Iron oxide enrichments were observed somewhere in the tuffs.

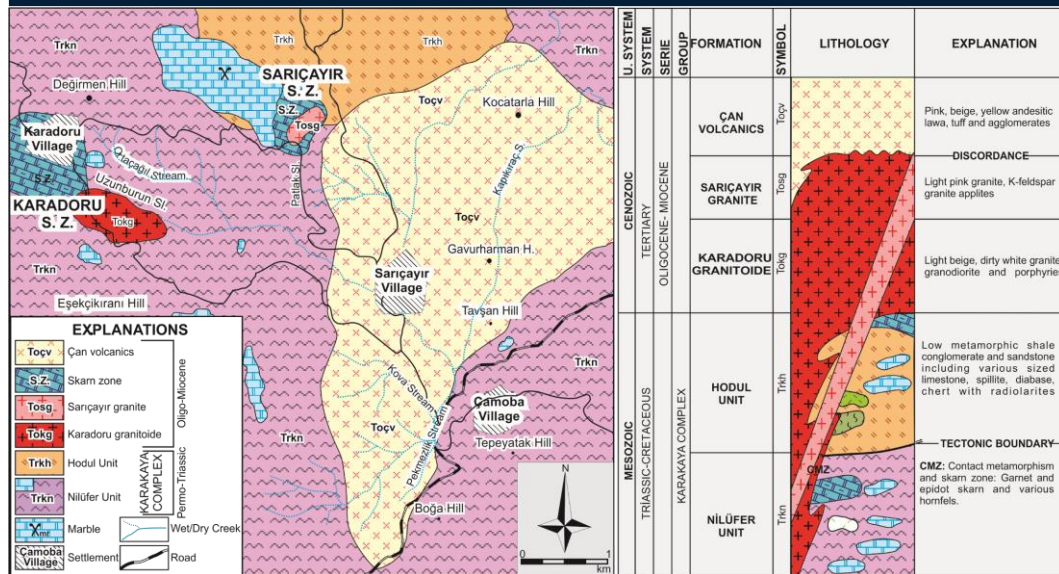


Figure 6. Geological map and tectono-stratigraphical section of the study area (After, Arik ve Akis, 2013)

### 3.2. Skarn Mineralization

Nilüfer and Hodul units were affected by the intrusion of Karadoru Granitoid and Sarıçayır alkali granite. Contact metamorphism and skarn type mineralization were developed adjacent to contacts of granitoids with the carbonate rocks of Nilüfer units. Skarn mineralization was approximately 1 km<sup>2</sup> area (e.g. [5], [7]). Garnet - epidote skarn was formed at the contact of granite and marble (Figure 3). Contact metamorphism appears to have extended from albite-epidote hornfels to hornblende hornfels facies. Epidote and quartz fillings are observed within fractures and faults of the Sarıçayır alkali granite. Garnets have generally andradite-rich composition. As a result of contact metamorphism minor amount of pyrite and magnetite and rarely chalcopyrite was formed in the skarn zone. Garnets are responsible for the iron enrichments while lead and copper enrichments were caused by the epidotes (e.g. [18]).

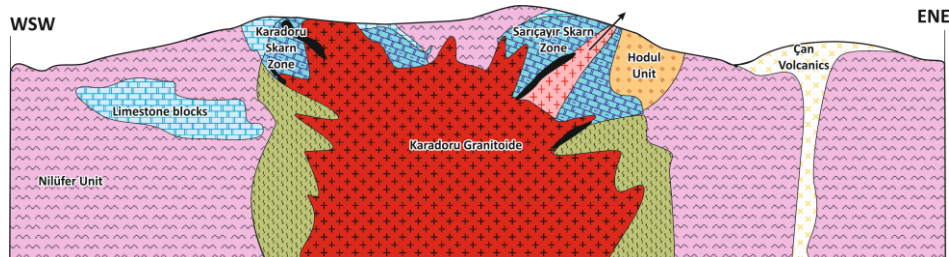


Figure 7. Schematic Cross Section model of Kızıltepe (Aladag) Skarn Zone (Modified from [7]).

The rocks in the Sarıçayır skarn zone investigated in 3 sections from intrusive rocks to outside zones; 1) Intrusive rocks (granite aplites), 2) skarn zone (epidote, garnet, diopside hornfels) and 3) carbonate rocks of Nilüfer Unit (e.g. [5]-[7]).

Garnets (andradite), epidote (epidote and epidote-Pb) and magnetite were identified in the skarn zone (e.g. [18]). In places, K-feldspar is concentrated and these rocks are called K-feldspar-epidote hornfels, garnet-epidote hornfels and garnet-hornfels. The spaces between the large crystal garnets are filled with quartz (e.g. [6], [7]). In the petrographic examinations of the epidote rich samples; epidote, plagioclase, biotite and opaque minerals were observed. These holocrystalline textured rocks are generally called epidote-skarn. Some of the samples were found to be entirely composed of epidote and these rocks are called epidosite (e.g. [6]). Pyrite, (py), Chalcopyrite (cpy), Limonite (lm), Bornite (bn) as well as Magnetite (Mg) were Observed in the skarn zone especially Sarıçayır Region.





Figure 8. Schematic cross section and mineral paragenesis of the Saricayir and Karadoru skarn mineralization, A: Metabasic rocks and quartz vein of Nilufer Unit, B and C: Calcite and epidote in limestone blocks D: Shale of Hodul Unit, E: Plagioclase phenocrystal and microlites in dough phase of Can Volcanics (Thin section, +N), F: Plagioclase phenocrystals in dough phase of andesitic lava of Can Volcanics (Thin section, +N), G: Magnetite and cinnabar in the skarn zone (Polished section +N), H: Pyrite, chalcopyrite and digenite in the skarn zone (Polished section, +N), I: Pyrite, chalcopyrite, sphalerite and fahlore in the skarn zone (Polished section, +N), J: Granite aplite and FeO veinlets in the Saricayir Granite (Thin section, +N), K: Myrmekitic textured granite of Saricayir Granites (Thin section, +N), L: Cinnabar and magnetite in the skarn zone (Thin section, //N), M: Epidote and garnet and zoned plagioclase in the skarn zone (Thin Section, //N), N: FeO in the fissures in the garnet and zoned plagioclase in the skarn zone (Thin Section, +N) (After [7]).

### 3.3. Geochemical Features of the Granitoidic Rocks and Skarn Zone

The major oxides and some trace element analysis of the samples taken from the Granitoidic Rocks (Karadoru Granitoidic and Saricayir Granites), and skarn zones (Karadoru and Saricayir) (Tables 1 and 3).

#### Granitoidic Rocks:

The average contents of main oxides such as SiO<sub>2</sub>, Al<sub>2</sub>O<sub>3</sub>, Fe<sub>2</sub>O<sub>3</sub>, MgO, CaO, Na<sub>2</sub>O, K<sub>2</sub>O, TiO<sub>2</sub>, MnO and Cr<sub>2</sub>O<sub>3</sub> were 76%, 11.32%, 2.77%, 0.4%, 1.3 %, 1.32%, 3.61%, 0.4%, 0.001%; while average trace elements such as Ba, V, Mo, Cu, Pb, Zn, As, Sb and Au were 150 ppm, 55 ppm, 1.1 ppm, 22 ppm, 14 ppm, 40 ppm, 0.7 ppm and 2.4 ppb respectively (e.g. [5]-[7]).

Table 6. Major oxides (%) and some trace element (ppm, Au: ppb) analysis and statistical summaries of the granitoidic rocks (S.D.: Standard deviation, S.E.: Standard error, t<sub>n</sub>: Calculated t value: L.L.: The lower limit, U.L.: Upper limit, Sample number: 9, tt: Table t value: 1.86).

Sample	SiO <sub>2</sub>	Al <sub>2</sub> O <sub>3</sub>	Fe <sub>2</sub> O <sub>3</sub>	MgO	CaO	Na <sub>2</sub> O	K <sub>2</sub> O	TiO <sub>2</sub>	P <sub>2</sub> O <sub>5</sub>	MnO	Cr <sub>2</sub> O <sub>3</sub>	Ba	Co	Sr	V	W	Mo	Cu	Pb	Zn	As	Sb	Au	Hg	
N8	77.2	12.4	0.7	0.1	0.3	3.01	5.68	0.10	0.01	0.02	0.003	49	0.5	4.0	47	8	2.5	1.1	4	29	11	4	0.4	1.1	0.01
N40	75.6	11.8	3.8	0.8	0.1	0.04	3.43	0.42	0.11	0.01	0.005	513	1.9	4.0	8	42	2.4	0.4	14	22	45	47	0.3	0.5	0.06
N40-A	89.7	4.7	1.3	0.2	0.0	0.03	1.09	0.05	0.12	0.02	0.003	107	0.6	1.0	3	33	0.6	1.4	6	17	9	71	0.3	1.6	0.01
N41	82.4	9.9	1.0	0.5	0.0	0.03	3.07	0.15	0.13	0.01	0.004	235	0.5	2.0	8	29	0.7	2.3	2	7	1	69	0.2	2.2	0.45
N42	57.4	16.2	11.1	1.8	0.1	0.04	2.84	2.43	0.22	0.12	0.018	113	42.3	2.0	14	346	7.0	0.7	130	3	94	150	0.5	7.0	0.09
N12	77.5	12.3	0.5	0.0	0.6	3.13	5.12	0.08	0.01	0.02	0.002	132	0.3	3.0	62	8	1.7	1.1	5	15	6	3	0.3	5.6	0.01
N12-D	76.8	12.9	0.5	0.1	0.6	2.91	5.21	0.12	0.01	0.01	0.002	37	0.5	5.0	32	8	3.2	0.9	4	17	8	3	0.3	0.5	0.01
N14	75.9	12.7	0.7	0.1	0.9	2.69	5.81	0.14	0.01	0.02	0.002	172	1.1	5.0	77	10	4.8	0.9	28	11	5	7	0.2	2.5	0.36
N16	73.8	9.1	5.3	0.2	9.0	0.02	0.20	0.13	0.02	0.11	0.002	4	1.1	3.0	433	10	1.1	1.1	1	2	6	8	3.7	0.5	29.95
M.	76.2	11.3	2.8	0.4	1.3	1.32	3.61	0.40	0.07	0.04	0.005	151	5.4	3.2	76	55	2.7	1.1	22	14	21	40	0.7	2.4	3.44
S.D.	8.5	3.2	3.6	0.6	2.9	1.53	2.03	0.77	0.08	0.04	0.005	153	13.8	1.4	136	110	2.1	0.5	42	9	30	50	1.1	2.4	9.94
S.E.	2.8	1.1	1.2	0.2	1.0	0.51	0.68	0.26	0.03	0.01	0.002	51	4.6	0.5	45	37	0.7	0.2	14	3	10	17	0.4	0.8	3.31

In the correlation analysis SiO<sub>2</sub> has strong and weak negative correlation other components. Fe<sub>2</sub>O<sub>3</sub>; has strong positive correlation with MgO, TiO<sub>2</sub>, MnO, Cr<sub>2</sub>O<sub>3</sub>, Co, V, Cu, Pb and Zn while strong negative correlation with SiO<sub>2</sub>. Cu, TiO<sub>2</sub>, V, Pb and Zn show strong positive correlation almost all other components except SiO<sub>2</sub>. Hg has strong positive correlation together with CaO and Sb (Table 2).

Table 7. Correlation coefficients between the components of the granitoidic rocks

	SiO <sub>2</sub>	Al <sub>2</sub> O <sub>3</sub>	Fe <sub>2</sub> O <sub>3</sub>	MgO	CaO	Na <sub>2</sub> O	K <sub>2</sub> O	TiO <sub>2</sub>	P <sub>2</sub> O <sub>5</sub>	MnO	Cr <sub>2</sub> O <sub>3</sub>	Ba	Co	Sn	Sr	V	W	Mo	Cu	Pb	Zn	As	Sb	Au	Hg
SiO <sub>2</sub>	1.0	-0.8	-0.8	-0.7	-0.1	0.1	-0.1	-0.9	-0.4	-0.7	-0.8	0.1	-0.8	-0.1	-0.1	-0.8	-0.8	0.5	-0.8	0.4	-0.8	-0.4	-0.2	-0.6	-0.1
Al <sub>2</sub> O <sub>3</sub>		1.0	0.4	0.5	-0.2	0.4	0.6	0.6	0.1	0.2	0.5	0.1	0.6	0.5	-0.2	0.5	0.8	-0.5	0.6	-0.1	0.6	0.1	-0.2	0.5	-0.3
Fe <sub>2</sub> O <sub>3</sub>			1.0	0.9	0.2	-0.6	-0.5	0.9	0.7	0.9	0.9	0.0	0.9	-0.3	0.2	0.9	0.6	-0.4	0.8	-0.5	0.9	0.7	0.3	0.5	0.3
MgO				1.0	-0.2	-0.6	-0.3	0.9	0.9	0.6	1.0	0.3	0.9	-0.4	-0.2	0.9	0.6	-0.3	0.9	-0.4	1.0	0.9	-0.1	0.6	-0.2
CaO					1.0	-0.2	-0.6	-0.2	-0.3	0.6	-0.2	-0.4	-0.1	0.0	1.0	-0.2	-0.2	0.0	-0.2	-0.5	-0.2	-0.3	1.0	-0.3	1.0
Na <sub>2</sub> O						1.0	0.9	-0.4	-0.8	-0.4	-0.4	-0.3	0.7	-0.2	0.4	0.1	-0.2	-0.3	0.5	-0.4	-0.7	-0.3	0.0	-0.3	0.0
K <sub>2</sub> O							1.0	-0.1	-0.4	-0.5	-0.2	0.1	-0.1	0.7	-0.5	-0.2	0.4	-0.2	-0.1	0.5	-0.1	-0.4	-0.6	0.1	-0.6
TiO <sub>2</sub>								1.0	0.8	0.7	1.0	0.0	1.0	-0.3	-0.2	1.0	0.8	-0.3	1.0	-0.4	0.9	0.8	-0.1	0.7	-0.1
P <sub>2</sub> O <sub>5</sub>									1.0	0.4	0.8	0.3	0.7	-0.7	-0.4	0.8	0.3	0.1	0.7	-0.3	0.8	1.0	-0.2	0.4	-0.2
MnO										1.0	0.6	-0.4	0.7	-0.3	0.6	0.7	0.4	-0.2	0.6	-0.7	0.6	0.5	0.7	0.4	0.6
Cr <sub>2</sub> O <sub>3</sub>											1.0	0.1	1.0	-0.4	-0.2	1.0	0.7	-0.3	1.0	-0.4	1.0	0.9	-0.1	0.7	-0.2
Ba												1.0	-0.1	0.1	-0.4	0.0	0.0	-0.2	0.0	0.2	0.3	0.2	-0.4	-0.1	-0.4
Co													1.0	-0.3	-0.2	1.0	0.8	-0.3	1.0	-0.4	0.9	0.8	-0.1	0.7	-0.1
Sn														1.0	0.1	-0.4	0.3	-0.5	-0.2	0.3	-0.2	-0.7	-0.1	-0.4	-0.1
Sr															1.0	-0.2	-0.2	0.0	-0.2	-0.5	-0.2	-0.4	1.0	-0.3	1.0
V																1.0	0.7	-0.3	1.0	-0.4	0.9	0.9	-0.1	0.7	-0.2
W																	1.0	-0.6	0.9	-0.2	0.7	0.4	-0.2	0.5	-0.3
Mo																		1.0	-0.4	-0.2	-0.5	0.0	0.0	-0.1	0.0
Cu																			1.0	-0.4	0.9	0.8	-0.1	0.7	-0.2
Pb																				1.0	-0.2	-0.4	-0.5	-0.4	-0.5
Zn																					1.0	0.8	-0.1	0.6	-0.2
As																						1.0	-0.2	0.5	-0.2
Sb																							1.0	-0.3	1.0
Au																								1.0	-0.3
Hg																									1.0

### Skarn Zone

Average Fe<sub>2</sub>O<sub>3</sub>, Co, Sn, Cu, Pb, Zn, As, Sb and Au 19.6%, 46 ppm, 29 ppm, 364 ppm, 401 ppm, 205 ppm, 343 ppm, 4.3 ppm and 12 ppb respectively (e.g. [5]-[7]). Some samples have reached up 321 ppm for Sn, 382 ppm for W, 4656 ppm for Cu, 8101 ppm for Pb, 3692 ppm for Zn, 2463 ppm for As and 100 ppm for Hg (Table 3).

Table 8. Major oxides (%) and some trace element (ppm, Au: ppb) analysis and statistical summaries of the granitoidic rocks (M: Mean, S.S.: Standard deviation, S.E.: Standard error,  $t_c$ : Calculated t value: L.L: The lower limit, U.L: Upper limit, Sample number: 22,  $t_t$ : Table t value: 1.72).

Sample	SiO <sub>2</sub>	Al <sub>2</sub> O <sub>3</sub>	Fe <sub>2</sub> O <sub>3</sub>	MgO	CaO	Na <sub>2</sub> O	K <sub>2</sub> O	TiO <sub>2</sub>	MnO	Cr <sub>2</sub> O <sub>3</sub>	Ba	Co	Sn	Sr	V	W	Mo	Cu	Pb	Zn	As	Sb	Au	Hg
N6	98.5	0.3	0.7	0.02	0.03	0.03	0.05	0.01	0.01	0.002	16	1	1	2	8	1	1.0	2	2	2	1	0.1	0.5	0.01
N9	40.7	0.7	26.1	0.49	28.76	0.01	0.01	0.01	0.54	0.002	32	19	1	24	10	201	2.4	5	167	14	539	1.24	8.1	0.02
N10-B	85.0	0.7	4.3	1.12	2.15	0.03	0.07	0.01	2.38	0.003	70	31	1	13	12	4	1.7	988	1013	3692	17	2.0	1.2	0.04
N11	50.1	1.0	13.4	6.86	19.78	0.12	0.03	0.01	3.65	0.002	8	104	1	34	20	10	0.4	324	8	114	26	1.4	0.5	0.01
N13	10.5	0.4	55.6	0.12	8.19	0.01	0.01	0.01	0.13	0.003	1524	54	1	8	102	9.1	4656	81	21	2463	0.4	60.6	0.01	
N13-A	33.7	1.9	32.4	0.18	28.49	0.01	0.01	0.01	0.71	0.003	4	1321	1	17	382	14.5	428	11	3	1348	0.8	11.7	0.04	
N13-C	36.6	0.2	30.5	0.01	31.17	0.01	0.01	0.01	0.72	0.003	2	45	24	1	8	254	2.5	50	246	62	259	0.5	6.9	0.01
N13-D	18.8	1.2	57.5	0.05	16.34	0.01	0.01	0.01	0.33	0.003	3	27	31	3	10	187	3.1	259	23	11	496	0.9	11.2	0.02
N13-E	26.8	0.9	39.2	0.04	23.79	0.01	0.01	0.01	0.32	0.003	3	53	28	1	8	213	3.1	1898	40	3	781	0.75	5.2	0.01
N14-A	88.6	0.3	8.2	0.01	0.13	0.01	0.02	0.01	0.08	0.003	30	23	1	9	8	36	2.9	9	55	101	385	78.1	40.5	100.0
N15	39.0	6.4	22.8	0.59	29.24	0.01	0.01	0.10	0.47	0.004	23	5	3	2	26	84	1.6	11	3	6	253	0.4	0.7	7.30
N16-A	33.2	12.3	13.8	1.57	28.69	0.01	0.15	0.19	0.67	0.004	5	9	34	402	18	10	0.9	1	7	29	18	1.5	0.5	2.71
N17	47.9	1.3	15.3	8.04	23.18	0.06	0.01	0.01	2.23	0.002	23	76	1	26	8	21	0.5	3	2	31	132	1.7	0.5	1.03

N19	35.6	0.4	30.9	0.04	32.07	0.01	0.01	0.01	0.29	0.002	3	5	1	1	8301	0.8	7	8	2	223	0.3	1.8	0.07	
N20	37.0	0.0	1.3	0.73	39.02	0.01	0.02	0.01	4.48	0.002	2	10	1	48	8	1	0.7	1	19	11	27	0.5	0.7	0.68
N22-A	34.7	0.3	34.7	0.74	28.56	0.01	0.01	0.01	0.34	0.002	9	14	41	1	8	67	1.1	49	2	4	460	0.4	1.3	0.37
N23	74.5	12.2	4.1	1.20	0.42	0.68	3.30	0.42	0.16	0.006	385	14	2	49	64	3	0.8	45	22	28	45	1.1	2.2	0.22
N24	46.8	2.6	22.9	2.74	19.81	0.07	0.02	0.66	1.82	0.008	20	26	92	136	99	2	0.2	118	6	245	10	1.0	3.9	0.24
N25	46.7	18.0	10.3	2.30	18.32	1.08	0.17	0.54	0.89	0.008	25	10	33	307	63	2	0.9	2	6	28	57	1.1	1.8	0.88
N34-A	95.8	1.5	1.0	0.09	0.18	0.23	0.20	0.03	0.05	0.002	65	2	1	17	8	1	0.7	8	6	12	3	0.1	2.1	0.20
N45	95.0	0.8	2.6	0.06	0.03	0.01	0.04	0.01	0.01	0.002	8	0	1	224	1	0.7	11	1	8	6	0.5	3.6	0.33	
N45-A	81.4	7.6	4.4	1.00	0.12	0.04	0.52	0.22	0.62	0.005	83	16	1	2445	1	0.6	15	27	86	6	0.1	3.5	0.09	
M.	52.6	3.2	19.6	1.27	17.20	0.11	0.21	0.11	0.95	0.003	37	46	29	5022	86	2.3	364	402	205	343	4.3	11.8	5.2	
S.D.	27.0	4.9	17.1	2.15	13.28	0.26	0.70	0.19	1.22	0.002	81	110	69	104	24	116	3.3	1041	1721	781	577	16.5	19.5	21.2
S.E.	5.7	1.1	3.7	0.46	2.83	0.06	0.15	0.04	0.26	0.000	17	23	15	22	5	25	0.7	222	367	166	123	3.5	4.2	4.5
t <sub>c</sub>	9.1	3.1	5.4	2.78	6.07	2.02	1.43	2.59	3.66	8.541	2	2	2	2	4	3	3.2	2	1	3	1.2	2.8	1.1	
L.L.	40.6	1.0	12.0	0.32	11.31	0.00	-0.10	0.02	0.41	0.003	1	-3	-1	4	11	34	0.8	-98	-361	-141	87	-3.0	3.1	-4.2
U.L.	64.5	5.4	27.2	2.22	23.09	0.23	0.52	0.19	1.49	0.004	73	95	60	96	33	137	3.8	825	1165	551	599	11.6	20.4	14.6

In the correlation analysis SiO<sub>2</sub> has strong and weak negative correlation with Fe<sub>2</sub>O<sub>3</sub> and CaO. Fe<sub>2</sub>O<sub>3</sub>; has strong positive correlation with W, and As while strong negative correlation with SiO<sub>2</sub>. Pb and Zn have not got any correlation with others. Hg has strong positive correlation with Sb; Au has strong positive correlation with Cu and As. According to these results SiO<sub>2</sub> shows different behavior in the geochemical process (Table 4).

Table 9. Correlation coefficients between the components of the skarn samples

	SiO <sub>2</sub>	Al <sub>2</sub> O <sub>3</sub>	Fe <sub>2</sub> O <sub>3</sub>	MgO	CaO	Na <sub>2</sub> O	K <sub>2</sub> O	TiO <sub>2</sub>	MnO	Cr <sub>2</sub> O <sub>3</sub>	Ba	Co	Sn	Sr	V	W	Mo	Cu	Pb	Zn	As	Sb	Au	Hg
SiO <sub>2</sub>	1.0	0.0	-0.8	-0.1	-0.8	0.1	0.2	0.0	-0.1	0.0	0.4	-0.4	-0.3	-0.1	0.1	-0.5	-0.4	-0.4	0.3	0.3	-0.5	0.3	-0.3	0.3
Al <sub>2</sub> O <sub>3</sub>		1.0	-0.3	0.1	-0.1	0.8	0.5	0.7	-0.1	0.7	0.4	-0.2	-0.1	0.8	0.6	-0.3	-0.2	-0.2	-0.1	-0.1	-0.3	-0.1	-0.3	-0.1
Fe <sub>2</sub> O <sub>3</sub>			1.0	-0.2	0.4	-0.3	-0.3	-0.2	-0.3	-0.1	-0.3	0.5	0.3	-0.2	-0.2	0.7	0.5	0.6	-0.2	-0.2	0.7	-0.2	0.5	-0.2
MgO				1.0	0.1	0.2	0.0	0.2	0.6	0.1	0.0	0.1	-0.1	0.2	0.2	-0.3	-0.3	-0.1	0.0	0.0	-0.3	-0.1	-0.3	-0.1
CaO					1.0	-0.2	-0.3	-0.1	0.4	-0.1	-0.4	-0.1	0.2	0.2	-0.2	0.5	0.1	-0.1	-0.2	-0.3	0.1	-0.3	0.0	-0.3
Na <sub>2</sub> O						1.0	0.5	0.7	-0.1	0.7	0.5	-0.1	-0.1	0.5	0.5	-0.3	-0.2	-0.1	-0.1	0.1	-0.2	-0.1	-0.2	-0.1
K <sub>2</sub> O							1.0	0.4	-0.2	0.4	1.0	-0.1	-0.1	0.0	0.4	-0.2	-0.1	-0.1	0.0	0.0	-0.2	-0.1	-0.1	-0.1
TiO <sub>2</sub>								1.0	0.0	1.0	0.4	-0.1	0.1	0.6	1.0	-0.4	-0.3	-0.2	-0.1	-0.1	-0.3	-0.1	-0.2	-0.1
MnO									1.0	-0.1	-0.1	0.0	-0.1	0.1	0.0	-0.3	-0.2	-0.2	0.3	0.3	-0.3	-0.1	-0.3	-0.2
Cr <sub>2</sub> O <sub>3</sub>										1.0	0.4	-0.1	0.1	0.6	0.9	-0.3	-0.1	-0.1	0.0	0.0	-0.2	0.0	-0.1	0.0
Ba											1.0	-0.1	-0.2	0.0	0.4	-0.3	-0.2	-0.1	0.1	0.1	-0.2	0.0	-0.2	0.0
Co												1.0	0.0	-0.1	-0.2	0.0	0.4	0.9	0.0	0.0	0.8	0.0	0.6	-0.1
Sn													1.0	0.0	0.1	0.6	0.8	0.2	-0.1	-0.1	0.5	-0.1	0.1	-0.1
Sr														1.0	0.4	-0.3	-0.2	-0.2	-0.1	-0.1	-0.3	-0.1	-0.2	-0.1
V															1.0	-0.3	-0.2	-0.2	-0.1	0.0	-0.3	-0.1	-0.3	-0.1
W																1.0	0.6	0.2	-0.1	-0.2	0.5	-0.1	0.3	-0.1
Mo																	1.0	0.5	0.0	-0.1	0.8	0.0	0.4	0.0
Cu																		1.0	-0.1	-0.1	0.9	-0.1	0.7	-0.1
Pb																			1.0	1.0	-0.1	0.0	-0.1	-0.1
Zn																				1.0	-0.1	0.0	-0.1	0.0
As																					1.0	0.0	0.7	0.0
Sb																						1.0	0.3	1.0
Au																							1.0	0.3
Hg																								1.0

#### 4. CONCLUSIONS

Triassic to Holocene aged metamorphic, magmatic and sedimentary units exposed in the study area. Permo-Triassic Nilufer unit was formed by metamorphic detritic and carbonate rocks in the greenschist facies, constitutes the lowest structural slice of the Karakaya complex. Cretaceous, low grade metamorphic Hodul Unit covers the Nilufer unit with tectonic contact. Oligocene Karadoru Granitoide cut the Nilufer and Hodul Units. Oligocene Saricayir granite is represented by pinkish-colored, fine-to medium-grained alkali feldspar granite, and aplitic granites. Miocene Can Volcanics represented by beige, yellowish beige and pink colored andesite, dacite and rhyodacitic lava, tuff and agglomerates.

Nilufer and Hodul units were affected by the intrusion of Karadoru Granitoide and Saricayir alkali granite. Contact metamorphism and skarn type mineralization were developed adjacent to contacts of granitoids with



the carbonate rocks of Nilufer units. Garnet - epidote skarn was formed at the contact of granite and marble and epidote skarn in the clastic rocks. Contact metamorphism appears to have extended from albite-epidote hornfels to hornblende hornfels facies. As a result of contact metamorphism minor amount of pyrite and magnetite and rarely chalcopyrite were formed in the skarn zone. Garnets are responsible for the iron enrichments while lead and copper enrichments were caused by the epidotes. Average Fe<sub>2</sub>O<sub>3</sub> 20%, Sn 29 ppm, Cu 364 ppm, Pb 400 ppm, Zn 205 ppm, As 343 ppm, Sb 4 ppm, Au 12 ppb and Hg 5 ppm. Some samples have reached up to 320 ppm for Sn, 380 ppm for W, 4660 ppm for Cu, 8100 ppm for Pb, 3700 ppm for Zn, 2500 ppm for As and above 100 ppm for Hg. According to the findings obtained from the field, mineralogical, petrographical, geochemical and statistical studies performed in the Karadoru and Saricayir Skarn deposits, granitoidic rocks of the Karadoru Granitoid and Saricayir Granites intruded into the clastic and carbonate rocks of the Bozalan formation and the Hodul Units, formed a contact metamorphic zone in this region. Karadoru and Saricayir Skarn Deposits and their near environs should be detailedly investigated for copper, lead, zinc and iron formations.

### ACKNOWLEDGMENT

*The Authors wish to thank Scientific Research Project Coordination Unit of Selcuk University for supports timely (BAP Project Numbers: 09201131 and 12701434).*

### REFERENCES

- [1]. Duru, M., Pehlivan, S., Senturk, Y., Yavas, F. and Kar, H., 2004. New results on the lithostratigraphy of the Kazdag massif in Northwest Turkey. *Turkish Journal of Earth Science*, 13, 2, 177-186.
- [2]. Donmez, M., Akcay, A.E., Genc, S.C. and Acar, S., 2005. Middle-Upper Eocene volcanism and marine ignimbrites of Biga Peninsula, *Journal of Min. Res. Expl. Inst. of Turkey*, 131 49-61.
- [3]. Bingol, E., Akyurek, B., Korkmazer, B., 1973, *Geology of Biga Peninsula and Karakaya formation characteristics*. 50th Anniversary Geology Congress of Republic's, 1973, Ankara.
- [4]. Okay, A. I., Siyako, M., and Burkan K. A., 1990, *Geology and tectonic evolution of Biga Peninsula*, *Bulletin of Turkey Petroleum Geologist Association*, 2/1 83-121.
- [5]. Akis, I., 2011, *Geological and geochemical features of the skarn deposits around the Saricayir (Yenice-Canakkale)*, MSc thesis Selcuk University, Graduate Natural and Applied Sciences, Geological Engineering Main Science Branch 108 pp.
- [6]. Arik, F., 2011, *Geological and geochemical characteristics of the skarn deposits around the Saricayir (Yenice-Canakkale)*, Selcuk University Scientific Research Projects Coordination Unit 09201045, 117 pp.
- [7]. Arik, F. and Akis, I., 2013, *Geological and geochemical features of the Saricayir (Yenice/Canakkale) Skarn deposits*, *Goldschmidt2013 Conference Abstracts*, 614.
- [8]. Genc, S.C., Donmez, M., Akcay, A.E. and Altunkaynak, S., 2004, *The middle Eocene to late Miocene magmatic evolution of the Biga Peninsula, NW Turkey*. 32nd. *IGC Florence 2004 –Sci. Sess.: Abstracts (part 2)* -1298.
- [9]. Robertson, A.H.F., Ustaomer, T., Pickett, E.A., Collins, A.S., Andrew, T., Dixon, J.E., (2004), *Testing models of Late Paleozoic – Early Mesozoic orogeny in Western Turkey: support for an evolving open – Tethys model*. *Journal of Geological Society, London, Vol. 161*, pp. 501–511.
- [10]. Okay, A.I., Satir, M., Maluski, H., Siyako, M., Monie, P., Metzger, R. and Akyuz, S., 1996, *Paleo- and Neotethyan events in northwest Turkey*. In: Yin A, Harrison M(eds) *Tectonics of Asia*. Cambridge University Press, Cambridge, 420-441.
- [11]. Okay, A.I., and Satir, M., 2000, *Coeval plutonism and metamorphism in a latest Oligocene metamorphic core complex in Northwest Turkey*. *Geological Magazine*, 137, 495-516.
- [12]. Okay, A.I., ve Goncuoglu, M.C., 2004, *The Karakaya Complex: A Review of data and concepts*. *Turkish Journal of Earth Sciences*, Vol.13, pp. 77-95
- [13]. Ongen, S., 1982, *Petrology of the Yenice (Canakkale) granitoids and wall rocks*, Istanbul Univ. Graduate Natural and Applied Science Institute, Associate Professor Thesis, 234 pp.
- [14]. Aysal, N. 2005, *Petrology of the Mesozoic-Tertiary Magmatism and Metamorphism East of Biga (Canakkale)* PhD. Thesis, Istanbul Univ. Graduate Natural and Applied Science Institute, 195 pp.
- [15]. Ongen, S., Azaz, D. and Aysal, N., 2002, *Petrography of the Oligocene aged Namazgah Granitoid and vessel rocks Yenice (Canakkale)*. 55th. *Turkey Geological Congress, Proceedings*, 204- 206.
- [16]. Ercan, T., Satir, M., Steinitz, G., Dora, A., Sarifakioglu, E., Adis, C., Walter, H.J. and Yildirim, T., 1995. *NW Anatolia Tertiary volcanism in Biga Peninsula, Gokceada, Bozcaada and Tavsan peninsulas characteristics*, *Journal of Min. Res. Expl. Inst. of Turkey, Ankara*, 117, 55-87.
- [17]. Lacin, D., 2003, *Formation, mineralogical and deposition features of the halloysites of the Biga Peninsula (Canakkale-Balikesir)* PhD. Thesis, Istanbul Univ. Graduate Natural and Applied Science Institute 162 pp.
- [18]. Aysal, N., Ongen, S. and Hanilci, N., 2006, *Petrography of the Karadoru Granitoid Pluton and its wall rocks and characteristics of the skarn zone (Yenice-Canakkale)*, *Istanbul Univ. Engineering Faculty, Journal of Geosciences* 19, (2), 183-194.

## The Landscape Design Project of Sey Bath Geosite (Kizilcahamam-Camlidere) Under Geopark and Geotourism Concept

Nurhan Kocan<sup>1</sup>, Tugba Yildiz<sup>2</sup>, Sinan Surun<sup>3</sup>

### Abstract

*As people become acquainted with nature their awareness of nature and knowledge about their surroundings are increase. With the developing technology, people who are sick of city life and need to rest in natural areas to spend their free time more efficiently. Various examples of geological and geomorphological structures are interesting for scientists and nature lovers. These mysterious formations, called geological heritage are a source of natural wealth and geotourism for the region they are in. Thanks to geotourism, people living in these areas are able to market their local products and rural development and economic development are achieved. Therefore, existing geological heritage areas should be regulated and tourism must be ensured and thus protected. In this study, Seyhamami Geocide was examined by geological and geomorphological aspects and proposal projects were prepared by evaluating in terms of landscape planning and design. Coreldraw, Auto Cad 2014, Photoshop CS5, Sketch Up and Lumion programs were used for drawing. The proposed projects were presented with three-dimensional visuals in the form of a landscape design project. It is believed that the project prepared for the applicable nature will contribute to the development of the study area.*

**Keywords:** Geotourism, Geopark, Landscape Planning, Landscape Design, Seyhamami Geositi (Ankara).

### 1. INTRODUCTION

If some of the areas where geological processes and phases are realized in destroy under the threat of human or natural impact that can be lost from the earth. So proof of the Earth starting from this day onwards will be extinction. This deletion can be a huge loss both scientifically and culturally.

The reasons for the conservation of natural areas in our country; education and scientific researches, the provision of natural resources and cultural-traditional-symbolic sustainability, the protection of species and genetic diversity, the protection of these natural and cultural areas with special importance against the disturbing effects in the environment, the improvement of environmental conditions, tourism and recreational purposes [1].

Geoparks are important places because of their scientific and educational significance, where geological and geomorphological formations are regarded as cultural heritage and at the same time they provide socio-economic development in the rural sense. In landscape planning and design, it is essential to make plan decisions for the most rational use of land, taking ecological factors into consideration. While geoparks are being planned; the preservation of the geological heritage for future generations, the training of people about geology and environment and the development of rural economy are the first things to be considered.

Scientific researchers can be done better by organizing and conserving geoparks and education, genetic diversity can be ensured and species can be saved, environmental conditions can be improved in every sense, natural resources sustainability and tourism opportunities can be provided, socio-economic development is supported. Development is not only in economic sense but in socio-cultural contexts. The continuity of scientific and educational work within the geopark area is essential. In addition, geoparks will increase the local awareness of the local people.

The purpose of this research is; the evaluation of the Seyhamami Geosite (Kizilcahamam-Camlidere) in terms of landscape design, to ensure that the geopark is a place where it is possible to meet the recreational needs of

the people who visit the scientific and touristic purpose and to have a good time, to contribute to the rural development of the local people and to prevent them from consuming / destroying geological heritage areas.

### ***1.1 Concepts of Geological Heritage, Geosite, Geotourism and Geopark***

It is hard to repair geological heritages in the event of its disappearance and in danger of extinction. It is all kinds of geological formations that can be regarded as valuable in terms of the documentation of the earth's geological history. These structures have been transformed into geological heritages under the influence of geomorphological factors and processes that have been going on for millions of years [2].

Geosite is a geological heritage element that carries natural inheritance in a geopark. The geosite may cover all or a small part of the geological heritage item associated with it. Not only geological or morphological elements but also earthquake-related associations which are associated with geological history and culture, are considered in the definition of geosite [3].

Geotourism is a trip in geological heritage areas that include scientific, educational, natural heritage, economic, conservation, geological and ecological items [2]. Geotourism is an area of social activity that has developed rapidly in recent years in addition where nature conservation and nature education can also be achieved and economic income can be provided [3].

Geoparks are areas that are protected by natural and cultural heritage. The socio-economic development aims especially in geological heritage zones. Geoparks are open spaces that can be visited by pedestrians or vehicles in the same geographical area [3].

### ***1.2 Planning and Design Approach in Geoparks***

Rural settlements are important with their natural surroundings and unique settlement characteristics. Rural landscape planning balancing between the natural characteristics of the rural area and the needs and desires of the society. The most important strength of rural recreation is the local culture that is in the people's daily life process. Recreational activities are being carried out in rural areas where the culture be lived, experienced and monitored [4]. The planning of rural areas for tourism and recreation is important for ensuring adequate and effective use of natural resources. Planning / design stage, in general be formed determination of problem and purpose, current situation analysis (survey), area usage diagram, evaluation / results.

There are some approaches to be applied in geopark planning and some criteria to be considered. These can be listed briefly as follows [5];

Geopark planning requires multidisciplinary studies. It will be more effective by working together for a planning group, including geological engineers, landscape architects and social science professions. Geological formations should not be damaged when planning the area. Adjusting the protection-use balance is a guide for regulations to be made in the area. Secondly it is important in terms of presentation of the area. It is necessary to explain the geological formations to the visitors and to inform them about the protection. Local people need to understand and learn well the subject in order to protect the area and to be able to own it.

The presentation of the site should be well done because this should be the beginning of the planning principles. They should be in the areas of geological heritage which are important in the scientific direction, rarely encountered and high aesthetic value. In addition to these, other important archaeological, ecological and historical aspects of the area should be considered as items. All of these archeological, historical, cultural and geological items in the area should be related to each other and arrangements should be made to inform the future tourists about the region. Walking, promenades and scenic navigation points should be determined, information panels and signs describing scientific features should be placed, transportation should be provided, brochures should be prepared, if necessary, relevant museums should be established and trips should be arranged by guides.

Participation in planning should be ensured in the local people. Local people can create new business opportunities by producing and selling some products belonging to that region. Thus, the quality of life increases, the economy develops, immigration can be prevented in large measure, the indigenous people have their own territory and thus the local identity is strengthened. Any use of the area should be planned and

implemented so as not to adversely affect the formation. The features that should be found in the accessories used in the designs in general are as follows [5, 6, 7];

Functional and aesthetic features should be taken into consideration in designing as well as original designs should be as possible; It must be easy to maintain or require too much maintenance; Must be in accordance with certain standards in terms of ergonomics and various physical properties; Must be suitable in terms of portability, mobility and availability of spare parts; It must be fast and robust; It should be resistant to vandalism.

## 2. MATERIAL METHOD

Seyhamami Geosite which is connected to Kizilcahamam-Camlidere Districts in Central Anatolia Region, Ankara, constitutes the study area and material. In the study, journals and books, reports, thesis studies, notices and articles were used as auxiliary materials. MTA's 1 / 100.000 scale Ankara H29-G29 sheet was used for area analysis, making plan decisions and creating landscaping pads. Ankara H29a4 and G29d3 topographic maps in 1/25000 scale covering Seyhamami were obtained from Ankara University Geological Engineering Department and used in conjunction with Google Earth images during the basin formation phases. The study area was visited within the scope of survey studies and photographs of the area were taken.

The fact that the Seyhamami geosite has not lost its historical feature and is still being preferred and used within the scope of health tourism in order to find healing by people has been the factor of choice. Landscape planning decisions and landscape design principles have been put forward in order to evaluate the geopark and geotourism potential of Seyhamami.

Topographic maps of the area were overlaid with Google Earth satellite imagery and drawn in Coreldraw and Auto Cad programs. The sketches with hand drawings were created after the base was created. These drawings were formed with Auto Cad 2014, Photoshop CS5, Sketch Up and Lumion programs and three dimensional landscape design models.

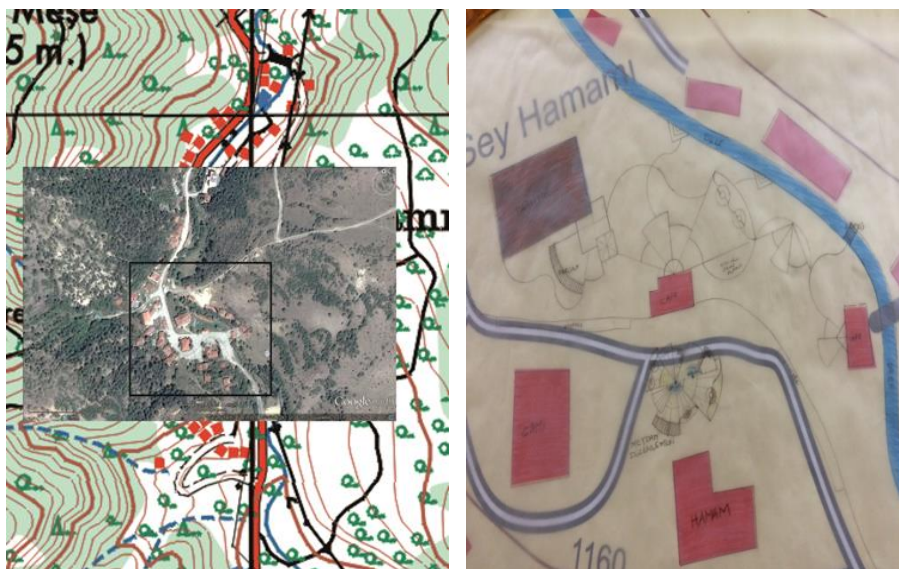


Figure 1. Overlaying the Google Earth image with a 1 / 25,000 topography map

Figure 2. View from Seyhamami Geosite landscape project sketch study

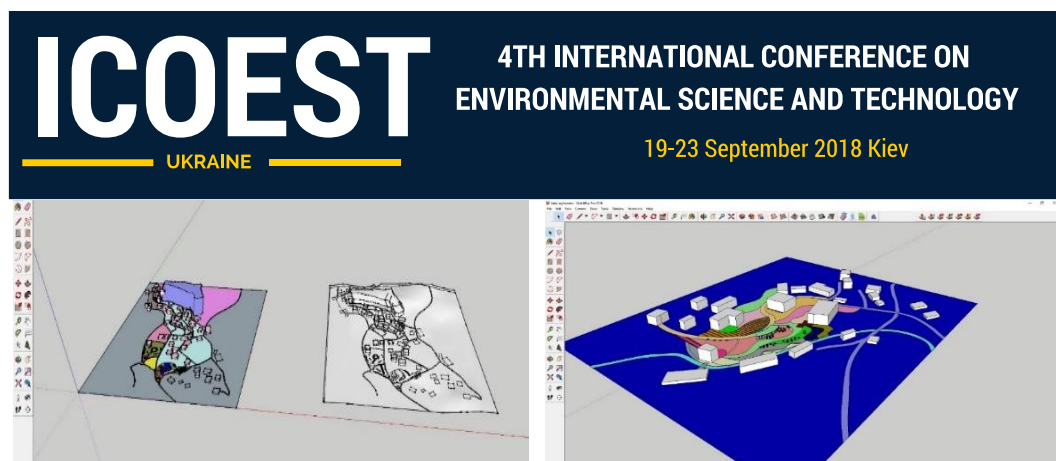


Figure 3, 4. A view from the Sketch Up stage of the project

### 3. RESULTS

#### 3.1 General Properties of Workspace

The study area is located between  $40^{\circ}28'(N)$  northern latitudes and  $32^{\circ}39'(E)$  eastern longitudes in terms of mathematics [8]; Seyhamami is 25 km from Kizilcahamam and 103 km from Ankara [9].

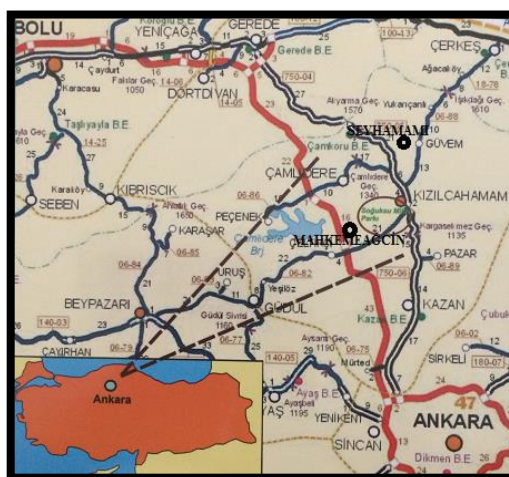


Figure 5. Location of the study area [11]

Kizilcahamam is located in the transition zone between Central Anatolia and Black Sea region. In this respect, climate characteristics of both regions are encountered [11]. The altitude of the Kizilcahamam is 975 m. The average annual temperature of the study area is  $9.9^{\circ}C$ . The amount of precipitation is 578,3 mm [10]. The average rainfall for many years is 545 mm. and the average humidity is 66% [12].

Kizilcahamam creates a transition between Central Anatolia and the Black Sea Region in terms of vegetation. In the middle of the creek is *Salix caprea* L., *Rubus caesius* L. On the roadside is *Rubus canescens* D.C., *Rosa foetida* J. Herm., *Prunus spinosa* L., *Acer campestre* L., *Acer hyrcanum* Fisch & Mey., *Ribes uva-crispa* L., *Populus tremula*, *Cornus mas*, *Acer campestre*, *Robinia pseudoacacia*, *Crataegus orientalis* var. *orientalis*, *Pyrus elaeagnifolia*. In the Kizilcahamam forests, the composition usually composed of natural landscape elements; *Pinus sylvestris*, *Pinus nigra*, *Abies* sp., *Quercus* sp. In general, the soil structure of Kizilcahamam is 6-7. class forest soil. The land of the Kizilcahamam valley is covered with an alluvium layer containing sand, silt and lava fragments. Under these alluviums the land forms the vicinity of the valley. Mainly calcareous brown forest soils are there in large land groups [10].

The volcanic cones, calderas, dikes, lava flows, pyroclastics and sediments such as tuffs and aglomas are the products of the volcanism that develops between 23-5 million years (Miocene) in the area [12].



The Hamam Stream, which is named from the city flows on the edge of Seyhamami. (K-G) directional fault extending along Hamamdere and a fault extending perpendicular to it (D-B). The temperature at the surface of the water is 44 °C. The bath was installed the exit of water. The water temperature and chemical composition is very suitable for hot spring tourism.

It is said that the Seyhamami Spas were built by German armies during the Crusades. The former name of the village of Sey Hamami is the Church. During the region of Iskender (the second half of XV) the church collapsed and a mosque was built at the same time. This mosque has been restored a number of times in the past. It was originally restored by the General Directorate of Foundations in 2007 and is still used as a mosque [12].

The population of Kizilcahamam is 25,021 by the year 2016. This population consists of 12,448 men and 12,573 women [11]. People living in rural areas generally provide their economical lives depending on the products and services they obtain from agricultural, forest and pasture lands [5]. Despite the presence of spas, the district is an officer and retirement settlement. Because the tourism revenues are under the expectation. As a result of these negative situations, the people in the region have migrated to other places, especially in Ankara. It is thought that it is possible for the district to become stronger in terms of the economic standpoint thanks to the tourism sector.



*Figure 6,7. Historical rural architecture in Seyhamami is a sample houses*



*Figure 8,9. Historic mosque and bath in Seyhamami*

### **3.2 Study Area Landscape Design Project**

The study area and its surroundings are very rich in geological respect. Natural, cultural, historical buildings, rich geological diversity and landscapes create opportunities in terms of geotourism. The use possibilities for health-tourism in Seyhamami Geosite are important uses of thermal-mineral waters. The landscape design of the area, which can be considered as thermal tourism, is important in terms of effective use of the area and meeting human needs in the most appropriate way.

The determination of natural, cultural and recreational landscape resource values and diversity of the study area, conservation and sustainable use of existing natural landscape was taken as a basis in consideration of conservation principle as well as aesthetic and functional area. People like these areas because of fresh air, silence, visual appeal of nature and so on. Day-to-day use and tent camping sites, especially in rural recreation areas where dominate forest, mountain and water landscapes, offer economical recreational activities with low cost to urban people.

Within the recreation programs organized by various tourism organizations, university nature clubs, photography clubs, mountaineering clubs, scout groups; there are scientific recreational uses such as camping, bird watching, taking nature photographs, nature walks which are introduced in nature guides. We will rank these areas according to the intensity of the activities they have visited; picnicking, watching the scenery, taking photos, walking, riding a bicycle, watching and examining animals and plants.

When you look at the area in general; the bath, the historical mosque and the pavilion around the area used as a pension in Seyhamami. There is no other vegetative element in this square and a huge hard surface appears that disturbs the human being. There is not a place where people can spend their time in this area where they are busy because of the people who come to take advantage of the summer bath.



Figure 10. An open space next to the Seyhamami pension



Figure 11. Current view of the area considered as a square arrangement in Seyhamami

The large pension is next to Seyhamami was thought picnic area, children's playground, viewing terrace and seating units. The existing large boarding house has been proposed to renew the facade in accordance with the area and other residences that are examples of regional architecture. In addition, a sales unit and a café where people can meet their needs are also considered. The area used as sales unit in the present is protected.

It is aimed to increase the visual values of the connection paths connecting these areas by creating the floor difference. Hamam Creek loses its water in the summer but still there are wooden terraces on the opposite side of the area. It has been considered to place new wooden bridges in order to pass the houses used by the people who come to the bath and to make activities such as taking pictures. It is thought that the picnic units intended to be used in this area are two-storeyed in the form of a pit and the lower parts are used for shading purposes.

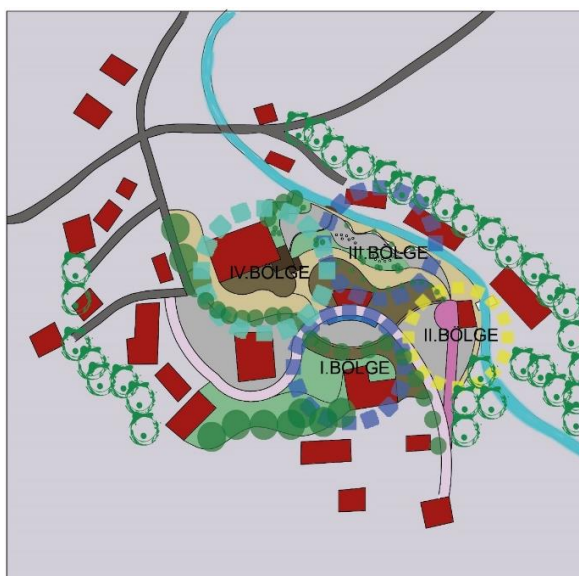


Figure 12. The landscape project stain plan study for Seyhamami





Figure 13. The landscape project definite plan study for Seyhamami

Existing plants have been tried to be preserved and new ones have been selected from natural species. Designed as a square in the middle of area which is aimed to utilize the visual effects of plants and water to break the monotony of the area in design while there is no plant in the area in now. The water was used in spacious area in front of the historical spa building because it reflects the value of the bath and because of its relaxing effect. The hard image of the area has been tried to soften with trees in the area. By creating flooring differences, the visual value of the area is increased and the pedestrian-vehicle path is separated from each other.

The trees and bushes used in project phase works: *Abies bornmulleriana*, *Acer campestre*, *Buxus sempervirens*, *Cornus mas*, *Pinus sylvestris*, *Pinus nigra*, *Populus tremula*, *Prunus spinose*, *Robinia pseudoacacia*, *Salix* sp., *Syringa vulgaris*, *Thuja orientalis*, *Rhododendron* sp., *Viburnum tinus*, *Quercus* sp.

The project has been modeled in 3-D programs in order to better determine the place and usage in the final project. In order to better understand these modeling studies, images were taken from different points of the field.



Figure 14. The landscape project for Seyhamami (in front of historical bath)



Figure 15. The landscape project for Seyhamami (view from the picnic area beside the pension, sitting units, viewing terrace)



Figure 16. The landscape project for Seyhamami (view from the picnic area, sitting units and the cafeteria)

#### 4. CONCLUSIONS AND RECOMMENDATIONS

The aim of the workshop is to provide a balanced design for recreation and art, which can be applied in a wide range of ways to meet the needs of the visitors, foreseeable for effective use of the available resources on the ground.

They can take nature walks and photo shoots on the Kavakozu chimneys near Seyhamami Geosite. Also, the Basalt Columns are on the road in tourism route. These geocide stops in the vicinity to Seyhamami will be a different activity for people who come for hot spring tourism.

The brochures to guide the people coming to the spa should be distributed and tours organized. The area can encourage people of all kinds who come to nature for a science while they are having fun where they can learn. These include activities such as botanical tourism, mountain climbing, mountain biking, rock climbing, nature photography, nature walk, photoperiod, wildlife observation, bird watching, hobby activities, picnic, camping tourism and grow numerous medical and aromatic plants naturally.

There are historical houses of old rural architecture in Seyhamami. These dwellings are usually rented as pensions to the arriving people. Apart from these house pensions, there is a big pension but this pension does not seem to be enough in terms of functionality and exterior appearance. This hostel can be restored to be more harmonious with nature and its functionality can be further increased. In addition, these original architectural structures have been restored and they can serve as boutique hotel and restaurant where regional specialties are served. It is thought that the number of visitors may increase if the area develops from this direction.

### REFERENCES

- [1]. Gul, A.. Korunan Dogal Alanlarin Planlama Sorunlari ve Ekolojik Yonetim Plani Onerisi. Cevre ve Orman Bakanligi 1. Cevre ve Ormancilik Surasi Tebligleri, (4),1421-1429, 2005.
- [2]. Acar, D. Jeoparklar: Pamukkale Ornegi. Uzmanlik Tezi, Kultur ve Turizm Bakanligi Yatirim ve Isletmeler Genel Mudurlugu, Ankara, 2008.
- [3]. Suludere, Y. ve Mulazimoglu, N. Kizilcahamam (Ankara) Bolgesinde Uygulamali Jeolojik Miras, Jeopark ve Jeoturizm Egitimi. Tubitak Bilim ve Toplum Projeleri Destekleme Programi, Ankara, 2011.
- [4]. Cinar, M. Kirsal Arazi Planlamalarinda Peyzaj Planlamasinin Yeri ve Onemi. Yuksek Lisans Tezi, Ataturk Universitesi, s. 118, Erzurum, 2007.
- [5]. Yilmaz, A. Jeolojik Mirasimiz. Bilim ve Teknik, 416, 92-93, Ankara, 2002.
- [6]. Guney, A., Erdem, U., Turkyilmaz, B. ve Hepcan. S. Peyzaj Konstruksiyonu, Ege Universitesi Ziraat Fakultesi Yayinlari, 147, Izmir, 1996.
- [7]. Saglik, A., Saglik, E. ve Kelkit, A. Kentsel Donati Elemanlarinin Peyzaj Mimarligi Acisindan Irdelenmesi Canakkale Kent Merkezi Ornegi, 1. Uluslararası Kentsel Planlama-Mimarlik Kongresi. 1023-1035, Kocaeli, 2014.
- [8]. 2016, URL 8. <https://tr.wikipedia.org/wiki/Kizilcahamam>
- [9]. 2016, URL 10. <http://www.yerturk.com/yer-sey-hamami-kizilcahamam-ankara.html#ad-image-0>
- [10]. Kizilcahamam Orman Isletme Mudurlugu, Soguksu Milli Parki Uzun Devreli Gelisme Plani, Analitik Etud Raporu, 2010.
- [11]. Kizilcahamam Belediyesi Yayinlari, Kizilcahamam-Camlidere Jeoparki, Ankara, 2016.
- [12]. Kazanci, N., Suludere, Y., Mulazimoglu, N., Tuzcu, S., Mengi, H., Hakyemez, H. Y. ve Mercan, N. Soguksu Milli Parki ve Cevresi Jeositleri, Milli Parklarda Jeolojik Miras- 1, Doga Koruma ve Mili Parklar Genel Mudurlugu Jeolojik Mirasi Koruma Dernegi, Ankara, 2007.

# A Study on the Determination of the Effects of Carbon Structures of FAME Fuels on Fuel Properties

*Mustafa Acaroglu<sup>1</sup>, A. Engin Ozcelik<sup>1</sup> Hasan Aydogan<sup>1</sup> Metin Cinar<sup>2</sup>*

## Abstract

*In the present study, two different types of safflower (Dincer and Remzibey-05), palm, mustard, cottonseed and rapeseed ME produced through transesterification were selected as the research material. FAME fuels produced by the transesterification method, the measured density, kinematic viscosity, heating value and cetane number, determined by gas chromatography according to the chemical structure and the carbon bonds, these equations are calculated, and the availability of statistical re-examined with empirical equations. Safflower measured fuel density, kinematic viscosity, HHV and CN 880 kg/m<sup>3</sup>, respectively, 3.98 mm<sup>2</sup> / s, 40 MJ / kg, 49.3, 885.31 kg/m<sup>3</sup>, while the calculated values, 4.00 mm<sup>2</sup> / s, 38.86 MJ / kg and found to 49.339.*

**Keywords:** biodiesel, cetane number, density, fuel properties, kinematic viscosity, HHV

## 1. INTRODUCTION

The world-wide development of biofuels today is a challenging and complex endeavor that gives rise to a number of questions that originate from the multitude of stakeholders and complex trade-offs that the production, distribution, and utilization of biofuels involves. The current interest in biofuels development stems from a major global reevaluation of traditional energy sources. Potential feedstocks include safflower, rapeseed, canola, jatropha, and palm oil. Biodiesel is used to substitute for diesel. It focuses on ethanol, the most commonly used biofuel to substitute for gasoline, and biodiesel, a substitute for diesel [1,2].

**Table 1** Chemical composition of FAME and diesel fuels

Properties	Diesel fuel	Rapeseed Methyl Ester
Formula	C <sub>12,226</sub> H <sub>23,29</sub> S <sub>0,0575</sub>	C <sub>19</sub> H <sub>34</sub> O <sub>2</sub> (or C <sub>19</sub> H <sub>36</sub> O <sub>2</sub> )
Composition (% per mass)	C:H:O (86.6: 13.4:0)	C:H:O (77.6:11.5:10.9)
Molecular weight (g/mol)	120-320	~295

Biodiesel fuels display higher density than diesel fuels, which is also reflected by the respective limits within the FAME (Fatty Acid Methyl Ester) standard (860-900 kg/m<sup>3</sup> at 15 C) and the petrol diesel fuel norm EN 590 (820-845 kg/m<sup>3</sup> at 15 C). Besides, biodiesel density values may differ depending on the measured temperature (Table 2). EN ISO 3675 standards apply in the density measurements with hydrometers and EN ISO 12185 standards apply in the density measurements performed using an oscillating U-tube [3-13].

<sup>1</sup> Selcuk University, Technology Faculty, Mechanical Engineering Department, 42031 Campus Konya Turkey

<sup>2</sup> CNR Consulting

*Table 2 Density of the selected FAME*

FAME	Density (kg/m <sup>3</sup> )	FAME	Density (kg/m <sup>3</sup> )
<b>C6:0</b>	889 (15)	<b>C16:0</b>	884 (20)
<b>C8:0</b>	881 (15)	<b>C18:0</b>	852 (38)
<b>C10:0</b>	876 (15)	<b>C18:1</b>	874 (20)
<b>C12:0</b>	873 (15)	<b>C18:2</b>	894 (15)
<b>C14:0</b>	867 (20)	<b>C18:3</b>	904 (15)

Kinematic viscosity is one of the most important features of biodiesel fuels. The viscosity of biodiesel fuels is generally higher compared to that of diesel fuel. At 40 °C temperature by FAME standards, these values vary between 3.50 - 5.00 mm<sup>2</sup>/s, while the viscosity values of diesel fuel vary between 2.00 - 4.50 mm<sup>2</sup>/s. There is a strong relationship between the kinematic viscosity values and the fatty acid compositions of biodiesels (Table 3) [14-22].

*Table 3 Kinematic viscosity of FAME*

FAME	C14:0	C16:0	C18:0	C18:1	C18:2	C18:3
Kinematic Viscosity at 40 °C (mm <sup>2</sup> /s)	3.24	4.32	5.56	4.45	3.64	3.27

By both the EN 14214 biodiesel standard and EN 590 diesel fuel standard, the minimum cetane number expected from the fuel is 51. Cetane number measurements yield fairly high values as 62 for palm, 62 for coconut and 58 for tallow FAME. Biodiesel fuels have advantages over diesel fuel in terms of cetane number (Table 4) [4, 22-33].

*Table 4 Cetane Numbers (CN) of selected FAME fuels*

	C10:0	C12:0	C14:0	C16:0	C18:0	C18:1	C18:2	C18:3
CN	47.9	60.8	73.5	74.3	75.7	55.0	42.2	22.7

The examination of fatty acid compositions show that cetane number values show an increase as the level of saturation of fatty acids decrease. However, a significant decrease is observed in the cetane number of biodiesel fuels with the increase of fatty acid contents especially after the C18:0 compositions. Considering the effect of cetane number on fuel combustion in diesel technology vehicles, the use of fuels with high CN but low viscosity and density such as palm, tallow and coconut by mixing with fuels that have good viscosity and density values like linseed and safflower would help in solving the problem [2].

Higher heating value (HHV) is determined via a bomb calorimeter. It includes the energy which is released by the condensation of water vapor produced during combustion and is therefore higher than Lower Heating Value (LHV), which is calculated from HHV. According to EN 14214 standards, the minimum HHV value for biodiesel fuels is expected to be 35.0 MJ/kg. Unsaturated fatty acid and carbon length are highly determinative factors for calorific value in FAME fuels (Table 5) [25, 30, 34-48].

*Table 5 Calorific values for Fatty Acid Supply Chain*

	C12:0	C14:0	C16:0	C18:0	C18:1	C18:2	C18:3
Calorific value (MJ/kg)	37.0	38.3	39.6	40.3	38.9	38.7	39.9

## 2. MATERIAL AND METHODS

In the present study, two different types of safflower (Dincer and Remzibey-05), palm, mustard, cottonseed and rapeseed ME produced through transesterification were selected as the research material. Methanol was used as alcohol and NaOH was used as catalyst in the transesterification process [49-54]. Three different procedures were used to examine Safflower ME [from Dincer], (SME-D). First, SME-D was not subjected to any procedures (washing drying) but directly analyzed following the transesterification process. In the second

procedure, SME-D was not subjected to washing but heated up to 97 °C. In this way, the methanol and water that might have remained were evaporated. In the third procedure, SME-D was subjected to washing and drying following the transesterification process. Carbon structures of the biodiesel oils investigated. These are measured individually (Table 6) [39, 49-60]. Methyl esters of the samples were prepared through transmethylation using KOH 2 mol/Liter in methanol and n-heptane in accordance with the method of ISO-5509 [57]. Density, kinematic viscosity, heat value and cetane number of the FAME fuels that were produced through transesterification were calculated using the coefficients given in Tables 1 to 5 with respect to fatty acid components.

**Table 6 Carbon structure for Fatty Acid Methyl Esters**

	Safflower Biodiesel	Safflower-2	Safflower-unwashed	Safflower-washed-drying	Palmoil Biodiesel	Palmoil Biodiesel - 10% additive	Rapeseed-00 Biodiesel	Mustard Biodiesel	Cottonseed Biodiesel
<b>C 10:0</b>	0	0.01	0.02	0.01		0.02		0.01	0.01
<b>C 12:0</b>	0	0	0.01	0.11	0.13	0.02		0.01	0.02
<b>C13:0</b>					0.26	0.23	0.1		
<b>C 14:0</b>	0.07	0.08	0.07	0.01	1.21	1.05		0.68	0.68
<b>C 16:0</b>	6.17	6.31	6.19	7.09	39.35	39.71	6.00	21	20.54
<b>C16:1</b>							0.37		0.81
<b>C17:0</b>							0.11		
<b>C 18:0</b>	2.7	2.66	2.63	2.6	3.8	3.26	1.50	1.85	1.85
<b>C 18:1</b>	33.06	32.74	32.48	32.76	44.86	44.92	63.12	20.27	20.45
<b>C 18:2</b>	58	58.2	58.59	57.41	10.38	10.8	19.08	56.17	55.91
<b>C. 18:3 n-3</b>							7.66		

### 3. RESULTS AND DISCUSSION

Laboratory measurement results are given in Table 7. The values calculated separately with respect to fatty acid content are presented in Table 8- Table 12.

**Table 7 Measured Fuel Properties of Methyl Esters**

	Density (kg/m3)	Kinematic Viscosity (at 40 °C mm <sup>2</sup> /s)	Heat Combustion (MJ/kg)	Cetane Number
SME-RB (Remzibey-05)	880	3.98	40	49.03
Safflower (Dincer) (SME-D)	883	4.03	39.6	49.80
SME-D unwashed	885	4.03	39.6	49.00
SME-D (washed +dried)	885	4.00	39.98	50
Palm oil ME (PAME)	880	5.89	37.0	60
Palm oil ME + 10% additive	868	5.45	36.4	57
Rapeseed ME	875	4.4	37.1	56
Black Mustard ME (BMME)	887	5.96	40.35	55.8
Cottonseed ME (COME)	872	4.95	37.20	51

**Table 8 Density values of Methyl Esters calculated based on fatty acid content**

Factor	SME-RB	SME-D	SME-D unwashed	SME-D (W+D)	PAME	PAME + 10% additive	RME	BMME	COME
<b>C6:0</b>	889.00	0	0	0	0	0	0	0	0



<b>C8:0</b>	881.00	0	0	0	0	0	0	0	0	0
<b>C10:0</b>	876.00	0	0.01	0.01	0.01	0	0.02	0	0.01	0
<b>C12:0</b>	873.00	0	0	0	0.11	0.11	0.02	0	0.01	0.02
<b>C13:0</b>	870.00	0	0	0	0	0.26	0.23	0.1	0	0
<b>C14:0<sup>&amp;</sup></b>	886.57	0.07	0.08	0.07	0.01	1.22	1.05	0	0.68	0.69
<b>C16:0<sup>&amp;</sup></b>	883.56	6.17	6.31	6.18	7.09	39.37	39.7	6.47	21	20.27
<b>C18:0<sup>&amp;</sup></b>	850.07	2.73	2.67	2.67	2.66	3.8	3.28	1.54	1.86	1.86
<b>C18:1<sup>&amp;</sup></b>	873.57	33.02	32.72	32.45	32.71	44.87	44.93	63.12	20.27	20.44
<b>C18:2</b>	894.00	58	58.21	58.60	57.40	10.37	10.77	19.09	56.17	55.91
<b>C18:3</b>	904.00	0	0	0	0	0	0	9.68	0	0
<b>Density (kg/m<sup>3</sup>)</b>	885.31	885.47	885.36	885.29	878.88	879.09		880.69	886.79	879.59

<sup>&</sup> re-calculated for a temperature of 20 °C

**Table 9** Kinematic viscosity values calculated based on fatty acid content

	Factor	SME- RB	SME- D	SME-D unwashed	SME- D (W+D)	PAM E	PAME +10% additive	RM E	BMME	COM E
<b>C14:0</b>	3.24	0.07	0.08	0.07	0.01	1.22	1.05	0	0.68	0.69
<b>C16:0</b>	4.32	6.17	6.31	6.18	7.09	39.37	39.7	6.47	21	20.27
<b>C18:0</b>	5.56	2.73	2.67	2.67	2.66	3.8	3.28	1.54	1.86	1.86
<b>C18:1</b>	4.45	33.02	32.72	32.45	32.71	44.87	44.93	63.12	20.27	20.44
<b>C18:2</b>	3.64	58	58.21	58.6	57.4	10.37	10.77	19.09	56.17	55.91
<b>C18:3</b>	3.27	0	0	0	0	0	0	9.68	0	0
<b>kinematic viscosity (mm<sup>2</sup>/s)</b>		4.001	3.998	3.994	3.999	4.325	4.322	4.185	3.979	3.946

**Table 10** HHV values calculated based on fatty acid content

	Factor	SME-RB	SME-D	SME-D unwashed	SME-D (W+D)	PAME	PAME + 10% additive	RME	BMME	COME
<b>C12:0</b>	37.0	0	0	0	0.11	0.11	0.02	0	0.01	0.02
<b>C14:0</b>	38.3	0.07	0.08	0.07	0.01	1.22	1.05	0	0.68	0.69
<b>C16:0</b>	39.6	6.17	6.31	6.18	7.09	39.37	39.7	6.47	21	20.27
<b>C18:0</b>	40.3	2.73	2.67	2.67	2.66	3.8	3.28	1.54	1.86	1.86
<b>C18:1</b>	38.9	33.02	32.72	32.45	32.71	44.87	44.93	63.12	20.27	20.44
<b>C18:2</b>	38.7	58	58.21	58.60	57.40	10.37	10.77	19.09	56.17	55.91
<b>C18:3</b>	39.9	0	0	0	0	0	0	9.68	0	0
<b>HHV (MJ/Kg)</b>		38.861	38.860	38.851	38.862	39.097	39.098	38.986	38.952	38.636

**Table 11** Cetane Number values calculated based on fatty acid content

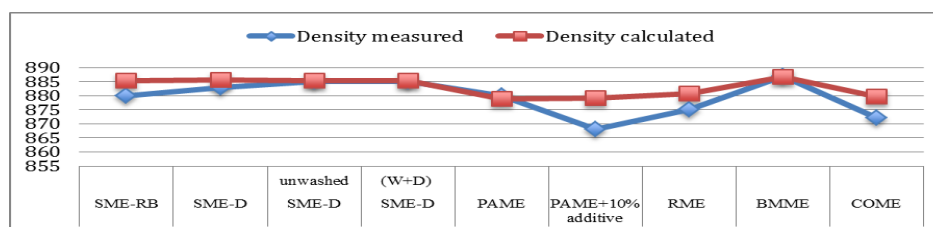
	Factor	SME-RB	SME-D	SME-D unwashed	SME-D (W+D)	PAME	PAME+10 % additive	RME	BMME	COME
--	--------	--------	-------	-------------------	----------------	------	-----------------------	-----	------	------

<b>C10:0</b>	47.9	0	0.01	0.01	0.01	0	0.02	0	0.01	0
<b>C12:0</b>	60.8	0	0	0	0.11	0.11	0.02	0	0.01	0.02
<b>C14:0</b>	73.5	0.07	0.08	0.07	0.01	1.22	1.05	0	0.68	0.69
<b>C16:0</b>	74.3	6.17	6.31	6.18	7.09	39.37	39.7	6.47	21	20.27
<b>C18:0</b>	75.7	2.73	2.67	2.67	2.66	3.8	3.28	1.54	1.86	1.86
<b>C18:1</b>	55.0	33.02	32.72	32.45	32.71	44.87	44.93	63.12	20.27	20.44
<b>C18:2</b>	42.2	58	58.21	58.6	57.4	10.37	10.77	19.09	56.17	55.91
<b>C18:3</b>	22.7	0	0	0	0	0	0	9.68	0	0
<b>Cetane Number</b>	49.339	49.334	49.246	49.574	62.147	62.029	50.94	52.373	51.820	

*Table 12 Measured and calculated values of FAME fuels*

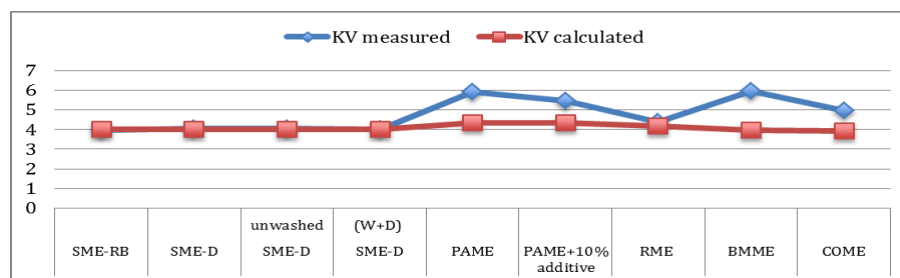
Properties	SME-RB	SME-D	SME-D unwashed	SME-D (W+D)	PAME	PAME+10 % additive	RME	BMME	COME
Density measured	880	883	885	885	880	868	875	887	872
<b>Density calculated</b>	<b>885.31</b>	<b>885.47</b>	<b>885.36</b>	<b>885.29</b>	<b>878.88</b>	<b>879.09</b>	<b>880.69</b>	<b>886.79</b>	<b>879.59</b>
KV measured	3.98	4.03	4.03	4.00	5.89	5.45	4.4	5.96	4.95
<b>KV calculated</b>	<b>4.00</b>	<b>3.99</b>	<b>3.99</b>	<b>3.99</b>	<b>4.32</b>	<b>4.32</b>	<b>4.18</b>	<b>3.97</b>	<b>3.94</b>
HHV measured	40	39.6	39.60	39.98	37.00	36.40	37.10	40.35	37.20
<b>HHV calculated</b>	<b>38.86</b>	<b>38.86</b>	<b>38.85</b>	<b>38.86</b>	<b>39.09</b>	<b>39.09</b>	<b>38.98</b>	<b>38.95</b>	<b>38.63</b>
CN measured	49.03	49.80	49.00	50.00	60.00	57.00	56.00	55.80	51.00
<b>CN calculated</b>	<b>49.34</b>	<b>49.33</b>	<b>49.25</b>	<b>49.57</b>	<b>62.15</b>	<b>62.03</b>	<b>50.94</b>	<b>52.37</b>	<b>51.82</b>

It can be seen from Figure 1 that there were not large variations in both measured and calculated values for safflower ME, but negligible variations were observed. However, the calculated density value was found to be higher than the measured value in Palm Methyl Ester with 10% additive.



*Figure 1 Density Variations*

Figure 2 shows that measured and calculated kinematic viscosity values were identical in all safflower ME samples. However, measured kinematic viscosity was higher than calculated kinematic viscosity in Palm and Mustard ME fuels with high saturated fatty acid content. The reason for this difference is that the coefficients of fatty acid values have a nominal distribution within themselves.



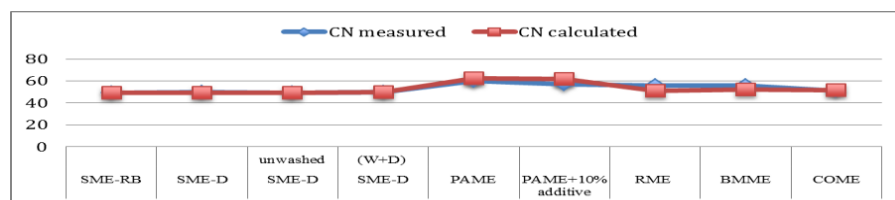
*Figure 2 Kinematic viscosity variations*

In Safflower ME, measured HHV values were found to be slightly higher than calculated HHV values. Measured HHV values were found to be smaller than calculated HHV values in PAME, PAME+10% and COME (Figure 3).



*Figure 3. HHV variations*

Figure 4 does not show a difference in CN variations. Measured CN values are equivalent to calculated CN values.



*Figure 4 CN variations*

Analysis of the measured results and the calculated results are consistent and are in close proximity. Accurate and precise measurement result in the multiple structures biofuel carbon fuels and fuel characteristics can be determined by using fatty acid components.

#### 4. ACKNOWLEDGEMENT

Selcuk University Scientific Research Projects Coordinating Office (Project Number 18701256) supports this study.

#### REFERENCES

- [1] M Acaroglu, Renewable Energy Sources, (Second Edition), Nobel Publishers, 609 pages, ISBN: 9786053950479, Ankara, 2007
- [2] M Acaroglu, M Unaldi Encyclopedia of Energy Research and Policy, Chapter 20. The Energy Balance and Fuel Properties of Biodiesel, pp. 589-602, Nova Publishers, USA, 2009
- [3] EN 590 Automotive fuels - Diesel - Requirements and test methods
- [4] EN ISO 3675 Crude Petroleum and Liquid Petroleum Products - Laboratory Determination of Density or Relative Density – Hydrometer Method
- [5] EN ISO 12185:1996. Crude petroleum and petroleum products - Determination of density - Oscillating U-tube method, 1<sup>st</sup> Edition
- [6] CW Bonhorst, PM Althouse, HO Triebold, Esters of Naturally Occurring Fatty Acids, Industrial and Engineering Chemistry (1948) 40 (12), 2379-2384, 1948
- [7] NL Drake, JR Spies, Croton resin III. The combined acids, Journal of the American Chemical Society 57, 184-187, 1935
- [8] KY Liew, CE Seng, LL Oh, Viscosities and Densities of the Methyl Esters of Some n-Alconic Acids. Journal of American Oil Chemists'Society, 69 (2), 155-158, 1992
- [9] FA Norris, DE Terry, Precise laboratory fractional distillation of fatty acid esters, Oil and Soap 22, 41-46, 1945

- [10] W Treibs, Autoxidation of oxygen-active acids. II Viscosimetric analysis of the addition of oxygen to methyl esters. *Berichte der deutschen chemischen Gesellschaft* 75B, 331-335, 1942
- [11] DH Wheeler, RW Riemenschneider, Preparation and properties of highly purified methyl olate, *Oil and Soap* 16, 207-209, 1939
- [12] ME Tat, JH Van Gerpen, The Specific Gravity of Biodiesel and Its Blends with Diesel Fuel, *J. Am. Oil Chem. Soc.* 77 (2), 115-119, 2000
- [13] ME Tat, JH Van Gerpen, The Kinematic Viscosity of Biodiesel and Its Blends with Diesel Fuel, *J. Am. Oil Chem. Soc.* 76 (12): 1511-1513, 1999
- [14] EN ISO 3104:1994. Petroleum products - Transparent and opaque liquids - Determination of kinematic viscosity and calculation of dynamic viscosity
- [15] CAW Allen, KC Watts, RG Ackman, MJ Pegg, Predicting the Viscosity of Biodiesel Fuels from Their Fatty Acid Ester Composition, *Fuel*, 78: 1319-1326, 1999
- [16] M Canakci, A Monyem, JH Van Gerpen, Accelerated oxidation process in biodiesel, *Trans. ASAE* 42(6): 1565-1572, 1999
- [17] S Kerschbaum, G Rinke, Measurement of the temperature dependent viscosity of biodiesel fuels. *Fuel*, 83(3): 287-291, 2004
- [18] A Srivastava, R Prasad, Triglycerides-based diesel fuels, *Renewable and Sustainable Energy Reviews*, 4, 111-133, 2000
- [19] O Syassen, Diesel engine technologies for raw and transesterified plant oils as fuels: desired future qualities of the fuels, p. 47-63. In Martini, N. and Schell, J. S. (ed.), *Plant oils as fuels*. Springer-Verlag, Heidelberg, 1998
- [20] G Vellguth, Pflanzenöl als Dieselkraftstoff-Substitut. Sonderdruck aus *Landbauforschung Volkenrode* 1, 12-16, 1998
- [21] M Worgetter, H Prankl, J Rathbauer, Eigenschaften von Biodiesel. *Landbauforschung Volkenrode. Sonderheft 190 (Biodiesel-Optimierungspotentiale und Umwelteffekte)*, p: 31-43, ISSN: 04586859, 1998
- [22] EN ISO 5165:1998. Petroleum products - Determination of the ignition quality of diesel fuels - Cetane engine method
- [23] EN 14214 Automotive fuels - Fatty acid methyl esters (FAME) for diesel engines - Requirements and test methods
- [24] EN 14213 - Heating fuels - Fatty acid methyl esters (FAME) - Requirements and test methods
- [25] W Korbitz, Biodiesel Production in Europe and North America, An Encouraging Prospect, *Renewable Energy* 16, 1079-1083, 1999
- [26] G Knothe, RO Dunn, Recent Results from Biodiesel Research at the National Center for Agricultural Utilization Research, *Landbauforschung Volkenrode, Sonderheft 190 (Biodiesel. Optimierungspotential und Umwelteffekte)*, 69-78, 1998
- [27] G Knothe, Einfluss der Struktur von Fettsäurealkylestern auf die Kraftstoffeigenschaften des Biodiesels, in Munack, A., and J. Krahel (eds.) *Biodiesel. Potenziale, Umweltwirkungen, Praxiserfahrungen*. Braunschweig: Landbauforschung Volkenrode, 115-124, 2002
- [28] G Knothe, RO Dunn, MW Shockley, MO Bagby, Synthesis and characterization of some long-chain diesters with branched or bulky moieties. *J Am Oil Chem Soc.*, 77(8):865-71, 2000
- [29] B Freedman, MO Bagby, H Khoury, Correlation of Heats of Combustion with Empirical Formulas for Fatty Alcohols, *J. Am. Oil Chem. Soc.*, 66: 595-596, 1989
- [30] JC Thompson, CL Peterson, DL Reece, SM Beck, Two-Year Storage Study With Methyl And Ethyl Esters Of Rapeseed, *Transactions of the ASAE* 41 (4), 931-939, 1998
- [31] JH Van Gerpen, Cetane number testing of biodiesel. *Proc. 3rd Conf. ASAE Liquid Fuel*, September 15-17, 197-206, Nashville, TN, USA, 1996
- [32] B Freedman, MO Bagby, Predicting Cetane Numbers of n-Alcohols and Methyl Esters from Their Physical Properties. *Journal of the American Oil Chemists' Society*, 67 (9): 565-571, 1990
- [33] WE Klopfenstein, Effect of Molecular Weights of Fatty Acid Esters on Cetane Numbers as Diesel Fuels, *J. Am. Oil Chem. Soc.*, 62: 1029-1031, 1985
- [34] CS Hawkins, J Fuls, Comparative Combustion Studies on Various Plant Oil Esters and the Long Term Effects of an Ethyl Ester on a Compression Ignition Engine, *ASAE publications* 4, 184-197, 1982
- [35] SJ Clark, L Wagner, MD Schrock, PG Piennaar, Methyl and ethyl esters as renewable fuels for diesel engines, *JAOCS*, 61:1632-1638, 1984
- [36] SC Borgelt, TS Kolb, LG Schumacher, "Biodiesel: World Status," *Liquid Fuels, Lubricants and Additives from Biomass, Proceedings of an Alternative Energy Conference*, Ed. by B.E. Dale, ASAE, 16-17 June 1994, Kansas City, MO, pp. 67-76, 1994
- [37] A Munack, J Krahel, H Speckmann, A Fuel Sensor for Biodiesel, Fossil Diesel Fuel, and Their Blends, 2002 ASAE Annual Meeting/CIGR XVth World Congress, paper no. 026081, Chicago, 2002
- [38] M Mittelbach, C Remschmidt, *Biodiesel the comprehensive handbook*, Second Edition, Boersdruck Ges.m.b.H., Vienna, 2005
- [39] B Freedman, MO Bagby, TJ Callahan, TW Ryan III, Cetane Numbers of Fatty Esters, Fatty Alcohols and Triglycerides Determined in a Constant Volume Combustion Bomb, *SAE Technical Paper Series 900343*, SAE, Warrendale, PA, 1990

- [40] E Goering, W Schwab, J Daugherty, H Pryde, J Heakin, Fuel properties of eleven vegetable oils. Trans. ASAE, 25:1472–1483, 1982
- [41] TH Gouw, JC Vlugter, CJA Roelands, Physical Properties of Fatty Acid Methyl Esters. VI. Viscosity, J. Am. Oil Chem. Soc., 43: 433–434, 1966
- [42] WE Klopfenstein, HS Walker, Efficiencies of Various Esters of Fatty Acids as Diesel Fuels, Journal of American Oil Chemists' Society 60 (8), 1596-1598, 1983
- [43] G Knothe, AC Matheaus, TW Ryan III, Cetane numbers of branched and straight-chain fatty esters determined in an ignition quality tester. Fuel 82, 971–975, 2003
- [44] G Knothe, MO Bagby, and TW Ryan III, Precombustion of fatty acids and esters of biodiesel, A possible explanation for differing cetane numbers, J. Am. Oil Chem. Soc., 75, 1007-1013, 1998
- [45] G Knothe, MO Bagby, TW Ryan III, Cetane Numbers of Fatty Compounds: Influence of Compound Structure and of Various Potential Cetane Improvers, SAE Technical Paper Series 971681, in State of Alternative Fuel Technologies, SAE Publication SP-1274, SAE, Warrendale, PA, 1997, pp. 127–132
- [46] GM Pischinger, AM Falcon, RW Siekmann, FR Fernandes, Methyl esters of plant oils as diesel fuels, either straight or in blends. Vegetable Oil Fuels, ASAE Publication 4-82, St. Joseph, MI: Amer. Soc. Agric. Eng, 1982
- [47] AW Schwab, MO Bagby, B Freedman, Preparation and properties of diesel fuels from vegetable oils, Fuel, 66:1372–1378, 1987
- [48] M Acaroglu, A Demirbas, Relationships between viscosity and density measurements of Biodiesel Fuels, Energy Sources, Part A, 29, 8, 705 – 712, 2007
- [49] Y Ali, MA Hanna, SL Cuppett, Fuel properties of tallow and soybean oil esters, JAOCS (1995) 72:1557–1564, 1995
- [50] BK Bala, Studies on biodiesels from transformation of vegetable oils for diesel engines, energy Edu. Sci. Technol., 15:1–43, 2005
- [51] G Knothe, KR Steidley, Kinematic viscosity of biodiesel fuel components and related compounds. Influence of compound structure and comparison to petrodiesel fuel components. Fuel, 84, 1059-1065, 2005
- [52] G Knothe, RO Dunn, Dependence of oil stability index of fatty compounds on their structure and concentration and presence of metals, J. American Oil Chem. Soc., 80(10): 1021–1026, 2003
- [53] F Ma, MA Hanna, Biodiesel production: A review. Bioresources Technology, 70:1–15, 1999
- [54] G Knothe, Dependence of biodiesel fuel properties on the structure of fatty acid alkyl esters. Fuel Proc. Technol., 86, 1059-1070, 2005
- [55] ASTM D 6584 Determination of Free and Total Glycerine in B-100 Biodiesel Methyl Esters by Gas Chromatography
- [56] EN 14331 Liquid petroleum products, Separation and characterization of fatty acid methyl esters (FAME) by liquid chromatography/gas chromatography (LC/GC)
- [57] ISO-5509, International Organization for Standardization (1978), Animal and Vegetable Fats and Oils-Preparation of Methyl Esters of Fatty Acids, ISO Geneve, Method ISO 5509, p. 1-6.
- [58] C Mariani, P Bondioli, S Venturini, E Fedeli, Vegetable Oil Derivatives as Diesel Fuel. Analytical Aspects, Note 1: Determination of Methyl Esters, Mono-, Di-, and Triglycerides, Riv. Ital. Sostanze Grasse, 69: 549–551, 1991
- [59] M Mittelbach, Diesel Fuel Derived from Vegetable Oils, V [1]: Gas Chromatographic Determination of Free Glycerol in Transesterified Vegetable Oils, Chromatographia, 37:623–626, 1993
- [60] prEN 14538 Fat and oil derivatives, FAME, Determination of Ca and Mg content by optical emission spectral analysis with inductively coupled plasma (ICP OES)

## Comparison of Performance and Combustion Characteristics of Methyl Ester and Ethanol Used In a Common Rail Diesel Engine

Hasan Aydogan<sup>1</sup>, Mustafa Acaroglu<sup>1</sup>, A. Engin Ozcelik<sup>1</sup>

### Abstract

*The use of oxygen fuels as alternative diesel fuels or in fossil fuels has always been on the agenda in reducing exhaust emissions from internal combustion engine vehicles. In fact, despite the fact that Rudolf Diesel originally used African origin ground oil as a diesel fuel, fossil-based fuels with higher energy content and higher energy content have become more widely used in diesel engines. Biodiesel is based on vegetable or animal fats is defined as the mono alkyl ester of the fatty acid chain. In this study, the effects of the engine power and torque performance of the Camellia biodiesel fuels by transesterification on fuel. Combustion characteristics of these fuels collationed to diesel fuel were identified at B20D80 and B20E15D65 ratios. With diesel fuel and all other fuel mixtures, the maximum engine power is achieved at 2500 rpm. At 2500 rpm, the engine power was reduced by the use of B20D80 fuel and by the use of B20E15D65 fuel compared to petrol diesel. This is due to the low heating value of the fuel. The maximum torque was found at 2000 rpm. At 2000 rpm, the engine torque was found at 181 Nm using petrol diesel fuel. The engine torque was found as 172 Nm with the B20D80 fuel and 161 Nm with the B20E15D65 fuel.*

**Keywords:** Diesel Engine Performance, Cameline Biodiesel, Combustion Characteristics

### 1. INTRODUCTION

Diesel engines have a bigger footprint in today's developing and developing countries, especially with the development of technology in the field of transportation. In 1997, the Kyoto Protocol was signed in Kyoto, Japan by 30 developed states to reduce carbon dioxide (CO<sub>2</sub>) emissions, which are greenhouse effect at global warming [1-7]. With the Kyoto protocol, a significant reduction in greenhouse emissions is anticipated by 2012. The EU Commission also issued Directive 2003/30 / EC on 8 May 2003 promoting the production of biofuels for use in the transport sector. Governments have had to take increasingly stringent measures on emissions, especially after the Kyoto Protocol. As a result of these measures, automotive manufacturers are also constantly working on vehicle and engine development to reduce emissions. The European Union (EU) has introduced and implemented Euro norms [8-11].

Today, vehicle manufacturers use exhaust emissions from diesel engine vehicles in acceptable limits to meet Euro norms by using systems such as high pressure fuel injection systems, gradual spraying, three-way catalytic converters, exhaust gas recycling, particulate filters, diesel engine management and control of spray initiation trying to pull [12-16].

Biodiesel is a renewable alternative diesel fuel and its usage has become more popular in the world. The alcohol which is used in the biodiesel production is very important and it directly affects the fuel properties. Different fuel properties may cause different injection and combustion characteristics in diesel engines. Camelina sativa plant is grown in summer and winter. Camelina sativa relatively resistant to standing, except for heavy clay and organic soil in very different areas with soil structure, it can be grown [16-19]. The pure form of ethanol is liquid, clear, colorless and has a characteristic smell. Ethanol can be produced from plants such as cane and corn [16].

<sup>1</sup> Corresponding author: Selcuk University Technology Faculty, Department of Mechanical Engineering, Camous, Selcuklu Konya, Turkey. [haydogan@selcuk.edu.tr](mailto:haydogan@selcuk.edu.tr)



## 2. MATERIAL AND METHOD

In this paper, diesel fuel camelina methy ester and ethanol were used as material. The characteristic of camelina oil and petrol diesel fuel are shown in Table 1. Camelina oil was converted to the methyl ester by transesterification method. Methyl alcohol and NaOH as the catalyst are used. Measurements are made according to EN 14214 [10].

Table 1. Comparison of the properties of raw camelina oil and diesel fuel

Properties	Raw camelina oil	Diesel
Density 15 °C (kg/m <sup>3</sup> )	918	838
Kinematic viscosity 40 °C mm <sup>2</sup> /s	24	2.92
Flash point °C	>220	102
Lower heating value (MJ/kg)	38	42.3
Ash (% mass)	0.0025	0.01
sulfur (mg/kg)	13.85	9
Water content (mg/kg)	710	43.8
Acid value (mg KOH/g)	1.39	-
Iodine number (g.I <sub>2</sub> /100 g)	151.5	-

A 1.9 multijet diesel engine was used in engine tests (Table 2). The tests were carried out on the hydraulic engine dynamometer with the specifications presented in Table 3.

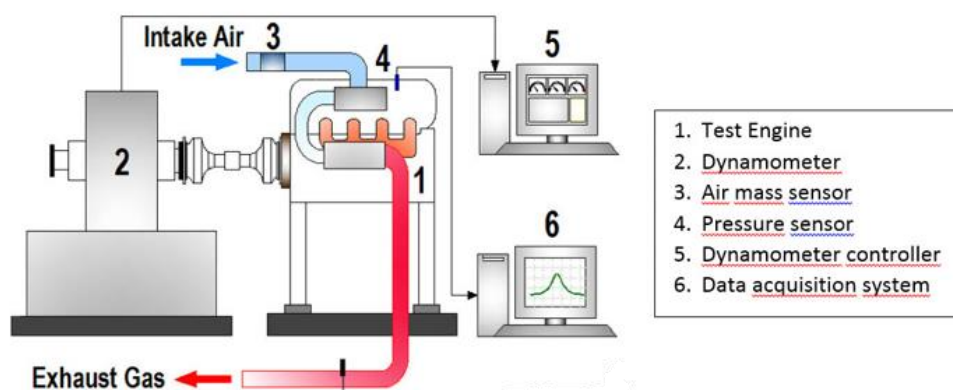
Table 2. Technical specifications of the test engine

ENGINE	1.9 Multijet diesel engine
Cylinder number and layout	4, in-line transverse
Cylinder volume (cc)	1910
Compression ratio	18.5:1
Maximum power HP – rpm	105 - 4000
Maximum torque Nm (kgm) - rpm	200 - 1750
Fuel	Diesel
Fuel feed	Electronically controlled Common Rail type Multijet direct injection, turbo and intercooler
Ignition	Compression
Diameter x Stroke (mm)	82 x 90.4

Table 3. Technical specifications of the hydraulic dynamometer used in the study

Brake model	BT-190 FR
Maximum brake power	100 kW
Maximum speed	6000 d/d
Maximum torque	750 Nm
Brake water operating pressure	0-2 kg/cm <sup>2</sup>
Water needed for maximum power	2,3 m <sup>3</sup> /hr
Brake water exit maximum temperature	80 °C
Torque measurement	Electronic load-cell
Rotation direction	Right and left rotation

Engine power, specific fuel consumption, engine torque, and engine in-cylinder pressure numbers were found. The test setup is shown in Figure 1. Three different fuels were used in the experiments. These fuels are diesel fuel, B20D80 (volume by 20% biodiesel, 80% diesel fuel) and B20D65E15 (20% biodiesel, 65% diesel fuel, 15% ethanol).



### 3. DISCUSSION AND CONCLUSIONS

Depending on engine speed diesel fuel, B20D80 and B20E15D65 Camellina methyl ester fuels the variation of engine power values are presented in Figure 2. Engine power increases with engine speed. Diesel fuel and other fuel blends were valid from the highest engine power of 2500 rpm. From a general standpoint, the engine power values found with diesel fuel and B20D80 and B20E15D65 mixtures were found to be near to each other at engine speeds. However, the 3000 RPM engine power obtained with B20D80 has been found to be 5% lower and the engine power is 15% lower than the diesel fuel obtained by B20E15D65. This result is due to the lower heating value of fuel.

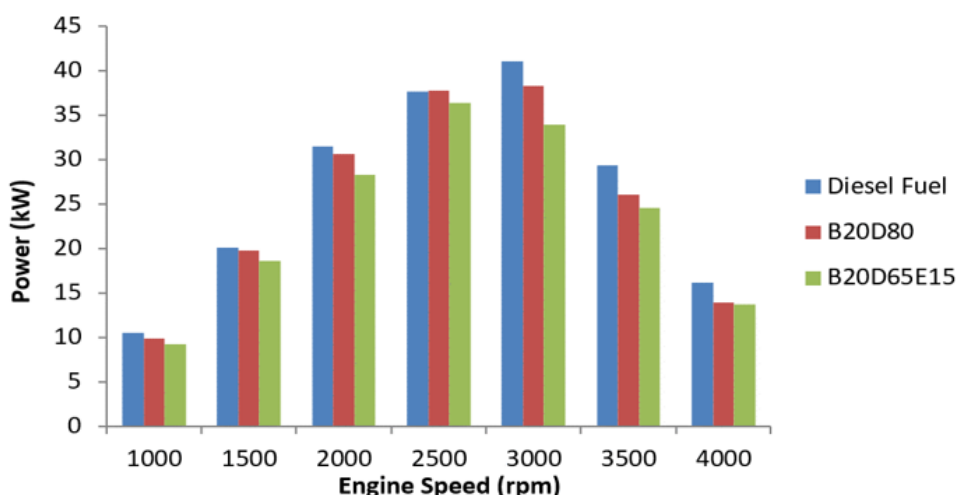


Figure 2. Variation of engine power with engine speed

The changing of the engine torque values is shown in Figure 3. The engine torque numbers showed a reduction with the reduction of the engine brake power. When this shape is analyzed, it can be shown that the max. torque

numbers is gain at 2000 rpm. Engine torque at 2000 rpm is measured as 185 nm with diesel fuel use. The engine torque is found as B20D15 fuel with B20E15D65 fuel and 175 Nm with 160 Nm. The cause for the decrease in engine torque is lower thermal energy of biodiesel mixtures.

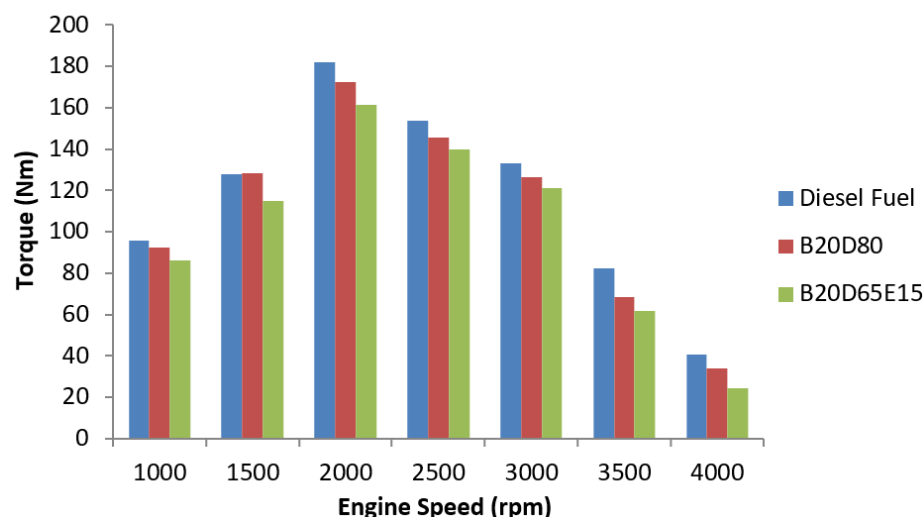


Figure 3. Variation of engine torque with engine speed

The values of specific fuel consumption according to engine speed can be seen in Figure. 4. The lowest specific fuel consumption with all fuels was achieved in the range of 1950-2500 rpm. At this rpm, the B20D15 with the use of the B20E15D65 compared to the diesel fuel and the specific fuel consumption values up to 13% by the use of 20% increased. Due to the low heating value of the B20E15D65 and B20D80 fuels, the fuel consumption and specific fuel consumption of the pump increases by using diesel fuel, sending more gasoline owing to the pump to gain near power. Additionally, the great viscosity of B20D80 fuel collated to other fuels is shown as another reason.

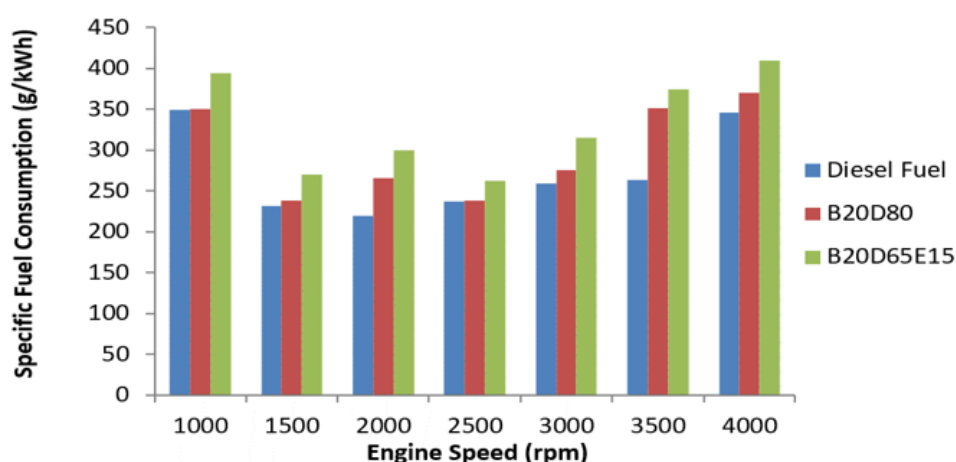


Figure 4. Relationship between specific fuel consumption and engine speed

In-cylinder gas pressures were investigated as combustion characteristics. As a result of burning of any fuel in an internal combustion engine, the spreading of mechanical loads in the cylinder according to the crank angle

is expressed with in-cylinder gas pressure curves [17-21]. The in-cylinder gas pressures of the test engine were measured at 2500 rpm, at which the maximum used torque value was obtained in cycles. Figure 5 shows the variation of the cylinder gas pressure amount for similar engine fuels with relevance to the crank angle. In the cylinder pressure measurement, the pressure values were recorded for every 120 cycles of the crankshaft in every 0.5 degree and the averages were taken. When the figure is analyzed, it can be seen that the gas pressures at 2500 rpm are quite likeness to one in all fuel types. The highest pressure is 9.8 MPa in diesel fuel; while the lowest value was measured at B20E15D65 with 9.2 MPa.

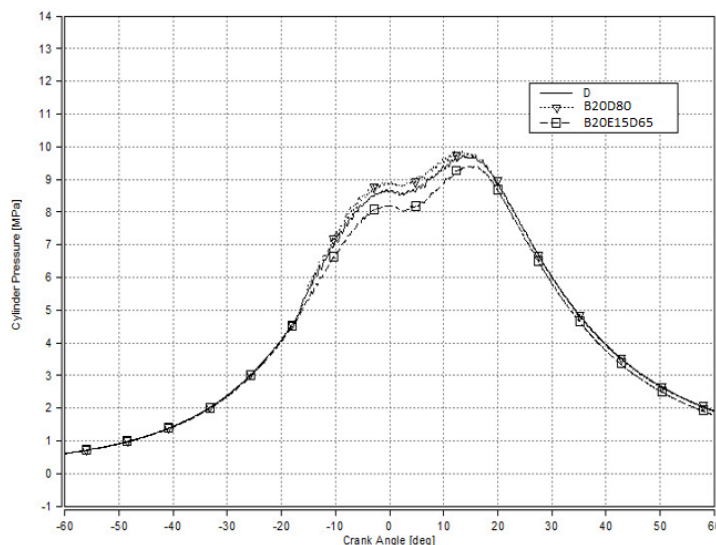


Figure 5. Variation of cylinder gas pressure values with respect to crank angle (2500 rpm)

#### 4. CONCLUSIONS AND SUGGESTIONS

In the paper, four-cylinder, four-stroke, four-stroke, turbocharged, rail-fueled diesel engines with performance, emission and combustion characteristics in relation to cylinder internal pressure numbers were investigated. Camelina methyl esters (B20D80 and B20E15D65) and petrol diesel fuel mixtures were used as fuel.

When examining the results gained in this paper, different biodiesel mixtures are of great importance on account of engine performance when the with regard to environment are taken into account. But, with regard to improving engine performance, there has been a serious need for new engine variants and combustion chambers that have been applied to the engine, rather than the proportions of the biodiesel blends according to the proportions of the design that fuel the aircraft today. This will make the combustion factors more efficient and ensure that the specific energy values of the fuel are used optimally.

#### ACKNOWLEDGMENT

*This study was supported by The Scientific and Technological Research Council of Turkey (TUBITAK) (project no 114M838) and the Scientific Research Foundation of Selcuk University. The authors would like to thank the individuals who were involved in making this work possible.*

### REFERENCES

- [1] Demirbas A, 2005. Biodiesel production from vegetable oils via catalytic and non-catalytic supercritical methanol transesterification methods. *Progress in Energy and Combustion Science*, 31, 5–6, 466-87.
- [2] Drenth AC, Olsen DB, Cabot PE, Johnson JJ, 2014. Compression ignition engine performance and emission evaluation of industrial oilseed biofuel feedstocks camelina, carinata, and pennycress across three fuel pathways. *Fuel*, 136, 143-55.
- [3] Atadashi, I.M., Aroua, M.K. and Aziz, A.A., 2010, High Quality Biodiesel And Its Diesel Engine Application: A Review, *Renewable and Sustainable Energy Reviews*, 14, 1999–2008
- [4] Alptekin, E., Canakci, M., Ozsezen, A.N., Turkcan, A., Sanli, H., 2015, Using waste animal fat based biodiesels–bioethanol–diesel fuel blends in a DI diesel engine, *Fuel*, 157:245-254
- [5] Abdel-Rahman, A.A., On the emissions from internal-combusiton engines: A Review, *International Journal of Energy Research*, 1998; 22, 483-513
- [6] Agarwal, A.K., 2005, Experimental Investigations Of The Effect Of Biodiesel Utilization On Lubricating Oil Tribology In Diesel Engines, *Automobile Engineering*, Vol:219, 703-713
- [7] Agarwal, A.K. and Rajamanoharan, K., 2009, Experimental Investigations Of Performance And Emissions Of Karanja Oil And Its Blends In A Single Cylinder Agricultural Diesel Engine, *Applied Energy*, 86, 106-112
- [8] Bannister, C.D., Hawley, J.G Ali, H.M., Chuck, C.J., Price, P., Chrysafi, S.S., Brown, A. and Pickford, W., 2009, The Impact Of Biodiesel Blend Ratio On Vehicle Performance And Emissions, *Automobile Engineering*, Vol:224, 405-421
- [9] European Commissions, 2014, The certification of the mass fraction of the ester, linolenic acid methyl ester, monoglyceride, diglyceride, triglyceride, total glycerol and water content, density, viscosity, oxidation stability, acid value, iodine value and flash point of biodiesel: ERM- EF001, Certification Report, 2014 Belgium
- [10] EN 590, European Standard, Automotive fuels- Diesel- Requirements and test methods, September 2013, 92 pages, Brussels
- [11] EN 14214, Liquid petroleum products - Fatty acid methyl esters (FAME) for use in diesel engines and heating applications - Requirements and test methods. European Committee for Standardization, 2012, Brussels
- [12] Singh, G., Singh, A.P., Agarwal, A.K., Experimental investigations of combustion, performance and emission characterization of biodiesel fuelled HCCI engine using external mixture formation technique, *Sustainable Energy Technologies and Assessments*, 2014; vol 6, 116–128
- [13] Allen, C., Toulson, E., Tepe, D., Schock, H., Miller, D., Lee, T., Characterization of the effect of fatty ester composition on the ignition behavior of biodiesel fuel sprays, *Fuel*, 2013; vol 111, 659–669
- [14] Sun Y, Ponnusamy S, Muppaneni T, Reddy HK, Patil PD, Li C, Jiang L, Deng S, 2014. Optimization of high-energy density biodiesel production from camelina sativa oil under supercritical 1-butanol conditions. *Fuel*, 135, 522-9.
- [15] Anastasov A, 2014. Biodiesel—Basic Characteristics, Technology and Perspectives. *Biotechnology & Biotechnological Equipment*, 23, sup1, 755-9.
- [16] Aydogan H, 2015, Performance, Emission And Combustion Characteristics Of Bioethanol-Biodiesel-Diesel Fuel Blends Used In A Common Rail Diesel Engine, *Journal of Thermal Science and Technology*, 35, 2, 19-27, ISSN: 1300-3615.
- [17] Benjumea, P., Agudelo, J.R., and Agudelo, A.F., 2011, Effect of the Degree of Unsaturation of Biodiesel Fuels on Engine Performance, Combustion Characteristics, and Emissions, *Energy Fuels*, 25, 77–85
- [18] Ozcelik AE, Aydogan H, Acaroglu M, 2015. Determining the performance, emission and combustion properties of camelina biodiesel blends. *Energy Conversion and Management*, 96, 47-57.
- [19] Saez-Bastante J, Ortega-Roman C, Pinzi S, Lara-Raya FR, Leiva-Candia DE, Dorado MP, 2015. Ultrasound-assisted biodiesel production from Camelina sativa oil. *Bioresour Technol*, 185, 116-24.
- [20] Drenth AC, Olsen DB, Deneff K, 2015. Fuel property quantification of triglyceride blends with an emphasis on industrial oilseeds camelina, carinata, and pennycress. *Fuel*, 153, 19-30.
- [21] Ciubota-Rosie C, Ruiz JR, Ramos MJ, Perez A, 2013. Biodiesel from Camelina sativa: A comprehensive characterisation. *Fuel*, 105, 572-7.



## Improvement of Engineering Properties of Sandy Soils by *Bacillus simplex*

*Baki Bagriacik<sup>1</sup>, Esra Sunduz Yigittekin<sup>2</sup>, Fatima Masume Uslu<sup>2</sup>,  
Sadik Dincer<sup>3\*</sup>*

### Abstract

*In this study, serious tests have been applied in the laboratory to investigate the availability of sandy soils with *Bacillus simplex* for increasing the bearing capacity and decreasing consolidation settlement. In the examinations, sand samples which were taken from river bed were used. Experiments were performed at Cukurova University Central Laboratory and soil mechanics laboratory of Civil Engineering Department on oven-dried sand samples. The sand was classified as uniform clean sand (SP). At experiments, *B. simplex* have been injected into the sandy soil with low bearing capacity. *B. simplex* is a bacterium that produces calcium carbonate. The *B. simplex* has been fed for adherence to the sandy soil. Then they have been dried in an oven fed and engineering experiments have been carried out. As a result of study, it was observed that the engineering properties of the sandy soils could be improved by injecting *B. simplex* into the soil.*

**Keywords:** Soil Improvement, *Bacillus Simplex*, Sandy Soils

### 1. INTRODUCTION

As many of construction is concentrated in populated urban areas, there is increasing need to construct on soft subsoils, which were considered unsuitable for construction just a couple of decades ago. Soft soils have been made in recent years in advanced constitutive modeling of such materials. For high subgrade constructions, selection of appropriate materials for embankment construction is the more important issue not only in terms of cost but also expected engineering performance. Loadings, excavations and transportation of these materials are the most important component of the total cost during embankment building process. At conventional approach, the soft soils at geotechnical engineering are removed and replaced by gravel or squashed rock layer. The embankment, subbase and base materials are provided that receive sites resulting in important cost increases. Using onsite soils is the most economical touch particularly in comparison to bringing choose borrow materials from faraway locations. It is reasonable that stabilization of borderline on-site soils and improvement of their engineering properties can be a well-balanced alternative to take on loan plant. Soil stabilization methods are important in dealing with for geotechnical engineering and transportation engineering departments. In addition to that, soil stabilization is becoming an alternative for increasing the strength properties of cohesionless soils. There are a lot of stabilization methods and one of the most important stabilization methods is the soil stabilization with *B. simplex*. There are a lot of studies about different soil stabilization methods [2, 17] but there is restrict study [18,19] about stabilization with *B. simplex* in the literature for geotechnical engineering and transportation engineering departments.

<sup>1</sup> Cukurova University, Engineering Faculty, Department of Civil Engineering, 01330, Adana, Turkey.  
[bbagriacik@cu.edu.tr](mailto:bbagriacik@cu.edu.tr)

<sup>2</sup> Cukurova University, Science and Letter Faculty, Department of Biology, 01330, Adana, Turkey  
[esra-gokyuzu@hotmail.com](mailto:esra-gokyuzu@hotmail.com) , [fmasure@hotmail.com](mailto:fmasure@hotmail.com)

<sup>3\*</sup> Corresponding author: Cukurova University, Science and Letter Faculty, Department of Biology, 01330, Adana, Turkey, [sdincer@cu.edu.tr](mailto:sdincer@cu.edu.tr)

### 2. MATERIAL AND METHODS

In the experiments, sand samples which were taken from Cakit River bed in Cukurova District were used. Experiments were performed at soil mechanics laboratory of Cukurova University on oven-dried sand samples. The sand was classified as uniform clean sand (SP) according to TS 1500 [20]. Test results of the sieve analysis are given in Table 1 [21]. Experimental studies were performed at the soil mechanics laboratory of Cukurova University using a direct shear test. At experiments, *B.simplex* have been used for soil improvement. *B.simplex* is a bacterium that produces calcium carbonate. Soil samples were collected from Thuja and Pinus pinea trees and 2 gr from each samples have weighed and homogenized in 10 ml sterilized serum physiologic by vortexing then, soil suspension have incubated for 15 min at 85 ° C to eliminate non-spore forming bacteria. At the end of the incubation, 100 µl from each samples were seeded onto urea agar plate by spread method and incubated for 24 hours at 37 ° C. Identifying has been conducted with molecular sequence-based identification, for this purpose isolated microorganisms' 16S ribosomal DNA sequence has been submitted to an online database (NCBI DNA sequence database) for comparison with known sequences. For the experimental study urea medium has been used [22]. Components of urea medium have been described below. All component of urea medium have been mixed in 900 mL of distilled water until dissolved, and the pH of the resulting urea medium solution has been adjusted to 6.0 and distilled water has been added to reach the final required volume (1 L) then, medium was autoclaved (at 120 for 15 minute). At the end of the autoclave process a 20-ml volume of calcium chloride solution has been added to the urea medium. After these procedure, the *B.simplex* has been injected into the sandy soil and fed for 15 days for adherence to the sandy soil. Then they have been dried in an oven fed and engineering experiments have been carried out. After preparation of both sandy soil and *B.simplex* treated sand mixtures. Direct shear tests were performed using only sandy soil and sandy soil with *B.simplex*. The direct shear test is the main engineering property of soil which controls the stability of a soil mass under vertical loads. It is a major interest in the design of different geotechnical and transportation structures to determination of the soil shear strength parameters. Figure 1 shows the direct shear test machine which was used to run the shear test. The shear box has a 60 × 60 mm horizontal cross section area, and the specimen height is 25 mm. The tests were conducted according to ASTM D-3080 [23] at constant displacement rate of 1.00 mm/min. The shear stress was recorded as a function of horizontal displacement up to an average shear strain of 12.50%. Tests were performed at three different vertical normal stresses of  $\sigma_N = 28$  kPa, 56 kPa and 112 kPa in order to completely define the shear strength parameters such as the friction angle ( $\phi$ ) for both sandy soil and *B.simplex* treated sand mixtures. In addition to these, microscopic examination (SEM) and chemical analyzes were performed for both sandy soil and *B.simplex* treated sand mixtures at Cukurova University Central Laboratory.

*Table 1. Soil properties [21]*

Granulometric Parameters	Unit	Value
Percentage of Medium Grained Sand	%	46.40
Percentage of Fine Grained Sand	%	53.60
Effective Grain Size, $D_{10}$	M	0.0018
$D_{30}$	M	0.0030
$D_{60}$	M	0.0050
Coefficient of Uniformity, $C_u$	-	2.78
Coefficient of Curvature, $C_c$	-	1.00
Soil Class	-	SP
Maximum Dry Specific Gravity	kN/m <sup>3</sup>	17.06
Minimum Dry Specific Gravity	kN/m <sup>3</sup>	15.03
Specific Gravity	kN/m <sup>3</sup>	26.80



Figure 9. Direct shear test machine

### 3. FINDINGS AND DISCUSSION

Serious tests have been applied in the laboratory to investigate the availability of both only sandy soils and sandy soils with *B.simplex* for soil improvement in this study. The images of *B.simplex* injected into the sandy soils after 2 days, 4 days, 6 days, 8 days, 10 days and 15 days are shown in Figure 2 and the images of microscopic examination (SEM) for 50  $\mu\text{m}$ , 5  $\mu\text{m}$ , 4  $\mu\text{m}$  and 2  $\mu\text{m}$  are shown in Figure 3. The chemical analyzes results are shown in Table 2. The direct shear test results are shown at Figure 4.

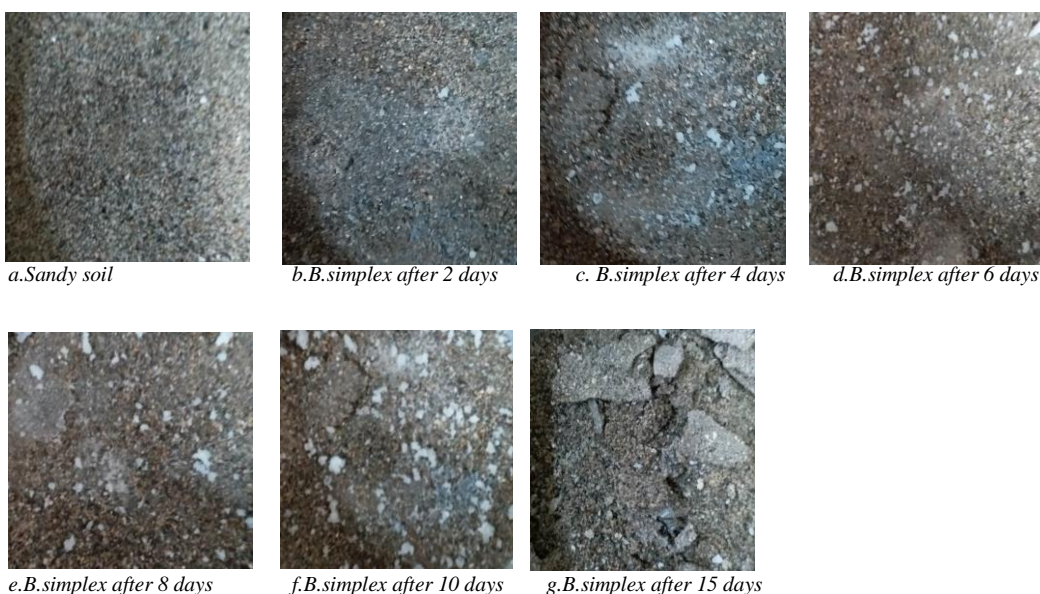
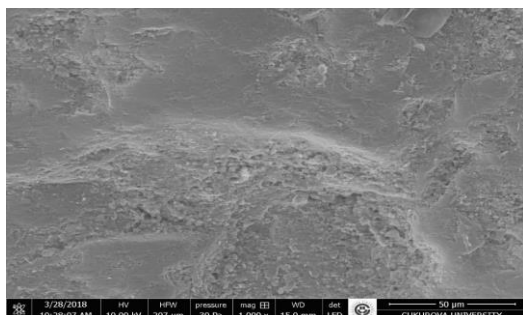


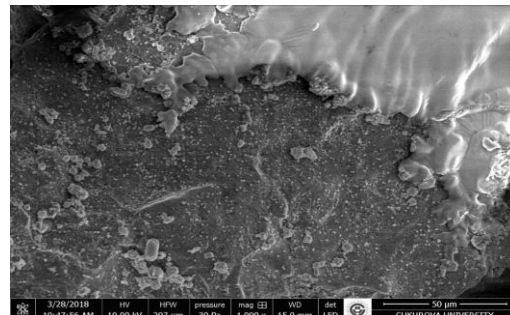
Figure 2. The images of both sandy soil and sandy soil with *B.simplex*

It was determined that white particles in the sand ground were formed as the number of days increased in the sand-blasted *B.simplex*. The side of the white particles produced in this *B.simplex* is believed that calcium

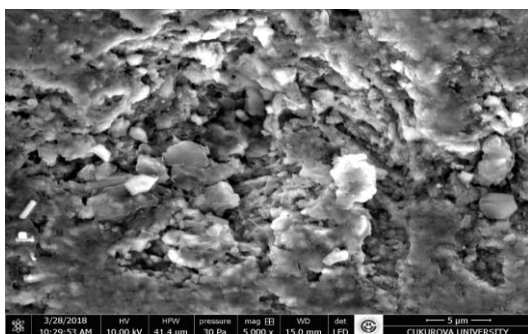
carbonates. Finally, it was seen that the amount of calcium carbonate increases as the number of days increases on bacterial injected sandy soil from Figure 2.



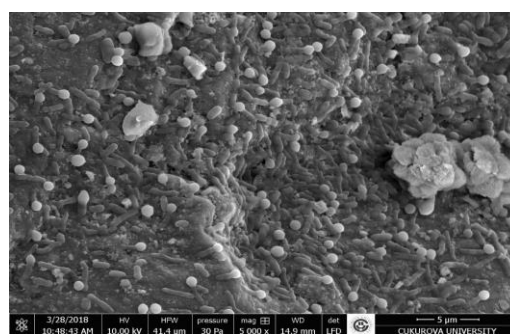
a. Sandy soil for 50 μm



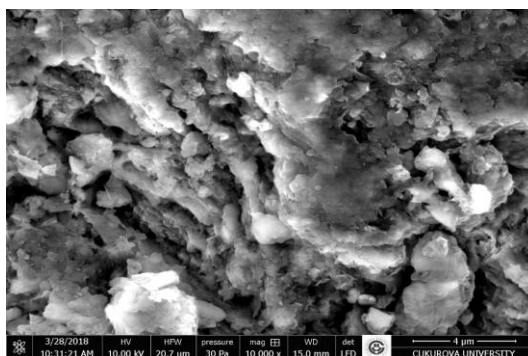
b. Sandy soil with *Bacillus* sp. for 50 μm



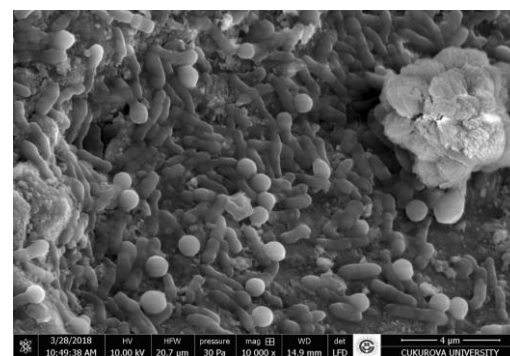
c. Sandy soil for 5 μm



d. Sandy soil with *B. simplex* for 5 μm



e. Sandy soil for 4 μm



f. Sandy soil with *B. simplex* for 4 μm



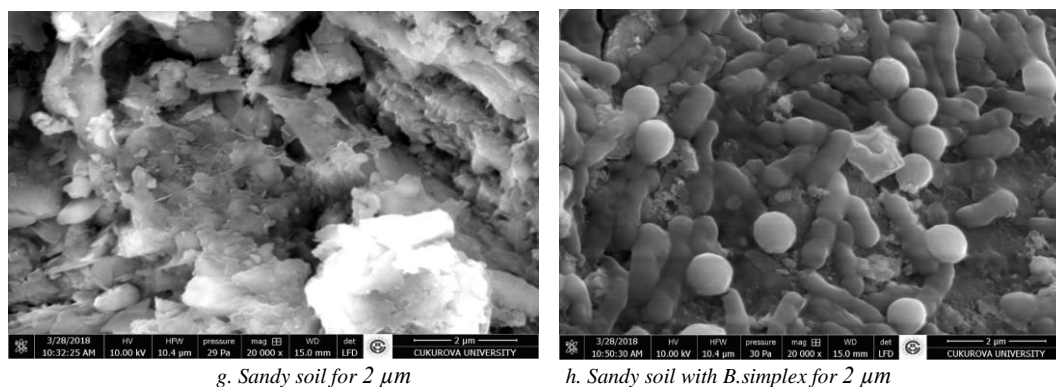


Figure 3. The images of microscopic examination (SEM) both sandy soil and sandy soil with *B.simplex*

As a result of microscopic investigations (Figure 3), it was determined that no calcium carbonate material was found on the sand that was not injected with *B.simplex*. However, a significant amount of calcium carbonate material was observed at the end of the 15 days after *B.simplex* injected sand. When microscopic examination of the *B.simplex* on the injected ground was carried out, it was determined that these calcium carbonate formations were spread to the ground at considerable rates.

Table 2. The chemical analyzes results

Element	Weight (%)	
	Only Sandy Soils	Sandy Soils with <i>B.simplex</i>
<b>Ca K</b>	<b>1.44</b>	<b>33.72</b>
O K	45.54	35.56
Mg K	20.55	0.84
Al K	1.22	0.55
Si K	19.21	1.51
CK	6.36	-

According to the results of chemical analysis at table 2, 1.44% calcium carbonate amount was found on sandy soil. When the *B.simplex* injected to sandy soil, it was seen that this rate increased to 33.72%.



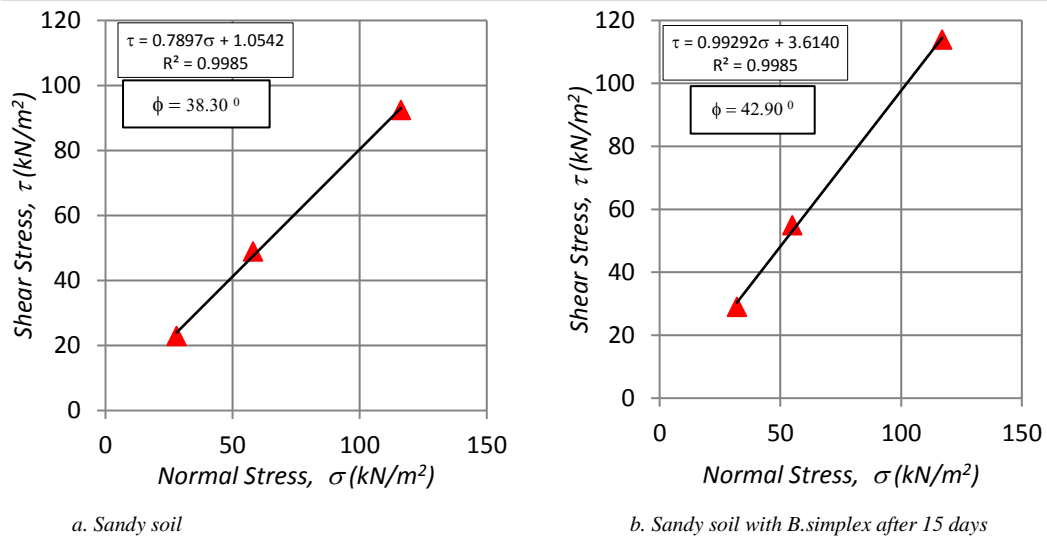


Figure 4. The direct shear test results

The frictional angle was found to be 38.30 degrees for only sandy soil. It was determined that the frictional angle increased to 42.9 degrees, when the *B.simplex* injected to sandy soils (Figure 4). It was also observed that the amount of cohesion (from 1.0542 kN/m<sup>2</sup> to 3.6140 kN/m<sup>2</sup>) to on the sandy soil increased with the injection of *B.simplex*. As a result, it was observed that the properties of the sandy soils could be improved by injecting *B.simplex* into the soil.

#### 4. CONCLUSIONS

This paper has presented to investigate the availability of both only sandy soils and sandy soils with *B.simplex* for soil improvement. Microscopic examination (SEM), chemical analyzes and direct shear test were performed for both sandy soil and *B.simplex* treated sand mixtures at Cukurova University Central Laboratory and at soil mechanics laboratory of Civil Engineering Department. The general results obtained at the conclusion of this study are presented below:

- It was determined that no calcium carbonate material was found on the sand that was not injected with *B.simplex*.
- A significant amount of calcium carbonate material was observed at the end of the 15 days after *B.simplex* injected sand.
- When microscopic examination of the *B.simplex* on the injected ground was carried out, it was determined that these calcium carbonate formations were spread to the ground at considerable rates.
- 1.44% calcium carbonate amount was found on sandy soil. When the *B.simplex* injected to sandy soil, it was seen that this rate increased to 33.72%.
- It was observed that the frictional angle increased from 38.30 to 42.9 degrees, when the *B.simplex* injected to sandy soils and the amount of cohesion (from 1.0542 kN/m<sup>2</sup> to 3.6140 kN/m<sup>2</sup>) to on the sandy soil increased with the injection of *B.simplex*.
- As a result of this study, it was observed that the engineering properties of the sandy soils could be improved by injecting *B.simplex* into the soil.

### REFERENCES

- [1]. E. T. Kowalski, D.W. Starry, "Modern Soil Stabilization Techniques," Characterization and Improvement of Soils and Materials Session of the 2007 Annual Conference of the Transportation Association of Canada Saskatoon, Saskatchewan, 2007.
- [2]. A. Ajayi-Majebi, W.A. Grissom, L.S. Smith, and E.E. Jones, "Epoxy-Resin-Based Chemical Stabilization of a Fine, Poorly Graded Soil System," *In Transportation Research Record 1295*, TRB, National Research Council, Washington, D.C., 1991.
- [3]. D. N. Little, "Handbook for stabilisation of pavement sgrades and base course with lime," United States of America Lime association of Texas, 1995.
- [4]. J. R. Prusinski and S. Bhattacharja, "Effectiveness of Portland cement and lime in stabilizing clay soils," *Transportation Research Record*. Issue-1652, pp 215-227, 1999.
- [5]. S. Bhattacharja and J. I. Bhatti, "Comparative performance of the Portland cement and lime stabilization of moderate to high plasticity soils," *Portland cement association*, 2003.
- [6]. J.S., Tingle and R.L., Santori, "Stabilisation of clay soils with non traditional additives," National Research Council, Washington D.C., *Transportation Research Record No. 1819*, pp. 72-84, 2003.
- [7]. M. C. Geiman, G. M. Filz and T. L. Brandon, "Stabilization of Soft Clay Subgrades in Virginia," *Phase I Laboratory Study Virginia Transportation Research Council*, 2005.
- [8]. S. Vitton, "Introduction to soil stabilization," Michigan Technological University, 2006.
- [9]. C. Jung and A. Bobet, "Post-Construction Evaluation of Lime-Treated Soils," *Indiana Department of Transportation State Office*, 2008.
- [10]. M. Mirzababaei, S. Yasrobi and A. Al-Rawas, "Effect of polymers on swelling potential of expansive soils," *Proceedings of the ICE Ground Improvement* 162(3), pp. 111-119, 2009.
- [11]. M. D. Liu, S. Pemberton and B. Indraratna, "A study of the strength of lime treated soft clays," 2010 .
- [12]. R. Brooks, F. F. Udoeyo, V. K. Takkalapelli, "Geotechnical properities of problem soils stabilized with fly ash and lime stone dust in Philadelphia," *American Society of Civil Engineers*, Vol. 23, No. 5, pp. 711-716, 2011.
- [13]. B. Celauro, A. Beviacqua, D. L. Bosco and C. Celauro, "Design procedures for soil-lime stabilization for road and railway embankments: Part 1, Review of design methods," *Elsevier*, 53, 755-764, 2012.
- [14]. S. A. A. Khattab and Y. A. Hussein, "The durability of fine grained soils stabilized with lime," *Al-Rafidain Engineering* 20 (1), pp. 85-92, 2012.
- [15]. A. S. Negi, M. Faizan, D. P. Siddharth and R. Singh, "Soil stabilization using lime," *International Journal of Innovative Research in Science, Engineering and Technology*, 2 (3), pp. 448-453, 2013.
- [16]. B. Bagriacik, "The Experimental Study on Soil Improvement with Additive Materials on Highways", *International Journal of Science and Research*, 6 (6), pp.2185 – 2189, 2017.
- [17]. B. Bagriacik, "Ulasim Yapilari Temel Zeminlerinin Katki Maddeleri ile Stabilizasyonu," *1st International Mediterranean Science and Engineering Congress*, pp. 4581-4586, 2016.
- [18]. E. Jr. Kavazanjian, , I. Karatas, "Microbiological improvement of the physical properties of soil". *6th International Conference on Case Histories in Geotechnical Engineering*, Arlington, VA, August 11-16, 2008.
- [19]. V. Ivanov, J. Chu, "Applications of microorganisms to geotechnical engineering for bioclogging and biocementation of soil in situ". *Reviews in Environmental Science and Biotechnology*, 7, 139-153, 2008.
- [20]. TS 1500, Insaat Muhendisliginde Zeminlerin Siniflandirilmesi.
- [21]. B. Bagriacik, "Zeminlerdeki Gerilme Durumlarının Deneyisel ve Teorik Olarak Incelenmesi". MSc Thesis, Cukurova University, Adana, Turkiye, 2010.
- [22]. Canakci, H., W. Sidik, and I. H. Kilic. 2015. "Effect of bacterial calciumcarbonate precipitation on compressibility and shear strength of organic soil." *Soils Foundations*. 55 (5): 1211–1221.
- [23]. ASTM D 3080, Standard test method for direct shear test of soils under consolidated drained conditions, American Society for Testing and Materials, West Conshohocken, 2005.

# Environmental Risks of Bumblebee Commercialization and Suggestions for Prevention

Ayhan Gosterit<sup>1</sup>, Fehmi Gurel<sup>2</sup>, Cengiz Erkan<sup>3</sup>

---

## Abstract

Bumblebees are an important pollinator of wild flora as well as agricultural crops and are increasingly used as an effective commercial pollinator in greenhouses crops mainly in tomatoes all over the world. Eurasian *Bombus terrestris* L. is the most reared subspecies for commercial pollination and has been used outside its natural distribution area. Very early after commercial introduction, it was recognized that this species is invasive and may disturb local ecosystems. There are many invasive characteristics of *B. terrestris* such as high migration ability, early seasonal emergence, high adaptability under adverse climatic conditions in various habitat, polylectic foraging strategies and regulation of life cycle in a year in newly colonized area. A single commercially produced *B. terrestris* colony may produce more than a hundred of new queens which may escape from greenhouses and found nest in native flora. The invasion and the increase in population of introduced *B. terrestris* in the new areas have caused some problems, such as competition with native pollinators for floral resources and nest sites, the introduction of parasites and pathogens, and hybridization with native species. Therefore their potentially effects on the environment are also being observed carefully. The aim of this report is to raise awareness about the environmental risks of bumblebee commercialization and make suggestions for prevention of this possible ecological damage.

**Keywords:** Bumblebee, *Bombus terrestris*, Commercialization, Invasion, Ecology

---

## 1. INTRODUCTION

Contributions of bees which commonly known as beneficial insects to pollination of flowering plants cannot be ignored. Bees which include about twenty thousand species are most important insect group and have 8 or 9 families according to morphological characters [1]. Honeybees (*Apis mellifera* L.) are most effective pollinator insects of native flora due to their extensive rearing all over the world. Bumblebees, of which about 250 species have been determined, are in second place for pollination of many flowering plants. This bee genus is used for the pollination of many cultivated plants in many countries [2, 3]. Because of their rearing is easier and their colony population is larger than the others, *Bombus terrestris* is the most year round reared species, in comparison to other bumblebee species. This species which includes nine subspecies is used mainly for greenhouse tomato pollination. They reduces pollination labor costs and improves the quality and quantity of crops. Commercially reared *B. terrestris* colonies are used in many countries, including some outside of its native range [4, 5].

Bumblebees are indispensable pollinator. However, *B. terrestris* has an invasion potential into new locations where they are non-native. Early seasonal emergence, high adaptability under adverse climatic conditions in a range of habitats, generalist or polylectic foraging strategies, and great phenological flexibility are most important invasive characteristics of *B. terrestris*. Soon after its commercial introduction, it was recognized that this species is invasive, can spread into new locations, and may disturb local ecosystems [6, 7]. Competition with native pollinators for floral resources and nest sites, the introduction of parasites and pathogens,

---

<sup>1</sup> Corresponding author: Applied Sciences University of İsparta, Faculty of Agricultural Sciences and Technologies, Department of Animal Science, İsparta, Turkey. [ayhangosterit@sdu.edu.tr](mailto:ayhangosterit@sdu.edu.tr)

<sup>2</sup> Akdeniz University, Faculty of Agriculture, Department of Animal Science, Antalya, Turkey. [fgurel@akdeniz.edu.tr](mailto:fgurel@akdeniz.edu.tr)

<sup>3</sup> Van Yüzüncü Yıl University, Faculty of Agriculture, Department of Animal Science, Van, Turkey. [cerkan@yyu.edu.tr](mailto:cerkan@yyu.edu.tr)

---

hybridization with native species and alteration of natural pollination systems are major problems that caused by invasion and the increase in population of introduced *B. terrestris* in the new areas. A single commercial *B. terrestris* colony is capable of producing more than a hundred new queens, which potentially could escape from greenhouses and form nests among the native vegetation [8, 9]. Therefore, these environmental risks should be taken seriously.

## 2. ECOLOGICAL FLEXIBILITY OF *B. TERRESTRIS*

*B. terrestris* has a broad spread area in the world. The natural distribution range of *B. terrestris* is the Palaearctic region between latitudes 60°N and 30°N and longitudes 10°W and 105°E. About ten geographically separated subspecies have been recognized in this distribution range. It is known that this species adapts better to hot and dry climate [4, 10, 11]. Commercial rearing of *B. terrestris* started to about thirty five years ago and this industry has developed rapidly. Colonies are produced by more than 30 suppliers and marketed to all over the world. We estimated that total number of colonies that use for pollination is to be around two millions per year.

*B. terrestris* has also speed and broad invasive potential related to other bumblebee species. Invasion speed of this species differs to their population density and ecological conditions. Researches displayed that *B. terrestris* has spread at 90 km in New Zealand, at 30 km in Israel, and at 25 km in Tasmania [12, 13]. It is also proved that *B. terrestris* can visit the flowers of many plants for pollen and nectar resources from sea level to 1500 m in altitude, containing all of the major native vegetation types [2, 13, 14].

*B. terrestris* shows great ecological flexibility, particularly in terms of diapause responses [12, 15]. Bivoltinism has been reported for some Mediterranean *B. terrestris* populations [15]. New Zealand *B. terrestris* populations are largely bivoltine and that nest founding by *B. terrestris* is possible any time of the year in some parts of New Zealand due to the variety of plants which provide some pollen and nectar throughout winter [1]. Similarly, two distinct generations have been found in Tasmania in the same season [16]. Our previous study that conducted in Mediterranean Coastal Region of Turkey showed that, native *B. terrestris* populations forage on 47 flowering plant species from 20 families. Two of the plant species (*Arbutus unedo* L. and *Vitex agnus-castus* L.) have long flowering periods and play a crucial role in the life cycle of native *B. terrestris* populations. The emergence of queens at the aestivation site was synchronized with the flowering of *Arbutus unedo* L., while the emergence of sexuals coincided with the flowering of *Vitex agnus-castus* L. [14].

## 3. RISKS OF BUMBLEBEE COMMERCIALIZATION

As a result of the contribution of humans, the potential of crossing geographical obstacles of living organisms has reached a level that cannot be predicted. Although a part of introduced species are beneficial for human health and that they cause little environmental damage, the other part of them quickly spread to new areas and have done great ecological harm [13]. The best example in this regard is the European honeybee, *Apis mellifera* L., which taken afterwards to America. Numerous studies have demonstrated that *A. mellifera* displaces native anthophiles and contributes to the pollination of weeds [17, 18]. The potential of *B. terrestris* to invade many habitat around the world raises concerns because of this species have similar harmful environmental impacts like honeybees. Possible negative effects of *B. terrestris* invasion are competition with native pollinators for floral resources, competition for nest sites, introduction of parasites and pathogens that may infect native organisms, disruption of pollination of native plants, and the hybridization with native species [6, 11].

Different organisms such a birds, insects and mammals that living in a specific region are fed by pollen and nectar gathered from flowers. One of the most important group of insects is bees. Foods of all bee species include pollen and nectar collected from flowers. Therefore, introduction of new species to a specific region or extreme increase of exotic species in this region make competition inevitable with host bee species in terms of the use of plant sources [11].

*B. terrestris* has the potential to compete for floral resources with host bee species, as a consequence of its polylectic foraging behavior. Many of these plants constitute the significant portion of food resource of other many native bee species. Life cycle and ecology of *B. terrestris* overlap with the foraging profiles of all other bee subgenera. Foraging period of bumblebees that forage during the spring and summer is longer than other pollinators. They have also capable of more use the pollen and nectar resource according to other pollinators [19]. Furthermore, *B. terrestris* that the most reared species for commercial pollination may has an advantage for competition of floral resource using because of its crowded colony population [11]. *B. terrestris* has comparatively larger and more hairy body than many other bee species. Bees that have a large body also take an advantage in cold weather because of their high ability to protect temperatures. *B. terrestris* can work very long hours, forage from dawn to dusk even on cold, rainy or foggy days. Overlap in floral resources is shows

that there is a competition between the *B. terrestris* and other bee species. However, if the nectar and pollen resources are not scarce, competition may not appear [20].

Other critical resource for bees in native fauna is nest site. There may be competition between the introduced *B. terrestris* and native organisms for nest sites. Sexuals (young queens and males) are produced in bumblebee colonies towards the end of the colony cycle in late summer. After mating, the young queens go into diapause while the founding queen. The following spring, the queens that survived hibernation seek the nest site for found their colonies. *B. terrestris* generally found their colonies in existing cavities below ground, often using abandoned rodent holes and spaces beneath man-made structures such as garden sheds [6]. The time of diapause termination varies according to region where native populations live. For example, in Mediterranean Region of Turkey, while queens of a native populations emerge from diapause in autumn at the Phassalis site (coastal region), queens of other native populations emerge from diapause in in spring at the Termessos site (500 – 700 m altitude) [14]. Founding nest site takes place in an ecological balance in native fauna. However, queens produced in commercial colonies potentially could escape from greenhouses and form nests among the native vegetation where using of commercial colonies for pollination agent is common. This case may increase the competition for nest site by disrupting the ecological balance.

Invasions and increased populations of introduced *B. terrestris* into new areas have also caused the transmission of parasites and pathogens. *Locustacarus buchneri*, *Nosema bombi*, *Crithidia bombi* and *Apicystis bombi* are some important pest and diseases which are determined in commercially reared colonies. In Japan, determination of endoparasitic mite, *L. buchneri*, in introduced colonies of *B. terrestris* clearly reveals the risk that the transfer of parasites and diseases [21]. Transfer of parasite and diseases may affect the not only native bumblebee species but also other insect species.

Another negative effect of bumblebee invasion is disturbing the pollination of native flora [6]. There must be a harmony between the morphology of the flower and pollinator for effective pollination. Flower of plant are visited by many pollinator and pollination quality of these pollinators is different. *B. terrestris* visits the different species of plant and sometimes provide the poor quality pollination. *B. terrestris* that as known also nectar robbing obtain the nectar of flowers with long corolla by making perforations at the base of the corolla tube. This behavior inhibits the visiting the flower by other pollinator and finally seed set [22]. Very few of plants that visited by bumblebees are host plants of the region where they live. Therefore, they may cause to increasing of pollination of exotic plant. It is inevitable that increasing of exotic plants causes to ecological and economic harm [23].

Interspecific hybridization between non-indigenous *B. terrestris* and indigenous bumblebee species was demonstrated [24]. Negative effects of inter-subspecific hybridization on native ecosystems have also been evaluated [25]. Our previous study revealed that hybridization between commercial and native genotypes generally resulted in intermediate expression of the colony traits. Maternal genotype primarily determines the colony traits. Our results imply that hybridization with the commercial genotype affected some colony traits of native *B. terrestris* colonies [9]. However, information about consequences of nearly 30-year history of commercialization of bumblebee respect to their hybridization level is not sufficient.

#### 4. CONCLUSION AND SUGGESTIONS

Bumblebees have become an indispensable pollinator, especially for greenhouse tomato production, because of its pollination efficiency, which reduces pollination labor costs and improves the quality and quantity of crops. Currently, about 250 species of true bumblebees have been identified. *B. terrestris* is the most commonly commercially reared species. This species is also one of the most abundant and widespread bumblebees throughout continental Europe and many Mediterranean and Atlantic island. It easily adapts to cloudy weather and to small enclosed areas, such as greenhouses. Commercially reared *B. terrestris* colonies are excellent pollinators and have been used in many countries for pollination agency. However, their negative effects on native ecological systems have been intensely discussed. Especially, negative effects of their commercialization such as competition with native pollinators for floral resources and nest sites, introduction of parasites and pathogens, disruption of pollination of native plants, and the hybridization with native species must be taken into attention for ecological sensitivity. Industry of bumblebee rearing and pollination service has an economic and sociological importance. Therefore, it is clear that prevention or restriction of use of commercially reared bumblebee colonies not rational and possible. However improve structural conditions of greenhouses, using covering nets, killing colonies and then burning the hive after use, using queen excluder and using colonies with health certificate can be suggested as a solution to decrease the negative ecological impacts of bumblebee commercialization.



### REFERENCES

- [1]. B.J. Donovan, "Interactions between native and introduced bees in New Zealand," *New Zealand Journal of Ecology*, vol. 3, pp.104-116, 1980.
- [2]. T. Benton, *The Bumblebees of Essex*, The Nature of Essex Series, No: 4, Essex: Loginga Books, 2000.
- [3]. P.H. Williams, "An annotated checklist of bumblebees with an analysis of patterns of description," *Bulletin of the Natural History Museum: Entomology Series*, vol. 67, pp. 79-152, 1998
- [4]. H.H.W. Velthuis and A. van Doorn, "A century of advances in bumble bee domestication and the economic and environmental aspects of its commercialization for pollination," *Apidologie*, vol. 37, pp. 421-451, 2006.
- [5]. P. Rasmont, A. Coppee, D. Michez and T. de Meulemeester, "An overview of the *Bombus terrestris* (L.1758) subspecies (Hymenoptera:Apidae)," *Annals de la Societe Entomologique de France*, vol. 44, pp. 243-250, 2008.
- [6]. D. Goulson, "Effects of introduced bees on native ecosystems," *Annual Review of Ecology, Evolution and Systematics*, vol. 34, pp. 1-26, 2003.
- [7]. A. Dafni, P. Kevan, C.L. Gross and K. Goka, "*Bombus terrestris*, pollinator, invasive, and pest: An assessment of problems associated with its widespread introductions for commercial purposes," *Applied Entomology and Zoology*, vol. 45, pp. 101-113, 2010.
- [8]. R.E. Owen, "Rearing bumble bees for research and profit: practical and ethical considerations," *Beekeeping and Bee Conservation Emerson Dechechi Chambo, IntechOpen*, DOI: 10.5772/63048, 2016.
- [9]. A. Gosterit and V.C. Baskar, "Impacts of commercialization on the developmental characteristics of native *Bombus terrestris* (L.) colonies," *Insectes Sociaux*, vol. 63, pp. 609-614, 2016.
- [10]. S. Goodwin and M. Steiner, "*Introduction of Bombus terrestris* for biological pollination of horticultural crops in Australia" Gosford IPM Services, 1997.
- [11]. A. Gosterit and F. Gurel, "Effects of invasion of *Bombus terrestris* (Hymenoptera: Apidae) on the ecosystem," *Uludag Bee Journal*, vol. 5, pp. 115-121, 2005.
- [12]. A. Dafni, "The threat of *Bombus terrestris* spread," *Bee World*, vol. 79, pp. 113-114, 1998.
- [13]. A. Hingston, J. Marsden-Smedley, D. Driscoll, S. Corbett, J. Fenton, R. Anderson, C. Plowman, F. Mowling, M. Jenkin, K. Matsui, K. Bonham, M. Iłowski, P. McQuillan, B. Yaxley, T. Reid, D. Storey, L. Poole, S. Mallick, N. Fitzgerald, J. Kirkpatrick, J. Febey, A. Harwood, K. Michaels, M. Russell, P. Black, L. Emmerson, M. Visoiu, J. Morgan, S. Breen, S. Gates, M. Bantich and J. Desmarhelier, "Extent of invasion of Tasmanian native vegetation by the exotic bumblebee *Bombus terrestris* (Apoidea: Apidae)," *Austral Ecology*, vol. 27, pp. 162-172, 2002.
- [14]. F. Gurel, A. Gosterit and O. Eren, "Life-cycle and foraging patterns of native *Bombus terrestris* (L.) (Hymenoptera, Apidae) in the Mediterranean region," *Insectes Sociaux*, vol. 55, pp. 123-128, 2008.
- [15]. A. Estoup, M. Solignac, J.M. Cornuet, J. Goudet and A. Scholl, "Genetic differentiation of continental and island populations of *Bombus terrestris* (Hymenoptera: Apidae) in Europe," *Molecular Ecology*, vol. 5, pp. 19-31, 1996.
- [16]. R.E. Buttermore, "Observations of successful *Bombus terrestris* (L.) (Hymenoptera: Apidae) colonies in southern Tasmania," *Australian Journal of Entomology*, vol. 36, pp. 251-254, 1997.
- [17]. I.M. Parker, "Pollination limitation of *Cytisus scoparius* (Scotch Broom), an invasive exotic shrub," *Ecology*, vol. 78, pp. 1457-1470, 1997.
- [18]. C.L. Gross and D. Mackay, "Honeybees reduce fitness in the pioner shrub *Melastoma affine* (Melastomataceae)," *Biological Conservation*, vol. 86, pp. 169-178, 1998.
- [19]. A. B. Hingston and P.B. McQuillan, "Does the recently introduced bumblebee *Bombus terrestris* (Apidae) threaten Australian ecosystems?" *Australian Journal of Zoology*, vol. 23, pp. 539-549, 1998.
- [20]. A. Dafni and A. Schmida, "*The possible ecological implications of the invasion of Bombus terrestris* (L.) (Apidae) at Mt Carmel, Israel. In: *The conservation of bees*," The Linnean Society, London, pp. 183-200, 1996.
- [21]. K. Goka, K. Okabe, M. Yoneda and S. Niwa, "Bumblebee commercialization will cause worldwide migration of parasitic mites," *Molecular Ecology*, vol.10, pp. 2095-2099, 2001.
- [22]. R.E. Irwin and A.K. Brody, "Nectar-robbing bumble bees reduce the fitness of *Ipomopsis aggregata* (Polemoniaceae)," *Ecology*, vol. 80, pp. 1703-1712, 1999.
- [23]. M.E. Hanley and D. Goulson, "Introduced weeds pollinated by introduced bees: Cause or effect?", *Weed Biology and Management*, vol. 3, pp. 204-212, 2003.
- [24]. Y. Kanbe, I. Okada, M. Yoneda, K. Goka and K. Tsuchida, "Interspecific mating of the introduced bumblebee *Bombus terrestris* and the native Japanese bumblebee *Bombus hypocrita sapporoensis* results in inviable hybrids," *Naturwissenschaften*, vol. 95, pp.1003-1008, 2008.
- [25]. T.C. Ings, N.L. Ings, L. Chittka and P. Rasmont, "A failed invasion? Commercially introduced pollinators in Southern France," *Apidologie*, vol. 41, pp. 1-13, 2010.

## Determination of the microbial composition of 1-year shelf-life lyophilized bacteria with DGGE method

*Didem Aksu<sup>1 2\*</sup>, Guven Ozdemir<sup>2</sup>*

### Abstract

*Lyophilization has been used for long-term storage of bacteria. Cryoprotectants should be used to obtain high viability of the bacteria and provide the cryoprotection to the cells during the freezing process. In this lyophilization study, the bacterial consortium was used which are biodegraded p-toluic acid (p-tol), 4-carboxybenzaldehyde (4-cba) and terephthalic acid (TA). The effects of different cryoprotectants on the viability of bacterial consortium were investigated. Furthermore, the microbial composition of these products were determined by Denaturing Gradient Gel Electrophoresis (DGGE) method after 1 year. According to the results of colony counts of bacteria, the survival rates showed that skim milk + sodium glutamate could still reach  $10^7$  cfu/mL after 12 months. Sequence analysis results of bands of DGGE were *Raoultella planticola* and *Pseudomonas alkyphenolica* dominated.*

**Keywords:** Cryoprotectant, DGGE, Lyophilization, PTA, Wastewater.

### 1. INTRODUCTION

Terephthalic acid produced by oxidation p-xylene. P-tol and 4-cba are formed during the reaction. These chemicals are carcinogen, toxic and mutagenic [1]. So, we have to removed chemicals in the environment. Other methods which are mechanical and chemical methods can also be used remove hydrocarbons but these methods have limited effectiveness and expensive. Bioremediation is an important technology for the treatment of these contaminated sites since it is economic and will lead to complete mineralization [2,3].

Lyophilization is preferred for long-term storage of bacteria. Besides the choice and concentration of cryoprotectant. There are many factors influence the success of lyophilization. These factors are the growth, preservation and rehydration medium, microbial growth rate, initial cell concentration, the rate of freezing temperature settings during lyophilization [4,5].

Complex microbial community analysis can be determined by molecular methods such as Denaturing Gradient Gel Electrophoresis (DGGE). In this method, the same length PCR products are separated in polyacrylamide gels containing a linearly increasing gradient of denaturants [6,7]. The aim of the study was to evaluate the success of lyophilization and determined the microbial structure of the bacterial product with DGGE at the end of 1-year shelf life.

### 2. MATERIAL AND METHODS

In this study we have used various bacteria obtained from previous studies [8,9,10,11]. Total 16 bacteria are shown Table 1.

<sup>1</sup> Corresponding author: Ege University Application and Research Center for Testing and Analysis, İzmir, Turkey. [didem.eroğlu@ege.edu.tr](mailto:didem.eroğlu@ege.edu.tr)

<sup>2</sup> Ege University, Faculty of Science, Department of Biology, Bornova, İzmir, Turkey. [guven.ozdemir@ege.edu.tr](mailto:guven.ozdemir@ege.edu.tr)

*Table 1. Bacteria used in the study*

Chemicals (used for biodegradation from previous studies)	Microorganisms	
	TA	<i>Pseudomonas</i> sp.
		<i>Chryseobacterium</i> sp.
		<i>Arthrobacter nicotinae</i>
		<i>Pseudomonas putida</i>
	p-tol	<i>Pseudomonas alkylphenolica</i>
		<i>Pseudomonas putida</i>
		<i>Pseudomonas alkylphenolica</i>
	4-cba	<i>Comamonas testosteroni</i>
		<i>Pseudomonas putida</i>
		<i>Chryseobacterium indolegenes</i>
	ANT (Anthracene)	<i>Pseudomonas fluorescens</i>
		<i>Arthrobacter protophormiae</i>
	FLO (Flourene)	<i>Acinetobacter</i> sp.
		<i>Micrococcus luteus</i>
	PYR (Pyrene)	<i>Aeromonas hydrophila</i>
	Fluoranthene	<i>Raoultella planticola</i>

Microorganisms were all cultured with 3 L nutrient broth in a fermentor (10%). Cells were harvested at the beginning of the stationary phase (12h) by centrifugation at 4000 rpm for 5 min at 30°C .

The initial cell concentration before lyophilization was  $6,2 \times 10^8$ . Several protectants were tested to improve the survival of bacterial consortium after freeze-drying. Protective agents protect against the harmful effect of lyophilization. protective agents which internal and external are divide in two group. External agents are more used in lyophilization studies of bacteria. Protective agents used in our studies are skim milk, sucrose, trehalose, sodium glutamate, polyvinyl alcohol, yeast and maltodextrin. After freeze drying, the samples were rehydrated Phosphate Buffer Solution (20 mL). After 15 min on the bench, the serial dilution technique was employed the determine the colony forming units on Plate Count Agar plate and added (1,25 mL) Nutrient Broth in (25 mL) Erlenmeyer flask. After the incubation time, DNA was extracted from samples taken from the Nutrient Broth.

DNA samples were prepared by two-step PCR. For the nested PCR, the bacterial forward primer 11F and universal reverse primer 1492R were used for the first-step. 338F (GC clamp) and 805R primer were used in second-step (Table 2) [12].

*Table 2. 16S rRNA gene primers used for PCR-DGGE fingerprinting.*

<b>Primers</b>	
<b>Bacteria</b>	
<b>11F-</b>	5'- GTTTGATCCTGGCTCAG – 3'
<b>1492R</b>	5'-TACGGCTACCTTGTTACGACTT-3'
<b>Bacteria</b>	5'CGCCCGCCGCGCGCGGGCGGGCGGGGCGGGGGCACGGGGGG
<b>338 F-GC</b>	ACTCCTACGGGAGGCAG-3'
<b>805 R</b>	5'- GACTACCAGGGTATCTAATCC – 3'

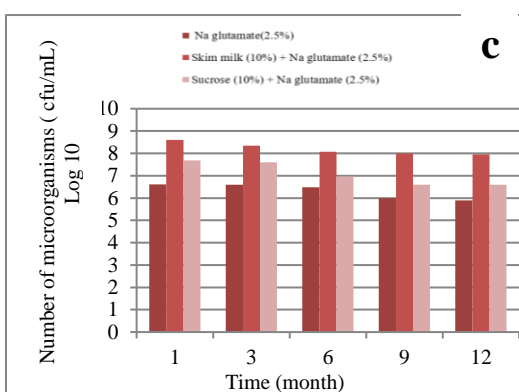
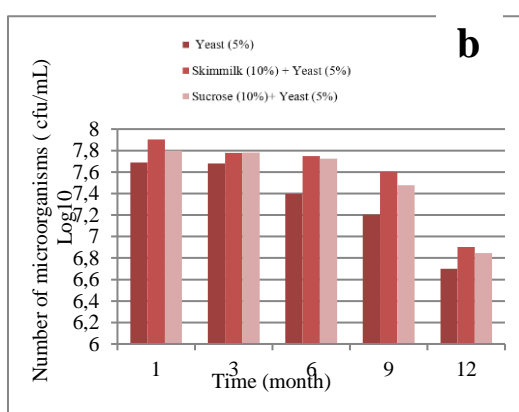
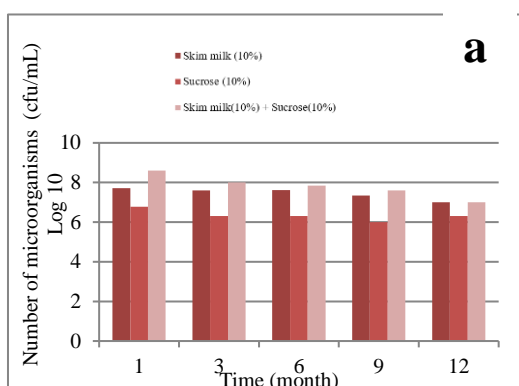
PCR products were separated by DGGE, which was conducted using the DCode™ Universal Mutation Detection System. PCR products were all separated in 8% acrylamide gel with a denaturing gradient from 40% to 60%. Gels were running in 1×TAE (Tris– acetate, EDTA) buffer at 60°C and at a constant voltage of 85 V for 16 h. The gel was stained for 15 min in 1X TAE containing Gel Green solution and examined under UV light in UVP Biospectrum Bioimaging Systems (Ultra-Violet Products Ltd.,Cambridge UK). The major DGGE bands were excised and purified to determine sequences.

### 3.RESULTS AND DISCUSSION

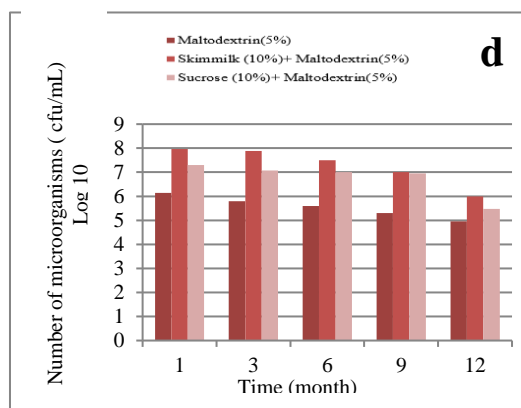
At the end of 12 months shelf life, the best viability was seen in skim milk and sodium glutamate (c) contains vial. In the previous lyophilization studies, skim milk powder is often chosen as drying medium. Because skim milk creates a porous structure in the freeze-dried product that makes rehydration easier; it is also believed that proteins in milk provide a protective coating for the cells [13].

The worst results were seen when maltodextrin was used as a preservative. When we look at the results in general, it was observed that use of skim milk in combination with preservatives increased the viability.

In this study, PVA was found to be ineffective in preserving the viability of the bacteria when used as a cryoprotectant. The lyophilized product, which does not contain cryoprotectant, showed no viability even at the end of one - month shelf life. Therefore, it is mandatory to use appropriate preservative in the lyophilization of bacteria.







**Figure 1.** Viability of lyophilized microorganisms after 12 months storage.

DNA fragments of the same length but with different sequences can be separated on polyacrylamide gel. According to the results of sequence analysis, it was observed that different series were different in maltodextrin and skim milk product groups than the others (Figure 2). *Pseudomonas alkylphenolica*, *Raoultella planticola* and *Comamonas* species were seen dominated than other bacteria in lyophilization vials.



**Figure 2.** Results of DGGE band pattern.



*The authors wish to thank Republic of Turkey, Ministry of Science, Industry of Technology under the grant SANTEZ-00719 STZ 2014 and Ege University, Scientific Research Projects Fund, Project no: (BAP 2016 FEN 008 ) for the financial support of this study. The support program of the Scientific and Technological Research Council of Turkey.(TUBITAK-BIDEB 2211-D) supported this study. This work supported by Ministry of Development Ege University Application and Research Center for Testing and Analysis (EGE-MATAL :2010K120810).*

### REFERENCES

- [1]. Verma, S., Prasad, B. and Mishra, I.M. Thermochemical treatment (Thermolysis) of petrochemical wastewater: COD removal mechanism and floc formation. *Ind. Eng. Chem. Res.* 50 (9), 5352–5359, 2011.
- [2] Liang, D.W., Zhang, T., Fang, H. H. P. and He, J. Phthalates biodegradation in the environment. *Appl Microbiol Biotechnol*, 80:183-198p, 2008.
- [3] Das, N. and Chandran, P. Microbial degradation of petroleum hydrocarbon contaminants: an overview. *SAGE-Hindawi Access to Research Biotechnology Research International Volume*, 13 doi:10.4061/2011/941810eme, 5 (1): 95-101, 2011.
- [4]. Y. Zhan, Q. Xu, M.M. Yang, H.T. Yang, H.X. Liu, Y.P. Wang, and J.H. Guo, "Screening of freeze-dried protective agents for the formulation of biocontrol strains, *Bacillus cereus* AR156, *Burkholderia vietnamiensis* B418 and *Pantoea agglomerans* 2Re40". *Lett Appl Microbiol.* 54(1):10-7. 2011.
- [5]. J. Palmfeldt, P. Radstrom, and B. Hahn-Hagerdal, "Optimisation of initial cell concentration enhances freeze drying tolerance of *Pseudomonas chloroaphis*" *Cryobiology* 47, 21–29, 2003.
- [6]. Muyzer, G., Waal, E.C. and Uitterlinden, A.G.. Profiling of complex microbial populations by denaturing gradient gel electrophoresis analysis of polymerase chain reaction-amplified genes coding for 16S rRNA. *Appl. Environ. Microbiol.*, 59, 695–700, 1993.
- [7]. Muyzer, G. and Smalla, K. Application of denaturing gradient gel electrophoresis (DGGE) and temperature gradient gel electrophoresis (TGGE) in microbial ecology. *Antonie Van Leeuwenhoek*;73(1):127-141., 1998.
- [8] Saygili, B. Isolation, Identification And Investigation Of Biodegradation Efficiencies Of The Microorganisms Which Have The Degradation Abilities Of Fluorene And Acenaphthene, *Msc In Biology*, Ege University June 2012, 80 Pages, 2012.
- [9] Tunc, E.. Analysis of Biodegradability of P-toluic Acid and 4-carboxybenzaldehyde in Petrochemical Industry Wastewater, *Msc In Biology*, Ege University, 91 pages., 2014.
- [10] Cay, H. Production of adapted liquid inoculate culture for wastewater treatment and determination of biodegradation efficiency and shelf life. *Msc In Biology*, Ege University, 142 pages, 2017.
- [11] Eroglu, D.. Analysing the biodegradation of terephthalic acid and 1,2 dichloroethane via some microorganism which was isolated from petrochemical system. *Msc In Biology*, Ege University, 93 pages, 2013.
- [12] Zwieler, J., Lassl, C., Hippe, B., Pointner A., Switzeny, O.J., Remely, M., Kitzweger, E., Ruckser R., Haslberge, A.G.. Changes in Human Fecal Microbiota Due to Chemotherapy Analyzed by TaqMan-PCR, 454 Sequencing and PCR, 2011.
- [13] Abadias M., Benabarre A., Teixidó N., Usall J., Viñas I. Effect of freeze-drying and protectants on viability of the biocontrol yeast *Candida sake*, *Int. J. Food Microbiol.* 65, 173–182., 2001.

## Chemical And Mineralogical Properties Of Salt And Soda Lake Muds Used As Peloids In Konya Basin, Turkey

*Muazzez Celik Karakaya<sup>1</sup>, Necati Karakaya<sup>1</sup>,*

### *Abstract*

Tuz Golu is the largest salt lake of Turkey and there are also some soda lakes of different sizes near the lake located in the closed Konya basin in central Anatolia. The muds formed under these salt and soda layers are used by the local people in various diseases in different forms such as mud baths, masks, and cataplasms. The purpose of the study is to determine the mineral types and chemical composition of the muds. The mineralogical compositions of the muds were investigated using X-ray diffraction, and chemical composition of waters and muds were determined by ICP-EAS to determine possible toxicity and suitability of the muds for peliotherapeutic cures. The water of the Salt Lake is enriched by Mg-Na-Cl-SO<sub>4</sub>, Mg-Cl and Na-Cl and their electrical conductivity (EC) values range from 141500 to 227000  $\mu$ S/cm while the soda lakes are enriched by Na-Mg-Cl-SO<sub>4</sub> and Na-Mg-SO<sub>4</sub>-HCO<sub>3</sub>, respectively. EC values of the lakes are between 148000 and 20200  $\mu$ S/cm. The mineralogical composition of the lakes is composed of mainly halite, thenardite, mirabilite, glauberite, gypsum/anhydrite, calcite, and aragonite. Dolomite, rarely konyaite, hexahydrite, bloedite and starkeite are found in some samples. Smectite, palygorskite, sepiolite, illite, kaolinite are common clay minerals in the lake muds. According to the preliminary results, it was determined that it cannot be cause no problems in terms of chemical composition but it may cause some skin problems such as scratching, dryness, and redness of the skin especially due to the high content of non-clay minerals.

**Keywords:** Clay, Konya, muds, peloids, Turkey, Tuz Golu

### 1. INTRODUCTION

It is also known as spa therapy, balneotherapy and peliotherapy which is used as an alternative treatment. Its demand is increasing nowadays and researches on this subject is more concentrated. Spa treatment or cure is usually applied to the patient through the treatment of natural clay and/or clay-mixed organic matter (peloid) mixed with hot water or thermal mineralized water and climate-induced natural therapeutic agents by mud bathing, mud mask, mud bandage, cataplasms or entering into mud pools. Peliotherapy or peloidotherapy, which is a sub-branch of balneotherapy, refers to the application of therapy to the patient in certain sessions and periods after maturation of the peloid, which is a natural mud of geological or partially biological origin, with mixed mainly thermal or saline waters.

Tuz Golu (namely Salt Lake) is in the central Anatolia and is one of the largest permanent hypersaline lakes in the world and the largest lake in the Middle East. It extends as much as 100 km from north to south and is as wide as 65 km east to west during high water periods. In the region there are also some permanent salt and soda lakes around the Tuz Golu in different size. These lakes are formed in tectonically controlled and parallel subsidence basins. The muds used in Salt Lake (Tuz Golu) and soda lakes (Bolluk and Tersakan) are usually formed under the evaporite sediments which are approximately 1-3 cm thick in salt or soda lakes (Figure 1).

The lakes in closed Konya basin are located in central Anatolia is one of the important regions of our country with salt potential and tourism. In the region, where active tectonic movements in central Anatolia and the volcanism in the Tertiary to Quaternary period are widely observed (Figure 1). The Late Eocene to Quaternary basaltic, andesitic, dacitic, and rhyolitic lavas and pyroclastic rocks are covered by Upper Miocene to Pliocene lacustrine and fluvial sediments. The volcanic and volcanoclastic sediments are generally observed in upper level of the basin sediments and interlayered mostly with detrital sediments.

<sup>1</sup> Corresponding author: Konya Technical University, Department of Geological Engineering, 42039 Selcuklu/Konya, Turkey. [muazzezck@gmail.com](mailto:muazzezck@gmail.com)

In the study area, it was observed that the mud which was formed naturally by partially alluvial soils consisting of the clay-silt sized sediments. The sediments are also containing salt crystals in small sized (0.1 to 1.0 cm). The mud is dark gray or black in color and has a good plasticity and is smell bad because it probably contains sulfuric bacteria or organic matter (Figure 2). The use of sludge is not based on any scientific research, especially people think that it is good for skin problems, especially to the feet. The use of sludge is not based on any scientific research, especially when people think that skin problems, such as eczema, fungus, acne, especially on their feet and partly on their hands and face. Some people use the sediment by covering some of their bodies with mud, waiting to dry under the sun and believes that mud is good for muscular-joint and rheumatic pain.

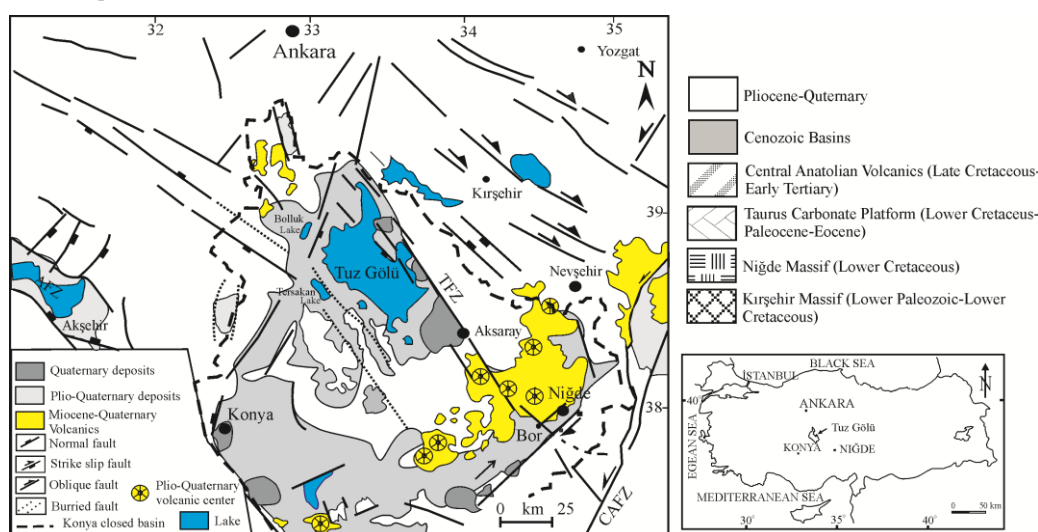


Figure 1. Simplified geology (after [1]) and location maps of study area.



Figure 2. Mud formation in Salt lake of the studied spas.

The therapeutic action of the clays essentially depends upon their mineralogical and chemical composition, as well as the physical, physicochemical properties. It was aimed to determine the suitability of the muds by determining of many properties, e.g. mineralogical composition and mineral content, chemical composition, consistency parameters. It is also aimed to investigate the properties and to determine its suitability of the muds for treatments in especially skin diseases, e.g. eczema, sebora, dermatitis, acne, etc. and to made recommendations.



### 2. MATERIALS AND METHODS

According to the purposes, the muds taken from the salt and soda lakes in the lakes. In order to determine the mineralogical composition, samples were collected and milled, and all samples and clay-sized fraction were analyzed by the Rigaku D / Max 2200 PC X-ray diffraction (XRD) at the Hacettepe University Laboratories. In the detailed clay analysis, three diffractograms were carried out from the oriented samples to normal, ethylene glycol, and baked at 490 ° C for four hours. The main and trace element analyzes of the investigated peloid samples were made in Acme (Canada) Laboratory. In the analyzes ICP-MS and EAS (Inductive Couple Plasma Mass Spectrometry, Emission Spectrometry) were used for the analysis of the main oxides and trace elements, loss on fire and LECO analysis for total C and S analyzes. Apparent viscosities of the samples, which were kept in a peloid-water mixture and kept in a 40°C hot water bath, were measured on a Brookfield LVDVIII + PRO ultra-rheometer. Two parallel measurements were performed at 30-minute intervals and at different cutting rates. The samples were incubated in the hot water bath at 40°C and the measurements were repeated after 24 hours. The consistency of the muds was determined with the Casagrande system using the Atterberg method in accordance with the ASTM 4318-00 standard ([2]). The temperature, pH, Eh, and conductivity water of the lakes were determined on site using WTW Multi 340i instruments and electrodes (pH, SenTix ORP) with automatic temperature compensation. The pH electrode was used after stabilization in a buffer solution at pH 4 and 7 for 24 h, followed by in-situ calibration (buffers at pH 4, 7, and 10).

### 3. RESULTS AND DISCUSSIONS

The saline mud samples are fine- to medium sized, and mineral fraction was predominantly composed of an amorphous phase, mostly halite, dolomite, gypsum, clay minerals, quartz, mica, and feldspar, and rarely pyrite (Table 1). The clay mineral composition identified oriented preparation by XRD, is formed from smectite, palygorskite, chlorite, and kaolinite analysis. Content of smectite and partially palygorskite are higher than the other minerals (Figure 3). The mineralogical composition of the investigated muds is not similar to commercial herbal clay (CHC), natural clay (NC) and pharmaceutical clay (PC) ([3]). The contents of carbonate minerals, e.g., calcite and dolomite lower than 20% in the samples is not negatively affect the required physicochemical properties of the muds.

Table 1. Whole rock and clay-size mineralogical composition of the muds.

Sample Number	Mineralogical composition	Clay Minerals
TL-1	Thenardite+Clay	Pa
TL-2/1	Dolomite+Palygorskite+Gypsum+Bloedite +Quartz+Calcite+Kaolinite	Pa+Chl
TL-2/2	Clay+Albite+Halite+Quartz	Pa
TK-1	Halite+Albite+Quartz+Calcite+Illite	Illt+Kln
TL-2/3	Halite+Calcite+Quartz+Albite+Clay	Chl+Illt+Kln
TL-4	Halite+Calcite+Clay+Dolomite	Sme+Illt+Chl+Kln
CH-3	Halite+Calcite+Clay+Quartz	Chl+Illt+Kln

\*: Chl: chlorite, Illt: illite, Kln: kaolinite, Sme: smectite, Pa: palygorskite (abbreviations from [4]).

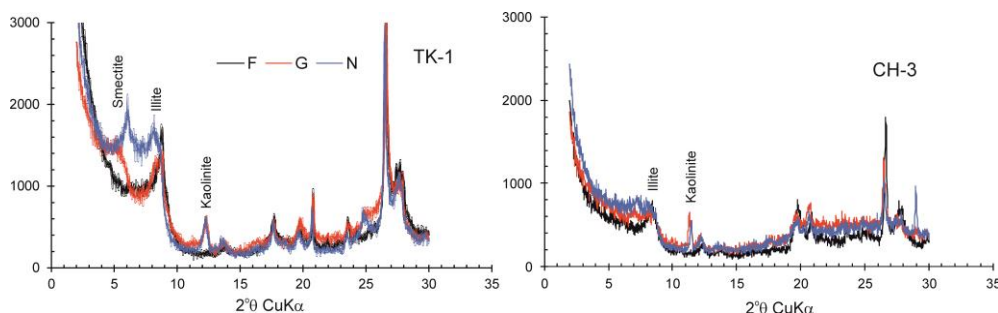


Figure 3. Representative X-ray diffraction pattern of <2 μm fraction oriented in natural condition (N), after heated at 490 °C(F) and solvated in ethylene glycol atmosphere (G).

The saline water pH and electrical conductivity (EC) are vary from 6.30 to 8.16 and 20.2 to 227 mS/cm, respectively. The water of the Salt Lake is enriched by Mg-Na-Cl-SO<sub>4</sub>, Mg-Cl and Na-Cl. The soda lakes are enriched by Na-Mg-Cl-SO<sub>4</sub> and Na-Mg-SO<sub>4</sub>-HCO<sub>3</sub>, respectively. The water of the lakes is neutral to weakly

alkaline. The high pH and electrical conductivity values classify the analyzed samples of the Salt Lake muds contain strong electrolytes.

Major and some trace element concentration of the samples are not similar. Major elements are also different those of the commercial (CHC), pharmaceutical (PC) and partially natural clay (NC) ([3]). Sulfur was enriched in the most of mud samples, and is enriched than those of the CHC, PC, and partially NC in some of the mud samples. The investigated sulfur-rich muds can thus be used for the treatment of some skin diseases. The Ba contents of the samples are range from 72 to 371 ppm which is partially higher than the CHC and especially PC and NC (Table 2). Considering this, Ba may not cause any skin problems and can be used in masks, baths, cures, patches, etc. Some hazardous element contents (As, Ba, Cd, Co, Cr, Pb, Ni, Zn) of the studied muds are partially higher than those of CHC, PC, and NHPG used in treatment ([5]). The As content exceeded the contents of CHC in all of the mud samples while Pb exceeded in one sample than those of the CHC (Table 2).

The toxic and partially toxic elements (As, Ba, Cd, Co, Hg, Pb, Ni, Se, Sb, Te, Tl, Zn) and less harmful elements (Li, Rb, Sr, Cr, Mo, V, Zr, REEs) are not admitted in cosmetic products and peloid therapy, therefore the elements should not be found in these type of materials and required measurements should be make ([3], [5], [6], [7], [8], [9]).

Table 2. Chemical composition of mud samples from the lakes.

	Unit	TL-1	TL-2/1	TL-2/2	TK-1	TL-2/3	TL-4	CH-3	CHC
Al	%	1.48	1.58	2.60	0.87	1.44	0.80	1.13	7.12
As	ppm	<b>11.30</b>	<b>17.17</b>	<b>27.96</b>	<b>16.89</b>	<b>32.21</b>	<b>17.93</b>	<b>17.39</b>	<b>2.88</b>
B	ppm	250.97	1143.67	166.92	318.06	804.04	743.60	440.85	ng
Ba	ppm	291.48	107.38	162.69	117.66	137.45	72.20	136.05	248
Ca	%	<b>15.66</b>	4.03	7.10	<b>31.10</b>	<b>18.41</b>	<b>10.95</b>	<b>14.96</b>	9.92
Cd	ppm	0.10	<b>0.39</b>	<b>0.59</b>	0.20	<b>0.52</b>	<b>0.35</b>	<b>0.35</b>	0.18
Co	ppm	5.68	7.50	<b>13.42</b>	3.47	5.13	3.48	11.91	13.3
Fe	%	1.32	1.53	2.93	0.67	1.14	0.66	1.80	3.65
K	%	0.91	<b>2.71</b>	0.90	0.27	0.73	0.55	0.55	1.80
Li	ppm	74.36	417.72	65.47	99.74	134.61	102.85	42.49	ng
Mg	%	<b>5.89</b>	<b>10.89</b>	<b>2.23</b>	<b>12.05</b>	<b>11.52</b>	<b>6.22</b>	<b>3.03</b>	1.21
Na	%	<b>3.84</b>	<b>6.96</b>	<b>17.66</b>	<b>6.95</b>	<b>3.19</b>	<b>7.70</b>	<b>4.20</b>	0.36
Ni	ppm	38.63	<b>43.45</b>	<b>76.91</b>	18.04	28.26	16.58	<b>58.71</b>	40
Pb	ppm	5.07	6.78	9.40	1.18	4.05	5.15	<b>13.42</b>	11.9
SO <sub>4</sub>	%	<b>20.07</b>	<b>6.98</b>	1.51	1.34	<b>10.26</b>	<b>23.45</b>	<b>20.99</b>	1.41
SiO <sub>2</sub>	%	<b>20.36</b>	15.56	<b>37.75</b>	15.33	17.72	14.24	<b>27.51</b>	19.52
Sr	ppm	336	<b>1469</b>	468	<b>3414</b>	4287	2538	1692	695
Br	ppm	15.37	763.76	411.12	411.10	301.81	149.71	71.26	ng
Cl	%	5.91	10.72	27.22	10.71	4.92	11.86	6.47	ng

Note: ng: not given, high values are shown in bold.

Some elemental contents, e.g., Br, Cl, K, Li, Mg, Na, S, and Si of the water taken from salt and soda lakes were compared with those of sea water. Nearly all of the elements contents in the investigated water were found several times above than those of the sea water (Table 3). Tuz Golu water is enriched crucial elements, including bromine, calcium, chloride, lithium, magnesium, sodium, potassium, and sulfur. These elements are important for skin metabolism of human body (Table 4), ([10]). NaCl has an emollient effect on skin

(Yoshizawa et al. 2001) and useful for acute irritant contact dermatitis due to significant reduction occur in transepidermal water loss (after [11]). Bromine content is higher than those of sea water and

Table 3. Composition of sea water (ppm) at 3.5% salinity (after [12]) and Tuz Golu.

	Na	Mg	Si	S	K	Sr	Ca	Cl	Br	Li
<b>Sea Water</b>	10800	1290	2.9	904	29	8.1	411	19400	67	0.17
<b>Salt Lake</b>	66440	4992	16.2	1299	1534	19.5	466	36643	248	439

Table 4. General Functions of Various Sea Water Minerals (after [11])

Element	General functions in skin
Chloride	Vital for proper metabolism
Sodium	Helps fight free radicals formed in the skin; mitigates skin aging
Magnesium	Increases the production of antioxidants; insufficient levels of manganese may lead to dermatitis
Sulfur	Important for collagen synthesis and for healthy skin keratinization
Calcium	Strengthens cell membranes; aids skin cell metabolism; essential for healing wounds preventing infection; helps cleanse pores
Potassium	Regulate the transfer of nutrients through cell membranes; helps prevent the formation of free radicals; helps prevent acne
Bromine	Simulates the skin's natural process; acts as a natural antibiotic; helps relive the discomfort associated with skin disorders
Boron	Plays a crucial role in maintaining transmembrane functionality
Strontium	Plays a role in connective tissue formation, reduces sensory irritation such as stinging, burning, itching, and inflammation
Silicon	Important for maintaining proper skin thickness and strength, as well as for the production of collagen

Different consistency parameters of the muds were measured. Plastic limit separates semi-solid and plastic behaviors and the liquid limit defines the second from viscous behavior. The consistency parameters are indication of the adhesion between particulate materials. Therefore, the slip resistance against load and stability and changing rigidity may be interpreted from these consistency parameters. At the same time, the liquid limit and the plasticity index are significant indicators swelling potential of the material. The liquid limit and plastic limit values of the samples are not similar (Table 5). Liquid limit and plasticity index are generally related to possible swelling and, the swelling potential of the material was classified as low, intermediate or high swelling capacity. The muds are mostly low plasticity indexes below 15% and also liquid limits under 50%, and are therefore they are not suitable for use as peloids, except one sample (TL-2/2). The high plastic index of the sample TL-2/2 is due to having high clay content than those of the other samples. The material having high plasticity index is more easily handled, easier to remove from the skin and also well adheres to the skin and maintains its property without being dispersed.

Table 5. Consistency limits and other physical characteristics of the peloid samples.

Sample	Liquid	Plastic	Plasticity	Expandability	Activity	Consistency	Consistency
Number	Limit	Limit	Index	Potential	Index	Index	Status
TL-1	28	15	13	LP/LS	0.15	0.34	Rigid
TL-2/1	27	15	12	LP/LS	0.15	0.33	Rigid
<b>TL-2/2</b>	<b>84</b>	<b>27</b>	<b>57</b>	<b>HP/HS</b>	<b>0.58</b>	<b>0.73</b>	<b>Semi rigid</b>
TK-1	46	20	26	MP/MS	0.23	0.29	Rigid
TL-2/3	38	14	24	MP/MH	0.24	0.26	Rigid
TL-4	39	21	18	LP/LS	0.17	0.42	Rigid

Note: \*: HP: plastic clay, MP: moderately plastic clay HS: high swelling, MS: medium swelling.

## 4. CONCLUSIONS

The investigated saline muds are contained clay minerals in partially acceptable percent used in pelotherapy. The water of the salt and other lakes and their muds in particular with abundant mineral salts, especially chloride and sulfate (sulfur) and iron compounds and bromine and the right amount of salt and multiple organic matter is reflected to be one of the finest lakes for medical treatments. The water of this lakes is extremely comforting, sedative and regulate blood flow by causing peripheral vasodilatation. The investigated muds contain especially high As and partially Co, Ni, Cr are not safe for user, therefore the people should be informed about the toxic elements. The muds having high NaCl, KCl, bromine, magnesium which are vital in especially preventing of skin irritation and dermatitis can be used healing these types of discomfort. As a result, muds of Tuz Golu have good properties in especially high content of some vital element for human body, therefore suitability of the muds should be investigated for therapeutic application in detail.

## ACKNOWLEDGMENT

The study was funded by the Selcuk University Scientific Research Projects support program (BAP 17401029).

## REFERENCES

- [1]. K. Dirik, O. Erol. Tuzgolu ve civarinin tektonomorfolojik evrimi, Orta Anadolu-Turkiye. (Haymana-Tuzgolu-) Ulukisla Basenleri Uygulamali Calisma. Turkiye Petrol Jeologlari dernegi Ozel Sayi 5, 2000.
- [2]. ASTM, *Annual Book of ASTM Standards, Standard Test Methods for Laboratory Determination of Liquid and Plasticity Index of Soils*, D 4318, Philadelphia, 1994.
- [3]. N. Mascolo, V. summa, F. Tateo. Characterization of toxic elements in clays for human healing use. *Applied Clay Science*, 1999, vol. 15.
- [4]. D.L. Whitney, B.W. Evans, Abbreviations for names of rock-forming minerals. *American Mineralogist*, 2010, vol. 95.
- [5]. R. Sanchez-Espejo, C. Aguzzi, P. Cerezo, I. Salcedo, A. Lopez-Galindo, C. Viseras, Folk pharmaceutical formulations in western Mediterranean: Identification and safety of clays used in pelotherapy. *Journal of Ethnopharmacology*, 2014, vol. 155.
- [6]. F. Tateo, A. Ravaglioli, C. Andreoli, F. Bonin, V. Coiro, S. Degetto, A. Giaretta, A. Menconi Orsini, C. Puglia, V. Summa, The in-vitro percutaneous migration of chemical elements from a thermal mud for healing use. *Applied Clay Science*, 2009, vol. 44.
- [7]. M.I. Carretero, M. Pozo, J.A. Martin-Rubi, E. Pozo, F. Maraver, Mobility of elements in interaction between artificial sweat and peloids used in Spanish spas. *Applied Clay Science*, 2010, vol. 48.
- [8]. M. Robelo, M. Viseras, A. Lopez-Galindo, F. Rocha, E. Ferreira da Silva, Rheological and thermal characterization of peloids made of selected Portuguese geological materials *Applied Clay Science*, 2011, vol. 51.
- [9]. M. Mattioli, L. Giardini, C. Roselli, D. Desideri, Mineralogical characterization of commercial clays used in cosmetics and possible risk for health. *Applied Clay Science*, 2016, vol. 119.
- [10]. Z. Ma'or, S. Yehuda, and W. Voss. 1997, Skin smoothing effects of Dead Sea minerals: comparative profilometric evaluation of skin surface. *International Journal of Cosmetic Science*, vol. 19 (3).
- [11]. J.H. Kim, J. Venkatesan, P.N. Sudha, *Sea Water and Sea: Mud Cosmeceutical Applications*. Marine Cosmeceuticals, Trends and Prospects, Taylor Francis, Boca Raton, 2011.
- [12]. K.K. Turekian, *Oceans*, Prentice-Hall, Englewood Cliffs, NJ, 1968.

## Lithofacies And Geochemical Properties Of Neogen Deposits At South Of Tuzgolu- Turkey

Arif Delikan<sup>1</sup>, Muazzez Celik Karakaya<sup>1</sup>, Necati Karakaya<sup>1</sup>, Hatice Unal  
Ercan<sup>1</sup>, Ayla Bozdogan<sup>1</sup>

### Abstract

The Tuzgolu Basin located at the Central Anatolia (Turkey) is bounded by Ankara uplift at the north, the Kirsehir massif from the east and the Sivrihisar-Bozdogan massive at the west. In the study area which is located at the South of the Tuzgolu, the Paleogene and Mesozoic marine carbonates and igneous rocks underlies the Neogene sequences. Neogene deposits consist of Kizilbayir, Katrandetepe and Bestepeler formations which are conformable with each other. 10 different lithofacies were identified within the Neogene sequence by considering sedimentation conditions, lithology, sedimentary structure and fossil content.; Grain-supported conglomerate facies (Gcu), Convolute bedded sandstone facies (Sk), Thick-bedded sandstone facies (St), Gray-purple colored thick layered mudstone facies (Mt), Oolitic limestone facies (OC), Alternating gypsum-anhydrite-mudstone-micritic limestone facies (Cmag), Bituminous shale facies (Bs), Halite-mudstone facies (Hm), Massive and parallel laminated tuff facies (Pmlt), Alternating mudstone-sandstone facies (Ms). The facies analysis show that sedimentation in the study area began with fluvial sediments (Kizilbayir formation) and followed by sediments of shallow lake which was often interrupted by sediments from land (Katrandetepe formation), and by the interbedded mudstone, sandstone, conglomerates and tuff at the closure of the lake (Bestepeler formation). According to the geochemical analysis results obtained from lake carbonate and evaporite deposits (Halite, anhydrite and gypsum), REE, LILE and HFSE values are more abundant in clayey samples than those in other evaporitic sediments. The Sr contents of halites (1-1539 ppm) are lower than sulfate (183-4378.04 ppm) and carbonates (922-12365 ppm). Halite minerals contain very high Cl (505686-615905 ppm) and low Br (5-637 ppm) indicating that they are products of dissolution, mixing and re-precipitation.

**Keywords:** Tuzgolu, Lithofacies, Halite, Gypsum, Anhydrite

### 1. INTRODUCTION

The Anatolian plateau was formed by the collision of the Arabian and Eurasian plates ([2] and [3]). The study area is located at the Central Anatolia is an inner enclosed basin and is bounded by Ankara uplift in the north, the Kirsehir massif from the east and the Menderes massif from the west (Figure.1). During this time, two major fault systems in the area, the Tuz Golu and the Sultanhanli faults, developed as south-west dipping, NW–SE striking, normal faults. At some time in the Late Miocene-Early Pliocene, during regional subsidence, a previously unreported phase of contraction occurred, which led to the development of a north-east–vergent thrust sheet, the culmination of which forms the morphologic ridge to the east of the Tuz Golu Lake ([2], [3], [4], [5], [6], [7], [8] and [9]).

The Tuz Golu Basin is located in the south-eastern part of Central Anatolia (Figure 1). Evaporitic and carbonate (limestone and dolomite) deposits are deposited from Na, Ca, Mg, Cl, CO<sub>3</sub>, and SO<sub>4</sub> in different contents and most of them were precipitated in inner continental basin, tectonically active (slump folding, chaotic structure and collapse deposits) and arid lacustrine environments which effected time to time intake of seawater ([1], [2], [3]). In this study area, more thicknesses of salt and soda than a few hundred meters were deposited during Miocene period.

<sup>1</sup> Corresponding author: Konya Technical University, Department of Geological Engineering, 42031, Selcuklu/Konya, Turkey. [adeli@selcuk.edu.tr](mailto:adeli@selcuk.edu.tr)

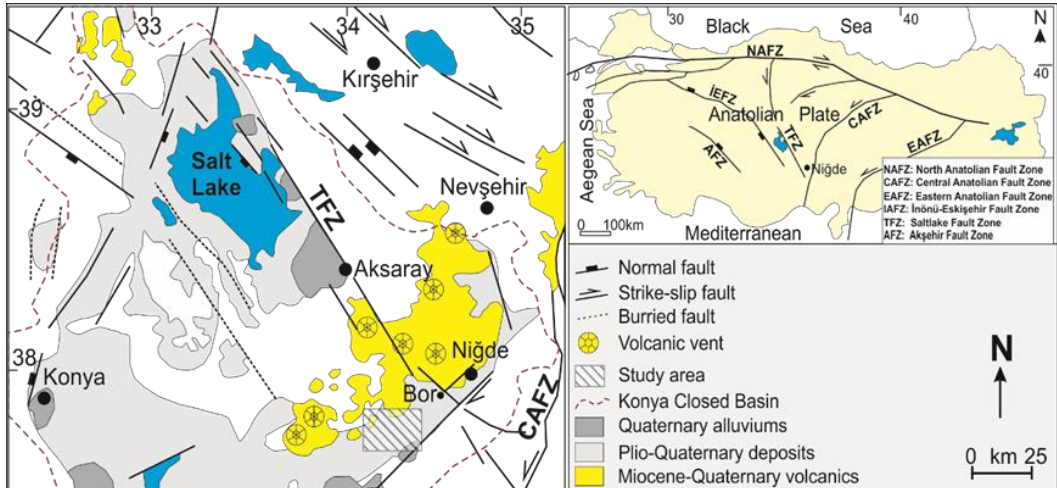


Figure 1. Simplified geology map (after [1])

## 2. RESULT AND DISCUSSION

### 2.1 STRATIGRAPHY

There are sediments of more than 3000 meters deposited in the Paleozoic-Quaternary period at the base of the Tuz Golu basin and various rock assemblages settled with volcanic activity (Figure 1).

### 2.2 Basement Rocks

Paleocene (Serenkaya formation), Eocene (guney formation) and Paleozoic aged metamorphic and sedimentary rocks (Asagidedigi formation) are found at the base of the late Miocene aged Lake formations (Figure 2 and 3)

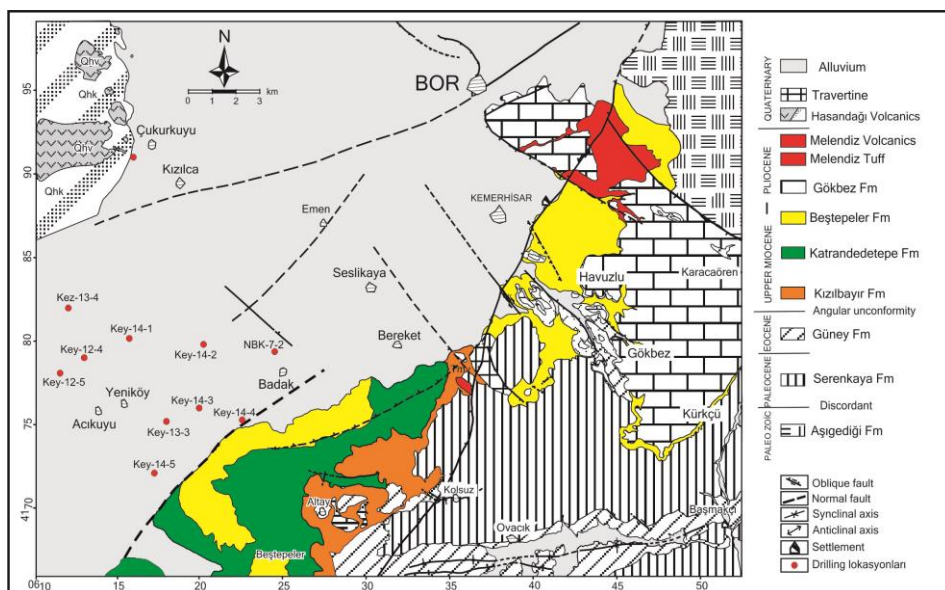


Figure 2 Geological map of study area (from [4], [5], [6], [7],) and drill locations

















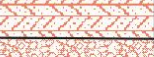








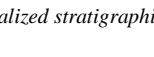

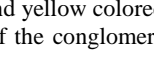

ERATHM	SYSTEM	SERIES	STAGE	FORMATION	THICKNESS	LITHOLOGY	EXPLANATION
CENOZOIC	QUATERNARY	PLIOCENE	UPPER	YULIUM	20-30		Gravel-sand-mud accumulating in valley bottoms
				15-20			Poorly cemented gravel and sand
				HASANDAG VOLCANICS			Pyroclastic-Basalt and andesites
				MELLENDEZ VOLCANICS			Basalt and andesites
				GÖKBEZ			Tuff and aglomera of Melendez volcanics
							Abundant plant fossiliferous mudstone-marl alternation
							Tuff and aglomera of Melendez volcanics
				BESTEPELER	400-450		Green-gray colored sandstone with gypsum and anthracite bands Mudstone alternation
							Polygenic conglomerate and sandstone with large gravels alternations
				KATRANDEDETEPE	700-1400?		Beige-Green lacustrine limestone marl-mudstone alternations
							Gypsum and mudstones starting with the basal conglomerate
							Anhydrite and mudstone alternation with coal level.
							Glauberite-anhydrite and halite-mudstone alternation
							Bituminous shale with dark brown oil spill. Dolomite and clayey limestone
							Carbonized level with a thickness of about 30 cm
NEOGENE	MIOCENE	UPPER	KIZILBAYIR	200-350			Reddish green colored claystone-siltstone alternation
							Green colored, cross-bedded and laminated sandstones
							Well cemented polygenic conglomerate
							Gray colored mudstone, thick bedded sandstone and shale alternations
							Sedimentary facies with limestone blocks
							Conglomerate-sandstone with normal grading and Shale alternation
							Coarse-grained conglomerate contain magmatic rock pebbles
							Metagabro
							Crystalline limestone
							Crystalline limestone
MESOZOIC	CRETACEOUS			SINERIZYAYLA METAGABRO			Metagabro
PALEOZOIC				AŞICEDİĞİ			Crystalline limestone

Figure 3. Generalized stratigraphic section of the study area (from [4], [5], [6], [7]).

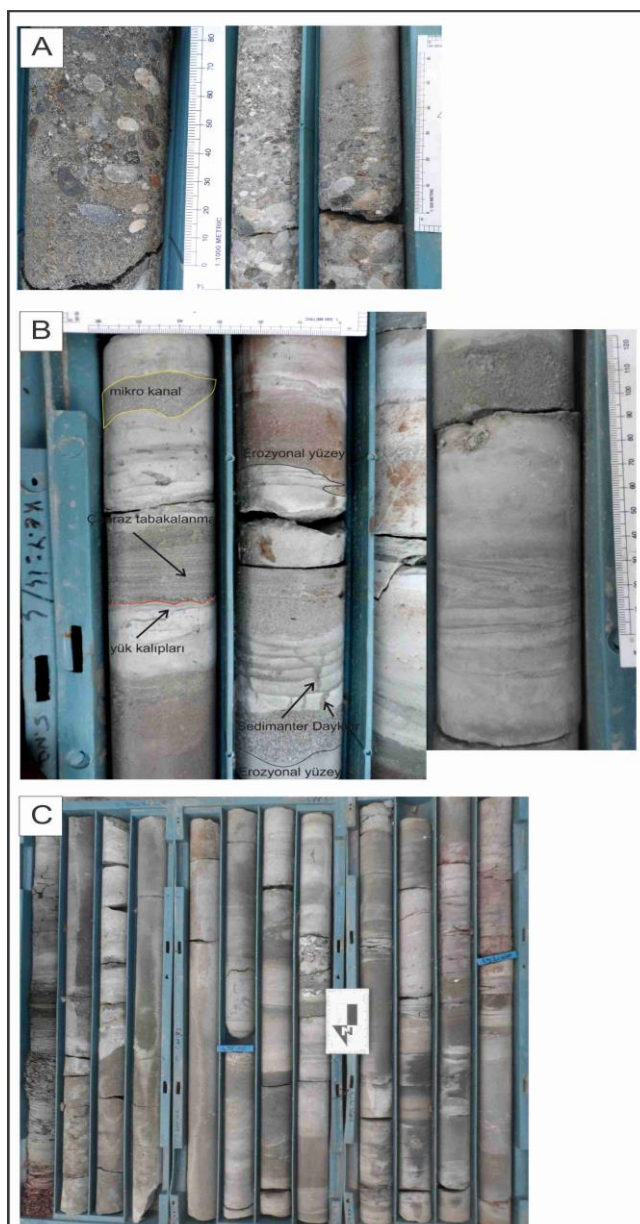
### 2.3 Kizilbayir formation

The formation comprises reddish and yellow colored conglomerate, sandstone and mudstone. Additionally, in the drilling logs, normal grading of the conglomerates, cross bedding and lamination in the sandstones are observed.

The Kizilbayir formation was deposited in a tectonically very active basin so that depositional conditions changed frequently and several different facies were deposited.

Three lithofacies were defined within the Kizilbayir Formation;

1. Clast-supported conglomerate lithofacies (Figure 4)
2. Convolute bedding sandstone lithofacies (Figure 4)
3. Gray-claret colored thick-bedded mudstone lithofacies (Figure 4)

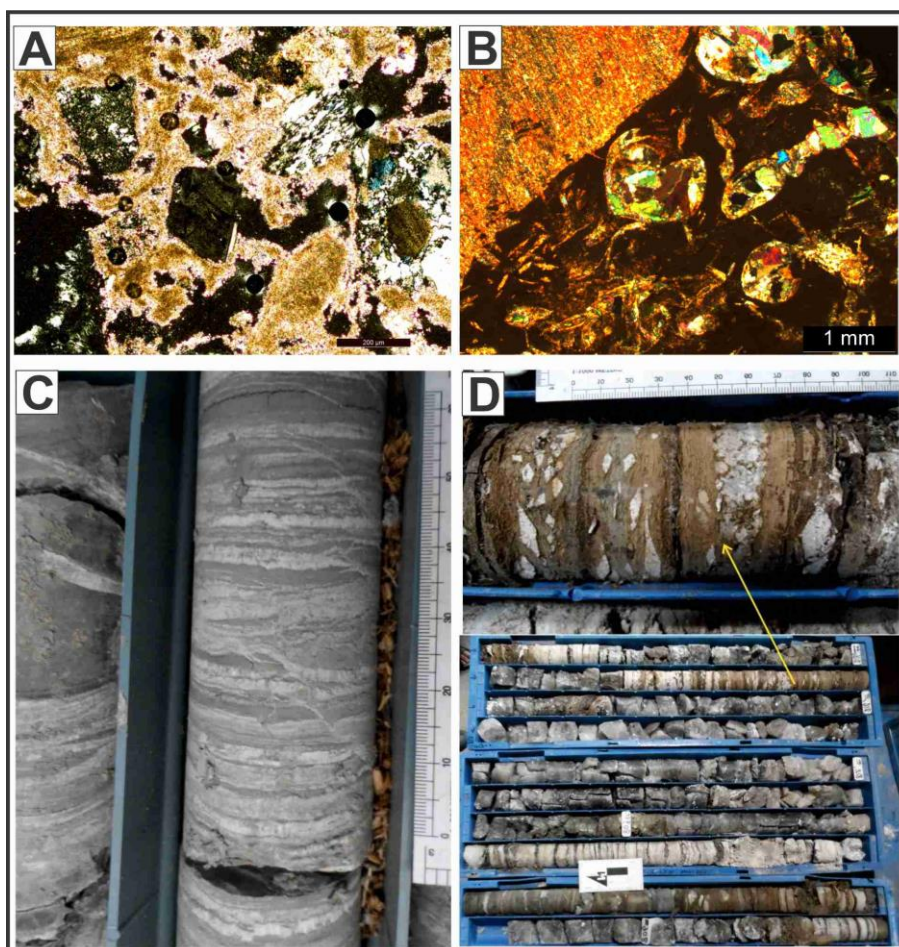


**Figure 4** Lithofacies of Kizilbayir formation; A. Clast-supported conglomerate lithofacies (Normal graded conglomerate), B. Convolute bedding sandstone lithofacies, C. Gray-claret colored thick-bedded mudstone lithofacies

## 2.4 Katrandedetepe formation

Formation consists of halite, gypsum, anhydrite, gulberite, mudstone, limestone, dolomite, bituminous, petroliferous sandstone, siltstone and sandstone. The formation commonly contains deformational structures. Such as salt diapirs, slump folds, and load cast structures. Three lithofacies were defined within the Katrandedetepe formation;

1. Oolitic limestone lithofacies (Figure 5)
2. Anhydrite, gypsum –mudstone –micritic limestone lithofacies (Figure 5)
3. Bituminous, petroliferous sandstone (Figure 5)



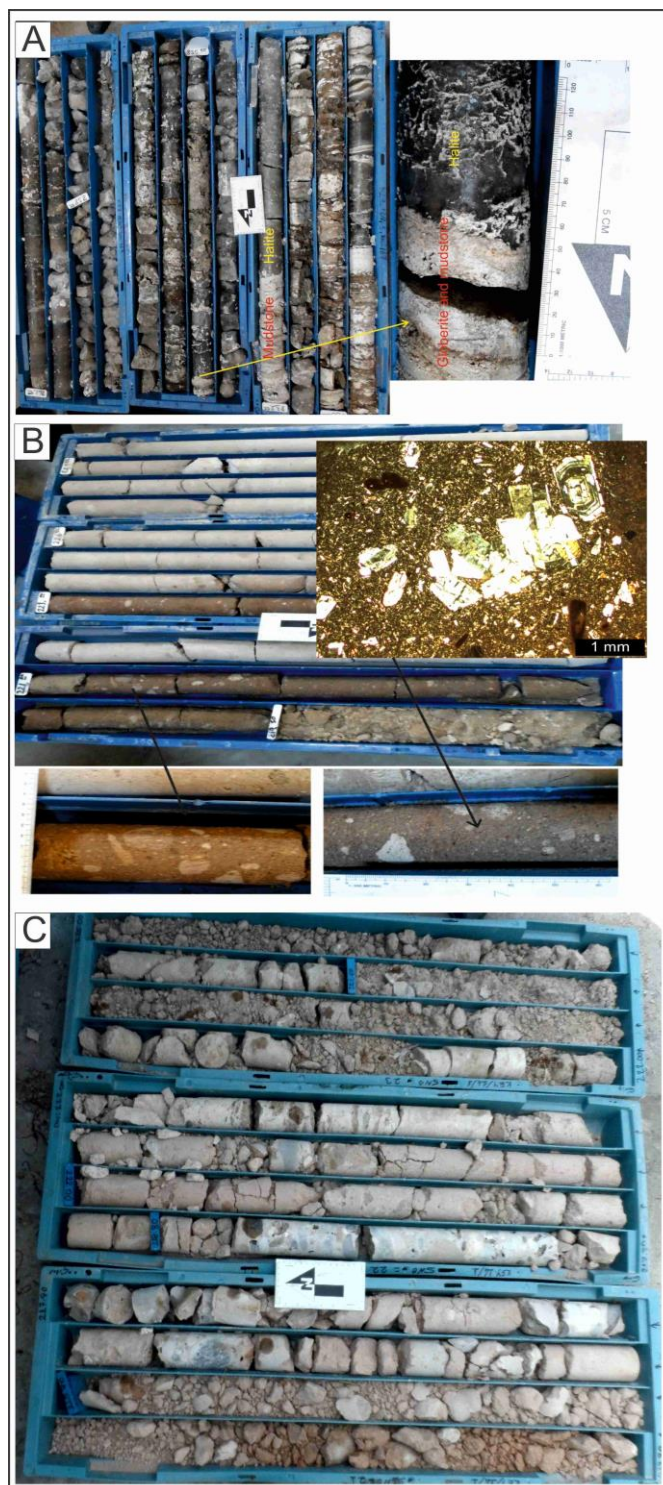
**Figure 5** Lithofacies of Katrandedetepe formation; A. Oolitic limestone lithofacies (Thin section photos), B. Anhydrite, gypsum –mudstone –micritic limestone lithofacies (Gastropoda shell was filled by anhydrite), C. Bituminous, petroliferous sandstone Lithofacies

## 2.5 Bestepeler formation

The formation includes light green mudstone, siltstone, sandstone, conglomerate, cream colored tuff and tuffite. Three lithofacies were defined within the Bestepeler formation;

1. Halite-mudstone-lithofacies (Figure 6)
2. Masiv and tabular bedding lapilli tuff lithofacies (Figure 6)
3. Mudstone-sandstone alternate lithofaciess (Figure 6)





**Figure 6** Lithofacies of Bestepeler formation; A. Halite-mudstone-lithofacies, B. Masiv and tabular bedding lapilli tuff lithofacies, C. Mudstone-sandstone alternate lithofaciess

### 3. GEOCHEMICAL PROPERTIES

According to petrographic and geochemical analyzes, 3 groups of minerals were identified. distribution of minerals according to depths in drilling log (Figure 7). Three groups are Sulphates, carbonates and Halite-Globerite

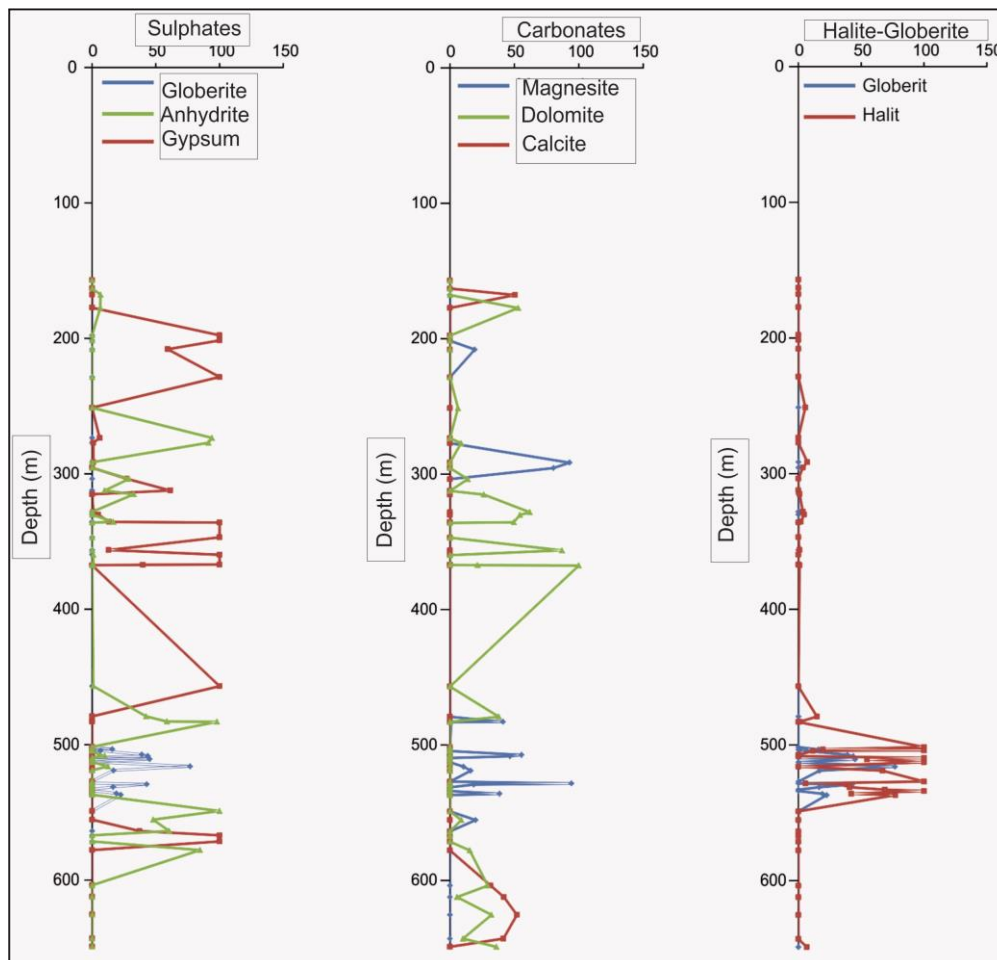


Figure 7. Changes of mineral contents of TG3 drilling.

### 4. CONCLUSION

1. The regional subsidence phase in the study area started in Tortonian times. A sediment sequences (Bestepe, Katrandetepe and Kizilbayir formations) which is more than 1000 m thick deposited from Late Miocene and possibly into Pliocene times
2. Facies properties and the synsedimentary structures (such as slump folding, chaotic levels, sedimentary dykes ect.) in the Katrandetepe formation show that the region was tectonically controlled.
3. The sequences comprise alternating evaporitic deposits (the cycle of the halite, gypsum, anhydrite) and siliciclastic deposits. This indicate that there was a continuous sedimentation which was mainly controlled by paleoclimatic changes

### REFERENCES

- [1] Goncuoglu, M. C., Turhan, N., Senturk, K., Uysal, S., Ozcan, A. & Isik, A. Orta Sakarya'da Nallihan Saricakaya Arasindaki Yapisal Birliklerin Jeolojik Ozellikleri. Maden Tetkik ve Arama Derleme Rapor No: 10094, Ankara (yayimlanmamis), 1996.
- [2]. Fernández-Blanco, D., Bertotti, G., Ciner, T.A. 2013. "Cenozoic Tectonics of the Tuz Golu Basin (Central Anatolian Plateau, Turkey)", Turkish Journal of Earth Science, 22, 715-738.
- [3] Yoldas, R. Ulukisla (Nigde) Bitumlu sist alaninin jeolojik ve ekonomik olanaklari, MTA rapor no: 5050, 1973.
- [4] Oktay, F. Y. Stratigraphy and Geological evolution of the Ulukisla and Surrounding Area. Geological Bulletin of Turkey, vol. 25, pp 15-23, 1982. Physical Geography
- [5] Demirtasli, E., Turhan, N., Bilgin, A. Z. & Selim, M. Geology of the Bolkar Mountains. In: Tekeli, O. & Goncuoglu, M.C. (Eds.), Geology of the Taurus Belt, Proceedings of the International Symposium on the Geology of the Taurus Belt, pp. 125-141, 1984.
- [6] Goncuoglu, M. C. Geochronological data from the Southern Part (Nigde Area) of the Central Anatolian Massif: Bulletin of Mineral Research and Exploration Institute of Turkey (MTA), vol. 105/106, pp 111-124, 1986.
- [7] Atabey, E. & Ayhan, A. Nigde-Ulukisla-Camardi-Ciftehan Yoresinin Jeolojisi, MTA Derleme no: 8064, 1986.
- [8] Muller, D.W. & Mueller, P.A. Origin and age of the Mediterranean Messinian evaporites: implications from Sr isotopes. Earth Planet. Sci. Lett., vol. 107, pp 1-12, 1991.
- [9] Gorur, N. & Tuysuz, O. Cretaceous to Miocene Palaeogeographic Evolution of Turkey: Implications for Hydrocarbon Potential. Journal of Petroleum Geology, vol. 24, pp 119-146, 2001,1.

### CURRICULUM VITAE

**Name Surname:** Assist Prof. Dr. Arif DELIKAN

**Occupation:** Researcher and lecturer in Konya Technical University Engineering and Natural Science Faculty, Geological Engineering Konya TURKEY

**Teaching Activities:** I have been giving various courses in undergraduate, master and doctoral students since 2004.

**Experience:** My MS and PhD thesis were related to Sedimentology, sedimentary rocks, general geology. I completed above 2 national projects supported by TUBITAK and University. My studies published in SCI-indexed (4 papers). I presented my results above 50 international and national symposiums. My publications were cited over 20 indexed publications.

**Areas of interest:** My research activities especially on sedimentary rocks, Basin analysis, Facies analysis, Stratigraphy, Tufa and Travertine



## Tannase Production and Enzyme Characterization from *Bacillus coagulans*

Esra Sunduz Yigittekin<sup>1</sup>, Sadik Dincer<sup>1\*</sup>

### Abstract

In this study, the tannase from *Bacillus* sp. strains isolated from soil samples were produced and characterized. Tannase production of these strains were determined by production of clear zones around the colonies on the tannic acid containing medium, after 96 hours incubation at 37°C. The enzymes isolated from *Bacillus* sp. 2.11 strain used in this study because it showed the best activity. *Bacillus* sp. 2.11 was determined to be *Bacillus coagulans* with the VITEK-2 Compact System. Three bands with molecular weights of 17 kDa, 14 kDa and 5 kDa were detected by SDS-PAGE analysis of the tannase produced from *Bacillus coagulans* strain. *Bacillus coagulans* enzyme activity was determined to be 0.313 µmol/mL, enzyme showed optimum activity at 30°C and pH 4.2. The *Bacillus coagulans* enzyme was able to maintain its activity for 64% at 80 °C for 15 minutes. The enzyme activity of *Bacillus coagulans* was able to maintain its activity with 1mM HgCl<sub>2</sub> (74.7%) and was significantly inhibited with 1mM and 5mM MnCl<sub>2</sub> and 5mM FeCl<sub>2</sub> (0%). According to these results, due to the characteristics property of tannase produced from *Bacillus coagulans*, it can be suggested that the enzyme is appropriate for industrial applications. This study was supported project by Cukurova University Scientific Research Project Coordinator with coded FYL-2015-3782.

**Keywords:** *Bacillus coagulans*, tannase, tannic acid, characterization

### 1. INTRODUCTION

Tannins are naturally occurring and water-soluble polyphenols in plants. It is usually found in the fruits, leaves, roots, trunk and seeds of plants. Tannins are gallic acid and glucose esters and have the chemical formula C<sub>14</sub>H<sub>10</sub>O<sub>9</sub> ([1]-[3]). They bind to proteins and precipitate. It has a great influence on the food and feed quality of many food consumed by humans and animals. Tannins inhibits many microorganisms thanks to inhibition of enzyme activity and their development resistance to microbiological attack ([4]-[6]). Tannins are classified as Condensed Tannins, Hydrolysable Tannins (Gallotannins, Ellagitannin), and Complex Tannins.

Tannin acyl hydrolase (EC 3.1.1.20), known as tannase, catalyzes the hydrolysis of debacle bonds in gallic acid esters and hydrolysable tannins such as tannic acid. As a result of hydrolysis of tannic acid with tannase occurs gallic acid and glucose ([7]- [9]). Resources of tannase are plants, animals and microorganisms (bacteria, fungi, yeast). Tannase is used for various industrial application such as, ready tea and cold tea production, wine and beer production, gallic acid production, animal feed additive and industrial wastewater treatment. In this study, it was aimed that production and characterization of tannase from *Bacillus* strain showing the best tannase activity. In this study, it was aimed that production of tannase which appropriate for using removing and clarifying of foam occurring during the production of cold tea, beer and wine, increasing the digestibility of tannins in animal feed industry, with gain of Gallic acid ensure that its using at pharmacology, remove organic pollutant tannins from industrial wastewater.

\* Corresponding author: Cukurova University, Science and Letter Faculty Biology Department, 01330, Saricam/Adana, Turkey. [esra-gokyuzu@hotmail.com](mailto:esra-gokyuzu@hotmail.com) [sdincer@cu.edu.tr](mailto:sdincer@cu.edu.tr)

<sup>1</sup> Cukurova University, Science and Letter Faculty Biology Department, 01330, Saricam/Adana,

## 2. MATERIALS AND METHODS

### 2.1. Isolation of *Bacillus* sp.

Soil samples were taken from *Platanus orientalis*, *Thuja orientalis* and *Cupressus arizonica* trees and 2 gr from each samples were weighed and homogenized in 10 ml sterilized saline with vortex. For the isolation of bacteria two different Isolation process is carried out .in the one of them before the inoculation soil samples incubated for 15 min at 85°C to eliminate non spore forming bacteria. 1ml of each soil suspension samples were inoculated to 10 mL bullion containing tannic acid (Tannic acid, 10 g/L; K<sub>2</sub>HPO<sub>4</sub>, 0,5 g/L; KH<sub>2</sub>PO<sub>4</sub>, 0,5 g/L; MgSO<sub>4</sub>, 0,5; NH<sub>4</sub>Cl, 1 g/L; CaCl<sub>2</sub>, 0.01 g/L; D-Glucose, 0,5 g/L) ([10]) and allowed to grow at 37°C in orbital shaker at 150 rpm for 72 hours. At the end of the incubation, these mediums were seeded onto PCA plate by reduction method and incubated for 24 hours at 37 °C. The single colony was seeded onto PCA again and incubated at 37°C for 24 hours. After incubation, plates were stored in t refrigerator at 4°C.

### 2.2. Determination of Tannase Producer Microorganism

The isolated bacteria were spotted on tannin agar plate and incubated for at 37 °C. for 72 hours. After incubation, to determine the biodegradation zone, plates were respectively staining with 0.01 M FeCl<sub>3</sub> and washing with 1M NaCl ([11]).

### 2.3. Identification of Bacteria

Gram-stained bacteria were identified by VITEK-II Compact System.

### 2.4. Production of Tannase Enzyme in Liquid Media

Tannase positive bacteria strains on solid medium were transferred liquid enzyme production medium and incubated at 37°C, 150 rpm for 48 hours. After incubation, the bacterial culture was centrifuged at 10,000 rpm for 15 minutes at + 4 °C (Sigma 2-16 K) the supernatant which containing tannase enzyme was used for enzyme activity assays.

### 2.5. Production of Tannase in Liquid Medium and Determination of Tannase Activity

To determine tannase activity from the isolated enzyme, first of all the enzyme, substrate and 0.05 M citrate buffer were incubated separately at 30°C for 5 minutes. Then Enzyme samples (250 µl enzyme + 250 µl substrate), blank (250 µl 0.05 M citrate buffer + 250 µl substrate) and control group solutions (250 µl substrate) were prepared and incubated at 30°C for 5 minutes. End of the incubation 300 µl of Rhodanin was added to each solution and incubated at 30°C for 5 minutes. After that ,200 µl 0.5 N KOH was added to each solution and incubated for 5 minutes at 30°C. in the next step 250 µl of enzyme (previously incubated at 30 °C for 5 minutes.) was added to only the control group. Finally, 4 mL of pure water was added to each tube and incubated at 30 °C for 5 minutes. End of the reactions. Tannase activity was measured at a wavelength of 520 nm with 96-well 'Multiskan <sup>TM</sup> FC Microplate Photometer' (Thermo Scientific <sup>TM</sup>). Incubation experiment were performed in a Bioer ThermoCell cooling & heating block and water bath. At the end of the measurement, tannase activity was calculated according to the following equation ([8]).

$$\text{Activity} = (\text{Enzyme Sample-Blank}) - (\text{Control-Blank}) \mu\text{mol/mL}$$

### 2.6. Characterization of Enzyme

#### 2.6.1. Determination of the optimum pH Value for the Enzyme Activity

To determine the optimum pH of the enzyme activity, experiments were carried out at various pH values using citrate (pH 3.0-5.8), Tris-Maleat (pH 6.2-7.4), Tris (pH 7.6-9.0) and Carbonate-Bicarbonate (pH 9.2-10.7) buffers containing methyl gallate substrate (0.01 M concentration) was prepared and standard enzyme activity was determined.

#### 2.6.2. Determination of Optimum Temperature Value of Enzyme

To determine the optimum temperature value of the enzyme activity, experiments were carried out at various temperatures (20, 30, 40, 50, 60, 70, 80, 90 and 100 °C). the experiments that temperature range 20°C from to 80°C were conducted in the Bioer ThermoCell Cooling&Heating Block and temperature range from 90-100°C

experiments were conducted in oil bath. Standard activity assay was carried out using substrate prepared at optimum pH.

### 2.6.3. Determination of Thermal (Temperature) Stability of Enzyme

For the detection of thermal (temperature) stability, the enzyme was pre-incubated at 80,90 and 100°C for various times (5,10,15,20 and 30 minute) After preincubation, activity experiment was carried out at optimum temperature and pH values.

### 2.6.4. The Effect of Inhibitor and Divalent Cations on Enzyme Activity

For the determination of the divalent cations effect on the tannase activity, stock metal solutions were prepared such as MgCl<sub>2</sub>, CuCl<sub>2</sub>, CoCl<sub>2</sub>, HgCl<sub>2</sub>, NiCl<sub>2</sub>, MnCl<sub>2</sub>, CaCl<sub>2</sub>, FeCl<sub>2</sub> and ZnCl<sub>2</sub> also metal and enzyme solution mixtures were prepared for pre-incubation of enzyme. Final volume of these mixtures were 100µl and final cation concentrations were prepared as 1mM and 5 mM. Pre-incubation of enzyme was carried out at 37°C. As an enzyme inhibitor, EDTA's effect on enzyme activity was investigated with same method. The activity experiments were carried out at the temperature which the optimum activity was observed and the substrate prepared at the pH value which the optimum activity was achieved.

### 2.7. Determination of Enzyme Molecular Weight by SDS-PAGE Method

The molecular weight of the tannase was determined with SDS-PAGE and Zymogram analyzes ([12],[13]).

## 3. RESULTS AND DISCUSSION

### 3.1. Identification of Bacteria

As a result of gram staining, *Bacillus* sp. 2.11 strains were defined as gram-positive and rod-shaped bacteria with microscopic examination. According to VITEK-2 Compact System results, isolated microorganism was identified as *Bacillus coagulans* strain.

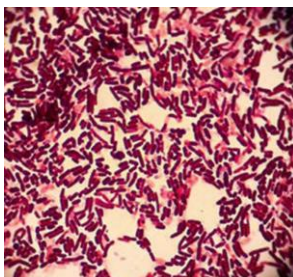


Figure 1. Microscopic appearance of gram stained *Bacillus* sp. 2.11



Figure 2. Result of VITEK-II Compact System type identification test

### 3.2. Determination of Tannase Producing Microorganism in Solid Media

Bacteria was spot-seeded onto Tannic Acid-Agar plates and incubated for 72 hours at 37°C. At the end of the incubation, the medium was stained with 0.01 M FeCl<sub>3</sub> and photographed before and after staining. It was observed that there is positive tannase activity considering, occurring transparency zone around the bacteria.



Figure 3. The appearance of the tannase positive microorganism before and after staining

### 3.3. Determination of The Strain Showing Tannase Activity

*Bacillus coagulans* enzyme activity was determined as spectrophotometric measurements at 0.313  $\mu\text{mol} / \text{mL}$ .

### 3.4. Effect of pH on Tannase Activity

In this study the highest enzyme activity was found at pH 4.2 (100%) in citrate buffer (Figure 4). While the enzyme showed an average of 92.5% activity in pH 4.2-4.6, activity average at pH 5.0-9.0 decreased to 49.42% and at pH 9.2-10.4 to 27.5%.

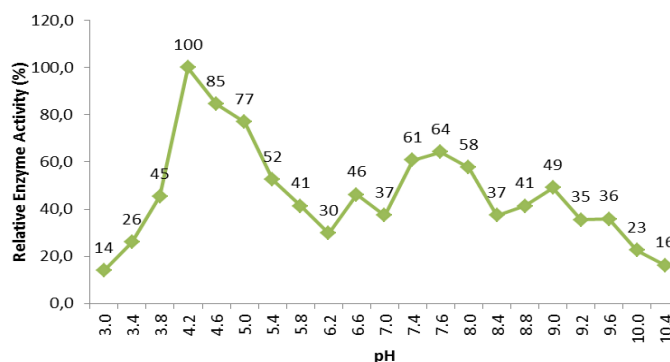


Figure 4. Optimum pH value of tannase enzyme activity produced from *Bacillus coagulans*

In other studies, optimum activity pH value of tannase produced from *Aspergillus niger* LCF 8 was determined to be 5 ([14]), optimum tannase activity of *Bacillus* sp. was obtained at pH 4.5 ([15]), the optimum tannase activity of *Bacillus subtilis* at pH 6 and the tannase which was cloned to *Lactobacillus plantarum* was observed at pH 5 ([16]).

Considering these results, it can be say that the enzyme is appropriate for using in acidic conditions.

### 3.5. Effect of Temperature on Tannase Activity

The optimum enzyme activity of *Bacillus coagulans* was showed at 30 °C (Figure 5). At the other temperatures it is observed that enzyme activity maintained 22% at 20 °C, 55% at 40 °C, 59% at 50 °C, %54 at 60 °C, 47% at 70 °C, 20% at 80 °C, 10% at 90 °C and 0% at 100 °C. While the average activity of the %range from 20 to 70 °C was % 56.28 decreased to 8.9% at range from 80 to 100°C. Considering these results, the *Bacillus coagulans* enzyme has a high activity in the range of 20-70°C and has a mesophilic property.

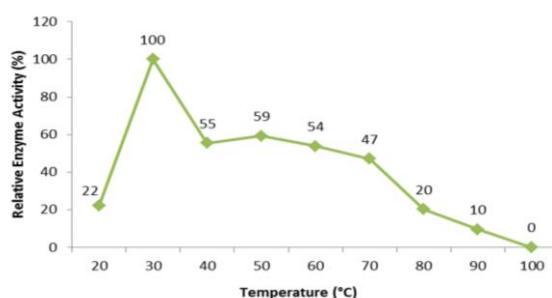


Figure 5. Optimum temperature value of tannase enzyme activity produced from *Bacillus coagulans*

In study of Yao et al. (2011), they obtained tannase from tannase-coded tan410 gene and purify, then optimum tannase activity temperature was determined to be 30°C ([17]). In another study tannase gene was cloned to *Lactobacillus plantarum* then the tannase produced from that microorganism showed optimum activity at 45°C ([16]) and in the study conducted with tannase produced from *Bacillus cereus* KBR9 strain, optimum activity temperature of enzyme was determined 40°C ([18]).

### 3.6. Findings on the Thermal Stability of Enzyme *Bacillus coagulans*

The *Bacillus coagulans* enzyme was able to maintain its activity 64.80% at 80 °C for 15 minutes (Figure 6). Considering the obtained data, it can be say that *Bacillus coagulans* enzyme maintained its activity an average of 39.75% after preincubation period of 0-30 minutes at all temperature values. This result revealed that the enzyme is mesophyll.

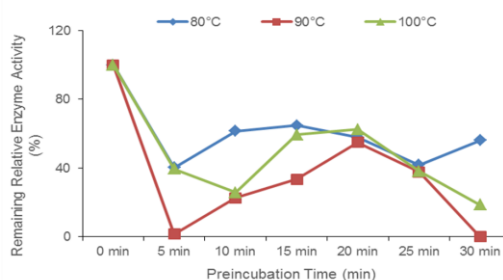


Figure 6. Thermal stability of enzyme *Bacillus coagulans*

Zakipour-Molkabadi et al. (2013) in their study partially purified and characterized the tannase which produced from *Penicillium* sp. EZ-ZH190 and they observed that the enzyme activity maintained 50% of the maximum activity at 50°C ([19]). The GALLO\_1609 gene from *Streptococcus gallolyticus* UCN34 cloned to *Escherichia coli* BL21 (DE3) and expressed as an active protein then its determined that the enzyme maintained its activity of 25% at 45°C ([20]).



### 3.7. Effect of Inhibitor and Divalent Cations on Enzyme of *Bacillus coagulans*

The tannase enzyme maintained its activity 74.7% after preincubated in 1mM concentration of  $\text{CuCl}_2$ . Enzyme activity was totally inhibited with both 1mM and 5mM concentration of  $\text{MnCl}_2$  and 5mM concentration of  $\text{FeCl}_2$ . Experiments results related with effects of inhibitors and divalent cations on enzyme activity were given Table 1.

Table 1. Effect of inhibitor and divalent cations on enzyme of *Bacillus coagulans* activity

Chemical	Relative Remaining Activity (%) (%) 1mM Concentration	Relative Remaining Activity (%) 5 mM Concentration
Control	100	100
EDTA	26,1	45,4
$\text{CaCl}_2$	18,3	13,3
$\text{HgCl}_2$	74,7	35,6
$\text{MnCl}_2$	0	0
$\text{ZnCl}_2$	37,6	30,4
$\text{MgCl}_2$	48,4	46,2
$\text{NiCl}_2$	10,3	52,2
$\text{CuCl}_2$	43	22,1
$\text{CoCl}_2$	41,4	28
$\text{FeCl}_2$	20,5	0

The study of Dincer et al. (2015), tannase cloned to *Lactobacillus plantarum* and tannase produced that microorganism pre incubated with  $\text{ZnCl}_2$  then it is revealed that the enzyme was significantly stimulated with  $\text{ZnCl}_2$  (105%) ([16]). In the study conducted with *Klebsiella*, tannase production, purification and characterization from *Klebsiella pneumoniae* KP715242 strain was conducted. in this study it is determined that He had the most inhibitory effect on tannase activity and  $\text{Zn}^{+2}$ ,  $\text{Mg}^{+2}$ ,  $\text{Mn}^{+2}$  had the enhancing effect on enzyme activity and any significant effect of EDTA no found ([21]).

### 3.8. Findings Related to SDS-PAGE Analysis

The protein bands obtained from the SDS-PAGE (10%) analysis of the *Bacillus coagulans* enzyme are shown in Figure 7. SDS-PAGE analysis revealed a three bands which molecular weights are 17 kDa, 14 kDa and 5 kDa. To determine molecular weights of protein bands, standard protein markers (Broad Range Markers: sc-2361- 500 UL 200 kDa 97 kDa 66 kDa 44 kDa 29 kDa 17 kDa 14 kDa 6 kDa) were used.

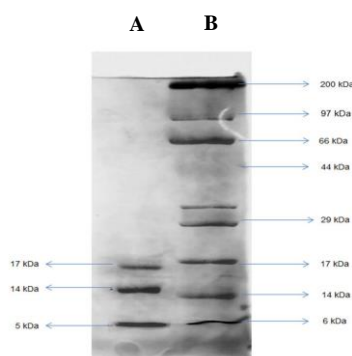


Figure 7. SDS-PAGE and zymogram result of *Bacillus coagulans* enzyme (A: Protein bands of *Bacillus coagulans* B: marker proteins)

In the other studies tannase produced from *Bacillus subtilis* PAB2 had the 52 kDa molecular weight ([22]), and tannase produced from *Enterococcus faecalis* had 45 kDa molecular weight ([23]).

#### 4. CONCLUSIONS

According to the results of this study, it was revealed that *Bacillus coagulans* is a tannase producer microorganism. Thanks to the characteristics of this enzyme, it can be recommended that use it in many industrial fields. also its use supply economically advantage. As a result, microbial tannase of produced can be used that cold tea, beer and wine production of the occurring in the removal of foam and clarify, hydrolyzed of excess tannins present in plant leaves and feed that consumed by ruminant animals, gain of gallic acid which used in the pharmacology area, also in the elimination of tannins that are organic pollutants in industrial wastewater.

#### ACKNOWLEDGMENT

This study was supported by Cukurova University Scientific Research Project Coordinator with project coded FYL-2015-3782. Thanks to the Biologist Fatima Masume Uslu for their contribution to the study.

#### REFERENCES

- [1]. C. N. Aguilar, R. Rodriguez, S. G. Gutierrez, C. Augur, T. E. Favela, B. L. A. Prado, C. A. Ramirez, E.J.C. Contreras, "Microbial tannases: Advances and perspectives," *Appl. Microbiol. Biotechnol.*, vol. 76, pp. 47-59, Aug. 2007.
- [2]. L. Mingshu, H. Qiang, J. Dongying, "Biodegradation of gallotannins and ellagitannins," *Journal of Basic Microbiology*, vol. 46, pp. 68-84, Feb. 2006.
- [3]. Albertse, "Cloning, expression and characterization of tannase from *Aspergillus* species," Phd thesis, University of The Free State, South Africa, 2002.
- [4]. R. A. Kumar, P. Gunasekaran, M. Lakshmanan, "Biodegradation of tannic acid by citrobacter freundii isolated from a tannery effluent," *Journal of Basic Microbiology*, vol. 39, pp. 161-168, Jun. 1999.
- [5]. I. Mueller-Harvey, "Analysis of hydrolysable tannins," *Animal Feed Science and Technology*, vol. 91, pp. 3-20, May. 2001.
- [6]. G. Goel, A.K. Puniya, K. Singh, "Tannic acid resistance in ruminal Streptococcal Isolates," *Journal of Basic Microbiology*, vol. 45, pp. 243-245, May. 2005.
- [7]. P. K. Lekha and B. K. Lonsane, "Production and application of tannin acyl hydrolase: State of the art," *Advances in Applied Microbiology*, vol. 44, pp. 216-260, Jan. 1997.
- [8]. S. Sharma, T. K. Bhat, R.K. Dawra, "A spectrophotometric method for assay of tannase using rhodanine," *Analytical Biochemistry*, vol. 279, pp. 85-89, Aug. 2000.
- [9]. X. Yu, Y. Li, D. Wu, "Enzymatic synthesis of gallic acid esters using microencapsulated tannase: Effect of organic solvents and enzyme specificity," *Journal of Molecular Catalysis B: Enzymatic*, vol. 30, pp. 69-73, Aug. 2004.
- [10]. K. C. Mondal, D. Banerjee, M. Jana, B. R. Pati, "Colorimetric assay method for determination of the tannin acyl hydrolase (EC 3.1. 1.20) activity," *Analytical Biochemistry*, vol. 295, pp. 168-171, Aug. 2001.
- [11]. R. Kumar, A. Kumar, R. Nagpal, J. Sharma, A. A. Kumari, "Novel and sensitive plate assay for screening of tannase-producing bacteria," *Annals of Microbiology*, vol. 60, pp. 177-179, Mar. 2010.
- [12]. G. Temizkan and N. Arda, 2008. *Nobel Tip Kitabevi*, 3rd ed., Istanbul Universitesi Biyoteknoloji ve Genetik Muhendisligi Arastirma ve Uygulama Merkezi, Istanbul, 2008.
- [13]. H. Rodriguez, J. M. Landete, J. A. Curiel, B. De Las Rivas, J. M. Mancheño, R. Muñoz, "Characterization of the P-Coumaric acid decarboxylase from *Lactobacillus plantarum* CECT 748T," *Journal of Agricultural and Food Chemistry*, vol. 56, pp. 3068-3072, Apr. 2008.
- [14]. C. Barthomeuf, F. Regerat, H. Pourrat, "Production, purification and characterization of a tannase from *Aspergillus niger* LCF 8," *Journal of Fermentation and Bioengineering*, vol. 77, pp. 320-323, 1994.
- [15]. O. Ileri, S. A. Adebuyose, O. O. Amund, B. O. Oyeteran, "A study of tannic acid degradation by soil bacteria," *Pakistan Journal of Biological Sciences*, vol. 10, pp. 3224-3227, Sep. 2007.
- [16]. S. Dincer, S. Ulusoy, E. S. Yigittekin, "Characterization and cloning of tannase from *Lactobacillus plantarum*," *Journal of Biotechnology*, vol. 208, pp. 64-65, Aug. 2015.
- [17]. J. Yao, X. J. Fan, Y. Lu, Y. H. Liu, "Isolation and characterization of a novel tannase from a metagenomic library," *Journal of Agricultural and Food Chemistry*, vol. 59, pp. 3812-3818, Mar. 2011.
- [18]. K. C. Mondal, D. Banerjee, R. Banerjee, B. R. Pati, "Production and Characterization of tannase from *Bacillus cereus* KBR9," *The Journal of General and Applied Microbiology*, vol. 47, pp. 263-267, Oct. 2001.

- [19]. E. Zaki pour-Molkabadi, Z. Hamidi-Esfahani, M. A. Sahari, M. H. Azizi, "A new native source of tannase producer, *Penicillium* sp. EZ ZH190: Characterization of the enzyme," *Iranian Journal of Biotechnology*, vol. 11, pp. 244-250, Aut. 2013.
- [20]. N. Jiménez, J. M. Barcenilla, F. L. De Felipe, B. De Las Rivas, R. Muñoz, "Characterization of a bacterial tannase from *Streptococcus gallolyticus* UCN34 suitable for tannin biodegradation," *Applied Microbiology and Biotechnology*, vol. 98, pp. 6329-6337, Jul. 2014.
- [21]. M. Kumar, V. Beniwal, R. K. Salar, "Purification and characterization of a thermophilic tannase from *Klebsiella pneumoniae* KP715242," *Biocatalysis and Agricultural Biotechnology*, vol. 4, pp. 745-751, Oct. 2015.
- [22]. A. Jana, C. Maity, S. K. Halder, A. Das, B. R. Pati, K. C. Mondal, P. K. D. Mohapatra, "Structural characterization of thermostable, solvent tolerant, cytosafe tannase from *Bacillus subtilis* PAB2," *Biochemical Engineering Journal*, vol. 77, pp. 161-170, Aug. 2013.
- [23]. G. Goel, A. Kumar, V. Beniwal, M. Raghav, A. K. Puniya, K. Singh, "Degradation of tannic acid and purification and characterization of tannase from *Enterococcus faecalis*," *International Biodeterioration&Biodegradation*, vol. 65, pp. 1061-1065, Oct. 2011.

## Effect of Nano-Silica Addition on Kaolin-Based Brick Properties

Gokhan Gorhan<sup>1</sup>, Gokhan Kurklu<sup>2</sup>

### Abstract

*In this study, brick samples were produced by adding nano-silica to 0.1% - 0.3% of kaolin clay by weight. In the study, 500 µm fine kaolin clay obtained from Canakkale-Can/Turkey region was used as raw material and HDK-N20 pyrogenic nano silica was used. The samples were formed in 25 mm cylinder molds using a hydraulic hand press at 70 bar pressure and using 50 g of wet materials. The shaped samples were dried until the laboratory samples reached constant weight, then the samples were fired at 700, 800 and 900 °C (with firing speed for 2.5 °C/min.) in laboratory-type electric ovens at one hour in the final temperatures. Following the firing process, the samples were placed in a water tank to determine their physical properties. According to the Archimedes principle, water absorption, porosity, unit volume weight and apparent density values of the samples were determined. Then, the compressive strengths of the relevant samples were determined in an automatic computer controlled cement press. According to findings; the apparent porosity, water absorption and apparent density values of the samples increased with increasing firing temperatures. However, it was observed that the increasing firing temperatures did not increase linearly in the sample compressive strengths. As a result, the compressive strength of the samples increased with the increase of nano-silica addition in the brick samples fired at 700 °C. However, in the samples fired at other temperatures, the effect of nano-silica addition was observed to be variable.*

**Keywords:** Nano-silica, kaolin, brick, firing.

### 1. INTRODUCTION

Clay minerals are known to partially or completely lose their crystal lattice structure due to dehydroxylation when they are subjected to thermal activation between 600 and 900 °C, and to be susceptible to a highly reactive form of phase transition [1].

Clay is the most reactive when the calcination temperature deteriorates the clay structure by causing the loss of hydroxyl [1]. Hence, clay is the most reactive under conditions in which clay structure precipitates and deteriorates, due to the calcination temperature resulting in the loss of hydroxyl (O'Farrell et al., 2006). This reactivity requires a calcination temperature of between 600 and 900 °C [1, 2].

Clay residues include the impurities of non-clay minerals such as mixtures of different clays and quartz, calcite, feldspar, mica, anatase and sulfides [3]. He et al. (1995) stated that after the heat treatment, kaolin and some montmorillonites have the highest pozzolanic activity and the rest of the clay minerals may show low pozzolanic activity. The optimum thermal process for the activation of different clays is determined by measuring the pozzolanic activity of the calcined material [3].

Kaolinite is stated to be the most reactive clay mineral. Some studies also investigated the effect of calcination parameters such as time and temperature on the pozzolanic reactivity of metakaolin for potential industrial applications [4, 5]. However, studies on the pozzolanic activity of the calcined clay minerals in the process of decomposition are limited [6].

<sup>1</sup> Corresponding author: Afyon Kocatepe University, Faculty of Engineering, Department of Civil Engineering, Afyonkarahisar, Turkey. [ggorhan@aku.edu.tr](mailto:ggorhan@aku.edu.tr)

<sup>2</sup> Afyon Kocatepe University, Faculty of Engineering, Department of Civil Engineering, Afyonkarahisar, Turkey. [kurklu@aku.edu.tr](mailto:kurklu@aku.edu.tr)

Nanotechnology, which has been an area of interest in recent years, is defined as the monitoring and structuring of nanometer-sized materials in order to produce materials with new properties and functions. It is reported that the use of nanomaterials in concrete increases the demand for water. However, nano materials are expected to improve cement-based material properties [7].

Not only science and engineering branches but also the construction industry keeps up with the latest developments in nanotechnology. It is stated that nanoparticles can accelerate nucleation events during the early age hydration of, especially, cement-based materials [8].

The aim of this study is to investigate the effect of nano-silica addition at certain rates on kaolin-based brick properties. Thus, it is hoped that this study will fill the gap in the literature and provide insight into the effect of nano-silica, which is generally used in cement-based materials, on clay structure.

## 2. MATERIALS AND METHODS

In this study, kaolin-based bricks were produced. First, optimization was performed to determine the nano silica content and optimum compression pressure for brick specimens to be prepared using a hydraulic hand press. Optimization showed that nano silica can be added to clay in 0.1% and 0.3% by weight.

In optimization, kaolin clay with a fineness of 500 micron supplied from Canakkale-Can region was used as raw material and HDK-N20 pyrogenic nano silica was used.

The specimens were compressed using a hydraulic hand press at 70 bar pressure, and 50 g wet materials were cast in cylinder molds with a diameter 25 to meet the slenderness ratio of 2. The specimens were dried in a lab-type oven until constant-weight and then kept in lab-type electric ovens at 700, 800 and 900 °C and at final temperatures for 1 h, and were fired at 2.5 °C/min.

After firing, the specimens were placed in a water tank to determine their physical properties. Porosity, unit volume weight and apparent density values were measured using TS EN 772-4 [9] and water absorption values were measured using TS EN 771-1 [10] according to Archimedes' principle. The mechanical properties of the brick specimens were determined according to TS EN 196-1 [11]. In the physical and compressive strength tests, the mean of three specimens was used for each specimen group. Table 1 shows the materials and mixture ratios used for the specimens.

*Table 1. Materials and Mixture Ratios*

No	Serial Code	Specimen size (mm)	Clay (gr)	Water (gr)	Nano silica (%)
1	R700	25 x 50	550	50	-
2	R800	25 x 50	550	50	-
3	R900	25 x 50	550	50	-
4	0.1 700	25 x 50	550	50	0.1
5	0.1 800	25 x 50	550	50	0.1
6	0.1 900	25 x 50	550	50	0.1
7	0.2 700	25 x 50	550	50	0.2
8	0.2 800	25 x 50	550	50	0.2
9	0.2 900	25 x 50	550	50	0.2
10	0.3 700	25 x 50	550	50	0.3
11	0.3 800	25 x 50	550	50	0.3
12	0.3 900	25 x 50	550	50	0.3

## 3. RESULTS AND DISCUSSION

Firing temperatures of 700 and 800 °C had an effect on the results. In all the series, the porosity of only the specimens fired at 900 °C increased linearly with an increase in the amount of added nano-silica. Given the fact that, under normal conditions, open porosity of specimens should not be too high, increasing the amount of nano-silica may have a negative effect on durability properties. It should, however, be noted that the increases in the porosity of the specimens were small. The apparent porosity of the specimens ranged from 32.3% to 35.1%. The results are shown in Figure 1.



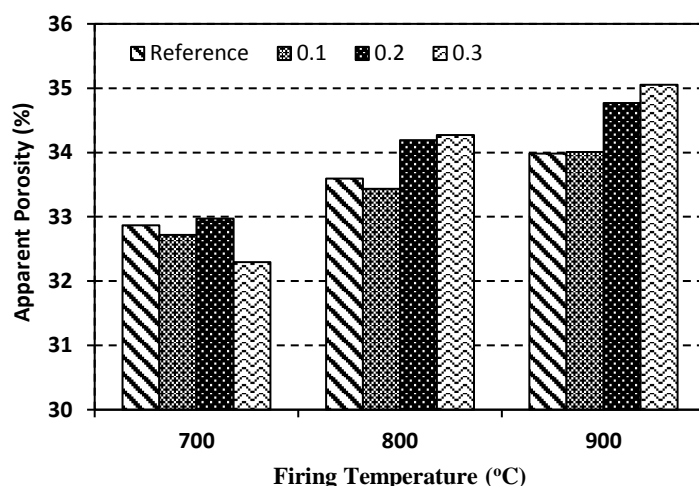


Figure 1. Apparent Porosity of Specimens

The rates of water absorption and apparent porosity of the specimens were similar. However, the effect of nano-silica addition on the brick specimens was unclear and unstable at all firing temperatures. The effect of nano-silica addition on water absorption rates is, therefore, unclear. The data showed that the water absorption rates of the specimens varied between 19.1% and 21.0%. The results are shown in Figure 2.

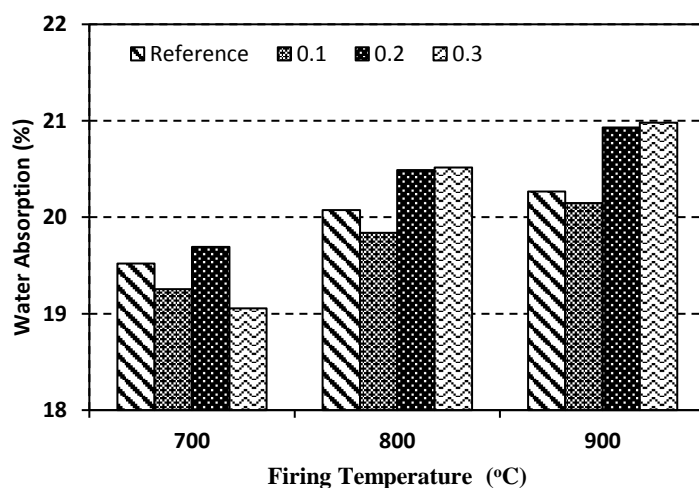


Figure 2. Water Absorption of Specimens

The unit volume weight and apparent density values are shown in Figures 3 and 4, respectively. In general, nano-silica addition did not have an effect on the density values. While 0.1% nano-silica added brick specimens fired at 700 °C had the highest unit weight (1699.1 kg/m<sup>3</sup>). 0.2% nano-silica added brick specimens fired at 900 °C had the lowest unit weight (1661.2 kg/m<sup>3</sup>). The unit weight of the specimens ranged from 1661.2 kg/m<sup>3</sup> to 1699.1 kg/m<sup>3</sup>.

The apparent density values showed that nano-silica addition linearly increased the density values of the brick specimens fired at 800 °C. The effect of nano-silica addition was unclear at other temperatures. 0.3% nano-silica added brick specimens fired at 900 °C had the highest apparent density (2572.4 kg/m<sup>3</sup>). However, the apparent density of the specimens did not change significantly in general (Figure 4).

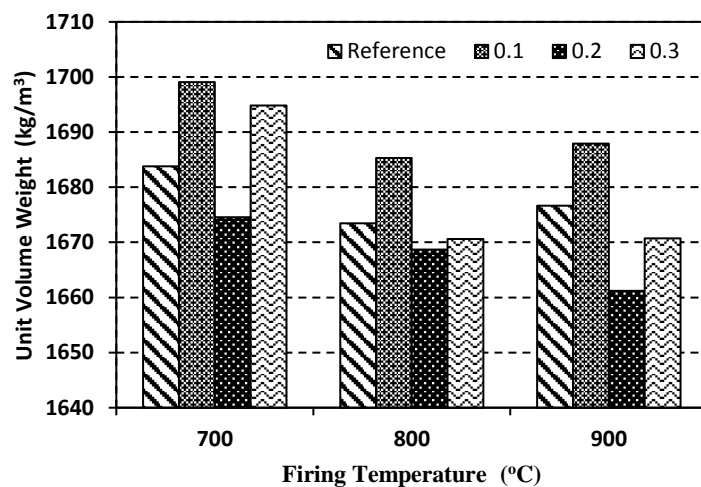


Figure 3. Unit Volume Weight Values

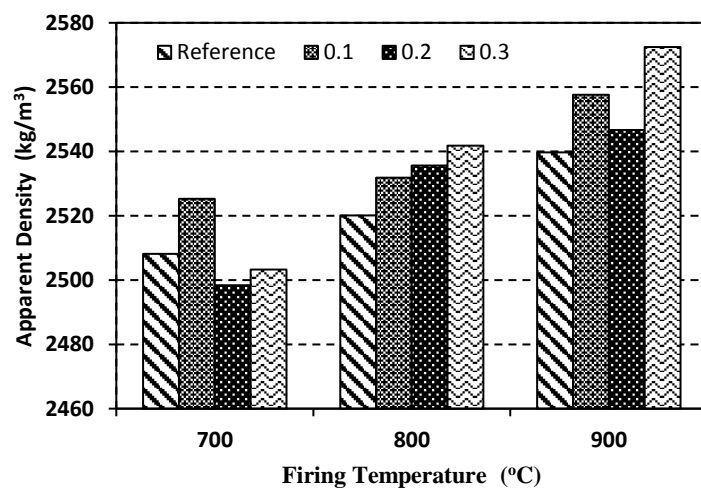


Figure 4. Apparent Density Values

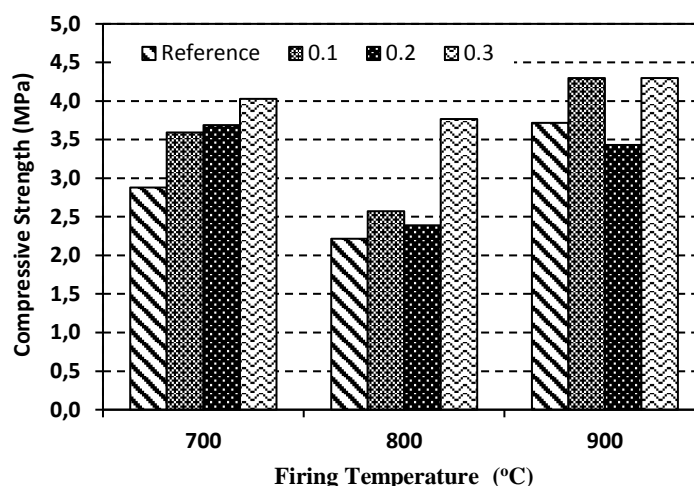


Figure 5. Compressive Strength Values

Compressive strength, which is an important mechanical property, is a measure of the resistance of the material to breaking. The higher the compressive strength, the more durable the material and the better the properties thereof. Though not as much as cement based materials, such building materials as bricks are expected have a certain compressive strength.

Figure 5 shows the compressive strength graph of the specimens. The specimens fired at 900 °C had the highest compressive strength (4.3 MPa). In general, the addition of 0.3% nano-silica slightly affected the compressive strength of the specimens. In all specimen groups, the compressive strength of only the specimens fired at 700 °C increased with an increase in the amount of added nano-silica. The compressive strength values of the specimens ranged from 2.2 MPa to 4.3 MPa.

#### 4. CONCLUSION

The results indicate that the addition of nano-silica did not cause a significant change in kaolin-based brick properties. Due to fact that, unlike the production of cement based materials, brick production involves thermal firing, nano-silica additions had no sufficient effect on compressive strengths. However, low nano-silica addition had a significant effect on these results. In conclusion, the use of nano-silica in kaolin-based brick production did not significantly affect physical properties. The compressive strengths of the brick specimens fired at 700 and 900 °C were similar. The addition of nano-silica increased the compressive strength of the specimens fired at 700 °C. Nano-silica-added bricks fired at these temperatures can be used for partition wall applications in the buildings.

#### ACKNOWLEDGEMENTS

The authors would like to thank the Scientific Research Projects Coordination Unit of Afyon Kocatepe University (AKU, BAPK, Project No: 17. KARIYER. 223) for supporting this work.

#### REFERENCES

- [1]. Sabir B B, Wild S & Bai J 2001 Metakaolin and calcined clays as pozzolans for concrete: a review Cement and Concrete Composites 23(6) 441-454.
- [2]. O'Farrell M, Sabir B B & Wild S 2006 Strength and chemical resistance of mortars containing brick manufacturing clays subjected to different treatments Cement and Concrete Composites 28(9) 790-799.
- [3]. Tironi A, Trezza M A Scian A N Irassar E F 2013 Assessment of pozzolanic activity of different calcined clays Cement and Concrete Composites 37 319-327.
- [4]. Shvarzman A, Kovler K, Grader G S, Shter G E 2003 The effect of dehydroxylation/amorphization degree on pozzolanic activity of kaolinite Cement and Concrete Research 33 (3) 405-416.
- [5]. Badogiannis E, Kakali G Tsivilis S 2005 Metakaolin as supplementary cementitious material Journal of Thermal Analysis and Calorimetry 81(2) 457.
- [6]. Fernandez R, Martirena F Scrivener K L 2011 The origin of the pozzolanic activity of calcined clay minerals: a comparison between kaolinite, illite and montmorillonite Cement and Concrete Research 41(1) 113-122.

- [7]. Yaltay, N., (2017). Nano Silika'nin Beton Basıncı Dayanımına Etkisinin İncelenmesi, Engineering Sciences (NWSAENS), 12(4):216-223, DOI: 10.12739/NWSA.2017.12.4.1A0388.
- [8]. Ozbora, A. A., Tarhan, M., & Engin, Y. (2013). Nanoteknolojinin Betonun Geleceğindeki Rolü. Beton 2013 Hazir Beton Kongresi Cagrili Bildirileri, 304,312, BETON 2013 Hazir Beton Kongresi Bildirileri, 21-23 Subat 2013-ISTANBUL
- [9]. TS EN 772-4, (2000). Methods of test for masonry units - Part 4: Determination of real and bulk density and of total and open porosity for natural stone masonry units. TSE, Ankara.
- [10]. TS EN 771-1, (2012). Specification for masonry units - Part 1: Clay masonry units. TSE, Ankara.
- [11]. TS EN 196-1, (2016). Methods of testing cement - Part 1: Determination of strength. TSE, Ankara.

## BIOGRAPHY

Assoc. Prof. Dr. Gokhan GORHAN was born in 1981 in Ankara. He completed his undergraduate degree in 2003 and his master's degree in 2006 in Afyon Kocatepe University. He earned his PhD in Ankara Gazi University in 2011. Dr. Gorhan is currently undertaking TUBITAK and BAP projects on various subjects related to building materials and is a faculty member of the Department of Civil Engineering of the Faculty of Engineering of Afyon Kocatepe University.

## Use of Alginate – Clinoptilolite Beads for the Removal of Mixed Heavy Metals: Effect of Clinoptilolite Size and Alginate – Clinoptilolite Ratio

Merve Yildiz<sup>1</sup>, Cigdem Kivilcimdan Moral<sup>2</sup>

### Abstract

Heavy metals are widely used in different industries. Effluents containing these metals should be treated due to their toxic properties even at low concentrations to protect water resources. Adsorption is one of the effective methods and alginate, a natural polymer adsorbent, has ability to capture metals. However, the removal efficiency of the metals by alginates is not high enough to use in real applications. Therefore, studies continue to seek better adsorbent combinations. For this purpose, clinoptilolite, which has abundant source in Turkey, is selected to increase heavy metal uptake capacity of alginate in this study. Similar to the alginate, clinoptilolite can be used for heavy metals removal by ion exchange. For these reasons, alginate – clinoptilolite (A – C) beads are formed for the removal of heavy metals ( $\text{Cu}^{2+}$ ,  $\text{Cd}^{2+}$ ,  $\text{Pb}^{2+}$ ) from a synthetic mixture using batch reactors. The results related with the effect of using different clinoptilolite sizes and A/C ratios are presented here. The results showed that the highest removal rates were obtained for  $\text{Pb}^{2+}$  ion.  $\text{Pb}^{2+}$  concentration could be reduced to  $4.3 \pm 2.5$  mg/L, which corresponds to over 95 % of removal, by using 300  $\mu\text{m}$  - 500  $\mu\text{m}$  clinoptilolite size in beads. On the other hand, there were no drastic changes on heavy metal reduction efficiencies at various A/C ratios (1/2, 1/1 and 2/1). Also, shape deterioration in A – C beads was observed at A/C ratio of 2/1 due to high viscosities of alginates.

**Keywords:** Adsorption, Biopolymer, Cadmium, Copper, Lead

### 1. INTRODUCTION

Environmental pollution has become an important issue with urbanization and increased parallel to industrialization. Particularly in the second part of twentieth century human population was increased and the problem is getting serious. There are lots of pollutants and heavy metals have significant role in this subject. Mining, energy and fuel production, pesticides and fertilizers, metallurgy, iron and steel plants, leather industry etc. contribute heavy metal pollution. Some of the metals used during production processes resulted in wastewaters and directly or indirectly they can reach to the environment which leads serious pollution problems [1]. These metals have adverse effects on both livings and the environment due to their toxic character and accumulation tendency in fatty tissues. For these reasons, it is very important to treat wastewaters containing heavy metals before discharges. There are different methods used for the removal of heavy metals. They can be listed as chemical precipitation, filtration, ion exchange, adsorption, membrane technologies, and evaporation [2]. Among them, adsorption would be a good alternative when natural, economic and easily available adsorbents are utilized in the process. In today's world, natural adsorbents are getting attention. Within this context, alginate, a biopolymer extracted from brown algae, is investigated for heavy metal removal. Alginates composed of mannuronic (M) and guluronic (G) acids (Figure 1) [3]. These blocks can be arranged as homopolymeric and heteropolymeric regions and particularly GG blocks have ability to form beads. Also, carboxyl and hydroxyl groups are the functional groups having ability to capture metals [4].

<sup>1</sup> Akdeniz University, Department of Environmental Engineering, Antalya, Turkey yldzmr23@gmail.com

<sup>2</sup> Corresponding author: Akdeniz University, Department of Environmental Engineering, Antalya, Turkey cigdemmoral@akdeniz.edu.tr



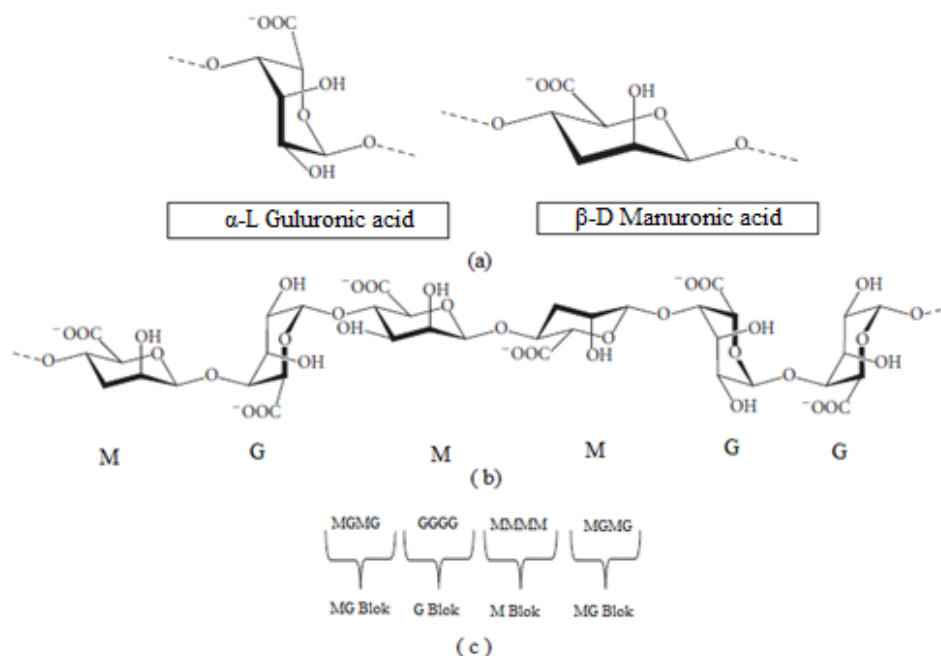


Figure 1. Structure of alginate; monomers (a) polymer chain; (b) block distribution (c) [5].

Alginate is mainly applied in bead form for heavy metal removal. And the recent trends in studies is to improve treatment efficiency of these polymeric beads by combining various materials. In this study, clinoptilolite was selected for this purpose. It is a natural zeolite being abundant in Turkey. Clinoptilolite has ability to take metals mainly by ion exchange. Thus, alginate-clinoptilolite (A-C) beads were formed to investigate heavy metal removal capacities in batch system. Then, A-C beads were used to elucidate the effect of clinoptilolite size and A/C ratio of the beads for the treatment of mixed heavy metals,  $\text{Cu}^{2+}$ ,  $\text{Cd}^{2+}$ ,  $\text{Pb}^{2+}$ , from a synthetic wastewater.

## 2. MATERIALS AND METHODS

In this study, different clinoptilolite sizes and A/C ratios were applied in formation of the beads and their effects on adsorption of heavy metals were investigated. Three different clinoptilolite sizes namely 100 $\mu\text{m}$ , 100-300 $\mu\text{m}$ , 300-500 $\mu\text{m}$  from Manisa-Gordes area were first conditioned. For this purpose, 10 g clinoptilolite was added into 1 M NaCl during 24 hours at 200 rpm. After that the zeolite was dried at 105 $^{\circ}\text{C}$  and stored in a desiccator before use.

Bead formation procedure can be summarized as follows: 2 % of alginate solution was added into  $\text{CaCl}_2$  solution (50 mM) dropwise at 1g/1g A/C ratio and then incubated overnight. After that these beads were filtered and dried at 35 $^{\circ}\text{C}$ .

In order to determine the effect of clinoptilolite size, 100 mg (i) 1g/1g A-C (<100 $\mu\text{m}$ ) beads (ii) 1g/1g A-C (100-300 $\mu\text{m}$ ) beads (iii) 1g/1g A-C (300-500 $\mu\text{m}$ ) beads were incubated into mixed heavy metal solution,  $\text{Cu}^{+2}$ ,  $\text{Cd}^{+2}$ ,  $\text{Pb}^{+2}$ , containing 100 mg/L of each metal at pH 4, 30 $^{\circ}\text{C}$  during 24 hours at 150 rpm.

In order to determine the effect of A/C ratio, 100 mg (clinoptilolite size <100 $\mu\text{m}$ ) (i) 1g/1g A-C beads (ii) 1g/2g A-C beads and (iii) 2g/1g A-C beads were incubated into the same heavy metal solution at pH 4, 30 $^{\circ}\text{C}$  during 24 hours at 150 rpm. Sampling were performed at the beginning and after 24 hours of experiments. This was

the equilibrium time previously determined from kinetic studies. These samples were acidified and stored at 4°C until analysis by ICP-MS.

### 3. RESULTS AND DISCUSSION

In this study, A-C beads were investigated for mixed heavy metals removal and the effect of clinoptilolite size on adsorption efficiency is shown in Figure 2. When the results were examined, there were no drastic changes for heavy metal adsorption efficiencies at various clinoptilolite sizes applied in the study. The beads first preferred to uptake lead, then copper and cadmium followed the others. Thus, the highest removal efficiency was observed for lead as 90 %. This value is corresponding to 45 mg Pb<sup>2+</sup>/g A-C beads. In literature, there are some evidences that claim decreasing particle size of the adsorbents improves adsorption capacity by increasing available surface area. However, similar to our study, only little variations were observed by changing zeolite size [6,7]. For the total surface area of a zeolite, one should consider both inner and outer surface area. When the particle size is increased by grinding, it only affects the outer surface area. Adsorbents having porous structure like zeolites, outer surface is considerably less than inner surface area. For these reasons, although the size and the outer surface area is increased by lowering the particles size, the adsorption efficiency might not be affected much.

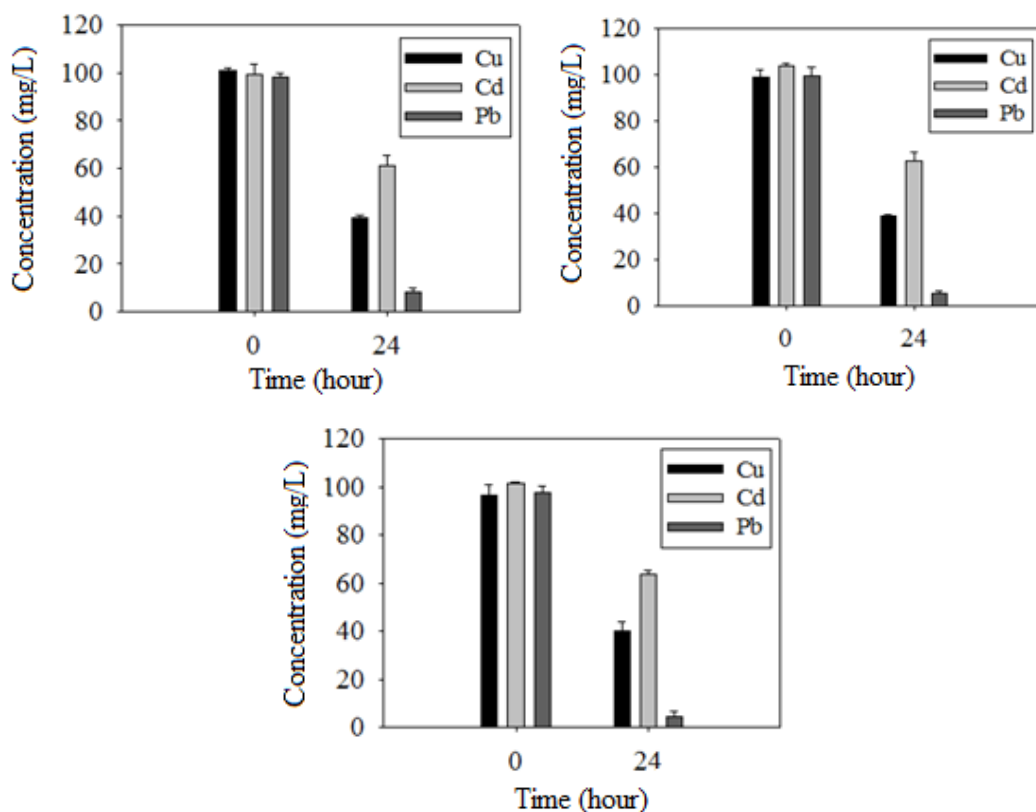


Figure 2. The effect of changing clinoptilolite size on heavy metal adsorption from a synthetic wastewater (a) (100µm<); (b) (100-300µm); (c) (300-500µm)

Another parameter which possibly have effect on heavy metal adsorption capacity of A-C beads is A/C ratio. That is the amount of alginate and clinoptilolite used to form the beads. Three different ratios were selected for this purpose and the results are presented in Figure 3. The study was started with 1g/1g A/C ratio and particularly lead was found to be effectively removed by A-C beads. Then, first the amount of clinoptilolite

was increased twice and 1g/2g A/C ratio was applied. For this case, removal rates were affected negatively particularly which was quite drastic for the case of cadmium because only 7 mg Cd<sup>2+</sup>/g A-C beads could be removed. Similarly, a study conducted to remove lead and nickel by using alginate-perlite showed that increase in perlite ratio reduced adsorption efficiency of heavy metals [8]. Therefore, this may probably due to limitation of heavy metals migration through alginate bead surface by increasing clinoptilolite concentration. On the other hand, when alginate concentration was increased twice and 2g/1g A/C ratio was applied, heavy metal removal efficiencies did not change much. Furthermore, high alginate concentration led to increase in viscosity that caused uneven shaped bead formation.

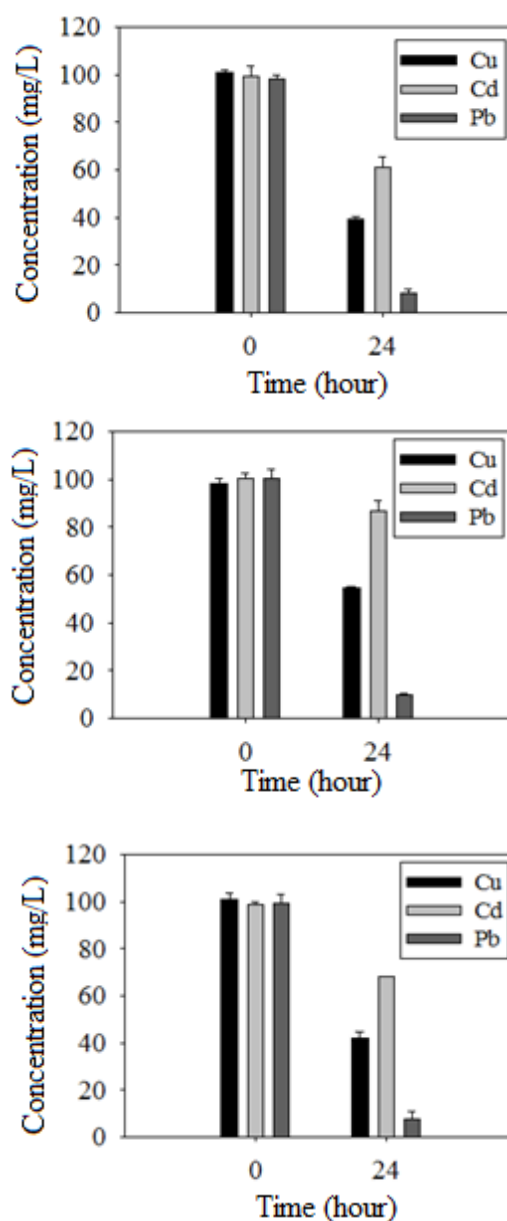


Figure 3. The effect of changing A/C ratio on heavy metal adsorption from a synthetic wastewater (a) (1g/1g); (b) (1g/2g); (c) (2g/1g).

### 4. CONCLUSIONS

In this study, A-C beads were examined as adsorbents for the removal mixed heavy metals from a synthetic wastewater in batch reactors. Common conclusions can be drawn from the study as follows:

- A-C beads were found effective in heavy metal reduction especially for the case of lead.
- Change in clinoptilolite size in the range of 100 and 500  $\mu\text{m}$  did not have drastic variation in heavy metal uptake levels.
- Increase in clinoptilolite ratio negatively affected adsorption rate especially for cadmium while increase in alginate did not improve heavy metal uptake.

### ACKNOWLEDGMENT

This study is supported by Akdeniz University Scientific Research Project Commission (FYL-2016-2001).

### REFERENCES

- [1]. San, "Agir Metal ve Boyar Madde Iceren Atikularin Rhodotorula Sp. Ile Aritimi," M. Turkish thesis, Ankara Universitesi Biyoteknoloji Enstitusu, August 2007.
- [2]. J. Wang, C. Chen, "Biosorbents for Heavy Metals Removal and Their Future," *Biotechnology Advances*, vol. 27, pp. 195-226, April 2009.
- [3]. I. D. Hay, Z. U. Rehman, A. Ghafoor, B. H. A. Rehm, "Bacterial Biosynthesis of Alginates," *Journal of Chemical Technology and Biotechnology*, vol. 85, pp. 752-759, March 2010.
- [4]. Draget, K. I., Smidsrød, O., Skjåk-Bræk, G. 2005. "Polysaccharides and Polyamides in the Food Industry. Properties, Production, and Patents.
- [5]. M. SzeKalska, A. PuciBowsk, E. SzymaNska, P. Ciosek, K. Winnicka, "Alginate: Current use and future perspectives in pharmaceutical and biomedical applications," *International Journal of Polymer Science*, vol. 2016, pp. 17, December 2016.
- [6]. M. I. Panayotova, "Kinetics and thermodynamics of copper ions removal from wastewater by use of zeolite," *Waste Management*, vol. 21, pp. 671-676, 2001.
- [7]. R. Leyva-Ramos, G. Aguilar-Armenta, L. V. Gonzalez-Gutierrez, R. M. Guerrero-Coronado, J. Mendoza-Barron, "Ammonia exchange on clinoptilolite from mineral deposits located in Mexico," *Journal of Chemical Technology and Biotechnolog*, vol. 79, pp. 651-657, 2004.
- [8]. H. Ture, K. Terzioglu, E. Tunca, "Characterization of alginate/perlite particles," *Suleyman Demirel Universitesi Fen Bilimleri Enstitusu Dergisi*, vol. 21, pp. 756-766, July 2017.

### BIOGRAPHY

Cigdem Kivilcimdan Moral is an Environmental Engineer graduated from Istanbul University, Turkey. Current working position is to be a faculty member at the Department of Environmental Engineering, Akdeniz University, Turkey as Assoc. Prof. Dr. The main areas of interest are water and wastewater treatment technologies, inorganic priority pollutants, production and application of biopolymers.

# Legislations of Ministry of Environment and Urbanization in Turkey for Sustainable Construction

*Serife Gokce<sup>1</sup>, Osman Aytekin<sup>2</sup>, Hakan Kusan<sup>3</sup>, Ismail Zorluer<sup>4</sup>*

---

## Abstract

Today, more than half of the world's population lives in cities. This ratio is expected to increase further in the future. The need for construction for social, cultural and similar activities, particularly the need for shelter, is increasing day by day depending on the increasing urbanization. The construction process, which requires the use of natural resources, energy and raw materials in high quantities, can lead to the emergence of various environmental problems during the supply and use of these resources. The productions, uses, maintenance-repair and demolition of constructions involve a long process. This long process causes the long-term interaction of the structures with the environment. For this reason, it is necessary that the structures must be compliance with environment and sustainable in order to eliminate or minimize the environmental effects caused by the constructs during their long life cycle. Today, almost every national government has departments or ministries that work within the scope of ensuring environmental sustainability. Ensuring sustainable environmental management in Turkey, planning and coordinating efforts for the establishment of settlements compatible with the environment is carried out by the Ministry of Environment and Urbanization. In this study, the legislations developed for ensuring the harmony of building-environment within the scope of sustainability targets has been researched. In the scope of the study, only the regulations that were carried out by the Ministry of Environment and Urbanization were addressed. The information obtained at the end of the study was assessed and the positive or negative aspects of the examined regulations and legislations were noted.

**Keywords:** Sustainability, sustainable construction, legislations, environmental sustainability.

---

## 1. INTRODUCTION

People need to structures for many purposes, especially for sheltering. Along with the developing technology, developments have begun to emerge in the process of building. Structures have begun to emerge as environmental elements that integrate high technologies and make people's lives easier. The fact that the world population tends to increase gradually increases the structure needs of people day-by-day. The rate of living in cities of the increasing population, is more than half of the total world population. This ratio is expected to increase further in the coming years.

Population growth and urbanization rates are similar to the increase in the world in terms of Turkey. With more than 80 million as of the end of 2017, 92.5% of Turkey's population lives in urban areas (Turkey Statistical Institute Address Based Population Registration System Results, 2017). Turkey has a very high rate of urbanization is expected to increase further in the future (World Urbanization Prospects The 2014 Revision).

As mentioned above, depending on factors such as population growth, urbanization, and the development of technology, the need for structuring and the expectation of people are increasing gradually. The increase in construction leads to an increase in the use of natural resources, energy and raw materials. In addition to these, constructions can have negative effects on the environment such as global greenhouse gas emission, environmental damage, pollution, solid waste generation (Ortiz et al., 2009). The removal of environmental

---

<sup>1</sup> Corresponding author: Afyon Kocatepe University, Department of Civil Engineering, 03000, Afyonkarahisar, Turkey. [sgokce@aku.edu.tr](mailto:sgokce@aku.edu.tr)

<sup>2</sup> Eskisehir Osmangazi University, Department of Civil Engineering, 26140, Eskisehir, Turkey. [oytekin@ogu.edu.tr](mailto:oytekin@ogu.edu.tr)

<sup>3</sup> Eskisehir Osmangazi University, Department of Civil Engineering, 26140, Eskisehir, Turkey. [hkusan@ogu.edu.tr](mailto:hkusan@ogu.edu.tr)

<sup>4</sup> Afyon Kocatepe University, Department of Civil Engineering, 03000, Afyonkarahisar, Turkey. [izorluer@aku.edu.tr](mailto:izorluer@aku.edu.tr)

damage caused by constructions, efficient use of natural resources, energy and raw materials during the production of structures, are possible thanks to achieve sustainability in construction works.

Sustainable construction is the implementation of sustainable development principles in the life cycle of infrastructures and superstructures and at the same time this implementation process aims to harmonize between the natural and structural environment (Hoskara and Sey, 2008).

Environmental problems and limited natural resources, energy, raw materials are global and significant problems that closely concern the whole world. For this reason sustainable construction is a global goal. Because world countries are at different levels of development, national organization and legal infrastructures are becoming important elements in order to move towards common global targets.

Today, almost every national government has departments or ministries that work within the framework of sustainability. Sustainable construction regulations in Turkey, mainly implements by the Ministry of Environment and Urbanization and the Ministry of Energy and Natural Resources. However, within the scope of this study, it was necessary to focus on the regulations that were carried out by the Ministry of Environment and Urbanization when considering the overall weight.

The regulations examined in the scope of the study were examined from the perspective of the construction sector, contributions to sustainable development were assessed and a number of suggestions were made for their development. The regulations that were in force but which have been removed from practice are excluded from the scope of the study.

## 2. FORMATION OF ENVIRONMENTAL LEGISLATION IN TURKEY AND SUSTAINABLE CONSTRUCTION

The construction sector, one of the key sectors of national economies, has an important place in achieving economic sustainability in terms of providing employment to people and contributing to the elimination of poverty (www.iso.org/); in achieving social sustainability goals when considering the impact of living spaces on people's quality of life; in achieving environmental sustainability goals due to the fact that the structures interact directly with the environment. Contribution to economic, social and environmental sustainability of the sector is made possible by achieving sustainable construction. As noted in the previous section, sustainable construction refers to a process in which the entire social, economic and environmental sustainability principles are integrated into the whole life cycle of infrastructures and superstructures. Having a long service life of the structures (Gultekin and Celebi, 2016) makes the sustainable construction production a complex process. At the same time, the fact that sustainable construction is a global goal is another criterion to consider. Therefore, in order to make the sustainable construction process easier to implement, various arrangements have been made, such as the development of various implementation tools, the development of standards, the construction of international contracts, the regulation of local legislation of countries, and the enforcement of legal sanctions. Within the scope of this study, sustainable construction is evaluated only in terms of environmental legislation. For this reason, the details of other regulations have not been addressed.

Turkey's environmental legislation is based on the 1982 constitution. The various items of the Constitution emphasize the issues related to the environment. The Environmental Law of 1983 became the most important resource in the development of environmental legislation. This law, which directly refers to environmental sustainability, considered as the first step towards sustainable construction in Turkey. Many regulations that are subject to environmental sustainability and sustainable construction today are based on Environmental Law. Legislation developed on the basis of this law is mentioned in the next chapter.

## 3. MINISTRY OF ENVIRONMENT AND URBANIZATION AND SUSTAINABLE CONSTRUCTION LEGISLATIONS

Ministry Of Environment and Urbanization aims to conduct business and operations with a regulatory, supervisory, participatory and solution-focused approach to create high-quality cities and settlements with a quality of life compatible with the sustainable environment in Turkey (<https://csb.gov.tr/>). The regulations, which are carried out by the Ministry of Environment and Urbanization, directly or indirectly related to sustainable construction, respectively; Environmental Impact Assessment Regulation , Regulation on Control of Excavation, Construction and Demolishing Wastes, Regulation on the Energy Performance of Buildings, Building Materials Regulation, Green Certificate Regulation for Buildings and Settlements.



### **3.1. Environmental Impact Assessment (EIA) Regulation**

The EIA regulation published for the first time on 07.02.1993 is based on the Environmental Law. It has got its current status which is in force today with the regulation on the amendment of the EIA regulation on 26.05.2017. EIA refers to the studies to be carried out in determining the positive and negative effects of the projects planned to be realized and the measures to be taken in order to prevent negative effects or to reduce the minimum wastage which will not cause damage to the environment and to identify and evaluate the selected places and technology alternatives and to monitor and control the implementation of the projects (EIA). This regulation is carried out by the Ministry of Environment and Urbanization. In article 6 sub-article 3 is written that *"For the projects subject to this regulation, unless the decision of the EIA is positive or the EIA is not required, the incentive, approval, permission, structure and usage license related to these projects can not be given, the investment for the project can not be started and can not be tendered."* (Regulation on the amendment of the EIA regulation). This article places a definite sanction on the construction projects falling within the scope of the regulation. Otherwise the realization of construction activities in the territory of Turkey is not possible. Decisions of "EIA Positive", "EIA Negative" or "EIA Not Required" are given by the Ministry.

### **3.2. Regulation on Control of Excavation, Construction and Demolishing Wastes**

The regulation effectuated on 18.03.2004 is based on the Environmental Law. It is carried out by the Ministry of Environment and Urbanization. The purpose of the regulation is to regulate the general rules that must be observed with the technical and administrative aspects of reducing, collecting, temporarily accumulating, transporting, recovering, evaluating and disposing of earth and earth and construction wastes in a way that will not harm the environment. In article 27 it is written that *"Recycling of construction / debris wastes in order to conserve natural resources, sustainable production, reduce the amount of waste to be stored and create economic value is essential."* With this article recycling of construction wreckage, in the production of new concrete, promotes to use primarily in construction of sports and play facilities and other filling and recreation works such as road, parking, pavement, walkways, drainage works, drainage pipes and filling materials in cable floors (Regulation on Control of Excavation, Construction and Demolishing Wastes).

### **3.3. Regulation on the Energy Performance of Buildings**

The regulation, which entered into force on 05.12.2008, replaced in the Thermal Insulation Regulations of Buildings. Various amendments were made and updated with the Regulation on the Amendment of the Energy Performance Regulations of Buildings on 28.04.2017. It is based on Energy Efficiency Law No. 5627. This regulation, which is carried out by the Ministry of Environment and Urbanization, has the aim of the efficient use of energy, the prevention of waste, the reduction of energy costs on the economy, and the enhancement of the efficiency of energy resources and the use of energy to protect the environment.

Due to population growth and urbanization, the number of buildings are increasing. Therefore, this regulation is an important legal regulation in order to prevent energy losses caused by buildings. Within the scope of the Regulation, the standards, methods and minimum performance criteria have been defined for the calculation methods for the preparation and implementation of building projects and energy identity documents in the buildings which are to be built (Regulation on The Energy Performance of Buildings).

#### **3.3.1. Energy Identity Certificate**

It is a certificate that includes the building's energy requirement and energy consumption classification, insulation properties, and minimum information on the availability of heating and / or cooling systems (Regulation on The Energy Performance of Buildings). In Building Bylaws article 65 sub-article 1 states that it is an obligation to have an energy identity certificate in order to obtain permission to use the building. Article 68 sub-article 8 states that the energy identity certificate has to be renewed at the end of any modification that will change the energy performance of the building (Building Bylaws). The Energy Identity Certificate is obligatory for the buildings that fall under the scope of the Regulation on The Energy Performance of Buildings. With the Building Bylaws, the necessity of having Energy Identity Certificate is increased in cases such as permission to use building, sale, renting.

### **3.4. Building Materials Regulation**

It first entered into force in 2002 and last updated on 10.07.2013. It is carry out by the Ministry of Environment and Urbanization.

It aims to generate performance data about the basic characteristics of building materials. It specifies the rules for attaching CE marking to materials. It determines the procedures and principles regarding the supply of building materials to the market (Building Materials Regulation). Under the topic of Annex-I Basic Requirements for Construction Work Hygiene, health and environment, it is written that;

Construction works should be designed and constructed in such a way as not to have a significant effect on the quality of the climates and the environment during the whole life cycle and after.

Construction work should be designed and constructed to require low energy consumption, use as little energy as possible during construction and dismantling, and ensure energy efficiency.

These two sentences promote sustainability and energy saving.

### ***3.5. Green Certificate Regulation for Buildings and Settlements***

This regulation, which is the most recent regulation for sustainable construction, was published on 23.12.2017 under the supervision of the Ministry of Environment and Urbanization. Regulation aims to make buildings and settlements use natural resources and energy efficiently. It regulates the procedures and principles for the establishment of evaluation and documentation systems to reduce the negative effects of buildings and settlements on the environment. Regulation includes assessing and documenting the environmental, social and economic performance and sustainability of existing and new buildings and settlements (Green Certificate Regulation for Buildings and Settlements).

This regulation, which is carried out by the Ministry of Environment and Urbanization, replaces the Regulation on Certification of Sustainable Green Buildings and Sustainable Settlements, which entered into force in 2014.

It is the legal basis for the production of environmentally friendly constructions. Obtaining a certificate is voluntary and evaluation and documentation procedures are carried out by the commission assigned by the Ministry.

## **4. CONCLUSIONS**

The formation and adoption of sustainable construction perception in our country is based on a recent past. The Environment Law, adopted in 1983, has a great importance for many regulations based on it, including sustainable construction, in the period after its adoption. So the perception of sustainability in Turkey began to form in 1983.

This study examined the regulations governing the implementation of the currently up-to-date by Ministry of Environment and Urbanization, which is concerned with sustainable construction. When repealed directives and regulations are also taken into account in Turkey sustainability has been involved in many legal arrangements. The frequent revision of the regulations can be evaluated both positively and negatively. Detecting the deficiencies and making updates shows that the matter has been carefully followed by the competent authorities and that the work continues on a continuing basis. On the other hand, however, there is a nonconformity in terms of tracking changes. For example, the inclusion of regulations that are not in force in the web sites of the Ministries conducting the work is confusing in reaching the current regulations.

The Ministry has developed sustainability projects as well as developing legislation. Not enough concrete output has been achieved because all these studies are based on a very recent past. Accordingly, it is possible to state that the incentives do not reach the adequate level.

It is anticipated that more holistic and enforced regulations will be made in the future, including environmental awareness and energy efficiency as well as all components of sustainability.

## **REFERENCES**

- [1]. Turkey Statistical Institute, Address Based Population Registration System Results. Publication date: 01.02.2018
- [2]. United Nations, Department of Economic and Social Affairs, World Urbanization Prospects The 2014 Revision.
- [3]. Ortiz, O., Castells F. and Sonnemann G., *Sustainability in the construction industry: A review of recent developments based on LCA*, Construction and Building Materials, 2009, vol. 23(1).
- [4]. Hoskara, E. and Sey, Y., *Ulkesel kosullar baglaminda surdurulebilir yapim*, itudergisi/a, mimarlik, planlama, tasarim, 2008, vol. 7(1).
- [5]. (2018) The ISO website. [Online]. Available: ([www.iso.org/](http://www.iso.org/)).

- [6]. Gultekin, A. B. & Celebi G. (2016). Yasam dongusu degerlendirme yontemi kapsaminda yapi urunlerinin cevresel etkilerinin degerlendirilmesine yonelik bir model onerisi. Duzce Universitesi Bilim ve Teknoloji Dergisi, 3, 1-36.
- [7]. (2018) The CSB website. [Online]. Available (<https://csb.gov.tr/>).
- [8]. Ministry of Environment and Urbanization, Regulation on the amendment of the Environmental Impact Assessment Regulation, Official Gazette Date: 26.05.2017, Number of Official Gazette: 30077.
- [9]. Ministry of Environment and Urbanization, Regulation on Control of Excavation, Construction and Demolishing Wastes, Official Gazette Date: 18.03.2004, Number of Official Gazette: 25406.
- [10]. Ministry of Environment and Urbanization, Regulation on the Energy Performance of Buildings, Official Gazette Date: 05.12.2008, Number of Official Gazette: 27075.
- [11]. Building Bylaws, Official Gazette Date: 03.07.2017, Number of Official Gazette: 30113.
- [12]. Ministry of Environment and Urbanization, Building Materials Regulation, Official Gazette Date: 10.07.2013, Number of Official Gazette: 28703.
- [13]. Ministry of Environment and Urbanization, Green Certificate Regulation for Buildings and Settlements, Official Gazette Date: 23.12.2017, Number of Official Gazette: 30279.

## Temporal Coastal Change Analysis in Kizilirmak Delta and Yesilirmak Delta

Aziz Sisman<sup>1</sup>, Elif Aldanmaz<sup>2</sup>

### Abstract

*Kizilirmak and Yesilirmak rivers are two of the most important rivers in Turkey they rise in Eastern part of Anatolia, pass through a lot of cities and emptying into the Black Sea. These two rivers form two important deltas in the Black Sea coast. Kizilirmak and Yesilirmak Delta have been occurred from the sediments carried by Kizilirmak and Yesilirmak Rivers for thousands of years. Kizilirmak Delta is an important wetland and 321 species of bird and a lot of plants lives in the delta area. The Kizilirmak River has 78.646 km<sup>2</sup> drainage area and 185 m<sup>3</sup>/s average flow value. Yesilirmak River has 37.823 km<sup>2</sup> drainage area and Yesilirmak Delta is an important wetland and also agricultural area for Turkey.*

*Last fifty years more than 30 regulators and dams were built on Kizilirmak River and the proportion of the alluvium flowing in the river significantly decreased. Therefore enlargement of Kizilirmak delta stopped and it began to shrink. Four dams and some power plant were built on Yesilirmak River and change of shoreline in Yesilirmak Delta is expected. The aim of this study is to investigate temporal changes in the Kizilirmak delta and Yesilirmak Delta coast, using aerial photo and satellite image in GIS.*

**Keywords:** Kizilirmak, Yesilirmak, Coastal Change, GIS

### 1. INTRODUCTION

A river delta is a landform which forms at the mouth of a river, where the river flows into an ocean, sea, lake or a reservoir. Kizilirmak and Yesilirmak deltas are two important wetlands and also agricultural areas in Turkey. These two deltas were formed by the sediment carried by Kizilirmak and Yesilirmak rivers for thousands of years.

Kizilirmak Delta is one of the most important plain in Turkey. The Delta is located in the central Black Sea region of Turkey, and covers an area of 50,000 ha that includes 15,000 ha of freshwater marshes and swamps, coastal lakes, and lagoons. The Delta has been declared a Ramsar site, which is a wetland of international importance [1].

The Kizilirmak River flows a total of 1,355 kilometers, rising in Eastern Anatolia then forming a wide arch, it joins Delice, Devrez and Gokirmak rivers, finally flowing through Samsun province Bafra district Kizilirmak Delta into the Black Sea. Kizilirmak has 78650 km<sup>2</sup> drainage area, it has an average flow rate of 185 m<sup>3</sup>/sn and it carries 831 million m<sup>3</sup> fresh water in to the black sea [2, 3].

The Yesilirmak River flows a total of 519 kilometers, rising in Eastern Anatolia in Sivas province Kose Mountain then it flowing through Samsun province Carsamba district Yesilirmak Delta into the Black Sea. Yesilirmak has 37823 km<sup>2</sup> drainage area, it has an average flow rate of 121 m<sup>3</sup>/sn. [4].

<sup>1</sup> Corresponding author: Ondokuz Mayıs University, Faculty of Engineering, Samsun, Turkey, asisman@omu.edu.tr

<sup>2</sup> General Directorate of Mapping, Ankara, Turkey, aldanmazeliff@gmail.com

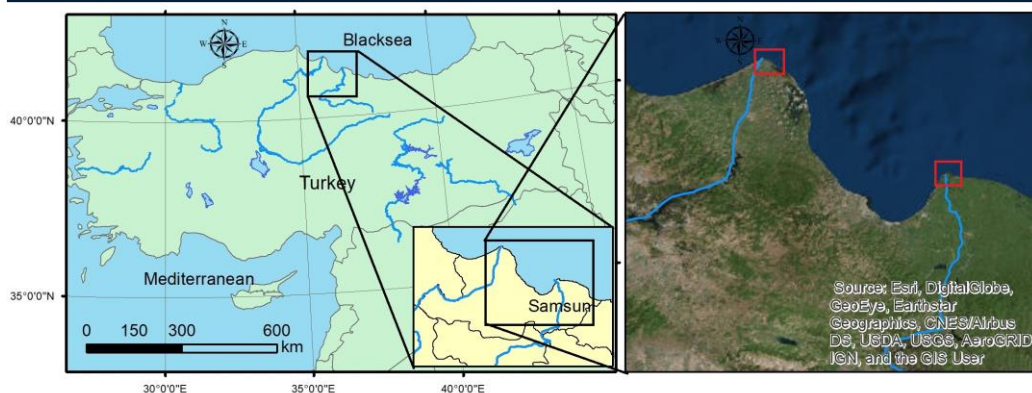


Figure 1. Study area

Kizilirmak and Yesilirmak rivers have shaped the formation of Kizilirmak Delta and Yesilirmak Delta and it continues. However, due to the many different reason, coastal line and also shape of these two deltas are changing.

Coastal line sometimes can be change. The coastal line progresses towards the sea or declines towards land because of some natural and artificial factors. Some natural factors cause change in coastal line are the change of rainfall, the change of wave and flow rate ect. The artificial factors are to remove of materials from the shore and to prevent of shore-feeding materials by some engineering structures such as dams.

The dams built on the rivers negatively affect the development of the deltas. The dams cause hydrological and morphological changes in the lower regions of the rivers with the amount of water and sediment they hold in proportion to their size. Research in this field is also rapidly increasing in Turkey [2, 5, 6, 7].

In this study, the coastal changes in the regions where Kizilirmak and Yesilirmak rivers flow into the sea (Figure 1) was investigated with aerial photographs and satellite images belong to the different years.

## 2. COASTAL LINE CHANGE

### 2.1. Kizilirmak River and Kizilirmak Delta

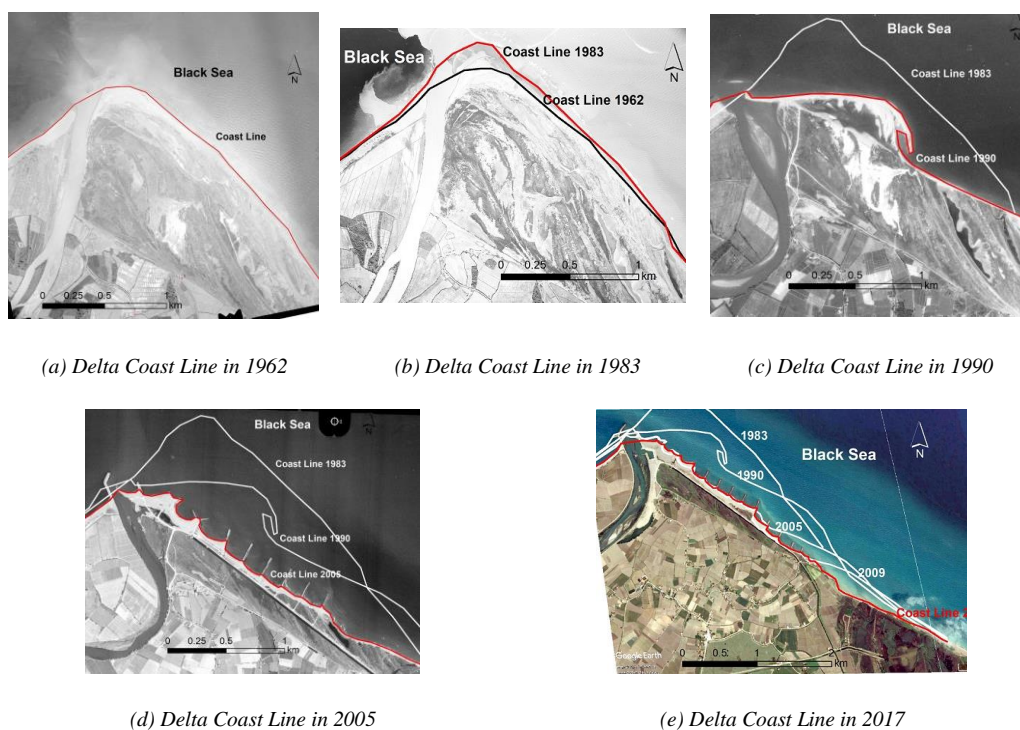
Kizilirmak river is the longest river which rising in Turkey and flowing in to the see in Turkey. There are 31 dams and regulators on the Kizilirmak River, 25 of them are in operation from the source to the mouth of the river. The most famous dams are Hirfanli Dam, Obruk Dam, Boyabat Dam and Antinkaya Dam.

Before 1960 a total amount of 23.1 million tons alluvium per year had been moved into the Black Sea by the Kizilirmak River (Figure 2a). Building dams on the river have caused to start reduction of the alluvium moved into the sea. After building Hirfanli Dam it was down to 18 million tons per year. But, enlargement of Kizilirmak Delta had continued until middle of the 1980's (Figure 2b). Alluvium moved in to the Black Sea was incredibly decreased, after building Altinkaya Dam in 1988 as shown in Figure 2c and Derbent Dam built in 1991, because these two dams are very close to the Delta coast. Altinkaya Dam is only 51 km and Derbent Dam is only 32 km far from the coast, for this reason Altinkaya and Derbent Dams have a significant effect on the Delta. Alluvium flowing in to the sea was decreased to the 0.46 million tons per year after these two dams built [8]. It was observed that only 0.30 million ton alluvium reach to the Black Sea in 2008 [2, 9].

The enlargement of Kizilirmak Delta stopped and a large coastal erosion has started and a huge amount of soil was disappeared in the study area after 1983 as shown in Table 1. Besides that, new plains have formed 120 km far from the coast, because of the alluviums accumulate behind the Altinkaya Dam.

*Table 1. Coastal line change in Kizilirmak Delta (Study Area)*

Year	Enlargement (ha)	Coastal Erosion (ha)
1962-1983	16.8	
1983-1990		65.2
1990-2005		102.1
2005-2017		50.0



*Figure 2. Kizilirmak Delta coast line by year*

To prevent coastal erosion in the Kizilirmak Delta, some coastal protection facilities were started to build in 1999 such as groins as shown in Figure 2d. The groins stopped the erosion where they were built, but coastal erosion effected beyond the groins, so coastal erosion only changed the location towards to the east of the Delta (Figure 2e). After building more than 15 groins coastal erosion slowed down but didn't stop and it was change the location. There are some important swamps, coastal lakes, and lagoons on the east side of the Delta, and some of the coastal lakes and lagoons are under threat of extinction because of the coastal erosion.

## **2.2. Yesilirmak River and Yesilirmak Delta**

There are a lot of studies about Kizilirmak River and Kizilirmak Delta in the literature but less study is observed about Yesilirmak River and Yesilirmak Delta. In this study, coastal change in a specific part of Yesilirmak Delta was determined using aerial photos, topographic maps and satellite images in between 1975 and 2017.

Yesilirmak River is one of the longest rivers which rising in Turkey and flowing in to the sea in Turkey. There are 18 dams and regulators on the river. The most famous dams are Hasan Ugurlu Dam, Suat Ugurlu Dam,



Almus Dam ve Atakoy Dam. After building dams and regulators flowing regime of the Yesilirmak river has changed, and it is effected the Yesilirmak Delta coastal line [10].

Enlargement of Yesilirmak Delta had continued until end of the 1970's (Figure 3a). Alluvium moved in to the Black Sea was decreased after building Hasan Ugurlu Dam in 1979 and Suat Ugurlu Dam in 1982, because these two dams are very close to the Yesilirmak Delta coast (Figure 3b). Suat Ugurlu Dam is only 47 km and Hasan Ugurlu Dam is only 66 km far from the coast, for this reason Suat Ugurlu and Hasan Ugurlu Dams have a significant effect on the Delta.

After building dams, especially Suat Ugurlu and Hasan Ugurlu, the proportion of the alluvium moved in the river decreased about %97 [11]. The enlargement of Yesilirmak has Delta stopped and coastal line has started to change in the study area. However, some enlargement is seen in east side of the Yesilirmak Delta as shown in Figure 3c, 3d and Table 2. It was thought that the reason of enlargement is direction of the dominant stream and wind regime. This situation should be investigated in the Delta using hydrographic surveying methods.

Table 2. Coastal line change in Yesilirmak Delta (Study Area)

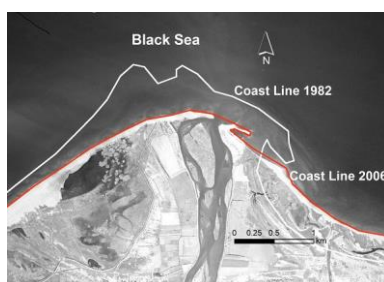
Year	Enlargement (ha)	Coastal Erosion (ha)
1975-1982	21.9	
1982-2017	94.1	
1982-2006		190.9
2006-2017		57.3



(a) Delta Coast Line in 1975



(b) Delta Coast Line in 1982



(c) Delta Coast Line in 2006



(d) Delta Coast Line in 2017

Figure 3. Yesilirmak Delta Coast Line by year

### 3. RESULTS AND CONCLUTIONS

Kizilirmak Delta and Yesilirmak Delta are the two most important deltas of Turkey and the Black Sea. After building some energy and irrigation facilities on the rivers which feeding these two deltas, it was observed that the enlargement undergoing for thousands of years in these areas has stopped and the contraction has begun.

The contraction is still continue in 2017. The coastal lakes and lagoons in the Kizilirmak Delta are under threat of extinction. If the regression seen on the shoreline cannot be prevented, the existing lagoons and wetland will disappear in near future.

This is a descriptive study, even if any energy and irrigation facilities will not be built on Kizilirmak and Yesilirmak rivers, the sediments will accumulate in the reservoirs behind of existing dams and it is expected that coastal erosion will continue in the future. Therefore, coastal protection facilities must be built in the risky area depends on hydrographic surveying and terrestrial surveying in the coast of two deltas.

### REFERENCES

- [1]. [1] Ataol M., Kole M., "Coastal Erosion of Kizilirmak Delta Between 2000 – 2015", 4<sup>th</sup> International Geography Symposium - GEOMED 2016 Book of Proceedings, 2016, ISBN: 978-605-66576-1-0
- [2]. [2] Yilmaz, C., "Kizilirmak Deltasinda Meydana Gelen Erozyonun Cografi Analizi", TURQUA - Turkiye Kuvaterner Sempozyumu V, Bildiriler Kitabı, O. Tuysuz, M. K. Erturac Editorler, 02–03 Haziran 2005 Istanbul.
- [3]. [3] Bahadır, M., "Kizilirmak nehri akim degisimlerinin istatistiksel analizi", Turkish Studies - International Periodical for the Languages, Literature and History of Turkish or Turkic Volume 6/3 Summer 2011, p. 1339-1356.
- [4]. [4] URL 1. Tubitak, Havza Koruma Eylem Planlarinin Hazirlanmasi-Yesilirmak Havzasi, [Online]. Available: <http://suyonetimi.ormansu.gov.tr/Files/Havzakormaeylemplanraporlari/Ye%C5%9Fil%C4%B1rmak%20Havzas%C4%B1.pdf>
- [5]. [5] Uzun, A., "Samsun Ili Kiyilarinda Antropojenik Degismeler", TURQUA Turkiye Kuvaterner Sempozyumu V, Istanbul Teknik Universitesi, Avrasya Yerbilimleri Enstitusu, 02-05 Haziran 2005, s. 183-190
- [6]. [6] Sisman A., Sisman Y., Kizilirmak Deltasi Kiyi Degisimlerinin Zamansal Analizi, Turkiye' nin Kiyi ve Deniz Alanlari IX. Ulusal Kongresi 14-17 Kasim 2012, Hatay-Antakya.
- [7]. [7] Beyazit, I., Ozturk, D., Kilic, F., "Kizilirmak Deltasi Kiyi Cizgisinin Zamansal Degisimi", 5. Uzaktan Algilama-CBS Sempozyumu (Uzal-CBS 2014), 14-17 Ekim 2014, Istanbul
- [8]. [8] Savran S. ve Otay, E. N., "Kizilirmak Deltasi Kiyi Erozyonunun Sayisal Modellemesi", IV. Kiyi Muhendisligi Ulusal Sempozyumu., Bildiriler Kitabı, Cilt: 2, 493-505, 2002, Antalya.
- [9]. [9] Zeybek, H.I., Uzun, A., Yilmaz, C., Ozdemir, S., "Kizilirmak deltasi'nda kiyi cizgisi degisikliklerinin sonuclari", Samsun Sempozyumu, 13-16 Ekim 2011 Samsun.
- [10]. [10] Atalay Dutucu A., Yesilirmak Deltasi'nda Jeomorfolojik Degisiklikler ve Gelecek ile Ilgili Ongoruler, Doktora Tezi Istanbul Universitesi Sosyal Bilimler Enstitusu, 2016 Istanbul
- [11]. [11] Jaoshvili, S., "The Rivers of the Black Sea", European Environment Agency Technical Report, 71, 2002.

## Effects of Catalysts on Bio-oil of Fast Pyrolysis of Greenhouse Vegetable Wastes

Hasan Merdun<sup>1</sup>, Ismail Veli Sezgin<sup>2</sup>

### Abstract

*In this study, GVWs were pyrolyzed in a laboratory-scale fast pyrolysis experimental system by using natural catalysts (calcite, dolomite, zeolite) under different process conditions to mainly produce bio-oil. Catalyst samples which maximized the bio-oil yields were selected and the average elemental (O, C, Ca, Mg) distribution on the surface of the selected catalysts were examined by using the scanning electron microscope (SEM) coupled with energy dispersive X-ray spectroscopy (EDX) technique. And also, gas chromatography-mass spectroscopy (GC-MS) analyses of bio-oil samples were made to determine the chemical compounds in bio-oil samples. SEM/EDX analyses were performed for the catalysts before (control) and after the experiments to investigate the effects of catalysts on the yield and quality of bio-oil samples. The study results showed that the % distribution of these elements on the catalysts surfaces was different from catalyst to catalyst compared to the control. Specifically, while O and Ca% on the catalysts surfaces decreased, C and Mg% increased (except Mg% on dolomite) after the experiments. The amount of some chemicals in bio-oil samples increased while the others decreased after using catalysts in the experiments.*

**Keywords:** Fast pyrolysis, bio-oil, catalyst, SEM/EDX.

### 1. INTRODUCTION

Energy is an indication of the development of a country and is a vital economic input in the industrial productions. Currently, for any kind of applications, energy is supplied from fossil fuel resources such as coal, oil, and natural gas. Fossil fuel resources have some limitations such as being depleted in the near future, heterogeneous distribution in the world, and contributing to global warming and climate change [1]. Therefore, biomass or bioenergy is an alternative to fossil energy sources due to its renewability and cleanness for environment [2], [3]. Biomass is any kind of materials obtained from plants and animals. In general, greenhouse vegetable wastes (GVWs), as one of the important biomass sources in the world and Turkey, are not evaluated effectively enough [4]. For example, in Turkey, GVWs are mostly left around greenhouses after harvesting, burned out in its place, and rarely transferred to landfills. All of these applications are problem for environment. Therefore, GVWs should be better evaluated for agriculture and environment.

Biomass such as GVWs can be evaluated in bioenergy production by either biochemical [5] or thermochemical [6] conversion processes. Fast pyrolysis, a kind of thermochemical conversion process, is commonly applied in the conversion of biomass into biofuels. Fast pyrolysis is the decomposition of organic materials into especially bio-oil (liquid fuel) in relatively high temperature and atmospheric pressure. Fast pyrolysis process has special characteristics such as relatively high temperature (500°C), small biomass particle size (1-2 mm), short reaction time (1-2 seconds) and fast cooling of pyrolysis vapor [7]. Catalysts are commonly used in this conversion process because it positively affects the yield and composition of bio-oil based on the feedstock type and particle size, pyrolysis temperature, and catalyst type and characteristics [8]. Bio-oil can be directly combusted in boilers or furnaces to get heat energy or upgraded to get benzene or diesel fuels to be used in transportation [9].

The objective of this study was to investigate the effects of natural catalysts (calcite, dolomite, zeolite) on bio-oil of fast pyrolysis of GVWs by using a laboratory-scale fast pyrolysis experimental system. To satisfy the

<sup>1</sup> Corresponding author: Akdeniz University, Department of Environmental Engineering, 07058, Antalya, Turkey, [merdun@alumni.clemson.edu](mailto:merdun@alumni.clemson.edu)

<sup>2</sup> Akdeniz University, Department of Environmental Engineering, 07058, Antalya, Turkey, [ivsezgin@gmail.com](mailto:ivsezgin@gmail.com)

objective, firstly, catalyst samples that maximized the bio-oil yields were selected. And then the average elemental (O, C, Ca, Mg) distribution on the surface of the selected catalysts were examined by using the scanning electron microscope (SEM) coupled with energy dispersive X-ray spectroscopy (EDX) technique. In addition, bio-oil samples were analyzed by gas chromatography-mass spectroscopy (GC-MS) to determine the chemical compounds in bio-oil samples.

## 2. MATERIALS AND METHODS

### 2.1. Materials

The wastes of greenhouse vegetables (tomato, pepper, eggplant, squash, and cucumber) were used in this study. After collecting GVWs from greenhouses in Antalya-Turkey, they were air-dried in laboratory and then milled and sieved to obtain the feedstock particle sizes of 0.3-0.5, 0.5-1.0, and 1.0-1.5 mm. The biomass sample of 15 g was obtained by mixing GVWs in the portions of 59.12% tomato, 4.16% pepper, 9.81% eggplant, 9.66% squash, and 17.25% cucumber based on their production potentials in Antalya. The samples were kept in air-tight glass cups for being used in fast pyrolysis experiments.

Natural catalysts such as calcite, dolomite, and zeolite were used in this study. After obtaining the catalysts from mines and chemical companies in Turkey; they were crushed, sieved to obtain particle size of 1.0-1.5 mm, dried, and calcinated.

### 2.2. Methods

A specially designed laboratory scale drop-tube reactor experimental system was used in fast pyrolysis experiments. The three main parts of the system was: feeding system, split/dualfurnace system, and condenser system. A quartz glass reactor with 120 cm length and 3 cm inside diameter was used in the system. Three different pyrolysis temperatures (450, 500, and 550°C), feedstock particle sizes (0.3-0.5, 0.5-1.0, and 1.0-1.5 mm), and a constant carrier gas (nitrogen) flow rate of 1450 mL/min were used in the experiments. The catalyst amount of 7.5 g and size of 1.0-1.5 mm were used with the pyrolysis reaction time of 5 min in all fast pyrolysis experiments. After each experiment bio-oil yield was calculated by mass balance equations.

Catalyst samples which maximized the bio-oil yields were selected and the average elemental (O, C, Ca, Mg) distribution on the surface of the selected catalysts were examined by using the scanning electron microscope (SEM) coupled with energy dispersive X-ray spectroscopy (EDX) technique. In addition, gas chromatography-mass spectroscopy (GC-MS) analyses of bio-oil samples were made to determine the chemical compounds in bio-oil samples and their relative abundances (peak areas). SEM/EDX analyses were performed for the catalysts before (control) and after the experiments to investigate the effects of catalysts on the yield and quality of bio-oil samples.

## 3. RESULTS AND DISCUSSION

The effects of natural catalysts (calcite, dolomite, and zeolite) on the yields and quality of bio-oil of fast pyrolysis of GVWs were investigated based on the accumulation of elements on the surface of the catalysts after the experiments. The deposition of elements on the surface of calcite, dolomite, and zeolite catalysts are shown in Figures 1-3, respectively. These catalysts were selected based on the highest bio-oil yields with the wt% of 34.27, 33.87, and 34.13% for calcite, dolomite, and zeolite catalysts, respectively. In general, the O concentration on the surface of catalysts was the highest, but the Mg concentration was the lowest (Figures 1-3). The C and Ca concentrations were between the two. While O and Ca% on the catalysts surfaces decreased, C and Mg% increased (except Mg% on dolomite) after the experiments. There was a consistent relationship between the concentrations before and after the experiments for a given element (Figures 1-3). The concentrations of O and Ca on the surface of calcite after the experiment decreased, whereas C concentration increased. On the other hand, the amount of Mg on calcite before and after the experiment was insignificant (Figure 1). The concentrations of O, Ca, and Mg on the surface of dolomite after the experiment decreased, whereas C concentration increased (Figure 2). However, there was no significant differences in the concentrations of elements O, C, Ca, and Mg on the surface of zeolite before and after the experiment (Figure 3). The study results showed that the % distribution of the elements O, C, Ca, and Mg on the catalysts surfaces was different from catalyst to catalyst compared to the control. The increase in the C concentration on the catalysts surfaces may be the result of the accumulation of high molecular weighted organic compounds (tar), whereas the decrease in the O concentration may be the result of the oxidation on the catalysts surfaces.

However, the changes in the concentrations of Ca and Mg on catalysts surfaces could not be reasoned at the moment.

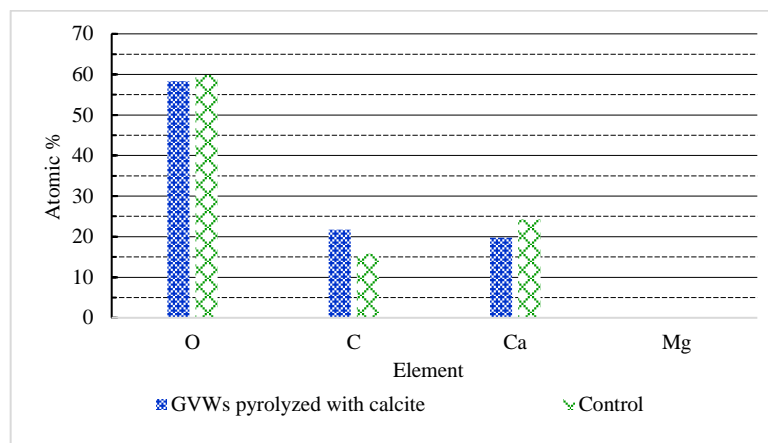


Figure 10. Calcite catalyst used in fast pyrolysis experiment of GVWs with the parameters of 1-1.5 mm and 500°C

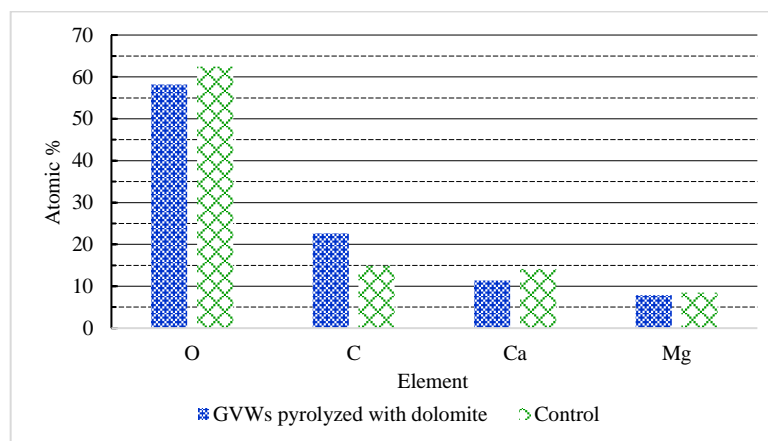


Figure 2. Dolomite catalyst used in fast pyrolysis experiment of GVWs with the parameters of 1-1.5 mm and 500°C

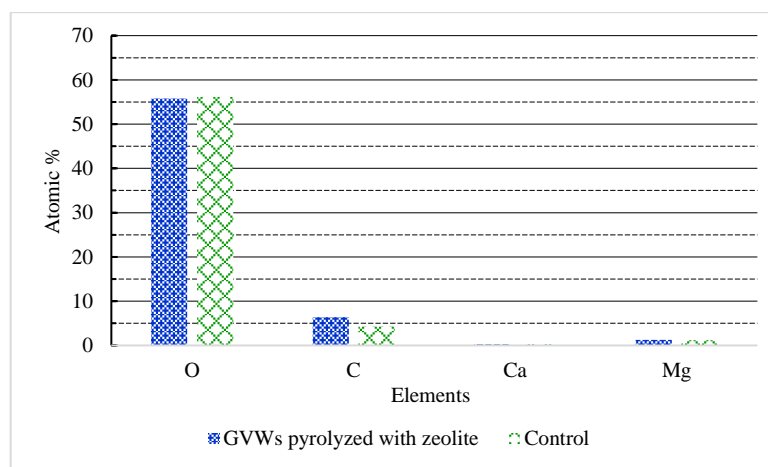


Figure 3. Zeolite catalyst used in fast pyrolysis experiment of GVWs with the parameters of 1-1.5 mm and 500°C

Chemical compounds and their relative abundances available in bio-oil samples obtained from fast pyrolysis of GVWs by using different catalysts and control are given in Table 1. In general, the amount of some chemicals in bio-oil samples increased while the others decreased after using catalysts in the experiments. Specifically, the amounts of 7 out of 12 (detected) chemicals increased when calcite was used as catalyst compared to the control, whereas the amounts of 4 out of 11 (detected) chemicals increased when zeolite was used as catalyst. However, the amounts of 3 out of 13 (detected) chemicals increased when dolomite was used as catalyst. Acetic acid and oxazole, 4,5-dihydro-2,4,4-trimeth had the highest amounts among the chemicals (Table 1).

Table 10. The names of chemical compounds and their relative abundances in bio-oil samples obtained from fast pyrolysis of GVWs with different catalysts

Name of Chemical Compound	Relative Abundance (%Area)			
	Calcite	Dolomite	Zeolite	Control
2-cyclopenten-1-one	<b>3.55</b>	<b>3.70</b>	<b>4.80</b>	3.07
2-cyclopenten-1-one, 2-methyl-	3.46	3.37	<b>4.63</b>	3.52
acetic acid	<b>12.64</b>	11.13	<b>14.67</b>	11.47
propanoic acid	-	-	2.55	-
2-cyclopenten-1-one, 3-methyl-	<b>4.88</b>	<b>4.60</b>	<b>3.64</b>	2.52
2,4-dimethyl-2-oxazoline-4-methanol	-	-	8.88	-
furfuryl alcohol	<b>3.30</b>	2.85	-	2.87
oxazole, 4,5-dihydro-2,4,4-trimeth	<b>11.79</b>	8.98	-	10.97
2(5H)-furanone	2.15	2.01	-	2.26
1,2-cyclopentanedione, 3-methyl-	5.52	5.27	5.40	5.67
guaiacol	<b>4.17</b>	<b>4.04</b>	3.55	3.87
phenol	2.70	2.34	3.00	-
2,6-dimethoxyphenol	<b>2.84</b>	2.61	2.11	2.81
3-pyridinol	2.19	-	2.01	-
1,4,7,10,13,16-hexaoxacyclooctadecane	-	3.60	-	3.85
1,4,7,10,13,16-hexaoxacyclooctadec	-	2.25	-	-

\*Bold values indicate that catalyst increases the amount of the corresponding chemical.

The parameters of experiments with calcite (GVWs, Ca., 1-1.5, 500), dolomite (GVWs, Do., 1-1.5, 500), zeolite (GVWs, Ze., 1-1.5, 500), GVWs: Greenhouse vegetable wastes, Ca: Calcite, Do: Dolomite, Ze: Zeolite, feedstock particle sizes (0.3-0.5, 0.5-1, and 1.1.5 mm), and temperatures (450, 500, and 550°C).

## 4. CONCLUSIONS

The effects of catalysts such as calcite, dolomite, and zeolite on the yields and quality of bio-oil of fast pyrolysis of GVWs were investigated by comparing the % accumulations of the elements O, C, Ca, and Mg on the surface of these catalysts before and after the experiments. The study results showed that the % amounts of the elements O, C, Ca, and Mg on the catalysts surfaces were different from catalyst to catalyst compared to the control. These interesting results suggest that different catalysts used in the fast pyrolysis of different feedstocks need to be further investigated or characterized.

## ACKNOWLEDGMENT

This study has been supported by Akdeniz University Scientific Research Project Commission (FBA-2018-3512).

## REFERENCES

- [1]. J.C. Serrano-Ruiz and J.A. Dumesic, J.A., Catalytic production of liquid hydrocarbon transportation fuels, (In: Catalysis for Alternative Energy Generation, Edited by Gucci, L. and Erdohelyi, A.), Springer Science and Business Media, New York.
- [2]. R. Saxena, D. Adhikari, H. Goyal, "Biomass-based energy fuel through biochemical routes: A review", Renewable and Sustainable Energy Reviews, 13, 167-178, 2009.
- [3]. M. Acaroglu and H. Aydogan, "Biofuels energy sources and future of biofuels energy in Turkey", Biomass & Bioenergy, 36, 69-76, 2012.
- [4]. F. Suarez-Estrella, "Effect of horticultural waste composting on infected plant residues with pathogenic bacteria and fungi: Integrated and localized sanitation", Waste Management, 27, 886-892, 2007.
- [5]. N.A. Perendeci, V. Yilmaz, B. Topkaya, U. Gunerhan, E. Us, L. Dumlu, H. Carrere, D. Patureau, M. Barret, N. Delgenes, H. Baskaya, O. Topac, S. Ucaroglu, "Sera atiklari ile evsel aritma camurlarından biyogaz eldesi ve sera atiklari uygulanan aritim alternatiflerinin sistem verimliliği üzerindeki etkilerinin değerlendirilmesi", TUBITAK Project (No: 107Y145) Final Report, 2010 (in Turkish).



- [6]. H. Merdun and I.V. Sezgin, "Products distribution of catalytic co-pyrolysis of greenhouse vegetable wastes and coal", *Energy*, 162, 953-963, 2018.
- [7]. A.V. Bridgwater, "Review of fast pyrolysis of biomass and product upgrading", *Biomass and Bioenergy*, 38, 68-94, 2012.
- [8]. F. French, S. Czernik, "Catalytic pyrolysis of biomass for biofuels production", *Fuel Processing Technology*, 91, 25-32, 2010.
- [9]. A. Veses, B. Puértolas, M.S. Callén, T. García, "Catalytic upgrading of biomass derived pyrolysis vapors over metal-loaded ZSM-5 zeolites: Effect of different metal cations on the bio-oil final properties", *Microporous and Mesoporous Materials* 209, 189-196, 2015.

## BIOGRAPHY

Dr. Hasan Merdun is currently serving as a faculty member at the Department of Environmental Engineering, Akdeniz University in Antalya, Turkey. His research interests include renewable energy, waste-to-energy, clean energy production, biomass, bioenergy, thermochemical conversion of biomass to biofuels, pyrolysis and gasification technologies, upgrading of biofuels, useful chemicals production from waste, and global warming and climate change. His research mission is to add value to the national and global bioenergy sector by applying an integrated biorefinery approach for the development of renewable energy technologies.

## Investigation of Catalysts and Bio-oil in Co-pyrolysis of Greenhouse Vegetable Wastes and Coal

Hasan Merdun<sup>1</sup>, Ismail Veli Sezgin<sup>2</sup>

### Abstract

*In this study, greenhouse vegetable wastes (GVWs) and lignite coal were co-pyrolyzed in a laboratory-scale fast pyrolysis experimental system by using calcite, dolomite, and zeolite as natural catalysts under different process conditions. Catalyst samples with the highest bio-oil yields were examined by using the scanning electron microscope (SEM) coupled with energy dispersive X-ray spectroscopy (EDX) technique to investigate the average elemental (O, C, Ca, Mg) distribution on the surface of the catalysts. In addition, bio-oil samples were analyzed by gas chromatography-mass spectroscopy (GC-MS) technique to determine the chemical compounds in the samples. The effects of catalysts on the yield and quality of bio-oil samples were investigated by SEM/EDX analyses by characterizing the catalysts before (control) and after the experiments. The study results showed that the catalysts had different amount of accumulation of these elements on the catalysts surface. After the experiments the amounts of O, Ca, and Mg (except Mg% on calcite)% on the catalysts surfaces decreased, but only C% increased. The catalysts had little positive effects on the amount of chemicals in bio-oil samples.*

**Keywords:** Co-pyrolysis, coal, bio-oil, catalyst, characterization.

### 1. INTRODUCTION

Energy can be obtained from two main sources such as fossil fuel sources and renewable energy sources. Nowadays, most of the energy (around 80%) is obtained from fossil fuel sources like coal, oil, and natural gas. However, fossil fuel sources have some limitations and adverse effects on environment. Instead of fossil sources, renewable energy sources such solar, wind, hydro, and biomass have taken attention in all over the world [1], [2]. Biomass is defined as all materials of plants and animal and their residues. The main components of plant biomass are cellulose, hemicellulose, lignin, extractives, and ash. Elemental composition of biomass includes carbon (C), oxygen (O), hydrogen (H), nitrogen (N), and chloride (Cl). Main sources of plant biomass are agricultural wastes and residues, agricultural wastes and residues, municipal solid wastes, and industrial processing wastes [3]. Greenhouse vegetables such as tomato, pepper, eggplant, squash, and cucumber are commonly planted in the world and Turkey. After harvesting these vegetables, their remainings or residues are mostly left around greenhouses, burned out in its place, and rarely transferred to landfills [4], [5]. Coal is a low calorific-valued fossil fuel with some problems for environment due to its high sulfur and ash contents [6]. Turkey has great potential of low calorific-valued coal [7]. When biomass like greenhouse vegetable wastes (GVWs) and low calorific-valued coal are utilized together with a modern technology such as fast pyrolysis, some synergic effects can be observed in the products [8], [9].

Biomass can be converted into different products (biofuels or useful chemicals) through either biochemical or thermochemical conversion technologies. Biochemical conversion technologies include anaerobic digestion and fermentation [10], whereas thermochemical conversion technologies include combustion, pyrolysis, gasification, and liquefaction [11]. Pyrolysis is the decomposition of organic materials into different products like biochar, bio-oil, gases under high temperature and atmospheric pressure. Fast pyrolysis is a special form of pyrolysis, where it requires small biomass particle sizes, relatively high temperature, short reaction time, and

<sup>1</sup> Corresponding author: Akdeniz University, Department of Environmental Engineering, 07058, Antalya, Turkey. [merdun@alumni.clemson.edu](mailto:merdun@alumni.clemson.edu)

<sup>2</sup> Akdeniz University, Department of Environmental Engineering, 07058, Antalya, Turkey, [ivsezgin@gmail.com](mailto:ivsezgin@gmail.com)

fast cooling of pyrolysis vapor [12]. Co-pyrolysis is the use of two different raw materials like GVWs and coal as in this case in the fast pyrolysis system so that some synergic effects are obtained on the yield and composition of the products [13]. The liquid product or bio-oil of fast pyrolysis has some problematic features such as high water and oxygen contents, high viscosity and acidity, and low energy potential. Therefore, catalysts are commonly used in getting rid of these undesired features of bio-oils by upgrading them [14].

The objective of this study was to investigate the effects of natural catalysts (calcite, dolomite, zeolite) on bio-oil of co-pyrolysis of GVWs and low calorific-valued coal by using a laboratory-scale fast pyrolysis experimental system. To do so, firstly, catalyst samples with the highest bio-oil yields were examined by using the scanning electron microscope (SEM) coupled with energy dispersive X-ray spectroscopy (EDX) technique to determine the average elemental (O, C, Ca, Mg) distribution on the surface of the catalysts. Then, bio-oil samples were analyzed by gas chromatography-mass spectroscopy (GC-MS) technique to determine the chemical compounds in the samples. Finally, the effects of catalysts on the yield and quality of bio-oil samples were investigated by SEM/EDX analyses by characterizing the catalysts before (control) and after the experiments.

## 2. MATERIALS AND METHODS

### 2.1. Materials

As feedstock the wastes of greenhouse crops (tomato, pepper, eggplant, squash, and cucumber) and lignite coal were used in this study. GVWs were collected from greenhouses in Antalya-Turkey, whereas lignite coal was purchased from a private coal company in Antalya-Turkey. GVWs were air-dried in laboratory and then milled and sieved to obtain the feedstock particle sizes of 0.3-0.5, 0.5-1.0, and 1.0-1.5 mm. The biomass sample of 15 g was obtained by mixing GVWs in the portions of 59.12% tomato, 4.16% pepper, 9.81% eggplant, 9.66% squash, and 17.25% cucumber based on their production potentials in Antalya. GVWs-coal blend samples were obtained by mixing 10 g GVWs with 5 g coal. The samples were kept in air-tight glass cups for being used in the fast co-pyrolysis experiments.

Catalysts (calcite, dolomite, and zeolite) used in this study were obtained from mines and chemical companies in Turkey. The obtained catalysts were crushed, sieved to obtain particle size of 1.0-1.5 mm, dried, and calcinated.

### 2.2. Methods

The fast co-pyrolysis experiments were performed in a specially designed laboratory scale drop-tube reactor experimental system. The system mainly composed of feeding system, split/dualfurnace system, and condenser system. A reactor made of quartz glass with 120 cm length and 3 cm inside diameter was used in the experimental system. A constant carrier gas (nitrogen) flow rate of 1450 mL/min and pyrolysis reaction time of 5 min were used in all fast co-pyrolysis experiments, whereas variable pyrolysis temperatures (450, 500, and 550°C) and feedstock particle sizes (0.3-0.5, 0.5-1.0, and 1.0-1.5 mm) were used in the experiments. The amount and size of catalysts used in the experiments were 7.5 g and 1.0-1.5, respectively. After each experiment bio-oil yield was calculated by mass balance equations.

Catalyst samples which maximized the bio-oil yields were selected and the average elemental (O, C, Ca, Mg) distribution on the surface of the selected catalysts were examined by using the scanning electron microscope (SEM) coupled with energy dispersive X-ray spectroscopy (EDX) technique. In addition, gas chromatography-mass spectroscopy (GC-MS) analyses of bio-oil samples were made to determine the chemical compounds in bio-oil samples and their relative abundances (peak areas). SEM/EDX analyses were performed for the catalysts before (control) and after the experiments to investigate the effects of catalysts on the yield and quality of bio-oil samples.

## 3. RESULTS AND DISCUSSION

The effects of different catalysts on the yields and quality of bio-oil of fast co-pyrolysis of GVWs and coal were investigated by considering the accumulation of elements O, C, Ca, and Mg on the surface of the catalysts. The accumulation of these elements on the surface of the catalysts are shown in Figures 1-3. The selected calcite, dolomite, and zeolite catalysts had the highest bio-oil yields with the wt% of 25.07, 25.07, and 26.13%, respectively. In general, the O and Mg concentrations on the surface of catalysts were the highest and lowest, whereas the C and Ca concentrations were between them (Figures 1-3). The concentrations of O, Ca, and Mg%

on the catalysts surfaces decreased, whereas C% increased after the experiments. The relationship between the concentrations before and after the experiments was constant for a given element (Figures 1-3). The concentrations of O and Ca on the surface of calcite after the experiment decreased, whereas C concentration increased. On the other hand, the amount of Mg on calcite before and after the experiment was almost the same (Figure 1). The concentrations of O, Ca, and Mg on the surface of dolomite after the experiment decreased, whereas C concentration increased (Figure 2). However, the differences in the concentrations of elements O, C, Ca, and Mg on the surface of zeolite before and after the experiment were so small (Figure 3). The study results showed that the catalysts had different amount of accumulation of the elements O, C, Ca, and Mg on the catalysts surface. Heavy molecular weight organic compounds such as tar may cause the increase in the C concentration on the catalysts surfaces, whereas the oxidation occurring on the catalysts surfaces may result in the decrease in the O concentration.

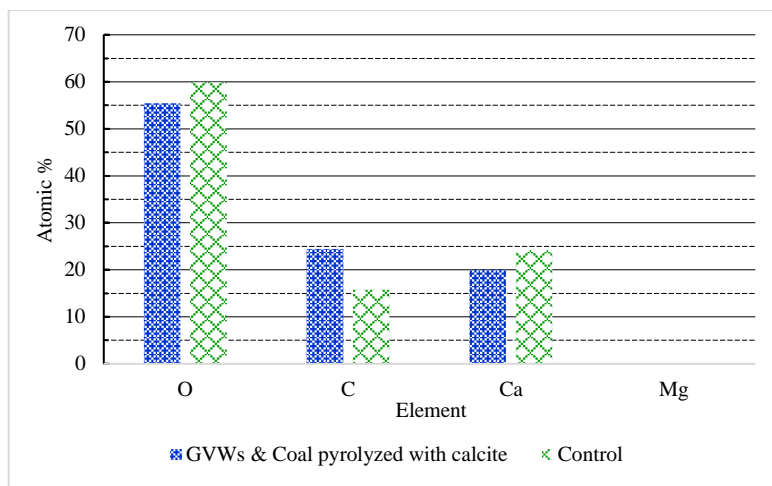


Figure 11. Calcite catalyst used in fast pyrolysis experiment of GVWs & coal with the parameters of 0.5-1.0 mm and 550°C

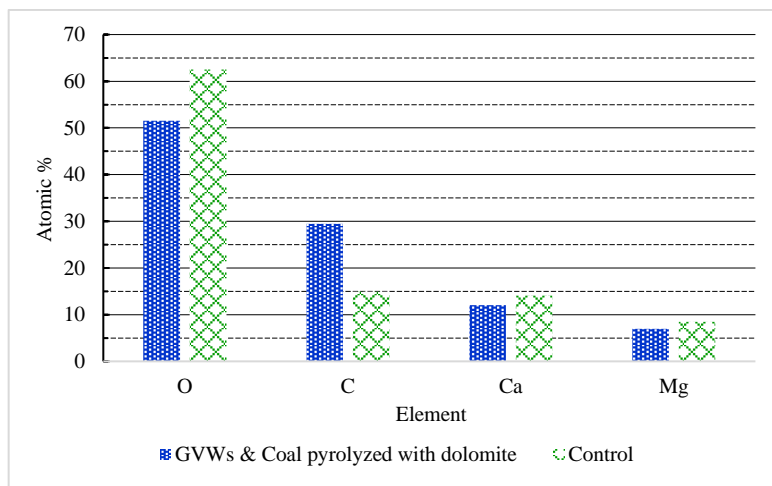


Figure 2. Dolomite catalyst used in fast pyrolysis experiment of GVWs & coal with the parameters of 1-1.5 mm and 550°C

The names of chemical compounds and their relative abundances in bio-oil samples obtained from fast pyrolysis of GVWs and coal with different catalysts are shown in Table 1. In general, the catalysts had little positive effects on the amount of chemicals in bio-oil samples. The amounts of 3 out of 11 (detected) chemicals increased when calcite was used as catalyst compared to the control, whereas the amounts of only 2 out of 11 (detected) chemicals increased when dolomite was used as catalyst. The most abundant chemical in bio-oil samples was acetic acid (Table 1).

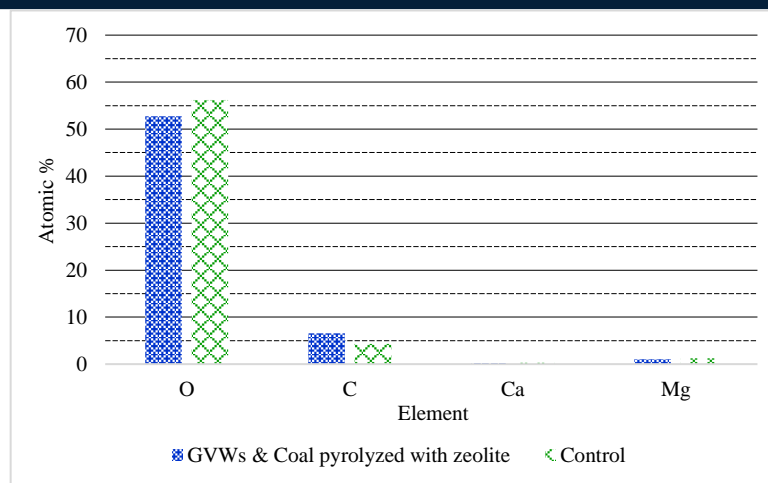


Figure 3. Zeolite catalyst used in fast pyrolysis experiment of GVWs & coal with the parameters of 1-1.5 mm and 550°C

Table 11. Chemical compounds and their relative abundances in bio-oil samples obtained from fast pyrolysis of GVWs and coal with different catalysts

Name of Chemical Compound	Relative Abundance (%Area)		
	Calcite	Zeolite	Control
2-cyclopenten-1-one	-	4.31	4.52
2-cyclopenten-1-one, 2-methyl-	2.86	3.68	4.45
acetic acid	10.80	13.42	14.84
propionic acid	-	<b>2.81</b>	2.53
2-cyclopenten-1-one, 3-methyl-	<b>4.91</b>	<b>3.48</b>	3.21
butanoic acid	-	2.27	-
5-methyl-2,4-dihydro-3h-pyrazol-3-one	-	3.88	-
furfuryl alcohol	3.56	-	3.63
2,4-dimethyl-2-oxazoline-4-methanol	4.00	-	9.76
1,2-cyclopentanedione, 3-methyl-	3.11	3.41	6.77
guaiacol	-	-	3.97
phenol	3.94	<b>4.86</b>	4.53
1,4:3,6-dianhydro-.alpha.-d-glucop uranose	4.23	-	-
3-pyridinol	<b>6.75</b>	2.25	2.25
2H-pyran, 2-(bromomethyl)tetrahydro-	2.55	-	-
1,4,7,10,13,16-hexaoxacyclooctadecane	4.91	4.43	-

\* Bold values indicate that catalyst increases the amount of the corresponding chemical.

The parameters of experiments with calcite (GVWs-C, Ca., 0.5-1.0, 550), zeolite (GVWs-C, Ze., 1-1.5, 550), GVWs: Greenhouse vegetable wastes, GVWs-C: Greenhouse vegetable wastes and coal blend, Ca: Calcite, Ze: Zeolite, feedstock particle sizes (0.3-0.5, 0.5-1, and 1.1.5 mm), and temperatures (450, 500, and 550°C).

## 4. CONCLUSIONS

The effects of natural catalysts on the yields and quality of bio-oil of fast co-pyrolysis of GVWs and lignite coal were investigated by comparing the % concentrations of the elements O, C, Ca, and Mg on the surface of the catalysts before and after the experiments. The study results showed that the catalysts had different amounts of accumulations of the elements O, C, Ca, and Mg on their surfaces when compared to the control. These results suggest that this ambiguity in the concentrations of the elements on the catalyst surfaces may be clarified by conducting the experiments in the future with different feedstocks and catalysts.

## ACKNOWLEDGMENT

This study has been supported by Akdeniz University Scientific Research Project Commission (FBA-2018-3512).

### REFERENCES

- [1]. A.K. Agarwal, "Biofuels (alcohols and biodiesel) applications as fuels for internal combustion engines", *Progress in Energy and Combustion Science*, 33, 233-271, 2007.
- [2]. H.B. Goyal, D. Seal, R.C. Saxena, "Bio-fuels from thermochemical conversion of renewable resources: A review", *Renewable and Sustainable Energy Reviews*, 12, 504-517, 2008.
- [3]. E. Bolyos, D. Lawrence, A. Nordin, "Biomass as an energy source: the challenges and the path forward", [www.ep.liu.se/ecp/009/003/ecp030903.pdf](http://www.ep.liu.se/ecp/009/003/ecp030903.pdf). [Accessed February, 2009].
- [4]. J. Olivier, CO<sub>2</sub>, CH<sub>4</sub>, and N<sub>2</sub>O emissions for 1990 and 1995; sources and methods. In: "CO<sub>2</sub> emissions from fuel combustion 1971-1999", 2001 Edition, pp. III.9-III.29. International Energy Agency (IEA), Paris, 2001.
- [5]. S. Parra, F.J. Aguilar, J. Calatrava, "Decision modelling for environmental protection: The contingent valuation method applied to greenhouse waste management", *Biosystem Engineering*, 99, 469-477, 2008.
- [6]. H. Haykiri-Acma, S. Yaman, "Synergy in devolatilization characteristics of lignite and hazelnut shell during co-pyrolysis", *Fuel*, 86, 373-380, 2007.
- [7]. <http://www.enerji.gov.tr/en-US/Pages/Coal>
- [8]. L. Zhang, S. Xu, W. Zhao, S. Liu, "Co-pyrolysis of biomass and coal in a free fall reactor", *Fuel*, 86, 353-359, 2007.
- [9]. D.K. Park, S.D. Kim, S.H. Lee, J.G. Lee, "Co-pyrolysis characteristics of sawdust and coal blend in TGA and a fixed bed reactor", *Bioresource Technology*, 101, 6151-6156, 2010.
- [10]. S. Achinas, V. Achinas, G.J.W. Euverink, "A technological overview of biogas production from biowaste, *Engineering*, 3, 299-307, 2017.
- [11]. N.L. Panwara, R. Kotharib, V.V. Tyagi, "Thermo chemical conversion of biomass - Eco friendly energy routes", *Renewable and Sustainable Energy Reviews*, 16, 1801-1816, 2012.
- [12]. H.S. Choi, Y.S. Choi, H.C. Park, "Fast pyrolysis characteristics of lignocellulosic biomass with varying reaction conditions", *Renewable Energy*, 42, 131-135, 2012.
- [13]. S. Li, X. Chen, A. Liu, L. Wang, G. Yu, "Co-pyrolysis characteristic of biomass and bituminous coal", *Bioresource Technology*, 179, 414-420, 2015.
- [14]. J.M. Encinar, J.F. Gonza'lez, G. Martinez, S. Roma'n, "Catalytic pyrolysis of exhausted olive oil waste", *Journal of Analytical and Applied Pyrolysis*, 85, 197-203, 2009.

### BIOGRAPHY

Dr. Hasan Merdun is currently serving as a faculty member at the Department of Environmental Engineering, Akdeniz University in Antalya, Turkey. His research interests include renewable energy, waste-to-energy, clean energy production, biomass, bioenergy, thermochemical conversion of biomass to biofuels, pyrolysis and gasification technologies, upgrading of biofuels, useful chemicals production from waste, and global warming and climate change. His research mission is to add value to the national and global bioenergy sector by applying an integrated biorefinery approach for the development of renewable energy technologies.



## Investigation of the Use of Adsorbents Derived from Waste Shells with Addition of PAn/K<sub>2</sub>S<sub>2</sub>O<sub>8</sub> in Laundry Wastewater Treatment by Adsorption Methods

Sevil Veli<sup>1</sup>, Ayla Arslan<sup>1</sup>, Eylem Topkaya<sup>1\*</sup>, Cisil Gulumser<sup>1</sup>, Hatice Kurtkulak<sup>1</sup>, Sehriban Zeybek, <sup>1</sup> Anatoli Dimoglo<sup>2</sup>

### Abstract

*In this study, the treatment of industrial laundry wastewater by adsorption process was investigated. The adsorbents used in this study were obtained from waste shells by using aniline and K<sub>2</sub>S<sub>2</sub>O<sub>8</sub>, which were walnut shell (WS/PAn+ K<sub>2</sub>S<sub>2</sub>O<sub>8</sub>), hazelnut shell (HS/PAn+K<sub>2</sub>S<sub>2</sub>O<sub>8</sub>), seed hull (SH/PAn+K<sub>2</sub>S<sub>2</sub>O<sub>8</sub>) and rice husk (RH/PAn+K<sub>2</sub>S<sub>2</sub>O<sub>8</sub>). In the experimental study, the performance of adsorption process was evaluated through color, turbidity, COD and detergent removal for two different pH values (pH 12 and pH 7). In the experiments conducted with original pH; the highest color, COD and detergent removals were obtained as 94%, 70% and 99% for SH/PAn+K<sub>2</sub>S<sub>2</sub>O<sub>8</sub>, respectively. Meanwhile, the highest turbidity removal was obtained 79% for HS/PAn+K<sub>2</sub>S<sub>2</sub>O<sub>8</sub>. When the initial pH was 7, the highest color and turbidity removals were achieved 98% for SH/PAn+K<sub>2</sub>S<sub>2</sub>O<sub>8</sub> and 89% for HS/PAn+K<sub>2</sub>S<sub>2</sub>O<sub>8</sub>, respectively. The highest COD removal was achieved 76% also for HS/PAn+K<sub>2</sub>S<sub>2</sub>O<sub>8</sub>. However, the highest surfactant removal was obtained 98% for WS/PAn+K<sub>2</sub>S<sub>2</sub>O<sub>8</sub>. According to these results, composites of seed hull aniline (SH/PAn+K<sub>2</sub>S<sub>2</sub>O<sub>8</sub>) and hazelnut shell aniline (HS/PAn+ K<sub>2</sub>S<sub>2</sub>O<sub>8</sub>) were determined to be used as adsorbents in the treatment of wastewater with high organic pollution load by adsorption method.*

**Keywords:** Adsorption, Laundry wastewater, PAn/K<sub>2</sub>S<sub>2</sub>O<sub>8</sub>, Waste shells adsorbents.

### 1. INTRODUCTION

Industrial laundry wastewater may have distinctive characteristics due to the industry's wide range of services for different institutions such as hotels, hospitals and restaurants. These wastewaters, which are included in the greywater class, usually contain high organic load for instance 1000 ppm suspended solids (TSS), 5000 ppm chemical oxygen demand (COD), 1100 ppm oil-grease and 1300 ppm biochemical oxygen demand (BOD) [1]. Laundry wastewater have high detergent concentration [2].

Laundry wastewater composition is very various and is toxic to aquatic organisms; hence laundry wastewater treatment is necessary before its discharge into aquatic environment [3]–[6]. There are many methods used for industrial laundry wastewater treatment. These methods can be primarily sorted as physical, chemical and biological systems. After emergent requirements for the environmental management, advanced treatment methods have been recently applied to these wastewaters along with or instead of the preceding systems. Bipolar electrocoagulation–electroflotation process [7], coagulation and membrane filtration [8], electrocoagulation/electroflotation [9], photocatalytic ozonation [10], coagulation–flocculation/ultraviolet photolysis [11], polyethersulfone/polyvinylpyrrolidone ultrafiltration membranes process [12], e-peroxone

<sup>1</sup> \*Corresponding author: Kocaeli University, Department of Environmental Engineering, 41380, Kocaeli, Turkey.  
[eylem.topkaya@kocaeli.edu.tr](mailto:eylem.topkaya@kocaeli.edu.tr)

<sup>1</sup> Kocaeli University, Department of Environmental Engineering, [sevilv@kocaeli.edu.tr](mailto:sevilv@kocaeli.edu.tr), [ataberk@kocaeli.edu.tr](mailto:ataberk@kocaeli.edu.tr), [cisil.gulumser@kocaeli.edu.tr](mailto:cisil.gulumser@kocaeli.edu.tr), [haticekurtkulak@gmail.com](mailto:haticekurtkulak@gmail.com), [zeybeksehrilan@gmail.com](mailto:zeybeksehrilan@gmail.com)

<sup>2</sup> Duzce University, Department of Environmental Engineering, [anatolidimoglo@duzce.edu.tr](mailto:anatolidimoglo@duzce.edu.tr)

process [13] and moving bed bio-reactor (MBBR) [14] processes are studies in literature about laundry wastewater treatment.

In this study, the treatment of laundry wastewaters by adsorption process was investigated via using polymeric composites produced from waste shells with  $K_2S_2O_8$  oxidizing agent as adsorbents. Treatment studies were evaluated in terms of color, turbidity, COD and surfactant parameters removals. So that, it is aimed to treat the laundry wastewaters, which have a high organic load and surfactant content, by adsorption process.

## 2. MATERIALS AND METHODS

### 2.1. Laundry Wastewater Characteristics

The wastewater used in this study was taken from a commercial laundry facility. The characterization of laundry wastewater was given in Table 1. All analyses of the parameters shown in Table 1 were conducted according to the standard methods [15].

*Table 1. Characteristics of laundry wastewater used in the study.*

Parameters	Results of Analysis
pH	11.39
Conductivity (mS/cm)	1.72
Temperature (°C)	20.5
Absorbance (abs- 228 nm)	1.829
Color (Pt-Co)	121
Turbidity (NTU)	169
TSS (mg/L)	99
COD (mg/L)	1251
TOC (mg/L)	270
Surfactant-MBAS (mg/L)	94
Alkalinity (mg $CaCO_3/L$ )	680
Orthophosphate (mg/L $PO_4^{3-}P$ )	0.514
Total Phosphate (mg/L $PO_4$ )	6.86
TKN (mg/L)	11
$NH_3-N$ (mg/L)	0
$NO_3-N$ (mg/L)	4.99
$NO_2-N$ (mg/L)	0.081
Total Nitrogen (mg/L)	16
Sulfate (mg/L)	94.8

## 2.2. Synthesis of the Composites via Polymerization

Different waste materials (walnut shells, hazelnut shells, seed hull and rice husk) used in this study. These shells were chemically activated with 100 mL aqueous solution of  $\text{H}_3\text{PO}_4$  (50%) at 80 °C in water bath for 4 hours, and then activated shells were dried at 105 °C for 12 hours. Subsequently, they were carbonized to obtain activated carbon. After acquiring the activated carbons, 1 g of each activated carbons were added into the 100 mL of continuously stirred  $\text{H}_2\text{SO}_4$  (1 M) solutions with 1 g of  $\text{K}_2\text{S}_2\text{O}_8$ . While stirring was on, 1 mL of aniline monomer was slowly added into this solution. After the homogenized mixtures had been obtained, these mixtures were put into the ultrasonic bath (Wise Clean WUC-AO6H) and polymerization was conducted at ambient temperature for 5 h. After this procedure, all samples were filtered through creped filter papers and washed for several times with distilled water. Finally, the polymerized activated carbons were dried in drying oven (Nuve FN500) at 60 °C for 24 h and then cooled in a desiccator. The synthesized polymeric composites were named as indicated in Table 2.

Table 2. The synthesized polymeric composites.

Substrate of Activated Carbon	Polymeric Composites Name
Walnut Shell (WS)	WS/ PAn + $\text{K}_2\text{S}_2\text{O}_8$
Hazelnut Shell (HS)	HS/ PAn + $\text{K}_2\text{S}_2\text{O}_8$
Seed Hull (SH)	SH/ PAn + $\text{K}_2\text{S}_2\text{O}_8$
Rice Husk (RH)	RH/ PAn + $\text{K}_2\text{S}_2\text{O}_8$

## 2.3. Experimental Procedure

100 mL of laundry wastewater sample was taken into a 250 mL Erlenmeyer flask and 1g of different adsorbents were added onto the sample. The samples were shaken in the water bath with 150 rpm stirring rate at room temperature (23°C) for 120 minutes. The experiments were conducted at two different pH values (7 and 12). The samples were separated from the adsorbents by filtration at the end of the agitation. The efficiency of the adsorption process was evaluated via color, turbidity, chemical oxygen demand (COD) and surfactant parameters. The spectrophotometer (HACH-LANGE Dr 5000) was used for measuring the color, turbidity and surfactant parameters in the experimental study. Color results were determined at the single wavelength of 455 nm in the spectrophotometer. The turbidity was measured by using the nephelometric method. The maximum absorbance was observed at 288 nm for the turbidity analysis. COD was measured by using the closed reflux method. Concentration of surfactant was measured by using the methylene blue anionic surfactant (MBAS) analysis. All analyses were carried on according to the standard methods for the water and wastewater examination [15].

## 3. RESULTS AND DISCUSSION

The treatment of laundry wastewater by adsorption process with the usage of adsorbents from different waste shells was investigated in this study. The efficiencies of the polymeric composites (WS/ PAn +  $\text{K}_2\text{S}_2\text{O}_8$ , HS/ PAn +  $\text{K}_2\text{S}_2\text{O}_8$ , SH/ PAn +  $\text{K}_2\text{S}_2\text{O}_8$  and RH/ PAn +  $\text{K}_2\text{S}_2\text{O}_8$ ) in the adsorption experiments at different initial pH values (the original pH=12 and pH=7) for 120 min duration were investigated in terms of color removal (Figure 1).

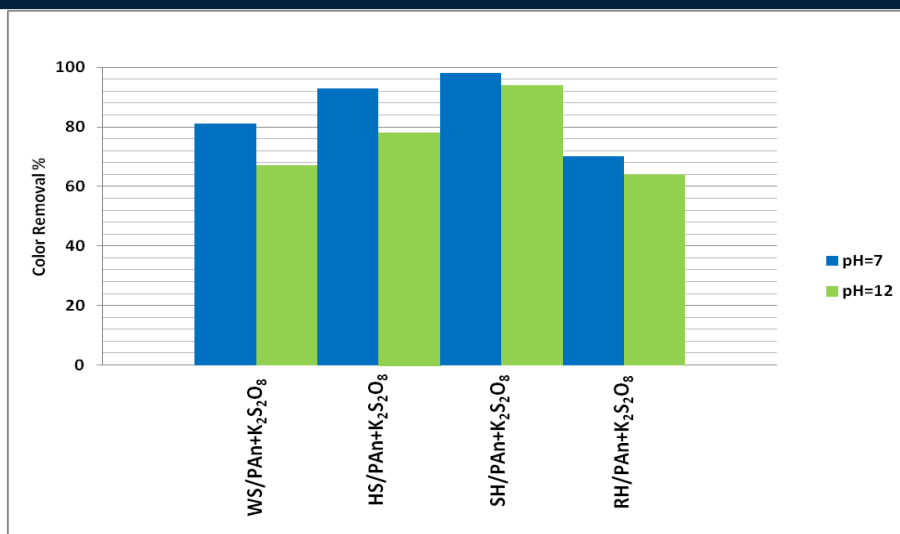


Figure 1. The effect of adsorbent on color removal yields (100 mL of Laundry wastewater, 1g of adsorbent amount, 120 min reaction time, 150 rpm stirring rate).

The highest color removal yields were achieved with the SH/PAn+K<sub>2</sub>S<sub>2</sub>O<sub>8</sub> composite at pH=7 and pH=12 with the results of 98% and 94%, respectively (Figure 1). The highest color removals for all adsorbent species were obtained at pH = 7.

The turbidity removal efficiencies of adsorbents for laundry wastewater treatment were also investigated with the same experimental conditions as seen in Figure 2.

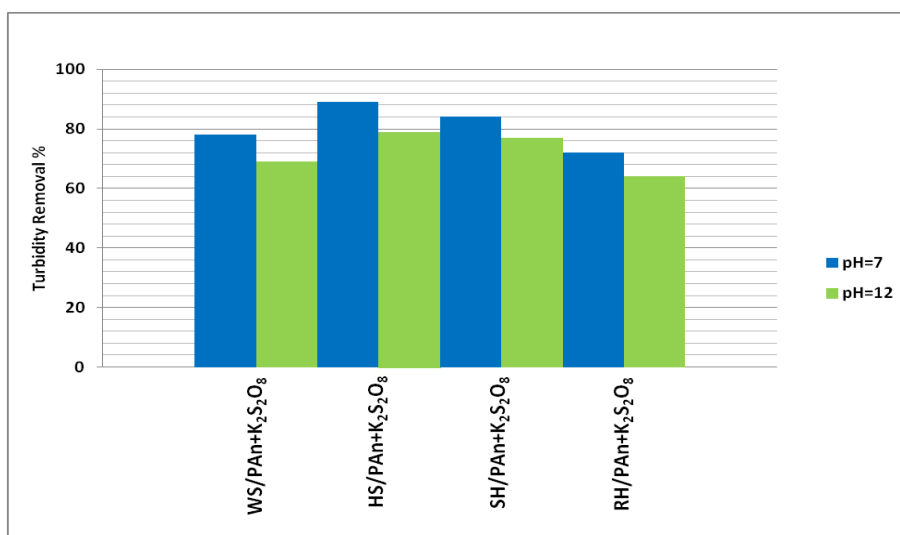


Figure 2. The effect of adsorbent on the turbidity removal yields (100 mL of Laundry wastewater, 1g of adsorbent amount, 120 min reaction time, 150 rpm stirring rate).

According to the Figure 2, the highest turbidity removal yields were achieved for the HS/PAn+K<sub>2</sub>S<sub>2</sub>O<sub>8</sub> and SH/PAn+K<sub>2</sub>S<sub>2</sub>O<sub>8</sub> composites at pH=7 with the results of 89% and 84%, respectively.

The efficiencies of polymeric composites were shown in Figure 3 in terms of COD removal for treatment of laundry wastewater by adsorption process.

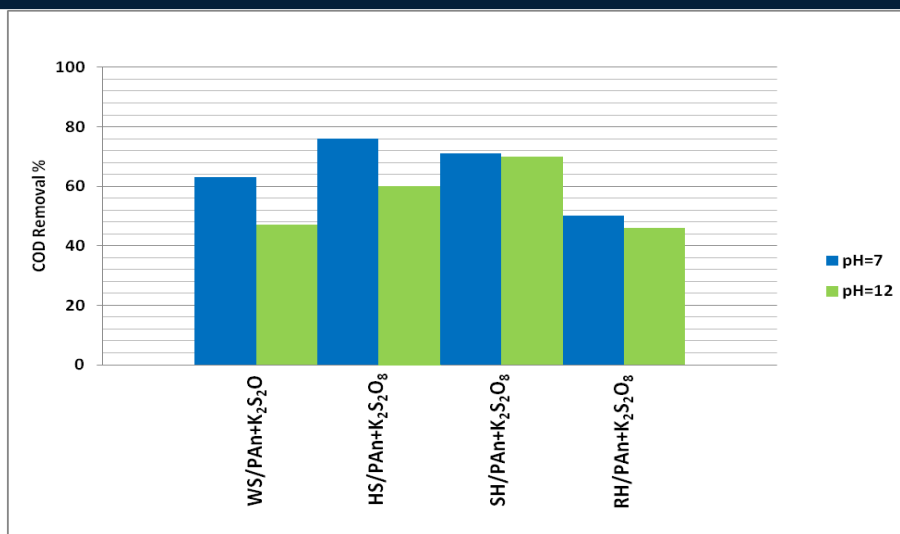


Figure 3. The effect of adsorbent on the COD removal yields (100 mL of Laundry wastewater , 1g of adsorbent amount, 120 min reaction time, 150 rpm stirring rate).

As seen from Figure 3, the highest COD removal yields in the laundry wastewater treatment were achieved at pH=7 by using the HS/PAn+K<sub>2</sub>S<sub>2</sub>O<sub>8</sub> and SH/PAn+K<sub>2</sub>S<sub>2</sub>O<sub>8</sub> composites with the results of 76% and 71%, respectively. Terechova et al. 2014, achieved also the same efficiency of COD removal in the treatment of laundry wastewater by using the coagulation–flocculation/ultraviolet photolysis process.

And at last, the efficiencies of all synthesized adsorbents were investigated in terms of surfactant removal in Figure 4.

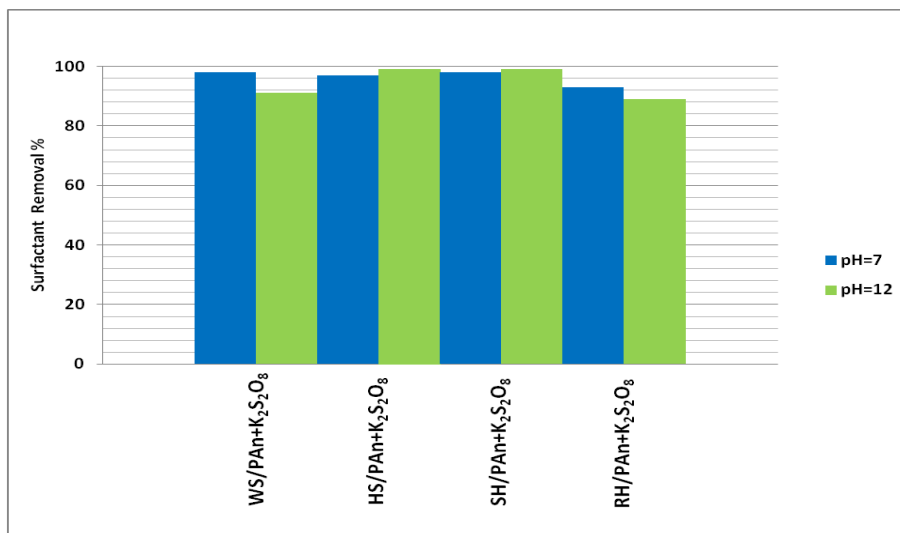


Figure 4. The effect of adsorbent on the surfactant removal yields (100 mL of Laundry wastewater , 1g of adsorbent amount, 120 min reaction time, 150 rpm stirring rate).

As seen from Figure 4, the highest surfactant removal yields in the laundry wastewater treatment were achieved over 90% removal efficiencies by using WS/PAn+K<sub>2</sub>S<sub>2</sub>O<sub>8</sub>, HS/PAn+K<sub>2</sub>S<sub>2</sub>O<sub>8</sub> and SH/PAn+K<sub>2</sub>S<sub>2</sub>O<sub>8</sub> composites at all pH values. Turkay et al. and Šostar-Turk et al. also obtained over 90% of efficiencies in terms of anionic surfactant removal by using different methods in the treatment of laundry wastewater.

### 4. CONCLUSION

In this study, the treatability of laundry wastewaters by adsorption process with using different adsorbents, which were prepared as polymeric composites from waste materials with  $K_2S_2O_8$  oxidant, was investigated in terms of color, turbidity, COD and surfactant parameters.

In the adsorption studies at both pH values, the highest color, COD and surfactant removal efficiencies were obtained with the utilization of SH/PAn+ $K_2S_2O_8$  composite. Maximum turbidity removals were also achieved with HS/PAn+ $K_2S_2O_8$  composite at both pH values. The highest surfactant removal efficiencies were obtained for the studies in which WS/PAn+ $K_2S_2O_8$  and SH/PAn+ $K_2S_2O_8$  composites were used as adsorbents at pH = 7. In general, the surfactant removal efficiencies were observed above 85% for all adsorbents used in the experiments at all pH values.

The polymeric composites of seed hull aniline (SH/PAn+  $K_2S_2O_8$ ), hazelnut shell aniline (HS/PAn+  $K_2S_2O_8$ ) and walnut shell aniline (WS/PAn+  $K_2S_2O_8$ ) were determined to be applicable as adsorbents in the treatment of wastewaters with high organic load by adsorption processes.

### ACKNOWLEDGMENT

The authors thank TUBITAK Research and Development Program with Priority Fields (1003) for their financial support to the main Project 115Y797 and sub-Project 115Y820.

### REFERENCES

- [1] F. Janpoor, A. Torabian, and V. Khatibikamal, "Treatment of laundry waste-water by electrocoagulation," *J. Chem. Technol. Biotechnol.*, vol. 86, no. 8, pp. 1113–1120, Apr. 2011.
- [2] J. K. Braga and M. B. A. Varesche, "Commercial Laundry Water Characterisation," *Am. J. Anal. Chem.*, vol. 05, no. 01, pp. 8–16, Jan. 2014.
- [3] J. K. Braga, F. Motteran, T. Z. Macedo, I. K. Sakamoto, T. P. Delforno, D. Y. Okada, E. L. Silva, and M. B. A. Varesche, "Biodegradation of linear alkylbenzene sulfonate in commercial laundry wastewater by an anaerobic fluidized bed reactor," *J. Environ. Sci. Heal. - Part A Toxic/Hazardous Subst. Environ. Eng.*, vol. 50, no. 9, pp. 946–957, Jul. 2015.
- [4] T. P. Delforno, A. G. L. Moura, D. Y. Okada, I. K. Sakamoto, and M. B. A. Varesche, "Microbial diversity and the implications of sulfide levels in an anaerobic reactor used to remove an anionic surfactant from laundry wastewater," *Bioresour. Technol.*, vol. 192, pp. 37–45, Sep. 2015.
- [5] G. Konnecker, J. Regelman, S. Belanger, K. Gamon, and R. Sedlak, "Environmental properties and aquatic hazard assessment of anionic surfactants: Physico-chemical, environmental fate and ecotoxicity properties," *Ecotoxicology and Environmental Safety*, vol. 74, no. 6, pp. 1445–1460, Sep. 2011.
- [6] M. Lechuga, M. Fernández-Serrano, E. Jurado, J. Núñez-Olea, and F. Ríos, "Acute toxicity of anionic and non-ionic surfactants to aquatic organisms," *Ecotoxicol. Environ. Saf.*, vol. 125, pp. 1–8, Mar. 2016.
- [7] J. Ge, J. Qu, P. Lei, and H. Liu, "New bipolar electrocoagulation-electroflotation process for the treatment of laundry wastewater," *Sep. Purif. Technol.*, vol. 36, no. 1, pp. 33–39, Apr. 2004.
- [8] S. Šostar-Turk, I. Petrinčić, and M. Simonić, "Laundry wastewater treatment using coagulation and membrane filtration," *Resour. Conserv. Recycl.*, vol. 44, no. 2, pp. 185–196, May. 2005.
- [9] C. T. Wang, W. L. Chou, and Y. M. Kuo, "Removal of COD from laundry wastewater by electrocoagulation/electroflotation," *J. Hazard. Mater.*, vol. 164, no. 1, pp. 81–86, May. 2009.
- [10] D. I. Kern, R. de O. Schwaickhardt, G. Mohr, E. A. Lobo, L. T. Kist, and E. L. Machado, "Toxicity and genotoxicity of hospital laundry wastewaters treated with photocatalytic ozonation," *Sci. Total Environ.*, vol. 443, pp. 566–572, Jan. 2013.
- [11] E. L. Terechova, G. Zhang, J. Chen, N. A. Sosnina, and F. Yang, "Combined chemical coagulation-flocculation/ultraviolet photolysis treatment for anionic surfactants in laundry wastewater," *J. Environ. Chem. Eng.*, vol. 2, no. 4, pp. 2111–2119, Dec. 2014.
- [12] A. Sumisha, G. Arthanareeswaran, Y. Lukka Thuyavan, A. F. Ismail, and S. Chakraborty, "Treatment of laundry wastewater using polyethersulfone/polyvinylpyrrolidone ultrafiltration membranes," *Ecotoxicol. Environ. Saf.*, vol. 121, pp. 174–179, Nov. 2015.
- [13] O. Turkay, S. Barisci, and M. Sillanpää, "E-peroxone process for the treatment of laundry wastewater: A case study," *J. Environ. Chem. Eng.*, vol. 5, no. 5, pp. 4282–4290, Oct. 2017.
- [14] S. Bering, J. Mazur, K. Tarnowski, M. Janus, S. Mozia, and A. W. Morawski, "The application of moving bed bio-reactor (MBBR) in commercial laundry wastewater treatment," *Sci. Total Environ.*, vol. 627, pp. 1638–1643, Jun. 2018.
- [15] A. Public Health Association, A. W. W. Association, and W. E. Federation, *Standard Methods for the Examination of Water and Wastewater 21st Edition*, vol. 552. 2005.



## Investigation of Bisphenol A Solutions Treatability by Using Ozone Based Oxidation Processes

Eylem Topkaya<sup>1</sup>, Ayla Arslan<sup>2</sup>

### Abstract

*In this study, treatability of bisphenol A (BPA), which is an endocrine disrupting chemical and widely used in many industries, was evaluated by examining the chemical oxygen demand (COD) and total organic carbon (TOC) parameters using by methods of O<sub>3</sub>, O<sub>3</sub>/UV, O<sub>3</sub>/UV/ZnO and O<sub>3</sub>/UV/Fe<sub>2</sub>O<sub>3</sub> advanced oxidation processes. The experimental studies were made of at 20 mg/L BPA concentration, at its own pH, at different reaction times (15-120 min), in the presence of 0.1 g of different catalysts (ZnO ve Fe<sub>2</sub>O<sub>3</sub>), at 5 ppm ozone dose and under the light source of 16 W UV lamp. The highest COD removal efficiencies were found as 55% over the 90 min reaction time in the O<sub>3</sub> process and as 67% at during the 60 min reaction time in the O<sub>3</sub>/UV/ZnO process. The highest TOC removal efficiencies were determined as 98% and as 96%, respectively as a result of O<sub>3</sub>/UV/ZnO and O<sub>3</sub>/UV processes during the 120 min reaction times.*

**Keywords:** Bisphenol A, COD removal, Ozone, TOC removal.

### 1. INTRODUCTION

Bisphenol A (BPA), which is one of the most widely used endocrine disrupters, is among the most important synthetic substances produced by human beings [1]. It is widely used in the production of polycarbonate plastics and epoxy resins. Epoxy resins; on the food contact surface of canned food, it is used for making jar lid, canned food and beverage bottles [2], [3]. Polycarbonate plastics; they play a role in the construction of materials such as baby and water bottles, CDs, medical equipment, and sunglasses [4]. BPA is available in the inlet and outlet of wastewater treatment plants and have access to the receiving environments with discharge [5].

Several studies have been conducted in the literature for the treatment of wastewater containing BPA. These are such as; adsorption and photocatalysis process [6], hot persulfate process [7], photocatalytic oxidation [8], [9], electrochemical advanced oxidation [10], electrochemical carbon-nanotube filter [11], fenton and fenton-like process [12]-[14], catalytic ozonation, photocatalytic ozonation and ozonation methods [15]-[17].

Advanced oxidation processes (AOPs) are chemical, photochemical and hydrothermal purification processes based on the formation of hydroxyl radicals (HO) with high oxidation potential. These processes can convert without discrimination of toxic pollutants and permanent organic substances into the final products such as CO<sub>2</sub> and H<sub>2</sub>O [18]-[21]. O<sub>3</sub>, O<sub>3</sub>/UV, O<sub>3</sub>/UV/ZnO and O<sub>3</sub>/UV/Fe<sub>2</sub>O<sub>3</sub> processes are one of the AOPs based on ozonation. Hydrogen radicals are formed by the degradation of ozone and these processes are highly effective methods for the oxidation of toxic and refractory compounds.

That's why, the treatability of 20 mg/L BPA was investigated in this study by using AOP methods of O<sub>3</sub>, O<sub>3</sub>/UV, O<sub>3</sub>/UV/ZnO and O<sub>3</sub>/UV/Fe<sub>2</sub>O<sub>3</sub> and removal efficiencies of these processes were evaluated on COD and TOC parameters.

<sup>1</sup> Corresponding author: Kocaeli University, Department of Environmental Engineering, 41380, Kocaeli, Turkey.  
[eylem.topkaya@kocaeli.edu.tr](mailto:eylem.topkaya@kocaeli.edu.tr)

<sup>2</sup> Kocaeli University, Department of Environmental Engineering, [ataberk@kocaeli.edu.tr](mailto:ataberk@kocaeli.edu.tr)

## 2. MATERIAL AND METHODS

### 2.1. Materials and samples

Bisphenol A (4,4'-(propane-2,2-diyl)diphenol, p,p'-Isopropylidenebisphenol, 2,2-Bis(4-hydroxyphenyl)propane -  $(\text{CH}_3)_2\text{C}(\text{C}_6\text{H}_4\text{OH})_2$  -  $M=228.29$  g/mole) was purchased from Sigma Aldrich. BPA aqueous solutions were prepared with pure water in the laboratory. BPA molecular structure is given in Figure 1. The ZnO and  $\text{Fe}_2\text{O}_3$  nanopowder (the brand of Sigma Aldrich) were used as an oxidants.

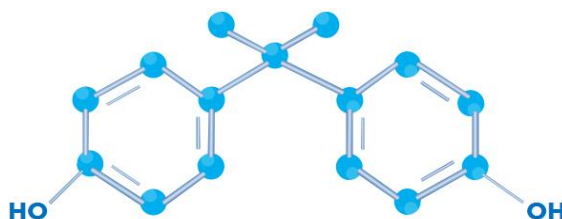


Figure 1. BPA molecular structure.

### 2.2. Experimental System

The used system is consisted of ozone monitor and generator, UV lamps and reaction tank. The ozone gas used in the experiments was produced by ozone generator using oxygen in the air. The produced ozone gas was fed into the reactor by means of a diffuser. 2 x 8W low-pressure mercury lamps were fitted in the reaction tank as to be UV light source. The experiments were carried out in a 2L volume quartz glass batch reactor. The reactor in which the experiments are made as follows Figure 2 [22].

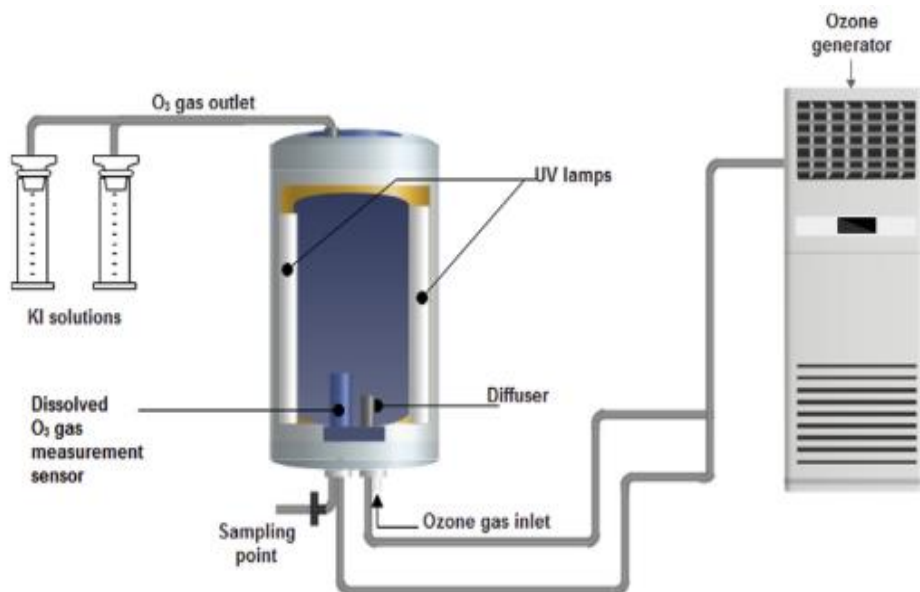


Figure 2. Ozone reactor system.

### 2.3. Analysis

The experiments were performed with 20 mg/L concentration of 1L BPA synthetic solution. Amount of 0.1g ZnO and  $\text{Fe}_2\text{O}_3$  oxidants were added into the reactor. Ozone dose was adjusted to be 5 ppm from the generator and UV lamps turned on. The experiments were performed during 120 min of reaction time. Samples were taken every 15 min during the first 60 min reaction. After 1 hour other samples were taken with 30 min intervals from the reactor. Degradation of BPA was measured by using the chemical oxygen demand (COD) and total

organic carbon (TOC) (Teledyne Tekmar), according to the standard methods for the examination of water and wastewater [23].

### 3. RESULTS AND DISCUSSION

In this study, treatability of pollutant Bisphenol A (BPA) was investigated with chemical and photochemical oxidation processes by using ZnO and Fe<sub>2</sub>O<sub>3</sub> catalyst. The experiments were carried out with 20 mg/L concentrations of BPA, 5 ppm ozone doses, pH 6.5-7, 16 W UV light effect, presence of 0.1 g ZnO and Fe<sub>2</sub>O<sub>3</sub> catalyst and constant of 120 min reaction time.

The effect of 5 ppm ozone dose and 16W UV light on 20 mg/L BPA treatment were determined to COD and TOC removal efficiencies and the result of the study were shown in Figure 3 and Figure 4.

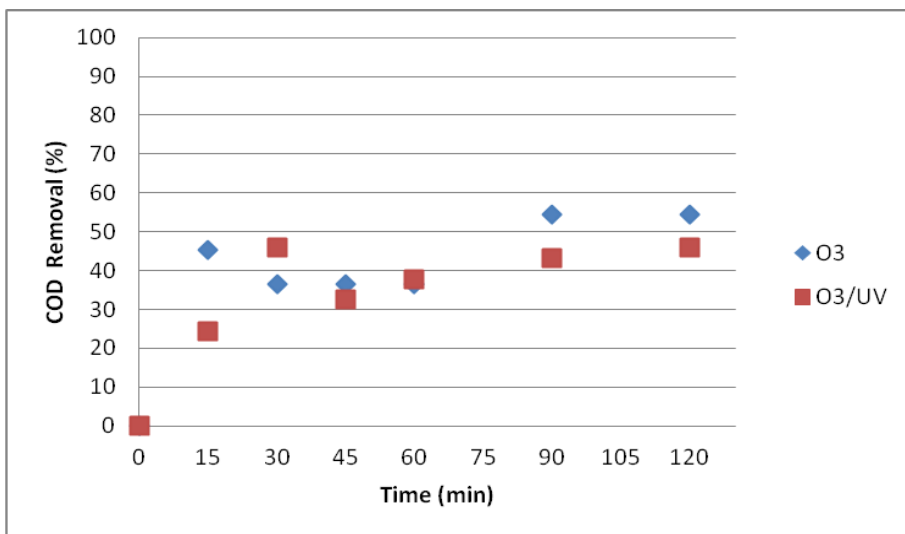


Figure 3. The effects of O<sub>3</sub> and O<sub>3</sub>/UV processes on COD removal for BPA treatment

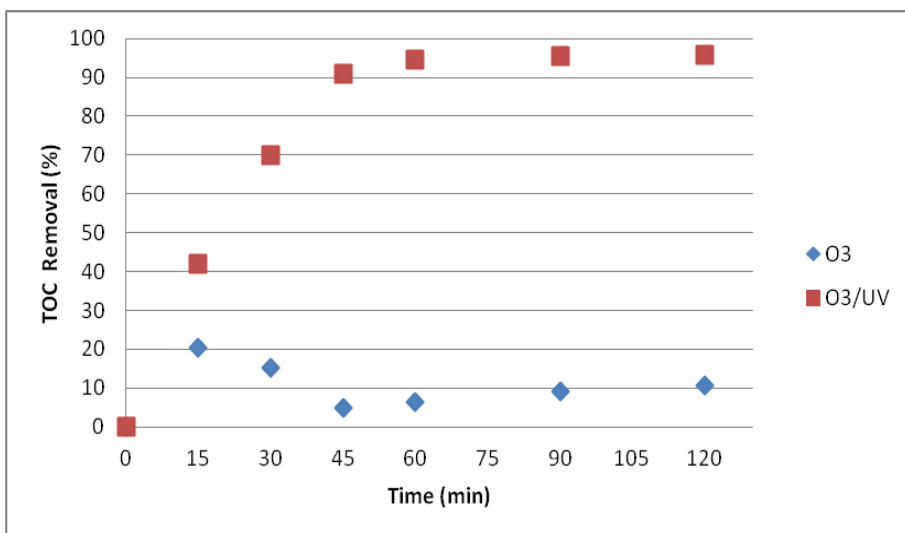


Figure 4. The effects of O<sub>3</sub> and O<sub>3</sub>/UV processes on TOC removal for BPA treatment

According to Figure 3 and Figure 4, using UV lamps were positive effect on COD and TOC removals in the first 30 min and 1 hour reaction times, respectively. In the O<sub>3</sub> process, the max COD removal was occurred

55% in the 90 minutes. But in the O<sub>3</sub>/UV process, the removal efficiency of COD decreased at the same reaction times. TOC removal efficiencies increased at first 60 min reaction time in O<sub>3</sub>/UV process. However, in the O<sub>3</sub> process, TOC removal increased for the first 15 minutes and there weren't observed removal along 120 min. It has been determined that the UV light has a positive effect in the first 30 to 60 minutes on the COD and TOC removal efficiencies at 20 mg/L BPA concentrations when the O<sub>3</sub>/UV process is used.

The removal of 20 mg / L BPA was also investigated using the photocatalytic ozone oxidation process. 0.1 g of ZnO and Fe<sub>2</sub>O<sub>3</sub> catalysts were used as catalysts. The results of the study were evaluated on COD and TOC removal efficiencies (Figure 5-6).

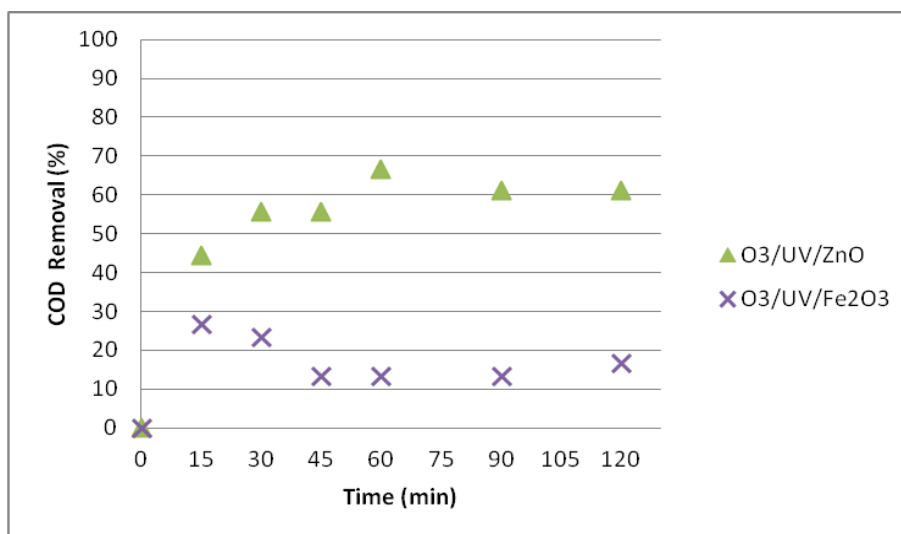


Figure 5. The effects of photocatalytic ozone processes on COD removal for BPA treatment

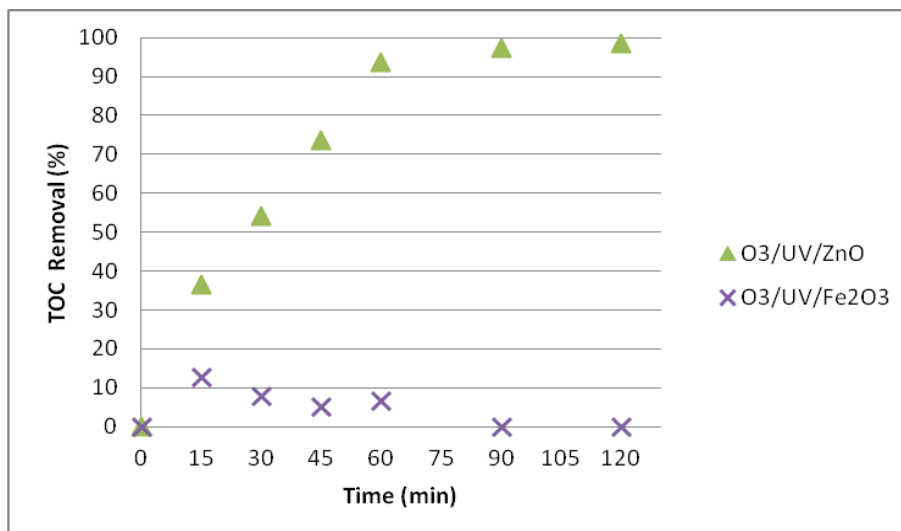


Figure 6. The effects of photocatalytic ozone processes on TOC removal for BPA treatment

As seen in Figure 5 and Figure 6; the use of ZnO catalyst caused the COD and TOC removals to increase by 67% and 97%, respectively, during the first 60 minutes. The prolongation of the reaction time to 120 min didn't change the removal efficiencies. Bechambi et al. 2015, they obtained that the highest TOC abatement is 63% with 4% C-doped ZnO photocatalytic degradation. The near result with literature was obtained in our study. The use of Fe<sub>2</sub>O<sub>3</sub> catalyst negatively affected the COD and TOC removals.

COD and TOC removal results of all ozone based oxidation processes at this works were evaluated collectively in Figure 7 and Figure 8.

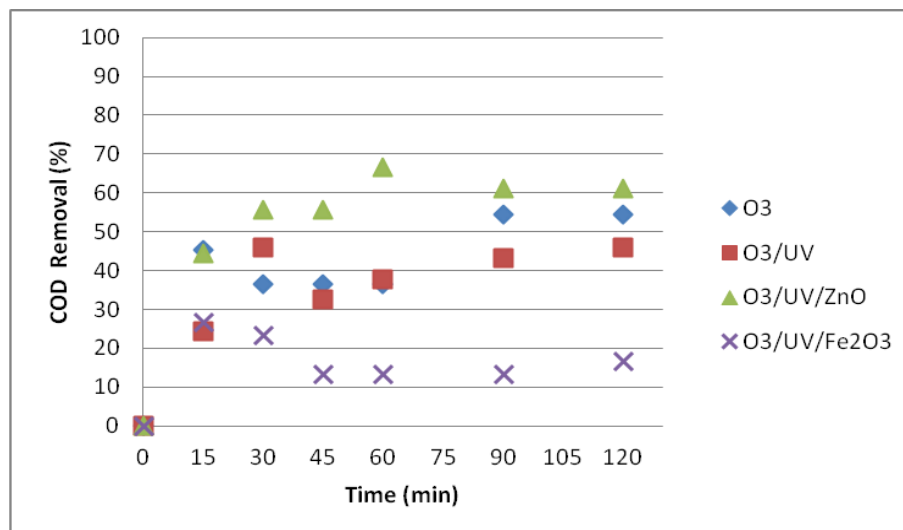


Figure 7. The effects of ozone based oxidation processes on COD removal for BPA treatment

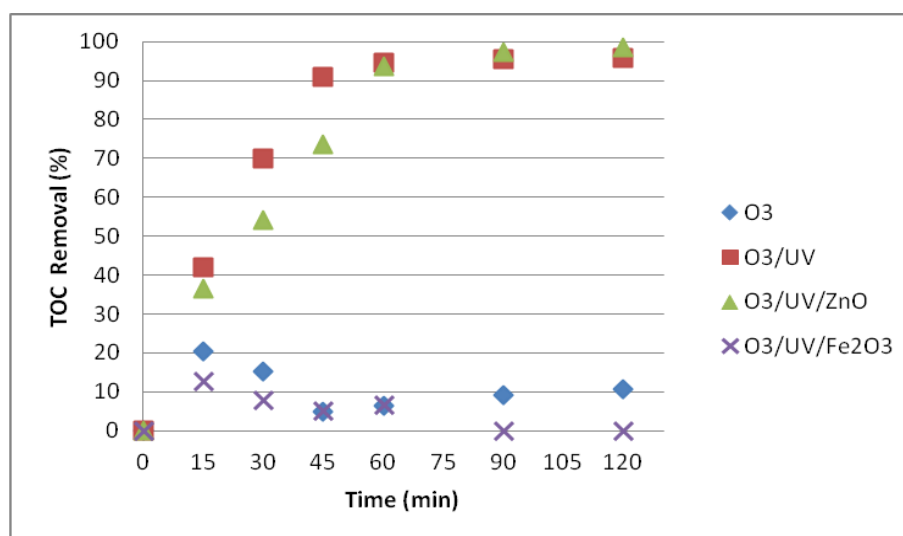


Figure 8. The effects of ozone based oxidation processes on TOC removal for BPA treatment

The highest COD removal efficiencies were obtained at reaction times of 60 min in  $O_3/UV/ZnO > O_3/UV > O_3 > O_3/UV/Fe_2O_3$  processes as 67%, 38%, 37% and 13%, respectively in Figure 7. The highest TOC removal efficiencies in the same reaction time were acquired 94% in  $O_3/UV/ZnO$  and  $O_3/UV$  oxidation processes in Figure 8.

The removal efficiencies of the BPA solution were also evaluated separately using the pseudo-first order kinetic rate model. The equation 1 was used to determine the relationship between the chemical concentration and the kinetic rate constant (k). The results of the calculations were given in Table 3.

$$-\frac{dC}{dt} = kC \quad (1)$$

Tablo 1. The pseudo-first order kinetic constants

Concentration	20 mg/L BPA			
Process	COD		TOC	
	Kinetic constants, k (min <sup>-1</sup> )	R <sup>2</sup>	Kinetic constants, k (min <sup>-1</sup> )	R <sup>2</sup>
O <sub>3</sub>	0,0081	0,253	0,0038	0,1398
O <sub>3</sub> /UV	0,0066	0,1483	0,0337	<b>0,7741</b>
O <sub>3</sub> /UV/ZnO	0,0114	-	0,0368	<b>0,9574</b>
O <sub>3</sub> /UV/Fe <sub>2</sub> O <sub>3</sub>	0,0021	-	0,0004	-

In Table 1, TOC data show that O<sub>3</sub>/UV/ZnO and O<sub>3</sub>/UV oxidation processes results were determined suitable for the pseudo-first order reaction kinetics. But, COD results weren't found suitable with this model. In different studies in the literature, the photocatalytic oxidation of 20 mg/L concentrations of bisphenol A degradation over different composites followed pseudo- first order kinetics model [25]-[28].

#### 4. CONCLUSION

In this study, the treatability of 20 mg/L concentration of Bisphenol A synthetic solution was investigated through the COD and TOC removal efficiency by using chemical and photochemical oxidation methods under the effect of 0.1g ZnO and Fe<sub>2</sub>O<sub>3</sub> catalysts, 5 ppm ozone dose and 16W UV light.

In the O<sub>3</sub> process, the 36% COD and 7% TOC removal efficiencies were obtained at optimum time of 60 minutes. At the optimum time, 38% COD and 95% TOC removals were determined in the O<sub>3</sub>/UV process. As a result of the O<sub>3</sub>/UV/ZnO photocatalytic ozone process were obtained 67% COD and 94% TOC removal efficiencies during the 60 min reaction time. The use of ZnO as a catalyst affects COD and TOC removals positively; but, the use of Fe<sub>2</sub>O<sub>3</sub> catalysts has been found to negatively affect the results of the study.

According to the results of this study; it may be said that the O<sub>3</sub>/UV/ZnO process can be used as an alternative treatment method in the treatment of commonly used micro pollutants like BPA.

#### ACKNOWLEDGMENT

The authors thank Kocaeli University, Scientific Research Project Funding (KOU BAP) for their financial support [Project number/code: 2017/082].

#### REFERENCES

- [1] E.J. Hoekstra, and C. Simoneau, "Release of bisphenol A from polycarbonate: a review", *Critical Reviews in Food Science and Nutrition*, vol. 53, pp. 386-402, 2013.
- [2] World Health Organization & Food and Agriculture Organization of the United Nations, "Toxicological and Health Aspects of Bisphenol A", Ottawa, Canada, 7-47, 2010.
- [3] J.H. Kang, F. Kondo, and Y. Katayama, "Human exposure to bisphenol A", *Toxicology*, vol. 226, pp. 79-89, Sep. 2006.
- [4] T. Geens, D. Aerts, C. Berthot, J.P. Bourguignon, L. Goeyens, P. Lecomte, G. Maghuin-Rogister, A.M. Pironnet, L. Pussemier, M.L. Scippo, J.V. Loco, A. Covaci, "A review of dietary and non-dietary exposure to bisphenol A", *Food and Chemical Toxicology*, vol. 50, pp. 3725-3740, Oct. 2012.



- [5] R.J. Meesters, and H.F. Schroder, "Simultaneous determination of 4-Nonylphenol and Bisphenol A in sewage sludge", *Anal. Chem.*, vol. 74(14), pp. 3566-3574, Jul. 2002.
- [6] L. Luo, J. Li, J. Dai, L. Xia, C.J. Barrow, H. Wang, J. Jegatheesan, and M. Yang, "Bisphenol A removal on TiO<sub>2</sub>-MoS<sub>2</sub>-reduced graphene oxide composite by adsorption and photocatalysis", *Process Safety and Environmental Protection*, vol. 112, pp. 274-279, Nov. 2017.
- [7] T. Olmez-Hanci, I. Arslan-Alaton, and B. Genc, "Bisphenol A treatment by the hot persulfate process: Oxidation products and acute toxicity", *Journal of Hazardous Materials*, vol. 263 (2), pp. 283-290, Dec. 2013.
- [8] B. Liu, M. Qiao, Y. Wang, L. Wang, Y. Gong, T. Guo, and X. Zhao, "Persulfate enhanced photocatalytic degradation of bisphenol A by g-C<sub>3</sub>N<sub>4</sub> nanosheets under visible light irradiation", *Chemosphere*, vol. 189, pp. 115-122, Dec. 2017.
- [9] T. Olmez-Hanci, D. Dursun, E. Aydin, I. Arslan-Alaton, B. Girit, L. Mita, N. Diano, D.G. Mita, and M. Guida, "S<sub>2</sub>O<sub>8</sub><sup>2-</sup>/UV-C and H<sub>2</sub>O<sub>2</sub>/UV-C treatment of Bisphenol A: Assessment of toxicity, estrogenic activity, degradation products and results in real water", *Chemosphere*, vol. 119, pp. 115-123, Jan. 2015.
- [10] R.C. Burgos-Castillo, S. Ignasi, M. Sillanpää, and E. Brillas, "Application of electrochemical advanced oxidation to bisphenol A degradation in water. Effect of sulfate and chloride ions", *Chemosphere*, vol. 194, pp. 812-820, Mar. 2018.
- [11] A. R. Bakr, and M. S. Rahaman, "Removal of bisphenol A by electrochemical carbon-nanotube filter: Influential factors and degradation pathway", *Chemosphere*, vol. 185, pp. 879-887, Oct. 2017.
- [12] W. Chen, C. Zou, Y. Liu, X. Li, "The experimental investigation of bisphenol A degradation by Fenton process with different types of cyclodextrins", *Journal of Industrial and Engineering Chemistry*, vol. 56, pp. 428-434, Dec. 2017.
- [13] M.P. Pachamuthu, S. Karthikeyan, R. Maheswari, A.F. Lee, and A. Ramanathan, "Fenton-like degradation of Bisphenol A catalyzed by mesoporous Cu/TUD-1", *Applied Surface Science*, vol. 393, pp. 67-73, Jan. 2017.
- [14] L. Zhang, D. Xu, C. Hu, and Y. Shi, "Framework Cu-doped AlPO<sub>4</sub> as an effective Fenton-like catalyst for bisphenol A degradation", *Applied Catalysis B: Environmental*, vol. 207, pp. 9-16, Jun. 2017.
- [15] X. Tan, Y. Wan, Y. Huang, C. He, Z. Zhang, Z. He, L. Hu, J. Zeng, and D. Shu, "Three-dimensional MnO<sub>2</sub> porous hollow microspheres for enhanced activity as ozonation catalysts in degradation of bisphenol A", *Journal of Hazardous Materials*, vol. 321, pp. 162-172, Jan. 2017.
- [16] G. Liao, D. Zhu, J. Zheng, J. Yin, B. Lan, and L. Li, "Efficient mineralization of Bisphenol A by photocatalytic ozonation with TiO<sub>2</sub>-graphene hybrid", *Journal of the Taiwan Institute of Chemical Engineers*, vol. 67, pp. 300-305, Oct. 2016.
- [17] J. Lee, H. Park, and J. Yoon, "Ozonation characteristics of bisphenol A in water", *Environ. Technol.*, vol. 24, pp. 241-248, 2003.
- [18] G. V. Buxton, C. L. Greenstock, W. P. Helman, and A. B. Ross, "Critical review of rate constants for reactions of hydrated electrons, hydrogen atoms, hydroxyl radicals (·OH/·O) in aqueous solution", *J. Phys. Chem. Ref. Data*, vol. 17, pp. 513-886, Oct. 2009.
- [19] O. Legrini, E. Olivers, and A. M. Braun, "Photochemical processes for water treatment", *Chem. Res.*, vol. 93(2), pp. 671-698, Mar. 1993.
- [20] S.J. Masten, and S.H.R. Davies, "The use of ozonation to degrade organic contaminants in wastewaters", *Env. Sci. Technol.*, vol. 28(4), pp. 180A-185A, Apr. 1994.
- [21] S. Esplugas, P. L. Yue, M. I. Pervez, "Degradation of 4-chlorophenol by photolytic oxidation", *Water Research*, vol. 28, pp. 1323-1328, Jun. 1994.
- [22] A. Arslan, E. Topkaya, D. Bingol, and S. Veli, "Removal of anionic surfactant sodium dodecyl sulfate from aqueous solutions by O<sub>3</sub>/UV/H<sub>2</sub>O<sub>2</sub> advanced oxidation process: Process optimization with response surface methodology approach", *Sustainable Environment Research*, vol. 28, pp. 65-71, Mar. 2018.
- [23] APHA, *Standard Methods for Examination of Water and Wastewater*, 21st ed., Washington, DC: American Public Health Association, 2005.
- [24] O. Bechambi, S. Sayadi, and W. Najjar, "Photocatalytic degradation of bisphenol A in the presence of C-doped ZnO: Effect of operational parameters and photodegradation mechanism", *Journal of Industrial and Engineering Chemistry*, vol. 32, pp. 201-210, Dec. 2015.
- [25] X. Xiao, R. Hao, M. Z. Liang, X. Zuo, J. Nan, L. Li, and W. Zhang, "One-pot solvothermal synthesis of three-dimensional (3D) BiOI/BiOCl composites with enhanced visible-light photocatalytic activities for the degradation of bisphenol-A", *Journal of Hazardous Materials*, vol. 233-234, pp. 122-130, Sep. 2012.
- [26] C. Chang, Y. Fu, M. Hu, C. Wang, G. Shan, L. Zhu, "Photodegradation of bisphenol A by highly stable palladium-doped mesoporous graphite carbon nitride (Pd/mpg-C<sub>3</sub>N<sub>4</sub>) under simulated solar light irradiation", *Applied Catalysis B: Environmental*, vol. 142-143, pp. 553-560, Oct.-Nov. 2013.

- [27] F. Chen, W. An, L. Liu, Y. Liang, W. Cui, “Highly efficient removal of bisphenol A by a three-dimensional graphene hydrogel-AgBr@rGO exhibiting adsorption/photocatalysis synergy”, *Applied Catalysis B: Environmental*, vol. 217, pp. 65-80, Nov. 2017.
- [28] C. Yu, Z. Wu, R. Liu, D.D. Dionysiou, K. Yang, C. Wang, and H. Liu, “Novel fluorinated Bi<sub>2</sub>MoO<sub>6</sub> nanocrystals for efficient photocatalytic removal of water organic pollutants under different light source illumination”, *Applied Catalysis B: Environmental*, vol. 209, pp. 1-11, Jul. 2017.

#### **BIOGRAPHY**

Eylem TOPKAYA; completed her undergraduate degree in 2004-2009 at Uludag University, Department of Environmental Engineering. She completed her master's degree in 2011-2014 at Gebze High Institute of Technology (GYTE), Institute of Natural and Applied Sciences, Department of Environmental Engineering. She has started her PhD education in 2014 at Kocaeli University, Institute of Natural and Applied Sciences, Department of Environmental Engineering and she is still in progress.

## Removal of Diclofenac from Aqueous Solution by Microwave Enhanced Persulfate Oxidation: Optimization Using Taguchi Design

Nevim Genc<sup>1</sup>, Elif Durna<sup>2</sup>

### Abstract

Diclofenac (DCF), an important non-steroidal anti-inflammatory drug, is widely used in human health care and veterinary industry. The main difficulty for the removal of DC from water is their high polarity and solubility in water. In this work, the performance of diclofenac (DCF), an anti-inflammatory analgesic, oxidation with activated persulfate (PS) by microwave was investigated. A optimization method was used Taguchi's robust design approach. Taguchi's L9 orthogonal array was planned for experimental design. The parameters for the L9 orthogonal array were determined as power (W), contact time (min), persulfate anion concentration (g/L) and pH. Removal process is optimized with the response characteristics of the DCF removal efficiency. The signal noise (SN) ratio was calculated for the response variable and the optimal combination level of the factors was obtained using Taguchi's orthogonal design. Analysis of variance (ANOVA) was used to describe the significance level of factors on the multiple performance characteristics considered. Ph has been found as the most effective factor and its contribution is 84.51% on multiple quality characteristics. The optimum conditions for DCF removal were determined as 0.5 g/L of PS, 1 min. of time, microwave power at 126 watt and pH at 3. As a result of the verification experiment, 94.74 % removal efficiency was obtained which was higher than the L9 Taguchi set.

**Keywords:** Microwave-persulfate, Diclofenac, multi-response S/N ratio, optimization, Taguchi methods, ANOVA

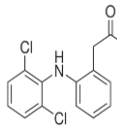
### 1. INTRODUCTION

A significant non-steroidal anti-inflammatory drug is diclofenac (DCF), it is widely used in human health and veterinary industries. In addition, the DCF has recently been included in the list of new priority hazardous substances by the European Commission [1]. The main difficulty in removing DCF from water is its high polarity and high solubility. Due to the polar variability, the DCF distribution in the environment is primarily due to the accumulation of aquatic environment and the accumulation of the food chain [2]. Under ambient pH conditions, DCF is present in an anionic form because the pKa value is in the range of 4.0-4.2. This limits the uptake of materials on earth and makes it very mobile in the natural environment [3]. It was reported that due to its low biodegradability and sorption character onto the activated sludge, typically only 21-40 percent of DCF is eliminated by traditional treatment plants [4],[5]. On the basis of the acid dissociation constant (pKa = 4.2) of DCF, two major species are present in the aquatic environment, the neutral form (DCF<sub>0</sub>) and the anionic form (DCF<sup>-</sup>). Where (DCF<sub>0</sub>) is the major form at pH < 4.2, whereas (DCF<sup>-</sup>) is predominant when pH > 6.0 [6]. Table 1 shows the properties of sodium diclofenac [7].

<sup>1</sup>Corresponding author: Kocaeli University, Department of Environmental Engineering, 41000, İzmit/Kocaeli, Turkey. ngenc@kocaeli.edu.tr

<sup>2</sup>Kocaeli University, Department of Environmental Engineering, 41000, İzmit/Kocaeli, Turkey. elif.durna@kocaeli.edu.tr

Table 12. Properties of sodium diclofenac

Diclofenac Sodium	pKa	LogKow	Molecular Weight (g/mol)	Excretion	Elimination half-life	Acute toxicity EC50	Detected Concentrations (µg/L)
	4.2	4.51	296.147	Biliary excretion: 65% of oral dosage excreted in urine	2 h	1–10 mg/L	surface water:1.2 drinking water:<10 underground water:0.59

Currently, several treatment technologies such as ozonation, photo-Fenton [8], sonolysis [9],[10], chlorination [11] and photocatalysis [12],[13] have been applied for the removal of DCF from contaminated water. However, these treatment processes still have several challenges such as generation of toxic by products, high operation cost and low treatment efficiency.

Advanced oxidation processes have considerable attention in the removal of recalcitrant organic pollutants such as pharmaceutical. Sulfate radical based advanced oxidation processes utilize highly-reactive sulfate radical ( $\text{SO}_4^{\cdot-}$ ). Generally,  $\text{SO}_4^{\cdot-}$  is generated by activation peroxydisulfate (PDS) or persulfate (PS). PS and PDS can be activated by a various activation methods, such as heat, UV, electron, alkaline, ultrasound, transition metal ions and carbo-catalysis [14].

Microwave technology has been widely used recently in the field of environmental engineering. Microwave irradiation can be considered an alternative to conventional heating methods because it triggers rapid heating and increases chemical reaction [15]. Microwave (MW) is an energy that consists of an electric field and a magnetic field. It is a form of electromagnetic waves with the wavelengths of 1 mm–1 m (frequency 300 MHz–300 GHz). MW energy can be combined with oxidants to increase the degradation efficiency of many pollutants and reduce the reaction time, as it is insufficient to disrupt the chemical bonds of many organic compounds by itself [16]. In the literature, microwave heating has been reported to give faster energy to accelerate persulfate activation, because microwave heating causes faster analyte degradation than conventional heating required for persulfate activation [14]. Nowadays MW coupled with advanced oxidation process, adsorbents and oxidants such as hydrogen peroxide and persulfate to increase the contaminant decomposition. Persulfate anions can be thermally activated to form a strong, nonspecific oxidant.

Radical-based photooxidation is one of the most efficient advanced oxidation processes used in removing contaminants. Recently, the AOPs induced by the sulfate radical have been of increasing interest. Due to its non-selective oxidation pattern and a significantly higher reduction potential of 2.6 V, it is lower than  $\text{OH}^{\cdot}$  (2.9 V) [17]. The sulfate radical is usually produced by activation of the persulfate salts using ultraviolet (UV) light, catalysts, high pH or heat [18].

In this study, Taguchi optimization was used for removal DCF from aqueous solution by microwave activated persulfate oxidation. The robust parametric design approach was used for optimization of DCF removal conditions.

### 1.1. Taguchi Methodology

Experimental design methods are used extensively to measure parameters that affect the response of an experimental study and to design experiments. Among the various experimental design methods used in the literature, the Taguchi method is seen as a widely used method to obtain results with fewer experiments and less cost compared to other methods.

Taguchi method suggests the use of the loss function to measure the performance characteristics deviating from the desired value. The value of the loss function is further converted into signal-to-noise (S/N) ratio. S/N ratio represents the desired part/wastage part. The optimum conditions should be calculated from the S/N ratio of the results obtained from experiments designed by orthogonal array technique [19].

In this study, the objective is to maximize DCF removal from the aqueous solution. The experimental values of quality characteristics are used to calculate the quality loss values for quality characteristic in all experimental

runs. Quality loss function can be of various types. In this study the higher Diclofenac removal are desired, therefore the quality loss function in  $i^{th}$  trial ( $l_i$ ) for higher-the-better case used which is given as follows [20].

$$l_i = \frac{1}{n} \sum_{i=1}^n \frac{1}{y_i^2} \quad (1)$$

where  $y_i$  is the observed data at the  $i^{th}$  experiment for a certain combination of control factor levels, and  $n$  is the number of experiment.

S/N ratio is used to indicate the quality index at each design point. S/N ratio corresponding to  $j$ th trial condition ( $\eta_j$ ) can be calculated from the total loss function [20,21].

$$\eta_j = -10 \log_{10}(L_j) \quad (2)$$

The mean S/N ratio for each parameter level is calculated. The aim is always to maximize the S/N. A parameter level corresponding to the maximum average S/N ratio is evaluated as the optimum level for that parameter. To predict and verify the performance characteristic with the selected optimum parameters, the predicted value of S/N ( $\eta_{opt}$ ) at optimum parameter levels is calculated by using Equation 3 :

$$\eta_{opt} = \bar{\eta} + \sum_{i=1}^k (\eta_{mi} - \bar{\eta}) \quad (3)$$

where  $\bar{\eta}$  is the mean S/N ratio of all experimental runs,  $k$  is the number of significant control factors, and  $\eta_{mi}$  is the average S/N for  $i$ th control factor corresponding to optimum parameter level. Confirmation experiment are performed at the optimum parameter levels recommended to verify the predicted response [20].

## 2. MATERIALS AND METHODS

The MW irradiation to activate the persulfate was provided by a domestic MW oven with microwave power of up to 700W at under atmospheric pressure. The tests were carried out in 150 ml glass beakers. The initial concentration of DCF was 50 mg/L. The mixture solution was placed in MW for a specific time. After each experimental run, the concentrations of DCF in solution were analyzed. Analysis: Treated samples after the MW irradiation were cooled to room temperature, added up to 50 mL with deionized water and analyzed. The concentration of DCF in the residual solutions was analyzed with a UV spectrometer (Hach-Lange DR 5000) at maximum wavelength.

Preliminary experiments have been carried out to determine the levels of Taguchi experimental parameters. These experiments were carried out at different time intervals with 0.5 g / L Persulfate concentration and 700 watt power of microwave irradiation. Taguchi experimental design method was used for optimization for diclofenac removal L9 orthogonal array, 3-level 4-factor design were chosen, the parameter levels are determined as the lowest (level 1), medium (level 2) and highest (level 3).

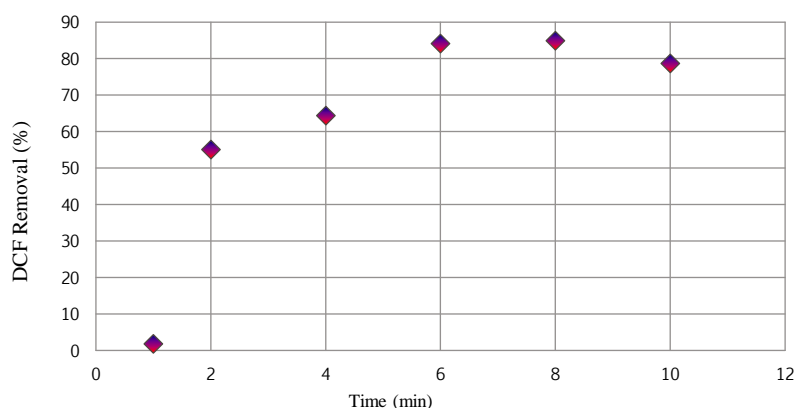


Figure 12. Preliminary experiments for determination of parameters

Table 2. Parameters chosen at three levels for Taguchi orthogonal experimental design

Factors	Symbol	Level 1	Level 2	Level 3
Persulfate concentration (g/L)	A	0.1	0.5	1
MW irradiation time (min)	B	1	2	4
Microwave Power (watt)	C	126	406	700
pH	D	3	6	9

### 3. RESULTS AND DISCUSSION

#### 3.1. Analysis of the Experimental Data

Process factors, their levels and obtained response of conducted experiments corresponding to L9 orthogonal array design were presented in Table 2. Results shows a wide range which is one of the goals of Taguchi methodology for determining the effects of parameters more correctly. The highest DCF removal was in experiment 5th and the lowest was at 3th experiment.

Table 3. Experimental design corresponding to L9 orthogonal array

Run	PS (g/L)	Time (min)	Power (W)	pH	Diclofenac Removal (%)
1	0.1	1	126	3	89
2	0.1	2	406	6	24.79
3	0.1	4	700	9	3.01
4	0.5	1	406	9	5.02
5	0.5	2	700	3	86.99
6	0.5	4	126	6	55.09
7	1	1	700	6	72.54
8	1	2	126	9	6.01
9	1	4	406	3	23.79

To determine the optimum level of combination, S/N ratio was used. The optimal levels of the control factors are the level with the greatest S/N ratio. The optimum levels are; contact time at level 3, power at level 3, pH at level 3 and citric acid addition at level 1 as shown in Table 3.

Table 4. Effect of factor level on S/N ratios

Factors	Symbol	Level 1	Level 2	Level 3	Max-Min
PS (g/L)	A	15.483	<b>19.20830</b>	16.7723	3.72512
Time (min)	B	<b>20.072</b>	17.41746	13.9735	6.09921
Power (W)	C	<b>19.797</b>	13.14249	18.5240	6.65471
pH	D	<b>25.103</b>	23.30617	3.05429	22.0490



The control factors effects on quality characteristic are shown in Figure 3. Overall mean value was calculated as 9.46 from all experiments.

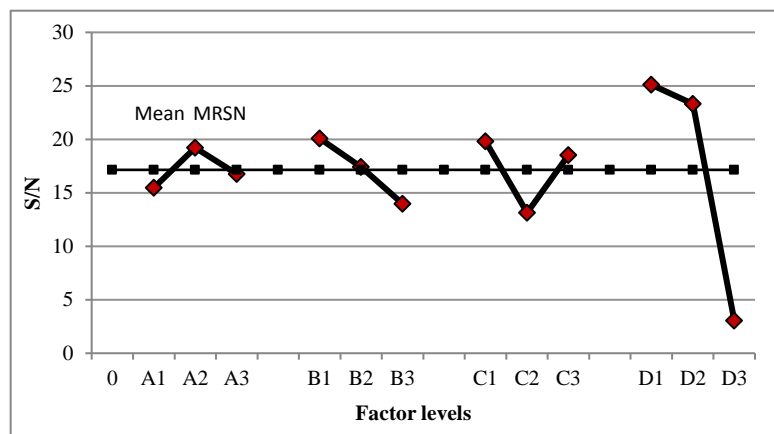


Figure 13. Effect of factor levels on S/N ratio

The optimum conditions for DCF removal were determined as 0.5 g/L of PS, 1 min. of time, microwave power at 126 watt and pH at 3.

### 3.2. Analysis of Variance

In order to see statistically significant control factors, the analysis of variance (ANOVA) is also performed. Table 4 shows the results of ANOVA obtained from S/N ratio. For L9 orthogonal array the total degree of freedom (DOF) is determined as 8. Besides the DOF for each parameter determined as 2 (3-1). From this, the DOF for the error calculated as 2.

Table 5. ANOVA Analysis

Factor	Degrees freedom	Sum of Square	Mean square	F value	Pure sum (%P)
PS (g/L)	2	21.4724	10.7362	1.00058	—
Time (Min)	2	56.1114	28.0557	2.6147	4.3139
Power (W)	2	74.8675	37.4337	3.4887	6.0968
pH	2	899.5276	449.7638	41.9164	84.4881
Error (SS <sub>E</sub> )	2	21.472	10736	1000.559	5.101
Total (SS <sub>T</sub> )	8	1051.979			100

(\*)The parameter which the percentage contribution falls less than 10% is considered statistically insignificant [22]. In this study, Persulfate concentration is considered insignificant and it is included in the error term.

F test is performed to define the meaningful effect of each factor on the response variable. The F value is a measure of the variance of the data to the mean. The large F value of any parameter indicates the importance on the response variable [23]. According to the results, the F ratio for microwave irradiation time and power are smaller than the pH F ratio.

This means that the variance of this factors is statistically insignificant. In ANOVA, the F ratio and P(%) values are helpful for the qualitative and quantitative evaluation of factorial effects, respectively [24]. As a result of ANOVA, MW irradiation time has been found as the most effective factor and its contribution is 35.4% on quality characteristics. The pH was the second most effective parameter by following the MW time with 34.5%.

### 4. CONCLUSIONS

The results obtained from the study are as follows:

- It has been found that microwave-activated PS oxidation is applicable for DCF removal but the effect of this combination is more dependent on pH.
- Due to the experimental design of the Taguchi, only a small number of experiments have been carried out and the four parameters affecting the result have been investigated.
- The optimum conditions for DCF removal were determined as 0.5 g/L of PS, 1 min. of time, microwave power at 126 watt and pH at 3.
- As a result of the verification experiment, 94.8 % removal efficiency was obtained which was higher than the L9 Taguchi set.
- The applicability of this method is generally financially dependent and will be considered in subsequent investigations.

### REFERENCES

- [1]. European Commission. (2013). Directive 2013/39/EU of the European Parliament and of the Council of 12 August 2013 amending Directives 2000/60/EC and 2008/105/EC as regards priority substances in the field of water policy. O J. L, 226, 1-17.
- [2]. V. Acuña, A. Ginebreda, J.R. Mora, M. Petrovic, S. Sabater, J. Sumpter, D. Barceló, "Balancing the health benefits and environmental risks of pharmaceuticals: Diclofenac as an example", *Environment International*, vol. 85, pp. 327-333, 2015.
- [3]. K. Sun, Y. Shi, X. Wang, J. Rasmussen, Z. Li, J. Zhu, "Organokaolin for the uptake of pharmaceuticals diclofenac and chloramphenicol from water", *Chemical Engineering Journal*, vol.330, pp.1128-1136, 2017
- [4]. J. Radjenović, M. Petrović, D. Barceló, "Fate and distribution of pharmaceuticals in wastewater and sewage sludge of the conventional activated sludge (CAS) and advanced membrane bioreactor (MBR) treatment" *Water Research*, vol.43(3), pp.831-841, 2009.
- [5]. Y. Zhang, S.U. Geißen, C. Gal, "Carbamazepine and diclofenac: removal in wastewater treatment plants and occurrence in water bodies" *Chemosphere*, vol.73, pp.151-1161, 2008.
- [6]. H.Y. Cheng, D. Song, H.J. Liu, J.H. Qu, "Permanganate oxidation of diclofenac: The pH-dependent reaction kinetics and a ring-opening mechanism", *Chemosphere*, vol.136, pp.297-304, 2015.
- [7]. N. Vieno, N., M. Sillanpää, "Fate of diclofenac in a municipal wastewater treatment plant: a review", *Environ. Int.*, vol.69, pp.2839, 2014.
- [8]. M.M. Sein, M. Zedda, J. Tuerk, T.C. Schmidt, A. Golloch, C. Sonntag, "Oxidation of diclofenac with ozone in aqueous solution" *Environ. Sci. Technol.*, vol. 42 (17), PP.6656-6662, 2008
- [9]. G. Tezcanli, Guyer, N.H. Ince, "Degradation of diclofenac in water by homogeneous and heterogeneous sonolysis" *Ultrasonics Sonochemistry*, vol.18(1), pp.114-119, 2011.
- [10]. J. Hartmann, P. Bartels, U. Mau, M. Witter, W. Tümping, J. Hofmann, E. Nietzschmann, "Degradation of the drug diclofenac in water by sonolysis in presence of catalysts" *Chemosphere*, vol.70(3), pp.453-461, 2008.
- [11]. M. Soufan, M. Deborde, B. Legube, "Aqueous chlorination of diclofenac: Kinetic study and transformation products identification" *Water Research*, vol.46(10), pp.3377-3386, 2012.
- [12]. L. Rizzo, S. Meric, D. Kassinos, M. Guida, F. Russo, V. Belgiorna, "Degradation of diclofenac by TiO<sub>2</sub> photocatalysis: UV absorbance kinetics and process evaluation through a set of toxicity bioassays" *Water Research*, 43(4), 979-88, 2008.
- [13]. D. Vogna, R. Marotta, A. Napolitano, R. Andreozzi, M. d'Ischia, "Advanced oxidation of the pharmaceutical drug diclofenac with UV/H<sub>2</sub>O<sub>2</sub> and ozone" *Water Research*, vol. 38(2), pp.414-422, 2004.
- [14]. L.W. Matzek, K.E., Carter, "Activated persulfate for organic chemical degradation: A review", *Chemosphere*, vol.151, pp. 178-188, 2016.
- [15]. Y. Kim J. Ahn, "Microwave-assisted decolorization and decomposition of methylene blue with persulfate", *International Biodeterioration & Biodegradation*, vol. 95, pp. 208-211, 2014.
- [16]. Y. Chou S. Lo J. Kuo C. Yeh, "Microwave-enhanced persulfate oxidation to treat mature landfill leachate", *Journal of Hazardous Materials*, vol. 284, pp. 83-91, 2015
- [17]. Q. Yang, H. Choi, Y. Chen, D. Dionysiou, "Heterogeneous activation of peroxymonosulfate by supported cobalt catalysts for the degradation of 2,4-dichlorophenol in water: the effect of support, cobalt precursor, and uv radiation", *Applied Catalysis B: Environmental*, vol. 77 (2-3), pp.300-307, 2008.
- [18]. D. Zhou, H. Zhang, L. Chen, "sulfur-replaced fenton systems: can sulfate radical substitute hydroxyl radical for advanced oxidation technologies", *J. Chem Technol Biotechnol.*, vol.90, pp.775-779, 2015.
- [19]. P.J. Ross, *Taguchi Techniques for Quality Engineering*, McGraw Hill Professional, 2<sup>nd</sup> edn. 1996.
- [20]. N. Aslan, I. Unal, "Multi-response optimization of oil agglomeration with multiple performance characteristics", *Fuel Processing Technology*, vol.92, pp. 1157, 2011.

- [21]. J. Antony, "Simultaneous optimisation of multiple quality characteristics in manufacturing processes using taguchi's qulaity loss function", *International Journal Advance Manufacturing Technology*, vol.17, pp. 134, 2001.
- [22]. R. Ramakrishnan, L. Karunamoorthy, "Multi response optimization of wire EDM operations using robust design of experiments" *International Journal Advance Manufacturing Technology*, vol. 29, pp.105, 2006.
- [23]. Sumit H. Dhawane A, Pratim B, Tarkeshwar K, Halder G., "Parametric optimization of biodiesel synthesis from rubber seed oil using iron doped carbon catalyst by Taguchi approach", *Renewable Energy.*, vol. 105, pp.616-624, 2017.
- [24]. Z.B. Gonder, Y. Kaya, I. Vergili, et al. "Optimization of filtration conditions for CIP wastewater treatment by nanofiltration process using Taguchi Approach", *Seperation and Purification Technology*, vol.70, pp. 265, 2010.

### BIOGRAPHY

Presenter Elif DURNA got her bachelors' degree in the Environmental Engineering Department at Kocaeli University, Kocaeli/Turkey in 2014, his master degree in the Environmental Engineering Department at Kocaeli University, Kocaeli/Turkey in 2018. She is currently a PhD candidate in the Environmental Engineering Department at Kocaeli University. She is still an academic member of the Environmental Engineering Department at Kocaeli University . Her major areas of interests are: Advanced Oxidation Techniques, Experimental Design Techniques, Membrane Treatment Methods.

## Microwave Assisted Sludge Disintegration: Optimization of Operating Parameters

Elif Durna<sup>1</sup>, Nevim Genc<sup>2</sup>

### Abstract

The high volume of sludge generated in wastewater treatment plants poses a problem for sludge processing and disposal. Sludge disposal is the reason for the 50% additional cost of total finance (Bougrier et al., 2005). Microwave (MW) disintegration has become an interesting subject in recent years as an innovative method applied on waste sludge. Using microwave energy can result in substantial waste volume reduction, process time reduction and energy savings. In this study, the efficiency of microwave disintegration on the sludge from a recycle line of a treatment plant was investigated. COD (chemical oxygen demand) was determined as the response parameter and the independent variables affecting the response were selected as microwave irradiation time, microwave power (watt), pH and organic acid addition (citric acid). For each selected parameter, 3 levels (low, medium, high) were determined and L9 orthogonal Taguchi experiment design was created with MINITAB 17. The optimum levels of control factors for maximum cell disruption were found as, microwave irradiation time at 5 min, microwave power at 700 watt, pH at 9 and citric acid addition at 0.5 ml. According to ANOVA analysis most effective control factors were found as microwave irradiation time and pH with contributions of 35.43% and 34.43% respectively. A confirmation experiment was performed to verify the effectiveness of the optimal combination. As a result of the optimization experiment performed, the higher COD value was achieved than the results in the L9 Taguchi experiment set, cell disruption was higher. It was concluded that the microwave disintegration could be an efficient option to break down the intracellular organic material and make the sludge more stable.

**Keywords:** Sludge Disintegration, Microwave, Taguchi Experimental Method

### 1. INTRODUCTION

Sewage sludge emerges as a by-product during or after the operation of water and wastewater treatment plants [1]. It is expected that the amount of global sludge will increase in the future due to increasingly stringent criteria for wastewater treatment and increased amount of wastewater. Typically, 0.2 to 0.3 kg of sludge is produced per m<sup>3</sup> of wastewater in a treatment plant, resulting in additional high costs for wastewater treatment. Half of the total cost is spent to dispose and treatment of the sludges [2],[3]. Treatment sludges resulting from the treatment of industrial or domestic wastewater are assessed in the hazardous waste category since they contain high levels of organic and inorganic contaminants. For this reason, the proper disposal of waste sludge is very important both in terms of environment and human health.

Anaerobic digestion is a well known technique for purification of excess waste sludge, stabilization of organic matter, reduction of biomass, and biogas production. However hydrolysis, which is the first step in anaerobic digestion, limits the rate and extent of the process. This restriction can be overcome by applying various pretreatment methods. Sludge disintegration has been developed as a pretreatment to eliminate the hydrolysis step, which is the rate limiting step prior to anaerobic digestion, and to increase the degree of stabilization of the sludge [4].

The disintegration can be performed by applying various physical, chemical or biological forces. Today, the most common disintegration methods can be listed as thermal, enzymatic digestion, use of detergents or organic

<sup>2</sup> Corresponding author: Kocaeli University, Department of Environmental Engineering, 41000, İzmit/Kocaeli, Turkey. ngenc@kocaeli.edu.tr

<sup>1</sup> Kocaeli University, Department of Environmental Engineering, 41000, İzmit/Kocaeli, Turkey. elif.durna@kocaeli.edu.tr

solvents, shearing, homogenization, sonication, grinding, differential centrifugation, rinsing with glass balls, osmotic shock and freezing / melting. Some of the innovative disintegration methods applied on waste sludge in recent years are: application of thermal energy, application of enzymes, ozonation, acidification / alkalization, high pressure application, ultrasonic application and microwave radiation application [5]. In recent years, conventional thermal methods for heating have been increasingly replaced by microwaves, which have much lower thermal losses in energy transfer and thus significantly reduce reaction times and energy requirements.

The mechanism of microwave irradiation includes a thermal effect and an athermal effect. The term 'athermal' for the microwave relates to an effect which is not usually associated with high temperature. "Thermal effect" refers to the process of generating heat as a result of the absorption of microwave energy by water or organic complexes while the microwave energy is transformed into heat derived from the internal resistance of rotation [6].

Microwave pretreatment also has the benefit of athermal effectiveness. Several studies have reported the presence of MW athermal effect on healing of activated sludge dissolution and biogas production [7],[8].

When microwave is used in sludge disintegration, it can significantly change the sludge flocks structure and character, as well as the numerous bacteria, protozoa, yeast, fungus and parasites that are seen in the sludge. Microwaves were additionally the result of decompose complex chemical compounds and convert them into simple compounds that could be easily degrade by microorganisms [9].

The microwaves can be directly heated internally, so that the heat loss can be minimized by convection and conduction. During conventional heating, the materials are heated from the outside, which means that heat can not be spread while the energy is transmitted.

One of the most obvious advantages of the microwave over traditional heating is its specific and non-contact heating, which eliminates the need for direct contact between the heating source and the heated material. MW heating can reach the desired temperature faster than conventional heating techniques while it consumes less energy. In addition to increasing sludge disintegration and biogas production efficiency, microwave system also provides destruction of fecal coliforms and many bacteria. Hong et.al. in their study they concluded that microwave irradiation 57 °C and 68 °C caused a faster reduction of bacterial activity compared to conventional heating [10]. Also they found that microwaves break down DNA in fecal coliform cells at lower temperatures than conventional heating. Based on these results, it can be said that microwave pre-treatment not only increases sludge stability and dewaterability, but also destroys harmful bacteria and pathogens unlike conventional heating. Due to all these reasons pre-treatment of the activated sludge with microwaves seems to be feasible and economical in terms of destroying pathogens and forming environmentally safe sludge.

There are some studies on microwave disintegration of sludge. However, these studies, were not described the optimization by a statistical design model. In this study, the effect of microwave disintegration on the waste activated sludge was investigated through the COD increase in supernatant and the optimization of the operating parameters was carried out by Taguchi methodology.

## 2. MATERIALS AND METHODS

### 2.1. Materials

The MW irradiation was provided by a domestic MW oven (CLATRONIC (Model MWG 786) with microwave power up to 700W at a frequency 2450 MHz under atmospheric pressure. The waste activated sludge was taken from the recycling line of a municipal waste water treatment plant which has initial COD value of 160 mg/L. Sodium hydroxide (NaOH), hydrochloric (HCL) are purchased from Merck company used for the pH adjustments in experiments. and citric acid ( $C_6H_8O_7$ ) was also purchased from Merck company used as an deflocculating agent.

The tests were carried out in 150 ml glass beakers. The mixture solution was placed in MW for a specific time. 0.1 N Citric acid was prepared for addition. Treated sludge samples after the MW irradiation were cooled to room temperature, added up to 100 mL with deionized water. Cooled samples were centrifuged at 3000 rpm for 20 minutes. The liquid (supernatant) on the centrifuged samples was taken into the sample containers with the aid of a pipette. COD analyzes have been carried out in accordance with the APHA standart methods [11].

## 2.2. Taguchi Methodolgy

In experimental design studies, factorial design, response surface method and Taguchi method are widely used today. Among these methods, Taguchi method is seen as a widely used method in the literature in terms of achieving a result with less number of experiments and less cost than other methods.

Taguchi method suggests the use of the loss function to measure the performance characteristics deviating from the desired value. The value of the loss function is further converted into signal-to-noise (S/N) ratio. S/N ratio represents the desired part/wastage part. The optimum conditions should be calculated from the S/N ratio of the results obtained from experiments designed by orthogonal array technique [12].

In this study, the objective is to maximize COD increase in the waste activated sludge. The experimental values of quality characteristics are used to calculate the quality loss values for quality characteristic in all experimental runs. Quality loss function can be of various types. In the present study the higher values of COD are desired, therefore the quality loss function in  $i^{th}$  trial ( $l_i$ ) for higher-the-better case used which is given as follows [13].

$$l_i = \frac{1}{n} \sum_{i=1}^n \frac{1}{y_i^2} \quad (1)$$

where  $y_i$  is the observed data at the  $i^{th}$  experiment for a certain combination of control factor levels, and  $n$  is the number of experiment.

S/N ratio is used to indicate the quality index at each design point. S/N ratio corresponding to  $j$ th trial condition ( $\eta_j$ ) can be calculated from the total loss function [13], [14].

$$\eta_j = -10 \log_{10}(L_j) \quad (2)$$

The mean S/N ratio for each parameter level is calculated. The aim is always to maximize the S/N. A parameter level corresponding to the maximum average S/N ratio is evaluated as the optimum level for that parameter. To predict and verify the performance characteristic with the selected optimum parameters, the predicted value of S/N ( $\eta_{opt}$ ) at optimum parameter levels is calculated by using Equation 3 :

$$\eta_{opt} = \bar{\eta} + \sum_{i=1}^k (\eta_{mi} - \bar{\eta}) \quad (3)$$

where  $\bar{\eta}$  is the mean S/N ratio of all experimental runs,  $k$  is the number of significant control factors, and  $\eta_{mi}$  is the average S/N for  $i$ th control factor corresponding to optimum parameter level. Confirmation experiments are conducted at recommended optimum parameter levels to confirm the predicted response [13].

In this study Taguchi experimental design method was used for optimization of microwave disintegration for waste activated sludge. L9 orthogonal array, 3-level 4-factor were chosen. Factors were microwave contact time (minute), microwave irradiation power (watt), pH and 0.1 N citric acid addition. Addition of an organic acid (citric acid) was also added as a parameter to increase the degradation by removal of extracellular polymeric substance (EPS) from the sludge. Since it is known from literature that citric acid addition increase the removal of extracellular polymeric substance (EPS) from waste activated sludge [15].

The factors and their levels are presented in Table 1. Experiments were carried out to determine the relationship between the response and controllable factors to enhance the COD increase in the supernatant.

Table 13. Parameters chosen at three levels for Taguchi orthogonal experimental design

Factors	Symbol	Level 1	Level 2	Level 3
Contact time (min)	A	1	3	5
Power (W)	B	126	406	700
pH	C	2	Original(6)	9
Citric acid addition (mL)	D	0.5	1	1.5



### 3. RESULTS AND DISCUSSION

#### 3.1. Analysis of the Experimental Data

Process factors, their levels and obtained response of conducted experiments corresponding to L9 orthogonal array design were presented in Table 2. Results of experiments shows a wide range which is one of the goals of Taguchi methodology for determining the effects of parameters more correctly. The highest COD solubility was in experiment 7 and the lowest COD solubility was in experiment 2.

Table 2. Experimental design corresponding to L9 orthogonal array

Run	Time (min)	Power (Watt)	pH	Citric Acid (mL)	COD (mg/L)
1	1	126	2	0.5	1600
2	1	406	Original (6)	1.0	800
3	1	700	9	1.5	3200
4	3	126	Original (6)	1.5	2080
5	3	406	9	0.5	3520
6	3	700	2	1.0	1920
7	5	126	9	1.0	4480
8	5	406	2	1.5	2560
9	5	700	Original (6)	0.5	3680

To determine the optimum level of combination, S/N ratio was used. The optimal levels of the control factors are the level with the greatest S/N ratio. The optimum levels are; contact time at level 3, power at level 3, pH at level 3 and citric acid addition at level 1 as shown in Table 3.

Table 3. Effect of factor level on S/N ratios

Factors	Level 1	Level 2	Level 3	Max-Min
Time	6.0206	9.5909151	<b>12.77397</b>	6.753372
Power	9.76128	7.657351	<b>10.96686</b>	3.309509
pH	7.90927	7.1848745	<b>13.29134</b>	6.106463
Citric Acid	<b>10.7149</b>	7.5226618	10.14789	3.192275

The control factors effects on quality characteristic are shown in Figure 3. Overall mean value was calculated as 9.46 from all experiments.

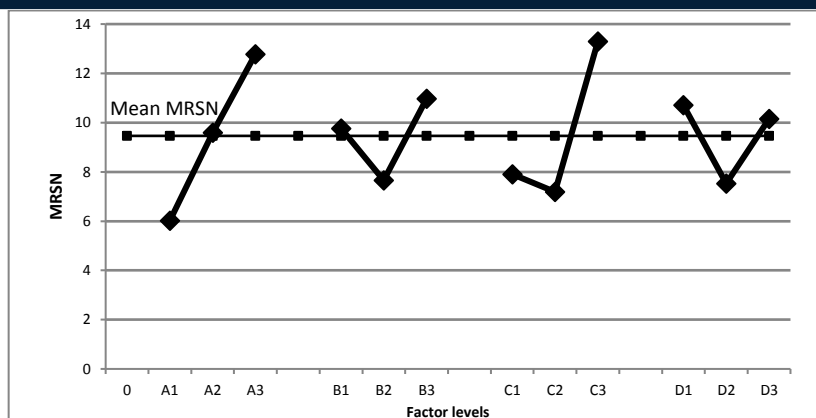


Figure 14. Effect of factor levels on S/N ratio

The optimum conditions for increase COD were determined as 5 min. for MW irradiation time, 700 watt for MW power, pH at 9 and citric acid addition at 0.5 mL. As a result of the optimization experiment performed under these experimental conditions, COD was found as 4800 mg/L.

### 3.2. Analysis of Variance

In order to see statistically significant control factors, the analysis of variance (ANOVA) is also performed. Table 4 shows the results of ANOVA obtained from S/N ratio. For L9 orthogonal array the total degree of freedom (DOF) is determined as 8. Besides the DOF for each parameter determined as 2 (3-1). From this, the DOF for the error calculated as 2.

Table 4. ANOVA Analysis

Factors	Degrees freedom	Sum of Square	Mean square	F value	Pure sum (%P)
Time	2	68.4870	34.2435	4.0686	<b>35.439</b>
Power*	2	16.8327	8.41639	1	-
pH	2	66.7802	33.3901	3.9672	<b>34.432</b>
Citric Acid	2	17.4039	8.7019	1.0339	5.3022
Error (SS <sub>E</sub> )	2	16.8327	8.4163	1	24.827
Total (SS <sub>T</sub> )	8	169.504	-	-	100

(\*)The parameter which the percentage contribution falls less than 10% is considered statistically insignificant [16]. In this study, Persulfate concentration is considered insignificant and it is included in the error term.

F test is performed to define the meaningful effect of each factor on the response variable. The F value is a measure of the variance of the data to the mean. The size of the F value that corresponds to the parameter indicates the importance of that parameter in the process [17]. According to the results, the F ratio for power and citric acid addition factors are smaller than the pH F ratio. This means that the variance of this factors is statistically insignificant. In ANOVA, the F ratio and P(%) values are helpful for the qualitative and quantitative evaluation of factorial effects, respectively [18]. As a result of ANOVA, MW irradiation time has been found as the most effective factor and its contribution is 35.4% on quality characteristics. The pH was the second most effective parameter by following the MW time with 34.5%.

### 4. CONCLUSIONS

Some of the results obtained from the study are as follows;

- MW irradiation effectively disintegrates the waste activated sludge and thus increasing the biodegradable portion in liquid phase of sludge.

-Combining MW with alkaline conditions increased the degree of disintegration.

- Optimization method using Taguchi's robust design approach and ANOVA technique were effective for investigate the relative effect of contact time, MW power, pH and citric acid addition factors on waste activated sludge disintegration.

- As a result of Taguchi experimental design optimum conditions for increasing COD were determined as as 5 min. for MW irradiation time, 700 watt for MW power, pH at 9 and citric acid addition at 0.5 mL (0.1 N).

- As a result of the confirmation experiment, 4800 mg/L COD was obtained in supernatant which was higher than the L9 Taguchi set.

### REFERENCES

- [1]. C. Cirakoglu, E. Dindar, F. Sagban, "Atik aktif camur dezentegrasyonu: mekanik, termal ve kimyasal yontemler", Uludag Universitesi Muhendislik Fakultesi Dergisi, vol. 22, pp. 29-38, 2016.
- [2]. K. G. Song, Y.K. Choungb, K.H. Ahtf, J. Cho, H. Yun, "Performance of membran bioreactor system with sludge ozonation process for minimization of excess sludge production", Desalination, vol. 157, pp. 353- 359, 2003.
- [3]. S. Saby, M. Djafer, G.H. Chen, " Feasibility of using a chlorination step to reduce excess sludge in activated sludge process", Water Research, vol. 36, pp. 656-666, 2002.
- [4]. C. Bougrier, C. Albasi, J.P. Delgenés, "Solubilisation of waste-activated sludge by ultrasonic treatment", Chemical Engineering Journal, vol.106, pp.163-169, 2005.
- [5]. K. Grübel, A. Machnicka, "Impact Of Microwave Disintegration On Activated Sludge, Ecological Chem Istry and Engineering", vol. 18(10), pp. 76-82, 2011.
- [6]. Q. Yu, H. Lei, Z. Li, H. Li, K. Chen, X. Zhang, R. Liang, "Physical and chemical properties of waste-activated sludge after microwave treatment", Water Research, vol. 44(9), pp. 2841-2849, 2010.
- [7]. C. Eskicioglu, N. Terzian, K. Kennedy, R. Droste, M. Hamoda, "Athermal microwave effects for enhancing digestibility of waste activated sludge" Water Research, vol. 41(11), pp. 2457-2466, 2007.
- [8]. S.A. Pino-Jelicic, S.M. Hong, J.K. Park, 2006. "Enhanced anaerobic biodegradability and inactivation of fecal coliforms and salmonella spp. in wastewater sludge by using microwaves" Water Environ. Res. vol. 78 (2), pp. 209–216, 2006.
- [9]. E. Wojciechowska, "Application of microwaves for sewage sludge conditioning", Water Research, vol. 39(19), pp. 4749-4754, 2005.
- [10]. S.M. Hong, J.K. Park, Y.O. Lee, "Mechanisms of microwave irradiation involved in the destruction of fecal coliforms from biosolids", Water Research, vol.38, pp.1615-1625, 2004.
- [11]. APHA, *Standard Methods for the Examination of Water and Wastewater*, 21st edn, American Public Health Association, Washington, DC., 2005.
- [12]. P.J. Ross, *Taguchi Techniques for Quality Engineering*, McGraw Hill Professional, 2<sup>nd</sup> edn. 1996.
- [13]. N. Aslan, I. Unal, "Multi-response optimization of oil agglomeration with multiple performance characteristics", Fuel Processing Technology, vol.92, pp. 1157, 2011.
- [14]. J. Antony, "Simultaneous optimisation of multiple quality characteristics in manufacturing processes using taguchi's qulaity loss function", *International Journal Advance Manufacturing Technology*, vol.17, pp. 134, 2001.
- [15]. T. Gayathri, S. Kavitha, S. Kumar, S. Kaliappan, I. Yeom, J. Banu, "Effect of citric acid induced deflocculation on the ultrasonic pretreatment efficiency of dairy waste activated sludge", *Ultrasonics Sonochemistry*, vol. 22, pp.330-340, 2015.
- [16]. R. Ramakrishnan, L. Karunamoorthy, "Multi response optimization of wire EDM operations using robust design of experiments" *International Journal Advance Manufacturing Technology*, vol. 29, pp.105, 2006.
- [17]. H. Sumit, A. Dhawane, B. Pratim, K. Tarkeshwar, G. Halder, "Parametric optimization of biodiesel synthesis from rubber seed oil using iron doped carbon catalyst by Taguchi approach", *Renewable Energy*, vol. 105, pp. 616-624, 2017.
- [18]. Z.B. Gonder, Y. Kaya, I. Vergili, et al. "Optimization of filtration conditions for CIP wastewater treatment by nanofiltration process using Taguchi Approach", *Seperation and Purification Technology*, vol.70, pp. 265, 2010.

### BIOGRAPHY

Presenter Elif DURNA got her bachelors' degree in the Environmental Engineering Department at Kocaeli University, Kocaeli/Turkey in 2014, his master degree in the Environmental Engineering Department at Kocaeli University, Kocaeli/Turkey in 2018. She is currently a PhD candidate in the Environmental Engineering Department at Kocaeli University. She is still an academic member of the Environmental Engineering Department at Kocaeli University . Her major areas of interests are: Advanced Oxidation Techniques, Experimental Design Techniques, Membrane Treatment Methods.

## Multi Response Optimization of Nanofiltration Process for Carbamazepine Removal

Ali Oguzhan Narci<sup>1</sup>, Ugur Ulukoylu<sup>2</sup>, Berna Kiril Mert<sup>2</sup>, Esra Can Dogan<sup>1</sup>

### Abstract

In recent years, the presence of micropollutants in aqueous environments is an increasing concern due to their potentially harmful effects on aquatic life. Conventional wastewater treatment technologies are ineffective in the treatment of pharmaceutical compounds such as carbamazepine at levels of ng/L and mg/L in surface and ground waters. Carbamazepine (CBZ), which is an anti-epileptic drug, is commonly present in municipal wastewater and it is not significantly removed during conventional biological treatment because of its resistance to biodegradation and low Log  $K_{ow}$ . For this reason, advanced treatment technologies should be considered which allow removal of carbamazepine from wastewater or destruction of its biological activity. In this study, the removal of carbamazepine from synthetic wastewater by nanofiltration process has been extensively investigated. Taguchi's robust design approach was used to optimize the system with the multi-response optimization method. Design factor and levels were selected as transmembrane pressure (TMP: 10, 15, 20 bar), membrane type (NF270, DS5DK, NP010), volume reduction factor (VRF: 1.5, 2.0, 3.0), and pH (6.12, 7, 10). L9 ( $3^4$ ) orthogonal array was used for experimental design and the-larger-the-better response category was applied to maximize carbamazepine removal and flux value. The optimum conditions were determined as the first level of membrane type (NF270), third level of TMP (20 bar), third level of VRF (3) and second level of pH (7). The most effective factor was found to be membrane type with 65.90%. Under these conditions, 91% carbamazepine removal and 134 L/m<sup>2</sup>.h flux value were obtained. These results showed significant improvement in performances of carbamazepine removal and flux by means of used the multi-response optimization, compared to initial value of carbamazepine removal (71.4%) and flux (95 L/m<sup>2</sup>.h).

**Keywords:** carbamazepine removal, nanofiltration process, multi-response optimization

### 1. INTRODUCTION

A recent study has shown that 631 different drugs and metabolites occur in 71 countries of the five United Nations regional groups in the world. It has been observed that there are remains of 16 pharmaceuticals, including diclofenac, carbamazepine, ibuprofen, sulphametoxazole, naproxen, estrone, estradiol, ethinylestradiol, trimethoprim, paracetamol, clofibrac acid, ciprofloxacin, ofloxacin, estriol, norfloxacin and acetylsalicylic acid [1]. Furthermore, because of the synergistic effects of micropollutions, even compounds persistence can cause undesirable effects on the environment. Once these pollutants have been consumed, they can be washed out of the human body or directly into the sewer system. Thus, they enter into surface water with untreated wastewater [2-3]. The micropollutants in wastewater are usually in the range of  $10^{-3}$ – $10^{-6}$  mg

<sup>1</sup> Corresponding author: Kocaeli University, Faculty of Engineering, Department of Environmental Engineering, 41380, Umuttepe/Kocaeli, Turkey. [alioguzhanmarci@gmail.com](mailto:alioguzhanmarci@gmail.com)

<sup>1</sup> Kocaeli University, Faculty of Engineering, Department of Environmental Engineering, 41380, Umuttepe/Kocaeli, Turkey. [esracdogan@gmail.com](mailto:esracdogan@gmail.com)

<sup>2</sup> Sakarya University, Faculty of Engineering, Department of Environmental Engineering, 54050, Esentepe/Sakarya, Turkey. [u.ulukoylu@gmail.com](mailto:u.ulukoylu@gmail.com), [bermakiril@gmail.com](mailto:bermakiril@gmail.com)

$L^{-1}$ , and their chemical and physical properties, ie solubility, volatility, absorbability, absorbability, biodegradability, polarity and stability, vary widely [4-5].

The removal of micro-pollutants is high for substances with high logKow efficiency, which facilitates adsorption and sludge removal. Low removal efficiency was observed for chemicals with low log K<sub>ow</sub> and acidic properties. Carbamazepine (CBZ) (5H-dibenzo[b,f]azepine-5-carboxamide), one of the 16 most commonly used drugs in water, is a drug sold under the name Tegretol, and its removal efficiency is low [6]. Carbamazepine is neutral substances that lack charge at the relevant pH and Carbamazepine has a log K<sub>ow</sub> value of 2.2 and is therefore not likely to adsorb to charged sludge surfaces, which may explain the low removal efficiencies. Also, carbamazepine has stable structures with delocalized electrons and is known to resist microbial degradation [7]. Municipal wastewater treatment plants (WWTPs) are generally not designed to purify pharmaceuticals. This is because they have been constructed to eliminate the easily and moderately biodegradable carbon, nitrogen and phosphorus compounds and microbiological organisms [8]. CBZ is ineffective by WWTPs and is often less than 10% treatment efficiency. For this reason, in order to be completely removed from wastewater, it has paved the way for different treatment applications, especially membrane filtration [9]. Membrane processes employing microfiltration (MF), nanofiltration (NF), ultrafiltration (UF), and reverse osmosis (RO) are widely used either separately or as a combination of membranes in series in wastewater reclamation/reuse and drinking water treatment to remove micropollutants. Microfiltration and ultrafiltration are generally not fully effective in removing pharmaceutical compounds. The studies on the use of NF and RO treatment showed that they have potential as efficient methods for removing pharmaceuticals from wastewater [10]. High pressure driven membrane processes as nanofiltration (NF) and reverse osmosis (RO) have appeared as useful options to remove a wide range of pharmaceuticals in terms of solute rejection [11-14]. Because membrane applications are costly treatment alternatives, it is an advantage to apply statistical experimental techniques to reduce the number of experiments in order to determine optimal conditions. Using design of experiment (DOE) methods based on the statistical techniques has been found to be an effective method for analysis the experimental results of a study to evaluate the individual contribution of controlling parameters on the objective functions. Also, these methods can be used for the purpose of process optimization. Taguchi method is known as a strong DOE method capable of funding an optimized design configuration [15]. Taguchi's parameter design is a simple and systematic approach to optimize design for performance, quality and cost. In most optimization studies have been done with only single quality parameter such that pollutant removal performance, however engineering applications and processes are composed of multiple responses [16].

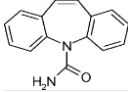
This study aims to optimization of nanofiltration (NF) process for carbamazepine removal from synthetic water by using Taguchi's robust design approach with the multi-response optimization method. The multi-response optimization for CBZ removal efficiency and membrane flux value simultaneously using Taguchi quality loss function has been done.

## 2. MATERIALS AND METHODS

### 2.1. Material

CBZ was selected because of it's wide existence in water sources and low removal efficiency which is below 10% in WWTPs [6-10]. CBZ, sold under the tradename Tegretol, is a medication used for treatment of epilepsy and neuropathic pain. In most sewage treatment plants, CBZ is poorly removed, due to its complex structure (containing strong electron withdrawing groups) that makes it extraordinary recalcitrant [17].

Tablo 1. Physical, chemical and pharmacological properties of carbamazepine [6]

PhAC	Carbamazepine (CBZ)
Molecular formula	C <sub>15</sub> H <sub>12</sub> N <sub>2</sub> O
Chemical Structure	
CAS No	298-46-4
Molecular weight (g/mol)	236
Usage	Antiepileptic, Analgesic
Water solubility (mg/L at 25 °C)	17,7
LogP	2,45

Three different commercial NF membranes (NF270, DS-5DK, NP010) were used in the experiments. NF270 and DS membranes are thin film composite membranes, NP010 membrane material is polyether sulfone. General properties of membranes were presented Table 2.

Table 2. General properties of membranes used in this study [18]

Membrane Type	Manufacturer	Material	MWCO (Da)	pH	Permeability (L/m <sup>2</sup> .h.bar) (20-25 °C)	Max. Pressure (Bar)	Max. Temperature (°C)
NF270	Filmtech (DOW)	Pap-TFC	300	2-11	22.3±0.8	41	45
DS-5DK	GE-Osmonics	TFC	150-300	2-11	4.2±0.5	41	50
NP010	Microdyn ®Nadir	PES	1000	0-14	>5	40	95

\*PES: Polyether sulfone; PAp: piperazine based semi-aromatic polyamide; TFC: Thin film composite

## 2.2. Experimental procedure

Synthetic feed solution was used and it was prepared by diluting a concentrated stock with Milli-Q water for the CBZ concentration would be 6 µg/L. CBZ was analyzed with LC-MS MS device and was performed using a liquid chromatography system (Agilent 6460 QQQ). The chromatographic separation was carried out on a Agilent Poroshell C-18 3x100x2.7µ column. The injection volume was 5 µl. A gradient elution program at 0.5 ml min<sup>-1</sup> flow, in which both reservoirs contained 5 mM ammonium formate+0.1% formic acid in (A) water and (B) Methanol, was used.

MS/MS experiments were performed on a ion mass spectrometer. The spectrometer was operated in positive ion mode with the multiple reaction monitoring (MRM) mode. MassHunter analyst software was used for instrument control and data acquisition. Nebulizer was adjusted 35 psi pressure and flow rate and temperature of drying gas were set 11 L/min and 300°C, respectively. The capillary voltage was set at 3,500 V and the source temperature at 400 °C. pH was analyzed by using Hach HQ40d multi parameter apparatus (Hach Co., USA).

A Sterlitech membrane filtration system (Model HP4750 Stirred cell, Sterlitech Corporation, USA) with an effective membrane area of 14.6 cm<sup>2</sup>, which is given figure 1, has used for all experiments. The feed volume capacity is 300 mL and it was stirred at 300 rpm for obtain cross-flow conditions. The TMP was adjusted by using nitrogen gas and the temperature was maintained at room temperature (25°C ± 1). Permeate collected in a beaker was measured by an electronic balance (Precisa XT2220M\_DR, Dietikon, Switzerland) and recorded by a computer using RsKey Ver. 1.34 software (A&D Comp. Ltd., Japan). Afterwards, the permeate fluxes (J: L/m<sup>2</sup>.h) were calculated using Eq 1. VRF and removal efficiency of CBZ were calculated Eq 2 and Eq 3, respectively.

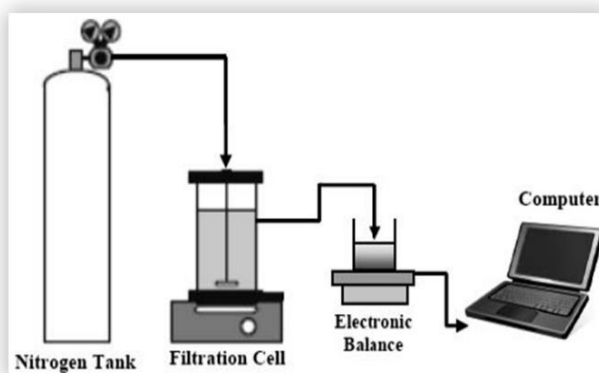


Figure 1. Schematic presentation of membrane process used in the experiments



$$J = \frac{1}{A} \frac{dV}{dt} \quad (1)$$

where A is effective membrane filtration area (m<sup>2</sup>), V is total volume of the permeate (m<sup>3</sup>), and t is filtration time (h), respectively.

$$VRF = \frac{V_f}{V_c} \quad (2)$$

where V<sub>f</sub> and V<sub>c</sub> are the initial volume of the feed and the final volume of the concentrate, respectively.

$$R(\%) = \left[ 1 - \frac{C_p}{C_r} \right] \times 100 \quad (3)$$

where C<sub>p</sub> is the CBZ concentration in permeate (mg/L) and C<sub>r</sub> is the CBZ concentration in the cell after the filtration (mg/L) [18].

### 2.3. Experimental design

Taguchi methods, a part of design of experiments related to robust design, have been earlier used in various fields like wastewater treatment, nano-technology etc. for optimization purposes [16]. In the present study, the multi-response optimization of CBZ removal efficiency and membrane flux value simultaneously using Taguchi quality loss function has been done. For this, 4 different factors with 3 levels were selected. The selected factors (trans-membrane pressure (TMP), volume reduction factor (VRF), pH and three different NF membranes) and their levels are given Table 3. Taguchi's L9 (3<sup>4</sup>) orthogonal arrays was employed for experimental planning. the higher value of both CBZ removal efficiency and flux value is desired, therefore higher-the-better response option is selected for used quality loss function which is given as follows [16,19]:

$$l_i = \frac{1}{n} \sum_{i=1}^n \frac{1}{y_i^2} \quad (4)$$

where y<sub>i</sub> is the observed data at the i<sup>th</sup> experiment for a certain combination of control factor levels, and n is the number of experiment.

Multiple S/N ratio (MSNR) is used to indicate the quality index at each design point. MSNR ratio corresponding to jth trial condition (η<sub>j</sub>) is calculated following [16,19]:

$$\eta_j = -10 \log_{10}(L_j) \quad (5)$$

A parameter level corresponding to the maximum average MSNR is evaluated as the optimum level for that parameter. The predicted value of MSNR (η<sub>opt</sub>) at optimum parameter levels is calculated by using Equation 6:

$$\eta_{opt} = \bar{\eta} + \sum_{i=1}^k (\eta_{mi} - \bar{\eta}) \quad (6)$$

where  $\bar{\eta}$  is the mean MSNR ratio of all experimental runs, k is the number of significant control factors, and η<sub>mi</sub> is the average MSNR for i<sup>th</sup> control factor corresponding to optimum parameter level. Confirmation experiments are conducted at determined optimum parameter levels to confirm the predicted response [16,19].

**Tablo 3. Factors, levels and their values used in experiments**

Factor	Symbol	Levels		
		1	2	3
Membrane type	A	NF270	DS-5DK	NP010
Transmembrane pressure TMP (bar)	B	10	15	20
VRF	C	1.5	2	3
pH	D	6.12	7	10

### 3. RESULTS AND DISCUSSION

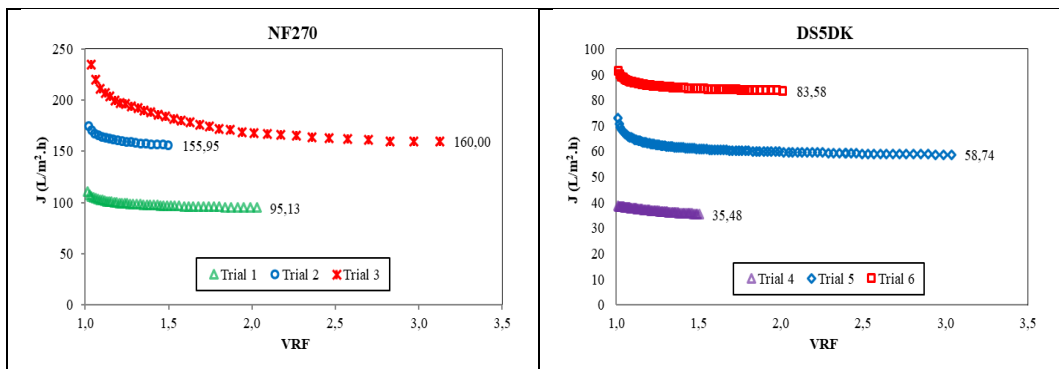
#### 3.1. Experimental results

Process factors, their levels, the obtained responses of the conducted experiments corresponding to L9 orthogonal array design and quality loss function values are given in Table 4. The highest CBZ removal performance was achieved with the DS5DK membrane, while the highest flux value was obtained with the NF270 membrane. This response parameters changed depending on some membrane properties (e.g., hydrophobicity, surface roughness and charge, molecular weight cut-off (MWCO)) and physicochemical characteristics of the compounds to be rejected (e.g., molecular weight, pKa, Kow and polarity), among others. Regarding the high pressure systems, the main characteristic of NF is the ion selectivity, where monovalent ions can pass through the membrane and multivalent anions are retained [20].

**Tablo 4.** L9 ( $3^4$ ) orthogonal array design by the Taguchi method for process optimization

Trial No	Membrane type	Transmembrane Pressure (bar)	VRF	pH	CBZ Removal (%)	Flux (L.m <sup>2</sup> /h)	Quality Loss Function (dB)	
							CBZ Removal (%)	Flux (L.m <sup>2</sup> /h)
1	NF 270	10	2	6.12	71.4	95	0.00020	0.00011
2	NF 270	15	1.5	7	40.0	155.65	0.00062	0.00004
3	NF 270	20	3	10	46.2	160	0.00047	0.00004
4	DS5DK	10	1.5	10	90.6	36	0.00012	0.00077
5	DS5DK	15	3	6.12	89.8	58.74	0.00012	0.00029
6	DS5DK	20	2	7	87.2	83.57	0.00013	0.00014
7	NP010	10	3	7	14.1	91.83	0.00502	0.00012
8	NP010	15	2	10	8.5	59.2	0.01376	0.00029
9	NP010	20	1.5	6.12	15.2	157.5	0.00431	0.00004

Figure 2 shows the permeate flux as a function of VRF under different operating conditions. The NF270 and NP010 membranes were found to be higher than the DS5DK membrane, depending on the pore diameter. In a short time, filtration, especially due to the increase in pressure, flux values, membrane contamination and pores occurred due to clogging.



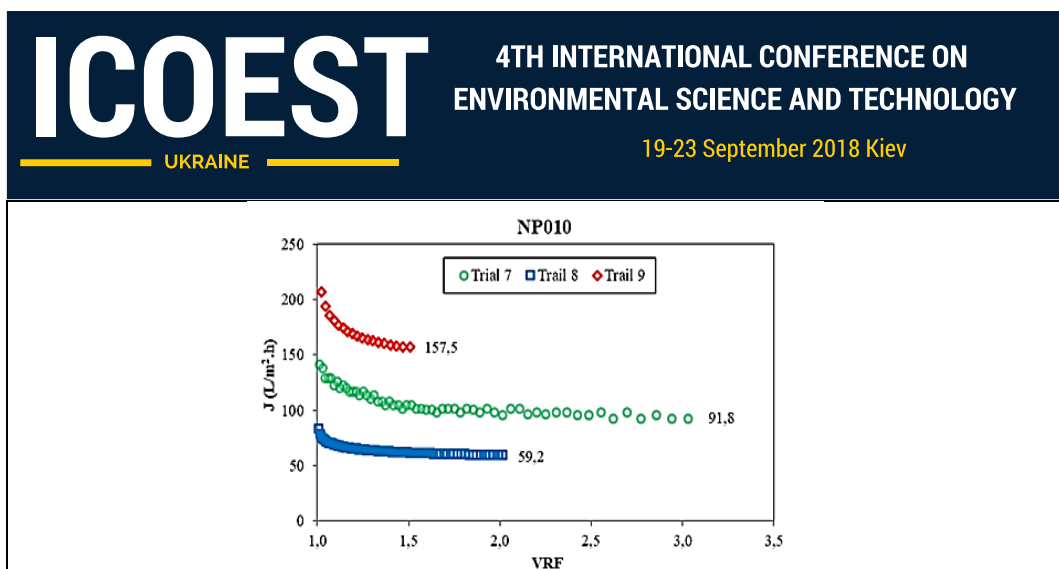


Figure 2. Flux values of membranes in experiment design

The effects of control factors (membrane type, TMP, VRF, and pH) on multiple quality characteristics are presented in Figure 3. In the Taguchi method optimum conditions are those that may result in the highest S/N. Levels with a high S/N ratio are those that represent the optimum conditions for a considered factor [21]. The maximum variation level was calculated as 7.64368 at membrane type. The optimum levels of control factors to obtain simultaneously the maximum rejection ratio and flux were determined as membrane type at level 1, TMP at level 3, VRF at level 3, and pH at level 2.

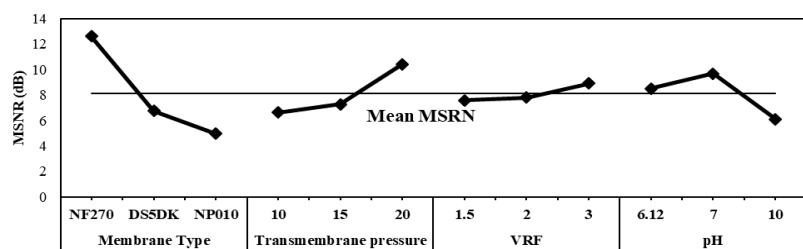


Figure 3. Effects of factor levels on MSNR

The most suitable membrane type was determined as NF270. The highest MRSN ratios were obtained at pH: 7, TMP: 20 bar and VRF: 3. MSNR values calculated for all factors and levels are given in Table 5.

Table 5. Effect of factor level on multiple S/N ratios

Factors	Symbol	Level 1	Level 2	Level 3	Delta
Membran Type	A	12.60678*	6.74641	4.96310	7.64368
TMP	B	6.62159	7.28843	10.40626*	3.78466
VRF	C	7.59299	7.80477	8.91853*	1.11375
pH	D	8.52299	9.67778*	6.11551	3.56226

\*Optimum Level

### 3.2. Analysis of variance

In order to investigate the relative contribution of factors or parameters on the responses, the analysis of variance (ANOVA) is performed. Table 6 shows the results of ANOVA obtained from calculated MRSN ratio. In ANOVA, the F ratio and P(%) values are tools that helpful for the qualitative and quantitative evaluation of factorial effects, respectively [19-22]. As shown in Table 6, the membrane type is the most influential factor since its percentage contribution is much higher than the other three. VRF has no significant effect due to very low percentage contribution. The most effective control factor is membrane type and its contribution is 65.90 % on multiple quality characteristics. It has been also seen that contribution of TMP and pH are 16.03% and 12.77%, respectively.

*Table 6. Analysis of variance (ANOVA) for response parameters*

Factor	DF	Adj SS	Adj MS	F	Pure sum (%P)
Membrane Type	2	95.950	47.975	31.538	65.90
Pressure	2	24.489	12.245	8.049	16.03
VRF	2	3.042	1.521	1.000	1.06
pH	2	19.819	9.910	6.514	12.77
Error (SS <sub>E</sub> )	2	3.042	1.521	-	-
Total (SS <sub>T</sub> )	8	143.301	-	-	-

### 3.3. Confirmation experiment

Confirmation experiments are recommended by Taguchi to verify experimental results [22]. A confirmation experiment was performed with optimal process parameters for compare to predicted and experimental results. The predicted, confirmation experiment and experimental run 1 response results are presented in Table 8. The results show considerable improvement in the quality and quantity of permeate with the multi response optimization used. CBZ removal efficiency and flux value increased from 71.4% and 95 L/m<sup>2</sup>.h to 91% and 134 L/m<sup>2</sup>.h, respectively.

*Table 7. Results of confirmation experiment at optimum parameter level*

	Initial Parameter Setting	Optimal Parameters		
		Prediction	Experiment	Improvement
Factor Levels	A <sub>1</sub> B <sub>1</sub> C <sub>1</sub> D <sub>1</sub>	A <sub>1</sub> B <sub>3</sub> C <sub>3</sub> D <sub>2</sub>	A <sub>1</sub> B <sub>3</sub> C <sub>3</sub> D <sub>2</sub>	-
Carbamazepine Removal (%)	71.4	-	91	19.6
Flux	95	-	134	39
MSRN (dB)	11.02806	17.29305	13.92814	2.90008

## 4. CONCLUSION

In the present study, “multi response optimization” method has been done to optimize NF process for CBZ removal.

The optimum levels of factors for maximum CBZ removal and permeate flux simultaneously obtained are membrane type at level 1, TMP at level 3, VRF at level 3 and pH at level 2.

The most effective control factor was found to be the membrane type by doing ANOVA analysis and its contribution is 66% on multiple quality characteristics.

The confirmation experiment was carried out with the optimal levels of parameters. The results show considerable improvement in the quality and quantity of permeate with the multi response optimization used. Removal efficiency of CBZ and membrane flux were increased from 71.4% and 95 L.m<sup>2</sup>/h to 91% and 134 L.m<sup>2</sup>/h, respectively with these optimum conditions. With the statistical study applied, an economical treatability study was conducted with fewer experiments.

It was determined that the multiple performance parameters (CBZ rejection ratio and flux of permeate) can be simultaneously improved through multi response optimization method. Also, with the statistical study applied, an economical treatability study was conducted with fewer experiments.

## ACKNOWLEDGMENT

*The authors acknowledge the support of Sakarya University Research Projects Department for this project (Project No 2014-01-12-004).*

### REFERENCES

- [1]. J.R. Andrade, M.F. Oliveira, M.G.C. Silva, and M. G. A. Vieira, "Adsorption of Pharmaceuticals from Water and Wastewater Using Nonconventional Low-Cost Materials: A Review," *Ind. Eng. Chem. Res.*, 57, 3103–3127, 2018.
- [2]. M. Farre, S. Perez, L. Kantiani, D.Barcelo, "Fate and toxicity of emerging pollutants, their metabolites and transformation products in the aquatic environment," *TrAC-Trends in Analytical Chemistry*, 27, 991-100, 2008.
- [3]. B. Kasprzyk-Hordern, R.M. Dinsdale, A.J. Guwy, "The occurrence of pharmaceuticals, personal care products, endocrine disruptors and illicit drugs in surface water in South Wales," *UK, Water Research*, 42, 3498-3518, 2008.
- [4]. B. Kiril Mert, N.Ozengin, E. Can Dogan and C. Aydinler, "Efficient Removal Approach of Micropollutants in Wastewater Using Membrane Bioreactor," <http://dx.doi.org/10.5772/intechopen.7518>, "Wastewater and Water Quality," ISBN:978-1-78923-621-7. 2018.
- [5]. P. Verlicchi, M.A. Aukidy, E. Zambello, "Occurrence of pharmaceutical compounds in urban wastewater: Removal, mass load and environmental risk after a secondary treatment—A review," *Science of the Total Environment*, 429, 123–155, 2012.
- [6]. Y.Zhang, S.W. Geiben, C. Gal, "Carbamazepine and diclofenac: removal in wastewater treatment plants and occurrence in water bodies," *Chemosphere*, 7, 1151–61, 2008.
- [7]. H. Ejhed, J. Fang, K. Hansen, L. Graae, M. Rahmberg, J. Magnér, E. Dorgeloh, G. Plaza, "The effect of hydraulic retention time in onsite wastewater treatment and removal of pharmaceuticals, hormones and phenolic utility substances," *Science of the Total Environment*, 618, 250–26, 2018.
- [8]. J. Tijani, O. Fatoba, L.F. Petrik, "A Review of pharmaceuticals and endocrine disrupting compounds: sources, effects, removal, and detections," *Water Air Soil Pollut.*, 224 (11), 1-29, 2013.
- [9]. D.P. Mohapatra, S.K. Brar, R.D. Tyagi, P. Picard, R.Y. Surampalli, "Analysis and advanced oxidation treatment of a persistent pharmaceutical compound in wastewater and wastewater sludge-carbamazepine" *Science of the Total Environment*, 470–47, 58–75, 2014.
- [10]. I. Vergili, "Application of nanofiltration for the removal of carbamazepine, diclofenac and ibuprofen from drinking water sources," *Journal of Environmental Management*, 127, 177-187, 2013.
- [11]. J. Radjenovic, M. Petrovic, F. Ventura, D. Barcelò, "Rejection of pharmaceuticals in nanofiltration and reverse osmosis membrane drinking water treatment," *Water Res.*, 42, 3601-3610, 2008.
- [12]. K. Boussu, C.Vandecasteele, B. Van der Bruggen, "Relation between membrane characteristics and performance in nanofiltration," *Journal of Membrane Science*, 310 (1-2), 51-65, 2008.
- [13]. M.J. Lo'pez-Mun'oz, A. Sotto, J.M. Arsuaga, B. Van der Bruggen, "Influence of membrane, solute and solution properties on the retention of phenolic compounds in aqueous solution by nanofiltration membranes," *Separation and Purification Technology*, 66 (1), 194-201, 2009.
- [14]. F. Marti'nez, M.J. Lo'pez-Mun'oz, J. Aguado, J.A. Melero, J. Arsuaga, A. Sotto, R. Molina, Y. Segur, M.I. Pariente, A. Revilla, L. Cerro, "Coupling membrane separation and photocatalytic oxidation processes for the degradation of pharmaceutical pollutants", *Water Research*, 1 -12, 2013.
- [15]. F. Googerdchian, A.Moheb, R. Emadi, M. Asgari, "Optimization of Pb(II) ions adsorption on nanohydroxyapatite adsorbents by applying Taguchi method," *Journal of Hazardous Materials*, 349, 186–194, 2018.
- [16]. N. Aslan, I. Unal, "Multi-response Optimization of Oil Agglomeration with Multiple Performance Characteristics" *Fuel Process. Technol.*, 92, 1157, 2011.
- [17]. M. Prado, L. Borea, A. Cesaro, H. Liu, V. Naddeo, V. Belgiorno, F. Ballesteros Jr., "Removal of emerging contaminant and fouling control in membrane bioreactors by combined ozonation and sonolysis", *International Biodeterioration & Biodegradation*, 119, 577 – 586, 2017.
- [18]. E. Can Dogan, C. Aydinler, B. Kiril Mert, A. O. Narci, O. Kilicoglu, E. Durna, U. A. Akbacak, "Kagit endustrisi atikularinin yeniden kullaniminda uygun nanofiltrasyon membranlarin belirlenmesi", *Pamukkale Univ Muh Bilim Derg*, 23(3), 279-287, 2017.
- [19]. N. Genc, E. C. Dogan, A. O. Narci, E. Bican, "Multi-Response Optimization of Process Parameters for Imidacloprid Removal by Reverse Osmosis Using Taguchi Design," *Water Environment Research*, 2017.
- [20]. M. O. Barbosa, N. F.F. Moreira, A. R. Ribeiro, M. F.R. Pereira, A. M.T. Silva, "Occurrence and removal of organic micropollutants: An overview of the watch list of EU Decision 2015/495," *Water Research*, 94, 257-279, 2016.
- [21]. A. Zirehpour, A. Rahimpour, M. Jahanshahi, M. Peyravi, "Mixed matrix membrane application for olive oil wastewater treatment: Process optimization based on Taguchi design method," *Journal of Environmental Management*, 132, 113-120, 2014.
- [22]. Z. B. Gonder, Y. Kaya, I. Vergili, H. Barlas, "Optimization of filtration conditions for CIP wastewater treatment by nanofiltration process using Taguchi approach", *Separation and Purification Technology*, 70, 265–273, 2010.

### BIOGRAPHY

Presenter Ali Oguzhan NARCI is currently a PhD student in the Environmental Engineering Department at Kocaeli University. He is still an academic member of the Environmental Engineering Department at Kocaeli University. His major study areas: Advanced Wastewater Treatment Techniques, Membrane Processes, Experimental Design Techniques and Techno-Economic Analysis of Treatment Processes.

## Mineralogical, Chemical And Physical Properties And Suitability For Therapy Of Peloids In Susurluk (Balikesir, Turkey)

*Necati Karakaya<sup>1</sup>, Muazzez Celik Karakaya<sup>1</sup>*

### *Abstract*

The mineralogical, chemical and physical properties of the peloids used for treatment and therapy purposes in the Susurluk province of Balikesir were investigated for their suitability. Morphological characteristics, mineral species and composition and chemical composition of the peloids were investigated by scanning electron microscopy, X-ray diffraction, and ICP-EAS, respectively. The peloids are composed of clay-silt-sized material and are generally composed of clay minerals (smectite, illite and kaolinite) calcite, quartz, feldspar and rarely gypsum, halite and more rarely pyrite minerals. Due to mineralogical composition controls the physical properties (viscosity, consistency limits, surface area, abrasivity, thermal properties, etc.) of the peloids have been examined. The peloids are high plastic and semi-rigid properties, with a cation exchange capacity of 28 meq / 100g and a BET surface area vary from 17 to 34 m<sup>2</sup>/ g, show similar viscosity and thixotropic properties as well as good fluidity. It has been determined that the peloids can maintain the heat for 15-20 minutes according to the original cooling values and the cooling kinetics, but the specific heat values are low. It has been determined that abrasive capacities may be partly a risk of skin starch, and water absorption and oil absorption capacities are close to natural peloids. According to the abovementioned properties, it is found that peloids used in the baths are not suitable for grain size and low clay content, chemical composition may not cause any problem and it can be used in therapy for some muscle problems in term of heat capacities.

**Keywords:** Balikesir, clay, peloid, thermal mud, Turkey

### 1. INTRODUCTION

It is also known as spa therapy, balneotherapy and pelotherapy which is used as an alternative treatment and its demand is increasing and gaining importance nowadays. Spa treatment or cure is usually applied to the patient through the treatment of natural (peloid), water and climate-induced natural therapeutic agents by bathing, drinking or by inhalation. The spa area is located about 10 km north of the Susurluk district, 50 km far from the northeast of Balikesir (Figure 1). There are also many hot water sources in the spa area which are partially using drinking, breathing. In Susurluk (Balikesir) spas, thermal waters have been using in the form of mud bath and inhalation (Figure 2). Pelotherapy or peloidotherapy, which is a sub-branch of balneotherapy, refers to the application of therapy to the patient in certain sessions and periods after maturation of the peloid, which is a natural mud of geological or partially biological origin, with thermal waters. In the study area, it was observed that the material which was formed naturally by partially alluvial soils consisting of the clay-silt sized sediments in the vicinity of the hot springs.

<sup>1</sup> Corresponding author: Konya Technical University, Department of Geological Engineering, 42039 Selcuklu/Konya, Turkey. [necati23@outlook.com](mailto:necati23@outlook.com)



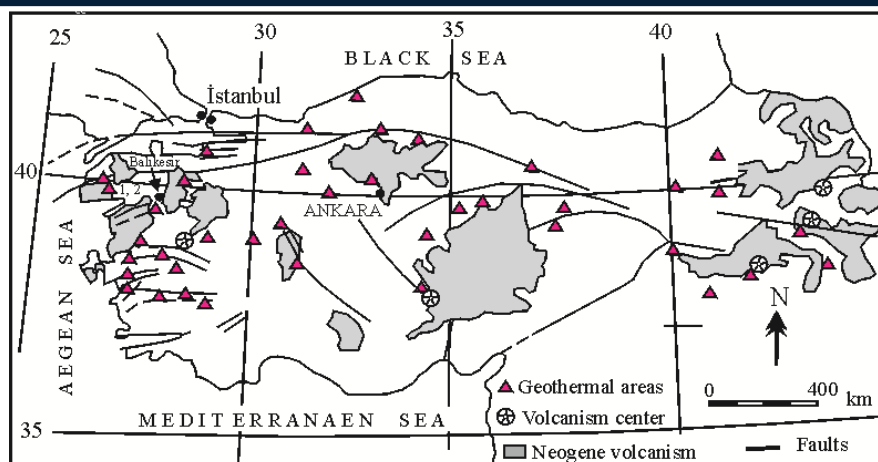


Figure 1. The location of Susurluk (Balikesir) spas and Turkey's active fault systems and geothermal fields (simplified from [1]).

The spas area in Susurluk are located is one of the important regions of our country with geothermal potential and thermal tourism. In the region where active tectonic movements in eastern Anatolia and the volcanism in the Tertiary period are widely observed, there are hot water outlets ranging from 50 to 60 °C in many areas. The Late Eocene to Middle Miocene basaltic, andesitic, dacitic, and rhyolitic lavas and pyroclastic rocks are covered by Upper Miocene to Pliocene lacustrine and fluvial sediments ([2], [3], [4]).

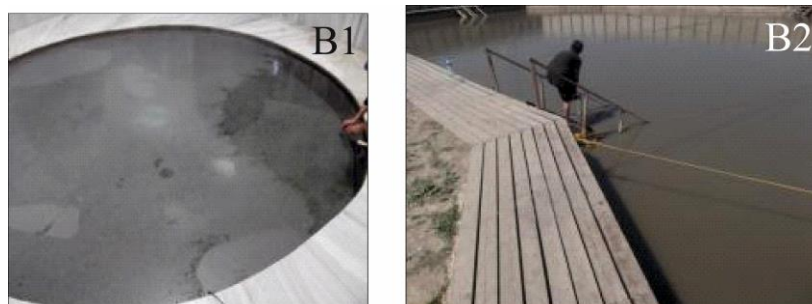


Figure 2. Mud pools of the studied spas in Susurluk.

The mud baths have been using to remedy some health problems, e.g. rheumatism, muscle-joint diseases, as well as cleanse and beautify to the skin. Some bodies covered themselves in the mud then wait for it to dry in the sun. There are two private facilities used by the patient, but the service quality is partially low. The muds which are used in mud ponds is formed by the interaction of tuffs, alluvial soils and rarely plant material with hot springs. Besides the skin diseases, especially in rheumatism, neuritis neurology, gynecological diseases, bone and calcification diseases, lumbago and metabolism disorders are used to treat such diseases.

The mud samples collected from two spas are close to the Aegean Sea, in both of them interaction of the thermal water with sea water is not clear. Some mineralogical, chemical and other basic characteristics of the mud / peloid used by the patients in Susurluk spas were investigated. In addition, it was aimed to determine the suitability of the muds by using the many technological properties. These include water-oil absorption capacity, humidity, swelling, heat holding capacity and cooling rate, surface area and cation exchange capacity. It is aimed to investigate the properties and to determine its suitability of the peloids for treatments and to made recommendations

## 2. MATERIALS AND METHODS

According to the purposes, the muds taken from the two mud pools used by the people in Susurluk spas and the muds from the alluvial soils around the hot springs. In order to determine the mineralogical composition, samples were collected and milled, and all samples and clay-sized fraction were analyzed by the Rigaku D / Max 2200 PC X-ray diffraction (XRD) at the Hacettepe University Laboratories. In the detailed clay analysis,

three diffractograms were carried out from the oriented samples to normal, ethylene glycol, and baked at 490 °C for four hours. The main and trace element analyzes of the investigated peloid samples were made in Acme (Canada) Laboratory. In the analyzes ICP-MS and EAS (Inductive Couple Plasma Mass Spectrometry, Emission Spectrometry) were used for the analysis of the main oxides and trace elements, loss on fire and LECO analysis for total C and S analyzes. The AI-1000 model Einlechner abrasion tester was used to measure the abrasive capacity of the samples. The consistency of the peloid and pure clay minerals was determined with the Casagrande system using the Atterberg method in accordance with the ASTM 4318-00 standard [5]. The original heat values were determined by Differential Scanning Calorimetry (DSC) device and cooling kinetics as defined by [6] and [7]. Surface area, pore size and pore volume measurements of peloid samples were determined by using Gemini VII 2390 V1.03 equipment (Micromeritics Instrument Corporation). The samples were exposed to a degassing method conducted at 150 °C under vacuum for 3 h to reach a constant weight. Apparent viscosities of the samples, which were kept in a peloid-water mixture and kept in a 40°C hot water bath, were measured on a Brookfield LVDVIII + PRO ultra-rheometer. Two parallel measurements were performed at 30-minute intervals and at different cutting rates. The samples were incubated in the hot water bath at 40°C and the measurements were repeated after 24 hours. The thixotropic index is defined as the ratio of the viscosity at 2.5 rpm to the viscosity at 20 rpm [8].

### 3. RESULTS AND DISCUSSIONS

The spas numbered as B1 and B2. The thermal water temperature, pH, EC of the B1 are 52.0-68.0 °C at the source, 7.3 to 8.0, 2.90 to 3.60 mS / cm, respectively. The physical parameters of the mud are 40 °C, 7.43, 2.61 mS / cm, respectively. The temperature, pH and EC of the B2 spas water are between 48.0-52.0 °C, 6.8-7.23, 2.80 mS/cm, while temperature, pH and EC of the mud are 40 °C, 7.70 and 2.84 mS / cm, respectively. This spa is similar to the B1 spa but has indoor mud pools.

Both of the peloids are fine- to medium sized, and composed mostly of clay minerals, quartz, mica, and feldspar, gypsum, halite, and rarely dolomite and pyrite. The smectite content of B1 is higher than the B2 (Table 1).

Table 1. Mineralogical composition of the spas (% wt.) (after [9])

Spa Name	Mineral types and composition (% wt.)*
B1	Sme(65)+Ms/Bt(8)+Fsp(8)+Kln(4)+Dol(1)+Gp(1)
B2	Sme(32)+Cal(27)+Ms/Bt(12)+ Fsp(11)+Qz(7)+Kln(4)+Py(4)+Hl(2)

Note: \*: Bt: Biotite, Cal: calcite, Dol: dolomite, Fsp: feldspars, Gp: gypsum, Hl: halite, Kln: kaolinite, Ms: muscovite, Qz: quartz, Sme: smectite, Py: pyrite (abbreviations from [10]).

The semi quantitative mineralogical composition of the commercial herbal clay (CHC) is somewhat similar to those of the peloids especially in terms of clay content while natural clay (NC) and mostly pharmaceutical clay (PC) [11], have different mineralogy from the investigated peloids. Quartz content in the spa B1 was not determined. The contents of carbonate minerals lower than 20% in both samples is not negatively affect the required physicochemical properties of the peloids.

Major and some trace element concentration of the samples are not similar. Major elements are also different those of the commercial, pharmaceutical and partially natural clays (Table 2a, b). Sulfur was not enriched in the peloid samples. CaO and LOI of the B2 spa are higher than those of B1 may be related to carbonate minerals.

Table 2a. Major element content (wt. %) of the peloids and some clay averages.

	SiO <sub>2</sub>	Al <sub>2</sub> O <sub>3</sub>	Fe <sub>2</sub> O <sub>3</sub>	MgO	CaO	Na <sub>2</sub> O	K <sub>2</sub> O	TiO <sub>2</sub>	P <sub>2</sub> O <sub>5</sub>	MnO	LOI*	Total	TOC	TOS
<b>B1</b>	54.95	14.95	5.92	2.87	4.30	1.47	2.50	0.74	0.16	0.11	11.80	99.76	5.27	0.04
<b>B2</b>	41.11	8.69	3.83	1.70	19.44	1.31	1.69	0.54	0.16	0.08	21.20	99.75	6.45	1.11
<b>CPC</b>	41.76	13.49	5.22	2.01	13.88	0.48	2.17	0.66	0.17	0.04	19.05	98.93	3.36	0.47
<b>PC</b>	47.91	12.81	3.06	2.96	1.27	0.37	0.23	0.24	0.05	0.03	30.08	99.01	6.11	0.04
<b>NC</b>	57.76	8.83	4.63	0.37	0.03	0.21	0.64	0.43	0.03	0.02	27.64	100.59	3.05	3.05

Note: \*: LOI: loss of ignition.

Table 2b. Trace (ppm) element content of the peloids and some clay averages.

	Sr	Ba	Co	Cr	Mo	Pb	Zn	Ni	As	Cd	Sb	Hg	Tl	Se
<b>B1</b>	286	<b>797</b>	<b>22.5</b>	<b>192</b>	0.2	<b>46.1</b>	69	<b>103.5</b>	<b>57.0</b>	0.2	<b>1.0</b>	<b>0.08</b>	<b>0.7</b>	<0.5
<b>B2</b>	733	<b>649</b>	<b>22.3</b>	<b>137</b>	1.1	<b>42.8</b>	50	<b>80.4</b>	<b>74.0</b>	<b>0.3</b>	<b>1.8</b>	<b>0.31</b>	<b>5.0</b>	<0.5
<b>CHC</b>	695	248	13.3	82	0.3	11.9	61	40	2.88	0.18	0.45	<0.01	<0.5	<0.2
<b>PC</b>	100	147	5	68	0.3	8.01	9	5	<0.3	0.02	0.22	<0.01	<0.5	<0.3

NC	42	75	28	96	2.1	27	58	324	140	1.3	12.3	61	7.5	20.8
NHPG	ng*	1300	5.0	1100	1.8	≤50	ng	60	≤8	3.0	5.0	1.0	0.8	17

Note: \*: ng: not given

The Ba content of the samples is higher than those of the CHC, PC, and NC (Table 2b). Considering this, Ba may not cause any skin problems and can be used in masks, baths, cures, patches, etc. Some hazardous elements (As, Ba, Cd, Co, Hg, Pb, Ni, Se, Sb, Te, Tl, Zn) of the peloids are higher than those of the CHC, PC, and Natural Health Products Guide (NHPG) ([11], [12]). The As content is exceeded the contents of CHC, PC, NC, and NHPG in all of the peloid samples while Pb is exceeded that of CHC, PC, and NC.

The presence of especially toxic and partially elements (As, Ba, Cd, Co, Hg, Pb, Ni, Se, Sb, Te, Tl, Zn) and less hazardous elements (Li, Rb, Sr, Cr, Mo, V, Zr, REEs) are not accepted in cosmetic products and peloid therapy, and great attention should be paid to the contents of such elements and necessary precautions should be taken ([7], [11], [12], [13], [14], [15]).

Consistency parameters of the peloids were measured. The liquid limit and plastic limit values of the samples are somewhat similar (Table 3). Liquid limit and plasticity index are good indicators of possible swelling and, the swelling potential of the material was classified as low, intermediate or high swelling capacity. The peloids have plasticity indexes above 15% and liquid limits above 50%, and are therefore suitable for use as peloids. The high plastic index of the sample B1 is due to having high clay content of them than those of the sample B2.

Table 3. Consistency limits and other physical characteristics of the peloid samples.

Sample Number	Liquid Limit (LL %)	Plastic Limit (PL %)	Plasticity Index (PI %)	Plasticity Expandability Potential*	Activity Index (AI %)	Consistency Index (I <sub>c</sub> )	Swelling (%)	Consistency Status
B1	63.00	22.12	40.88	HPL/HS	0.63	0.61	9.50	Semi rigid
B2	56.50	24.40	32.10	HPL/MS	0.42	0.73	6.10	Semi rigid

Note: \*: HPL: highly plastic clay, HS: high swelling, MS: medium swelling.

Clay pastes used in pelotherapy should have viscosities of about 4 Pa.s at 10 rpm and peloids with very low viscosities are not suitable for use in therapy ([7]). Viscosities of the peloids are mostly similar to the required viscosity values. B1 peloid is most suitable than the B2 and both of them show thixotropic property which is very important property because it leads to the use of clay or clay minerals in several semisolid products such as lotions, creams, pastes and make-up preparations (Figure 3) ([7]). And the properties cause to the peloids show flowing when mixed with water and preserve their shape when applied to skin. As a result, preparation of peloid materials should be selected precisely for the skin type and problem, and the mineralogical composition, mineral content, and physicochemical properties should be determined in detail.

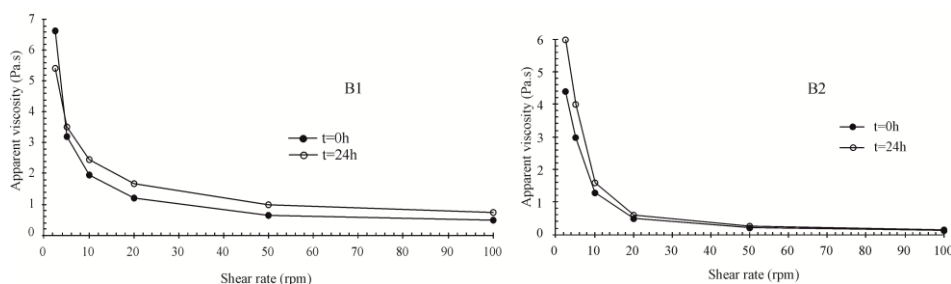


Figure 3. Apparent viscosity curves of some peloid samples.

Very high viscosity and thixotropy are not useful due to peloid converts too sticky and its fluency is greatly reduced and therefore shaping/working of the peloid becomes difficult, drying times are prolonged. And also it becomes more difficult to remove from skin and the container (or storage) after drying, and can be cause to an unpleasant situation.

Heat dissipation capacity is related to type and content of material and swelling. The capacity was determined of the peloids from every mixtures of muds with bidistilled waters, and duration of cooling temperature range from 31.5 to 49.0 minutes between 65 and 40 °C (Figure 4).

The cooling time is determined to define the suitability of the peloid to the heat therapy application on the body. Specific heat capacity of the muds range from 0.72 to 0.78 J/g.°C ([9]). The specific heat must be greater than

1.00 J/K.g and it is desired close to 2.00 J/K.g because the value is suitable for clays used in pelotherapy ([7]). The capacity may be accepted as suitable value for healing but lower than those of values in literature and pure clays'. The temperature of peloid should be above 5 °C the body temperature during the application and it's required to keep this temperature 15 to 20 minutes. The studied peloids examined in this aspect were determined to be suitable for heat therapy, rheumatologic, gynecological, muscular-joint disorder because of their heat retention times.

The property of surface area is important to determine the interaction of clay or clay minerals with applying area. Therefore, clays should exhibit a high specific surface area because the higher the surface area shows more interaction between the clay and the treated area. Surface areas and micro pore volume and diameter were measure and compared some pure clay minerals (Table 4) ([9]). BET surface area of the peloids vary from 17.34 to 30.40 m<sup>2</sup>/g and the values close to illite and kaolinite while lower than smectite and sepiolite. Because of the peloid samples containing smectite, illite and partially kaolinite besides to non-clay minerals caused to low surface and micropore areas.

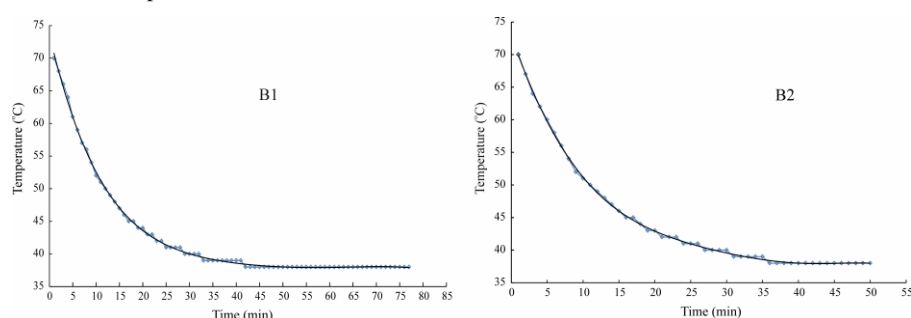


Figure 4. Cooling temperature and time.

Table 4. Surface area and micro pore properties of the peloids and some pure clay minerals ([9]).

Parameters	BET surface area (m <sup>2</sup> /g)	Langmuir surface area (m <sup>2</sup> /g)	Micro pore area (m <sup>2</sup> /g)	Micro pore volume (cm <sup>3</sup> /g)	Mean pore diameter nm (BET 4V/A)
				One Point Adsorption	Adsorption
B1	30.40	41.87	2.76	0.059	7.74
B2	17.34	22.62	3.13	0.042	9.69
Smectite	86.22	103.00	29.61	0.14	6.70
Illite	17.92	23.93	3.89	0.002	12.79
Sepiolite	198.88	260.12	81.45	0.04	10.28
Kaolinite	32.90	42.73	2.56	0.001	19.21

CEC of the investigated peloids are between 27.20 (B2) and 28.84 meq/100g (B1) close to Benetutti mud (30 meq/100g, ([16]) and higher than those of the Morinje mud (18 meq/100g, [17]). The abrasivity index of the B1 (155 g/m<sup>2</sup>) is lower than the B2 (195 g/m<sup>2</sup>) is related to high content of non-clay minerals, especially tectosilicates of the B2. The peloids having high abrasivity index may cause skin irritation or scratching when used as skin mask.

#### 4. CONCLUSIONS

Smectite content is lower in B1 than the B2, therefore the investigated thermal muds are contained clay minerals in partially acceptable percent used as pelotherapy. Contain some toxic and dangerous elements above the than values of the CHC and PC. Mineralogical, chemical and some physicochemical properties of mixture of illite, smectite and kaolinite and non-clay minerals (carbonates and some tectosilicates) show that preparation of peloids, are partially appropriate for improving or applying maturation treatments. The specific surface (owing to the high percentage of < 2 µm clay fraction) and cation exchange capacity, high CaO content (especially B2) of the thermal mud make them have to consider to improve the quality of peloid muds and use for therapy. The containing some toxic elements (As, Ba, Cd, Co, Hg, Pb, Ni, Se, Sb, Te, Tl, Zn) and less hazardous elements (Li, Rb, Sr, Cr, Mo, V, Zr, REEs) are not accepted in cosmetic products and peloid therapy, and great consideration should be paid to the contents of such elements. The handling and swelling potential of the B2 are better than the B1.

## ACKNOWLEDGMENT

The study was funded by The Scientific and Technological Research Council of Turkey (TUBITAK 110Y033) and the Selcuk University Scientific Research Projects support program (BAP 11401045).

## REFERENCES

- [1]. S. Simsek, "Dunya'da ve Turkiye'de jeotermal gelismeler". III. Geothermal Resources Symposium *PROC*, Ankara, Turkey, pp. 1-17.
- [2]. U. Gemici, G. Tarcan, Hydrochemistry of the Simav geothermal field, western Anatolia. *Journal of Volcanology Geothermal Research*, 2002, vol. 116.
- [3]. H. Mutlu. Constraints on the origin of the Balikesir thermal waters (Turkey) from stable isotope ( $\delta^{18}\text{O}$ ,  $\delta\text{D}$ ,  $\delta^{13}\text{C}$ ,  $\delta^{34}\text{S}$ ) and major-trace element compositions. *Turkish Journal of Earth Science*, 2007 vol. 16.
- [4]. M.C. Karakaya, N. Karakaya, Chemical composition and suitability of some Turkish thermal muds as peloids. *Turkish Journal of Earth Science*, 2018, vol. 27.
- [5]. ASTM, *Annual Book of ASTM Standards, Standard Test Methods for Laboratory Determination of Liquid and Plasticity Index of Soils*, D 4318, Philadelphia, 1994.
- [6]. C. Gomes, *Argilas: aplicoes na industria*, Aveiro, Portugal: O Liberal - Empresa de Artes Graficas (in Portuguese), 2002.
- [7]. M. Robelo, M. Viseras, A. Lopez-Galindo, F. Rocha, E. Ferreira da Silva, Rheological and thermal characterization of peloids made of selected Portuguese geological materials *Applied Clay Science*, 2011, vol. 51.
- [8]. A. Singer, E. Galan. *Palygorskite-Sepiolite. Occurrences, Genesis and Uses*. Developments in Sedimentology Amsterdam, the Netherlands, Elsevier, 1984, vol.37.
- [9]. M.C. Karakaya, N. Karakaya, S. Aydin, The physical and physicochemical properties of some Turkish thermal muds and pure clay minerals and their uses in therapy. *Turkish Journal of Earth Science*, 2017, vol. 26.
- [10]. D.L. Whitney, B.W. Evans, Abbreviations for names of rock-forming minerals. *American Mineralogist*, 2010, vol. 95.
- [11]. N. Mascolo, V. Summa, F. Tateo. Characterization of toxic elements in clays for human healing use. *Applied Clay Science*, 1999, vol. 15.
- [12]. R. Sanchez-Espejo, C. Aguzzi, P. Cerezo, I. Salcedo, A. Lopez-Galindo, C. Viseras, Folk pharmaceutical formulations in western Mediterranean: Identification and safety of clays used in pelotherapy. *Journal of Ethnopharmacology* 2014, vol. 155.
- [13]. F. Tateo, A. Ravaglioli, C. Andreoli, F. Bonin, V. Coiro, S. Degetto, A. Giaretta, A. Menconi Orsini, C. Puglia, V. Summa, The in-vitro percutaneous migration of chemical elements from a thermal mud for healing use. *Applied Clay Science*, 2009, vol.44.
- [14]. M. Mattioli, L. Giardini, C. Roselli, D. Desideri, Mineralogical characterization of commercial clays used in cosmetics and possible risk for health. *Applied Clay Science*, 2016, vol. 119.
- [15]. M.I. Carretero, M. Pozo, J.A. Martin-Rubi, E. Pozo, F. Maraver, Mobility of elements in interaction between artificial sweat and peloids used in Spanish spas. *Applied Clay Science*, 2010, vol. 48.
- [16]. S. Cara, G. Cargangio, G. Padalino, M. Palomba, M. Tamanini, The bentonites on pelotherapy: chemical, mineralogical and technological properties of materials from Sardinia deposits (Italy). *Applied Clay Science*, 2000, vol.16.
- [17]. G. Mihelčić, G. Kniewald, G. Ivanišević, R. Čepelak, V. Mihelčić, N. Vdović, Physico-chemical characteristics of the peloid mud from Morinje Bay (eastern Adriatic coast, Croatia): suitability for use in balneotherapy. *Environmental Geochemical Health*, 2012, vol. 34.

## Experiences on sustainable tourism development in Turkey

*Saniye Gul Gunes<sup>1</sup>*

### Abstract

*Turkey contains a great variety of natural habitats, ranging from Mediterranean, Aegean, and Black Sea beaches to towering coastal and interior mountains, from deeply incised valleys to expansive steppes, from fertile alluvial plains to arid, rocky hillslopes. She has also 18 asset in the UNESCO World Heritage list, 16 asset in the UNESCO Intangible Heritage list, 459 blue flag beaches and protected areas with different characteristics. Therefore, Turkey is a tourist destination with a lot of competitive advantage in terms of many types of tourism such as ecotourism, nature tourism, community-based tourism, cultural tourism, gastronomy tourism, health tourism, religious tourism etc. At this point; diversification of tourism, spread of it over a year, creation of different tourism destinations and alternatives, awareness raising on nature and culture conservation is very important. The United Nations has declared the year 2017 "International Year for Sustainable Tourism for Development" in order to emphasize the importance of sustainable tourism for the whole world. In particular, sustainable tourism approach have a vital importance for all types of tourism development in Turkey.*

*In recent years, there are different successful sustainable tourism practices in Turkey in the context of nationally/internationally funded projects, social responsibility studies, governmental and non-governmental enterprises. In this paper, current tourism statement of Turkey is evaluated; only two best practices- Kure Mountains National Park and Camili (Macahel) Biosphere Reserve- are explained in detail; and suggestions for ensuring sustainable tourism development in Turkey are established.*

**Keywords:** Turkey; Camili Biosphere Reserve; Kure Mountains National Park; sustainable tourism; development.

### 1. INTRODUCTION

Tourism comprises the activities of persons travelling to and staying in places outside their usual environment for not more than one consecutive year for leisure, business and other purposes, different from the exercise of an activity remunerated from within the place visited [1]. Over the last fifty years tourism has become one of the largest economic sectors globally, accounting for some 10% of the world's GDP. In many developing countries, tourism is the top export category. As a worldwide export category, tourism ranks third after chemicals and fuels and ahead of automotive products. International tourist arrivals grew 6.8% in 2017. A total of 1,323 million international tourist arrivals were recorded in destinations around the world, some 84 million more than in 2016. By region, Africa and Europe grew above average; Americas 209 million (+4%), Europe 671 million (+8%), Asia and Pacific 323 million (+6%), Africa 63 million (+9%), Middle East 58 million (+5%). By sub region, North Africa and Southern and Mediterranean Europe led results in 2017, reflecting strong demand for destinations along the Mediterranean [2].

According to UNWTO (United Nations World Tourism Organization), international tourism receipts increased 4.9% in real terms (adjusted for exchange rate fluctuations and inflation) to reach US\$ 1,340 billion in 2017. Strong outbound demand from both traditional and emerging markets fuelled growth in global receipts, which follows the positive trend recorded in international tourist arrivals (+7%). By region, the Middle East led growth in receipts, as some destinations rebounded strongly after weaker results in 2016. By sub region, growth was significant in South Asia and South-East Asia, as well as in Southern Mediterranean Europe and North Africa. Americas US \$326 billion (24%), Europe US\$ 519 billion (39%), Asia and Pacific US\$ 390 billion (29%), Africa US\$ 37 billion (3%), and Middle East US\$ 68 billion (5%) [2].

<sup>1</sup> Selcuk University, Department of Gastronomy and Culinary Arts, 42250, Selcuklu/Konya, Turkey, gulgunes@selcuk.edu.tr



Tourism expenditure is defined as the total consumption expenditure made by a visitor or on behalf of a visitor for and during his/her trip and stay at destination [1]. Table 1 shows top spenders in international tourism. China continues to lead global outbound travel in terms of expenditure. Tourism expenditure from the United States, the world's second largest source market, increased by US\$ 13 billion compared to 2016 (+9%), the largest increase in absolute terms among the top spenders. The Russian Federation rebounded strongly (+30%) after a few years of decline climbing three places to re-enter the top ten at number 8. All other source markets among the top ten recorded increases with particularly strong results in the Republic of Korea, Italy and Canada [2].

Table 1. Top spenders 2017 [2].

Country	US\$ billion
China	257.7
USA	135.0
Germany	89.1
United Kingdom	71.4
France	41.4
Australia	34.2
Canada	31.8
Russian Federation	31.1
Republic of Korea	30.6
Italy	27.7

UNWTO predicts that growth trends in world tourism will continue, with total arrivals reaching 1.8 billion by 2030. Again, emerging economies, including developing countries, stand to see the highest rate of growth. Further massive growth is predicted for tourism, providing excellent opportunities for spreading prosperity but presenting considerable challenges and potential threats to the environment and local communities if not well managed. Climate change is recognized as a major global issue, with significant implications for tourism. There is also an increasing appreciation of the potential role of tourism in addressing world poverty, by bringing sources of income to the heart of some of the poorest communities [3]. The United Nations has declared the year 2017 "International Year for Sustainable Tourism for Development" in order to emphasize the importance of sustainable tourism for the whole world. The UNWTO has noted that the tourism sector is in a position to be a leading change agent in the journey toward a green economy, provided it is afforded the right investment and guidance [4].

## 2. SUSTAINABLE TOURISM AS A DEVELOPMENT TOOL

Tourism is an exciting and dynamic sector that is constantly changing. It can affect people's lives in many different ways: for tourists it can be a source of lifelong memories, joy and fulfilment, and for businesses and destinations it is a source of income and employment. It is important to remember that tourism is an activity, as an economic sector and as an area of study, cannot be separated from the wider external environment within which it operates. Tourism is influenced by external issues that have a significant impact on the nature of its development, on the ability of tourism businesses to operate successfully, and on tourism's potential to benefit or to damage destinations [5]. The anticipated growth and the new trends observed in tourism have promoted the sector into such a strategic position that it may become the most important tool for the conservation of resources as well as to increase the environmental consciousness of the local people. These objectives can be achieved by generating financial resources which are necessary for conserving natural, historical and cultural assets by means of tourism, creating awareness and education programmes for visitors and local communities [6]. According to UNWTO and UNEP (United Nations Environment Programme); tourism is in a special position in the contribution it can make to sustainable development and the challenges it presents. Firstly, this is because of the dynamism and growth of the sector, and the major contribution that it makes to the economies of many countries and local destinations. Secondly, it is because tourism is an activity which involves a special relationship between consumers (visitors), the industry, the environment and local communities. This special relationship arises because, unlike most other sectors, the consumer of tourism (the tourist) travels to the producer and the product [4].

It can also help the sustainable management of protected areas, as a market-based alternative catering to the growing number of discriminating travellers trying to find, understand and enjoy a natural environment. Tourism can support the protection of natural resources, as local residents realise the value of their asset and want to preserve it. At the same time, our global heritage of living species is threatened as never before, as the protected areas that harbour so much of our biodiversity are exposed to the pressures of unsustainable development. The precautionary approach urges us to be especially concerned about tourism in protected areas,

given the risk of damage and destruction to this unique natural resource. Visitor impact management is ever more important as the number of tourist increases, and their distribution is often concentrated in major tourism destinations in ecologically vulnerable areas [7].

All of the above negative aspects underline the need for tourism to be very carefully planned and managed in developing countries. This requires governments to establish and implement clear policies on the control and management of the sector, in conjunction with all tourism stakeholders. In order to develop the tourism sector in a sustainable manner and enhance the local socio-economic impact from tourism, many developing countries have made tourism a priority in their national development policies, and are trying, with the support of donors and development organisations, to formulate and implement interventions to increase tourism's contribution to poverty reduction. A fundamental requirement of the tourism sector is that it should embrace the principles of sustainable tourism and focus on the achievement of sustainable development goals.

Sustainable tourism should not be regarded as a separate component of tourism, as a set of niche products, but rather as a condition of the tourism sector as a whole, which should work to become more sustainable. The UNWTO has defined sustainable tourism as "tourism that takes full account of its current and future economic, social and environmental impacts, addressing the needs of visitors, the industry, the environment and host communities" [3].

All tourism should be more sustainable. Sustainable tourism is not a discrete or special form of tourism. Rather, all forms of tourism should strive to be more sustainable. Making tourism more sustainable is not just about controlling and managing the negative impacts of the industry. Tourism is in a very special position to benefit local communities, economically and socially, and to raise awareness and support for conservation of the environment. Within the tourism sector, economic development and environmental protection should not be seen as opposing forces—they should be pursued hand in hand as aspirations that can and should be mutually reinforcing. Policies and actions must aim to strengthen the benefits and reduce the costs of tourism [4].

UNWTO and UNEP identified 12 aims for an agenda for sustainable tourism. Economic viability, local prosperity, employment quality, social equity, visitor fulfilment, local control, community wellbeing, cultural richness, physical integrity, biological diversity, resource efficiency and environmental purity. The order in which these twelve aims are listed does not imply any order of priority. Each one is equally important [4].

### 3. TOURISM IN TURKEY

Turkey contains a great variety of natural habitats, ranging from Mediterranean, Aegean, and Black Sea beaches to towering coastal and interior mountains, from deeply incised valleys to expansive steppes, from fertile alluvial plains to arid, rocky hillslopes. A myriad of community types and habitat mosaics occur, containing a rich mixture of plant and animal species, many of which are endemic [8]. The global importance of Turkey's biodiversity is exemplified by the fact that three ecoregions, two terrestrial (Caucasus and Irano-Anatolian) and one marine (Mediterranean), are classified as Global 200 Ecoregions considered by WWF as the most important ecoregions on earth in terms of their conservation values [9]. It is a scientific truth that Turkey has one of the richest natural heritage in temperate zone with approximately 11.707 plant taxa-3649 of them are endemic [10], 450 bird [11] and 413 butterfly [12] species and habitats provide living area for them.

She has also 18 asset in the UNESCO World Heritage list; 16 asset in the UNESCO Intangible Heritage list, two cities (Gaziantep and Hatay) in the UNESCO creative (gastronomy) cities list [13]; 459 blue flag beaches and 22 marinas [14]; and protected areas with different characteristics. Therefore, Turkey is a tourist destination with a lot of competitive advantage in terms of many types of tourism such as cultural tourism, ecotourism, nature tourism, community-based tourism, gastronomy tourism, health tourism, and religious tourism.

Turkey closed the 2015 with 39.5 million foreign visitors and was in the 6th place in Top 10 ranking by international tourist arrivals [15]. Turkish tourism sector have started to experience decreases as from 2015 September, as a result of the developments in its region, economic crises in the Russian Federation which one of its most important markets, some problems between two countries and some security concerns after the 2014 which hosted nearly 36 million foreign visitors and got significant share from the world tourism sector. Unfortunately, 25.3 million foreign guests visited Turkey in 2016. The losses in Russia and German markets caused a difficult year for the tourism sector. 2017 was a recovery year for Turkish tourism sector. According to the UNWTO, Turkey which decreased to the 10th place in 2016, rose to 8th place in 2017 in the international tourist arrivals in the world (Table 2) [2], [16].

According to UNWTO, when ranking the world's top international tourism destinations, it is important to consider both international tourist arrivals and international tourism receipts (Table 3). Seven out of the top ten

destinations appear on both lists, despite showing marked differences in terms of the type of tourist they attract, as well as the average length of stay and spending per trip and the night. Turkey is the eighth country in international tourist arrivals, but unfortunately not appear in top ten country in international tourism receipts in the world [2].

At this point; diversification of tourism, spread of it over a year, creation of different tourism destinations and alternatives, awareness raising on nature and culture conservation is very important. In particular, sustainable tourism approach is a crucial for all types of tourism development studies in Turkey.

Table 2. International tourist arrivals-2017 [4].

Country	Million
France	86.9
Spain	81.8
USA	75.9
China	60.7
Italy	58.3
Mexico	39.3
United Kingdom	37.7
<b>Turkey</b>	<b>37.6</b>
Germany	37.5
Thailand	35.4

Table 3. International tourism receipts-2017 [4].

Country	US\$ Billion
USA	210.7
Spain	68.0
France	60.7
Thailand	57.5
United Kingdom	51.2
Italy	44.2
Australia	41.7
Germany	39.8
Macao (China)	35.6
Japan	34.1

#### 4. EXPERIENCES ON SUSTAINABLE TOURISM DEVELOPMENT IN TURKEY

In recent years, there are different successful sustainable tourism practices in Turkey in the context of nationally/internationally funded projects, social responsibility studies, governmental and non-governmental enterprises. Local tourism development experiences such as Beypazari, Nallihan, Seferihisar, Camili and Kure Mountains and projects such as “Future Lies in Tourism” (initiated by Anadolu Efes) and DATUR (Eastern Anatolia Tourism Development Project) are some of them. Only two of them-Camili (Macahel) Biosphere Reserve and Kure Mountains National Park tourism development experiences- are explained in detail in this paper.

##### 4.1. Artvin-Camili (Macahel) Biosphere Reserve

The first steps for development and implementation of participatory management plans and effective governance mechanisms in protected areas of Turkey were taken during Biodiversity and Natural Resources Management (BNRM) Project. The project was implemented (2000-2008) by Turkish Ministry of Environment and Forestry (MEF) in collaboration with World Bank and supported by Global Environment and Facility (GEF). The objective of the project was to establish effective participatory planning and sustainable management of protected areas and natural resources at four selected protected areas, one of which is Camili (Macahel) Biosphere Reserve at the border of Turkey and Georgia. Macahel was the old name of Camili in Georgian language.

The Camili Basin is located within the municipal borders of Borcka District in the Province of Artvin, 45 km far from the district centre. The Camili Biosphere Reserve is surrounded by mountains on three sides, and meets the Georgian border on the fourth side to the north. There are three main valleys with the Biosphere Reserve. The main ecosystem types are boreal coniferous forest and temperate deciduous forest including tree species such as black alder (*Alnus glutinosa*), oriental spruce (*Picea orientalis*), Caucasus lime tree (*Tilia rubra* ssp.

caucasicus), hazelnut (*Corylus avellana*) and Sessile oak (*Quercus petraea*). The Camili basin is part of the Karcil Mountains Important Plant Area, which is one of the 122 Important Plant Areas defined in Turkey. The basin is the only area where the Caucasus bee race has remained without its purity being damaged. It is one of the three most important bee races in the world. The rangelands and alpine meadows are officially under the management responsibility of the Turkish Ministry of Agriculture and Rural Affairs (MARA). The site was also designated by the MARA as a genetic reserve in 2001 in recognition of the presence of the pure Caucasian bee race, which is one of the three important bee races in the world [17], [18], [19].

Many mammals are threatened by extinction because of habitat loss and illegal hunting. The brown bear (*Ursus arctos*), chamois (*Rupicapra rupicapra*) and roe deer (*Capreolus capreolus*) are among the main target species to be protected in the Camili region in Northeastern Anatolia, which is one of the few regions where they can find refuge. Important carnivore species in the area include wolf (*Canis lupus*), jackal (*Canis aureus*), red fox (*Vulpes vulpes*), badger (*Meles meles*), marten (*Martes foina*) and weasel (*Mustela nivalis*) which are evaluated as target species for securing the ecological balance. The Karcil Mountains with the Camili forests is one of the important habitats of the endemic Caucasian black grouse (*Tetrao mlokosiewiczii*).

There are six villages in the biosphere reserve and the permanent population is 1213 people (268 households). Due to the geographical conditions of the area the roads are blocked by snow for 4-6 months in winter. Local people are dependent on nature in order to perpetuate their living. Human-nature relations are built on traditional knowledge and experiences from the past. Besides traditional agriculture and animal husbandry, queen bee production, organic agriculture and ecotourism are considered as the basic activities for a potential economic development. Among the income generating activities, queen bee and honey production are the major activities in the basin [19].

The importance of the basin in terms of nature began with project called "Old Growth Forests of the Black Sea Region" implemented by WWF (World Wildlife Fund) between 1993-1996. Then, old growth forests in Efele and Gorgit area were declared as Nature Conservation Area by Ministry of Forestry in 1998 [20].

By the BNRM project, many components including activities like policy and programs, training and awareness and implementation and monitoring were realized. With the support of project;

- participatory management plan was prepared,
- training and awareness programs were carried out for local people and school children,
- local people had technical and financial support about alternative income generation activities,
- visitor centre and bird watching towers were constructed,
- traditional houses restored for accommodation of tourists,
- local ecotourism and beekeeping committee were established and
- the basin joined to the World Biosphere Reserve Network in 2005

Additionally, the project team received an extensive training on the basics of planning and implementation of sustainable tourism in protected areas and completed "Sustainable Tourism Development Plan" with contribution of local stakeholders. This document is a part of the overall management plan and has been an exemplary document for similar studies conducted in other protected areas throughout Turkey. As a supportive element for building local capacity for sustainability of the project results, a small grant programme was implemented for funding projects of local individuals and initiatives. In this context, fifty small-grant projects (on sustainable tourism, training and capacity building, bee-keeping and marketing, handicrafts, nature conservation and biodiversity conservation) were supported [18].

After BNRM project completed, the success story in Camili was not ended. Local producers have obtained the organic product certificate in 2010 with the support of the project titled "Certification of Local Products in Camili Biosphere Reserve". A documentary film for Camili Biosphere Reserve was prepared by a national documentary TV channel with the support of Turkish National Commission for UNESCO. With this documentary film, natural resources, biodiversity, cultural and historical values and traditional life style of Camili Basin and people are presented to the national public. In addition, land uses from past to present, traditional life, cultural and socioeconomic development of Camili Biosphere Reserve and people were presented in a book by a project titled "Biosphere Reserves in Education for Sustainable Development: Life in Camili" with support of Turkish National Commission for UNESCO. This book has been distributed to the related stakeholders. After declaration as a biosphere reserve, number of visitors has been increased. In 2000, while the number of tourists who visit the region was nearly zero, this figure has increased to one thousand after declaration of the area as biosphere reserve by UNESCO in 2005. The number of family pensions increased to twelve in 2006, and 25 in 2014. And the number of visitors in the basin increased to 2200 by 2006 and 6500 visitors in 2011 and approximately 30.000 visitors in 2013. And thus beekeeping, honey production,

production of natural products, bed and breakfast and guidance services activities were much appreciated in Camili Biosphere Reserve. Therefore, incomes of local people has been increased and through nature friendly economic activities, a model on sustainable development has been established. The family pensions consists of traditional wooden houses with local architecture. Houses are turned into family pensions with little modifications in order to protect local architecture. Pensions provide clean and natural accommodation facilities with warm and welcoming family environment for the guests. Local people is aware of the nature and its protection. Pensions provide locally produced food with a large menu for their guests. Most of local foods are produced by themselves or bought from their neighbors creating an economic circle that provides mutual benefits for all involved [20].

### ***4.2. Kastamonu-Bartın Kure Mountains National Park***

The Kure Mountains, located in the provinces of Kastamonu and Bartın, on the west of Black Sea Region — one of the largest protected areas in Turkey. Kure Mountains start from Bartın River on the west and runs 300 kilometers on to Kizilirmak River toward the east. Thanks to its varied topographical structure, the area hosts a diverse landscape. It owes its rich habitat, which include all the main ecosystem types such as forest, maquis, cliffs, caves, river, coastal and traditional agricultural areas, to being a part of the coastal mountain system that covers the north of Anatolia from one end to the other. There is both national and international importance of this area. Kure Mountains with a surface area of 37,753 hectares has been declared as national park in 2000. Daily life activities around the National Park do not spread into the boundaries of the National Park; consequently there are not any settlements within the boundaries. In other words, the National Park, located on an east-west axis, is a physical and social barrier for its surrounding. This area is located in “North Anatolia and Caucasia Temperate Zone Forests” that is prior to in terms of natural protection of WWF on a global scale. As one of the 9 Mediterranean forest hotspots in Turkey identified by the WWF, the national park is a contribution of the Turkish Government to WWF’s “Gifts to the Earth” initiative [21] , [22].

Alternative job opportunities compatible with education, awareness raising, and sustainable resource management in the area are of special interest for the local public. A number of projects were developed to involve local communities. The first was implemented by “The Kastamonu Foundation for Development, Health, Environment, Education and Tourism” with financial support from the WWF Mediterranean Programme in 2000. Involving local communities in protecting their environment was the primary aim of the project. Ecotourism was identified as one of the best options for developing alternative livelihoods for the local communities. Educational activities for local communities and the local authorities included seminars on the sustainable use of forest resources and conservation of biodiversity. In addition, a traditional village house was renovated as an ecotourism centre. After opening the Pinarbasi Ecotourism Center in 2001, tourist guide training courses were organized and certificates were issued to 20 local nature guides. In 2002, ecotourism guide maps were published to inform both domestic and international visitors about multifunctional forests in the Kure Mountains. In 2003, income from the maps was used to establish the Kastamonu Ecotourism Association, which brings local nature guides together and aims to enhance the attractiveness of the villages around the park for tourists. Both publication of the maps and the foundation of the Kastamonu Ecotourism Association helped to draw media attention to biodiversity conservation and ecotourism activities in the area [23].

Another successful undertaking is the Zumrut Village Ecotourism Project, financially supported by the GEF Small Grants Program and executed by the Kastamonu Ecotourism Association between 2004 and 2006. Zumrut village in Azdavay district in the southeast of the national park has more than 350 inhabitants, but only 35 of them live permanently in the village. Most of the people migrated to Istanbul to find a job or obtain education. The village has experienced economic loss as a result of the designation of the national park, which creates a negative attitude among local people towards the national park and nature conservation in general. This project aimed to improve ecotourism in the Kure Mountains and its environs in order to create alternative livelihoods for local people. The project contributed to awareness-raising about sustainable use of forest ecosystems and participation of local communities in the management of the national park. Ecotourism opportunities and threats were determined and potential nature-based ecotourism activities were identified, such as bird and wildlife watching, trekking, hiking, horseback riding, mountain biking, caving, and rock climbing. In 2006, a public awareness programme was finalized; one village house and one mansion with 25 beds were restored in the traditional architecture style. The old village school building was refurbished as the Visitor and Public Awareness Center. The village house and mansion are now operated by the local public; training courses on packaging and preparation of organic products are very popular among women. Probably the most important contribution of the project to the local community, especially for women, foresters, and unemployed youth was



to offer alternative livelihoods in local nature guidance, organic and traditional hand-made products, bicycle and horse rental, and accommodation in village houses [23].

Kure Mountains was pilot area of the Project titled “Enhancing Coverage and Management Effectiveness of the Subsystem of Forest Protected Areas in Turkey’s National System of Protected Areas” (2008-2012). The project -supported by GEF and implemented by MEF- has the following objectives related to tourism:

- To develop a National Park management plan, including a sustainable tourism development strategy through a consultative process involving government, NGOs and local communities.
- To ensure long-term financial sustainability of the park through a visitor management programme supported by education, interpretation and recreation facilities, and consider effective mechanisms for management of park revenues.
- To develop alternative livelihood options for local communities such as ecotourism, non-timber forest products in order to reduce pressure on forest resources.
- To improve environmental awareness of local communities and visitors by promoting natural and cultural values through awareness raising activities, media and outreach through local NGOs.

“Visitor and Information Centre”, “Information Centre” and gate entrance units were established in Bartın and Kastamonu. Infrastructure and guidance studies and introductory, informative and direction boards were installed in the scope of visitor management. Following the trainings on “Boarding House Keeping in Ecotourism”, 15 of the people who attended the trainings were supported for arranging one room of their house as boarding houses in Bartın. This project was declared as one of the 24 best practices on sustainable development and green economy implementations of Turkey in the Rio+20 (United Nations Sustainable Development Conference) in 2012. In 2012, Kure Mountains National Park also became the first in Turkey and the 13<sup>th</sup> in Europe to be granted an elite PAN Parks (Protected Area Network) certificate, recognizing its high value as a protected natural area and destination for sustainable tourism [24], [25], [26].

## 5. RESULTS AND DISCUSSION

Tourism is one of the largest and fastest growing economic sectors in the world, and has a considerable role to play in delivering sustainable development in many countries. At the same time it must be well managed so that it benefits local communities and the natural and cultural environments upon which it depends [3]. According to UNWTO 2017 statistics, Turkey is the 8th country in international tourist arrivals, but unfortunately not appear on top ten international tourism receipts list. Today, the vast majority of tourists come to the Mediterranean region with tour packages as part of mass tourism and almost spend all of the holidays at the hotel. In other words, these tourists mostly return to their countries without knowing Turkish culture and natural values of Turkey. According to Egresi, mass tourism has played a critical role in Turkey’s strategy for economic development. However, mass tourism development has not been without costs. Tourists tend to consume more vital resources than local people and generate more waste and pollution in Turkey. He also found that local people of Turkey have benefited very little from tourism development. The main benefit for them is the provision of jobs, but most of these are seasonal, part-time, low-skilled, and low-paying. Tourism has also brought them higher prices and a de facto segregation (from tourists in the coastal areas, where they appear to have lost the right to access beaches and other coastal lands which used to be public in the past but seem to be reserved for tourists nowadays [27].

In fact, Turkey's tourism potential, not simply from mass tourism in the Mediterranean. The Anatolian plateau is one of the cradles of civilization and has hosted many peoples throughout history. Turkey has an important position with respect to climate, the existence of natural resources and historical assets. Besides various local traditions and customs, the hospitality of the Anatolian people is an important aspect of the tourism offer. There are a number of other factors including a young and dynamic population, being one of the cradles of civilization, establishing a bridge between East and West, representing the exotic culture of the East, and having more modern and equipped accommodation facilities than other competitor countries in the Mediterranean have. Turkey has the capability of providing a variety of tourism activities (sea and thermal resorts, cultural and natural attractions, historical sites, etc.), as well as transportation facilities (via land, sea, and air) [28].

Tourism could be an instrument in sustainable development and nature conservation. With the support of careful planning, strategy formulation and management; negative impacts can be minimized and positive impacts can be maximised. 2017 has been declared by the United Nations as the “International Year of Sustainable Tourism for Development” and it is therefore opportune to consider how tourism may contribute to sustainable development of destinations in Turkey. The concept of sustainable tourism was first mentioned in 8th Five-Year Development Plan (2001-2005) in Turkey. In the 2023 Tourism Strategy also, the principle



of sustainability is often cited. Nowadays especially the Turkish Ministry of Culture and Tourism, NGO's and local authorities are increasingly starting to realize the importance of sustainable tourism development. And as a developing country, studies on this subject are increasing day by day and different experiences stand out. Experiences on tourism development in Kure Mountains National Park and Camili Biosphere Reserve are only two of them.

According to Cetinel and Yolal, the education and the awareness of the people, both the residents and the public, is also an important determinant for the success of the sustainable tourism development [29]. A capacity-building programme provides communities with the skills, expertise, and capital necessary to start and operate small-scale tourism enterprises and service quality. Programmes provide leadership training, and small loans to local residents for beekeeping, nature guiding, hotel operations and use of renewable energy sources [30].

On the other hand, policy makers and destination stakeholders must balance the economic impacts of tourism against damage to the socio-cultural fabric of the destination. Likewise, management of environmental sustainability is considered a critical element for the livelihood of residents and continued enjoyment for tourists.

In this process; it is also important that the plans of the areas where tourism develops are handled with a participatory approach. Successful tourism initiatives require the effective participation of all relevant stakeholders. Numerous types of actors and agents are involved in producing the goods and services that are consumed by visitors, and good governance is required for sustainable tourism at a destination. Governance can be defined as "an alternative system for government administration or a cooperative management system where various entities, including the government, businesses, and civil society, go beyond the traditional division of roles, share their experiences and knowledge, and ultimately build trust through participation, cooperation, and communication, all for the benefit of resolving common issues". There is a need to connect stakeholders and establish a virtuous circle for tourism development in order to achieve the goals of revitalizing regional economies, creating jobs, preserving local culture, developing local communities, and protecting the environmental ecosystem. For good governance, all stakeholders should be represented in the decision-making and empowered to contribute to those decisions [31].

## References

- [1]. M. Libreros, *A conceptual framework for a Tourism Satellite Account*, OECD Meeting of National Accounts Experts, OECD, STD/NA (98)20, 1998.
- [2]. UNWTO. (2018) Tourism Highlights Ed.2018 [Online]. Available: <http://marketintelligence.unwto.org/publication/unwto-tourism-highlights-2018>
- [3]. UNEP and UNWTO. *Making Tourism More Sustainable: A Guide for Policy Makers*, World Tourism Organization, 209 s, 2005.
- [4]. UNWTO. *Sustainable Tourism Governance and Management in Coastal Areas of Africa*. UNWTO, Madrid, 2013.
- [5]. C. Inkson and L. Minnaert. *Tourism Management-An Introduction*. London: Sage, 2012.
- [6]. N. Beunders, R. Klep, M. Tapaninen and G. Gunes. *Türkiye'deki Korunan Alanlar ve Çevresinde Sürdürülebilir Turizm Gelişim Stratejisi Rehberi*. Dumat Ofset Matbaacılık San. Tic.Ltd.Sti., 120s., Ankara, 2007.
- [7]. P.F.J. Eagles, S. F. McCool and C.D Haynes, *Sustainable Tourism in Protected Areas: Guidelines for Planning and Management*. IUCN Gland, Switzerland and Cambridge, UK. , 183pp, 2002.
- [8]. K. Guclu and F. Karahan, "A review: the History of Conservation Programs and Development of National Parks Concept in Turkey". *Biodiversity and Conservation* 13: 1373–1390, 2004.
- [9]. UNDP (2009) Turkey Monthly Newsletter. Special Edition, December 2009, [Online]. Available: <http://www.undp.org.tr>
- [10]. A. Guner, S. Aslan, T. Ekim, M. Vural, M.T. Babac (editors). *Türkiye Bitkileri Listesi (Damarlı Bitkiler)*. Nezahat Gökçigit Botanik Bahçesi ve Flora Araştırmaları Derneği Yayını, İstanbul, 2012.
- [11]. K. Isik. *Biyolojik Çeşitlilik*, ANG Vakfı Yayın No: 2, İstanbul, 224 pp, 2014.
- [12]. H. Yildirim. *Kocaeli'nin Kelebekleri*, T.C. Orman ve Su İşleri Bakanlığı, 2016.
- [13]. (2018) The UNESCO website [Online]. Available: <https://en.unesco.org/>
- [14]. (2018) The Blue Flag Turkey website [Online]. Available: <http://www.mavibayrak.org.tr/en/Default.aspx>
- [15]. UNWTO. (2016) Tourism Highlights Ed.2016 [Online]. Available: <http://marketintelligence.unwto.org/publication/unwto-tourism-highlights-2016-edition>
- [16]. TUROFED. *Turizm Raporu*. 2008/1, Ankara, 2018.
- [17]. C. Adem, S.Arancı and U. Zeydanlı. GEM-CON-BIO Case Study Report Camili Biosphere Reserve Turkey. Project title: Governance and Ecosystems Management for the CONservation of BIODiversity, Project acronym: GEM-CON-BIO Project, Project no: 028827, 64 pp, 2007.
- [18]. G. Gunes. "Governance and Participation in Camili Biosphere Reserve". *International Journal of Information Technology and Business Management*. 29th October 2012. Vol.6 No.1, 37-49, 2012.
- [19]. (2018) UNESCO The MAB Programme [Online]. Available: <http://www.unesco.org/mabdb/br/brdir/directory/biores.asp?mode=all&code=TUR+01>

- [20]. E.Erturk. (2014) "A Turkish Success Story in Sustainable Development: Camili Biosphere Reserve" [Online]. Available: <http://www.unesco.org/new/en/natural-sciences/environment/ecological-sciences/related-info/publications/research-papers/>
- [21]. DHKV (WWF Turkey). *Ormanlar ve Orman Urunleri*. Nature Footprints, Ana Basim A.S., Istanbul, 2000.
- [22]. C.Bastemur, G.Gunes. "Rural Tourism in Protected Areas: A Case Study from Kure Mountains National Park-Turkey", *Forestry Review*, 44:23-30, 2013.
- [23]. G.Gunes and L. Hens, "Ecotourism in Old-Growth Forests in Turkey: The Kure Mountains Experience". *Mountain Research and Development*, Vol 27. No: 3, Aug. 2007, pp. 281-283, 2007.
- [24]. Anonymous. *Turkey's Sustainable Development Report: Claiming the Future*, Ministry of Development, Ankara, 2012.
- [25]. UNDP-Turkey (2018), *Lighting the Way to Sustainability*. [Online]. Available: <http://www.tr.undp.org/content/turkey/en/home/ourwork/environmentandenergy/successstories/lightingthewaytosustainability.html>
- [26]. (2018). The GEF (Global Environment Facility) website [Online]. Available: <https://www.thegef.org/project/enhancing-coverage-and-management-effectiveness-subsystem-forest-protected-areas-turkey-s>
- [27]. I.Egresi, *Tourism and Sustainability in Turkey: Negative Impact of Mass Tourism Development*. In: Egresi I. (eds) *Alternative Tourism in Turkey*. GeoJournal Library, vol 121. Springer, Cham, 2016.
- [28]. I.Bircan, H.I. Ulker, G. Gunes, G.Karakoc, Z.Poyraz. "Tourism Destination Sustainability And Non-Governmental Organizations (NGO's): A Case Study Of Beypazari, Turkey". *Journal of Educational Travel*, Vol 1, No 1, January 2010, 17-32.
- [29]. F.Cetinel and M.Yolal, "Public Policy and Sustainable Tourism in Turkey". MPRA Paper No. 25418, posted 27. September 2010, [Online]. Available: <https://mpa.ub.uni-muenchen.de/25418/>
- [30]. UNWTO, *Sustainable Tourism for Development Guidebook-Enhancing Capacities for Sustainable Tourism for Development in Developing Countries*. European Commission, Madrid:UNWTO, 228 pp, 2013.
- [31]. UNWTO and Griffith University, *Managing Growth and Sustainable Tourism Governance in Asia and the Pacific*, UNWTO, Madrid, 2017.

**Biography:** Saniye Gul Gunes is a landscape architect and associated professor at Selcuk University, Konya, Turkey (from April 2017 on). Prior to her present position she was a research assistant in Ankara University (1993-2002); worked for Ministry of Environment and Forestry (2002-2007); part time lecturer at Bilkent University (2002-2003) and Ankara University, Department of Tourism Guidance (2003-2007); and full time academician at Atilim University, Department of Tourism and Hotel Management (2007-2017). Her research interests are environmental management, tourism and environment relations, tourism and local development, sustainable tourism, rural planning, cultural and natural heritage, and nature conservation and participatory management planning in protected areas.

## Quantification Of Microorganism Composition Of Biohydrogen Production From The Dry Fermentation System By Real- Time Q-Pcr

C. Vural<sup>1</sup>, D. Aksu<sup>1,2</sup>, T. Keskin<sup>3</sup>, H. Nalakath Abubackar<sup>3</sup>, G. Ozdemir<sup>1</sup>, N. Azbar<sup>4</sup>

### Abstract

The composition of microorganisms is an effective and fundamental factor in the production of biohydrogen. *Clostridium* species are frequently encountered in the production of biohydrogen. Four specific real-time PCR primers of *Clostridium butyricum*, *Clostridium pasteurianum*, *Clostridium tyrobutyricum* and *Clostridium* 16S rRNA genes responsible for hydrogen production were synthesized and quantitative and qualitative results were determined by Real-time PCR. It has also been found that *Clostridium* species are responsible for the hydrogenase gene in the production of hydrogen. For this reason, the primers of the hydrogenase gene were also synthesized and evaluated quantitatively in Real-time PCR. In this study, where hydrogen production is carried out from fruits and vegetables wastes; the effect of particle size has been investigated. Samples were taken from the dry fermentor reactor system depending on the varying amounts of biohydrogen produced in three different parameters (autoclaved – small particles, non-autoclaved – small particle and autoclaved- large particles). In these samples taken from the dry fermentor reactor system, the number of *Clostridium* species present was discussed by evaluating the particle sizes. In order to provide quantitative results in real-time Q-PCR applications; cloning of species which are dominant in hydrogen production and hydrogenase gene have been performed. Maximum hydrogen production is obtained by autoclaving - in the case of small particles; 44%. *C. pasteurianum* was not found in this sample. The gene for the hydrogenase enzyme responsible for the production of hydrogen is 10<sup>6</sup> copies of the gene. In addition, *C. butyricum* and *C. tyrobutyricum* counts were 10<sup>5</sup> gene copies / mL.

**Keywords:** Quantitative real-time PCR, Biohydrogen Production, Dry Fermentation, *Clostridium* sp., Microbial Community Structure

### 1. INTRODUCTION

Biological hydrogen production methods mainly include fermentative and photosynthetic hydrogen production. Although photosynthetic hydrogen production is theoretically perfect process that converts solar energy to hydrogen and is a theoretical process, it is difficult to apply in practice due to the low utilization efficiency of the light and the difficulties in reactor design for the production of hydrogen. On the other hand, fermentative hydrogen production, high hydrogen production speed and simple operation has advantages [1]. Characterization of mixed cultures and determination of microbiota in fermentative hydrogen production is very important. In culture-related studies, only a limited proportion of microorganisms can be recovered. Culture-independent methods such as denaturing gradient gel electrophoresis (DGGE) have improved the problems of cultural methods by characterization of microbiology; it is not successful in quantitatively determining microbial communities. Fluorescent in situ hybridization (FISH) can provide quantitative data on cell numbers microscopically; however, it is not as easy and practical as real-time analysis [2]. Therefore, it is

<sup>1</sup> Ege University, Faculty of Science, Dept. of Biology, Basic and Industrial Microbiology Section, Bornova, İzmir, Turkey.

<sup>2</sup> Ege University Application and Research Center for Testing and Analysis, İzmir, Turkey.

<sup>3</sup> Ege University, Faculty of Engineering, Dept. of Bioengineering, Bornova, İzmir, Turkey.

<sup>4</sup> University la Coruña, Faculty of Sciences And Center for Advanced Scientific Research (Cica), La Coruña, Spain.

the most accurate method to perform quantitative analysis of the dominant microorganism species that play a role in hydrogen production by real-time reverse transcriptase-polymerase chain reaction (RT-PCR).

Literature-based studies; *Clostridium* species play a major role in the production of hydrogen by dark fermentation [3,4]. The most common strains of *Clostridium butyricum*, *Clostridium pasteurianum*, *Clostridium tyrobutyricum* and *Clostridium beijerinckii* etc. are generally used in fermentative systems using inoculated anaerobic wastes dominated by *Clostridium* sp.. For example *Clostridium butyricum*; It is known to produce hydrogen using various carbon sources, including monosaccharides (such as glucose, galactose, mannose), disaccharides (such as sucrose, lactose, maltose, trehalose) and polysaccharides (such as starch, inulin) [5].

The hydrogenase enzyme, which is directly responsible for the production of hydrogen, is found in *Clostridia* and can be detected using real-time Q-PCR (Hsiao, 2009). Hydrogenases; according to the metal content of the active site, [Fe] -, [FeFe] - and [NiFe] -hydrogenases are divided into three groups. *Clostridium* species which produce hydrogen in the normally have [FeFe]- hydrogenases. [NiFe]- hydrogenases are found in microorganisms that generally consume hydrogen (such as a methanogenic arch), which are responsible for the conversion of H<sub>2</sub> to CH<sub>4</sub>. Conversely; *Clostridia* destroy the hydrogenase enzyme that catalyzes the recycled oxidation of hydrogen [3].

In this study; the qualitative and quantitative analyzes of these three *Clostridium* species (*C. pasteurianum*, *C. butyricum*, *C. tyrobutyricum*) and the *Clostridium* 16S rRNA gene in the samples taken from the dry fermenter system were performed by real-time Q-PCR. In order to give quantitative results in real-time Q-PCR applications, the species which are dominant in hydrogen production and the cloning of the hydrogenase gene were performed. Also; Qualitative and quantitative analysis of the hydrogenase gene, which is normally involved in hydrogen production, was determined by real-time Q-PCR.

## 2. METARIALS AND METHODS

### 2.1. Inoculum and substrate

The Fruit and Vegetable Wastes (FVWs) were supplied during the winter season from the main hall of Izmir Municipality, Turkey. The flocculated inoculum was collected from the percolation tank of a dry anaerobic fermentation system. The inoculum was used without any pre-treatment.

### 2.2. Analytical methods

Chemical oxygen demand (COD) and Volatile solids (VS) content were measured according to the Standard Methods [6]. The initial and final pH values of each sample were measured with pH meter (Sartorius, PB 11). Total biogas production was measured by a 100 mL glass syringe (Fortuna, Germany). H<sub>2</sub> content of the total biogas was determined by a GC (6890N Agilent) equipped with a thermal conductivity detector and HayesepD 80/100 packed column [7]. Organic acids were analyzed using a GC (6890N Agilent) equipped with a flame ionization detector and DB-FFAP 30 m 0.32 mm 0.25 mm capillary column (J&W Scientific). The trace element analysis was conducted by ICP-OES by IZSU (Izmir Water Analysis Laboratory, Turkey).

### 2.3. DNA extraction

50 mL bioreactor samples in falcon tubes were used for DNA extraction. For this purpose, 3 cycles of sonication were applied to these tubes containing the samples, for 10 s with 90% power applied with a sonication probe (Bandelin SONOPULS™ GM 2070 Digital Ultrasonic Homogenizer, Germany). DNA extractions of these samples were carried out by using ZR Fungal/Bacterial Miniprep Kit (Zymo Research, USA). The purity of the isolated DNAs was checked and quantification performed on Nanodrop 2000c (Thermo Scientific) and mean values were measured as approximately 50 ng/mL with 1.75-1.80 purities at 260/280 nm wavelength. To visualize DNA extracts, 2 mL of each extract was electrophoresed on 1% agarose gels in 1xTAE buffer, which were then stained with gel red (Biotium) and examined under UV light in UVP Biospectrum Bioimaging Systems (Ultra-Violet Products Ltd., Cambridge UK).

### 2.4. Cloning and Plasmid DNA Isolation

*C. pasteurianum* (DSM-525), *C. butyricum* (DSM-10702), *C. tyrobutyricum* (DSM-2637), *Clostridium* sp. 16S rRNA gene region, and hydrogenase gene region, Gem-T easy vector systems (pGem-T Easy Vector Systems - Promega) used in study. Gene regions were transferred to the plasmid following the kit's protocol. *E. coli* JM 109 cell was used as recipient cell.

Plasmid DNA isolations were performed using NORGEN Biotek kit. The plasmid DNAs were isolated following the transfer of each gene region to the plasmid. The amounts and purities of plasmid DNAs were determined by measuring them at 260/280 nm at Nanodrop 2000c (ThermoScientific). As a result of the analysis, it was observed that the purity of all plasmids DNA was between 1.7-1.9.

### 2.5. Real-Time Q-PCR

For real-time Q-PCR analysis, LightCycler 96 System (Roche, Germany) was used. The reaction mixture was prepared using RealQ Plus Master Mix Green (Ampliqon) content. The primary sets to be used in analyzes are; 16S rRNA-encoding DNA region (CHISF - CLUSTER), *C. pasteurianum* (CpasteurianumF- CpasteurianumR) and gene region responsible for the production of hydrogenase enzyme (HGr - HGf) belonging to *Clostridium* sp. The primers sets of *C. butyricum* (CbutyHYDAf-CbutyHYDAr) and *C. tyrobutyricum* (CtyroW428f-CtyroW428r) were synthesized by using Primer3 and NCBI databases in this project. Two primer pairs used for each gene region are given in Table1.

Table 1. Oligonucleotides used in qrt-PCR

Oligonucleotides	Sequence from 5'-3'	Specificity	References
Chis15'f	AAAGGRAGATTAATACCGCATAA	<i>Clostridium</i> sp. 16S rRNA gene	[8]
Clustlr	TTCTTCCTAATCTCTACGCA	<i>Clostridium</i> sp. 16S rRNA gene	[8]
HG-f	AAGAAGCTTTAGAAGATCCTAA	Hydrogenase gene	[9]
HG-r	GGACAACATGAGGTAAACATTG	Hydrogenase gene	[9]
CbutyHYDAf	AGTGTTCAAATGTTGGTAAATGTG	<i>C. butyricum</i>	This study
CbutyHYDAr	CTCTTGTTGTTGCCCTCAGTATTAG	<i>C. butyricum</i>	This study
CtyroW428f	TCTGCCTCAAGTGTTCTCT	<i>C. tyrobutyricum</i>	This study
CtyroW428r	TCCTCCGTATTTATCTGTCCTT	<i>C. tyrobutyricum</i>	This study
C.pasteurianumF	CTCATGTGGGACTTCAAGCA	<i>C. pasteurianum</i>	[10]
C.pasteurianumR	CACCAGGTGTTGTTTCTGGA	<i>C. pasteurianum</i>	[10]

## 3. RESULTS AND DISCUSSION

Among the literature-based studies, it was determined that *Clostridium* species (*C. pasteurianum*, *C. butyricum*, *C. tyrobutyricum*) were found to be dominant in the production of hydrogen [11,12] The results of these literatures were supported in our study and it was observed that *Clostridium* species were high in the presence of high H<sub>2</sub>.

Samples were taken from the dry fermentor reactor system depending on the varying amounts of biohydrogen produced in three different parameters (autoclaved-small particles, non-autoclaved-small particles and autoclaved-large particles). Generally, if we look at H<sub>2</sub> production, the best result is autoclaving-small particle.

Looking at the results of solid fermentor 1-day (Figure 1) were not detected *Clostridium* species and hydrogenase gene. Already this sample has not production of H<sub>2</sub>. Maximum H<sub>2</sub> production is obtained by autoclaving in the case of small particles (44%) but was not found in this sample *C. pasteurianum*.

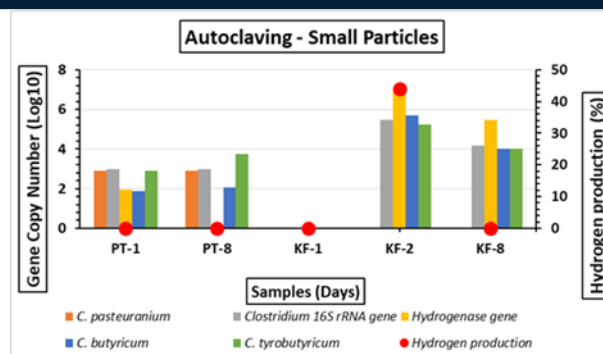


Figure 1. Results of the number of gene copy number and hydrogen production of autoclaving–small particle size samples.

As shown Figure 2, although the production of H<sub>2</sub> at percolation tank 17-day, the *Clostridium* species and hydrogenase gene were not detected. This situation is due to the presence of other organisms producing H<sub>2</sub> such as *Lactobacillus* species. When H<sub>2</sub> production is 13%, it was determined that there organisms were determined that gene copy number is 10<sup>4</sup>. But *C. pasteurianum* and *C. butyricum* was not. Although it had similar organism numbers with 12-days (KF) and 6-days, (KF) no H<sub>2</sub> was detected. This may be due to some microorganisms using hydrogen. Although the production of H<sub>2</sub> percolation tank 2-day, *Clostridium* species and hydrogenase gene were not detected.

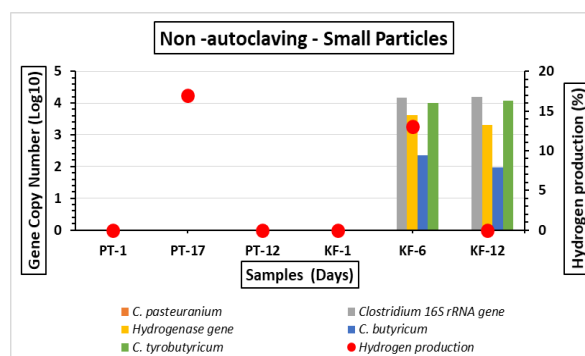


Figure 2. Results of the number of gene copy number and hydrogen production of non-autoclaving–small particle size samples.

As shown Figure 3, Looking at the results of solid fermentor (KF) 2.day, H<sub>2</sub> production is 36% and *C. butyricum* gene copy number is 10<sup>8</sup>.



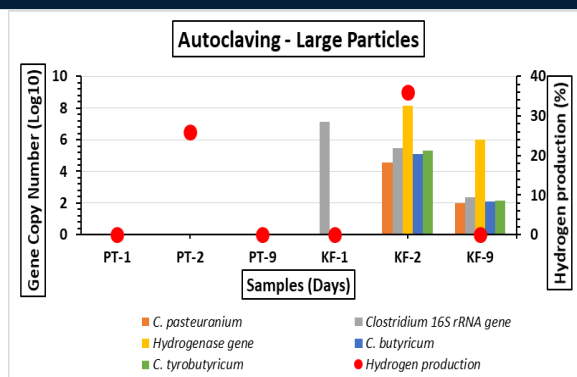


Figure 3. Results of the number of gene copy number and hydrogen production of autoclaving-large particle size samples.

*Clostridium* species are the main responsible for H<sub>2</sub> production in dark fermentation [13,14]. The organisms belonging to genus *Clostridium* such as *C.butyricum*, *C.tyrobutyricum*, *C.pasteurianum* are obligate anaerobe and spore forming organisms. The greatest difficulty with fermentative hydrogen production using mixed culture is the presence of hydrogen-consuming microorganisms in the same environment [15]. The result of the literature study has been found to solve this problem with high temperature application in many studies [16]. Samples were subjected to heat pre-treatment at 105 °C for 5 minutes in the autoclave. Looking at the results (Table 2) the level of hydrogen production was higher when autoclaved inoculum was used.

Table 2. Results of the number of gene copy number and hydrogen production of all of samples

		<i>C.pasteurianum</i>	<i>Clostridium</i> 16 S rRNA gene	Hydrogenase gene	<i>C.butyricum</i>	<i>C.tyrobutyricum</i>
Hydrogen production (%)	Sample name	Number of gene	Number of gene	Number of gene	Number of gene	Number of gene
Autoclaving- Small Particles						
-	PT Inoculum 1. Day	8.13E+02	9.56E+02	9.02E+01	7.38E+01	7.76E+02
-	PT 8. Day	8.33E+02	9.78E+02	0.00E+00	1.20E+02	5.48E+03
-	KF 1. Day	0.00E+00	0	0.00E+00	0.00E+00	0.00E+00
44	KF 2. Day	0.00E+00	2.93E+05	9.60E+06	4.84E+05	1.68E+05
-	KF 8. Day output	0.00E+00	1.53E+04	2.98E+05	1.06E+04	1.06E+04
Non autoclaving Small Particles						
-	PT Inoculum 1. Day	0.00E+00	0	0.00E+00	0.00E+00	0.00E+00
17	PT 17.day	0.00E+00	0	0.00E+00	0.00E+00	0.00E+00
-	PT 12. Day	0.00E+00	0	0.00E+00	0.00E+00	0.00E+00
-	KF inoculum 1.day	0.00E+00	0	0.00E+00	0.00E+00	0.00E+00
13	KF 6. Day	0.00E+00	1.51E+04	4.08E+03	2.22E+02	1.03E+04
-	KF 12. day output	0.00E+00	1.54E+04	2.04E+03	9.21E+01	1.17E+04

Autoclaving Large Particles						
-	PT Inoculum 1. Day	0.00E+00	0	0.00E+00	0.00E+00	0
26	PT 2. Day	0.00E+00	0	0.00E+00	0.00E+00	0
-	PT 9.day output	0.00E+00	0	0.00E+00	0.00E+00	0
-	KF inoculum 1.day	0.00E+00	1.42E+07	0.00E+00	0.00E+00	0
36	KF 2.day	3.77E+04	2.95E+05	1.39E+08	1.23E+05	1.95E+05
-	KF 9. Day output	1.02E+02	2.28E+02	9.75E+05	1.22E+02	1.34E+02

#### 4. CONCLUSIONS

During microbial consortium monitoring in tank with molecular methods, *Clostridium* species were monitored and dominated during the production of H<sub>2</sub>. Furthermore, with appropriate primer or probe design the method can be applied to different strains. Real-time PCR is applicable to any selected species in bioreactors and allows the determination of the microbial community structure during production of H<sub>2</sub> in reactor systems.

#### ACKNOWLEDGMENT

The authors wish to thank TUBITAK-MAG-215 M 314 for financial support of this study. We also thank to IZSU for their kind supports. HNA thanks the Xunta de Galicia (Spain) for his postdoctoral fellowship (ED 481B-2016/195-0).

#### BIOGRAPHY

Didem AKSU graduated from Biology Department at Ege University in 2009. She has a master and Ph.D. degrees in Basic and Industrial Microbiology Section at Ege University. In her Ph.D. work, she has investigated about biodegradation of wastewater. His main research interests are in the field of molecular biology, microbiology. Currently, she is a research assistant in Application and Research Center for Testing and Analysis at Ege University.

#### REFERENCES

- [1]. Genc, N. "Atik Aritma Camurlarından Biyohidrojen Uretimi", Journal of Engineering and Natural Sciences, Sigma 28, 235-248, 2010.
- [2]. Tolvanen, K. E. S., Koskinen, P. E. P., Ylikoski, A. I., Ollikkab P.K., Hemmila, I.A., Puhakka, J.A., Karpa, M.T. "Quantitative monitoring of a hydrogen-producing *Clostridium butyricum* strain from a continuous-flow, mixed culture bioreactor employing real-time PCR", International Journal of Hydrogen Energy 33:542-549, 2008. doi:10.1016/j.ijhydene.2007.10.005
- [3]. Vasconcelos de Sa, L.R., Oliveira, T.C., Santos, T.F., Matos, A., Cammarota, M.C., Morais Oliveira, E.M., Ferreira-Leita, S. "Hydrogenase activity monitoring in the fermentative hydrogen production using heat pretreated sludge: A useful approach to evaluate bacterial communities performance", International Journal of Hydrogen Energy 36:7543-7549, 2011. doi:10.1016/j.ijhydene.2011.03.119
- [4]. Hsiao, C.L., Chang, J.J., Wua, J.H., Chinc, W.C., Wenc, F.S., Huang, C.C., Chen, C.C., Lina, C.Y. "Clostridium strain co-cultures for biohydrogen production enhancement from condensed molasses fermentation solubles" International Journal of Hydrogen Energy, 34:7173-7181, 2009. doi:10.1016/j.ijhydene.2009.06.028
- [5]. Wang, J. and Yin, L. "Biohydrogen Production from Organic Wastes", Green Energy and Technology, Springer, Singapore, ISSN 1865-3529, 2017.
- [6]. American Public Health Association, APHA, AWWA. Standard methods for the examination of water and wastewater. 20th ed. 1998 [Washington DC, USA].
- [7]. Azbar N, Dokgoz FT, Keskin T, Eltem R, Korkmaz KS, Gezginy Akbal Z, et al. Comparative evaluation of biohydrogen production from cheese whey wastewater under thermophilic and mesophilic anaerobic conditions. Int J Green Energy 2009;6:2,192e200. https://doi.org/10.1080/15435070902785027.
- [8]. Cheng, C.H., Hung, C.H., Lee, K.S., Liao, P.Y., Yang, L.H., Lin, P.J. and Lin, Y. "Microbial community structure of a starch-feeding fermentative hydrogen production reactor operated under different incubation conditions" Int.J.Hydrogen Energy, 33:5242-5249, 2008.

- [9]. Wang, M. Y., Tsai, Y. L., Olson, B. H. & Chang, J. S. "Monitoring dark hydrogen fermentation performance of indigenous *Clostridium butyricum* by hydrogenase gene expression using RT-PCR and qPCR", *Int J Hydrogen Energy* 33:4730–4738, 2008.
- [10]. Savichtcheva, O., Joris, B., Wilmotte, A., Calusinska, M. "**Novel FISH and quantitative PCR protocols to monitor artificial consortia composed of different hydrogen-producing *Clostridium* spp.**", *Int J Hydrogen Energ.*, **36**: 7530-7542, 2010.
- [11]. Minton, N.P., Clarke, D.J. *Clostridia* (Volume 3), Biotechnology handbooks, New York: Plenum Press., 1989.
- [12]. Brosseau, J.D., Zajic, J.E. "Hydrogen gas production with *Citrobacter intermedium* and *Clostridium pasteurianum*", *Journal of Chemical Technology & Biotechnology*, 32, 496., 1982.
- [13]. Yokoi, H., Saito, A., Uchida, H., Hirose, J., Hayashi, S., Takasaki, Y. Microbial hydrogen production from waste potato starch residue. *J Biosci Bioeng*, 91 pp. 339-343, 2001.
- [14]. Noike, T., Takabatake, H., Mizuno, O., Ohba M. Inhibition of hydrogen fermentation of organic wastes by lactic acid bacteria *Int J Hydrogen Energy*, 27 pp. 1367-1371, 2002.
- [15]. Zhang, T., Liu, H. And Fang H., Biohydrogen production from starch in wastewater under thermophilic condition, *Journal of Environmental Management*, 69:149-156., 2003
- [16]. Van Ginkel, S., Sung, S., and Lay, J.J. Biohydrogen Production as a Function of pH and Substrate Concentration. *Environ. Sci. Technol.*, 35, 4726, 2001.

# Recent advances in membrane fouling control in wastewater treatment processes

*Amar Ćemanović<sup>1</sup>, Neslihan Manav<sup>2</sup>, Abdullah Kizilet<sup>3</sup>, Ozer Cinar<sup>4</sup>*

---

## Abstract

*Membrane bioreactors (MBRs) are systems performing biological wastewater treatment with membranes utilized for solids separation. These systems have a wide range of applications since they offer some important advantages over conventional processes (e.g. high solids removal, low sludge production etc.). One of their main drawbacks, however, is the occurrence of membrane fouling – the occlusion of membrane pores by the various components found in the mixed liquor. Factors contributing to this phenomenon are various and stem from all the aspects of the treatment process, including membrane-, biomass- and wastewater characteristics as well as operating conditions. Efficient fouling control requires a thorough insight into reactor operation and the mechanisms leading to membrane fouling in the first place. While there are some universal remedies, proper tackling of this problem requires an individual approach tailored to the system of concern, since best results originate from the utilization of several methods together. This review outlines novel and emerging methods having a potential to contribute to sustainable and economical membrane fouling mitigation in the future.*

**Keywords:** Biological processes, wastewater treatment, membrane bioreactors, membrane fouling.

---

## 1. INTRODUCTION

The first use of membrane bioreactor technology has been reported in 1969 by Smith et al. [1]. It was utilized with ultrafiltration membranes in a pilot-scale plant treating industrial wastewater. Even though the initial systems had many disadvantages, such as high capital costs and challenges in operation (mainly due to excessive membrane fouling), MBR slowly started to gain recognition and popularity. The advantages that allowed the MBR to start replacing many of the conventional systems widely in use are its low footprint (since no settling tank is necessary), high treatment efficiency, low sludge production, ease of retrofitting to existing systems etc.

Membranes utilized in MBR systems have a pore size range of  $10^3$  -  $10^{-4}$   $\mu\text{m}$ . Based on it, the process is called microfiltration (MF), ultrafiltration (UF), nanofiltration (NF) or reverse osmosis (RO). Another division among MBR systems takes into account the system setup. Namely, the membrane modules may be located in the treatment tank itself (submerged system) or in a separate tank (side-stream system). For either of the mentioned configurations, the membrane itself can be in the form of a flat sheet or hollow fibers. All of these options are an important aspect of reactor design and operation and need to be carefully chosen based on the specific needs of the system in question.

## 2. FACTORS AFFECTING MEMBRANE FOULING

Due to the vast number of factors involved in wastewater treatment, there is no single system which suits all applications. Each system comes with its inherent advantages and disadvantages, and the membrane bioreactor systems are no exception. Apart from the aforementioned advantages, there are certain drawbacks as well when

---

<sup>1</sup> Istanbul Technical University, Department of Environmental Engineering, Maslak/Istanbul, Turkey.

<sup>2</sup> Department of Bioengineering and Sciences, Kahramanmaraş Sutcu İmam University, 46100, Kahramanmaraş, Turkey,

<sup>3</sup> Yildiz Technical University, Department of Environmental Engineering, 34220, Esenler/Istanbul, Turkey.

<sup>4</sup> Corresponding author: Yildiz Technical University, Department of Environmental Engineering, 34220, Esenler/Istanbul, Turkey. [ocinar@yildiz.edu.tr](mailto:ocinar@yildiz.edu.tr)

compared to conventional systems (CAS). Those include process complexity, relatively high capital and operating costs, increased foaming propensity and, most prominently, membrane fouling.

Membrane fouling can best be described as occlusion of membrane pores leading to decrease in filtration flux (in case of constant pressure operation mode) or increase in transmembrane pressure (TMP; in case of constant flux operation mode). It is not to be confused with clogging which occurs between membrane sheets or fibers inside modules/cassettes. There are many factors that affect the fouling propensity of a given system, and they can be broadly grouped into: membrane-, wastewater-, and biomass characteristics, as well as operating conditions (Figure 1).

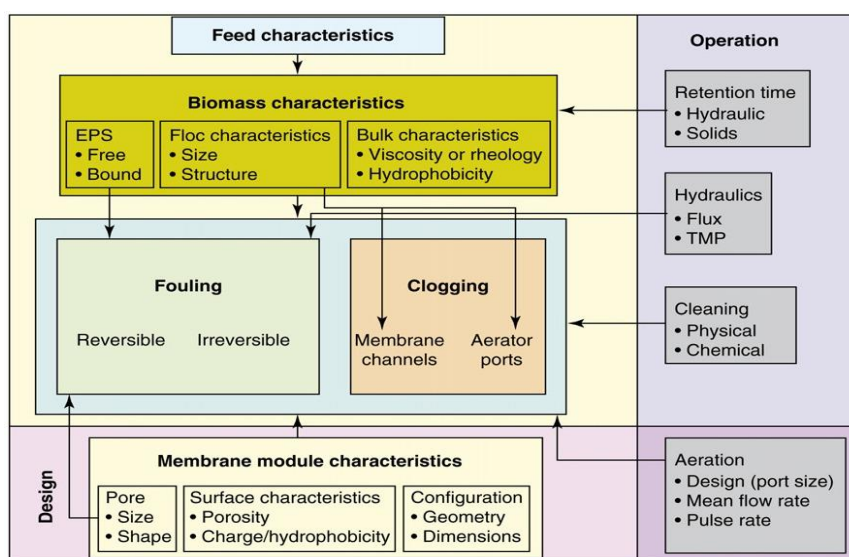


Figure 15. Interrelationship between MBR parameters and fouling [2]

## 2.1. Membrane characteristics

The proper choice of membranes for MBR systems is of crucial importance for the proper functioning and maintaining of the system. Membranes differ in the following aspects: material, pore size, porosity, hydrophobicity, charge, module etc. [3].

Membranes utilized in MBR systems are generally of polymeric nature, although inorganic membranes are also being used, as well as support materials (mostly textile) which are utilized for dynamic MBR (DMBR) systems. The main property they have to display is durability when exposed to various chemicals, varying pH levels, oxidants, varying temperatures as well as mechanical wear. While inorganic membranes are quite robust, their high price and limitations in their manipulation render them a relatively unpopular choice for MBRs. The most commonly used polymeric membrane material is PVDF (Polyvinylidene Difluoride), but others are also popular and include PTFE (polytetrafluoroethylene), polyolefins, PSF (polysulfonate), CA (cellulose acetate) etc. The support materials used for DMBR systems are generally of a larger pore size than commercial membranes and can be obtained at a much lower cost. They include different textile materials, woven and non-woven meshes etc.

Pore size has to be determined by considering the size of particles from the feed solution, since in the event that the two are similar, an increase in fouling probability occurs. Hereby, pore size distribution and the average pore size are the parameters considered. Porosity refers to the fraction of pores/voids in a material. Hydrophobicity is important since hydrophobic membranes are more prone to fouling, as they interact more closely with hydrophobic components of the feed solution. In order to alleviate this drawback, such membranes may be surface-modified. Charge is similarly important due to interactions on the membrane surface. Finally, module design and placement directly correlate with feed flow and particle occlusion, and have to be optimized in order to preclude fouling or clogging.

## 2.2. Wastewater characteristics

While domestic wastewater is mostly of similar composition everywhere, industrial wastewater is much more specific and differs largely based on the type of industry and the processes being applied. The influent wastewater affects both the biomass in the reactor as well as the membrane directly. Parameters such as turbidity and suspended solids concentration may represent the effect on the membrane, while COD, nutrient content, and potential toxicity exert their effect largely on the biomass. Other important parameters include temperature, pH, alkalinity etc.

## 2.3. Biomass characteristics

Biomass characteristics depend on its composition, the type of wastewater as well as the operating conditions. The main characteristics considered in MBR fouling studies include floc structure and floc size distribution, MLSS concentration, dissolved matter and EPS concentration etc. [3].

## 2.4. Operating conditions

The specific parameters that govern reactor operation and have a direct or indirect effect on membrane fouling are: aeration, HRT, SRT, F/M ratio, TMP/critical flux, hydrodynamics configuration, crossflow velocity etc. [3]. The reactor concentration of oxygen affects microbial growth and metabolism directly, but aeration in MBR systems also has an additional role. Namely, coarse air bubbles applied on the membrane surface in submerged systems cause shear stress which can maintain the thickness of the cake layer at a tolerable level [4]. When it comes to HRT, SRT and the F/M ratio, these parameters mostly affect the microbial biomass, i.e. its growth, flocking, EPS concentration etc. TMP and critical flux, on the other hand, are directly related to the fouling process and thus have to be closely controlled. Operating the reactor at a flux higher than the critical flux value leads to excessive fouling.

## 3. CLASSIFICATION OF MEMBRANE FOULING

There are various classifications of membrane fouling found in the literature. One of them is based on the possibility to remove fouling using specific cleaning processes. Namely, Park et al. [3] divide it into reversible and irreversible fouling, meaning that the former can be removed by physical or chemical cleaning (or a combination thereof), whereas the latter cannot be removed whatsoever. After irreversible fouling accumulates to a certain extent, the only way to recover initial flux/TMP values is to replace the membrane. Additionally, reversible fouling is further divided into recoverable and irrecoverable. Recoverable fouling can be removed by simple means, i.e. physical cleaning, backwashing etc., whereas irrecoverable requires the use of chemicals.

Another way fouling is classified is based on the place of its occurrence. Accordingly, it can be cake layer deposition or internal pore fouling. The former refers to the accumulation of solids on the surface of the membrane, whereby they form a so-called cake layer. That layer acts as a secondary membrane, with its own pores and permeability. This property is being exploited in DMBR systems, since the original membrane, called support material, has a relatively large pore size. On the other hand, internal pore fouling occurs when particles smaller than the pore diameter get stuck inside, thereby decreasing the amount of permeate that can pass through.

A further way of classification is according to the solids deposition pattern. Hereby, the solids that enter the pores of the membrane may either cause its narrowing or block it completely. Those that accumulate on the surface, however, form a cake layer, as previously mentioned (Figure 2).

## 4. ESTABLISHED MEMBRANE FOULING CONTROL METHODS

When it comes to membrane fouling control, there are two principle ways to approach the issue: membrane cleaning and fouling prevention.

Membrane cleaning can be physical in nature, including processes such as air sparging, intermittent aeration, backwashing (with air or permeate) as well as sponge scouring. It can also be chemical, which is usually the submersion of the membrane in an acid and/or basic solution. Physicochemical methods such as chemically enhanced backwashing are also in use.

Prevention of membrane fouling is performed in different ways, the most common of which is pretreatment of the influent wastewater. This involves methods such as coarse and fine screening, grit removal, primary



sedimentation etc. Pretreatment is performed in conventional systems as well, but has a special importance in MBR systems due to their propensity for fouling. Another way of fouling prevention is operation of the reactor at subcritical flux level, as well as close control of sludge parameters, including MLSS, HRT, SRT, DO, F/M ratio.

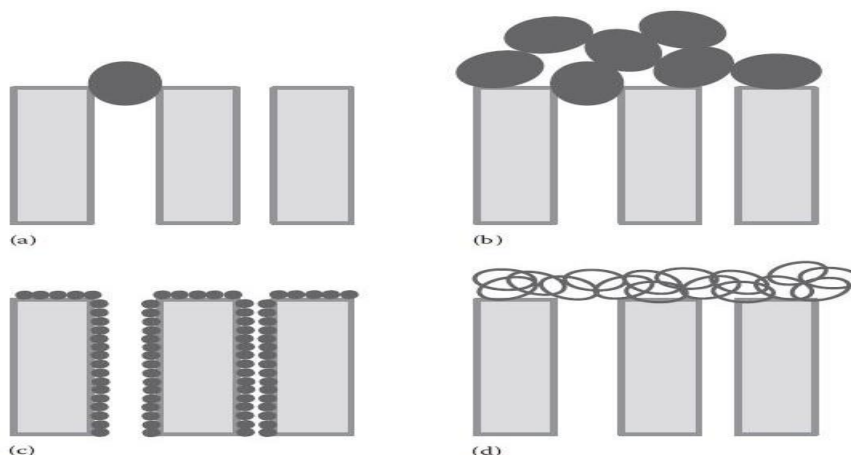


Figure 16. Mechanisms of membrane fouling according to solids deposition pattern: a) complete blocking, b) internal pore blocking, c) intermediate blocking, and d) cake formation [3].

One of the more advanced approaches to the problem of membrane fouling is biological control. There are several established methods, such as quorum quenching, enzymatic digestion, as well as utilization of nitric oxide (NO) and bacteriophages.

Quorum quenching is basically the inhibition of quorum sensing (QS), a means of bacterial communication through signal molecules which enables them to produce biofilms [5]. The main approaches hereby are prevention of the production of these signal molecules, interference with the receptor of the signal or inactivation of the signals [6]. An example of the latter can be found in studies [7] and [8].

When it comes to enzymatic digestion, it can be applied on different levels, be it to biodegrade the aforementioned signal molecules or the biofilm directly. The latter works by targeting EPS, the main building material that connects bacteria into a biofilm. Several groups reported success applying this approach ([9], [10], [11]), but some concerns remain due to the short catalytic lifetime and loss of free enzymes.

Nitric oxide is a biological messenger molecule which signals bacteria to disperse their biofilm [5]. It has been shown to work for a wide range of bacterial species. The downside to this approach is the low solubility of NO in water.

Bacteriophages are a type of virus which specifically attacks bacteria, wherein it propagates eventually killing its host. In wastewater treatment applications, they have been shown to inhibit or disrupt biofilm formation on membrane surfaces ([12], [13], [14]). One of the major disadvantages of this method is the high specificity of bacteriophages against the target bacteria.

Another important approach to fouling control is through the use of electricity-based methods, the most prominent being electrocoagulation and electrophoresis.

Electrocoagulation works in-situ by creating metal cations at the anode (e.g.  $\text{Fe}^{3+}$ ,  $\text{Al}^{3+}$  etc.) which then act as coagulating agents, reducing the charge difference between particles in the solution and thereby enabling them to coagulate into larger flocs. The method has been proven efficient ([15], [16]) and has a major advantage over chemical coagulation – no chemical sludge is produced. However, with this approach, care has to be taken to provide optimized conditions so as not to cause bacterial inactivation.

Electrophoresis applications, on the other hand, exploit the negative charge found on particles in the aqueous solution of the reactor. Namely, a direct current (DC) electric field applied close to the membrane drives off the particles from the membrane and towards the anode ([17], [18]). The main limiting factors in the utilization of this method are electrode corrosion and high energy consumption.

There is a variety of methods dealing with modifications of the properties of both membranes and modules. Membrane modification is most often performed by surface modification to decrease the hydrophobicity, which is performed either by coating or grafting a functional group. Another prominent method involves modification of the surface morphology to reduce microbial deposition. When it comes to module modification, it most often comes down to alterations of shape in order to create more favorable hydrodynamic conditions.

Finally, dynamic MBR systems are viewed as an improvement over conventional MBRs when it comes to cost and membrane fouling. These systems rely on support materials with a larger pore size, on top of which a secondary (cake) layer forms (dynamic membrane). This layer is composed of solids from the solution, and has a pore size comparable to that of microfiltration membranes. Due to the fact that mostly inexpensive textile materials and meshes are used as support material, these systems have a lower capital cost than conventional MBRs. Furthermore, since biomass retention is performed by the secondary layer, the support material is much less prone to fouling. Flux/TMP recovery is mostly as easy as removing the cake layer. However, the drawback of DMBRs is that initial effluent quality is low, until the secondary membrane is fully formed (unless pre-formed dynamic membrane is used).

## 5. RECENT DEVELOPMENTS IN MEMBRANE FOULING CONTROL

Being a major drawback of MBR systems, membrane fouling is being addressed by a considerable number of studies. New fouling control methods are being devised regularly, and the following sections describe some of the most promising among them.

### 5.1. Addition of adsorbents

Adsorbents are porous compounds having the ability to bind different molecules from the surrounding medium to their surface. When it comes to MBR systems, these compounds can help control membrane fouling by removing organics and other pollutants from solution, or providing a surface for attached growth of biomass. The most commonly applied adsorbents are powdered and granular activated carbon (PAC and GAC, respectively) [19]. PAC concentration has to be determined carefully, since the small size of the particles coupled with a high dosage can worsen the fouling of membranes. GAC, on the other hand, has a larger particle size and is therefore suitable as biologically activated carbon, which is covered in the next section.

### 5.2. Mechanically assisted membrane aeration scouring

This method encompasses the addition of abrasive particles to the reactor solution so as to enhance the membrane surface scouring. Most often used are GAC, plastic beads or other biofilm carriers. With the exception of GAC, they all perform a dual role, acting both as abrasive for the membrane and as a surface for attached growth of the biomass. GAC has the added property of being a potent adsorbent (in this context termed biologically activated carbon), and as such has been shown to be able to provide a 20-60% enhancement of flux ([20] and [21]). Additionally, the property of having both suspended and attached growth in the same reactor contributes significantly to the wastewater treatment efficiency of the system. Not all types of biofilm carrier work for all systems, though, so more research is needed in this field.

### 5.3. Novel membrane developments

Increase in turbulence near the membrane surface has been shown to be an efficient tool against membrane fouling. This is generally accomplished with rotating and vibrating membranes. The idea behind this is to provide a force that would be able to scour or shake off loosely bound particles on the surface of the membrane, before they achieve a stable integration into the existing cake layer/biofilm. Different studies showed the benefits of this approach, whereby a higher rotation speed has been associated with higher fouling mitigation, but only up to a certain threshold ([22], [23], and [24]).

### 5.4. Ultrasonic cleaning of membranes

An advanced method of physical cleaning of membranes is with the use of ultrasonic sound waves. These waves are in the frequency range of >20kHz and act by agitating the particles in the membrane, thereby loosening them and causing them to become detached. The main advantage of this method is high flux recovery and the possibility to apply it in-situ [25].

### **5.5. Cell immobilization**

This method limits the free movement of bacterial cells by one of two ways: attachment to a support (mostly biofilm carriers) or cell entrapment (CE) with the use of porous polymer matrices [26]. The former mainly refers to operating an attached growth system, whereas the latter can also offer some level of protection of the biomass from toxic compounds. Materials applied for the matrices range from natural materials such as alginate, agar, and carrageenan, to synthetic polymers including polyacrylamide, polyvinyl alcohol, xanthan gum etc. [5]. An important advantage of CE is that in addition to preventing the biomass from reaching the membrane, it also lowers the levels of bound SMP and EPS, which are known to contribute to fouling.

### **5.6. Improvements in chemical cleaning**

The main innovation when it comes to chemical cleaning of MBR membranes comes in the form a novel biosurfactant – rhamnolipids. These compounds offer advantages in the form of lower cost, higher solubility and less toxicity than conventional methods [5]. Their mode of action is based on biofilm reduction and detachment [27]. It was also reported that, when added during reactor operation, they increased contact between bacteria and lipid molecules, thereby enhancing their removal [28].

### **5.7. Novel biological control methods**

D-amino acids are compounds shown to be able to trigger biofilm disassembly even in trace amounts [29]. Since they can be produced and secreted by a number of bacterial species, they offer a low-cost strategy in fouling control. However, D-amino acids have been shown to be species-specific, which significantly limits their application. In addition, some naturally derived compounds have also shown promise in biofilm inhibition. Those include extracts from ginger [30], garlic [31], ginseng [32] and brominated alkylidene lactams [33]. Their advantage is that they have low- to no toxicity to the biomass, and may offer a cheap solution depending on their accessibility.

### **5.8. Addition of engineered nanomaterials (ENMs)**

Various engineered nanomaterials (ENMs) can be utilized in MBR systems for efficient fouling control. These materials have specific properties which make them particularly suitable for this purpose, such as antimicrobial ability, photocatalytic activity, and hydrophilicity. Among these ENMs are silver nanoparticles (NPs), graphene, graphene oxide, fullerenes, carbon nanotubes, titanium dioxide NPs etc. [34]. They can be used as membrane surface additions or supplied to the reactor directly. Some of the disadvantages of these systems include the potentially high cost and limited accessibility, as well as limited photocatalytic activity in systems with a high turbidity.

## **6. CONCLUSION**

Membrane fouling is the major disadvantage of MBR systems and has, accordingly, received much attention in the literature. A large number of factors contributes to this phenomenon, which makes its mitigation much harder a task. Apart from established methods, researchers all over the world are constantly devising new ways to enrich the toolbox of reactor operators in their struggle to get fouling under control. Often several methods have to be used in conjunction in order to achieve the best results, and there is no single approach which suits all systems. Therefore, a delicate balance has to be found between gains (lower fouling propensity, improved flux etc.) and losses (cost, higher sludge production etc.) in the application of fouling control methods.

## **ACKNOWLEDGEMENTS**

Author Amar Ćemanović is supported by the Scientific and Technological Research Council of Turkey (Tubitak) through the 2215 Graduate Scholarship Programme.

## **REFERENCES**

- [1]. C.V. Smith, D.D. Gregorio and R.M. Talcott, "The use of ultrafiltration membranes for activated sludge separation", 24th Annual Purdue Industrial Waste Conference, Lafayette, IN pp. 130-1310, 1969.
- [2]. S. Judd, "The status of membrane bioreactor technology", Trends in Biotechnology, 26, 2, 109 – 116., 2008.
- [3]. H.-D. Park, I.-S. Chang and K.-J. Lee, *Principles of Membrane Bioreactors for Wastewater Treatment*, Boca Raton, FL, USA: CRC Press, Taylor and Francis Group, 2015.
- [4]. P. Le-Clech, V. Chen, T.A. Fane, "Fouling in membrane bioreactors used in wastewater treatment." J. Membr. Sci. 284 (1), 17–53, 2006.

- [5]. M. Bagheri, S.A. Mirbagheri, "Critical review of fouling mitigation strategies in membrane bioreactors treating water and wastewater." *Bioresource Technology* 258, 318–334, 2018.
- [6]. T.B. Rasmussen, M. Givskov, "Quorum sensing inhibitors: a bargain of effects." *Microbiology* 152 (4), 895–904, 2006.
- [7]. D.M. Roche, J.T. Byers, D.S. Smith, et al., "Communications blackout? Do N-acylhomoserine-lactone-degrading enzymes have any role in quorum sensing?" *Microbiology* 150 (7), 2023–2028, 2004.
- [8]. K.-M. Yeon, W.-S. Cheong, H.-S. Oh, et al., "Quorum sensing: a new biofouling control paradigm in a membrane bioreactor for advanced wastewater treatment." *Environ. Sci. Technol.* 43 (2), 380–385, 2008.
- [9]. I.P. Molobela, "Protease and amylase enzymes for biofilm removal and degradation of extracellular polymeric substances (EPS) produced by *Pseudomonas fluorescens* bacteria." *Afr. J. Microbiol. Res.* 4 (14), 1515–1524, 2010.
- [10]. M. Loisel, K.W. Anderson, "The use of cellulase in inhibiting biofilm formation from organisms commonly found on medical implants." *Biofouling* 19 (2), 77–85, 2003.
- [11]. S. Te Poelle, J. Van der Graaf, "Enzymatic cleaning in ultrafiltration of wastewater treatment plant effluent." *Desalination* 179 (1–3), 73–81, 2005.
- [12]. A. Branch, T. Trinh, G. Carvajal, et al., "Hazardous events in membrane bioreactors—Part 3: impacts on microorganism log removal efficiencies." *J. Membr. Sci.* 497, 514–523, 2016.
- [13]. R.M. Chaudhry, K.L. Nelson, J.R.E. Drewes, "Mechanisms of pathogenic virus removal in a full-scale membrane bioreactor." *Environ. Sci. Technol.* 49 (5), 2815–2822, 2015.
- [14]. S. Purnell, J. Ebdon, A. Buck, et al., "Bacteriophage removal in a full-scale membrane bioreactor (MBR)—implications for wastewater reuse." *Water Res.* 73, 109–117, 2015.
- [15]. W. Den, C.-J. Wang, "Removal of silica from brackish water by electrocoagulation pretreatment to prevent fouling of reverse osmosis membranes." *Sep. Purif. Technol.* 59 (3), 318–325, 2008.
- [16]. K. Bani-Melhem, M. Elektorowicz, "Development of a novel submerged membrane electro-bioreactor (SMEBR): performance for fouling reduction." *Environ. Sci. Technol.* 44 (9), 3298–3304, 2010.
- [17]. L. Liu, J. Liu, B. Gao, B., et al., "Fouling reductions in a membrane bioreactor using an intermittent electric field and cathodic membrane modified by vapor phase polymerized pyrrole." *J. Membr. Sci.* 394, 202–208, 2012.
- [18]. J.-P. Chen, C.-Z. Yang, J.-H. Zhou, et al., "Study of the influence of the electric field on membrane flux of a new type of membrane bioreactor." *Chem. Eng. J.* 128 (2), 177–180, 2007.
- [19]. O. Kulesha, Z. Maletskyi, H. Ratnaweera, "State-of-the-art of membrane flux enhancement in membrane bioreactor." *Cogent Engineering*, 5: 1489700, 2018.
- [20]. M.A.H. Johir, R. Aryal, S. Vigneswaran, et al., "Influence of supporting media in suspension on membrane fouling reduction in submerged membrane bioreactor (SMBR)." *Journal of Membrane Science*, 374(1–2), 121–128, 2011.
- [21]. M.A. Johir, S. Shanmuganathan, S. Vigneswaran, et al., (2013), "Performance of submerged membrane bioreactor (SMBR) with and without the addition of the different particle sizes of GAC as suspended medium." *Bioresource Technology*, 141, 13–18, 2013.
- [22]. D.-Y. Zuo, H.-J. Li, H.-T. Liu, et al., "A study on submerged rotating MBR for wastewater treatment and membrane cleaning." *Korean J. Chem. Eng.* 27 (3), 881–885, 2010.
- [23]. T. Jiang, H. Zhang, D. Gao, et al., "Fouling characteristics of a novel rotating tubular membrane bioreactor." *Chem. Eng. Process.: Process Intensif.* 62, 39–46, 2012.
- [24]. T. Jiang, H. Zhang, H. Qiang, et al., "Start-up of the anammox process and membrane fouling analysis in a novel rotating membrane bioreactor." *Desalination* 311, 46–53, 2013.
- [25]. L. M. Ruiz, J. I. Perez, A. Gómez et al., "Ultrasonic irradiation for ultrafiltration membrane cleaning in MBR systems: operational conditions and consequences." *Water Sci Technol.* 75 (4): 802–812., 2016.
- [26]. C. Juntawong, C. Rongsayamanont, E. Khan, "Entrapped cells-based-anaerobic membrane bioreactor treating domestic wastewater: performances, fouling, and bacterial community structure." *Chemosphere* 187, 147–155, 2017.
- [27]. L.H. Kim, Y. Jung, S.-J. Kim, et al., "Use of rhamnolipid biosurfactant for membrane biofouling prevention and cleaning." *Biofouling* 31 (2), 211–220, 2015.
- [28]. L. Qin, G. Zhang, Q. Meng, et al., "Enhanced submerged membrane bioreactor combined with biosurfactant rhamnolipids: performance for frying oil degradation and membrane fouling reduction." *Bioresour. Technol.* 126, 314–320, 2012.
- [29]. I. Kolodkin-Gal, D. Romero, S.G. Cao, et al., "D-Amino Acids Trigger Biofilm Disassembly." *Science* 328 (5978), 2010.
- [30]. H.S. Kim, H.D. Park, "Ginger Extract Inhibits Biofilm Formation by *Pseudomonas aeruginosa* PA14." *PLoS One* 8 (9), 2013.
- [31]. T. Bjarnsholt, P.O. Jensen, T.B. Rasmussen, et al., "Garlic blocks quorum sensing and promotes rapid clearing of pulmonary *Pseudomonas aeruginosa* infections." *Microbiol. Sgm* 151, 2005.
- [32]. H. Wu, B. Lee, L. Yang, et al., "Effects of ginseng on *Pseudomonas aeruginosa* motility and biofilm formation." *Fems Immunol.* Med. Microbiol. 62 (1), 2011.
- [33]. U.A. Pereira, L.C.A. Barbosa, C.R.A. Maltha, et al., "Gamma-Alkylidene-gamma-lactones and isobutylpyrrol- 2(5H)-ones analogues to rubrolides as inhibitors of biofilm formation by Gram-positive and Gram-negative bacteria." *Bioorg. Med. Chem. Lett.* 24 (8), 1052, 2008–2008, 2014.
- [34]. F. Meng, S. Zhang, Y. Oh, et al., "Fouling in membrane bioreactors: An updated review." *Water Research* 114: 151–180, 2017.

## The Importance of Ventilation for Indoor Air Quality

*Bahtiyar Ozturk<sup>1</sup>, Hulya Aykac Ozen<sup>1</sup>, Hamdi Obekcan<sup>1</sup>*

### Abstract

*Indoor air quality (IAQ) has a pretty high importance for healthy indoor environment in which most people spend more than 90% of their daily time. We believe that the indoor air is more cleaner than outside because the building shelter us from harmful effects of substances exist in outside air. But, Environmental Protection Agency (EPA) indicated that concentrations of some pollutants may be 2-5 times, and occasionally more than 100 times higher than outside levels. Therefore, EPA ranked indoor air pollution (IAP) among the top five environmental risks to public health. The most common technique to reduce pollutant concentrations to acceptable levels in buildings is to feed fresh air into indoor environment either by natural or mechanical ventilation. In order to provide a healthy and comfortable indoor environment a suitable and effective ventilation system must be designed and operated. In this paper major principles of effective ventilation systems for indoor have been discussed and made clear.*

**Keywords:** ventilation, indoor air quality, ventilation design

### 1. INTRODUCTION

Indoor air pollution is the existing of particulate and gaseous constituents above the acceptable levels in an enclosed space. Good indoor air quality is the air free of pollutants which cause unhealthy and discomfort of occupants in an enclosed space. Good IAQ is defined by the absence of harmful or unpleasant constituents (ASHRAE, 2009). Thermal conditions, relative humidity and noise are also parameters that effect occupant comfort. Poor Indoor Air Quality (IAQ) is among the top five environmental risks (USEPA, 2016)

After energy crisis in mid 1970s, energy conservation became a key issue for residential, office, school and industrial buildings. One way to reduce energy requirement or consumption for enclosed spaces is to seal buildings from outside air by using more tight building equipments. This tightness of buildings resulted in the accumulation of pollutants inside, and exposure to pollutants caused health problems for occupants. According to WHO (2000a), diseases caused by poor IAQ are allergic and asthma symptoms, lung cancer, chronic obstructive pulmonary disease (COPD), airborne respiratory infections, cardiovascular disease (CVD), odour and irritation (SBS symptoms), and stress. Symptoms commonly attributed to indoor air quality (IAQ) problems include headache, fatigue and shortness of breath, sinus congestion, cough and sneezing, eye, nose, throat and skin irritation, dizziness and nausea [4]. Most people spent 90 percent of their daily time in indoors, and because of this, indoor air quality becomes an important health concern for human beings.

The concentration of pollutants in a closed area depends generally on the ventilation rate and emission rates. Heating, cooling, openings on the shell, ventilation system, emission from building materials, furniture, goods and belongings, thermal performance and weather condition are influenced by many factors [5]. In order to provide a good IAQ, source control for pollutants and feeding in the fresh air are the major goals. IAQ and ventilation are linked because good ventilation is one of the main methods of controlling IAQ. The agenda or topics regarding IAQ that were discussed in the study were directly informed by the literature review.

### 2. VENTILATION FOR GOOD IAQ

Ventilation of buildings in general may be done for several reasons, the most important is to remove or dilute the indoor generated pollutants and supply fresh air for human beings. The enclosed area must be ventilated either by natural or mechanical way to provide acceptable IAQ. A preferred ventilation system must supply

<sup>1</sup>Corresponding author: Ondokuz Mayıs University, Department of Environmental Engineering, 55200, Atakum/Samsun Turkey. [bozturk061@gmail.com](mailto:bozturk061@gmail.com)

enough fresh air and distribute to places where it is needed, and also must provide acceptable comfort by controlling moisture and temperature. The both methods have discussed below by comparing advantages and disadvantages.

## 2.1 Natural Ventilation

In natural ventilation, air diffuses in from openings of doors, windows and other slits in building shell by pressure or temperature, or both, difference between indoor and outdoor of the building. There is no external driving force for air movement, it can be achieved by structural controls. In order to supply enough fresh air from outside or to achieve a maximum human comfort in indoor maximum natural energy must be utilized. Different techniques can be used to drive fresh air inside or to push the polluted air to outside. These techniques are called as stack effect, wind tower and courtyard effect. In stack effect, temperature creates a pressure differences between outside and inside of the building. This pressure differences plays a driving force for air movement. Warm air moves up because of its lower density and it creates a lower pressure zone close to ground level and the fresh air flows into the room ground from outside because of its higher pressure and density (Figure 1a). The polluted air is vented out from an opening above the room. In wind tower, fresh and cooler air enters inside from one side of a tower and the polluted air leaves the room from other side of the tower (Figure 1b). In courtyard, buoyancy force plays important role especially in high-rise residential buildings. Cool air moves in the courtyard from ground level and moves up, then leaves the room (Figure 1c). For the courtyard ventilation, we must open more space in the ground floor than the upper floor near the roof. If the openings on the windward face of the building, courtyard ventilation works more effectively.

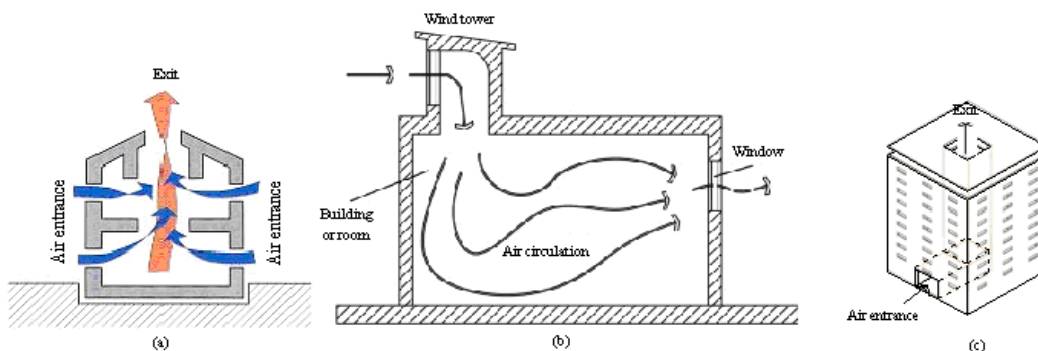


Figure 1. Fresh air intake applications in natural ventilation [6].

a) stack ventilation [6], b) wind tower [7], c) courtyard ventilation [8]

Orientation of building is important as much as architecture of the building in natural ventilation. The architectural characteristics of a building are position of openings, cross ventilation, size of openings and opening types. For the better ventilation, the opening size on the windward face of the building must be smaller than the opening size on the reverse side. The position of buildings in a city is also important, because close buildings to each other restricts the air flow between buildings and sometimes creates turbulence which affects the air flow direction.

## 2.2 Mechanical Ventilation

Feeding the fresh air into an enclosed area and pulling the polluted and unhealthy air out of the building are performed by using an electrical driven ventilator. Such a ventilation system is called as mechanical, forced or activated ventilation. In mechanical ventilation system the air can be supplied where ever we want in a controlled flow rate, but it consumes energy continuously during the activated status.

The most basic form of a mechanical ventilation system used industry is general or dilution ventilation which can be used if the contaminant(s) of interest is not highly toxic and if the rate of generation is predictable. It is generally used when contaminant sources scattered throughout the workplace or sources are mobile such as forklift trucks in a warehouse [9]. Sometimes we need to remove pollutants before spreading into the enclosed space. Such a ventilation application is called as local exhaust ventilation (LEV). Local exhaust systems are used in a wide variety of settings, from research laboratory hoods to commercial kitchens to foundries. LEV systems can, and should, be used in the vast majority of situations in preference over general exhaust [9]. Application of Local Exhaust and General Exhaust Ventilation systems are given in Table 1.



Table 1. Application of Local Exhaust and General Exhaust Ventilation [9].

Local Exhaust Ventilation	General Exhaust Ventilation
Contaminant is toxic	Contaminant has low order of toxicity
Workstation is close to contaminant release point	Contaminants are gases and vapors not particles
Contaminant generation varies over shift	Uniform contaminant release rate
Contaminant generation rate is high with few sources	Multiple generation sources, widely spaced
Contaminant source is fixed	Generation sites not close to breathing zone
	Plant located in moderate climate

Mechanical ventilation of buildings where people use it for their daily activities are different than industrial ventilation. Fresh air is mostly fed into the enclosed space through a duct after filtration, and sometimes air is cooled or heated before feeding. The replaced air needed sometimes heating in winter or cooling in summer, and sometimes must be conditioned. Such a ventilation system is called as heating, ventilation and air conditioning (HVAC) system. A mechanical ventilation design procedure must take into account the air flow rates, heat and cooling loads, air shifts according occupants and air supply principles must be applied. Fresh air supplied from ambient is not free of pollutants; therefore the air must be cleaned before feeding inside especially the building takes place in polluted area such as industrial place or in city centre.

There are two basic ways to take fresh air inside of building, namely displacement ventilation and mixing or dilution ventilation (Figure 2). In displacement ventilation cool and fresh air is introduced into a room close to floor level at low velocity (Figure 2a). Buoyancy forces ensure that this supply air pools near the floor level, allowing it to be carried up into the thermal plumes that are formed by heat sources. This type of air distribution is effective at delivering fresh air to occupants and removing many of the contaminants associated with heat sources, while creating a comfortable environment [10]. Fresh air is supplied into the room near the floor by displacement when the contaminants are warmer and/or lighter than the room air, supply air is cooler than the room air, the room height is 2.75 m or above and low noise levels are desired [10]. The fresh air is distributed into the room by a overhead air distributor if ceiling heights are below 2.4 m, disturbances to room air flow are strong, contaminants are colder and/or denser than the ambient air, cooling loads are high and radiant cooling is not an option [10]. Displacement ventilation is suitable for cooling not heating. In mixing or dilution ventilation uncontaminated fresh air supplied in dilutes the pollutant concentration inside the enclosed space. The fresh air is mixed with the contaminated air inside and vents out together with the polluted air (Figure 2b). The dilution of pollutants depends on how fresh air mixed with the contaminated air. Therefore, for the same amount of ventilating air, displacement ventilation provides better air quality than mixing ventilation. Mixing ventilation mixes pollutants through the room, but displacement ventilation allows pollutants to naturally convect upward.

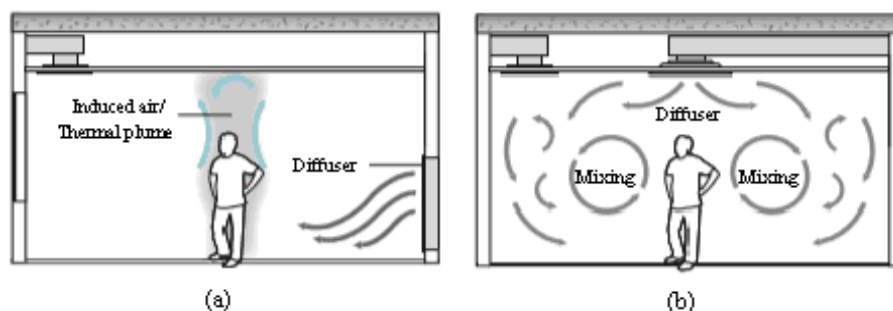


Figure 2. Mechanical ventilation application. A) displacement ventilation, b) mixing ventilation [10].

Designer of a ventilation system must also pay attention to the occupant comfort. Air flow rate, noise of ventilation system and humidity and temperature of the intake air can affect the occupant comfort. Unsuitability of these factors causes dissatisfaction and discomfort; therefore the air is needed to be conditioned sometimes. In order to have good ventilation all times the system requires regular planned maintenance and monitor the system performance.

Ventilation system consumes more energy, and hence an energy saving or recovery system can be designed. There are two kinds of energy saving in mechanical ventilation. One method is recovering of heat of exhaust air by transferring its heat to the cool intake air using a heat exchanger. The other method is the demand controlled ventilation by which air is supplied in when pollution levels of inside air reached to or exceeded the

limit value. This method is especially applied to the place where people live for their daily activities such as school, theatre, etc. The indicator pollutant is CO<sub>2</sub> in demand controlled ventilation. A CO<sub>2</sub> sensor is adjusted to a limit value that is recommended by regulation and the ventilation system is activated when the sensor measured the limit pollutant concentration.

## Conclusions

This study based on the literature review can be concluded by summarizing the effectiveness of the ventilation systems used daily life. Ventilation of closed areas is crucial for human health. Natural ventilation is an energy saving method but it is not effective for all kinds of buildings. Natural ventilation can be used when a building has a windward position, small size and openings suitable for air intake and exhausting. Mechanical ventilation supply enough air inside but consumes more energy. Designing of a good ventilation system is important for enough air supply and energy saving. Displacement ventilation is better than mixing ventilation when the room height is higher than 2.75 m. Demand controlled ventilation can be applied in most places people use for their daily activities.

## REFERENCES

- [1] ASHRAE, (2009). Indoor air quality guide: Best practices for Design, Construction, and Commissioning. Volume 101, Issue 6.
- [2] United States Environmental Protection Agency (USEPA) (2016). An introduction to Indoor Air Quality. <https://www.epa.gov/indoor-air-quality-iaq/introduction-indoor-airquality>
- [3] WHO, 2000a. The Right To Healthy Indoor Air. Bilthoven, The Netherlands,; Who Regional Office For Europe
- [4] Y. Zhang, *Indoor Air Quality Engineering*, CRC Press LLC, 2005, 7.
- [5] M. Hayashi, M. Enai, and Y. Hirokawa, "Annual characteristics of ventilation and indoor air quality in detached houses using a simulation method with Japanese daily schedule model", *Build. And Environ*, vol.36, pp. 721-731, 2001.
- [6] A. Aflaki, N. Mahyuddin, Z. A-C.M. Avad, and M.R. Baharun, "Relevant indoor ventilation by windows and apertures in tropical climate: a review study, E3S Web Conference 3, p.1-5, 2014.
- [7] A.R. Dehghani-sanij, M. Soltani, and K. Raahemifar, "A new design of wind tower for passive ventilation in buildings to reduce energy consumption in windy regions", *Renew. And Sustain. Energy Rev.*, vol. 42, pp. 182-195, 2015.
- [8] C. Wei-Hwa, and A. Duc Anh, "Natural ventilation inside courtyard-apartment building in Taiwan", Fourth German-Austrian IBPSA Conference, 22-24 September 2012, Berlin, Germany 392-399.
- [9] W.A. Burges, M.J. Ellenbecker, and R.D. Treitmen, *Ventilation for Control of the Work Environment*, Wiley Interscience, Second Edition, John Wiley & Sons Inc., New Jersey 2004.
- [10] F. Porges, *Displacement Ventilation: Engineering Guide*, **R. L. Craig Company, Inc. Louisville 2012.**

## Effect of Common-Rail Diesel Engine Bioethanol-Biodiesel-Eurodiesel Mixtures on Engine Performance and Emissions

*A.Engin Ozcelik<sup>1</sup>, Mustafa Acaroglu<sup>1</sup>, Hasan Aydogan<sup>1</sup>, Metin Cinar<sup>2</sup>*

### Abstract

*In recent years, many different studies have been conducted regarding the use of ethanol in both gasoline and diesel engines. As is known, ethanol is a clean fuel in terms of environmental pollution and is suitable for use by mixing gasoline because the number of ethanol octane is high. Ethanol, however, is very low in the number of Setan, it is not used by mixing directly into the diesel fuel. The biggest problem of the use of ethanol in the engines is the difficulty of working in the cold as a result of slow evaporation at low temperatures.*

*In this study, bioethanol produced from sugar beet was used. Biodiesel is manufactured by transesterification method from safflower oil. In all of the mixtures, biodiesel fuel and bioethanol rates of 20% were used as 20%, 30% and 50%. Fuel comparison fuel is accepted as Eurodiesel. The experiments used a diesel engine with a Common-rail fuel system. The results of the experiments were evaluated by comparing the motor performance and emissions values.*

**Keyword:** Biodiesel, bioethanol, Eurodiesel, engine performance, emissions

### 1. INTRODUCTION

The world's energy needs are increasing rapidly due to population growth and industrialization. The renewable fossil fuels will soon be over, and the negative impacts on the environment have been renewed and sought to "clean energy" in the world states. For this purpose, many scientific studies have been conducted and new energy policies have been established with legal regulations [1].

Bioethanol from these fuels; It is a clean, environmentally friendly and renewable fuel produced by the fermentation of high agricultural products such as corn, wheat, barley, rich in starch or sugar, sugar cane, sorghum, and adding a variety of chemicals and enzymes [2]. Biodiesel is a fuel that is environmentally friendly and renewable qualified liquid, which is covered with biofuels obtained from vegetable crude oils or used and by means of chemical methods from animal fats [3].

The use of biodiesel and bioethanol in diesel engines can be utilized in domestic sources, improvement in engine emissions and increase in fuel diversity. The high viscosity of vegetable oils from renewable energy sources, the low end of the aircraft, negatively impacts the use of diesel engines as fuel. This means that vegetable oils are not directly used in internal combustion engines due to their high viscosity. The atomization of the fuel worsens because the high viscosity negatively affects the spraying process [4]. Improper mixing of the air and vegetable oil causes the missing burn. High viscosity also has problems with clogging of injectors, carbon deposits in segments and degradation of lubrication oil. The high flash point indicates that the volatile feature is low. This leads to more accumulative in the combustion chamber, to clog Carbonization and Segman at the end of the injector. The high viscosity is low in the cold, causing the first movement difficulty, flame extinguish, and prolonged ignition delay period [5].

<sup>1</sup> Selcuk University / Faculty of Technology Department of Mechanical Engineering, Konya, Turkey

<sup>2</sup> CNR Consulting, Kloten – Zurich, Switzerland

In order to achieve maximum engine efficiency with minimal fuel consumption in internal combustion engines, the combustion process needs to be used to improve and withstand the use of fuel-resistant fuels. The heat content of alcohol is much lower than the gasoline. Nevertheless, many researchers stressed that low rates of alcohol-gasoline use do not adversely affect motor performance. The fact that alcohol has a higher octane number compared to gasoline-alcohol mixtures allows it to be used in a higher compression ratio spark ignition engines [6]. When the theoretical combustion reactions of alcohol are established, a lower stoichiometric air-fuel ratio is obtained compared to gasoline. This indicates that more alcohol can be burned with the air used for the combustion of the gas [7].

Fuel that can be used in internal combustion engines, inexpensive and abundant production, high thermal values, easy to store, move, high compression ratios to work and low-level exhaust Emissions. Alcohols have been used in motors since the years of the invention of automobiles [8]. Only biomethanol and bioethanol from non-petroleum-based raw materials are manufactured practically by the current technology. Bioethanol has a high octane number and is manufactured from agricultural products. Bioethanol is a suitable fuel for spark plug motors due to these properties and is used in motors by mixing at certain ratios alone or in gasoline [9].

In this study, safflower biodiesel has been mixed with bioethanol and eurodiesel fuel at different rates and various fuels have been obtained. In comparison with these fuels obtained, the engine performance values were examined by comparing eurodiesel as fuel.

## 2. MATERIAL AND METHOD

The safflower biodiesel used in this study was made by using the Transestrification method of the biodiesel safflower oil. Bioethanol was obtained from the Bioethanol factory in Cumra district of Konya, which belongs to Anadolu Birlik Holding. Obtained from these fuels were obtained from E20-B20-D60 (bioethanol rate 20%, biodiesel rate 20% and Eurodiesel rate 60%), E30-B20-D50 and E50-B20-D30. These mixtures were then compared with Eurodiesel fuel.

Experiments used a diesel engine with four-stroke, four-cylinder, electronic fuel injection system with COMMON-rail fuel system. The test mechanism used in the study is shown in Figure 1. The technical characteristics of the engine used in the study were given in table 1, characteristics of the motor dynamometer and exhaust emission device in table 2 and 3.

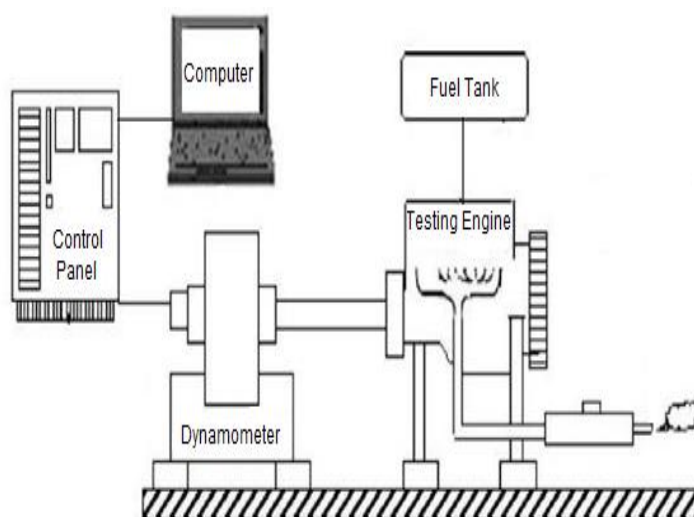


Figure 1 Schematic view of the Motor Test Assembly

Table 1. Technical specifications of the engine used in the study

Motor	1.9 Multijet
Number of cylinders and layout	4, a single row of the front transverse
Cubic capacity (cc)	1910
Compression ratio	5.18: 1
Maximum power hp - d / d	105 - 4000
Maximum torque Nm (kgm) - d/d	200 - 1750
Fuel	diesel
Fuel supply	Electronically controlled Common Rail type MultiJet direct injection, turbocharger and intercooler
Ignition	compressional
Bore x Stroke (mm)	82 x 90.4

Table 2. Technical specifications of the engine dynamometer

Model	BT-190 FR
Capacity	100 kW
Maximum speed	6000 rpm
Maximum torque	750 Nm

Table 3 Technical Specifications Of The Exhaust Emission Device

Parameters	Measurement Range	Sensitivity
HC	0-20.000 ppm	1 ppm
CO <sub>2</sub>	0-20%	0.1%
CO	0-15%	0.001%
O <sub>2</sub>	0-21.7%	0.01%
NO <sub>x</sub>	0-5000 ppm	1 ppm

Before starting measurements, the engine is heated to the operating temperature. Experiments were carried out at a full throttle position at different engine speeds. First, the experimental process was conducted using Eurodiesel fuel. Other fuels were then used as E20-B20-D60 (bioethanol rate 20%, biodiesel ratio 20% and eurodiesel ratio 60%), E30-B20-D50 and E50-B20-D30 mixtures respectively. The bioethanol used in the study was obtained from sugar beet.

### 3. RESULTS AND DISCUSSION

In the use of bioethanol-biodiesel-eurodiesel mixtures, variations of the engine torque values obtained depending on engine rpm are shown in Figure 2. Bioethanol and the thermal energy of the biodiesel are lower than the fuel of the Eurodiesel, leading to a decrease in motor torque. In experiments carried out at different engine speeds, the engine torque has increased depending on engine rpm, and the maximum engine torque is achieved at 2000 RPM engine speed in all fuels. In the use of the E50-B20-D30 fuel, the engine torque has been observed to fall by 17% according to Eurodiesel.

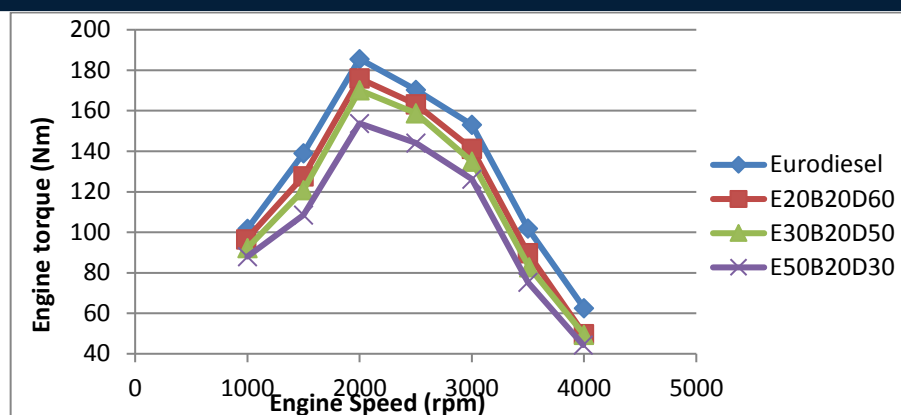


Fig. 2. Engine torque values according to engine RPM

In Figure 3, in the use of bioethanol-biodiesel-eurodiesel mixtures, effective power changes are observed depending on the era of the experimental engine. When the shape is examined, the motor's effective power increases depending on the motor rpm. When the engine power readings of all fuels are examined, the maximum engine power is 3000 rpm. The lowest values were obtained in the E50-B20-D30 fuel. The maximum engine power of the E50-B20-D30 fuel has decreased by 19% compared to the Eurodiesel fuel. This reduction depends on the decline in motor momentum.

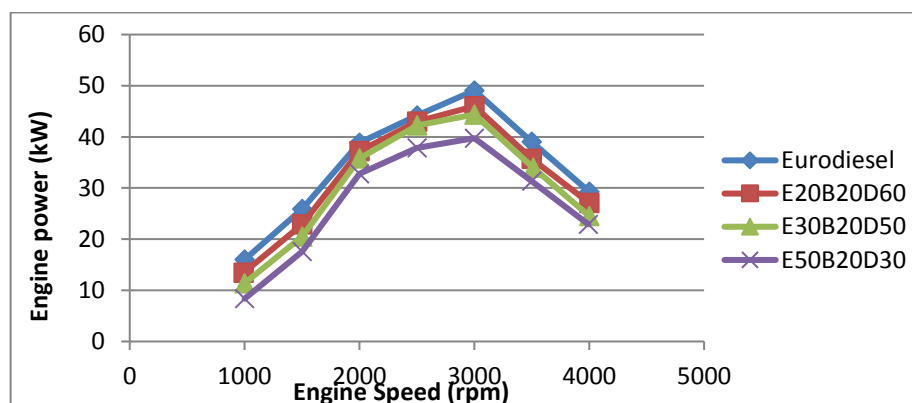


Fig. 3. Engine power values according to engine RPM

In Figure 4, in the use of bioethanol-biodiesel-Eurodiesel fuel mixtures, specific fuel consumption values are observed depending on engine rpm. The lowest specific fuel consumption values are obtained in the use of Eurodiesel fuel. When the specific fuel consumption values are examined, the 2000 rpm is the lowest value in all of the fuels. As the percentage of bioethanol in the fuel mixture increases, an average of 34% increase in specific fuel consumption values. The main reason for the high value of the specific fuel consumption of bioethanol mixtures is that bioethanol is lower than the eurodiesel fuel of the energy content.



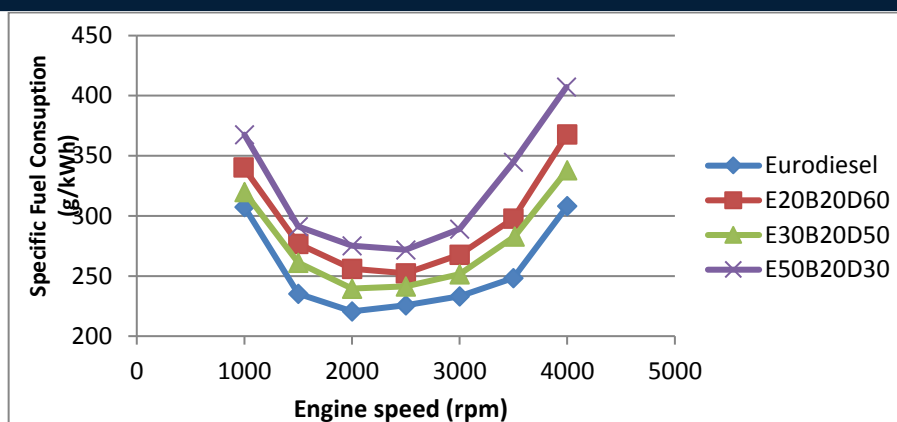


Fig. 4. Exchange of specific fuel consumption values according to engine RPM

The main reason for the presence of CO among combustion products is the inadequacy of oxygen or the absence of complete combustion. Figure 2 shows the variation of CO in the exhaust gases with respect to engine devine in the use of bioethanol-biodiesel-Eurodiesel fuels mixtures. When the figure is examined, it is seen that the amount of CO increases a little as the cycle increases. The use of E50-B20-D30 fuel seems to reduce CO by more than 42%. This reduction is due to the presence of oxygen in the contents of bioethanol and biodiesel.

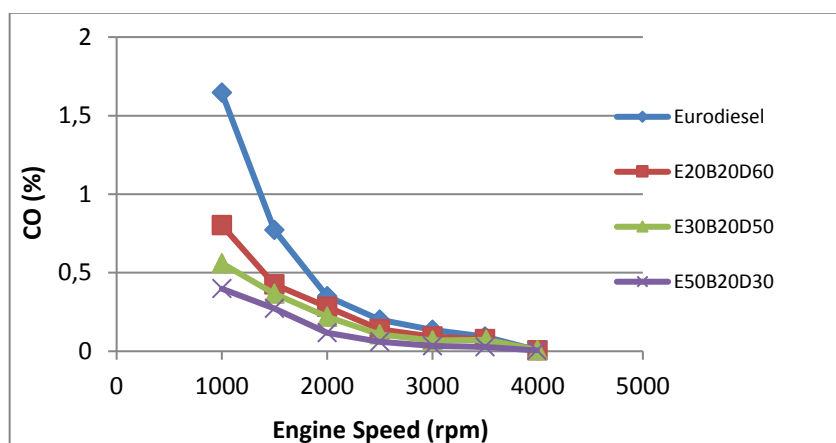


Fig.5. CO changes depending on engine speed

Figure 3 shows the variation of CO<sub>2</sub> values in the exhaust gases with respect to engine dynamics. The increase in the amount of CO<sub>2</sub> in the exhaust gases shows a good combustion. With the use of bioethanol, biodiesel and Eurodiesel mixtures, CO<sub>2</sub> emissions have been reduced by up to 15%. This decrease can be explained by the impoverishment of the mixture due to the presence of bioethanol and biodiesel in the content of O<sub>2</sub>.

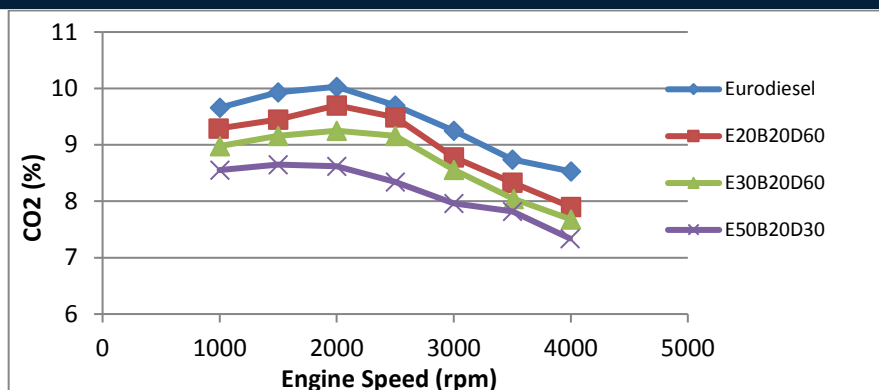


Fig.6. Change of CO<sub>2</sub> according to engine revolution

HC means unburned fuel. In Figure 7, the use of bioethanol-biodiesel-Eurodiesel mixtures shows a change in HC values relative to different engine revolutions. The lowest HC value is measured in E30-B20-D50 fuel use. In the use of Eurodiesel fuel, HC values decreased by more than 50%. This shows that you are better off.

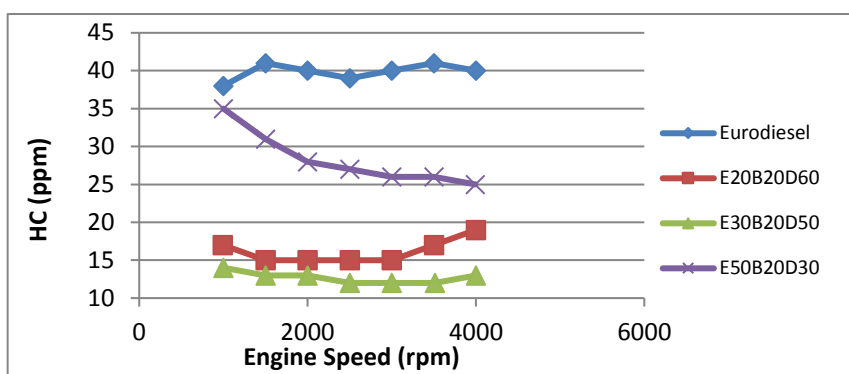


Fig.7. Change of HC according to engine speed

In Figure 8, the use of bioethanol-unleaded gasoline mixtures shows a change in NO<sub>x</sub> values relative to different engine revolutions. The highest NO<sub>x</sub> value was measured in the use of E50-B20-D30 fuel. The use of this fuel has shown that NO<sub>x</sub> values increase by more than 10%. This is an expected situation because of the presence of oxygen in the bioethanol and biodiesel and biodiesel.

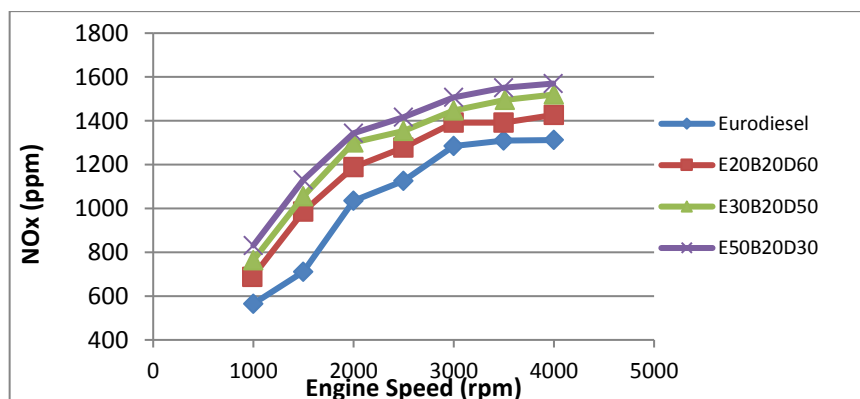


Fig.8. NO<sub>x</sub> change according to engine speed

### 4. RESULTS

In this study, the changes related to motor performance and emissions were investigated in the use of bioethanol-biodiesel-eurodiesel mixtures in a Common-rail diesel engine. In the use of bioethanol and biodiesel fuel, it was observed that the engine torque and engine power fell by an average of 10%, according to the fuel of the Eurodiesel. As the percentage of bioethanol in the fuel mixture increases, an average of 30% increase in specific fuel consumption values. There has been an increase in fuel consumption to achieve the engine power and torque values obtained in the use of Eurodiesel. As a result, the engine has been seen to be used with bioethanol, 20% biodiesel, up to 50% without any modifications, and there are no major effects on motor performance.

The use of mixture fuels E20-B20-D60 (bioethanol ratio 20%, biodiesel 20% and Eurodiesel 60%), E30-B20-D50 and E50-B20-D30 mixture fuels showed a 15% decrease in CO, CO<sub>2</sub> and HC values. When the test results are examined, it is seen that the bioethanol can be used without changing any of the diesel engines with Common-rail fuel system up to the E50-B20-D30 ratio and can contribute to the reduction of harmful emissions.

### ACKNOWLEDGMENT

*This work is supported by the Coordinatorship of Selcuk University's Scientific Research Projects.*

### RESOURCES

- [1] Imrag H. Investigation of the effects of bioethanol usage in gasoline engines and the effectiveness of exhaust emissions, Balikesir University, Department of Mechanical Engineering, 2006
- [2] Yamik, H., "Researching the possibilities of the use of oil esters as alternative fuel in diesel engines", PhD thesis, Gazi University Institute of Science, Ankara, (2002).
- [3] Neto, A.C., Guimarães, M.O.C., Freire, E., Business Models for Commercial Scale Second-generation Bioethanol Production, Journal of Cleaner Production, 20 February 2018
- [4] Park, S.H., Yoon, S.H., Lee, S.C., HC And CO emissions reduction By Early injection strategy in a bioethanol blended Diesel-fueled Engine With a narrow Angle injection System, Applied Energy, Volume: 107, July 2013, Pages: 81-88
- [5] Tgarguifa, A., Abderafi, S., Bounahmidi, T., Modeling and optimization of distillation to produce bioethanol, Energy Procedia, Volume 139, December 2017, Pages 43-48
- [6] Barabás, I., todorut, A., Băldean, D., Performance and emission characteristics of an CI Engine fueled With Diesel – Biodiesel – Bioethanol blends, Fuel, Volume 89, Issue 12, December 2010, Pages 3827-3832
- [7] Aytac, S., "a research on the determination of some performance values in the use of the proportional mixtures of diesel and vegetable oils as fuel in a small, strong engine", PhD thesis, Trakya University Institute of Natural Sciences, Edirne, (1997).
- [8] Acaroglu m., Oguz H., Unalik M., 2004. An alternative fuel for Turkey: bioethanol, fuel usage and

## Determination of Optimum Operational Conditions for the Removal of 2-Methylisoborneol and Geosmin from Drinking Water by Peroxone Process

Hazal Gulhan<sup>1,2</sup>, Malhun Fakioglu<sup>1</sup>, Mustafa Evren Ersahin<sup>1</sup>, Hale Ozgun<sup>1</sup>, Izzet Ozturk<sup>1</sup>

### Abstract

Two-methylisoborneol (2-MIB) and geosmin are two compounds, which cause taste and odor problems in surface water bodies. Since conventional water treatment processes are insufficient for the removal of these substances, advanced oxidation processes have gained importance recently. Peroxone process is an advanced oxidation process based on using ozone ( $O_3$ ) in conjunction with hydrogen peroxide ( $H_2O_2$ ) to produce an oxidizing hydroxyl radical ( $\bullet OH$ ) that removes 2-MIB and geosmin compounds from water. In this study, optimum operational conditions including hydrogen peroxide:ozone ratio ( $H_2O_2:O_3$ ) and contact time were investigated for the removal of 2-MIB and geosmin from drinking water by peroxone process in laboratory scale reactor. 2-MIB and geosmin compounds were spiked into the water samples obtained from the outlet of an aeration unit in a full-scale drinking water treatment plant. Supplied  $O_3$  concentration was 4 mg/L in all experiments. Firstly, the effect of  $H_2O_2:O_3$  ratio on 2-MIB and geosmin removal rates was investigated by applying different ratios of  $H_2O_2:O_3$  including 0.1, 0.3, 0.5 at a contact time of 10 min. Then, different contact times including 5, 7, 10 min were tested with the optimum  $H_2O_2:O_3$  ratio selected at the first stage. The overall results indicated that  $H_2O_2:O_3$  ratio of 0.1 and contact time of 5 min were the optimums for 2-MIB and geosmin removal with removal efficiencies of about 95% and 98%, respectively. According to the results,  $H_2O_2:O_3$  ratio was found to be more effective than contact time on 2-MIB and geosmin removal.

**Keywords:** 2-methylisoborneol, geosmin, peroxone process, water treatment

### 1. INTRODUCTION

Tap water quality is strongly dependent on raw water characteristics in the reservoirs, processes applied for water treatment, and conditions of water distribution network. Taste and odor problems related to some actinomycete and algae species in surface water bodies may lead to loss of customer confidence in water utilities, especially during warm/hot weather conditions [1], [2], [3]. 2-Methylisoborneol (2-MIB) and geosmin, referred as the two main compounds causing taste and odor problems in tap water, are identified in actinomycete culture.

Both 2-MIB and geosmin are volatile saturated tertiary alcohols, which can be detected at extremely low concentrations [4]. 2-MIB that is produced by *Actinomadura sp.*, *Streptomyces antibioticus*, *S. Griseus* etc. is a source for musty smell. Geosmin that is produced by *Actinomyces biwako*, *Microbispora rosea*, *Nocardia sp.* etc. causes earthy-musty smell in water [1]. Threshold odor values for 2-MIB and geosmin were reported to be between 6.3-15 ng/L and 1.3-4.0 ng/L, respectively. The low threshold of detection of these compounds may result in public health concern and complaints regarding taste and odor. Therefore, research has focused on the proper management strategies for the removal of these odorous metabolites

<sup>1</sup> İstanbul Technical University, Department of Environmental Engineering, 34469, Sariyer/İstanbul, Turkey.

<sup>2</sup> Corresponding author: İstanbul Technical University, Department of Environmental Engineering, 34469, Sariyer/İstanbul, Turkey. [gulhan@itu.edu.tr](mailto:gulhan@itu.edu.tr)

from drinking water supplies recently [4], [5]. Conventional treatment processes such as coagulation, flocculation, sedimentation and chlorination are insufficient for the removal of 2-MIB and geosmin. However, powdered activated carbon (PAC) adsorption, biofiltration and ozonation processes are capable of removing these taste and odor causing substances from water. Recent studies mainly focused on activated carbon adsorption and ozone ( $O_3$ ) based advanced oxidation processes for the removal of 2-MIB and geosmin [6]. For example, peroxone process is an advanced oxidation process, which is based on the use of  $O_3$  in conjunction with hydrogen peroxide ( $H_2O_2$ ) to produce an oxidizing radical called hydroxyl radical ( $\bullet OH$ ) [7].

Several studies have been conducted in both laboratory and pilot scale for the removal of 2-MIB and geosmin by using peroxone process. Studies showed that the rate of oxidation is slower for 2-MIB in comparison to geosmin. Besides, oxidation of each substance was promoted by the increased  $O_3$  and  $H_2O_2$  dose [8]. The study of Ferguson et al. [9] showed that removal efficiencies of 2-MIB and geosmin could reach up to ~90% and ~95%, respectively by applying peroxone process with 2 mg  $O_3$ /L (hydrogen peroxide:ozone ratio ( $H_2O_2:O_3$ )=0.2). Similar removal efficiencies were obtained by applying an  $O_3$  dose of 4 mg /L for the same water sample. Studies conducted to compare single ozonation process and peroxone process in terms of 2-MIB and geosmin removal showed that peroxone process had advantages over single ozonation process even though treatment performances of both processes were similar [9], [10], [11]. This conclusion was attributed to bromate formation, a disinfection byproduct, by the ozone oxidation process during water treatment. Studies on bromate formation during the removal of 2-MIB and geosmin indicated that formation of bromate was much lower in a peroxone process in comparison to a single ozonation process [9], [10], [11], [12]. Since bromate is limited by many regulations throughout the world due to its possible carcinogenic effects, minimizing bromate formation in water treatment plants by process selection is very crucial.

The aim of this study was to investigate optimum operational conditions including  $H_2O_2:O_3$  ratio and contact time for the removal of taste and odor causing compounds, 2-MIB and geosmin. For this purpose, 4 mg  $O_3$ /L was applied at a contact time of 10 minutes. Results obtained with different  $H_2O_2:O_3$  ratios, including 0.1, 0.3 and 0.5 and without addition of  $H_2O_2$ , were compared with each other. Following the selection of the optimum  $H_2O_2:O_3$  ratio, different contact times including 5, 7 and 10 min were tested in order to investigate the optimum contact time for the removal of 2-MIB and geosmin.

## 2. MATERIAL AND METHODS

### 2.1. Surface water samples and reagents

Surface water sample was obtained from the outlet of an aeration unit in a full-scale drinking water treatment plant. The characterization of the raw water used in the study is provided in Table 14. Concentrations of 2-MIB and geosmin were quite low (lower than 10 ng/L, which is commonly indicated as the limit concentration causing taste and odor problems [11], [13]) during the experimental period (Table 1). Lower concentrations of 2-MIB and geosmin in water sample might be related with the sampling period during winter since 2-MIB and geosmin concentrations are expected to be higher at warmer weather conditions. Therefore, 2-MIB and geosmin were spiked into the water sample and 2-MIB and geosmin concentrations of ~70 ng/L were maintained during the experimental study. In this study, chromatographic grade 2-MIB and geosmin standard (Supelco, USA) with a concentration of 100  $\mu g$ /ml methanol was used for maintaining the required concentrations of 2-MIB and geosmin in the water sample.  $H_2O_2$  solution (30%) used in the experiments was of analytical grade (Merck, Germany). All other reagents and solvents (e.g., hydrogen phthalate, potassium iodide, sodium hydroxide, ammonium molybdate tetrahydrate) required for the analytical and experimental procedures were at least of analytical grade (Sigma Aldrich, Germany), and all solutions were prepared with deionized water.

Table 14. Raw water quality

Parameter	Unit	Value
Chlorine	mg/L	20.1
Color	Pt-Co	0.2
Conductivity (25 °C)	$\mu S/cm$	310
pH	-	7.9
Iron	mg/L	0.194
Manganese	mg/L	0.027
Sulfate	mg/L	21.1
Sodium	mg/L	14.8

Total Organic Carbon (TOC)	mg/L	2.5
Turbidity	NTU	4.8
Ultraviolet Light at a Wavelength of 254 nm (UV <sub>254</sub> )	cm <sup>1</sup>	0.08
2-MIB	ng/L	<0.5
Geosmin	ng/L	2.3
Chlorophyll A	mg/m <sup>3</sup>	1.3
Bromide	mg/L	0.03
Total Dissolved Solids (TDS)	mg/L	185
Total Hardness	mg CaCO <sub>3</sub> /L	145
Total Alkalinity	mg CaCO <sub>3</sub> /L	132

### 2.2. Experimental set-up

A laboratory-scale reactor was used in the experimental study, which was made of glass with a volume of 1.5 L (height: 100 cm, diameter: 6 cm). The reactor included a ceramic diffuser located at the bottom part. The top part of the reactor was covered with a glass equipment to collect and analyze off-gas O<sub>3</sub>. O<sub>3</sub> was generated with an O<sub>3</sub> generator (Meo-20, Arcbull, Turkey), which had a capacity of 5-25 g/m<sup>3</sup>. An oxygen concentrator (Healthtime OC-5, Elmaslar, Turkey) was used to feed the O<sub>3</sub> generator. The schematic diagram of the experimental set-up is provided in Figure 17.

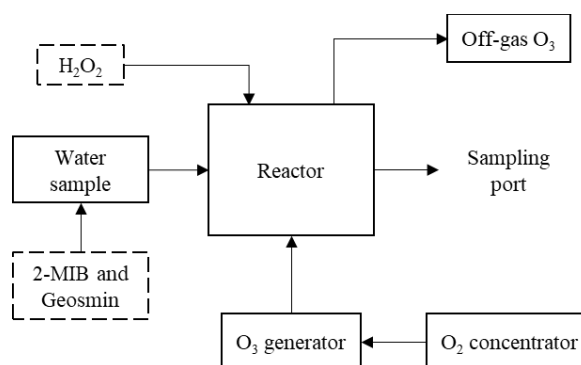


Figure 17. Schematic diagram of the experimental set-up.

### 2.3. Experimental plan

Experiments were performed at batch mode by feeding the reactor with 2-MIB and geosmin spiked water. For all the experiments, 4 mg/L of O<sub>3</sub> concentration was supplied. Before starting the experiments, the influent 2-MIB, geosmin and TOC concentrations were determined in 2-MIB and geosmin spiked water samples.

At the first stage of the experimental plan, experiments were conducted at 10 min of contact time. The aim of the first stage experiments was to determine optimum H<sub>2</sub>O<sub>2</sub>:O<sub>3</sub> ratio to remove 2-MIB and geosmin from water. Therefore, H<sub>2</sub>O<sub>2</sub>:O<sub>3</sub> ratio of 0.0 (ozonation only), 0.1, 0.3, and 0.5 were tested (Figure 18). Experiments to determine the removal efficiencies of 2-MIB and geosmin with ozonation only were conducted without H<sub>2</sub>O<sub>2</sub> dosage. However, calculated volume of H<sub>2</sub>O<sub>2</sub> solution was added into the reactor at the beginning of the experiments that were conducted to investigate the peroxone process performance. For each experiment, variations in O<sub>3</sub> and residual H<sub>2</sub>O<sub>2</sub> concentrations with time were also determined by taking samples at different times (1, 2, 3, 5, 6, 8, and 10 min for O<sub>3</sub> concentration; 0.5, 3, 5, and 10 min for residual H<sub>2</sub>O<sub>2</sub> concentration). At the end of each experiment conducted at first stage, effluent samples were taken in order to determine the removal efficiencies of 2-MIB, geosmin and TOC.

Following the determination of the optimum H<sub>2</sub>O<sub>2</sub>:O<sub>3</sub> for 2-MIB and geosmin removal, different contact times including 5, 7 and 10 min were tested in order to find the optimum contact time for the removal of 2-MIB and geosmin at the second stage of the experiments (Figure 18).



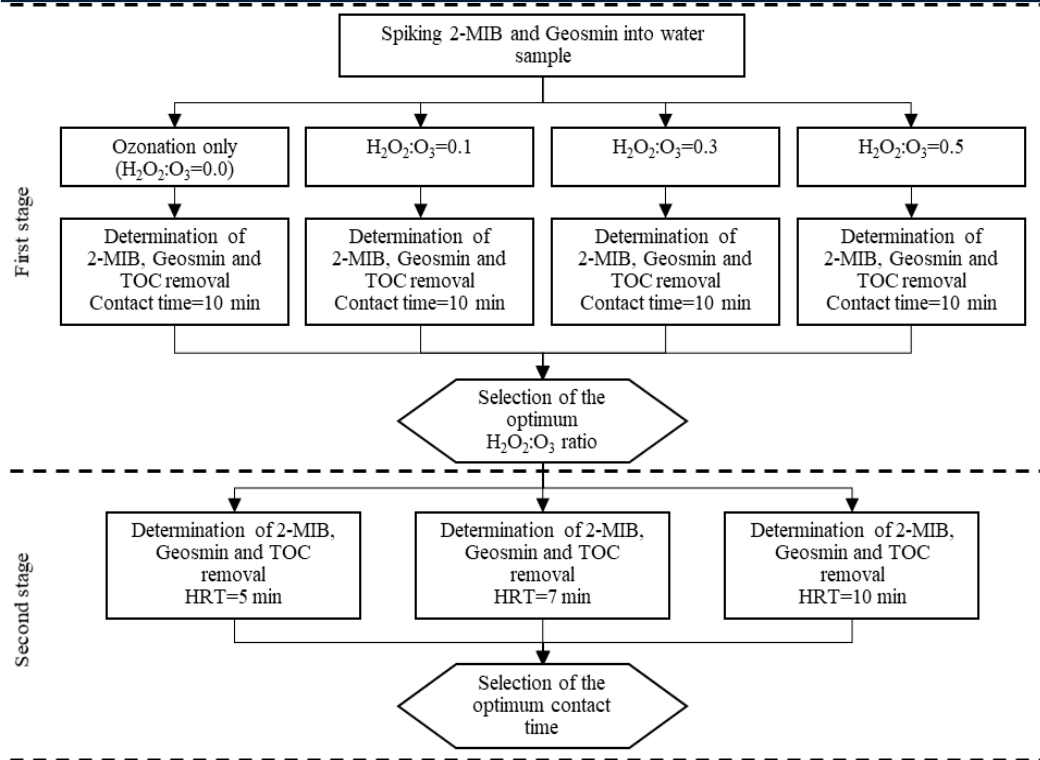


Figure 18. Schematic diagram of the experimental plan.

## 2.4. Analytical and instrumental procedures

Off-gas  $O_3$  concentration (gas phase) was determined with the iodometric titration method [14] and the dissolved  $O_3$  concentration (liquid phase) was analyzed with the indigo colorimetric method [15].  $H_2O_2$  concentration in the liquid phase (as residual) was measured by using the iodide/molybdate method [16]. 2-MIB and geosmin concentrations were analyzed by gas chromatography (Model: 7890B, Agilent Technologies, USA) using Method 8270D [17]. TOC analyzer (TOC-L Series, Shimadzu, Japan) was used to determine the TOC concentration.

## 3. RESULTS AND DISCUSSION

### 3.1. Variations in dissolved $O_3$ and residual $H_2O_2$ concentrations with time

Figure 19(a) presents the variations in dissolved  $O_3$  concentration depending on contact time. After 3 minutes, dissolved  $O_3$  concentration in the reactor was almost stabilized. Residual  $H_2O_2$  concentration in the reactor as a function of time is given in Figure 19 (b). For each  $H_2O_2:O_3$  ratio, residual  $H_2O_2$  concentration decreased dramatically after 3 minutes of contact time. Therefore, it may be concluded that minimum contact time of 3 minutes is required to achieve an effective ozonation for the tested conditions.

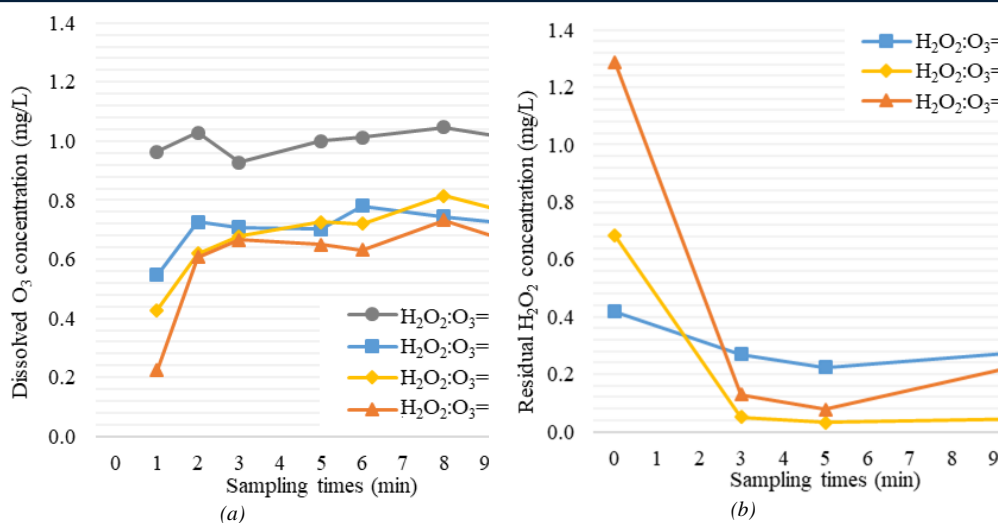


Figure 19. Variations in concentration depending on contact time: (a) Dissolved  $O_3$  concentration, (b) Residual  $H_2O_2$  concentration.

### 3.2. Impact of $H_2O_2:O_3$ ratio on treatment performance

Removal efficiencies of TOC, 2-MIB and geosmin as a function of different  $H_2O_2:O_3$  ratios are provided in Figure 20. It was apparent from Figure 20 that ozonation, with and without  $H_2O_2$  addition, was not effective in TOC removal. However, sole  $O_3$  application could achieve removal efficiencies of 90% and 95% for 2-MIB and geosmin without  $H_2O_2$  addition ( $H_2O_2:O_3=0$ ), respectively. Peroxone process resulted in an enhancement in removal efficiencies for both 2-MIB and geosmin compounds by increasing the removal efficiencies up to 96.2% and 98.5%, respectively at  $H_2O_2:O_3$  ratio of 0.1. Slightly higher removal efficiencies were achieved at  $H_2O_2:O_3$  ratio of 0.3 and 0.5. Thus,  $H_2O_2:O_3$  ratio of 0.1 was proposed as the optimum ratio for 2-MIB and geosmin removal considering the financial feasibility of the system. Higher removal efficiencies were achieved for geosmin in comparison to 2-MIB, which was consistent with the results obtained in the studies of Ferguson et al. [9] and Westerhoff et al. [18].

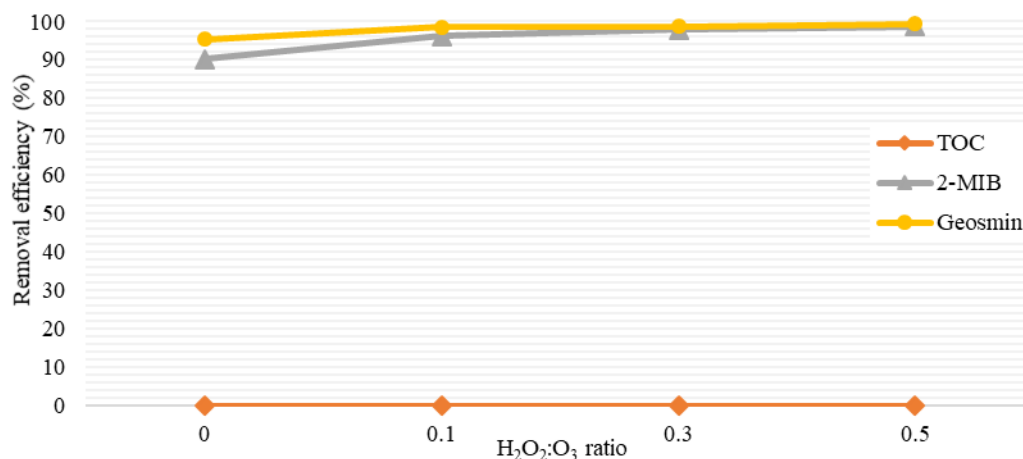


Figure 20. Removal efficiencies of TOC, 2-MIB and geosmin at different  $H_2O_2:O_3$  ratios (contact time: 10 min).

### 3.3. Impact of contact time on treatment performance

After the determination of the optimum  $H_2O_2:O_3$  ratio, different contact times were tested in order to determine the optimum contact time for the peroxone process. Removal efficiencies of >95% and >98%

were achieved for 2-MIB and geosmin, respectively for each contact times (5 min, 7 min and 10 min). Therefore, the optimum contact time was suggested as 5 min. According to the results, it can be concluded that the change in the ratio of  $\text{H}_2\text{O}_2:\text{O}_3$  was more effective on 2-MIB and geosmin removal in comparison to the change in the contact time.

#### 4. CONCLUSIONS

In this study, removal of TOC and taste and odor causing substances, including 2-MIB and geosmin, was investigated at a laboratory scale peroxone process. Trends in dissolved  $\text{O}_3$  and residual  $\text{H}_2\text{O}_2$  concentrations in the reactor depending on the contact time presented that 3 min of contact time was sufficient for the reaction of  $\text{H}_2\text{O}_2$  with  $\text{O}_3$ . The optimum  $\text{H}_2\text{O}_2:\text{O}_3$  ratio and contact time were determined as 0.1 and 5 min for the removal of 2-MIB and geosmin. By applying optimum operational conditions, peroxone process had a positive effect on 2-MIB and geosmin removal in comparison to the application of single ozonation process. The results indicated that the change in  $\text{H}_2\text{O}_2:\text{O}_3$  ratio was more effective on 2-MIB and geosmin removal in comparison to the change in contact time.

#### ACKNOWLEDGMENT

This research was funded by Istanbul Water and Sewerage Administration (ISKI). The authors express their gratitude to Fatih Turan, General Director of ISKI. The authors would like to thank the Head of the Water Treatment Department and all staff in the Water Treatment Department of ISKI for their support.

#### REFERENCES

- [1]. S. D. Faust, & O. M. Aly. Chemistry of Water Treatment. New York: Lewis Publishers, 1998.
- [2]. C. M. Palmer. Taste and Odor Algae. Algae and Water Pollution, 1980.
- [3]. A. Zamyadi, R. Henderson, R. Stuetz, R. Hofmann, L. Ho, and G. Newcombe. G. Fate of geosmin and 2-methylisoborneol in full-scale water treatment plants. *Water Research*, 2015, 83, 171-183.
- [4]. M. Drikas, M. Dixon, J. Morran, J. Removal of MIB and geosmin using granular activated carbon with and without MIEEX pre-treatment. *Water Research*, 2009, 43, 5151-5159.
- [5]. E. C. Wert, M. M. Dong, and F. L. Rosario-Ortiz. Using digital flow cytometry to assess the degradation of three cyanobacteria species after oxidation processes. *Water Research*, 2013, 47, 3752-3761.
- [6]. R. Srinivasan and G. A. Sorial. Treatment of taste and odor causing compounds 2-methyl isoborneol and geosmin in drinking water: A critical review. *Journal of Environmental Sciences*, 2010, 1-13.
- [7]. M. Fakioglu. Removal of Taste and Odor Causing Compounds in Drinking Water by Peroxone Process. Master's Thesis, Istanbul Technical University, 2017.
- [8]. M. Antonopoulou, E. Evgenidou, D. Lambropoulou, I. Konstantinou. A review on advanced oxidation processes for the removal of taste and odor compounds from aqueous media. *Water Research*, 2014, 53, 215-234.
- [9]. D. W. Ferguson, M. J. McGuire, B. Koch, R. L. Wolfe, and E. M. Aieta. Comparing PEROXONE and Ozone for Controlling Taste and Odor Compounds, Disinfection By-products, and Microorganisms. *American Water Works Association*, 1990, 181-191.
- [10]. Y. Wang, J. Yu, D. Zhang, and M. Yang. Addition of hydrogen peroxide for the simultaneous control of bromate and odor during advanced drinking water treatment using ozone. *Journal of Environmental Sciences*, 2014, 550-554.
- [11]. T. Mizuno, S. Ohara, F. Nishimura, and H. Tsuno.  $\text{O}_3/\text{H}_2\text{O}_2$  Process for Both Removal of Odorous Algal-Derived Compounds and Control of Bromate Ion Formation. *Ozone: Science & Engineering*, 2011, 121-135.
- [12]. A. H. Knol, K. Lekkerkerker-Teunissen, C.J. Houtman, J. Scheideler, A. Ried, and J. C. van Dijk. Conversion of organic micropollutants with limited bromate formation during the Peroxone process in drinking water treatment. *Drink. Water Eng. Sci.*, 2015, 8, 25-34.
- [13]. WQRA. Tastes and Odours in Reservoirs. Adelaide: Water Quality Research Australia, 2010.
- [14]. International Ozone Association. Iodometric Method for the Determination of Ozone in a Process Gas. Las Vegas: Quality Assurance Committee, 1996.
- [15]. APHA; AWWA; WEF. Standard Methods for the Examination of Water and Wastewater. Washington D.C.: American Public Health Association, 2005.
- [16]. N.V. Klassen, D. Marchington, and C.E. McGowan. Method HP-02 Analysis of Hydrogen Peroxide. *Anal. Chem.* 1994, 66: 2921-2925.
- [17]. USEPA. EPA Method 8270D. U.S. Environmental Protection Agency, 1998.
- [18]. P. Westerhoff, B. Nalinakumari, and P. Peng. Kinetics of 2-MIB and Geosmin Oxidation during Ozonation. *Ozone: Science and Engineering*, 2006, 28: 277-286.

## A Case Study for Waste to Energy Conversion: MCw Plasma Gasifier

Melda Ozdinc Carpinlioglu<sup>1</sup>, Aytac Sanlisoy<sup>2</sup>

### Abstract

*The critical importance of energy for the total economic infrastructure is apparent in reference to our daily life in integrity with transportation systems of goods and people, the site of manufacturers from enormous global industries to small-medium enterprises, and even for the policy-makers from independent social groups, local municipalities, governments to global organizations. The following inter-related-inter-influenced sub-cases are referred concepts:*

*-The transformation of existing linear economy to a circular one covering our life with the role of waste management and thereby*

*- Methodology for cleaner production*

*- Waste to energy conversion*

*In this respect ; operational characteristics of a research test system " MCw GASIFIER " as a case study for the disposal of a variety of solid wastes is the topic of the presentation. Microwave MCw plasma is generated by the commercial system of MUEGGE at a frequency of 2450 MHz under atmospheric conditions. The characteristics of the system hardware; plasma gasification process and the treatment of gasification process via measurements are described. The performance treatment of plasma gasification and the operational range of MCw GASIFIER are given. The covered ranges of the major variables are input MCw plasma power range  $P$ ;  $3000\text{ W} \leq P \leq 6000\text{ W}$  rate of plasma environment gas;  $Q$   $50\text{ l/min} \leq Q \leq 100\text{ l/min}$ .*

**Keywords:** Microwave Plasma Gasification, Waste to Energy Conversion, Gasification Performance

### 1. INTRODUCTION

Waste to energy conversion can be regarded as a topic in relevance with circular economy [1]. As can be described by Staehel [2] circular economy is a new relationship with our goods and materials that would save resources and energy . He denotes that in the last decade South Korea, China and the United States have started research programs to foster circular economics by boosting remanufacturing and reuse. EU Horizon 2020 program published their first call for circular economy proposals lately in 2014. Singh and Ordonez [3] discuss on the resource recovery from post-consumer wastes for upcoming circular economy. A revised model for recovery routes in society in which waste management is allocated an important role in facilitating material recirculation is presented in their study. They notice that circular economy as a sustainable alternative to current linear economic system can be identified through the basic difference between the so-called waste management and manufacturing-centered take-back systems. In terms of municipal solid waste, MSW and urbanization worldwide the current state of art can also be referred according to World Bank reports. It is estimated that by 2100 the growing global urban population will be producing three times as much waste as it does today. The level of waste should have– physical and fiscal consequences for cities around the world. Global solid waste generation is estimated to be more than 3.5 million tons per day in 2010, more than 6 million tons per day by 2025 and 11 million tons per day by 2100. The global cost of trash is \$205 billion a year in 2010 and \$375 billion by 2025. However there are some positive examples for waste reduction (San Francisco has an ambitious goal of "zero waste" by 2020 with

<sup>1</sup> Corresponding author: Gaziantep University, Department of Mechanical Engineering, 27310, Sehitkamil/Gaziantep, Turkey. [melda@gantep.edu.tr](mailto:melda@gantep.edu.tr)

<sup>2</sup> Gaziantep University, Department of Mechanical Engineering, 27310, Sehitkamil/Gaziantep, Turkey. [aytacsanlisoy@gmail.com](mailto:aytacsanlisoy@gmail.com)

aggressive recycling. Industries in Kawasaki, Japan, divert 565,000 tons of potential waste per year.) Although it is not possible to cover the total content of updated researches, two sample journals of Elsevier: The Journal of Cleaner Production (since 1993) and of Springer: Waste and Biomass Valorization (since 2010) can be referred to visualize the current trend on waste management. Therefore the disposal of a variety of wastes through different energy conversion systems is a fact. In the last decades researches directed to the relevant topics. Leckner [4] classified the waste to energy processing systems as i) Mass burning systems (Combustion) – Waste is burned in a furnace to recover heat energy. ii) Gasification systems- The sorted waste is sent to a gasification reactor – the product gases are cleaned from ash and heavy metals- clean gas is used as fuel in power systems to generate electricity. iii) Co-combustion systems- The produced syngas is mixed with a primary fuel and combusted in boiler to produce steam. iv) Melting plants -The ash in the products is melted and/or vitrified. The aim is reduce the ash and dioxin formation and as a new emerging v) Plasma gasification

Plasma gasification offers an environmental performance better than incineration and conventional gasification systems due to reduced volume of waste and with almost complete disposal of harmful wastes. Therefore handling of plastic wastes- harmful, toxic wastes and MSW seems to be possible. The solid waste conversion to syngas and ash in the plasma environment gas is achieved by a variety of (radio frequency RF, direct current DC and microwave MCw) excitation. The need of experimental research on MCw plasma gasification systems is determined [5]. It is known that the amount of plasma input power, conversion efficiency of waste and process characteristics are dependent on the physical- chemical characteristics of the waste and the plasma environment gas besides the system characteristics. The major problem associated with plasma gasification is the optimum operating conditions with a reduced amount of energy input. In this paper a micro -wave plasma gasification system MCw GASIFIER which was installed as a laboratory –sized pilot plant is discussed as a case study.

## 2. MCW GASIFIER PRESENTATION

MCw GASIFIER is an open cycle blower type atmospheric set-up which is given in Figure 1. The heart of set-up is microwave plasma generation and control system is of MUEGGE. The system is able to generate microwave plasma at a varying input power up to 6000 W at a frequency of 2450 MHz. Air is used as the plasma environment gas. Magnetron generates microwave signal through the waveguide to the plasma applicator at where plasma phase of the air is formed in the applicator. The isolator is used to protect the electrical components from dummy load and the stub tuner optimizes the signal for minimum reflection.

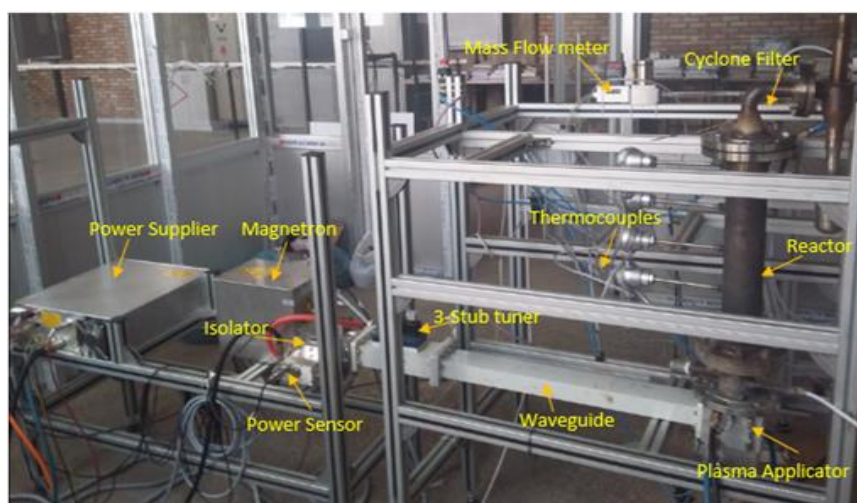


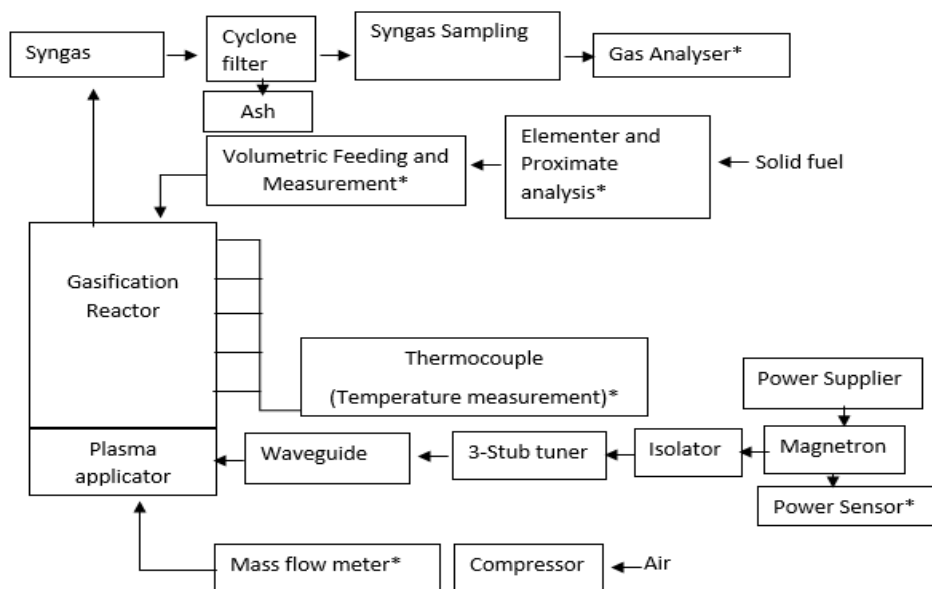
Figure 1. Photograph of MCw GASIFIER

Microwave plasma gasification system description is also given in Figure 2. The system consists of the following sub-components; microwave plasma system, solid waste feeding and air supply system, gasification reactor, process outputs collection system and the measurement - data acquisition system. Although the system explanation is available in [6] the following describes MCw GASIFIER briefly .

### 1) Microwave plasma system

Muegge MX6000D-110K model 6 kW power supplier

Muegge MH6000S-213BF model magnetron head (It provides the microwave signal up to 6 kW power at 2450 MHz frequency).



\*Indicates measurement systems

Figure 2. Block diagram of MCw GASIFIER

The measurement and data acquisition chain is described in Figure 3.

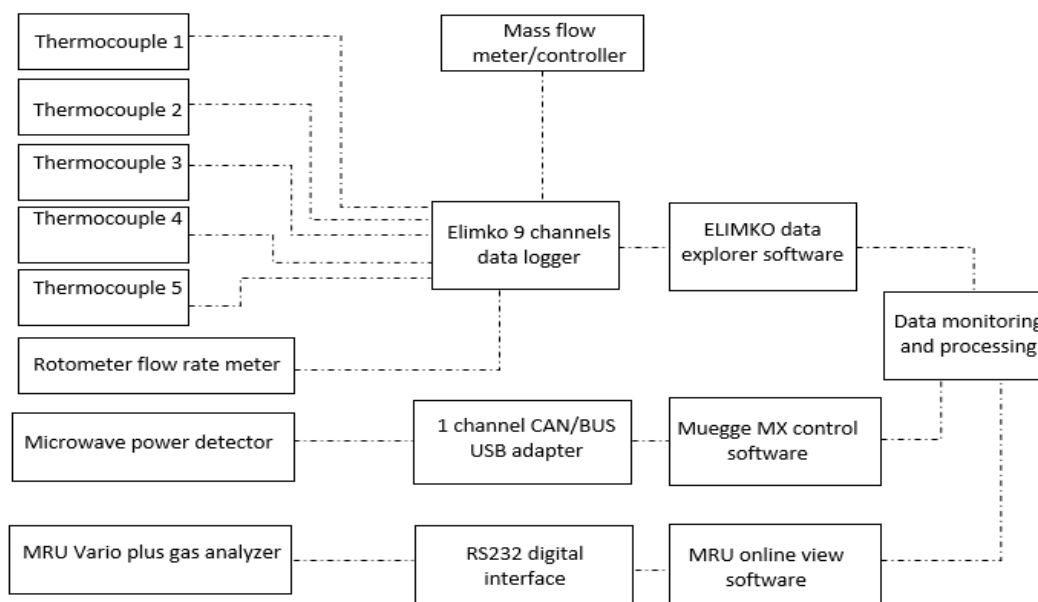


Figure 3. The measurement and data acquisition chain



Muegge isolator (Protects electrical components from dummy load)

Muegge stub-tuner (Adjusts the reflected and forwarded power)

Muegge waveguide (transfers microwave signal from magnetron head to plasma applicator)

Muegge plasma applicator (Microwave signal interact with air and plasma is formed)

2) KOCH PU-02 model volumetric feeding unit for waste feeding

Lupamat LKV 30/8 model single stage screw compressor (to provide air)

3 ) Gasification reactor (Custom-made, 81mm diameter, 625 mm total height)

4 ) Cyclone filter (Custom-made)

5) Measurement and Data Acquisition System( 5 Thermocouples located along the reactor , Syngas Analyzer: MRU Vario-Plus , ELIMKO data logger , Magnetron Power Sensor , Mass flow meter )

The local temperatures in the reactor is measured by using 5 B type of thermocouples with a sensitivity of  $\pm 4$  °C with 1 second intervals. The reactor length is 625 mm and the measurement locations with respect of height of reactor are  $y/h=(0.28,0.44,0.6,0.76 \text{ and } 0.92)$  . The produced syngas content is analyzed by using MRU Vario-plus Gas Analyzer at 2 seconds intervals. ELIMKO data logger is used to collect the data. The physical and chemical characteristics of solid waste determination are through proximate and ultimate analysis besides micro-structure SEM and EDX analysis. The amount of ash left the cyclone filter at the end of the gasification is measured by a sensitive mass balance at a sensitivity of  $\pm 0.24$  mg.

The solid waste samples are the powders of a variety of coal( CR,CSA,CTR) sawdust( HSD,PSD) and polyethylene ( PP) to symbolize different biomass . The gasified sample is called as fuel of the reactor meanwhile produced syngas is considered as an alternative gaseous fuel. Ash remained can be called as the waste of waste in case of future operation of system with MSW.

### 3. 3. RESULTS AND DISCUSSION

#### 4. 3.1. PLASMA GASIFICATION PROCESS DESCRIPTION

The gasification process description is based on the paper of Carpinlioglu and Sanlisoy [7]. The details of the conducted measurements are given in Ph. D thesis of Sanlisoy [8] and the analysis methodology and therefore description through the conducted research project advised by Carpinlioglu in [9]. In reactor fuel bed is fixed; plasma applied at the bottom center of the fuel bed as a swirling air inlet. The operation is under atmospheric pressure with STP conditioned air flow rate supply and with a steady state continuous power, P application.

The gasification process is determined by the local temperature measurements and syngas content analysis during process timely. The data are instantaneously recorded during the gasification time  $t_g$  which is determined by the syngas content variation. During gasification a continuous steady state air flow is generated with a continuous plasma power input, P however decomposition of the fuel bed is not steady. The end of gasification and thereby  $t_g$  is determined by recording pure air content in syngas measured by MRU Vario-plus Gas Analyzer.

A brief summary is given in Table 1 through the definitions and calculation methodology. As can be seen parameters are defined as waste-fuel parameters, syngas parameters, gasification- conversion parameters and thermodynamic analysis parameters. A transient analysis is applied in terms of mass and energy balance. Thermodynamic analysis parameters can also be regarded as performance parameters.

*Table 1. Parameters and definitions*

PARAMETER	DEFINITION AND DESCRIPTION
WASTE-FUEL BASED	Content analysis : Proximate - Ultimate analysis , SEM EDX analysis Density -size of particles – FUEL BED configuration Higher heating value HHV and lower heating value LHV of fuel

SYNGAS: AMOUNT  CONTENT DISTRIBUTION : (volumetric percentages of carbondioxide, carbon monoxide methane oxygen nitrogen ) HYDROGEN QUALITY OF SYNGAS H q %  TEMPERATURE OF SYNGAS  T <sub>syn</sub> (°C)  HHV  MOLECULAR WEIGHT	<p>Amount of syngas: <math>m_{syn} = m_{fuel} + m_{air} - m_{ash}</math> (kg)</p> <p>Content of syngas:</p> $\text{Syngas (\%)} = \frac{2}{t_g} \sum \text{Syngas}_{(t)}$ $H_q [\%] = \frac{m_{H_2}}{m_{syn}} \times 100$ $T_{syn} (°C) = \left( T_{y/h=0.28} + T_{y/h=0.44} + T_{y/h=0.6} + T_{y/h=0.76} + T_{y/h=0.92} \right) / 5 \text{ (°C)}$ $T_{y/h} = \frac{1}{t_g} \sum_{t=1}^{t_g} T_{(y,t)}$ $\sum \text{Syngas}(m \%) \cdot HHV_{\text{syngas}} = CO(m \%) \cdot HHV_{CO} + CO_2 (m \%) \cdot HHV_{CO_2} + H_2 (m \%) \cdot HHV_{H_2} + CH_4 (m \%) \cdot HHV_{CH_4} + O_2 (m \%) \cdot HHV_{O_2} + N_2 (m \%) \cdot HHV_{N_2}$ $\sum \text{Syngas}(n \%) \cdot M_{\text{syngas}} = CO(n \%) \cdot M_{CO} + CO_2 (n \%) \cdot M_{CO_2} + H_2 (n \%) \cdot M_{H_2} + CH_4 (n \%) \cdot M_{CH_4} + O_2 (n \%) \cdot M_{O_2} + N_2 (n \%) \cdot M_{N_2}$
GASIFICATION AND CONVERSION-BASED  TIME: t g CCE:content conversion	<p>Gasification time: t g by SYNGAS CONTENT MEASUREMENT</p> $\text{Syngas CCE}_{\text{syn}} [\%] = \frac{m_{syn}}{m_{fuel}} \times 100$ $\text{Hydrogen CCE}_{H_2} [\%] = \frac{m_{H_2}}{m_{fuel}} \times 100$ $\text{Ash CCE}_{\text{ash}} [\%] = \frac{m_{ash}}{m_{fuel}} \times 100$
THERMODYNAMIC ANALYSIS PERFORMANCE BASED  SYNGAS ENERGY FUEL ENERGY PLASMA ENERGY  PROCESS 1 <sup>ST</sup> LAW EFFICIENCY  SYSTEM 1 <sup>ST</sup> LAW EFFICIENCY	<p>Syngas Energy: <math>E_{syn} (kJ) = m_{syn} (kg) \cdot HHV_{syn} (kJ/kg)</math></p> <p>Fuel Energy: <math>E_{fuel} (kJ) = m_{fuel} (kg) \cdot HHV_{fuel} (kJ/kg)</math></p> <p>Plasma Energy: <math>E_{plasma} (kJ) = W_{plasma} (kW) \cdot t_g (s)</math></p> <p>First law efficiency of process:</p> $\eta_{EP} [\%] = \frac{m_{syn} (kg) \cdot HHV_{syn} (kJ/kg)}{m_{fuel} (kg) \cdot HHV_{fuel} (kJ/kg)} \times 100$ <p>First law efficiency of system:</p> $\eta_{ES} [\%] = \frac{m_{syn} (kg) \cdot HHV_{syn} (kJ/kg)}{m_{fuel} (kg) \cdot HHV_{fuel} (kJ/kg) + E_{plasma} (kJ)} \times 100$ <p>Hot gas efficiency of system:</p> $\eta_{HG} [\%] = \frac{m_{syn} (kg) \cdot [HHV_{syn} (kJ/kg) + c_{p(syn)} (kJ/kg \cdot K) \cdot (T_{syn} - T_o) (K)]}{m_{fuel} (kg) \cdot HHV_{fuel} (kJ/kg) + E_{plasma} (kJ)} \times 100$

### 5. 3.2 OPERATIONAL RANGE

The conducted operational range is described in Table 2. Hornbeam and pine sawdust HSD, PSD Russian, South African and Sirmak Turkish coal CR, CSA CTR and polyethylene particles PP are used as samples of different MSW. Air at different rates; 50, 75,100 L/min is used as plasma environment gas for plasma formation. Input power of plasma generator is varied sequentially from the lowest possible value, P =3 kW to its maximum value of 6 kW as 600 W intervals. The total number of gasification case is 108.

Table 2. Operational Range of MCw GASIFIER

CASE	
FUEL	Sawdust, Coal , Polyethylene
MCw POWER	3kW, 3.6 kW, 4.2 kW, 4.8 kW, 5.4 kW and 6 kW

### 3. CONCLUSION

The basics of MCw GASIFIER are presented as aimed in this paper. The details of sample operation with PP is the topic of the other paper during ICOEST 2018. Therefore without going into physical description of the gasification process the determined ranges of the important parameters can be given as a concluding session in Table 3.

Table 3. Selected limits of MCw GASIFIER operation with 250 g Fuel

Gasification time	Syngas Temperature	Amount of Syngas	Process Efficiency	System Efficiency
7- 17 min	621 - 1276 °C	0.66- 1.2 kg	30% - 86%	20% - 61%

The physical interpretation of waste decomposition by plasma gasification as a function of fuel type is a current topic of research.

### ACKNOWLEDGEMENT

The authors would like to acknowledge the financial support of this work by the Scientific and Technological Research Council of Turkey (TUBITAK) under the contract number 115M389. Also, authors are thankful for the financial support of University of Gaziantep BAP –RM16.01

### REFERENCES

1. Carpinlioglu , M.O., *Brainstorming: Symbiosis-Circular-Performance Economy-Alternative Fuels for Future*, in *1st International Conference on Alternative Fuels: Future and Challenges (ICAF'16)*. 2016: Kayseri, Turkey.
2. Stahel, W.R., *Circular Economy*. Nature 2016. **531**: p. 435–438.
3. Singh, J. and Ordoñez I, *Resource recovery from post-consumer waste : Important lessons for the upcoming circular economy*. Journal of Cleaner Production, 2016. **134**(SI): p. 342-353.
4. Leckner, B., *Process aspects in combustion and gasification Waste-to-Energy (WtE) units*. Waste Management, 2015. **37**: p. 13-25.
5. Sanlisoy, A. and Carpinlioglu M.O., *A review on plasma gasification for solid waste disposal*. International Journal of Hydrogen Energy, 2017. **42**(2): p. 1361-1365.
6. Sanlisoy, A. and Carpinlioglu M.O., *Presentation of a Microwave Plasma Gasification System "MCw Gasifier"* in *Fourth European Conference on Renewable Energy Systems (ECRES2016)*. 2016: Istanbul. p. 503-506.
7. Carpinlioglu, M.O and Sanlisoy A., *Performance assessment of plasma gasification for waste to energy conversion: A methodology for thermodynamic analysis*. International Journal of Hydrogen Energy, 2018. **43**(25): p. 11493-11504.
8. Sanlisoy, A., *An Experimental Investigation on Design and Performance of Plasma Gasification Systems*, Ph. D Thesis in Mechanical Engineering Department of Gaziantep University. 2018, Gaziantep University.
9. Carpinlioglu , M.O. , *Kati Atiklarin Enerji Donusumunde Plazma Gazlastirma Kullanimi ile Calisan Laboratuvar Olcekli Bir Test Duzeneginin (Mikrodalga Gazlastirici) "Mwgazlastirici" Tasarim Uretim ve Performans Degerlendirilmesi-Plazma Gazlastirma Teknolojisinin-Bilginin Urettilip Kullanilmasinda Bir Vaka* TUBITAK 115M389 Final Report, 2018.

## Microwave Plasma Gasification Process of Polyethylene

Melda Ozdinc Carpinlioglu<sup>1</sup>, Aytac Sanlisoy<sup>2</sup>

### Abstract

A microwave plasma gasification process designed for the determination of energy conversion characteristics of polyethylene through a laboratory-sized test system called as MCw GASIFIER is the concern of the presentation. An open cycle blower type atmospheric test system with a fixed bed updraft reactor using air as the plasma environment gas is used. The utilized microwave plasma input power is between 3 kW to 6 kW for a fixed amount (250 g) of polyethylene bed in the reactor. The gasification process for each case is determined by means of the instantaneous measurements of local temperatures along the reactor during the gasification (5 stations), gasification time from the start and end of process which is defined by means of the instantaneous syngas content analysis. Proximate-ultimate analysis of polyethylene, chemical content - available energy content of the produced syngas and ash of the gasification are given to determine energy conversion characteristics of the process through thermodynamic analysis.

**Keywords:** MCw GASIFIER, polyethylene, gasification, syngas, efficiency

### 1. INTRODUCTION

There are variety of ways to convert waste into energy such as incineration, gasification or the pyrolysis [1,2,3]. The issue of this paper is the conversion of polyethylene which is selected as plastics waste into syngas through a microwave plasma gasification process since the disposal of waste plastics is a current global problem. Plasma gasification system MCw GASIFIER is described in the previous article of the authors in the content of ICOEST 2018. The results of operation in the covered ranges of powers between 3 kW- 6 kW and air flow rates of 50 sL/min-100 sL/min are presented through the sample descriptions. The produced syngas energy and the consumed polyethylene energy potentials are calculated and the performance of the system is evaluated in terms of mass and energy content of the inputs and outputs.

### 2. MATERIALS AND METHODS

MCw GASIFIER (Figure 1) consists of the following sub-components; microwave plasma system, solid waste feeding and fluid supply systems, gasification reactor, process outputs collection system and the measurement - data acquisition system. The experimental system explanation can be found in the presented conference paper and articles [4, 5]. The air is supplied to the plasma applicator at desired flow rate from 50 to 100 sL/min. The temperature in the reactor is measured by using 5 B type thermocouples which can measure the temperature up to 1820°C with 1 second interval. The reactor length is of 625 mm and the measurement locations with respect of height of reactor are  $y/h = 0.28, 0.44, 0.6, 0.76$  and  $0.92$ . The ELIMKO data logger is used to collect the data. The produced syngas content is analyzed by using MRU vario-plus gas analyzer with 2 seconds interval. In order to determine thermodynamic analysis of the process the fuel- polyethylene content is examined by proximate and ultimate analysis and results are given in Table 1.

<sup>1</sup> Corresponding author: Gaziantep University, Department of Mechanical Engineering, 27310, Sehitkamil/Gaziantep, Turkey. [melda@gantep.edu.tr](mailto:melda@gantep.edu.tr)

<sup>2</sup> Gaziantep University, Department of Mechanical Engineering, 27310, Sehitkamil/Gaziantep, Turkey. [aytacsanlisoy@gmail.com](mailto:aytacsanlisoy@gmail.com)

Table 1. Proximate and ultimate analysis of the polyethylene

Moisture (%)	Volatile matter (%)	Fixed carbon (%)	Ash (%)	
0.19	94.90	0.91	5.44	
Carbon (%)	Hydrogen (%)	Oxygen (%)	Nitrogen (%)	Sulphur (%)
69.6	10.26	16.14	0.00	0.00

The beginning and end of the process is determined by variation of syngas content. Since before and after the process, the gas content is air during the process syngas content varies. The time of gasification  $t_g$  indicates the process time. The average of temperature for each thermocouple is determined by using equation 1. The average temperature of 5 thermocouples are called as syngas temperature (equation 2).

$$T_{y/h} = \frac{1}{t_g} \sum_{t=1}^{t_g} T_{(y,t)} \quad (1)$$

$$T_{syn} (^{\circ}C) = (T_{y/h=0.28} + T_{y/h=0.44} + T_{y/h=0.6} + T_{y/h=0.76} + T_{y/h=0.92}) / 5 \quad (^{\circ}C) \quad (2)$$

The average of each syngas component is determined by using equation 3.

$$Syngas (\%) = \frac{2}{t_g} \sum Syngas_{(t)} \quad (3)$$

The thermodynamic analysis of the system is performed based on the methodology explained in detail in [6,7,8]. For the thermodynamic evaluation of gasification system the gasification reactor is chosen as control volume. The mass and energy balance equations are derived. The air flow supplied to the reactor at steady conditions with steady power use. 250 g of polyethylene in the form of particles, PP is used as a stationary bed in the reactor.

Mass balance in the reactor can be derived by using transient process mass balance in equation 4a and it is reduced for the process to equation 4b:

$$m_{input} - m_{output} = (m_2 - m_1)_{CV} \quad (kg) \quad (4a)$$

$$m_{polyethylene} + m_{air} = m_{syn} + m_{ash} \quad (kg) \quad (4b)$$

The process performance is directly related to the decomposition of polyethylene into syngas and ash. Since the desired product is syngas, content conversion for the syngas ( $CCE_{syn}$ ) can be defined as ratio of syngas mass ( $m_{syn}$ ) to mass of polyethylene, ( $m_{polyethylene}$ ) as follows in equation 5:

$$CCE_{syn} [\%] = \frac{m_{syn}}{m_{polyethylene}} \times 100 \quad (5)$$

and the system energy efficiency is defined in equation 6.

$$\eta_{Es} [\%] = \frac{E_{syn} (kJ)}{E_{polyethylene} (kJ) + E_{plasma} (kJ)} \times 100 \quad (6)$$

The definition of syngas energy and fuel energy are given in equation 7 and 8. The input plasma energy is given in equation 9:

$$E_{syn} (kJ) = m_{syn}(kg).HHV_{syn}(kJ/kg) \quad (7)$$

$$E_{polyethylene} (kJ) = m_{polyethylene}(kg).HHV_{polyethylene}(kJ/kg) \quad (8)$$

$$E_{plasma} (kJ) = W_{plasma} (kW).t_g (s) \quad (9)$$

The heating value of various gases tabulated in a thermodynamic textbook [9] are used. Since system energy efficiency is based on the determination of higher heating value (HHV); HHV of the polyethylene is calculated by using equation 10 described by Channiwala and Parikh, 2002 [10].

In the system efficiency definition, the temperature of the syngas ( $T_{syn}$ ) is the critical parameter. Hot gas efficiency ( $\eta_{HG}$ ) is taken into account for the cases of syngas temperature ( $T_{syn}$ ) is higher than the ambient temperature ( $T_0$ ). The system hot gas efficiency ( $\eta_{HG}$ ) is given in equation 10.

$$\eta_{HG} [\%] = \frac{E_{syn} (kJ) + m_{syn}(kg). \left[ c_{p(syn)} \left( \frac{kJ}{kg.K} \right) \cdot (T_{syn} - T_0)(K) \right]}{E_{polyethylene} (kJ) + E_{plasma} (kJ)} \times 100 \quad (10)$$

### 3. RESULTS AND DISCUSSION

As can be seen from Table 1 polyethylene, PP mainly consists of carbon (69.6 %) and almost all the content is volatile (94.9%). The higher heating value (HHV) of polyethylene is determined as 34633 kJ/kg.

The temperature distribution in the reactor by varying the plasma power is given in Figure 1. While the temperature is highest near plasma flame, it reduces by going away from it. Because, the energy intensity is much higher near plasma flame. While the highest temperature is 1520 °C at  $y/h=0.28$  at 6 kW power, it reduces to 847 °C at  $y/h=0.92$  at 6 kW power. The plasma power increases the temperature in the reactor because of increasing the energy intensity. The lowest temperature is measured at  $y/h=0.92$  that is the outermost measurement location and 3 kW plasma power.

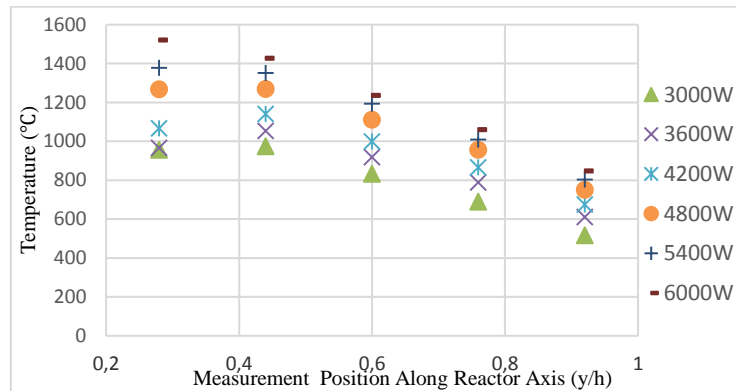


Figure 1. The temperature distribution for the gasification of Polyethylene (PP) in case of 50 sL/min air flow rate

During the gasification process, the inputs; weight of polyethylene and air are measured. Also, the ash output is measured. By using equation 4, the produced syngas amount is calculated. The variation of gasification time; air and syngas weights by changing the microwave plasma power are given in Table 2. The gasification time reduces by increasing the plasma power from 660 seconds to 520 seconds by increasing the plasma power from 3 kW to 6 kW. The reduction in gasification time causes the decreasing of the supplied air amount. Because, the air is supplied to the gasifier steadily at constant flow rate. If the



time reduces, the supply amount air reduces proportionally. It also effects the syngas production. Because the produced syngas amount is calculated through weight of inputs and outputs.

Table 2. Presentation of inputs and the outputs to the reactor and syngas temperature at 50 sL/min

Power (W)	$t_g$ (s)	$m_{air}$ (kg)	$m_{syngas}$ (kg)	$m_{ash}$ (kg)	$T_{syn}$ (°C)
3000	660	0.65	0.90	0.0021	793
3600	640	0.63	0.88	0.00201	867
4200	600	0.59	0.84	0.00187	949
4800	580	0.57	0.82	0.00163	1070
5400	560	0.55	0.80	0.00144	1147
6000	520	0.51	0.76	0.00116	1218

The syngas temperature increases from 793 °C to 1218 °C by increasing the plasma power from 3 kW to 6 kW. Because the increasing the plasma power rises the energy density in gasifier and the temperature increases by increasing the plasma power. The air flow rate has reverse effect on syngas temperature.

The variation of syngas content distribution by changing the plasma power between 3 kW – 6 kW is given in the Table 3. O<sub>2</sub> in syngas increases approximately 36 %, CO<sub>2</sub> in syngas reduces approximately 31 %, CO in syngas increases approximately 14 %, H<sub>2</sub> in syngas increases approximately 28 %, CH<sub>4</sub> in syngas reduces approximately 12 % and N<sub>2</sub> in syngas goes down approximately 1 % by increasing plasma power from 3 kW to 6 kW.

Table 3. Presentation of molar based syngas content distribution as example at 50 sL/min

Power(W)	$t_g$ (s)	O <sub>2</sub> ,%	CO <sub>2</sub> ,%	CO,%	H <sub>2</sub> ,%	CH <sub>4</sub> ,%	N <sub>2</sub> ,%
3000	660	1.12	16.21	19.62	9.80	2.12	51.13
3600	640	1.18	15.30	20.11	9.91	2.01	51.49
4200	600	1.32	14.62	20.67	10.03	1.98	51.38
4800	580	1.44	13.01	21.31	10.80	1.94	51.50
5400	560	1.43	12.54	21.94	11.32	1.95	50.82
6000	520	1.52	11.21	22.27	12.56	1.86	50.58

The variation of CCE<sub>syn</sub>, syngas energy, fuel energy and plasma energy at altered plasma power between 3 kW – 6 kW is given in the Table 4. Content conversion performance reduces by increasing power from 360 % to 305 % by increasing power from 3 kW to 6 kW. Syngas energy changes from 3298 kJ to 3327 kJ by increasing plasma power from 3 kW to 6 kW. The system energy efficiency ( $\eta_{ES}$ ) lowers from 31.00 % to 28.24 % by increasing plasma power from 3 kW to 6 kW. In addition to system efficiency parameters, the syngas energy includes both the chemical energy and sensible energy as a result of its high temperature in the hot gas efficiency ( $\eta_{HG}$ ). The magnitude of the hot gas efficiency ( $\eta_{HG}$ ) is higher than the system energy efficiency ( $\eta_{ES}$ ). Because, the sensible energy of the syngas is also considered in calculations of hot gas efficiency ( $\eta_{HG}$ ). The hot gas efficiency ( $\eta_{HG}$ ) slightly rises from 36.23 % to 36.54 % by increasing plasma power from 3 kW to 6 kW.

Table 4. Presentation of the CCE<sub>syn</sub>, syngas energy, fuel energy and plasma energy results for the polyethylene (PP) gasification process.

Plasma Power (W)	CCE <sub>syn</sub> (%)	Syngas energy (kJ)	Plasma energy (kJ)	System energy efficiency $\eta_{ES}$ [%]	System hot gas efficiency $\eta_{HG}$ [%]
3000	360	3298	1980	31.00	36.23
3600	352	3267	2304	29.80	35.61
4200	336	3187	2520	28.51	34.86
4800	328	3274	2784	28.62	36.03
5400	320	3321	3024	28.43	36.37
6000	305	3327	3120	28.24	36.54

## 4. CONCLUSION

In gasification of polyethylene at altered plasma powers between 3 kW and 6 kW the effects of air flow rate and plasma power on plasma gasification performance are revealed. The syngas content conversion parameter is varied between 305 % and 571 %. System energy efficiency is varied between 28.24 % and 31 %, the hot gas efficiency is varied between 36.23 % and 36.54 %.

## ACKNOWLEDGEMENT

*The authors would like to acknowledge the financial support of this work by the Scientific and Technological Research Council of Turkey (TUBITAK) under the contract number 115M389. Also, authors are thankful for the financial support of University of Gaziantep BAP –RM16.01.*

## REFERENCES

1. Leckner, B., Process aspects in combustion and gasification Waste-to-Energy (WtE) units. Waste Management, 2015. **37**: p. 13-25.
2. Sekiguchi, H. and Orimo T., Gasification of polyethylene using steam plasma generated by microwave discharge. Thin Solid Films, 2004. **457**(1): p. 44-47.
3. Tang, L. and Huang H., Decomposition of polyethylene in radio-frequency nitrogen and water steam plasmas under reduced pressures. Fuel Processing Technology, 2007. **88**(6): p. 549-556.
4. Sanlisoy, A. and Carpinlioglu M.O., Presentation of a Microwave Plasma Gasification System "MCw Gasifier" in Fourth European Conference on Renewable Energy Systems (ECRES2016). 2016: Istanbul. p. 503-506.
5. Sanlisoy, A. and Carpinlioglu M.O., Preliminary measurements on microwave plasma flame for gasification. Energy, Ecology and Environment, 2018 **3**(1): p. 32-38 .
6. Sanlisoy, A., An Experimental Investigation on Design and Performance of Plasma Gasification Systems, in Mechanical Engineering Department of Gaziantep University. 2018, Gaziantep University.
7. Carpinlioglu, M.O and Sanlisoy A., Performance assessment of plasma gasification for waste to energy conversion: A methodology for thermodynamic analysis. International Journal of Hydrogen Energy, 2018. **43**(25): p. 11493-11504.
8. Carpinlioglu M.O., Kati Atiklarin Enerji Donusumunde Plazma Gazlastirma Kullanimi ile Calisan Laboratuvar Olcekli Bir Test Duzeneginin (Mikrodalga Gazlastirici) "Mewgazlastirici" Tasarim Uretim ve Performans Degerlendirilmesi-Plazma Gazlastirma Teknolojisinin-Bilginin Uretilip Kullanilmasinda Bir Vaka TUBITAK 115M389 Final Report, 2018.
9. Cengel, Y.A. and Boles M.A , Thermodynamics: an engineering approach. 2007, USA: McGraw-Hill.
10. Channiwala, S.A. and Parikh P.P. , A unified correlation for estimating HHV of solid, liquid and gaseous fuels. Fuel, 2002. **81**(8): p. 1051-1063.

## The Effect of Environmental Pollutants on Honeybees (*Apis mellifera* L.)

Cengiz Erkan<sup>1</sup>, Ayhan Gosterit<sup>2</sup>

### Abstract

Honeybees (*Apis mellifera* L.) are prevalent in almost all regions on earth, except for polar regions, due to their high adaptability. The honeybees that deliver important products such as primarily honey and beeswax, royal jelly, bee venom and propolis for human consumption, while they improve crop quality and yield in plant propagation due to their contribution to pollination and provide sustenance for the plants through their effects on seed binding. On the other hand, the desire of humans to own and control everything on earth caused various damages on the world at various degrees since the gathering and hunting period. Especially during the 18th century, the rapid consumption of resources, which started with the industrial revolution, increased the above-mentioned damages significantly. In the present study that aimed to draw attention to several environmental pollutants such as heavy metals, electromagnetic radiation and pesticides, which are the most important causes of serious losses in honeybee colonies throughout the world, it was also aimed to assess the methods to prevent the honeybees that are utilized as bioindicators in determination of environmental pollution and bee products from the above-mentioned effects.

**Keywords:** Honeybee, *Apis mellifera*, Environmental pollution, Heavy metals, Electromagnetic fields, Pesticides

### 1. INTRODUCTION

Beekeeping of production that may be carried out by a smaller capital and in a shorter time in comparison to other agricultural activities. While there is no need for a robust structure in beekeeping, there is also no need for property ownership. In the case that it is well-planned, and collaboration is made with other types of production, it may easily become a second job. Beekeeping, which is usually considered to be an income-raising activity in small family establishments, also helps using the labor force in the family efficiently [1].

Honey bees provide their producers with significant contributions with their products with high nutritional contents that are used as raw materials in various branches of the industry such as especially honey, wax, pollen, royal jelly, propolis and bee venom, as well as sales of live material such as queens, swarms and package bees.

Bees help plants survive by acting as carriers for the pollination of fruits and vegetables that need external pollination. In order for plants to be able to produce seeds and fruits, their flowers need to be sufficiently pollinated. Honey bees are insect that have the best abilities for pollination especially in open spaces [2, 3]. The transition of honey bees to a system of feeding with nectar and pollen and formation of suitable organs by passing through various stages of evolution are believed to be related to meeting the needs of plants to be pollinated [3]. Therefore, bees, which are excellent pollinators as a result of their body structures and nutritional styles, are attracted by flowers that secrete nectar. Honey bees play an active role in the pollination of several plants, especially fruit species such as almond, apple, cherry, peach, pear, apricot and strawberry, field plants such as cotton, sunflower and anise, garden plants such as cantaloupe and watermelon, and feed plants such as clover and sainfoin [4]. Agriculturally developed countries which have

<sup>1</sup>Corresponding author: Van Yuzuncu Yil University, Faculty of Agriculture, Department of Animal Science, Van, Turkey. cernan@yyu.edu.tr

<sup>2</sup>Applied Sciences University of Isparta, Faculty of Agricultural Sciences and Technologies, Department of Animal Science, Isparta, Turkey. ayhangosterit@sdu.edu.tr

understood the need of plants for pollination and the importance of honey bees in pollination achieve more production and higher quality by leasing bee colonies in flowering periods.

The beekeeping activities of humankind which may be dated back to 8000 years ago and started by collection of honey from natural hives turned towards beekeeping activities by transportation of colonies into primitive hives made of mud in Ancient Egypt, and today, this resulted in the spread of beekeeping almost everywhere outside the polar circles [5].

Honey bees, which have a social lifestyle, consist of worker bees, male bees and queen bees based on their characteristics. Among bees that live in colonies, these three groups are specialized for different tasks. The yield of a honey bee colony is directly related to the beekeeping practices and the environment that it is affected by. The beekeeper usually cannot control the effect of the environment, while they aim to get a higher revenue.

Honey bees are constantly in interaction with their environment while collecting pollens and propolis and carrying water to the hive to be used for different tasks. This environment might have a radius of 10 km for one colony based on factors such as nutritional sources and geography [6].

In recent years, bee deaths that have been observed in several places in the world were mainly associated climatic changes [7], and these losses that contained several uncertainties were named Colony Collapse Disorder [8, 9, 10]. Additionally, the effect of pollutants on air, soil and water resources in the abnormal colony losses is undeniable.

Honey bees, who are the lead actors of the animal farming activity that is the most dependent on nature, transfer the contents of various plants from different species into their products [8, 11]. Therefore, the chemical contents of beekeeping products are closely related to the quality of the environment. Due to these characteristics, both honey bees and their products are used as bioindicators for detecting environmental pollutants [6, 12, 13].

## 2. ENVIRONMENTAL POLLUTANTS

Pollution is described as any factor that affects the utility obtained from environmental resources negatively. Mixing of substances that affect the living and inanimate elements of the environment negatively, inflict structural damages and deteriorate their qualities into air, water and soil to an intense degree is known as "environmental pollution [14].

Pollutants that harm the lives of living beings may be in the phases of solid, liquid or gas. The nature of the pollutant and its density determines the severity of pollution.

While there are different classifications on pollutions that have a negative effect on living beings, the following classification may mainly be the case.

- Air pollution
- Water pollution
- Soil pollution
- Noise pollution
- Nuclear hazards

Each type of pollution in this classification leads to damaging all living beings directly or indirectly by harming nature. Moreover, pollution of the environment triggers climate changes by disrupting the balance of the ecosystem.

## 3. EFFECTS OF POLLUTANTS ON HONEYBEES

While each living being may react to effects to different extents, honey bees which have high levels of sensitivity to the environment are in the position of a detector of environmental pollution due to their death rates and the residues of toxic substances in their products [11].

Plants which are the main requirement of life for bees, secrete volatile fragrance molecules via their roots, leaves, flowers and fruits. Each species of flower has a complex set of fragrances that does not resemble others. These fragrances are under the effects of biotic and abiotic factors. While biotic factors include the unique structure of the flower species, state of pollination and insect infestation, main abiotic factors include

temperature, radiation and CO<sub>2</sub>. Depending on these factors, the fragrances of flowers may change based on time and place [15]. Many insects have the ability to detect smells from long distance. Reduction and change in smells affect this distance [16]. The smells that are secreted by plants may be broken up by reacting with air pollutants such as ozone. Thus, bees are able to find less food although they spend more time. As air pollution changes smell intensity to a significant extent, the relationship between the bee and the plant gets harmed [15, 17].

Based on the study of a simulation, researchers reported that fragrance molecules may remain in a clean environment for 40 hours, while this duration is reduced to 10 hours when they are exposed to an ozone level of 6 parts per billion for one hour. Again, studies stated that, while it takes 10 minutes for bees to find fragrance molecules in an environment without ozone, this duration is increased up to 180 minutes at an ozone level of 20 parts per billion [15].

Air pollutants do not only have a negative effect on honey bees' access to nutritional resources. This also leads to an indirect reduction in human food resources depending on the reduction in pollination [15, 18].

With faster technological activities in the world, usage of heavy metals including metal raw materials has also increased. With this increase, heavy metal wastes have become a significant environmental problem. The most important reason that heavy metals are an important issue is that these metals have a different structure in comparison to others.

Heavy metals such as As, Cd, Cu, Fe, Hg, Pb and Zn pose a potential of harm for the lives of living beings. They may lead to poisoning or even death even in very small quantities [19, 20]. The most significant sources of heavy metal pollution are industries. Release of metals that are used in industries for various purposes into the external environment when they become unusable inflicts a great risk on natural life.

As honey bees collect nectar and pollen from plants, they are in a constant relationship with the environment. Wastes and toxic substances that lead to environmental pollution are absorbed by the plants that are around and accumulated in the body of the plants. Thus, honey bees are also affected by environmental pollution.

Excessive amounts of heavy metals in the body of a plant lead to an increase in the concentrations of toxic heavy metals in the contents of the honey produced by honey bees from the plant's nectar and the bodies of the bees [21]. While heavy metals affect the quality and physiological characteristics of bee products negatively, they also lead to excessive numbers of bee deaths [22].

Chemical and biological preparates that are used for the purpose of suppressing the diseases and harmful plants and weeds that limit plant production are generally known as pesticides [23]. In the international market, there has been a substantial increase in the share of pesticides, which have had a potential to increase in numbers and complexity since the 1940 based on the increase in yield of plant products. The negative effects of pesticides, which may have varying effects based on forms of application, times of application and formulations, on the ecosystem are undeniable due to their accumulation in nature and harm on organisms other than the target organism [24].

Honey bees, which may be biological determinants in studies on environmental pollution and agricultural pest control in terms of both colony deaths and residues in their products as their lives are completely dependent on nature [25, 26, 11, 27], are the living beings that are affected by pesticide applications the most. Excessive and irresponsible use of pesticides lead to diminishing of thousands of colonies, loss of yield and residues in beekeeping products each year [27]. As a result of pesticide application processes, in addition to excessive deaths of bees in colonies, behavioral disorders are also observed, and the desire of bees to clean themselves increases [28]. Because of this, the rates of returning to the hive in forager bees are significantly reduced, and colonies are weakened [29].

In order to protect colonies from pesticides, which constitute a stress factor for honey bees, the plant producer and the beekeeper must act in collaboration. For this purpose, there are some precautions that may be taken by plant producers such as using chemicals that have much lower toxic effects and only when it is absolutely needed, taking into account the flight activities of honey bees for timing the applications, avoiding usage of powder chemicals and paying attention to not polluting water resources. Beekeepers should also take precautions such as forming their bee yards away from possible pesticide application areas, moving colonies when needed and keeping a clean source of water around their bee yard [22, 30, 31].

Studies on the effects on the lives of honey bees focus on radiations which are a source of ongoing pollution. Radiations are classified as ionizing and nonionizing ones based on whether or not they remove electrons

from the substance when they interact with it. It is known that ionizing radiations with radioactive (nuclear) properties lead to fatal and permanent outcomes when they interact with living beings. Nonionizing radiations have lower degrees of influence on living beings. Cell phones that facilitate communication by using radio frequency waves use RF microwaves, which are nonionizing, when they contact base stations. The electromagnetic radiation with a GSM frequency that is released into the environment creates thermal and nonthermal effects on biological tissues as a result of the absorption of the energy it carries while it is moving in the body after contacting the living being. While thermal effects lead to increased temperatures in the body, nonthermal ones usually cause chemical, biological and psychological imbalances [32].

Beekeeping is an agricultural activity that is intertwined with nature. Considering the developments in communication technologies, the amounts of radiation that bees are exposed to is a topic that needs to be focused on. Limited numbers of studies so far have been conducted more on cell phones and DECT phones that work on analog lines, and their results were not generalized. These studies have found that the flight activities of bees decreased, the rates of return to the hive in forager bees were reduced, aggressiveness increased, and the probability of observing Colony Collapse Disorder increased.

Other important types of environmental pollution that impact the lives of honey bees are light and noise pollutions. Such pollutions that may occur or reach the colony especially during winterization, which is known as the resting period of a colony, lead to behavioral and physiological changes by disrupting the winterization system of the colony.

#### 4. CONCLUSION AND SUGGESTIONS

The desire of humankind to keep and control everything in the world has led it to harm the world to different extents since the hunter-gatherer communities up to our times. Rapid consumption of resources that started especially with the Industrial Revolution in the 18th century took the severity of these damages to even greater dimensions.

Despite several techniques and precautions that were developed with the purpose of receiving high yields from honey bees, increases in colony losses and decreases in yields directed all people who study this field towards focusing on all influential factors.

This study aimed to draw attention to air pollution, heavy metals, pesticides, electromagnetic radiation and other various environmental pollutants which are among the most important causes of substantial colony losses and yield problems that are observed in the world.

Exploitation of nature, which satisfies all the needs of living beings, by one species -humans- narrows down the living spaces of other living being, especially honey bees. It should be kept in mind that life will exist as long as bees exist.

#### REFERENCES

- [1]. H. Kiziltas, "Farkli kovanların propolis üretimine ve içerisine (Fenolik bileşim) etkisi", (master's thesis, unpublished). Van YÜ Graduate School of Natural and Applied Sciences, 2018.
- [2]. R. Sirali, A. Ugur, M. Turkmen, "Bal arılarının sebze üretimindeki rolü", *Aricilik Arastirma Dergisi*, vol. 3: pp. 3-6, 2011.
- [3]. F. Kaya, "Agri ilinde arıcılık yapısı ve Değerlendirme raporu", *Ataturk Universitesi Sosyal bilimler Enstitüsü Dergisi*, vol. 12 (2), pp. 35-55, 2008.
- [4]. E. Altunoglu, "0900 Ziraat kiraz cesidi polinasyonunda bal arisi (Apis mellifera L.) kullaniminin meyve kalitesi ve verimine olan etkisinin belirlenmesi", (master's thesis, unpublished). University of Adnan Menderes Graduate School of Natural and Applied Sciences, 2017.
- [5]. E. Crane, *Beekeeping: Science, Practice and World Recourses*, Heinemann, London, p. 640, 1990.
- [6]. C. Nisbet, A. Guler, G.F. Yarim, S. Cenesiz, Y. Ardali, "Cevre ve flora kaynaklarının arı ürünlerinin mineral madde içerikleri ile ilişkisi", *Turkish Journal of Biochemistry/Türk Biyokimya Dergisi*, vol. 38 (4), pp. 494-498, 2013.
- [7]. Y. L. Conte, M. Navajas, "Climate change: impact on honey bee populations and diseases," *OIE Revue Scientifique et Technique*, vol. 27 (2), pp. 485-510, 2008.
- [8]. R. Johnson, (2010) Honey Bee Colony Collapse Disorder, Congressional Research Service. Available: <http://www.fas.org/sgp/crs/misc/RL33938.pdf>
- [9]. B. Dainat, D. VanEngelsdorp, P. Neumann, "Colony collapse disorder in Europe", *Environ Microbiol Rep.*, vol. 4 (1), pp. 123-5 2012
- [10]. B. Bekic, M. Jelocnik, J. Subic, "Honey bee colony collapse disorder (Apis mellifera L.) – possible causes", *Scientific Papers Series Management, Economic Engineering in Agriculture and Rural Development*, vol. 14 (2), pp. 13-18, 2014.



- [11]. RM. Johnson, MD. Ellis, CA. Mullin, M. Frazier, "Pesticides and honey bee toxicity – U.S.A.", *Apidologie*, vol. 41, pp. 312-331, 2010.
- [12]. G. Celli B. Maccagnani, "Honey bees as bioindicators of environmental pollution", *Bulletin of Insectology*, vol. 56 (1), pp. 137-139, 2003.
- [13]. E. Skorbiłowicz, M. Skorbiłowicz, I. Ciesluk, "Bees as Bioindicators of Environmental Pollution with Metals in an Urban Area", *Journal of Ecological Engineering*, vol. 19 (3), pp 229-34, 2018.
- [14]. (2018) Ankara Belediyesi web sayfası. [Online]. Available: [https://www.ankara.bel.tr/files/7414/3695/0096/1-cevrebilgisi-16\\_SAYFA.pdf](https://www.ankara.bel.tr/files/7414/3695/0096/1-cevrebilgisi-16_SAYFA.pdf)
- [15]. JD. Fuentes, M. Chamecki, T. Roulston, B. Chen, KR. Pratt, "Air pollutants degrade floral scents and increase insect foraging times", *Atmospheric Environment*, vol.141, pp. 341-372, 2016.
- [16]. E. Pehlivan, "Boceklerde cesitli davranis sekilleri ve bunlardan yararlanma olanaklari", *Turkiye Bitki Koruma Dergisi*, vol. 5 (4), pp. 243-52, 1981.
- [17]. G. Farre-Armengol, J. Penuelas, T. Li, P. Yli-Pirila, I. Filella, J. Llusia, JD. Blande, "Ozone degrades floral scent and reduces pollinator attraction to flowers" *New Phytologist*, vol. 209, pp. 152-160, 2015.
- [18]. C. Brittan, C. Kremen, A. Garber, AM. Klein, "Pollination and plant resources change the quality of almonds for human health", *PLoS ONE*, vol. 9 (2), DOI:10.1371/journal.pone.0090082, 2014.
- [19]. PB. Tchounwou, CG. Yedjou, AK. Patlolla, DJ. Sutton, "Heavy Metals Toxicity and the Environment", *Natl. Inst. Health*, vol. 101, pp. 133-64, 2012.
- [20]. SC., Izah, IR. Inyang, TC. Angaye, IP., Okowa, "A Review of Heavy Metal Concentration and Potential Health Implications of Beverages Consumed in Nigeria", *Toxics*, vol. 5(1), pp. 1-15, 2016.
- [21]. A. Roman, "Levels of copper, selenium, lead, and cadmium in forager bees", *Polish Journal of Environmental Studies*, vol. 9(3), pp.663-69, 2010.
- [22]. Z. Barganska, M. Slebioda, J. Namiesnik, "Honey bees and their products: bioindicators of environmental contamination" *Crit Rev Environ Sci Technol.*, vol. 46, pp. 235-48, 2016.
- [23]. H. Ozbek, *Arlarin zirai mucadele ilaclarindan etkilenmeleri ve alinacak onlemler*, Zirai Mucadele ve Zirai Karantina Genel Mudurlugu Yayinlari, Ankara. 1983.
- [24]. M. Yildiz, O. Gurkan, C. Turgut, G. Unal, "Tarimsal savasmda kullnlanil pestisidlerin yol actigi cevre sorunlari", *TMMOB Ziraat Muhendisleri 6. Teknik Kongresi*, 3-7 January 2005, Ankara, p. 629-48.
- [25]. JJ. Bromenshenk, JL. Gudatis, SR. Carlson, JM. Thoma, MA. Simmons, M.A. "Population dynamics of honey bee nucleus colonies exposed to industrial pollutants", *Apidologie*, vol. 22, pp. 359-369, 1991.
- [26]. PG. Kevan, "Pollinators as bioindicators of the state of the environment: species, activity and diversity", *Agriculture, Ecosystems and Environment*, vol. 74, pp. 373-393, 1999.
- [27]. C. Porrini, AG. Sabatini, S. Girotti, F. Fini, L. Monaco, L., G. Celli, L. Bortolotti, S. Ghini, "The death of honey bees and environmental pollution by pesticides: the honey bees as biological indicators", *Bulletin of Insectology*, vol. 56 (1), pp. 147-52, 2003.
- [28]. H. Perveen, M. Alhariri, M. Ahmad, A. Suhail, "Insecticidal mortality, foraging behavior and pollination role of honeybee (*Apis mellifera* L.) on sarson (*Brassica campestris* L.) crop", *International J Agriculture & Biology*, vol. 2 (4), pp. 332-3, 2000.
- [29]. HM. Thompson, "Behavioural effects of pesticides in bees--their potential for use in risk assessment", *Ecotoxicology*, vol. 12 (1-4), pp. 317-30, 2003.
- [30]. B. Kovanci, Tarimsal savas ve aricilik, *Marmara Bolgesi I. Aricilik Semineri*, 10-11 February 1988, Bursa, p. 47-53.
- [31]. E. Tutkun, A. Bosgelmez, *Bal arisi zararilari ve hastaliklari teshis ve tedavi yontemleri*, Bizim Buro Basimevi Kizilay-Ankara, p 365, 2003.
- [32]. L. Sevgi. (2015) Cep Telefonlari ve Baz Istasyonlari Tartismalari Uzerine, (access 2015), [http://www3.dogus.edu.tr/lsevgi/LSevgi/EMC\\_YAZI/cbt4.pdf](http://www3.dogus.edu.tr/lsevgi/LSevgi/EMC_YAZI/cbt4.pdf).

## Comparison of the thermal performances of concretes containing waste rubber for energy efficient buildings

Recep Yumrutas<sup>1</sup>, Hasan Oktay<sup>2</sup>

### Abstract

*Due to the rapid depletion of available sites, the disposal of waste tires is becoming a serious environmental problem day by day. Assessment of waste rubbers in concrete is an innovative solution that meets both the challenge of the tire disposal problem and a demand for improved thermal performances of structural materials for energy efficient buildings. Therefore, in this study, an investigation is performed both to obtain new concrete types by using waste rubbers with high thermal insulating characteristics and to compare the thermal performance of those concretes with conventional ones. For this purpose, different types of concrete samples were prepared with a constant water-cement ratio, and normal aggregates replaced by rubber aggregates at different volume fractions between 0% and 60% of the total aggregate volume. In the experiments, all mechanical tests were conducted and the hot disk method was used to establish thermal property values of concrete samples. In order to determine the most suitable concrete samples, heat flows through the produced samples are calculated using a program developed in MATLAB. Calculation method for the heat flow is based on solution of transient heat transfer problem for the multilayer structures. The program is executed to calculate hourly heat gain values for these samples over a period of 24 h during design day for Batman, Turkey. The results indicated that the maximum reduction in heat gain value was obtained as 50.6 % for RC60 wall with commonly used thickness of 20 cm corresponding to conventional concrete.*

**Keywords:** Concrete, waste rubber, heat gain, thermal and mechanical properties.

### 1. INTRODUCTION

Disposal of waste tires has been a major environmental issue to cities all around the world. Rubber tires not only consume significant landfill space, but the risk of fire poses a serious threat to the environment. Besides, they provide breeding grounds for mosquitoes that may carry disease [1]. Hence, a series of the problems generate significant pressure to the local authorities identifying the potential application for these waste products. Assessment of waste rubbers as building materials appears to be innovative solution not only to such pollution and disposal problem but also to the problem of economical design of buildings. Therefore, the use of waste rubber particles in cementitious materials has great potential to positively affect the properties of concrete in a wide spectrum. In general, concrete has many limitations such as low tensile strength, low ductility, and low energy absorption. Concrete also tends to shrink and crack during the hardening and curing process. The brittle nature of concrete and its low properties has prompted the use of waste tire particles as a concrete aggregate to possibly remedy or reduce these negative attributes [2].

Concrete building structures, the most economical building material that is used as one of the most versatile and universal [3]. Due to this fact, the construction industry is always trying to increase its uses and applications and improving its properties, while reducing cost. An important way to obtain more energy efficiency in buildings is to improve the thermal insulation properties. Reduction of the heat loss in buildings decreases the consumption of energy, thus, reduces the cost of heating and cooling. As a result of the lower use of energy, improvements in thermal insulation also affect sustainability. Addition of waste

<sup>1</sup> Corresponding author: Gaziantep University, Department of Mechanical Engineering, 27310, Gaziantep, Turkey. [yumrutas@gantep.edu.tr](mailto:yumrutas@gantep.edu.tr)

<sup>2</sup> Batman University, Department of Mechanical Engineering, 72100, Batman, Turkey. [hasan.oktay@batman.edu.tr](mailto:hasan.oktay@batman.edu.tr)

tire particles into cementitious composites is known to improve thermal insulation performance with almost no extra material cost and can thus provide an alternative cost-effective solution for today's energy efficient buildings. It also provides an alternative safe way of utilizing a waste material to help environmental protection [4].

The importance of recycling of waste tires coupled with the interest in overcoming the aforementioned concrete defects have motivated a significant body of research pertaining to rubberized concrete. A review of the literature revealed that several investigations into rubberized concrete have been previously performed. Fattuhi et al. [5] mentioned in his report that the concrete made with low grade rubber concrete had lower compressive strength compared with high grade rubber concrete. These similar observations were also made by Topcu et al. [6] and this could be caused by weak interfacial bonds between the cement paste and tire rubber. Piti et al. [7] outlined that crumb rubber responses were found to denote greater flexibility and toughness with larger deflection at peak load, longer post-peak load responses and higher fracture energy. Benazzouk et al. [8] conducted an investigation about the effects of waste rubber particles on the thermal properties of concrete were studied. Different concrete mix designs with different rubber particle replacements of aggregate with a ratio of 10%, 20%, 30%, 40% and 50% were used. It was found that the addition of rubber particles reduced the thermal conductivity and density of samples. Also, they reported that the thermal insulating effect of rubber particles is most attractive and indicates a high and promising potential for development. In addition, experimental studies have shown that the bricks with a high content of crumb rubber with conventional sand aggregate showed a high energy absorption capacity drastically reduced density and offered a smooth surface as compared with current concrete bricks. The improvements insulation characteristics vary from 5 to 11% depending on the amount of rubber crumb used [9]. An explorative study was conducted to investigate thermal benefits of scrap-tire materials into building envelope. A room whose exterior walls are fully made with scrap-tire added concrete is constructed here for obtaining better thermal protection. It was verified in the study that the introduction of the scrap-tire pieces into building walls reduces the heat transfer through them by increasing their thermal insulation characteristics [10].

The literature about the use of tire rubber particles in cement-based materials generally focuses on the use of tire rubber as an aggregate in concrete and evaluates only the mechanical properties. Despite its potential advantage, not much attention has been given in investigating thermal performance of rubberized cementitious products. Therefore, in this study, an investigation is performed both to obtain new concrete types by using waste rubbers with high thermal insulating characteristics and to compare the thermal performance of those concretes with conventional ones.

## 2. MATERIALS AND METHODS

### 2.1. Materials and composition

The materials were used to obtain different concrete building structures were locally available ordinary Portland cement (PC) (CEM I 42.5R), silica fume, fine and coarse aggregates, waste rubber particles, superplasticizer and air-entraining admixtures, which are used to purposely introduce and stabilize microscopic air bubbles in concrete. Rubber particles ranging in a size from 4.75 mm to 0.075 mm was generated from waste tire without steel fibers with a cracker mill process. Then, mixtures were designed with a constant water–cement ratio of 0.48 and total cement content of 350 kg/m<sup>3</sup>. Silica fume is used as an amount of 10% by weight of cement in this study. Natural aggregates were replaced by rubber particles at different volume fractions between 0% and 60% of the total aggregate volume. Because of having low strengths of rubber aggregates, rubberized concrete with higher than 60% ratios are formed as a concrete for non-structural purposes and were not cased in this study. In totally, 84 pieces were produced and cured water at room temperature of 20 ± 2°C.

### 2.2. Test methods

Thermophysical and mechanical tests were carried out to establish the hardened properties of the concretes regarding the compressive and splitting tensile strength, the bulk density, and the thermal conductivity tests. The mechanical tests were performed on air-dry specimens at the age of 28 days. The thermal conductivity test was performed on air dried samples at the age of 35 days. The measurement of the thermal property tests is performed by TPS (Transient Plane Source) technique (Figure 1). Experimental studies on both aggregate and concrete were determined according to TSE and ASTM International standards.



Figure 1. The thermal property measurement device used in the study (TS EN 12667)

### 2.3. Heat gain formulation for comparison

In order to decide whether any one of building wall elements is the best or not in view of heat transfer, it is necessary to compare heat gain or loss for these elements. In this study, heat gain values for the produced building wall elements are calculated by using measurement values of thermophysical characteristics of the elements. The heat gain values for each element will be compared with those of the other building elements. Any element or elements having the lowest heat gain values are recommended to applicants. Since the lowest energy consumption for heating and cooling of any space is the most important for humanity or environment protection or pollution.

One-dimensional transient heat transfer problem for a building element is formulated by a differential equation and boundary conditions. Solution of the problem is used to find temperature of inside surfaces of the building walls. The transient heat transfer problem is put into dimensionless form and CFPT is applied to the dimensionless formulation of the problem. Schematic view of a multilayer wall consisting of a finite number of layers is shown in Figure 2. The building wall consists of  $N$  layers, and the  $n$ th layer of which has a thickness of  $L_n$ .

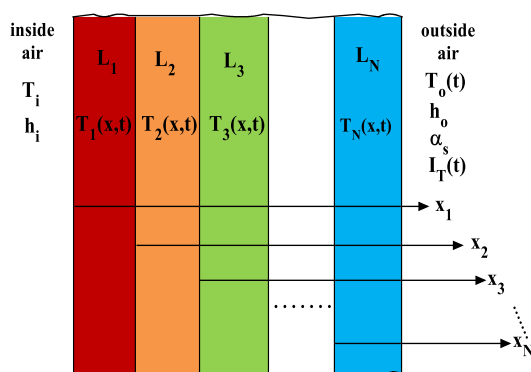


Figure 2. Schematic view of a multilayer wall.

Heat gain through any wall can be given as a function of interior surface temperatures of building wall, interior design air temperature and convective heat transfer coefficient. That is, it can be calculated by multiplying of convection coefficient and temperature difference. Thus, the heat flux can be expressed as:

$$q_c = h_i[T_1(0, t) - T_r]$$

The temperature difference represents the difference of temperature between the inside surface of the wall,  $T_I(0,t)$  and interior air temperature,  $T_r$  which is commonly taken as 25 °C for cooling season. Since temperature of the inside wall surface,  $T_I(0,t)$  can be obtained, heat transfer to the room then can be calculated. Transformed formulation is solved to obtain periodic solution and presented in the following expression.

$$T_n(z_n, \tau) = \sum_{n=-M}^{n=M} T_{nj}(z_n) e^{i\omega_j \tau} \quad \omega_j = 2\pi j$$

where  $T_n(z_n, \tau)$  is the temperature profile for the wall and  $M$  is the large number, and it is generally taken as 60. The transient temperature profile and its expression and also calculation procedure are presented in Yumrutas et al. [11,12].

## 2.4. Hourly Solar Radiation Incident on Exterior Wall Surface

Solar radiation incident on the building surfaces is a very effective parameter for heat gain. Because solar radiation is a factor in the calculation of the cooling load, the equations are required to calculate the solar radiation values measured on an hourly basis from the horizontal surfaces. In the study, one of the hottest day of the summer season was selected as the climate data (July 26) of 2016 in Batman province. In order to obtain radiation and temperature measurement data, the meteorological measurement system was established in Batman University (Figure 3). The pyranometer used in the measurement system was connected to a data logger with the help of a solar cell assisted battery.



Figure 3. The meteorological system in Batman University (39.79 latitude; 41.06 longitude).

## 3. RESULTS AND DISCUSSION

In this study, an investigation is performed both to obtain new concrete types by using waste rubbers with high thermal insulating characteristics and to compare the thermal performance of those concretes with conventional ones. Thermophysical and mechanical tests were carried out to establish the hardened properties of the concretes regarding the compressive and splitting tensile strength, the bulk density and the thermal conductivity tests.

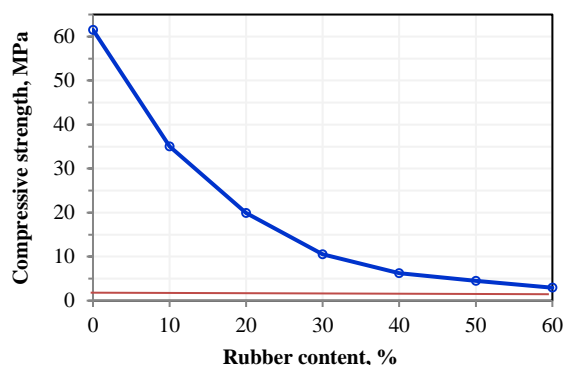


Figure 4. Effect of rubber content on compressive strength

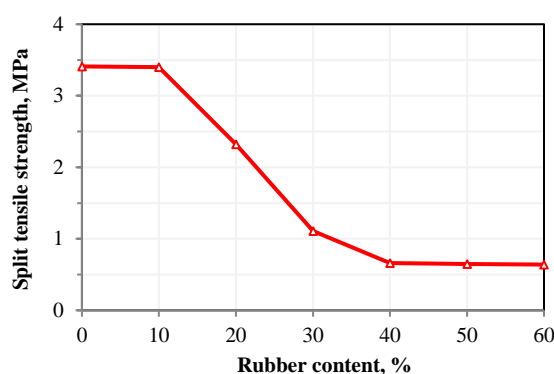


Figure 5. Effect of rubber content on split tensile strength

Figure 4 and Figure 5 present the results for the 28-day compressive and split tensile strength tests values of the concrete samples that varied from 2.94 to 61.52 MPa for compressive strength test and varied from 0.64 to 3.41 MPa for split tensile strength test at different volume fractions between 0% and 60% of the total aggregate volume. There was a significant reduction in both strength tests compared with the control concrete. The reason for the greatest reductions could be attributed both to a reduction of quantity of the solid load carrying material and to the lack of adhesion between the rubber particles and the paste. On the contrary, the reason for the lower reduction in the tensile strength than compressive strength values is considered due to the fiber effect of the waste tires in the concrete that prevents the sample to be divided into the pieces.

The oven-dried density decreased with increasing rubber aggregate ratios as shown Figure 6. From the results, it was found out a reduction up to 32 % of the density was observed when 60% by volume of the normal aggregate was replaced by rubber chips in the sample. Such a reduction in the bulk density can have significant advantages from the point of earthquake resistance.



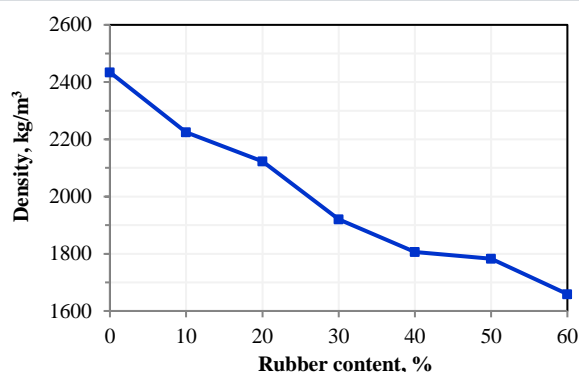


Figure 6. Effect of rubber content on the density.

Thermal conductivity of a material is the quantity of heat transmitted through a unit thickness in a direction perpendicular to a surface of unit area, due to a unit temperature gradient under given conditions. Generally, low thermal conductivity corresponds to high insulating capability. The variation of the thermal conductivity with respect to rubber particle content is displayed in Fig. 7. It was observed that the addition of rubber particles into the cement matrix reduces the thermal conductivity of the composite. Values decreased from 2.08, for the control specimen, to 0.55 W/mK for RC50 corresponding to a decrease of 73.56 %. This was due to the insulating effect of rubber particle, which had a lower thermal conductivity compared to that of cement matrix.

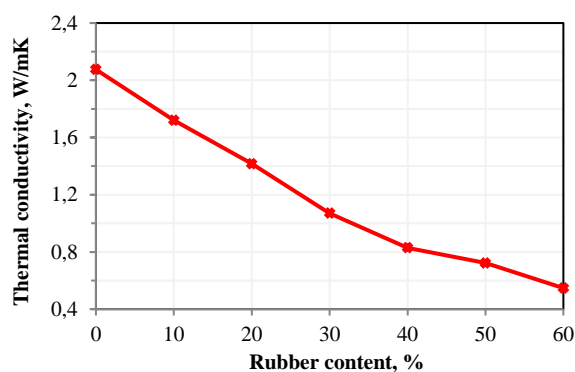


Figure 7. Effect of rubber content on the thermal conductivity.

In order to determine the most suitable concrete samples, a periodic solution of unsteady heat transfer problem for a building wall is used to calculate heat gain from the produced samples. Therefore, a computer program in MATLAB was prepared by using input data. The program is executed to calculate hourly heat gain values for these samples over a period of 24 h during design day for Batman, Turkey. Heat gain fractions in the present study are defined as the ratio of heat gain value of each wall construction to the heat gain value of the reference wall sample. It is seen from Figure 8 that the maximum reduction in heat gain value was obtained as 50.6 % for RC60 wall (concrete wall within 60 % rubber particles) with commonly used thickness of 20 cm corresponding to conventional concrete. The lowest heat gain value was obtained due to the lowest thermal conductivity of RC60 wall.

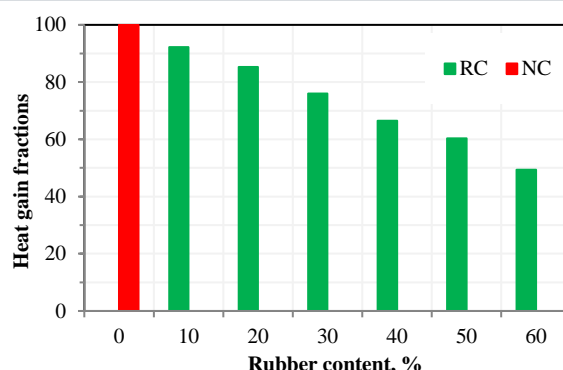


Figure 8. The percentages of max. heat gain fractions for each south-wall construction with different rubber ratios.

Daily variations of heat gain values of the NC and RCC walls with different RCA ratios are illustrated in Figure 9. NC (normal concrete wall) wall constructions have the highest amplitude of the heat gain value and this is followed by RC10, RC20, RC30, RC40, RC50 and RC60, respectively. The lowest and highest heat gain values are obtained for the RCC50 and NC walls with the values of 32.56 W/m<sup>2</sup> and 65.91 W/m<sup>2</sup>, respectively. It can be concluded from the Figure 9 that rubberized concrete walls will contribute to the reduction of the building space cooling load and the capacity of air-conditioning system. Considering that the amount of energy consumption of the buildings is such enormous, hence the thermal insulating effect of those elements is most attractive and indicates a high and promising potential.

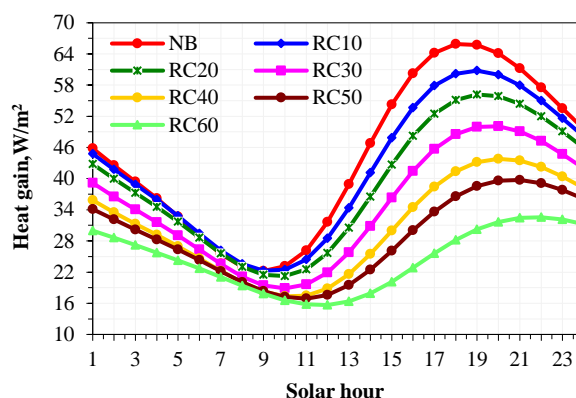


Figure 9. Variation of the highest heat gains with thickness of south-wall constructions.

## 4. CONCLUSION

The main conclusions obtained from both experimental and theoretical studies can be summarized as follows:

1. Compressive and split tensile strength values decreased with the increase of the amount of rubber particle in concrete. This reduction is generally due to the lack of adhesion between the rubber particles and the paste.
2. The oven-dried density values decreased with increasing rubber aggregate ratios. Such a reduction can have significant advantages from the point of earthquake resistance.
3. The reduction in thermal conductivity of composite was due to the insulating effect of rubber particle, which had a lower thermal conductivity compared to that of cement matrix.
4. The results indicated that the maximum reduction in heat gain value was obtained as 50.6 % for RC60 wall with commonly used thickness of 20 cm corresponding to conventional concrete. Use

of waste rubber particles in a masonry construction can help reduce the building space cooling load and the capacity of air-conditioning system.

5. Consequently, addition of waste tire particles into concrete provides not only an alternative cost-effective solution for today's energy efficient buildings, but also an alternative safe way of utilizing a waste material to help environmental protection.

### REFERENCES

- [1] M. W. Tantala, Lepore, J. A., and I. Zandi, "Quasi-Elastic Behavior of Rubber Included Concrete," in *Proceedings, 12th International Conference on Solid Waste Technology and Management*, 1996.
- [2] M. Venu and P. N. Rao, "Study of Rubber Aggregates in Concrete: An Experimental Investigation", *International Journal of Civil Engineering & Technology (IJCIET)*, vol. 1, no. 1, pp. 15 – 26, 2010.
- [3] N. Siva linga Rao, "Investigations on Properties of Lightweight Aggregate Concrete with Cinder", *International Journal of Earth Sciences and Engineering*, vol. 4, no. 6, pp. 907-912, 2013.
- [4] R. Siddique and T. R. Naik, "Properties of Concrete Containing Scrap-Tire Rubber—An Overview", *Waste Management*, vol. 24, pp. 563–569, 2004.
- [5] N. Fattuhi and L. Clark, "Cement based materials containing shredded scrap truck tire rubber", *Construction and Building Materials*, vol. 10, no. 4, pp. 229-236, 1996.
- [6] I. B. Topcu, "The Properties of Rubberized Concrete", *Cement and concrete Research*, vol. 25, no. 2, 1995.
- [7] P. Sukontasukkul, "Properties of Concrete Pedestrian Block Mixed with Crumb Rubber" *Department of Civil Engineering, King Mongkut's Institute of Technology –North Bangkok*: pp. 450-457, 2006.
- [8] A. Benazzouk, O. Douzane, K. Mezreb, B. Laidoudi, and M. Quéneudec, "Thermal Conductivity of Cement Composites Containing Rubber Waste Particles: Experimental Study and Modelling", *Construction and Building Materials*, vol. 22, no. 4, pp. 573-579, 2008.
- [9] P. Turgut, and B. Yesilata, "Physico-Mechanical and Thermal Performances of Newly Developed Rubber-Added Bricks", *Energy and Buildings*, vol. 40 no. 5, pp. 679-688, 2008.
- [10] B. Yesilata, H. Bulut, and P. Turgut, "Experimental Study on Thermal Behavior of A Building Structure Using Rubberized Exterior-Walls", *Energy and Buildings*, vol. 43 no. 2, pp. 393-399, 2011.
- [11] R. Yumrutas, O. Kaska and E. Yildirim, "Estimation of Total Equivalent Temperature Difference Values for Multilayer Walls and Flat Roofs by Using Periodic Solution", *Building and Environment*, vol. 42, pp. 1878–85, 2007.
- [12] R. Yumrutas, M. Unsal and M. Kanoglu, "Periodic Solution of Transient Heat Flow Through Multilayer Walls and Flat Roofs by Complex Finite Fourier Transform Technique", *Building and Environment*, vol. 40, pp. 1117–1125, 2005.

# Mathematical Modeling and Performance Analysis of Solar Assisted Heat Pump Wheat Drying System with Energy Storage Tank

*Recep Yumrutas<sup>1</sup>, Hatem Ismaeel<sup>2</sup>*

## Abstract

*An analytical model is presented to predict the long term performance of a solar assisted drying system with a heat pump and an underground spherical thermal energy storage (TES) tank. The system consists of a wheat dryer, heat pump, TES tank and solar collectors. The analytical model is based on a proper coupling of each model for the wheat dryer, the heat pump, solar collectors, and the TES tank. An analytical model was developed to obtain the performance of the system. Therefore, a computational model was written in MATLAB program. The results obtained from the analysis indicate that 4-6 years operational time span is necessary before the system can attain an annually periodic operating condition. Results also indicate a decrease in solar collector area leads to a decrease the storage tank temperature and COP. Carnot efficiency (CE) has a small effect on the TES tank temperature while having a stronger effect on the COP of the heat pump.*

**Keywords:** Wheat; Dryer unit; Solar system modeling; Solar energy; Energy storage; Heat pump drying

## 1. INTRODUCTION

Drying is used in a wide variety of applications ranging from food drying to wood drying. In drying, heat and moisture transfer occur simultaneously. The direct contact heat and mass transfer method has been adopted in many engineering fields by using different heat transfer media [1]. Grains can be divided into three groups; cereals (maize, wheat, millet. Rice, etc), pulses (beans, peas, cowpeas, etc.), and oil seeds (soyabeans, sunflower, linseed, etc) [2].

Using heat pump system in convective hot air dryers has been recognized as an ideal area for HP applications [3]. Mrema et al. [4] found that Heat Pump Drying system (HPDs) consume 60–80% less energy than conventional dryers operating at the same temperature. Schmidt [5] classified HPD applications to three types Air source heat-pump drying systems, Ground source heat-pump drying systems and Chemical heat-pump drying systems. It may be concluded that the most preferred method used to determine the HPD efficiency is SMER, while in recent years exergetic analysis method has been widely used. A comparative study on the mathematical modeling of the drying characteristics of wheat grains investigated to estimate the suitable mathematical model of the drying behavior of the wheat at different operating parameters [6]. Drying experiments were carried out with different operating parameters such as inlet air temperature (55, 60 and 65°C), air velocity (2.2, 2.4 and 2.6 m/sec) and initial moisture content of wheat (27.5, 30 and 32.5%) of total solid weight. Among different model considered, the logarithmic model presented a better agreement with the data attained from the experiments [6].

Previous studies indicate that there is limited information on ground heat pump drying systems, despite the many studies that have been undertaken [7]. Especially with taking into account transient operational behavior of these systems starting from their first day of operation until such systems reaches an annually

<sup>1</sup> Corresponding author: Gaziantep University, Department of Mechanical Engineering, 27310, Gaziantep, Turkey. [yumrutas@gantep.edu.tr](mailto:yumrutas@gantep.edu.tr)

<sup>2</sup> Duhok Polytechnic University, Bardarash Technical Institute, Duhok, Iraq. [bardarashi77@gmail.com](mailto:bardarashi77@gmail.com)

periodic regime, and this is the subject of the present investigation. The objective of this study is to give an analytical model for the solar assisted heat pump drying system to find performance of the whole system.

## 2. DESCRIPTION OF THE SYSTEM

The scheme of the thermal system is described in Figure.1. The system consists of four main components which are wheat dryer, heat pump, solar collectors and TES tank located in Gaziantep, Turkey. The TES is to be used for seasonal storage of solar energy for use by the heat pump. The TES is assumed to be spherical and buried underground. Solar collectors absorb solar energy and charge it into the TES tank during the whole year. Solar collectors operate whenever there is useful solar energy is available. Heat pump is coupled to the TES tank used as a heat source. Heat will be supplied to the dryer by the heat pump. It is considered that the heat is supplied to the dryer by heat pump condensor, then via air heating and passing through moist product in the dryer unit to evaporate undesired water available in the wheat.

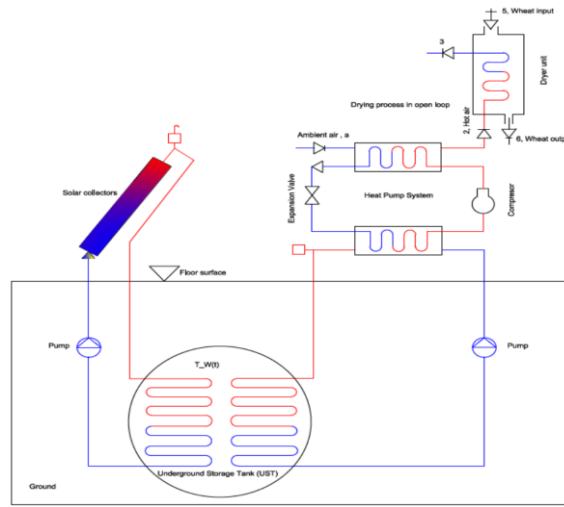


Figure 1. Heat pump wheat drying system assisted by solar collectors and TES tank

## 3. ANALYTICAL MODELING OF THE SYSTEM

### 3.1. Dryer unit

Schematic of the dryer unit is illustrated in Figure 2. Mass and energy balances can be written for the dryer unit, and treated as a control volume. We can write mass balances for the dryer given above for three flows: (1) product, (2) dry air, and (3) water [8].

$$\text{Product: } \dot{m}_{p_z} = \dot{m}_{p_s} = \dot{m}_p$$

$$\text{Air: } \dot{m}_{a_z} = \dot{m}_{a_s} = \dot{m}_a$$

Water:

$$\omega_2 \dot{m}_a + \dot{m}_{w_z} = \omega_3 \dot{m}_a + \dot{m}_{w_s} \quad (1)$$

An energy balance can be written for the entire system with insulated drying chamber by equating input and output energy terms [8]:

$$\dot{m}_a h_2 + \dot{m}_p h_{p_z} + \dot{m}_{w_z} h_{w_z} = \dot{m}_a h_3 + \dot{m}_p h_{p_s} + \dot{m}_{w_s} h_{w_s} + \dot{q}_l \quad (2)$$

The enthalpy of air mixture can be written as the following [9].

$$h = 1.006 T + \omega(2501 + 1.86 T) \quad (3)$$

The specific enthalpy term of the product (wheat) in the energy rate balance can therefore be expressed as follows:

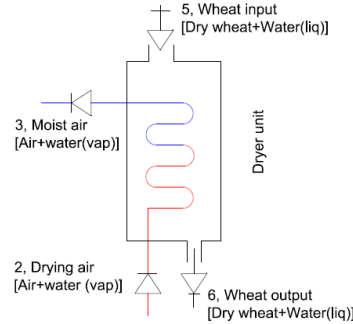


Figure 2. Schematic of dryer unit.

$$(h_{p_4} - h_{p_2}) = C_{p_{wheat}}(T_6 - T_5) \quad (4)$$

Therefore eq. (2) can be written as following:

$$\dot{m}_a(h_2 - h_3) = \dot{m}_p C_{p_{wheat}}(T_6 - T_5) + \dot{Q}_{evap} \quad (5)$$

The heat transfer rate due to phase change is:

$$\dot{Q}_{evap} = \dot{m}_w \times h_{fg} \quad (6)$$

where  $h_{fg}$  is latent heat of vaporization of water (kJ/kg) at the average temperature of the moist material.

$$T_{average} = \frac{T_5 + T_6}{2}$$

The wheat kernel specific heat given by Kazarian and Hall [10].

$$C_{p_{wheat}} = 1398.3 + 4090.2 \left( \frac{M_p}{1 + M_p} \right) \quad (7)$$

$$M_p = \frac{W_5 - W_6}{W_6} \times 100$$

where  $W_5$  is weight of material before drying (kg),  $W_6$  is weight of material after drying (kg) and  $M_p$  is moisture content of material on a dry basis (kg water/kg solid). Another equation will be used to find the weight of material after drying as following [11]:

$$W_6 = W_5 - \left[ W_5 \frac{(M_{p_5} - M_{p_6})}{100 - M_{p_6}} \right] \quad (8)$$

where  $W_5$  &  $W_6$  in kg representing weight of wheat product before and after drying respectively.

Drying temperatures are typically in the range of 0–70°C. However, for special purposes, the lower temperature limit can be shifted down to –10°C. Inlet relative humidities of the air are usually kept ~30 to 40% [12], [13].

### 3.2. Energy requirement of the heat pump

A heat pump extracts heat from a source and transfers it to a sink at a higher temperature [14]. The heat pump extracts heat from the TES tank, and supplies heat to the ambient air by air cooled condenser. Then air is passing through moist wheat in the dryer, the wheat temperature increased and water vapor will be released to the environment as a result of contact between them. Heat supplied to the dryer can be expressed by the product of the coefficient of performance (COP) of the heat pump and heat pump work:

$$Q_{cond}(t) = W(t)(COP) \quad (9)$$

$$COP = \frac{Q_{cond}(t)}{W(t)} \quad (10)$$

COP of the heat pump was calculated using the approach given in [15]. The Carnot efficiency,  $\eta_c$  is equal to the ratio of actual COP of a heat pump to Carnot COP.



$$\eta_c = \frac{COP}{COP_c} \quad (11)$$

Carnot  $COP_c$  may be expressed as a function of source ( $T_h$ ) and sink ( $T_c$ ) temperatures as:

$$COP_c = \frac{T_h(t)}{T_h(t) - T_w(t)} \quad (12)$$

Combining above two equations, yields:

$$COP = \eta_c \left( \frac{T_h(t)}{T_h(t) - T_w(t)} \right) \quad (13)$$

$$\dot{Q}_{cond} = \dot{m}_a C_{p_n} (T_2 - T_a) \quad (14)$$

The eq.14 can be used to find mass flow rate of air  $\dot{m}_a$  entering to the dryer.

$$\dot{m}_a = \frac{\dot{Q}_{cond}}{C_{p_n} (T_2 - T_a(t))} \quad (15)$$

$$\dot{Q}_{cond} = (UA)_{hs} (T_h(t) - T_c) \quad (16)$$

where  $(UA)_{hs}$  and  $T_h(t)$  are UA-value for the load side heat exchanger (condenser) and  $T_c$  mean temperature of fluid in the load side heat exchanger located in the dryer unit.

$$T_c = \frac{T_2 + T_a}{2} \quad (17)$$

Where  $T_a$  represents the minimum ambient temperature in the year for Gaziantep city (Turkey) to estimate  $T_c$ , and  $T_2$  is supply air temperature to moist wheat in the dryer. Now it can be combine the Eqs. (14) and (16) and solve for  $T_h$  then insert the result of  $T_h$  in Eq.18, gives:

$$COP = \eta_c \left( \frac{u(\phi_c + 1) + \phi_2 - \phi_a(t)}{u\phi_c + \phi_2 - \phi_a(t) - u\phi_w(t)} \right) \quad (18)$$

Inserting Eqs. (18) and (14) into Eq. (9), the dimensionless compressor work may,  $w$ , be obtained in dimensionless form as follows:

$$w = \frac{[\phi_2 - \phi_a(t)][u\phi_c + \phi_2 - \phi_a(t) - u\phi_w(t)]}{\eta_c [u(\phi_c + 1) + \phi_2 - \phi_a(t)]} \quad (19)$$

$$u = \frac{(UA)_{hs}}{\dot{m}_a C_{p_n}} = \frac{T_2 - T_a(t)}{T_h(t) - T_c} \quad (20)$$

For drying, a more appropriate efficiency parameter is the specific moisture evaporation (extraction) rate (SMER) defined by [2]

$$SMER = \frac{\text{amount of water evaporated}}{\text{energy used}} = \frac{\dot{m}_w}{E_{input}} \quad (21)$$

Alternatively, the reciprocal of the SMER is reported as the heat pump dryer efficiency (HPDE), which is the energy required to remove 1 kg of water. The SMER depends on the maximum air temperature in the dryer, the air's relative humidity, the evaporation and condensation temperatures, and the efficiency of a refrigeration system [9]. Where  $E_{input}$  is the energy input to the drying system (KW).

### 3.3. Transient temperature field problem around the TES tank

The water is considered to be initially at the deep ground temperature  $T_{\infty}$ , and fully mixed at a spatially lumped time varying temperature  $T_w(t)$ . The energy balance of the underground TES tank is shown in Figure 3.

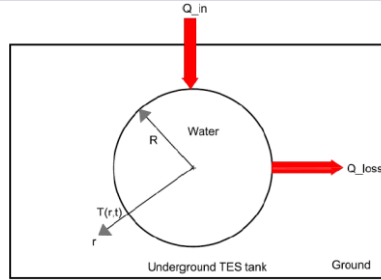


Figure 3. The energy balance of the underground TES tank.

The transient heat transfer problem given by [17], with temperature of water in the TES tank at the  $n$ th time increment to yield:

$$\phi_w(\tau_n) = \frac{q(\tau_n) + \left[ \frac{P}{\Delta\tau} + \frac{1}{\sqrt{\pi\Delta\tau}} \right] \phi_w(\tau_{n-1}) - \sum_{i=1}^{n-2} \frac{\phi_w(\tau_i + 1) - \phi_w(\tau_i)}{\sqrt{\pi\Delta\tau(n-i)}}}{1 + \frac{P}{\Delta\tau} + \frac{1}{\sqrt{\pi\Delta\tau}}} \quad (22)$$

Eq. (22) will be used to calculate the water temperature of the spherical TES. The term  $q(\tau)$  in Eq. (22) represents the dimensionless net heat input rate to the TES tank [17]. The heat input rate to the TES tank,  $q(\tau)$  is the difference between dimensionless heat collection rate by the solar collectors and the energy extracted by the heat pump, which is given as [18], [19]

$$q(\tau) = q_u(\tau) - q_c(\tau) + \frac{w(\tau)}{\gamma} \quad (23)$$

where  $\gamma$  is dimensionless parameter  $\left( \frac{4\pi Rk}{\dot{m}_a C_{p,a}} \right)$ , and  $q_u(\tau)$  is the dimensionless available solar energy rate collected by the solar collectors.  $q_c(\tau)$  and  $w(\tau)$  are the dimensionless heat requirement of the dryer and the heat pump work, respectively.

### 3.4. Hourly useful solar energy collection rate

Flat plate solar collectors are considered to charge solar energy into the storage tank. It can be obtained from the expression for useful energy collection rate. The hourly useful energy collection rate,  $Q_u(t)$  can be calculated with the formula given by [22].

$$Q_u(t) = \eta_{fp}(t) I_T(t) \quad (24)$$

where  $\eta_{fp}$  is the efficiency of a flat plate solar collector and it can be calculated as in [20]. Procedure calculation details for remaining parameters is given in [22].

## 4. RESULTS AND DISCUSSION

A computer program based on the analytical model was prepared in MATLAB to carry out the numerical computations. All data for computation of the system performance parameters are taken from Gaziantep Meteorological Station and from Ref. [6], [20], [23], and [24].

Figure 4 is depicted for comparing effect of the thermophysical properties of the three earth types on store temperature [23]. It shows that both thermal conductivity and thermal diffusivity values for coarse grained earth are lower than corresponding values of these properties for the other types of earth. Also, heat capacity of coarse grained earth is greater than those values for the other types of earths. It is also seen from the Fig. that there is rapid variation of TES tank temperatures during the first few years of operation. Variations of the TES tank temperatures decrease up until the fourth year of operation for all geological structures, and they do not change after fourth year of operation indicating periodic operating conditions thereafter. Fig. 5 indicates annual variation of the TES tank temperature for limestone type earth during the first, second, fifth, and sixth years of operation. It is seen that annually periodic operating conditions are reached after the fourth year of operation.

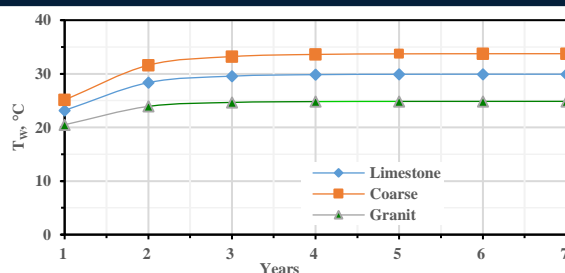


Figure 4. variation of the TES tank temperature for September ( $A_c=30 \text{ m}^2$ ,  $CE=40\%$ ,  $V=200 \text{ m}^3$ ,  $W_s=20 \text{ kg/hr}$ )

Fig. 6 shows annual variation of water temperature in the TES tank during the fifth year of operation for three different geological earth types; coarse graveled earth, limestone, and granite. It is seen that the highest temperatures are at the end of summer and the lowest ones are at the end of winter. Heat pump does not operate in summer months while the TES tank is charged by solar resulting in an increase in the tank temperature. As a result of energy extraction from the TES tank by the heat pump during winter season, the tank temperature decreases gradually toward the end of the winter season, and the lowest store temperature occurs at the end of winter. It is clear that the highest store temperatures are obtained when the TES tank is surrounded with coarse graveled earth, and the lowest one is obtained for the granite. These observations are in agreement those presented in [17] and [19] for annually periodic operation of the system.

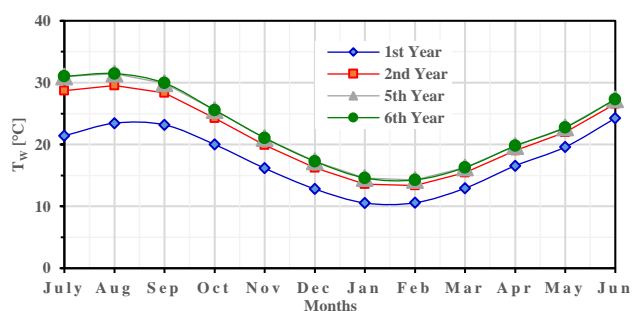


Fig. 5. Variation of the TES tank temperature with years (limestone,  $A_c = 30 \text{ m}^2$ ,  $CE = 40\%$ ,  $V = 200 \text{ m}^3$ ,  $W_s=20 \text{ kg/hr}$ ).

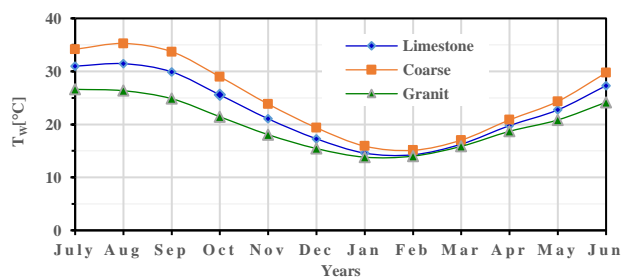


Figure 6. Effect of earth type on water temperature in the TES tank during fifth year of operation

( $A_c = 30 \text{ m}^2$ ,  $CE = 40\%$ ,  $V = 200 \text{ m}^3$ ,  $W_s=20 \text{ kg/hr}$ ).

CE values are recommended in Ref. [25] in the range of 0.30 and 0.50 for small electric heat pumps. In this study, three CE values are used as 0.30, 0.40 and 0.50. Results obtained for monthly variation of the TES tank temperature during the fifth year of operation and long term variation of COP are shown in Figs. 7 and 8, respectively. Higher CE values yield lower TES water temperatures [21], and this is depicted in Fig. 7. A higher CE means a higher amount of heat extraction from the tank for the same heating load, and as a result of this, the TES temperature decreases. Effect of CE on the TES tank temperature is small as it is seen in Fig. 7. COP increases with years up until annually periodic operational conditions are attained. Effect of the CE on the TES tank temperatures reported in this study are in agreement with results in [17] and [21].

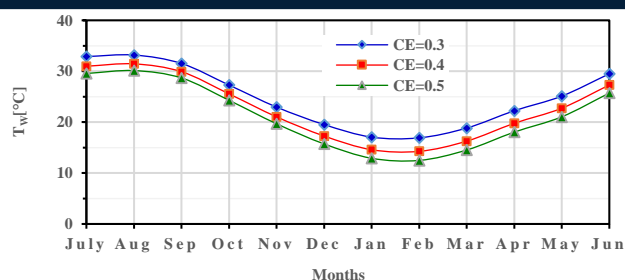


Figure 7. Effect of CE on TES tank temperature during fifth year of operation

(limestone,  $A_c = 30 \text{ m}^2$ ,  $V = 200 \text{ m}^3$ ,  $W_5 = 20 \text{ kg/hr}$ )

Effects of collector area on the TES tank temperature and on the COP of the heat pump are shown on Figs. 9 and 10. It is seen in both figures that the TES tank temperature and COP increase with increasing collector area. It is observed from the Fig. 10 that the heating system reaches an annually periodic operating condition within 4 or 5 years for the system parameters considered in this study. Total annual energy supplied to the system during a whole year is solar energy and heat pump work. Total annual energy supplied is partially stored in the tank, partially lost into the surrounding earth, and the remaining portion used for dryer unit.

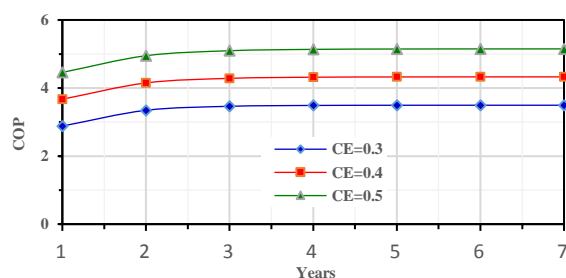


Figure 8. Effect of CE on COP of the heat pump (limestone,  $A_c = 30 \text{ m}^2$ ,  $V = 200 \text{ m}^3$ ,  $W_5 = 20 \text{ kg/hr}$ ).

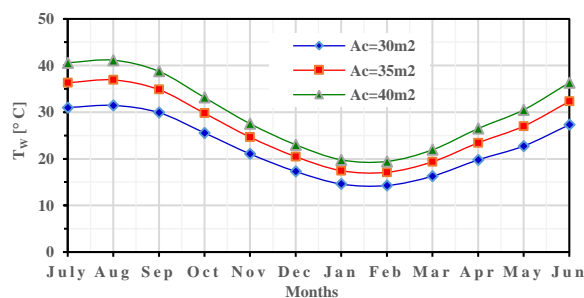


Figure 9. Effect of collector area on the TES tank temperature during fifth year of operation

(limestone,  $CE = 40\%$ ,  $V = 200 \text{ m}^3$ ,  $W_5 = 20 \text{ kg/hr}$ ).

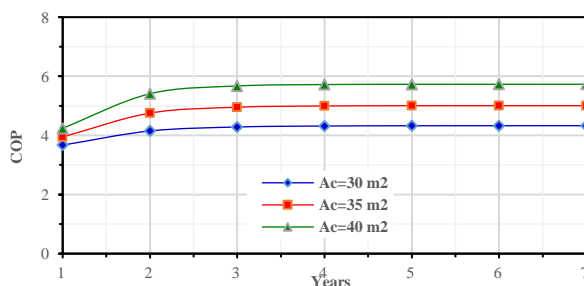


Figure 10. Effect of collector area on heat pump COP (limestone,  $CE = 40\%$ ,  $V = 200 \text{ m}^3$ ,  $W_5 = 20 \text{ kg/hr}$ ).

Energy fractions in the present study are defined as the ratio of each energy component to the total annual energy supplied to the system. Annual energy balance of the system during the first, third and fifth years of operation is shown in Figs. 11. It indicates an increase in solar energy fraction and a corresponding increase in the fraction used at the load with years.

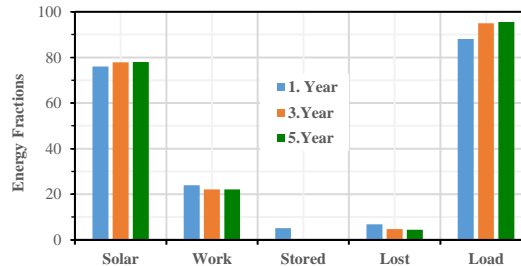


Figure 11. Variation of energy fractions with years (limestone,  $A_c=30 \text{ m}^2$ ,  $CE=40\%$ ,  $V=200 \text{ m}^3$ ,  $W_s=20 \text{ kg/hr}$ ).

### 5. CONCLUSION

A computer code based on the analytical model was developed, and used to investigate the effects of operation number of years, thermophysical properties of earth surrounding the TES tank, Carnot Efficiency (CE) of the heat pump and collector area on the TES tank temperature on thermal performance of the system. Results indicate that an operational time span of 4–6 years will be sufficient for the system under investigation to reach an annually periodic operating condition. Thermophysical properties of earth around the tank effects the performance of the system and coarse grained earth yields the best thermal performance from within the three earth types considered in this study. CE has a small effect on the TES tank temperature while having a stronger effect on the COP of the heat pump.

### Nomenclature

A area ( $\text{m}^2$ )

c specific heat ( $\text{J}/(\text{kg K})$ )

COP coefficient of performance of heat pump

HPD heat pump drying

k thermal conductivity of earth ( $\text{W}/(\text{m K})$ )

R tank radius (m)

q dimensionless heat transfer to the tank

Q heat transfer to the tank (W)

t time (s)

$T_a$  ambient air temperature (K)

$T_2$  condenser outlet temperature (K)

$T_5$  moist wheat temperature (K)

$T_6$  dry wheat temperature (K)

$T_w$  water temperature in storage tank (K)

$T_\infty$  deep earth temperature (K)

u dimensionless parameter,  $(UA)_{he}/\dot{m}_a C_{p,a}$

$(UA)_{he}$  product of heat transfer coefficient and area for heat pump condenser (W/K)

w dimensionless compressor work

W compressor work (W)

x	dimensionless radial distance
re	monthly average reflectivity of earth
Greek letters	
$\alpha$	thermal diffusivity of earth (m <sup>2</sup> /s)
$\eta_c$	Carnot efficiency
$\eta_{fp}$	efficiency of a flat plate solar collector.
$\phi$	dimensionless temperature, $\phi = \frac{T-T_\infty}{T_\infty}$
$\rho$	density (kg/m <sup>3</sup> )
$\tau$	dimensionless time

### REFERENCES

- [1] Inaba H; Aoyama S; Haruki N; Horibe A; Nagayoshi K (2002) Heat and mass transfer characteristics.
- [2] Mrema, G. C., Gumbe, L. O., Chepete, H. J., & Agullo, J. O. (2012). *Rural structures in the tropics: design and development*. Food and Agriculture Organization of the United Nations.
- [3] Schmidt EL, Klocker K, Flacke N, Steimle F. Applying the transcritical CO<sub>2</sub> process to a drying heat pump. *Int J Refrig* 1998;21 (3):202–11.
- [4] Strommen I, Eikevik TM, Alves-Filho O, Syverud K, Jonassen O. Low temperature drying with heat pumps new generations of high quality dried products. In: 13th International drying symposium; 2002.
- [5] Colak, N., & Hepbasli, A. (2009). A review of heat-pump drying (HPD): Part 2–Applications and performance assessments. *Energy Conversion and Management*, 50(9), 2187-2199.
- [6] Sundaram, P., Sudhakar, P., & Yogeshwaran, R. (2016). Experimental studies and mathematical modeling of drying wheat in fluidized bed dryer. *Indian Journal of Science and Technology*, 9(36).
- [7] Kivevele, T., & Huan, Z. (2014). A review on opportunities for the development of heat pump drying systems in South Africa. *South African Journal of Science*, 110 (5-6), 01-11.
- [8] Dincer, I., & Rosen, M. A. (2012). *Exergy: energy, environment and sustainable development*. Newnes.
- [9] Alves-Filho, O. (2015). *Heat pump dryers: Theory, design and industrial applications*. CRC Press.
- [10] Kazarian, E. A., & Hall, C. W. (1962). *Thermal properties of grain* (Doctoral dissertation, Michigan State University of Agriculture and Applied Science. Dept. of Agricultural Engineering).
- [11] Mrema, G. C., Gumbe, L. O., Chepete, H. J., & Agullo, J. O. (2012). *Rural structures in the tropics: design and development*. Food and Agriculture Organization of the United Nations
- [12] Strommen, I. 1980. Drying of heavily salted codfish. Ph.D. Thesis. The Norwegian Institute of Technology, Division of Refrigeration Engineering, Trondheim, Norway (in Norwegian).
- [13] Magnussen, O. M. and Strommen, I. 1981. Heat pump drying of heavily salted codfish. *Nordic Refrigeration Meeting*, Copenhagen, May 21 – 23 (in Norwegian).
- [14] ASHRAE, H. (2000). *Systems & Equipment Handbook 2000. SI Edition*.
- [15] Tarnawski, V.R., 1989. Ground heat storage with double layer heat exchanger. *International Journal of Energy Research* 13, 137 – 148.
- [16] Zogou, O., & Stamatelos, A. (1998). Effect of climatic conditions on the design optimization of heat pump systems for space heating and cooling. *Energy Conversion and Management*, 39(7), 609-622.
- [17] Yumrutas, R., & Unsal, M. (2012). Energy analysis and modeling of a solar assisted house heating system with a heat pump and an underground energy storage tank. *Solar Energy*, 86(3), 983-993.
- [18] Yumrutas, R., & Unsal, M. (2000). Analysis of solar aided heat pump systems with seasonal thermal energy storage in surface tanks. *Energy*, 25(12), 1231-1243.
- [19] Yumrutas, R., Kunduz, M., & Ayhan, T. (2003). Investigation of thermal performance of a ground coupled heat pump system with a cylindrical energy storage tank. *International journal of energy research*, 27(11), 1051-1066.
- [21] Yumrutas, R., Kanog˘lu, M., Bolatturk, A., Bedir, M.S., 2005. Computational model for a ground coupled space cooling system with an underground energy storage tank. *Energy and Building* 37, 353–360.
- [20] Yumrutas, R., & Kaska, O. (2004). Experimental investigation of thermal performance of a solar assisted heat pump system with an energy storage. *International journal of energy research*, 28(2), 163-175.
- [22] Duffie, J. A. (1991). Beckman. *Solar Engineering of thermal process*. WA, New York.
- [23] Ozisik, M.N., 1985. *Heat Transfer: A Basic Approach*. McGraw-Hill, New York.
- [24] Elminir, H.K., Ghitass, A.E., El-Hussainy, F., Hamid, R., Beheary, M.M., Abdel-Moneim, K.M., 2006. Optimum solar flat-plate collector slope: case study for Helwan. *Egypt, Energy Conversion and Management* 47, 624–637.
- [25] Zogou, O., Stamatelos, A., 1998. Effect of climatic conditions on the design optimization of heat pump systems for space heating and cooling. *Energy Conversion and Management* 39 (7), 609–622.



## Adsorption of methylene blue by using activated carbon prepared by olive seed

Aysegul Pala<sup>1</sup>, Ceren Melis Karakivrak<sup>1</sup>, Gunes Kursun<sup>2</sup>,

### Abstract

*In this study, the adsorption of methylene blue (MB) from its aqueous solution onto activated carbon prepared by olive seeds were investigated. Morphology, surface properties, bond structures and elemental ratios of activated carbon were determined by using SEM, BET, FTIR and XPS analysis, respectively. The adsorption characteristics of activated carbon were investigated as a function of initial dye concentration and adsorption dosage. Activated carbon was prepared from olive seed by chemical activation. The activation process was performed by using %30 Na<sub>2</sub>CO<sub>3</sub> and %5 H<sub>3</sub>BO<sub>3</sub> with olive seed. In order to obtain activated carbon, 750°C activation temperature and 60 minute carbonization time were selected. The optimum conditions for the adsorption of MB were found as follows: adsorbent dosage of 0,5 g/L, initial MB concentration of 10 mg/L. As a result of adsorption 97.27 % removal of MB was reached. According to experiments the best fit isotherm was determined as Langmuir isotherm with R<sup>2</sup> = 0,9533.*

**Keywords:** Adsorption, Methylene Blue, Olive Seeds, Activated Carbon

### 1. INTRODUCTION

Discharging of dyes into water media even in low amounts can affect the aquatic life, prevent light to get in and decrease the performance of photosynthesis. Dye effluents comes from plastics, rubber, paper, textile, cosmetics and leather industries (1). Activated carbon has been favourable as an adsorbent for MB removal from wastewater due to its large specific surface area, low density, chemical stability, suitability for large scale production, variety of structural forms, and its ability to modify the pore structures (2). Due to the low cost, high adsorption capacity, low clay ingredients and enough mechanic strength, activated carbon is producing from agricultural wastes (3). Activated carbon from olive stones were used for water purification (4). Riham Hazzaa and Mohamed Hussein has been reported olive stones from activated carbon for adsorption of cationic dye (5).

### 2. MATERIAL AND METHODS

#### 2.1. Preparation

Preparation process was separated into 3 steps, activation, which is the enlargement of the pores and improvement of the surface functional groups, dehydration is the loss of the water and carbonization is the transformation of organics to elemental carbon and loss of non-carbon compounds.

In the first stage of the preparation step, olive seed has been extracted from Kusadasi, Aydin, Turkey. Olive seeds prepared with 1-4 mm size.. 30 % Na<sub>2</sub>CO<sub>3</sub> solution and 5 % H<sub>3</sub>BO<sub>3</sub> solution was prepared. Na<sub>2</sub>CO<sub>3</sub> solution was done with stirring speed of 250 rpm for 4 hours and was impregnated. In the second stage of the preparation step, H<sub>3</sub>BO<sub>3</sub> solution was done with the stirring speed of 250 rpm for 2 hours on a 80 °C water bath and was impregnated. After second stage, samples were dehydrated in the incubator at 105 °C.

<sup>1</sup>Corresponding author: Dokuz Eylul University, Department of Environmental Engineering, 35160, Buca/İzmir, Turkey. [aysegulpala@deu.edu.tr](mailto:aysegulpala@deu.edu.tr)

<sup>2</sup> Dokuz Eylul University, Applied Sciences, 35160, Buca/İzmir, Turkey.

## 2.2. Carbonization

In order to transform olive seed to activated carbon, Samples were carbonized in the nitrogen gas atmosphere. 750°C carbonization temperature and 60 minutes time was preferred. After carbonization; samples were washed with pure water at the pH=6,5 and dehydrated on a 105 °C stove. After these steps, activated carbon olive seeds were prepared.

## 2.3. Characterization

In order to measure XPS of samples, Thermo Scientific K-Alpha XPS was used. SEM micrographs of the samples were examined in COXEM EM-30 Plus. FTIR analysis was performed in Thermo Scientific Nicolet IS10. For characterization of samples, SEM (Scanning Electron Microscope), XPS (X-Ray Photoelectron Spectroscopy), FTIR (Fourier Transform Irradiation), BET (Brunauer Emmett Teller) tests were performed.

## 3. RESULT AND DISCUSSION

### 3.1. Carbonization

After carbonization process, the sample was shown in Figure 1.



Figure 1. The sample of olive seeds after carbonization process

### 3.2. SEM ( Scanning Electron Microscope)

According to SEM results, the activated carbon olive seeds have micro and macro pores. It has high adsorption capacity.

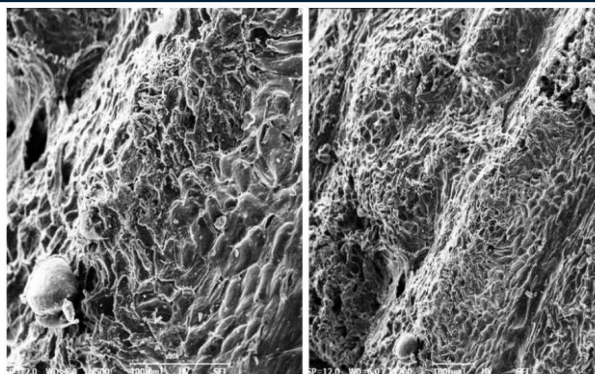


Figure 2. SEM morphology of olive seed for x200 and x500, respectively

### 3.3. FTIR ( Fourier Transform Irradiation)

According to FT-IR results alcohols, ketons and carboxyl groups were occurred as shown in Figure 3.

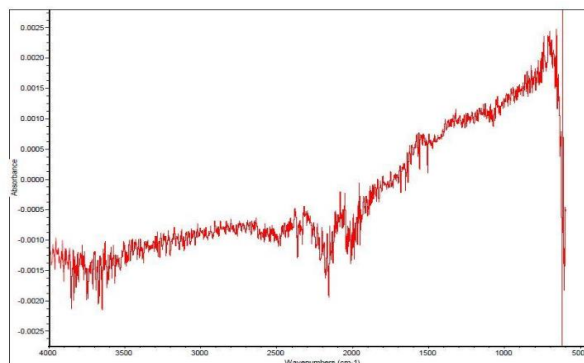


Figure 3. FTIR sample

### 3.4. XPS (X-Ray Photoelectron Spectroscopy)

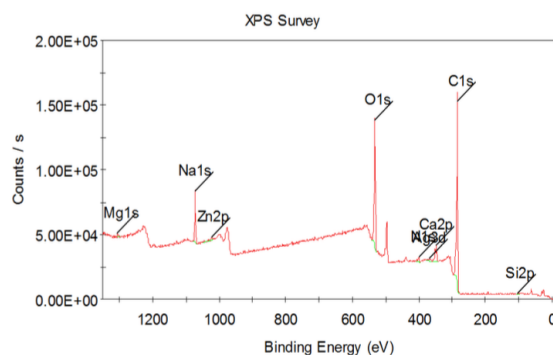


Figure 4. XPS result of the sample

According to XPS result, the carbon, oxygen, calcium and sodium were found to be 58.32, 26.66, 5.12, 4.87 %, respectively. XPS results of activated carbon olive seeds were shown in Figure 4-5.

Name	Peak BE	FWHM eV	Area (P) CPS.eV	Weight %	Q
C1s	285.20	2.84	468624.15	58.32	1
O1s	532.16	3.56	388836.60	26.66	1
Na1s	1072.04	2.58	99504.65	4.87	1
Ca2p	347.97	3.69	70624.49	5.12	1
N1s	399.85	4.34	24447.46	2.29	1
Ag3d	368.01	4.20	15582.34	0.83	1
Si2p	103.38	3.42	2867.25	0.83	1
Mg1s	1305.03	0.33	6321.16	0.38	1
Zn2p	1022.74	2.10	16443.27	0.70	1

Figure 5. XPS result of the sample

### 3.5. BET (Brunauer Emmett Teller)

According to BET results, BET Surface Area was measured as 441,0890 m<sup>2</sup>/g, Single-point adsorption was measured as 0,233865 cm<sup>3</sup>/g, Adsorption average pore diameter (4V/A by BET): 21,208 Å, Desorption average pore diameter (4V/A by BET): 21,319 Å, BJH Adsorption average pore width (4V/A): 30,667 Å, BJH Desorption average pore width (4V/A): 27,719 Å measured, respectively.

### 3.6. Adsorption

Activated carbon prepared from olive seeds were produced and 10 mg/L methylene blue solution was tested for colour removal. Increased amount of activated carbon as 0,1 g, 0,3 g and 0,5 g were put into 50 ml flasks for each samples. Adsorption and colour removal efficiency results were shown in Table 1. The adsorption effect of activated carbon on MB were illustrated in Figure 6.

Table 15. Adsorption Results

Sample	g/l	Absorbance	Absorbance	Colour Removal efficiency (%)
Olive seed	0,1	2,161	0,11	94,91
Olive seed	0,3	2,161	0,087	95,97
Olive seed	0,5	2,161	0,059	97,27
Blank sample		2,161	2,128	1,53



Figure 6. The effect of adsorption

### 3.7. Adsorption Kinetics

According to Langmuir isotherm of olive seeds,  $R^2$  was found to be 0,9533. Langmuir isotherm was illustrated in Figure 7. For Freundlich isotherm  $R^2$  was found to be 0,8803 and illustrated in Figure 8. With reference to Figure 9, when the dye concentration was increased, the adsorption capacity was found to be increased.

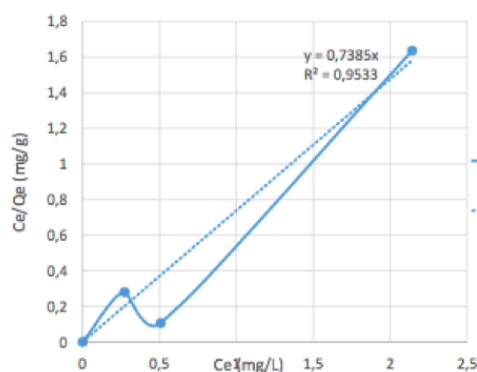


Figure 7. Langmuir isotherm of olive seeds

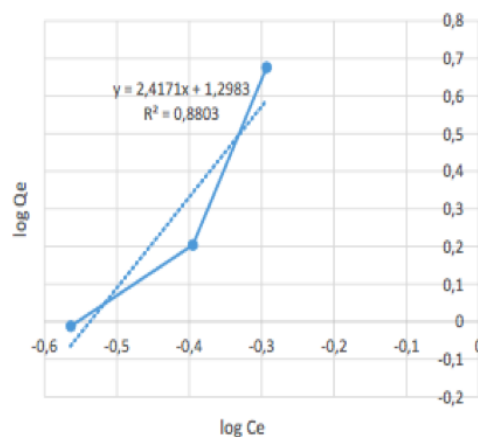


Figure 8. Freundlich isotherm of olive seed

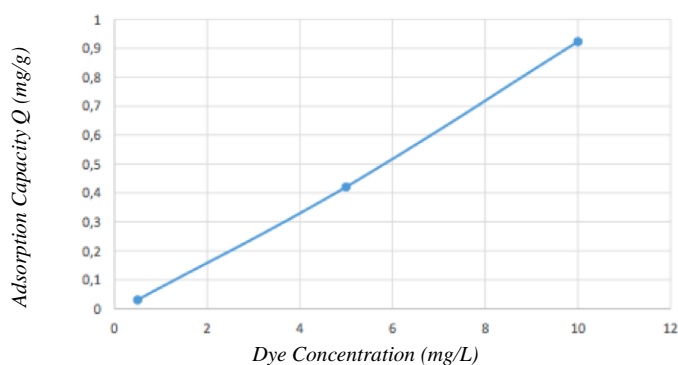


Figure 9. Adsorption capacity vs. dye concentration

### 4. CONCLUSIONS

In this study, activated carbon prepared from olive stone has been successfully produced. Activated carbon used as an adsorbing agent for the removal of MB dye from aqueous solutions. From this study, obtained results given in below.

- According to SEM micrographs, olive seed activated carbon samples have macro and micro pores.
- FTIR results showed that alcohols, ketons and carboxyl groups were occurred.
- According to BET results surface area was found to be 441,0890 m<sup>2</sup>/g and single-point adsorption was found to be 0,233865 cm<sup>3</sup>/g.
- XPS results indicates that C, Na, O, Mg, Si, B, N, Ca, Zn, Ag, K elements were found.
- The best result of MB removal was achieved as 97,27 % with 0,5 g/l olive seed.
- The adsorption capacity was found to be increased, when the dye concentration was increased.
- The best fit isotherm was determined as Langmuir isotherm with  $R^2 = 0,9533$

### REFERENCES

- [1]. M. Ugurlu , A.Gurses and M. Acikyildiz, Comparison of textile dyeing effluent adsorption on activated carbon activation, *Microporous Mesoporous Mater.* 111, 2008, 228–235.
- [2]. M. Rafatullah, O. Sulaiman, R. Hashim and A. Ahmad , Adsorption of methylene blue on low-cost adsorbents: A review, *J. Hazard. Mater.* 177, 2010, 70–80.
- [3]. O. Ioannidou and A. Zabaniotou, 2007. Agricultural residues as precursors for activated carbon production – A review, *Renewable & Sustainable Energy Reviews*, 11, 1966–2005.
- [4]. V. Vadivelan and K. Vasanth Kumar, Equilibrium, kinetics, mechanism, and process design for the sorption of methylene blue onto rice husk, *J. Colloid Interf. Sci.* 286, 2005, 90–100.
- [5]. R. Hazzaa and M. Hussein, Adsorption of cationic dye from aqueous solution onto activated carbon prepared from olive stones, *Environmental Technology & Innovation*, Volume 4, 2015, 36-51.



## The Microwave Oven Curing of Fly Ash-Based Geopolymer Mortars

Gokhan Kurklu<sup>1</sup>, Gokhan Gorhan<sup>2</sup>

### Abstract

Industrial wastes such as fly ash or blast furnace slag, where dissolved silica and alumina species are present, are commonly used alumina silicate materials. Activation of aluminosilicates with alkaline solutes, particularly when the activating solution does not contain soluble silica, requires the external energy to be supplied as heat to form the alkaline aluminosilicates. This energy transfer, which takes place over a wide temperature range of 40 to 90 °C and a curing time of 2 to 48 hours, is generally carried out with conventional techniques and with the help of an oven. This can cause irregular heat build-ups that can affect the mechanical properties of the material that gives thermal energy to the material surface by radiant or convection heating. As an alternative, microwave curing in which microwave energy is transmitted directly to the material through interactions at the molecular level with the electromagnetic field is proposed in this work. This curing method has been tried in the production of geopolymer mortar. Foam as binder and NaOH solution as alkali activator. Two different molarities were produced in the microwave furnace series with NaOH solution (3M and 9M), three power levels (200, 300, 400 W) and two different curing times (25 and 50 min). The physical and mechanical test results obtained indicate that the microwave oven curing method produces satisfactory results, and the molarity, the energy and the curing temperature are effective in the results. The highest compressive strength was obtained at 9M for 25 minutes and 23.1 MPa for 200 W series.

**Keywords:** Fly ash, microwave, geopolymer mortar.

### 1. INTRODUCTION

In the production of concrete and mortar, activation of alkalis referred to as geopolymers is an alternative method to cement and binder obtained by its hydration. An inorganic material obtained using this method has an amorphous semi crystalline polymeric structure and is synthesized by alkali activation of amorphous aluminosilicates at ambient temperature or slightly higher temperatures [1] [2]. Geopolymerization is based on an aluminosilicate chain and is a polymeric reaction between a certain amount of alumina and silica with a strong alkaline solution (NaOH, KOH, water glass, or combination thereof, etc.). Geopolymerization is generally referred to as alkali activation and converts the amorphous components of a material into a composite with strong bonding properties [3] [4]. Concrete and mortars produced with this composition provide not only comparable performance to conventional Portland cement concrete but also mechanical strength, small drying shrinkage, high fire resistance, superior acid resistance, effective immobilization, resistance to hazardous substances, significantly reduced energy use and greenhouse gas emissions [5] [6]. The three most common classes of materials used in geopolymerization are calcined clay, coal slag and fly ash [7]. Fly ash is an industrial waste with pozzolanic properties obtained from thermal power plants. It contains amorphous silica and alumina dissolved in high amounts when a soluble alkali solution is used [8]. It is a suitable industrial waste for geopolymer synthesis and can be found all over the world. The use of fly ash-based geopolymers is still not widespread, despite extensive research on them. One of the main reasons for this is that fly ash varies depending on its source. On the other hand, most research focuses on the analysis of differences in geopolymer synthesis [9]. Resulting in low binding and early strength development, low reactivity of fly ash is another factor that limits its use for geopolymerization. Final

<sup>1</sup> Corresponding author: Afyon Kocatepe University, Department of Civil Engineering, 03200, ANS Campus/Afyonkarahisar, Turkey. [kurklu@aku.edu.tr](mailto:kurklu@aku.edu.tr)

<sup>2</sup> Afyon Kocatepe University, Department of Civil Engineering, 03200, ANS Campus/Afyonkarahisar, Turkey. [ggorhan@aku.edu.tr](mailto:ggorhan@aku.edu.tr)

hardening usually occurs before fly ash dissolution is achieved [10]. Fly ash-based geopolymers gain higher compressive strength when cured between 40 and 85 °C [11].

Unlike the curing method used in the production of conventional concrete and mortar, geopolymers are cured in ovens. An alternative to this curing method is microwave oven curing. Owing to its superior penetration depth, high-frequency electromagnetic heating, such as microwaves, can reduce irregularity in curing [12]. Microwave energy generates heat in cementitious materials due to the dielectricity of water, and is, therefore, a promising alternative to accelerate geopolymerization. The microwave process has several advantages over other curing methods. First, microwave energy can heat a specimen homogeneously and volumetrically, regardless of the heat conductivity of the specimen. Second, microwave energy can accelerate evaporation more easily, better control energy absorption, and optimize the overall heating process prior to desorption. Finally, microwave energy can potentially improve the ultimate performance of geopolymer materials to achieve long-term goals [13]. Numerous studies have investigated the effect of microwave curing on fly ash, cement and geopolymer materials. In one study, isothermal heating methods were used to determine the effects of microwave curing. Appropriate amounts of pozzolanic materials such as furnace slag, silica fume or class F fly ash were added to Type I Portland cement mortars. The mortars were isothermally cured with feedback temperature control at several temperatures. Curing times were determined using instrumented penetration test and compressive strength values were measured for 28 days. Optimum curing conditions were found at 40 and 60 °C, however, microwave curing at 80 °C was found to be unsuitable [14].

Another study investigated the acceleration of microwave curing of cement paste using a continuous band dryer. The microwave power was provided by 14 800-W compressed air-cooled magnets, each with a maximum 11.2 kW. The aim of this study is to apply microwave curing to improve cement paste properties by heat transfer occurring during compressive strength and to compare the cement paste with conventional cement paste. Test results show that microwave energy accelerates the early pressure regime of the cement paste and does not affect the compressive strength at the later age [15]. Somaratna et al. focused on the compressive strength and microstructure development of fly ash mortars activated with microwave-cured NaOH, and associated them with the absorption of microwave energy. Results showed that mortars cured for 48 h at 75 °C were comparable to or higher than those microwave cured for less than 120 minutes at higher temperatures. The rate of energy absorption was relatively constant for a significant portion of the microwave curing time, which can be attributed to the decrease in the dielectric loss factor as a consequence of the loss of moisture resulting from the increase in internal electric field. The compressive strength was related to the microwave energy absorbed by the specimens, especially when free water was present in the system.

This study suggests microwave curing where microwave energy is transmitted directly to the material through interactions with the electromagnetic field at the molecular level. This curing method was used in the production of geopolymer mortars. Fly ash was used as a binder and NaOH solution was used as alkali activator. This study investigated the effect of molarity, microwave power level and curing time on the physical and mechanical properties of fly ash based geopolymer mortars.

## 2. MATERIAL METHOD

### 2.1. Material

In this study, fly ash obtained from Seyitomer Thermal Power Plant located in Kutahya was used as binder in the production of mortar specimens. The chemical composition and XRF results of the fly ash are shown in Table 1 and Figure 1, respectively. Quartz sand was used as aggregate in the preparation of the mortar. The specific gravity and the largest particle diameter of the sand were 2.62 and 4 mm, respectively. NaOH and 3 modules of sodium silicate (SS) were used as alkali activator. Table 2 shows the properties of NaOH and SS solutions.

Table 1. Chemical composition of fly ash

Oxide (%)	SiO <sub>2</sub>	Al <sub>2</sub> O <sub>3</sub>	Fe <sub>2</sub> O <sub>3</sub>	MgO	Na <sub>2</sub> O	K <sub>2</sub> O	SO <sub>3</sub>	CaO	LOI	Total
Fly Ash	49.81	18.50	13.40	4.56	0.55	1.84	1.45	4.31	3.52	97.94

### 2.2. Preparation of Mortars

3 and 9 M NaOH solutions were used to prepare the mortars. NaOH in pellet form was dissolved in distilled water and prepared at the desired ratio and was used after it was allowed to stand at room temperature for 24 h. During the preparation of the mortar, the fly ash and NaOH and SS solutions to be activated were first mixed for 3 minutes, and then the sand was added and stirred for another 3 min. Teflon molds were used so that the mixture would not be affected by the microwave. 50x50x50 mm and 40x40x160 mm specimens were produced for the compression test and bending test, respectively. The liquid/binder ratio was 0.72 and the NaOH/SS ratio was 0.5. The mixing ratios of the mortars are given in Table 3.

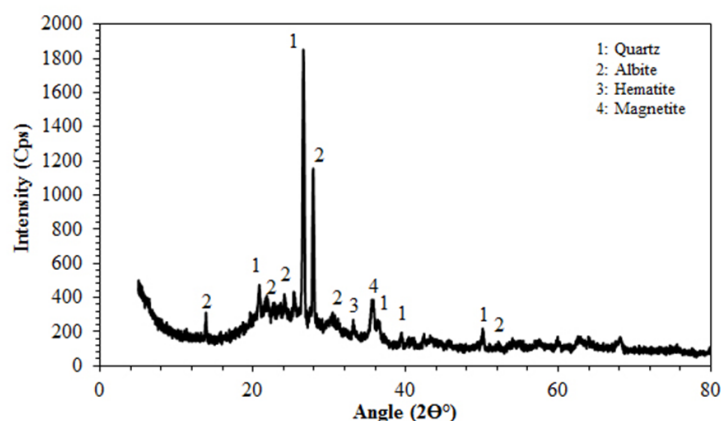


Figure 1. X-ray diffractogram of fly ash

Table 2. Chemical properties of alkaline activators

Sodium silicate solution (water glass)	Sodium hydroxide (NaOH)
Na <sub>2</sub> O: 7.5–8.5 %	14 M
SiO <sub>2</sub> : 25.5–28.5 %	M: 40 g/mol
Density (20 °C) 1.296–1.396 g/ml	NaOH ≥ 97.0%
Fe ≤ 0.005 %	
Heavy metals: (as Pb) ≤ 0.005 %	

Table 3. Mix proportion of mortars.

Serial	Molarity	Curing Time (min)	Watt	Sand (g)	Fly ash (g)	Sodium silicate solution (ml)	Solution of NaOH (ml)
1	9M	25	200	750	250	120	60
2	9M	25	300	750	250	120	60
3	9M	25	400	750	250	120	60
4	9M	50	200	750	250	120	60
5	9M	50	300	750	250	120	60
6	9M	50	400	750	250	120	60
7	3M	25	200	750	250	120	60
8	3M	25	300	750	250	120	60
9	3M	25	400	750	250	120	60
10	3M	50	200	750	250	120	60
11	3M	50	300	750	250	120	60
12	3M	50	400	750	250	120	60

### 2.3. Microwave Process

After the mortars were placed in the molds, curing was carried out using a home microwave oven with a 20-liter capacity, 800 W output and 50Hz power source. The basic principle of this method is that the interaction of the electromagnetic field with the material structure leads to energy transfer. Microwave-material interactions result in translational motions of free or bound charges and transformation of dipoles. Inertia, elastic and friction forces which resist these movements cause the volumetric heating of the material. The effect of the electromagnetic field on the material is mainly due to the complex dielectric permeability of the material.

The effectiveness of heating a material using microwave energy depends on the amount and rate of energy absorption of the material. The energy absorption rate defined as power per unit volume is one of the important parameters for microwave processing of materials. Dielectric properties have a significant effect on the absorbed energy and thus affect the volumetric heating of the material. A significant portion of the energy to be absorbed is converted into heat in the material [16]. In this study, three different energy levels (200, 300 and 400 W) and two different curing times (25 and 50 min) were used for curing. Immediately after these processes, the outer surface temperatures of the specimens were measured using laser thermometers.

#### 2.4. Physical and Mechanical Tests

After microwave curing, geopolymer mortars were kept at room temperature in laboratory conditions until physical and mechanical tests. The tests were carried out on 7-day geopolymer mortar specimens. Three specimens from each specimen group were used and their mean values were calculated for the physical tests. The Archimedes principle was used to determine the physical properties of the geopolymer specimens. The apparent porosity, bulk density and apparent density of the specimens were determined by tests carried out in accordance with TS EN 772-4 [17]. The water absorption of the specimens was determined using the TS EN 771-1 [18] standard.

### 3. RESULTS AND DISCUSSION

Figures 2 show the apparent porosity and water absorption of the mortars microwave cured for 9M and 3M, respectively. The porosity of the mortars prepared using 9M ranged from 18.3% to 20.7%. It is not possible to establish a linear relationship for this change between the series in terms of cure time or cure energy. The water absorption values varied between 10% and 11.8%, at the lowest 300 W and at the highest 400 W levels. Unit volume weight and apparent density values for 9M and 3M are given in Figures 3, respectively.

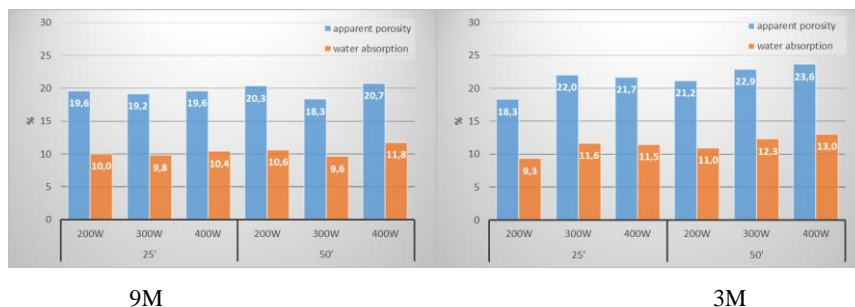


Figure 2. Apparent porosity and water absorption of the mortars

The unit volume weights for 9M ranged from 1952 to 1760 kg/m<sup>3</sup> depending on the heating energy. A similar situation applied to apparent density. The unit volume for 3M ranged from 1962 to 1815 kg/m<sup>3</sup>.

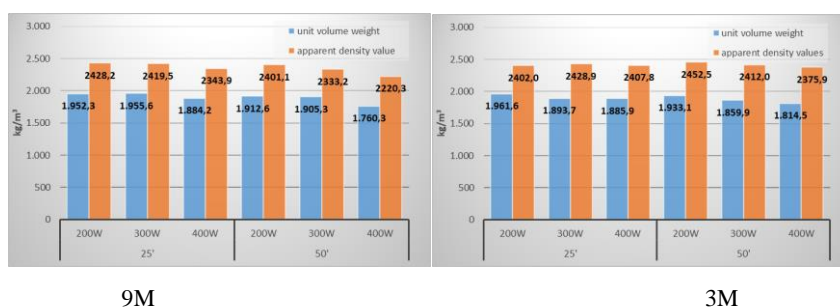


Figure 3. Unit volume weight and apparent density values of the mortars

Figures 4 show the compressive strength values for 9M and 3M, respectively. The compressive strength for 9M showed a linear change depending on the microwave energy. In the 3M series, the compressive strength fluctuated due to the curing time and energy. The compressive strength of all series ranged from 8.2 to 23.1 MPa.

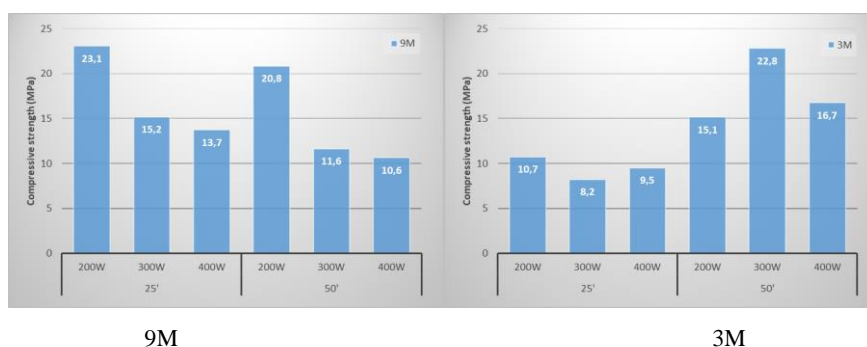


Figure 4. The compressive strength values of mortars

Figures 5 show the flexural strength graphs. The flexural strength of the specimens varied between 3.6 and 5.8 MPa. One of the main reasons for these physical and mechanical changes is that the temperature of the specimens and the continuation of this temperature cause geopolymerization to be completed early or not to be completed.

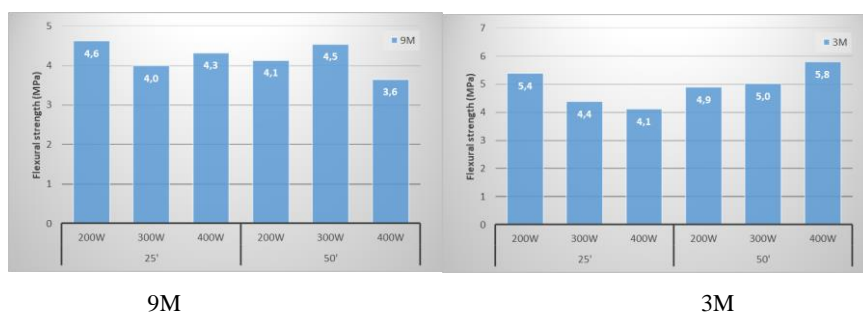


Figure 5. The flexural strength of mortars

The final temperatures of the specimens are given in Figure 6 to better understand this phenomenon. The temperature in the microwave increased with energy and time. The graph on Figure 6 clearly shows why 25 and 50 min were chosen as curing times. Figure 7 shows the time-independent temperatures. Accordingly, the changes in physical and mechanical properties observed in Figures 8, 9 and 10 became meaningful.



Figure 6. The final temperatures of microwave oven

Figure 7. Average final temperature

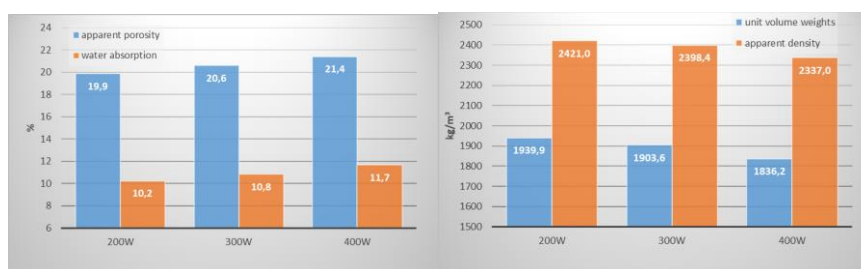


Figure 8. Average apparent porosity and water absorption

Figure 9. Average unit volume weights and apparent density

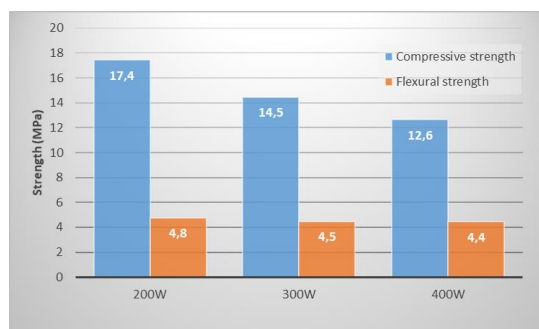


Figure 9. Average compressive strength and flexural strength

#### 4. CONCLUSION

The main subject of interest in the production of geopolymer mortar and concrete is raw material selection and curing. Curing time and curing methods are issues to be overcome due to the fact that the on-site production of geopolymers is limited. This study proposed a microwave curing method to cure fly-ash based geopolymer mortars in a short period of time to overcome these issues. This curing method did not adversely affect the physical properties of the mortar. At low energy levels, compressive strength over 20 MPa was achieved in 25 min. In this study, increasing the microwave energy and curing time was sufficient to obtain similar results when the NaOH molarities in the mixtures decreased. The results indicate that microwave curing of geopolymer mortars is an approach that needs to be considered. It is recommended that further studies address internal structure changes and process optimization.

#### ACKNOWLEDGMENT

The authors would like to thank the Scientific Research Projects Coordination Unit of Afyon Kocatepe University (AKÜ, BAPK, Project No: 17. KARİYER. 215) for supporting this work.



### BIOGRAPHY

The author was born in 1980 in Ankara. He received his undergraduate, graduate and doctoral degrees from the Technical Education Faculty of Afyon Kocatepe University. Dr. Kurklu is currently undertaking TUBITAK and BAP projects on various subjects related to building materials and is a faculty member of the Department of Civil Engineering of the Faculty of Engineering of Afyon Kocatepe University. He is married with two children.

### REFERENCES

- [1]. Van Deventer, J. S., Provis, J. L., & Duxson, P. (2012). Technical and commercial progress in the adoption of geopolymer cement. *Minerals Engineering*, 29, 89-104.
- [2]. Pacheco-Torgal, F., Abdollahnejad, Z., Camões, A. F., Jamshidi, M., & Ding, Y. (2012). Durability of alkali-activated binders: a clear advantage over Portland cement or an unproven issue? *Construction and Building Materials*, 30, 400-405.
- [3]. De Vargas, A. S., Dal Molin, D. C., Vilela, A. C., Da Silva, F. J., Pavao, B., & Veit, H. (2011). The effects of Na<sub>2</sub>O/SiO<sub>2</sub> molar ratio, curing temperature and age on compressive strength, morphology and microstructure of alkali-activated fly ash-based geopolymers. *Cement and concrete composites*, 33(6), 653-660.
- [4]. Mo, B. H., Zhu, H., Cui, X. M., He, Y., & Gong, S. Y. (2014). Effect of curing temperature on geopolymerization of metakaolin-based geopolymers. *Applied clay science*, 99, 144-148.
- [5]. Rangan BV. Fly ash- based geopolymer concrete. Research report, Engineering faculty, Curtin University of Technology, Australia, 2008.
- [6]. Wallah SE, Rangan BV. Low-Calcium Fly Ash-Based Geopolymer Concrete: Long-Term Properties, Research Report GC2, Faculty of Engineering, Curtin University of Technology, Perth, 2006.
- [7]. Duxson, P., & Provis, J. L. (2008). Designing precursors for geopolymer cements. *Journal of the American Ceramic Society*, 91(12), 3864-3869.
- [8]. Hwang, C. L., & Huynh, T. P. (2015). Effect of alkali-activator and rice husk ash content on strength development of fly ash and residual rice husk ash-based geopolymers. *Construction and Building Materials*, 101, 1-9.
- [9]. Nikolić, V., Komljenović, M., Bašcarević, Z., Marjanović, N., Miladinović, Z., & Petrović, R. (2015). The influence of fly ash characteristics and reaction conditions on strength and structure of geopolymers. *Construction and Building Materials*, 94, 361-370.
- [10]. Mucsi, G., Kumar, S., Csöke, B., Kumar, R., Molnár, Z., Rácz, Á., ... & Debreczeni, Á. (2015). Control of geopolymer properties by grinding of land filled fly ash. *International Journal of Mineral Processing*, 143, 50-58.
- [11]. Bakharev, T. (2005). Geopolymeric materials prepared using Class F fly ash and elevated temperature curing. *Cement and concrete research*, 35(6), 1224-1232.
- [12]. W.H. Sutton, *Am Ceram Soc Bull* 68(2) (1989) 376-386.
- [13]. S.M. Christo, M.S. Thesis, Northwestern University, Evanston, IL, 1989.
- [14]. Sohn, D., & Johnson, D. L. (1999). Microwave curing effects on the 28-day strength of cementitious materials. *Cement and Concrete Research*, 29(2), 241-247.
- [15]. Rattanadecho, P., Suwannapum, N., Chatveera, B., Atong, D., & Makul, N. (2008). Development of compressive strength of cement paste under accelerated curing by using a continuous microwave thermal processor. *Materials Science and Engineering: A*, 472(1-2), 299-307.
- [16]. Clark, D. E., Folz, D. C., & West, J. K. (2000). Processing materials with microwave energy. *Materials Science and Engineering: A*, 287(2), 153-158.
- [17]. TS EN 772-4, Kagir birimler- Deney metotları- Bolum 4: Tabii taş kagir birimlerin toplam ve gorunen porozitesi ile boşluksuz ve boşluklu birim hacim kutlesinin tayini (Methods of test for masonry units - Part 4: Determination of real and bulk density and of total and open porosity for natural stone masonry units) TSE, Ankara-Turkey (2000)
- [18]. TS EN 771-1: 2011+A1 Kagir birimler, ozellikler- Bolum 1: Kil kagir birimler (Tuğlalar) (Specification for masonry units – part 1: clay masonry units) TSE, Ankara-Turkey (2015)

## Use of 3D City Modeling Techniques in Urban Planning : A Case Study of Selahiye

*Mehmet Fatih Docker<sup>1</sup>, Ahmet GUu<sup>2</sup>, Remziye Emel Akduman<sup>3</sup>*

### Abstract

*The Earth has been changed and altered from past to present by human activities. Agriculture, transport, industry, mining and settlements are human activities that are effective in the transformation of natural landscape into cultural landscapes. The settlement areas have caused significant changes in the Earth since the human being's settled passion. Natural unsettled areas are opened to settlement construction activities with each passing day. However, this situation is much more unplanned and painful today with increasing population pressure. As long as unplanned settlement and use of the natural environment contrary to the physical space organization continues, mankind will continue to lose natural resources that cannot be recovered. At this point, a sustainable urban planning approach gains importance. In the recent past, planning studies with classical methods have gained a different dimension with developing technology. Urban models obtained by 3D modeling also change the planning process. We have significantly improved the way we visualize urban objects, visualize and plan our sustainable future environments. In this study, planning studies conducted in rural settlements located close to the city's area of influence, were analyzed in 3D city models. The obtained numerical data was prepared with geographic information systems software and modeled in Esri CityEngine software. Thus, what kind of cultural landscaping will be revealed as a result of planning is revealed visually. The 3D urban information system infrastructure has been created along with the attribute information added to the created 3D model.*

**Keywords:** 3D City Modeling, Urban Planning, GIS, Sakarya

### 1. INTRODUCTION

Accelerating industrialization activities in the second half of the 20th century increased the migration from rural areas to cities and caused the population to be collected in urban areas. Urbanization rate and urban population reached high levels especially in developing countries. While 55.3% of the world's population lives in cities, this ratio is over 75% in our country (Birleşmiş Milletler, 2018). The rural-urban migration, lack of employment in the agricultural sector, factors such as repellency of rural areas and attractiveness of the city has accelerated the increase in urban population. This situation led to the emergence of cities away from infrastructure and planning, and to the emergence of a lots spatial problems such as transportation, environmental pollution and lack of natural resources in urban areas. The bigger and complexity of data in urban areas leads to the failure to find solutions to these spatial problems by classical methods. Therefore, the need for Geographical Information Systems (GIS), where the data of physical and human geography is collecting, storing and analyzed, is increasing. GIS helps to find the best solutions for spatial problems by processing the data obtained with the spatial data infrastructure and transforming it into geographical information.

The space is the place where all human activities are carried out and all experiences are experienced. Geography, which is a space science, has also been mentioned as a focal point (Tümertekin & Özgüç, 2011). Two-dimensional (2D) print maps, which they produce in order to understand the space and communicate the information in the best way, have been insufficient in applications using advanced technologies. (Rüstemov, 2014). To understand the space, need to think three-dimensional. Today, many

<sup>1</sup>Corresponding author: Sakarya University, Department of Geography, 54050, Serdivan/Sakarya, Turkey. [fdoker@sakarya.edu.tr](mailto:fdoker@sakarya.edu.tr)

<sup>2</sup> Sakarya University, Department of Geography, 54050, Serdivan/Sakarya, Turkey. [ahmet.gul6@ogr.sakarya.edu.tr](mailto:ahmet.gul6@ogr.sakarya.edu.tr)

<sup>3</sup>Sakarya University, Department of Geography, 54050, Serdivan/Sakarya, Turkey. [remziye.akduman@ogr.sakarya.edu.tr](mailto:remziye.akduman@ogr.sakarya.edu.tr)

studies have two dimensions. It is not possible to handle the third dimension with two-dimensional prepared materials. Therefore, it is easier to understand the space with 3D modeling. The aim of this study is to make a two-dimensional studies is insufficient and create a three-dimensional urban information system has found the right. This 3D representation, which will form the basis for the City Information System, is for geographic data management. The use of this at local, regional and national level is indispensable in today's technologies in order to provide decision-support services to the economy and administrative managers from local to national and international levels. Visualizing objects of the city in three dimensions is changing the way we understand and plan our sustainable future environments. The general vision and scenario of the city for the future allows us to save time and money. By making virtual visualization as realistic as possible during the design phase, it is possible to foresee errors and minimize errors in their realization. Recently, there are various applications using Geographic Information Technologies and virtual reality and 3D building models. The most important of these is undoubtedly virtual cities and 3D street maps. In virtual cities, three-dimensional solid block models of buildings, roads, vegetation, land and many other objects are located (Sümer & Türker, 2010).

National scale of 1/100 000 and 1/25 000 scale Environmental Plan was completed today in Turkey. Local governments are planning to implement master plans in accordance with these plans. The 2-D drawings they have used in the regions they plan in new are not sufficient to understand the state of the region. The use of 2D mapping for GIS and City Information Systems by public institutions and/or private companies is still insufficient. 3D maps are more effective in understanding the space compared to 2D maps, and their use is not developed enough. Particularly in the context of the application of Article 18, the fact that the future of the city will not be exactly perceived causes serious problems during planning. World and in Turkey are seen scale similar to 3-D modeling studies. The techniques used in these modeling studies vary. In these studies, it is observed that the data collection phase mainly carried out terrestrial optical recording systems and terrestrial laser scanners. (Tiryakioğlu, ve diğerleri, 2016). Other method is called in the 3D city model as photorealistic visualization where the buildings are modeled and supported by facade photographs. Thus, the existing texture is reflected in the model (Yıldırım, 2012). Another work can only be done by "computer-generated models" with programs in the web browser plug-in at CityGML. (Yücel & Selçuk, 2009). In this study, the city model created in the City Engine software can be easily transferred to the web interface. In this way, time and cost gains can be obtained and the changes made in the City Engine program can be updated dynamically on the internet. Today, resources are many have been consumed by people around the world. Therefore, use of natural resources with caution is required. Today, people do not know the value of the land and quickly destroy them. The use of land in this way brought many problems in cities. The use of fertile land for housing, the inability to improve urban living areas, the inability to create an environment that everyone can use in a healthy way, and the fact that uninterrupted infrastructure services cannot be delivered to people are some of these problems. In order to solve the problems caused by lack of planning with 3D model, well-prepared Land Management Systems, Urban Information Systems and the most current 3D Modeling technologies are needed by experts who can be dominant in the whole country. As a result of all these, it will contribute to many other areas such as the welfare of the society, economic development, inter-institutional communication and regular use of environmental resources.

## 2. MATERIALS AND METHODS

### 2.1. Study Area

Selahiye, which forms the project area, is located in the Çatalca-Kocaeli Department in the east of the Marmara Region. The whole settlement is located in Serdivan within the administrative boundaries of Sakarya province. The mathematics position is between 40°46'50" and 40°47'06" parallels and 30°19'14" and 30°20'20" meridians. In the administrative sense, the bird flight to the Serdivan is 3 km away. It is in the situation area of the city of Serdivan (Figure 1). The settlement located to the north and east of the Adapazarı plain, and to the north of the Serdivan hill, is surrounded by the Sapanca lake in the south and the Kocaeli plateau to the west. The

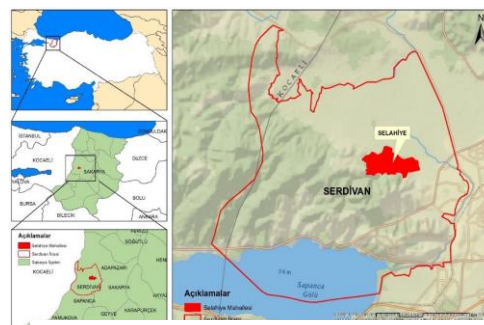


Figure 1 Location of Selahiye

settlement began in the semi-uneven mountainous area, and nowadays is spreading to the fertile plain. In addition to having a road network connecting Kocaeli and Sakarya in terms of transportation, the fact that it is located close to important centers such as Istanbul and Ankara made the site suitable for human activities.

### 2.2. Veri ve Yöntem

ArcInfo, ArcEditor 10.x, Sketchup Pro 2017/18, Google Earth Pro, MapCad, NetCad software used in image processing algorithms to determine the general framework of the study area. The city has been modeled Esri CityEngine program. Esri CityEngine CGA (Computer Aided Architecture) shape grammar is a unique programming language specified for creating architectural 3D content. The term CGA means "Architecture Produced by Computer". The idea of grammar-based modeling is to define rules or CGA rules for recursively refining a design by creating more details within CityEngine (Esri, 2018).

CityEngine works mainly on grammar-based modeling. Grammar-based modeling means visualization of commands entered into the software. This is done with the syntax of the CGA, as many software draws it, making it graphically. The main steps in such image-based modeling are: (Figure 2)

- 1-Obtain building facade photographs,
- 2-Create a rule file,
- 3-Building road networks and parcels,
- 4-Layer creation,
- 5-Texturing of building facades,
- 6-Production of the final textured photorealistic 3D building.

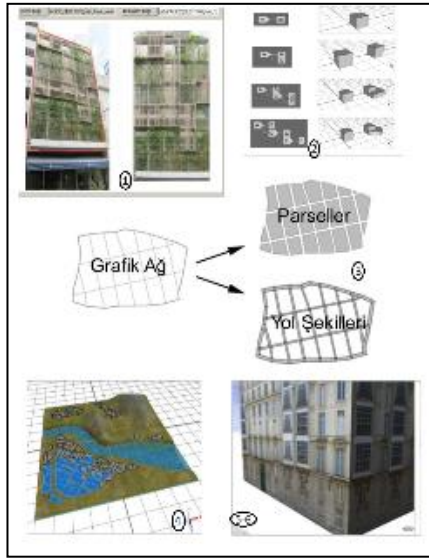


Figure 2 Grammar-Based Modelling

The shape file, street network and other layers were created in the CityEngine environment. The production of wireframe models, which are building facades with texture and updating of building data, are the main steps of this process (Singh, Jain, & Mandla, 2014). In order to make a good urban modeling of the study area 3D Modeling, Master Plans, Geographical Information Systems (GIS) and orthophoto methods were determined. Studies with 3D Modeling, GIS and orthophoto methods have been supported by field observations in the study area.

In the study, 1/1000 scale application maps and cadastral situation processed application development plans were used. These maps, which are prepared in accordance with the master application principles, include the islands of the region, order, density and application stages, principles and all other information. Orthophoto, elevation information, map edge information, grid elevation curves, location and position names and cartographic information were obtained. Since the study area includes a local study area, the images of the study area have been tried to be optimized by using the necessary technological facilities. Field studies were carried out to determine the city components for the purpose of realization of the modeling process. The aim of the field study is to see the lifestyle in the existing land, to take into consideration the needs of the people and the region, and to make the 3D practice towards them.

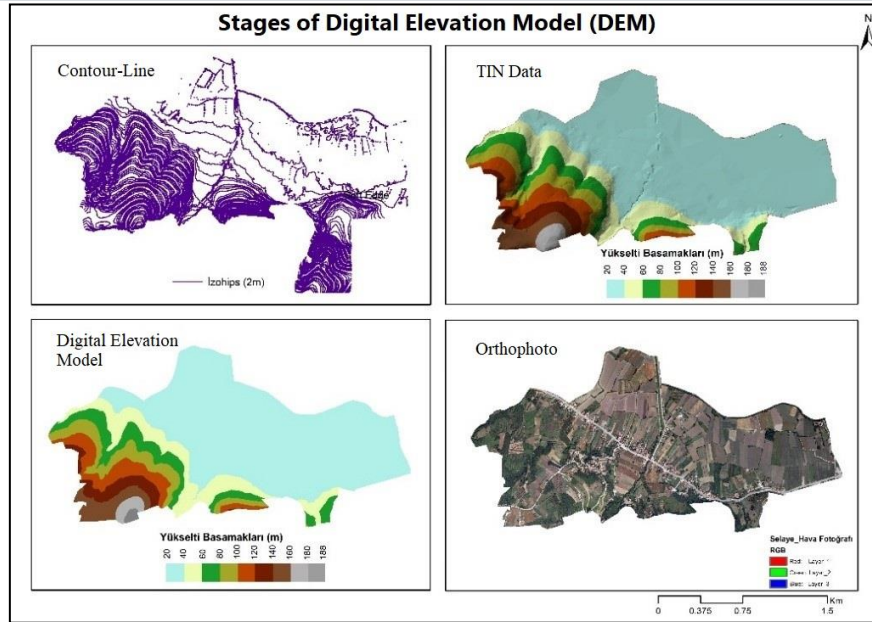


Figure 3 Digital Elevation Model And Orthophoto

Since the project area is a local region, it is foreseen to use orthophotos due to high resolution requirement. Aerial photographs covering the land were obtained from the local municipality. The digital elevation model is a regular field measurement data, measured at certain intervals from the terrain and within a given system. This numerical land modeling in the raster data structure consists of a whole set of cells sorted in column and row order. Digital Elevation Model is created based on remote sensing and field measurement data. (Turoğlu, 2016) In this study, Digital Elevation Model was obtained by converting the contour line within the master plan to the data of TIN (Triangulated Irregular Network) and then into a raster data via Arcmap 10.x program (Figure 3). It was then used as terrain in CityEngine software. Terrain is formed by overlapping of both elevation model and land photograph produced by orthophoto or similar method. The registration phase is among the capabilities of CityEngine software. 1/1000 master plans taken from the municipality contain a lot of information for the settlement area (Figure 4). Obtaining the most necessary data from this is important at this stage. Roads, sidewalks, residential settlements, housing development, trade, parking, public institutions, etc. all data is converted to required formats. Building areas have been issued with the rules set out in the master regulations of parcels or public lands.

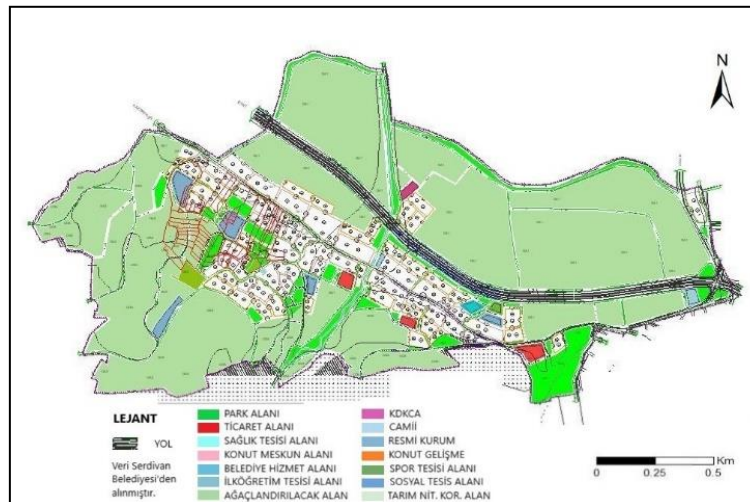


Figure 4 1/1000 Master Plan



## 3. RESULTS AND DISCUSSION

### 3.1. Results

One of the objectives of the study is to serve public institutions and organizations, to make the right decisions in the development of the city, to serve the decision making process in the production of housing factors come from. The population of Selahiye reached 1123 in 2017 according to TUIK(Turkey Statistical Institute) data. Due to the presence of the city of Serdivan, it is expected that the settlement will be accelerated in the near future due to population growth and will result in an unplanned settlement in the immediate vicinity of the city. In the modeling stage, all the soil part of the study boundary is modeled in the future prediction. Infrastructure work within the study area is not yet organized. However, all infrastructure superstructure area planning has been done and a suitable modeling has been done. In urban areas, recreational areas are very important for people to enjoy their leisure activities. In this settlement, which has not yet been planned, there is no park and recreation area but according to the master plan, Selahiye Creek, as in Figure 5, is modeled as a recreation and listening area.



Figure 5 Developed of Selahiye Stream



Figure 6 Izmit highway passing through Selahiye modeling



Figure 7 Findings after three-dimensional modeling

The six-lane Izmit Motorway (Figure 6), viaducts, mosques, trade centers, health facilities, primary education, sports facilities, official institutions, residential parcel areas, and the areas to be afforested in a city are modeled. In addition, the recreation areas have been formed by arranging the rivers and surrounding

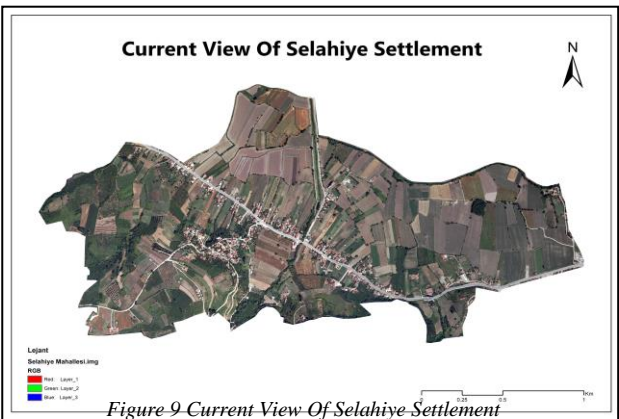


areas within the working area boundaries. The main aim of the study is to plan a sustainable city. All these activities are the common requirements of sustainable cities.

Two-dimensional studies are insufficient in city planning and third dimensional studies are not considered in terms of the two dimension so many errors and problems are encountered. Therefore, it is necessary to revise the master plans before 3D modeling. Because the third dimension, which is not considered when the plans are drawn, presents problems in modeling and, most importantly, in the settlement phase. As in Figure 7, it is determined that the high slope areas are designated as parking area or the roads drawn as two dimensional in the master plans are located on sloping land as a result of 3D application. This suggests that 3D modeling is necessary before settlement. If it is settled without planning, the people who will live here will turn to non-agricultural activities. Existing agriculture and stockbreeding activities will decrease and their basic economic activities will change direction. However, with the 3D modeling, the tissue will be preserved and the fertile lands here will continue to be evaluated. Thanks to the CityEngine program, the modeling can be accessed on the internet without any need for different software. According to the study, it is possible to reach the future of Selahiye easily. One of the findings that can be obtained from the study is to see a city or administrative neighborhood in terms of settlement before than building a building model the construction, and then it is aimed that the problems that may occur during the settlement development are taken beforehand. Building modeling is based on the City Engine training data, which Esri has introduced. Some public buildings, sports facilities etc. determined in Selahiye master plan the program is transferred from other data formats.

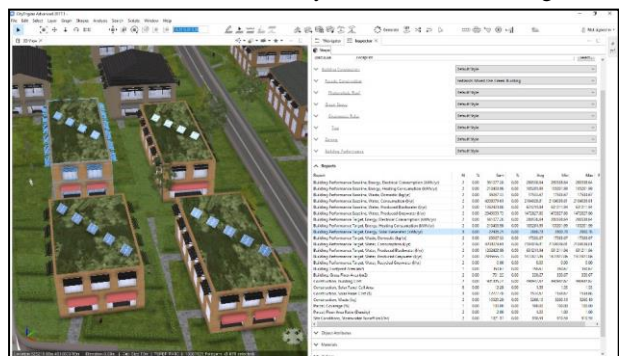
Before starting to construction with City Engine, all calculations related to the parcel area are done within the system. At this stage, City Engine software has the ability to calculate and report the cost of a construction's excavation costs and volume calculations, the retaining wall and the cost of infrastructure, the cost of all operations from the building to the sale of the building.

Although the Selahiye is located in the south of the mountainous region in the opposite direction to the direction of the sun, a large part of the settlements are in the northeast. The solar panel modeling on the roofs of the solar-powered buildings was done in Figure 8 and the calculations were carried out.



### 3.2. Current Settlement of Selahiye and Comparison of 3D Modeling

The current status of the Selahiye is close to the city center but not yet developed in terms of urbanization and it has the status of village. As a result of the field study, it was observed that the site settlements were new. Due to the fact that the city is located in the enlargement area, it is considered appropriate to model



the study area according to the existing master plan.

In the Selahiye, which was established as a road-length settlement, just behind the settlements, agricultural lands were observed as shown in Figure 9. The existing residences in Selahiye do not correspond exactly with the master plan. At the moment, new residential areas have been established next to this highway.

In the modeling study of Selahiye, the priority data master plan was made.

Figure 8 Panels in the Roof of Buildings

Then, the human characteristics of the Selahiye were taken into consideration. According to these data, a city modeling has been made for the needs.

The main economic activities of the people in Selahiye neighborhood are agriculture and animal husbandry. Selahiye, which is just beginning to urbanization, is modeled not only in the region of construction but also as a settlement area which can make agricultural production. In urbanization, it is now possible to turn agricultural land into a residential area.

Because this area is not only in the area of agricultural land, but in fact it has a planning where settlement and agriculture are together. Therefore, it can be considered neither a residential area nor an agricultural area. With this modeling, it is aimed that the people will continue their lives without being cut off from agriculture and from where they live. In this direction, the settlement is mostly concentrated in the sloping area. Slopes should be taken into consideration for future sites. The city model of Selahiye includes all the components of the city. These include social activity areas, parks, central trade areas, public bazaar, bakery, local businesses and so on. City components are modeled. The people living here will be able to meet all food and other needs without being connected to the city center.

According to other information obtained in the field studies related to Selahiye, people first want to get rid of the dependence on the city center in the newly established and developing settlements. Today's master plans are prepared by taking these expectations into consideration. Preparation of master plans in this way reduces the density in the city center and eliminates the problems caused by the crowd. With this modeling, this residential area, which is expected to have a population of 10,000 in the future, is not able to break down from the city center while providing a number of functions in itself. Because industry, education, service sector is not a development zone, functional relations with city centers will continue.

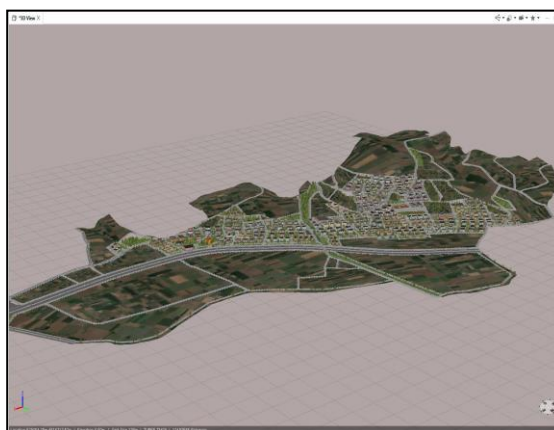


Figure 10 3D Scene which is created with CityEngine

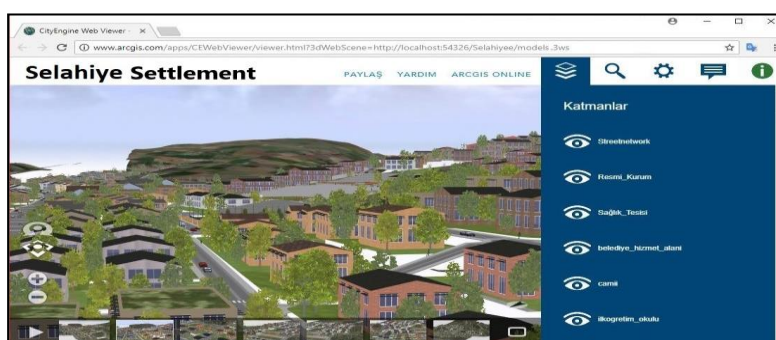


Figure 11 Web Presentation Of City Engine

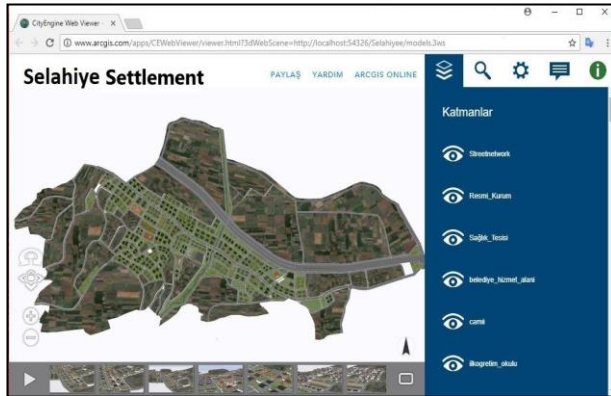


Figure 12 Web Presentation Of City Engine

provide internet presentation. As a result, the .cej software is transformed into .3ws format, as shown in Figure 11, when switching to a 3D model / city Internet environment. Selahiye's city modeling can easily be presented to the web easily without needing different software thanks to the integration of the program.

While transferring the database and all the city components to the web environment in the software, it is possible to access the attributes of the components within the model or city as shown in Figure 12. It also offers the possibility to offer this to multiple users.

#### 4. CONCLUSIONS

In our age, technologies are rapidly developing and changing. Keeping up with the technologies that show continuous improvement and change is inevitable in urban planning studies. Geographic Information Systems together with location-based developing technologies and three-dimensional modeling has begun to develop. In this study, 3-dimensional urban modeling was performed by visualizing the changing criteria in the development of temporal and spatial development in the Selahiye and visualizing the social and spatial texture without distorting the social and spatial texture. With the city modeling, the current situation is compared with the future situation. By comparison, the current situation will be predicted in the future by supporting the field studies. Urban components, especially agriculture, which is an economic activity, are brought together without disturbing the texture. Selahiye, which has a village status in terms of settlement geography, will start to gain urban functions in a short time due to its proximity to the district center. Therefore, the future status is modeled in the city status.

During the city modeling, the characteristics of the citizens who will live in the working area were tried to be taken into consideration and they were raised to the third dimension based on the planning according to the master plan. Due to the fact that all the plans made especially for the master plan were two-dimensional, many errors were encountered during the modeling process. It is also possible to use the height by drawing attention to the fact that two dimensions are not sufficient here. Due to the inadequacy of two-dimensional works, it is easier to understand the space with the three-dimensional modeling needed. In order to understand the real sense, it is necessary to perceive three-dimensional. For this reason, three dimensional modeling should be used in planning studies. With the modeling, the problems that will arise in the future will be prevented without realizing the problems that will arise in the future. In this way, everything is premeditated for the well-being of the people who will live by saving time and cost in order to prevent the washing and demolition. There are various property rights violations arising from the rapid development of cities. With these three-dimensional information system, these violations can be viewed and necessary measures can be taken without losing time (Bal, 2007). Thanks to this system, illegal construction of the city will be controlled. The timely provision of other fees such as taxation and property fees will be easier and more systematic. The three-dimensional modeling studies are made not only for the city modeling in this study, but also for the modeling of historical and tourism-oriented structures, disaster management, environment and urban regulations, universities, real estate market. Many 3D modeling software is available. However, due to its dynamic nature, various calculations and image quality, Esri City Engine program was used for city modeling in Selahiye. In addition to the road, housing, mosque, sports facility,

All information obtained provides a base for creating a city model. After modeling, it is foreseen that there will be some error margins during the implementation phase of the study. Other disciplines related to the subject must test the applicability of the model in real life and work to eliminate the margin of error. Esri City Engine 2017.1 software not only works as a desktop application, but keeps pace with the developing technology. Therefore, this software was used to design the study in three dimensions.

City Engine software Esri cloud integration with the 3D work done in the software makes it possible to

trade centers, as well as infrastructure services modeled in the work with City Engine program can be modeled. The necessary plans can be modeled in three dimensions by program.

The three-dimensional measurements and inquiries can be made from these bases and especially in terms of the sensitivity of the measurements in the city master activities and a number of construction work required for the survey of land and even without the use of any measuring instrument in the field is intended (Uçar & Ergün, 2004). City Engine software includes these features in the current version. These features are provided in more advanced dimensions. In order to meet the demands of the local governments to create rapidly increasing City Information System, there is a need to prepare the Urban Information System infrastructure and standards required for our country without losing more time (Çete, 2002). For this reason, in this field, self-made elements and technical tools are needed. With the technical personnel and hardware, the problems of the City Information System in local governments should be minimized and temporal and spatial deformation should be avoided.

### ACKNOWLEDGEMENTS

This study was supported by TÜBİTAK(The Scientific And Technological Research Council Of Turkey)2209/A University Students Research Projects Support Program.

### REFERENCES

- [1]. Bal, M. A. (2007, Ekim). Kent Bilgi Sistemlerinin Üç Boyutlu Görselleştirilmesi Ümitköy-Çayyolu Örneği. Yüksek Lisans Tezi.
- [2]. *Birleşmiş Milletler*. (2018). Dünya Kentleşme Araştırmaları: <https://esa.un.org/unpd/wup/>
- [3]. Çete, M. (2002). Kent Bilgi Sistemi Tasarımı Ve Uygulaması: Pelitli Belediyesi Örneği . Trabzon: Jeodezi ve Fotogrametri Müh. Anabilim Dalı Yüksek Lisans Tezi.
- [4]. Esri. (2018, 07 13). *City Engine Manual*. <http://desktop.arcgis.com/en/cityengine/latest/get-started/cityengine-faq.htm#anchor11>
- [5]. Rüstemoğlu, V. (2014). Coğrafi Bilgi Sistemleri ve 3D Modelleme. *KMÜ Sosyal ve Ekonomik Araştırmalar Dergisi*, 146-150.
- [6]. Singh, S. P., Jain, K., & Mandla, R. (2014, Ocak). Image based Virtual 3D Campus modeling by using CityEngine. *American Journal of Engineering Science and Technology Research*, 2(1).
- [7]. Sümer, E., & Türker, M. (2010). 3B Bina Modelleri İçin Otomatik Bina Yüz Dokusu Çıkarımı. *HKMO Jeodezi, Jeoinformasyon Ve Arazi Yönetimi Dergisi* 5(3), 11-16.
- [8]. Tiryakioğlu, İ., Uysal, M., Erdoğan, S., Yalçın, M., Polat, N., & Toprak, A. S. (2016). 3 Boyutlu Bina Modelleme ve Web Tabanlı Sunumu : Ahmet Necdet Sezer Kampüsü Örneği. *Afyon Kocatepe Üniversitesi Fen Ve Mühendislik Bilimleri Dergisi*, 16(1), 107-114.
- [9]. Turoğlu, H. (2016). *Coğrafi Bilgi Sistemlerinin Temel Esasları*. İstanbul: Çantay Kitabevi.
- [10]. Tümerterkin, E., & Özgüç, N. (2011). *Beşeri Coğrafya: İnsan, Kültür, Mekan*. İstanbul: Çantay Kitabevi.
- [11]. Uçar, E., & Ergün, B. (2004). Fotogrametride Üç Boyutlu Şehir Modelleme Teknikleri Ve Cbs Kullanımı. *Harita Genel Komutanlığı Harita Dergisi*(132), 48-56.
- [12]. Yıldırım, E. (2012). Üç Boyutlu Kent Modelleri ve İnternet Erişimi. *Yıldız Teknik Üniversitesi Harita Mühendisliği Anabilim Dalı YL Tezi*. İstanbul.
- [13]. Yücel, M. A., & Selçuk, M. (2009). Farklı Ayrıştırma Düzeylerinde 3 Boyutlu Kent Modelleme Ve CityGML. *Journal of Yasar University*, 4(15), 2337-2355.

# ICOEST

UKRAINE

4TH INTERNATIONAL CONFERENCE ON  
ENVIRONMENTAL SCIENCE AND TECHNOLOGY



**TURKISH  
AIRLINES** 

**CNR**GROUP

**EUROPE  
CONGRESS**  
[www.europecongress.org](http://www.europecongress.org)